



**University of
Reading**

Novel strategies for the characterisation and diagnosis of snakebite envenomation

Harry Fonseca Williams

Thesis submitted for the Degree of Doctor of Philosophy

**School of Chemistry, Food and Pharmacy
Institute for Cardiovascular and Metabolic Research**

August 2019

“All good stories start with a snake”

-Nicholas Cage

Contents

Acknowledgments.....	1
Abbreviations.....	2
Declaration.....	4
Abstract.....	5
Publications and presentations.....	6
1. Introduction.....	8
1.1 Definition of snakebite envenoming.....	8
1.2 Generalise pathology of SBE.....	9
1.3 Toxic synergy of methaemoglobin production as a result of SBE.....	10
1.4 Delays in muscle regeneration following SBE.....	11
1.5 Current state and necessity of diagnosis in treating SBE.....	13
1.6 Summary.....	14
2. Additional introductory chapters.....	17
2.1 The urgent need to develop novel strategies for the diagnosis and treatment of snakebites.....	18
Introduction.....	19
The Complexity of Snake Venom.....	24
Antivenom and its associated problems.....	29
Diagnosis of snakebites.....	31
Future treatment approaches for snakebite envenoming.....	33
Diagnostics feeding into treatment.....	35
Conclusion.....	36
References.....	37
2.2 Challenges in diagnosing and treating snakebites in a rural population of Tamil Nadu, India: The views of clinicians.....	48
Introduction.....	49
Methods.....	49
Results and Discussion.....	50
Conclusions.....	51
References.....	51
3. Aims and objectives.....	52
4. Experimental chapters.....	55
4.1 Impact of Naja nigricollis Venom on the Production of Methaemoglobin.....	56
Introduction.....	57

Results.....	59
Discussion.....	62
Materials and Methods.....	65
References.....	66
4.2 Mechanisms underpinning the permanent muscle damage induced by snake venom metalloprotease.....	69
Introduction.....	71
Materials and Methods.....	72
Results.....	75
Discussion.....	82
References.....	86
4.3 Effects of batimastat and marimastat on a group I metalloprotease from the venom of Crotalus atrox.....	90
Introduction.....	91
Materials and Methods.....	93
Results.....	98
Discussion.....	106
References.....	107
4.4 The detection of snake venom serine proteases using a peptide-based approach.....	112
Introduction.....	114
Materials and Methods.....	117
Results.....	122
Discussion.....	129
References.....	133
4.5 Toxin-specific antibodies for the detection of snake venom metalloproteases in clinical samples obtained from snakebite victims.....	136
Introduction.....	138
Methods.....	141
Results.....	145
Discussion.....	154
References.....	157
5. General discussion.....	161
6. Appendix.....	174
Doctors questionnaire.....	175
Coauthored papers.....	177

Acknowledgements

First and foremost, I would like to acknowledge a huge debt of thanks to my supervisor and thalaivar Dr Sakthivel Vaiyapuri who gave me an opportunity to pursue this PhD in an act of blind faith. Without his support the transition between field zoologist and conservationist to laboratory-based researcher would have been unbearable. He has provided endless support to me throughout every step of my PhD and his passion for this subject has been incredibly contagious. I cannot begin to thank him enough.

I would also like to thank my second supervisor Dr Andrew Bicknell for his infrequent but most valuable intellectual and experimental input as well as unfailing good humour. Professor Ketan Patel also deserves huge thanks for putting up with my amateur muscle work and providing constant assistance from his group during the muscle damage study presented herein (a big thank you particularly to Ben Mellows and Robert Mitchell). The other PIs of Hopkins particularly Professor Phil Knight, Dr Keith Foster, Dr Graeme Cottrell and Dr Alister McNeish were invaluable in the lending of equipment, expertise and patience.

A massive thanks is also bestowed upon Venomtech UK - without our collaboration my PhD would have involved a much narrower range of venoms and have far lesser implications for snakebite in the real world. The CEO Steve Trim was also instrumental with his constant intellectual support and willingness to assist us in every way.

My fellow lab-mates Thomas Vallance, Divyarashree Ravishankar, Eman Alzahrani, Dina Albadawi, Kahdr Alatawi, Maryam Salamah and Radhika Pothi have all supported me in a number of platelet-based ways and my team venom partner Harry Layfield who was essential to the final year of my PhD and in assisting me in teaching our endless students. The BSc, UROP, MPharm and work experience students: Alice Filipe, Rae Ahamed, Peter Banks, Nicola Spence, Melina Akhbari, Marco Yung, Alison Wong, Kitty Lun, Felix Townsend, Chloe Small, Alex Soundy and of course Ipsitiger Sarkar for teaching me to teach and appreciating my passion and forgiving any occasionally passive aggressive or impatient behaviour.

I also extend my thanks to the other PhD students and postdocs of Hopkins, particularly my masseuse in chief Anna Roashan, as well as Daniella Vaughan, Jono Sheard, Wouter Eilers, Mhairi Laird, Shirley Keaton, Roashan Limbu, Yuhan Hu, Charlotte Day, Andrew Parnell, Feroz Ahmed, Khalid Alyodawi and Marie-Theres Zeuner amongst others for stimulating conversation. Penultimately, the Co-Op/Eat at the Square for occasional necessary tasty indulgences and finally my family, who have been unceasing in their support of me. I never would have started and certainly never would have finished this PhD without them.

Abbreviations

Abbreviation	Acceptation
3FTX	Three-finger toxin
ABScaff	Alternative Binding Scaffolds
ANOVA	Analysis of Variance
ASV	Anti-snake venom (antivenom)
BAAMC	N α -Benzoyl- L-Arginine-7-Amido-4-methylcoumarin hydrochloride
BM	Basement Membrane
CAMP	<i>Crotalus atrox</i> metalloprotease
CAMP2	<i>Crotalus atrox</i> metalloprotease 2
CLN	Centrally Located Nuclei
CRiSP	Cysteine-rich secretory protein
CRP-XL	Cross Linked Collagen Related Peptide
CSL-SVDK	Commonwealth Serum Laboratory Snake Venom Detection Kit
CT	Cholera Toxin
CTX	Cardiotoxin I from <i>Naja pallida</i>
DALYs	Disability Adjusted Life Years
DAPI	4, 6-diamidino-2-phenylindole
DTT	Dithiothreitol
DMEM	Dulbecco's Modified Eagle Medium
DNA	Deoxyribose Nucleic Acids
ECM	Extra Cellular Matrix
ED ₅₀	Median Effective Dose
EDL	Extensor Digitorum Longus
EGF	Endothelial Growth Factor
ELISA	Enzyme Linked Immunosorbent assay
Fab	Fragment Antigen-binding
F(ab') ₂	Fab dimer resulting from pepsin digestion
FPLC	Fast Protein Liquid Chromatography
GDP	Gross Domestic Product
Hb	Haemoglobin
HPLC	High Performance Liquid Chromatography
IgG	Immunoglobulin G
KSPi	Kunitz Type Serine Protease Inhibitor

LAAO	L-Amino Acid Oxidase
LFA	Lateral Flow Assay
mAb	Monoclonal antibody
MetHb	Methaemoglobin
MS	Mass spectrometry
MYH3	The gene for embryonic skeletal muscle myosin heavy chain 3
NGF	Nerve growth factor
NP	Natriuretic peptides
NTD	Neglected Tropical Disease
PAR	Protease activated receptor
PBS	Phosphate buffered saline
PBS-T	PBS containing Tween® 20
PEG	Polyethylene Glycol
RBC	Red Blood Cell
RNA	Ribonucleic Acid
ROS	Reactive Oxygen Species
SAVP	South Africa Vaccine Producers
SBE	Snakebite envenoming
SC	Satellite Cell
scFvs	Single Chain Variable Fragments
SDS-PAGE	Sodium Dodecyl Sulphate Polyacrylamide Gel Electrophoresis
SFCM	Single Fibre Culture Medium
SLEP	Shelf life extension program
SMT	Small Molecular Therapeutics
SVSP	Snake venom serine protease
SVMP	Snake venom metalloprotease
TA	Tibialis Anterior
TLSP	Thrombin-like serine protease
T-VDA ^{CV}	Targeted venom discovery array for Cardiovascular system
PLA2	Phospholipase A2
SNACLEC	Snake C-type lectin
VAP	Vascular Apoptosis Inducing Protein
V _H H	Single domain antibody fragments
WBCT	Whole blood clotting time/test
WHO	World Health Organisation

Declaration

Declaration of original authorship

I confirm that this is my own work and the use of all material from other sources has been properly and fully acknowledged.

Harry Fonseca Williams

Abstract

Globally, snakebite envenoming (SBE) kills in excess of 100,000 people annually and causes sequelae to over 450,000. Improvements to treatment, and even much of our understanding of the pathologies surrounding snakebite have gone little improved in over a century. This thesis aims to uncover more of the mysteries surrounding SBE and outline methodologies for the improvement of diagnostics for snakebites. Clinicians are crippled by a lack of reliable diagnostical tools and have nothing by which to treat any of the underlying conditions associated with SBE. Here we aim to answer two questions, what are these underlying conditions and are future therapeutics likely to be efficacious; and can toxin-specific antibodies be developed to identify venom components and diagnose SBE? To answer the first, we focus on venom-induced muscle damage and oxidative stress through characterising collagenolytic activities of snake venom metalloproteases (SVMP) and methaemoglobin production respectively (methaemoglobin is a toxic product of the oxidation of haemoglobin). This latter effect, was found to be a potential result of a wide range of venoms and particularly pronounced in an Elapid, *Naja nigricollis*, challenging the assumption that this effect is only seen in viper venoms. In addition to this, the route by which SVMPs induce permanent skeletal muscle damage was elucidated via the purification of a P-III SVMP and its treatment in skeletal muscles of mice. The three causative factors contributing to the prevention of muscle regeneration seen were found to be 1. destruction of collagen and a range of other basement membrane components, 2. Damage of blood capillaries causing delayed macrophage infiltration and blockade of blood supply to the affected regions, and 3. reduced proliferation, migration and abundance of satellite cells, thereby preventing the muscle regeneration. The use of matrix metalloprotease inhibitors, marimastat and batimastat were found to inhibit a P-I SVMP. The administration of such therapeutics requires careful diagnosis, and thus our second focus was developing means by which to detect snake venoms in victims. The use of a sequence-structure-function and phylogenetic approach in synthesising peptides from which to make toxin-specific antibodies showed some promise but yielded ineffectual antibodies for use in the two-site immunoassay they were designed for. Using antibodies instead raised against purified toxins was more successful, allowing the development of relatively specific two-site enzyme-linked immunosorbent assays and lateral flow assays. Together, this study forms a solid basis in order to characterise SBE in more detail and develop diagnostic platforms using novel strategies to not only improve the diagnosis and treatment of snakebites but also to better understand the pathophysiology of SBE.

Publications and presentations

The following originated within the timeframe of this doctorate:

& included in this thesis *Authors contributed equally to the work

Review articles

1. **The urgent need to develop novel strategies for the diagnosis and treatment of snakebite.**

&**Williams, H. F.**, Layfield, H. J., Vallance, T., Patel, K., Bicknell, A. B., Trim, S & Vaiyapuri, S.
Toxins 20 June 2019 11(6): 363

2. **Toll-Like Receptor 4 Signalling and Its Impact on Platelet Function, Thrombosis, and Haemostasis.**

Vallance, T. M., Zeuner, M. T., **Williams, H. F.**, Widera, D., & Vaiyapuri, S.
Mediators of Inflammation (2017) Vol: 2017

Short Communications

3. **Challenges in diagnosing and treating snakebites in a rural population of Tamil Nadu, India: The views of clinicians.**

&**Williams, H. F.**, Vaiyapuri, R., Gajjeraman, P., Hutchinson, G., Gibbins, J. M., Bicknell, A. B., & Vaiyapuri, S.
Toxicon (2017) 130: p.44-46

Research Articles

4. **Impact of *Naja nigricollis* venom on the production of methaemoglobin.**

&**Williams, H. F.**, *Hayter, P., Ravishankar, D., Bains, A., Layfield, H. J., Croucher, L., Work, C., Bicknell, A., Trim, S. & Vaiyapuri, S.
Toxins (2018) 10(12), p.539

5. **Mechanisms underpinning the permanent muscle damage induced by snake venom metalloprotease.**

&**Williams, H. F.**, *Mellows, B. A., *Mitchell, R., Sfyri, P., Layfield, H. J., Salamah, M., Vaiyapuri, R., Bicknell, A. B., Collins-Hooper, H., Matsakas, A., Patel, K., & Vaiyapuri, S.
PLOS Neglected Tropical Diseases (2019) 13(1), p.e0007041

6. **Environmental factors affecting the distribution of African elephants in the Kasigau wildlife corridor, SE Kenya.**

Williams, H. F., Bartholomew, D. C., Amakobe, B., & Githiru, M.
African Journal of Ecology (2018), 56(2) p.244-253

7. **Roadkill scavenging behaviour in an urban environment.**

Schwartz, A. L., **Williams, H. F.**, Chadwick, E., Thomas, R. J., & Perkins, S. E.

Journal of Urban Ecology (2018), 4(1), pp.1-7

8. Impact of specific functional groups in flavonoids on the modulation of platelet activation.

Ravishankar, D., Salamah, M., Akimbaev, A., **Williams, H. F.**, Albadawi, D. A., Vaiyapuri, R., Greco, F., Osborn, H., & Vaiyapuri, S.

Scientific Reports (2018) 8(1), p.9528

9. Ruthenium-conjugated chrysin analogues modulate platelet activity, thrombus formation and haemostasis with enhanced efficacy.

Ravishankar, D., Salamah, M., Attina, A., Pothi, R., Vallance, T., Javed, M., **Williams, H. F.**, Alzahrani, E., Kabova, E., Vaiyapuri, R., Shankland, K., Gibbins, J., Strohfeld, K., Greco, F., Osborn, H., & Vaiyapuri, S.

Scientific reports (2017) 7(1), p5738

10. The endogenous antimicrobial cathelicidin LL37 induces platelet activation and augments thrombus formation.

Salamah, M. F., Ravishankar, D., Kodji, X., Moraes, L. A., **Williams, H. F.**, Vallance, T. M., Albadawi, D., Vaiyapuri, R., Watson, K., Gibbins, J., Brain, S., Perretti, M., & Vaiyapuri, S.

Blood advances (2018) 2(21), pp.2973-2985

Posters

11. Williams, H. F., Bicknell, A., and Vaiyapuri, S. (2017) The use of synthetic flavonoids in the treatment of snakebites. Reading School of Pharmacy Research Showcase.

12. Williams, H. F., Mellows, B., Mitchell., Layfield, H. J., Salama, M., Vaiyapuri, R., Bicknell, A., Patel, K., and Vaiyapuri, S. (2018). Mechanisms underpinning permanent skeletal muscle damage induced by snake venom metalloproteases. Leiden, Naturalis. Snakebite: from science to society

Talks

13. Williams, H. F., Bicknell, A., and Vaiyapuri, S. (2017) Developing a diagnostic kit for snakebite envenomation. Reading School of Pharmacy Research Showcase.

14. Williams, H. F., Bicknell, A., and Vaiyapuri, S. (2018) Developing a diagnostic kit for snakebite envenomation. Hopkins Seminar Series.

15. Williams, H. F., Mellows, B., Mitchell., Layfield, H. J., Salama, M., Vaiyapuri, R., Bicknell, A., Patel, K., and Vaiyapuri, S. (2018). Mechanisms underpinning permanent skeletal muscle damage induced by snake venom metalloproteases. Yerevan, Armenia. European Section on the International Society for Toxinology.

16. Williams, H. F (2019). Snakebite: a vascular journey of destruction? Pint of Science – Reading.

1. Introduction

1.1 Definition of snakebite envenoming

Snakebite is the product of bites from approximately 4,000 species of snakes. It can lead to psychological trauma, infections, bleeding and other undesirable effects, but only a certain proportion of these bites will involve envenomation [1]. Less than 20% of the snake species found globally are venomous, and bites from these species can lead to Snakebite Envenomation (SBE). SBE involves much more serious pathologies and frequently results in death [2]. Even in the case of bites from venomous species, outcomes ranging from dry bites, where no venom is injected, to full envenomations, with the injection of all venom available in the glands, can occur, leading to a broad range of pathologies.

SBE kills an estimated 100,000 people or more every year [3], causes physical and psychological trauma to many more and is now receiving unprecedented attention from the media and research funders. SBE is nevertheless likely to remain a hugely distressing and common disease in the rural tropics for many decades to come.

It is the rapid injection of the most toxicologically complex, naturally occurring cocktail on earth and associated with such a diverse range of effects that animal-derived antivenom treatments have been very difficult to improve upon. The lack of education, protective clothing and effective antivenoms all also contribute to this dire state of affairs [4]. Clinicians feel somewhat powerless, without protocols or any diagnostical methods and treatment does, to a large extent, depend upon the individual clinician's experience with bites and somewhat trial and error approaches from their past. Clinicians recognise antivenoms inefficacy at treating the local effects and are unequivocally in need of adjunctive treatments for the reduction of mortality, permanent physical disabilities, disfigurement and other SBE associated morbidity [5]. Snake venoms are hugely diverse arsenals, and the result of millennia of evolution with natural selection guiding snake venoms to both kill their prey and begin digestion from within as efficiently as possible [6]. Venoms typically contain multiple enzymatic and non-enzymatic

components from ten major toxin families, each eliciting a range of effects [7]. The full variety of effects induced by each family is far from being understood, but the future of therapeutics which must target morbidity as well as mortality, depends upon understanding exactly which systems a venom can attack, and how best this can be prevented or ameliorated.

1.2 Generalised pathology of SBE

After injection from venom glands via fangs, venom is typically deposited in the interstitial fluid, where the non-locally acting components slowly travel through the lymphatic system (aided in some cases by hyaluronidases in the venom cleaving the hyaluronic acid of the interstitial fluid) before reaching the blood stream [1]. The vast range of effects can then be grouped loosely into systemic haemotoxic and neurotoxic effects and local cytotoxicity. Viper venoms are typically a combination of both haemotoxic and cytotoxic components: upon reaching the blood, haemotoxic venoms act on vessels and the blood itself, collagenolytic enzymes begin cleaving blood vessels and causing haemorrhaging (snake venom metalloproteases [SVMPs]). Simultaneously, a range of compounds will start affecting the blood directly, both inhibiting or activating platelets (disintegrins, snake venom serine proteases [SVSPs], cysteine rich secretory proteins [CRiSPs], L-amino acid oxidases [LAAO], phospholipase A₂ [PLA₂]) cleaving fibrinogen to cause unstable clots (SVMP and SVSP) and making the blood uncoagulable – intensifying haemorrhaging – and lysing red blood cells to release haemoglobin (PLA₂ and three finger toxins [3FTX]), and then oxidising this to form the toxic hypoxic compound methaemoglobin (LAAO and others). The consequential reduction in circulating blood causes hypotension and can at the extreme cause hypovolemic shock and heart failure [4]. This is frequently combined with cytotoxic effects involving venom components attacking the muscle and other tissues which are exposed following haemorrhaging or surrounding the bite site. The basement membrane of muscle fibres and cell membranes of individual myocytes are frequently targeted causing necrosis and impairing

muscle regeneration [8, 9]. The lack of blood supply from the haemotoxic effects then further exacerbate this cytotoxicity [10].

This is in contrast to elapid envenomation, which, while frequently involving some degree of haemotoxic/cytotoxic effects, more typically centre on neurotoxicity. Following the slow release from the lymphatic system to the blood, their, largely non-enzymatic components, primarily target synapses (PLA₂, 3FTX and kunitz type peptides), preventing nerve transmission and frequently paralysing victims of bites [11].

This highlights the huge complexity of SBE, which despite being considered one disease, gives rise to a range of different disorders. SBE is recognised as a neglected tropical disease (NTD), but by comparison to other NTDs it has many more impediments to treatment: it has a much greater range of causative toxins; just one far more antiquated treatment option; and almost no diagnostical methods by which to not only improve treatment, but also allow the collection of more robust epidemiological data – which is currently lacking [2].

1.3 Toxic synergy of methaemoglobin production as a result of SBE

An incomplete understanding of all the underlying pathophysiology of SBE mean there are no therapies yet to be considered realistic alternatives to antivenom. Local to the bite, many venoms will have such destructive effects on the vasculature in the tissues they enter, that antivenoms are unable to reach the areas in need and fail to ameliorate the hypoxia, local tissue damage and other secondary effects [12]. One compounding factor to the cytotoxic nature of many venoms is methaemoglobin production. The generation of this toxic haemoglobin species is currently associated with few (mostly viper) venoms [13, 14] but is actually the result of a large range of both viper and elapid venoms [15]. This production of such a toxic compound can exacerbate hypoxia from haemorrhage induced ischaemia and cause oxidative stress, particularly at the bite site where the majority of necrosis and local tissue damage occurs. Use of the antioxidant melatonin has been proposed as one possible

means of ameliorating the effect [13, 16]. However, melatonin is also associated with lowering of the blood pressure [17] and has the potential to act in synergy with hypotensive venom toxins, intensified by haemorrhaging caused by SVMPs and increasing the chances of hypovolemic shock occurring. Therefore, the safe administration of melatonin is likely to rely on specific diagnosis in order to rule out envenoming from hypotensive venoms. This effect on haemoglobin is also likely to add significantly to local hypoxic conditions, adding to delayed muscle regeneration and furthering the cell death and necrosis common to the tissues local to the bite site. Muscles already starved of oxygen from haemorrhaging of vasculature and ischaemia are provided with an oxidised and unrelinquishing haemoglobin species, that promotes oxidative stress in already necrotic and dying tissues.

1.4 Delays in muscle regeneration following SBE

The effects of venoms on muscles can be attributed to three main toxin families, PLA₂, 3FTXs and SVMPs. As pore forming molecules the myotoxic nature of PLA₂s and 3FTXs is rapid depolarisation of myocytes, effecting the myofibres without effecting the basement membrane (BM) surrounding them [18]. The BM is an essential element skeletal muscle and provides the medium for satellite cell functionality and consequential successful muscle regeneration [19] (see Figure 1). Satellite cells are the multipotent precursors to myocytes which move to sites of damage before proliferating and differentiating into renewed muscle [20]. This causes PLA₂ and 3FTX induced muscle damage to undergo much faster regeneration than SVMP-induced muscle damage, due not only to the destruction of collagen and other muscular basement membrane components by SVMPs, but also haemorrhaging from the cleavage of collagen found in the vascular endothelium [21].

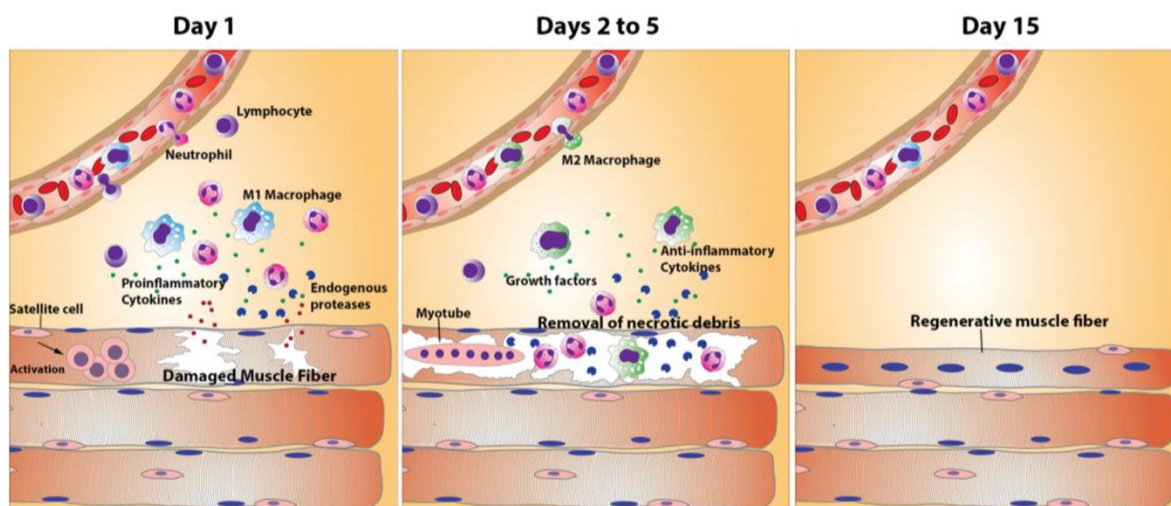


Figure 1. Schematic showing normal skeletal muscle regeneration. Taken from Gutierrez *et al.* (2018) [23]. After muscle damage and consequential necrosis, an inflammatory response is triggered involving an influx of resident immune cells including neutrophils and macrophages to clear necrotic debris. Resident multipotent satellite cells are then activated and replicate, regenerating the damaged muscle fibre. Under viperid envenoming, haemorrhaging prevents leucocyte efficacy and damage to the basement membrane prevents normal satellite cell function thereby hindering regeneration.

Secondary to a venom's directly myotoxic actions on the BM, can be the haemorrhagic and consequently ischaemic and hypoxic conditions which can in themselves cause cytotoxicity through the lack of toxin clearance, reduction in nutrients and oxygen, and lack of debris clearance by macrophages [22]. Therefore, SVMPs are a key target when addressing the local effects of snakebite in order to ensure functioning vasculature through which a healthy blood supply can pass and if necessary, drugs can be administered. A range of potential small molecular therapeutics (SMTs) targeting SVMPs have been proposed, though none are yet to have been approved for clinical usage.

Suggested future therapeutics combatting SVMP related cyto- and haemotoxic effects are currently limited to two groups: the metal chelators, for example EDTA [24], which are able to chelate the zinc found within SVMPs - an ion which is essential to their function; and the matrix metalloprotease inhibitors (MMPis), which mimic the natural substrate of metalloproteases, binding permanently and blocking their function [25]. Their ability to effect

endogenous metalloproteases has implications for their use *in vivo*, however there is a growing body of evidence suggesting such SMTs could significantly ameliorate the haemorrhagic and collagenolytic effects of the SVMPs – which may outweigh any negative effects on endogenous proteins. This would reduce ischemia, hypoxia and other SVMP-associated local effects. The significant homogeneity between SVMPs and endogenous matrix metalloproteases mean these are also inhibited by these compounds. The MMPs have been associated with a decrease in vascular growth and the other endogenous functions of these proteases [26]. Therefore, care must be taken when administering such drugs and ascertaining the state of envenomation by an SVMP-containing venom is essential before administration of potentially detrimental compounds [2].

1.5 Current state and necessity of diagnosis in treating SBE

Diagnostical devices for snakebite envenoming are virtually non-existent. Given the lack of diversity in treatments, with typically only one polyvalent antivenom available in a region, some scientists deem the development of such products unnecessary. However, in the future, alternative treatments will become available.

In order to facilitate the toxin-specific approaches that most of these future therapeutics are currently focussed on, cheap, indicative, point-of-care devices are in need of development. This will not only take the onus off clinicians making the right decision on treatment, but prevent drug wastage and unnecessary hospital bills [2]. This can potentially inform on the exact species in some locations and indicate toxin-specific treatments where available.

By furthering our understanding of some of the lesser known effects of venoms and assessing the ability of available drugs to ameliorate the negative effects we can rapidly alleviate some of the morbidity associated with SBE. The use of drugs will undoubtedly have consequences on physiology, some of which may not be beneficial, therefore benefits should be weighed up against negatives, and diagnostics need to be improved to allow

administration, only when certain that perceived benefits are justified and that the drug indicated will be beneficial to the victim of that specific envenomation.

1.5 Summary

In this thesis SBE is shown to be an incredibly complex malady, particularly when compared to other neglected tropical diseases. Clinicians feel somewhat powerless, in part due to rarely having an understanding of the offending snake species, how much venom has been injected and therefore what to expect from a given envenomation. SBE also has underlying and currently untreated side effects, including methaemoglobin production and associated hypoxia. The production of which we show to be common amongst snake venoms. Methaemoglobin is likely to exacerbate local tissue damage and muscle regeneration. The musculature is already damaged due to a range of myotoxic venom components, and regeneration is known to be delayed in SVMP-containing venoms. We found this delayed regeneration to be a result of basement membrane destruction which has consequences for satellite cell mobility and efficacy – an essential aspect to effective regeneration. This is unlike smaller pore forming myotoxins which allow muscles to regenerate with relative ease and pace. We found metalloprotease inhibitors and chelators to effectively prevent the collagenolytic activity of a P-I SVMP *in vitro*, suggesting these compounds could aid in the amelioration of SVMP-induced long-term skeletal muscle damage. Finally, we show two possible methods for developing simple point of care devices indicating the presence of specific toxins. These can be developed using purified proteins, or peptides based on conserved regions of proteins and immediately feed into protocols, indicating antivenom, as well as helping in the collection of rigorous epidemiological data.

References

1. Warrell, D.A., *Snake bite*. The Lancet, 2010. **375**(9708): p. 77-88.
2. Williams, H.F., et al., *The Urgent Need to Develop Novel Strategies for the Diagnosis and Treatment of Snakebites*. Toxins, 2019. **11**(6): p. 363.
3. Kasturiratne, A., et al., *The global burden of snakebite: a literature analysis and modelling based on regional estimates of envenoming and deaths*. PLoS Med, 2008. **5**(11): p. e218.
4. Gutiérrez, J.M., et al., *Snakebite envenoming*. Nature Reviews Disease Primers, 2017. **3**: p. nrdp201763.
5. Williams, H.F., et al., *Challenges in diagnosing and treating snakebites in a rural population of Tamil Nadu, India: The views of clinicians*. Toxicon, 2017. **130**: p. 44-46.
6. Casewell, N.R., et al., *Complex cocktails: the evolutionary novelty of venoms*. Trends in ecology & evolution, 2013. **28**(4): p. 219-229.
7. Tasoulis, T. and G.K. Isbister, *A Review and Database of Snake Venom Proteomes*. Toxins, 2017. **9**(9): p. 290.
8. Xiong, S. and C. Huang, *Synergistic strategies of predominant toxins in snake venoms*. Toxicology Letters, 2018. **287**: p. 142-154.
9. Ferreira, B.A., et al., *Inflammation, angiogenesis and fibrogenesis are differentially modulated by distinct domains of the snake venom metalloproteinase jararhagin*. International Journal of Biological Macromolecules, 2018. **119**: p. 1179-1187.
10. Gutiérrez, J.M., et al., *Experimental pathology of local tissue damage induced by Bothrops asper snake venom*. Toxicon, 2009. **54**(7): p. 958-975.
11. Ranawaka, U.K., D.G. Lalloo, and H.J. de Silva, *Neurotoxicity in Snakebite—The Limits of Our Knowledge*. PLOS Neglected Tropical Diseases, 2013. **7**(10): p. e2302.
12. Gutiérrez, J.M., et al., *Neutralization of local tissue damage induced by Bothrops asper (terciopelo) snake venom*. Toxicon, 1998. **36**(11): p. 1529-1538.
13. Sharma, R.D., et al., *Oxidative stress-induced methemoglobinemia is the silent killer during snakebite: a novel and strategic neutralization by melatonin*. Journal of pineal research, 2015. **59**(2): p. 240-254.
14. Meléndez-Martínez, D., et al., *Rattlesnake Crotalus molossus nigrescens venom induces oxidative stress on human erythrocytes*. Journal of Venomous Animals and Toxins including Tropical Diseases, 2017. **23**(1): p. 24.
15. Williams, H.F., et al., *Impact of Naja nigricollis Venom on the Production of Methaemoglobin*. Toxins, 2018. **10**(12): p. 539.
16. Katkar, G.D., et al., *Melatonin alleviates Echis carinatus venom-induced toxicities by modulating inflammatory mediators and oxidative stress*. J Pineal Res, 2014. **56**(3): p. 295-312.
17. Scheer, F.A., et al., *Daily nighttime melatonin reduces blood pressure in male patients with essential hypertension*. Hypertension, 2004. **43**(2): p. 192-197.
18. Gutiérrez, J.M.a. and C.L. Ownby, *Skeletal muscle degeneration induced by venom phospholipases A2: insights into the mechanisms of local and systemic myotoxicity*. Toxicon, 2003. **42**(8): p. 915-931.
19. Caldwell, C., D. Matthey, and R. Weller, *Role of the basement membrane in the regeneration of skeletal muscle*. Neuropathology and applied neurobiology, 1990. **16**(3): p. 225-238.
20. Otto, A., et al., *Canonical Wnt signalling induces satellite-cell proliferation during adult skeletal muscle regeneration*. Journal of cell science, 2008. **121**(17): p. 2939-2950.

21. Williams, H.F., et al., *Mechanisms underpinning the permanent muscle damage induced by snake venom metalloprotease*. PLOS Neglected Tropical Diseases, 2019. **13**(1): p. e0007041.
22. Gutiérrez, J.M., et al., *Hemorrhage induced by snake venom metalloproteinases: biochemical and biophysical mechanisms involved in microvessel damage*. Toxicon, 2005. **45**(8): p. 997-1011.
23. Gutiérrez, J., et al., *Why is skeletal muscle regeneration impaired after myonecrosis induced by viperid snake venoms?* Toxins, 2018. **10**(5): p. 182.
24. Ainsworth, S., et al., *The paraspecific neutralisation of snake venom induced coagulopathy by antivenoms*. Communications Biology, 2018. **1**(1): p. 34.
25. Escalante, T., et al., *Effectiveness of batimastat, a synthetic inhibitor of matrix metalloproteinases, in neutralizing local tissue damage induced by BaPI, a hemorrhagic metalloproteinase from the venom of the snake Bothrops asper*. Biochemical pharmacology, 2000. **60**(2): p. 269-274.
26. Zhu, W.-H., et al., *Regulation of vascular growth and regression by matrix metalloproteinases in the rat aorta model of angiogenesis*. Laboratory Investigation, 2000. **80**(4): p. 545.

2. Additional introductory chapters

2.1 The urgent need to develop novel strategies for the diagnosis and treatment of snakebites

Harry F. Williams, Harry J. Layfield, Thomas Vallance, Ketan Patel, Andrew B. Bicknell, Steven Trim and Sakthivel Vaiyapuri

Toxins 2019

2.2 Challenges in diagnosing and treating snakebites in a rural population of Tamil Nadu, India: The views of clinicians

Harry F. Williams, Rajendran Vaiyapuri, Prabu Gajjeraman, Gail Hutchinson, Jonathon M. Gibbins, Andrew B. Bicknell and Sakthivel Vaiyapuri

Toxicon 2017

2.1 The urgent need to develop novel strategies for the diagnosis and treatment of snakebites

Harry F. Williams¹, Harry J. Layfield¹, Thomas Vallance¹, Ketan Patel², Andrew B. Bicknell², Steven Trim³ and Sakthivel Vaiyapuri¹

¹School of Pharmacy, University of Reading, Reading, United Kingdom

²School of Biological Sciences, University of Reading, Reading, United Kingdom

³Venomtech Private Limited, Sandwich, United Kingdom

Toxins 2019 - Open Access

Conclusion of this chapter

Snakebite envenoming is one of the most complex of the neglected tropical diseases. The diversity in toxicological profiles and resulting pathologies is unprecedented in other diseases and clinicians are somewhat powerless in diagnosing and treating it. Currently, polyvalent antivenoms are the only treatment option and aim at preventing the life-threatening aspects of envenomation but have few effects on the local tissue damage and morbidity associated with snakebite. An added issue is that diagnosis is usually based on symptoms, making the rapid administration of antivenom (which is essential to minimising local effects and minimising risk of death) a rare occurrence. There are however a range of emerging therapies as both adjunctive and alternative treatments to antivenom, but the commonality of adverse effects - such as unwanted inhibition of endogenous proteins - make proper diagnosis a necessity before administering potentially harmful drugs. Such diagnostical tools are in desperate need of development as none are currently commercially available in the areas most in need.

Contribution to this chapter

General contribution (85%)

- Analysis and interpretation of data
- Writing of the manuscript
- Preparation and design of figures

Review

The Urgent Need to Develop Novel Strategies for the Diagnosis and Treatment of Snakebites

Harry F. Williams ¹, Harry J. Layfield ¹, Thomas Vallance ¹, Ketan Patel ², Andrew B. Bicknell ², Steven A. Trim ³ and Sakthivel Vaiyapuri ^{1,*}

¹ School of Pharmacy, University of Reading, Reading RG6 6AH, UK; h.f.williams@pgr.reading.ac.uk (H.F.W.); harrylayfield@gmail.com (H.J.L.); t.m.vallance@pgr.reading.ac.uk (T.V.)

² School of Biological Sciences, University of Reading, Reading RG6 6AH, UK; ketan.patel@reading.ac.uk (K.P.); a.b.bicknell@reading.ac.uk (A.B.B.)

³ Venomtech Ltd, Discovery Park, Sandwich, Kent, UK; s.trim@venomtech.co.uk

* Correspondence: s.vaiyapuri@reading.ac.uk

Received: 30 May 2019; Accepted: 18 June 2019; Published: 20 June 2019

Abstract: Snakebite envenoming (SBE) is a priority neglected tropical disease, which kills in excess of 100,000 people per year. Additionally, many millions of survivors also suffer through disabilities and long-term health consequences. The only treatment for SBE, antivenom, has a number of major associated problems, not least, adverse reactions and limited availability. This emphasises the necessity for urgent improvements to the management of this disease. Administration of antivenom is too frequently based on symptomatology, which results in wasting crucial time. The majority of SBE-affected regions rely on broad-spectrum polyvalent antivenoms that have a low content of case-specific efficacious immunoglobulins. Research into small molecular therapeutics such as varespladib/methyl-varespladib (PLA₂ inhibitors) and batimastat/marimastat (metalloprotease inhibitors) suggest that such adjunctive treatments could be hugely beneficial to victims. Progress into toxin-specific monoclonal antibodies as well as alternative binding scaffolds such as aptamers hold much promise for future treatment strategies. SBE is not implicit during snakebite, due to venom metering. Thus, the delay between bite and symptom presentation is critical and when symptoms appear it may often already be too late to effectively treat SBE. The development of reliable diagnostic tools could therefore initiate a paradigm shift in the treatment of SBE. While the complete eradication of SBE is an impossibility, mitigation is in the pipeline, with new treatments and diagnostics rapidly emerging. Here we critically review the urgent necessity for the development of diagnostic tools and improved therapeutics to mitigate the deaths and disabilities caused by SBE.

Keywords: snakebite envenoming (SBE); venom; diagnostics; therapeutics; toxin neutralisation; neglected tropical disease

Key Contribution: This review highlights the key factors contributing to the gross mortality and morbidity associated with snakebite envenoming. The current research taking place to overcome this complex disease and the urgent need to develop improved diagnostics and therapeutics for snakebites are also discussed.

1. Introduction

Snakebite envenomation (SBE) is a life threatening and traumatising affliction that is unequivocally associated with the world's most impoverished people [1]. Mortalities from SBE are concentrated in the rural tropics where snakes are in abundance and the agricultural work force is

poorly protected. The limited recognition of the scale of the crisis by health authorities around the globe afforded SBE a place on the World Health Organisation's list of neglected tropical diseases in 2009 (NTD). This was followed by a contentious removal before again being reinstated in 2017 and quickly being made a priority NTD [2,3]. The confusion surrounding SBE as an NTD is somewhat justified: SBE is not limited to the tropics and all other NTDs are caused by pathogens entering the body: protozoa, helminths, bacteria and viruses [4]. Thus, the causative agents are easier to identify and study by comparison to the diversity of pathologies associated with SBE. Indeed, Australia classes snakebite as a non-intentional injury rather than a disease, but with an average of two deaths a year, it is unlike the crisis seen in more impoverished countries [5]. The extent of SBE taking place every year is estimated to be between 1.8–2.7 million [6]. The actual deaths from SBE are purported to be between 81,000–137,000 [7] and nearly 50,000 of these deaths are estimated to take place in India alone [8]. There are a further 8,000 in Pakistan and 6,000 in Bangladesh [9], while in the Americas despite 60,000 snakebites taking place annually, deaths are estimated to only be in the hundreds [10]. While shocking, the deaths frequently hide a potentially greater issue, which is the disability and consequential loss to the economic workforce. Delays in seeking medical assistance are common, and postponements for just a couple of days can lead to gangrene, compartmental syndrome and amputation [11]. Surviving SBE can also have mental health implications, with survivors seeing a three-fold increase in depressive disorders compared to the general population [12]. Post-traumatic stress disorder also occurred in a further 20% of SBE victims surveyed in Sri Lanka [12]. In West Africa, the disability-adjusted life years (years lost due to disability or early death) from SBE are estimated to be over 300,000 [13]. These figures are ever increasing, due to past data suffering from flaws from under-reporting and victims avoiding hospitals for cheaper and more convenient traditional herbalists.

This staggering epidemiology is unsurprising when compared to more typical diseases. The marked difference between SBE and many of the other NTDs is the diversity involved in the range of associated toxins seen globally. Cholera, for example, (not limited to the tropics and therefore sometimes ignored as an NTD), like SBE causes many thousands of deaths every year (Table 1). Cholera has such a dramatic effect on its victims primarily through one toxin (cholera toxin/CT) released by strains of the *Vibrio cholerae* bacteria. CT triggers a cascade of events which culminate in an influx of salts and water into the intestine, causing the diarrhoea that aids in transmission of the disease to others, and leaves victims to die by dehydration [14]. The disease is the result of one toxin, from one species of bacteria, with one simple and effective treatment. The nematode infections (shown in Table 1) are all a result of roundworms, which have evolved to inhabit the gastrointestinal tract of humans. Despite resulting from a range of species, the same anti-helminthic drugs can easily treat this disorder [15]. In stark contrast, SBE can be the result of bites from hundreds of different snake species, each possessing a multitude of different toxin profiles and leading to a vast array of different pathologies [16]. Treatment is consequently far more complex than the rehydration required to beat the majority of cholera infections [17], and simple prophylactics required to prevent many of the other NTDs (Table 1) [18]. SBE has proved to be an incredibly complex disease to accurately diagnose and treat appropriately.

Table 1. A comparison of snakebite envenomation (SBE) alongside other traditional major neglected tropical diseases. Sorted based on deaths. Adapted and updated from Hotez et al. (2007) [19].

Disease (Source of Data)	Causal Species	Estimated Deaths/An	Global Prevalence	Population at Risk	Clinical Manifestations	Treatment	Diagnostics
Snakebite Envenomation [7]	Snakes: >90 Genera, >700 Species	81,000–137,000	Up to 2,700,000	6–7 Billion	Neurotoxicity and paralysis or cardiovascular toxicity and hypovolemic shock. Cytotoxicity leading to tissue damage and amputation.	Anti-venom	Fang marks, local tissue damage, immunoassay (Aus) Clinical/laboratory markers give other indications
Cholera [20,21]	Bacterium: <i>Vibrio cholerae</i>	68,400	2,800,000	1.4 Billion	Watery diarrhoea	Oral or intravenous rehydration	Stool examination
Leishmaniasis [20]	Protist: <i>Leishmania</i> spp. Transmitted by female sandflies; <i>Phlebotomus/Lutzomyia</i> spp.	24,200	12,000,000	350 Million	Cutaneous and mucocutaneous disease, kala-azar	Anti-moniales, amphotericin B, pentamidine, miltefosine	Biopsy
Chagas' Disease [20]	Protist: <i>Trypanosoma cruzi</i>	8000	5,700,000	70 Million	Cardiomyopathy, megacolon, Mega esophagus	Benznidazole, nifurtimox	Blood smear
Schistosomiasis (Bilharzia) [20]	Trematodes: <i>Schistosoma</i> spp.	4400	207,000,000	779 Million	Hematuria and urogenital disease, intestinal and liver fibrosis, growth and cognitive delays	Praziquantel	Stool examination
Human African Trypanosomiasis [20]	Protist: <i>Trypanosoma brucei</i> amongst other species. Transmitted by tsetse flies; <i>Glossina</i> spp.	3500	300,000	60 Million	Sleeping sickness	Pentamidine, suramin, melarsoprol, eflornithine	Biopsy or blood smear
Ascariasis [20]	Nematode: <i>Ascaris lumbricoides</i>	2700	807,000,000	4.2 Billion	Malnutrition, growth and cognitive delays	Albendazole/mabendazole	Stool examination
Trichuriasis [22,23]	Nematode: <i>Trichuris trichiura</i>	Deaths rarely direct	604,000,000	3.2 Billion	Inflammatory bowel disease, growth and cognitive delays	Albendazole/mabendazole	Stool examination
Hookworm Infection [22,23]	Nematodes: <i>Ancylostoma duodenale/Necator americanus</i>	Deaths rarely direct	576,000,000	3.2 Billion	Anemia, malnutrition, growth and cognitive delays, poor pregnancy outcome	Albendazole/mabendazole	Stool examination
Lymphatic Filariasis [24,25]	Nematodes: <i>Wuchereria bancrofti</i> , <i>Brugia</i> spp.	Deaths rarely direct	120,000,000	1.3 Billion	Adenolymphangitis, lymphedema, hydrocele	Ivermectin/diethylcarbamazine (plus albendazole)	LFA test strip (Alere)
Trachoma [19]	Bacterium: <i>Chlamydia trachomatis</i>	Deaths rarely direct	84,000,000	590 Million	Trachomatous folliculitis and inflammation, trichiasis, blindness	Surgery, azithromycin	Clinical diagnosis using loupes (magnifiers)

Onchocerciasis [26]	Nematode: <i>Onchocerca volvulus</i> . Transmitted by blackflies; <i>Simulium</i> spp.	Deaths rarely direct	37,000,000	90 Million	Onchocerca, skin disease, blindness	Ivermectin	Biopsy/slit lamp examination/antibody tests
Leprosy [27]	Bacterium: <i>Mycobacterium leprae</i>	Deaths rarely direct	200,000	ND	Lepromatous leprosy, tuberculoid leprosy	Multidrug therapy, rifampicin, clofazimine, dapsone	Biopsy
Dracunculiasis [28]	Nematode: <i>Dracunculus medinensis</i>	Deaths rarely direct	30	ND	Disfiguring ulcer, secondary bacterial infection	Metronidazole/thio bendazole adjunctive to self-care and stick therapy	Clinical presentation

Venoms are essentially cocktails of toxic and non-toxic components: proteins, peptides, metal ions and small organic molecules, including nucleotides, secreted by animals to predate on or defend against other animals. In snakes, venom is a modified form of saliva produced from a pair of venomous glands and delivered by fangs, and found in species from a number of taxa. All venomous reptiles have been grouped in a clade called Toxicofera, within which, another clade, Caenophidia holds all the venomous snakes (Figure 1). The strictly venomous families are Elapidae (elapids) that includes the snakes with fixed front fangs e.g., cobras, kraits, mambas, taipans and sea snakes (sometimes grouped in the subfamily, Hydrophiinae) amongst others; and Viperidae (vipers) which have hinged front fangs allowing longer fangs and deeper tissue penetration. The vipers are further divided into two subfamilies, Viperinae (the true vipers, e.g., Gaboon viper and European adder) and Crotalinae (the pit vipers, e.g., rattlesnakes and lanceheads). Additionally, two other families contain venomous species, although the majority of these families are made up of non-venomous snakes. The first is Colubridae (colubrids), a loose grouping containing over half of described snake species with reported deaths arising from at least five species: the boomslang (*Dispholidus typus*); twig snake (*Thelotornis capensis*); tiger keelback (*Rhabdophis tigrinus*); South American green racer (*Philodryas offersii*) and Peruvian slender snake (*Tachymenis peruviana*) [29], though many others have potentially occurred. The second mixed family is Lamprophiidae (lamprophiids), which contains several venomous (e.g., Atractaspidinae) and non-venomous subfamilies, of note is the genus *Atractaspis*: the stiletto snakes or burrowing asps [16,30,31]. Venomous bites from *Atractaspis* occur across most of sub-Saharan Africa (and some western Asian counties) and occasionally cause fatalities [32] due in part to a lack of specific antivenom over most of the genus' range. The majority of lethal bites are, however, almost exclusively from members of Viperidae and Elapidae families [33]. The impact of these two families can be oversimplified as largely neurotoxic in the case of elapid bites and haemotoxic in the case of viper bites. Flaccid paralysis and respiratory failure often result from elapid bites. Hypovolemic shock (the loss of >20% blood) leading to heart failure [34,35] alongside acute kidney injury [36] are potential causes of death in viper bites. However, there are some vipers that rely on neurotoxic components, such as the atypical South American rattlesnake (*Crotalus durissus terrificus*) the venom of which contains crotoxin, and Russell's viper, *Daboia russelii*, which contains U1-viperitoxin-Dr1a [37]. Both of these viperid neurotoxins are pre-synaptically active neurotoxic phospholipase A₂ (PLA₂) [38] which are generally seen more commonly in elapid venoms (other neurotoxic viper venoms are known [39–41]). Elapids are also not without their exceptions to the rule, in particular the Australian elapids for which the cause of death is frequently cardiac arrest, and coagulopathy is also common due to the high proportion of prothrombin activators in their venoms [5,42,43].

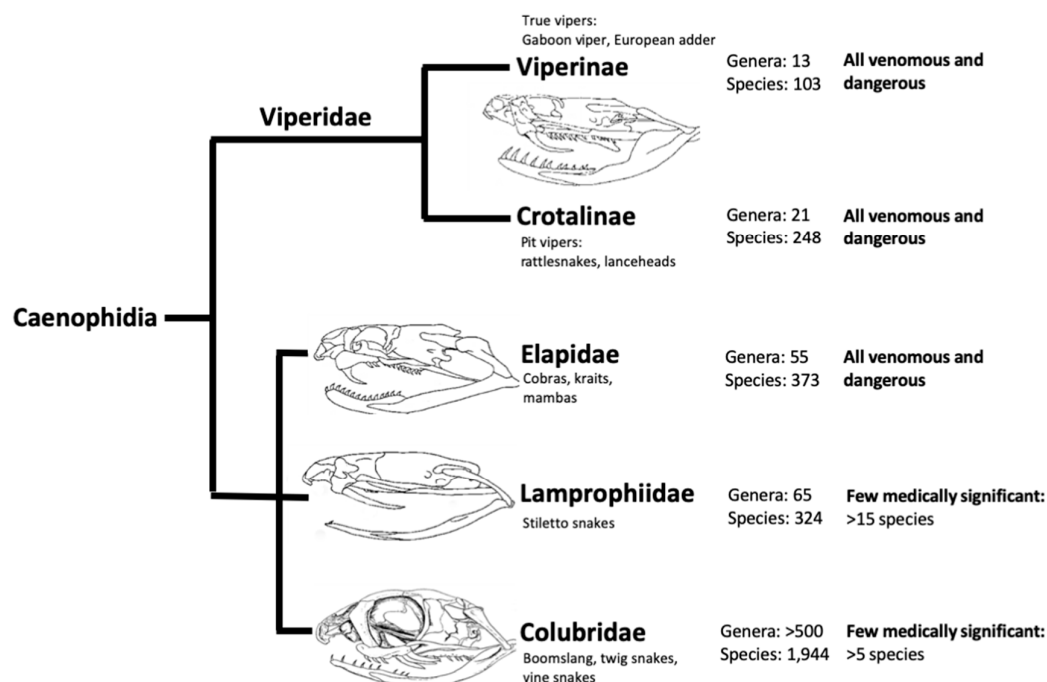


Figure 1. Phylogenetic tree adapted from Reyes-Velasco et al. (2014) [44]. Shows the Caenophidia, a clade including all venomous snakes. The skull diagrams were adapted from published images [45,46]. Number of species and genera were taken from the reptile database [47].

2. The Complexity of Snake Venoms

One of the major difficulties in treating snakebites is the hugely diverse geographic and taxonomic nature of venomous snakes and the consequential variability of venoms [48–50]. Many of the 680 or so venomous species of snakes are further split into subspecies each with added levels of diversity in venom compositions to their congeners [51]. As well as this, many undiscovered cryptic species may also exist providing yet further diversity of venom and undiscovered venom components [52]. The variation in venom between these subspecies leads to differences in symptomatology [53] as well as varying levels of antivenom efficacy [54]. Therefore, a thorough knowledge of serpentine systematics is crucial for effective treatment of snakebites [55]. Despite their differences, snake venoms do have many similarities. They are all complex mixtures of hydrolytic enzymes, biologically active non-enzymatic proteins and peptides—these are responsible for the spectrum of their toxic effects (Figure 2) [16].

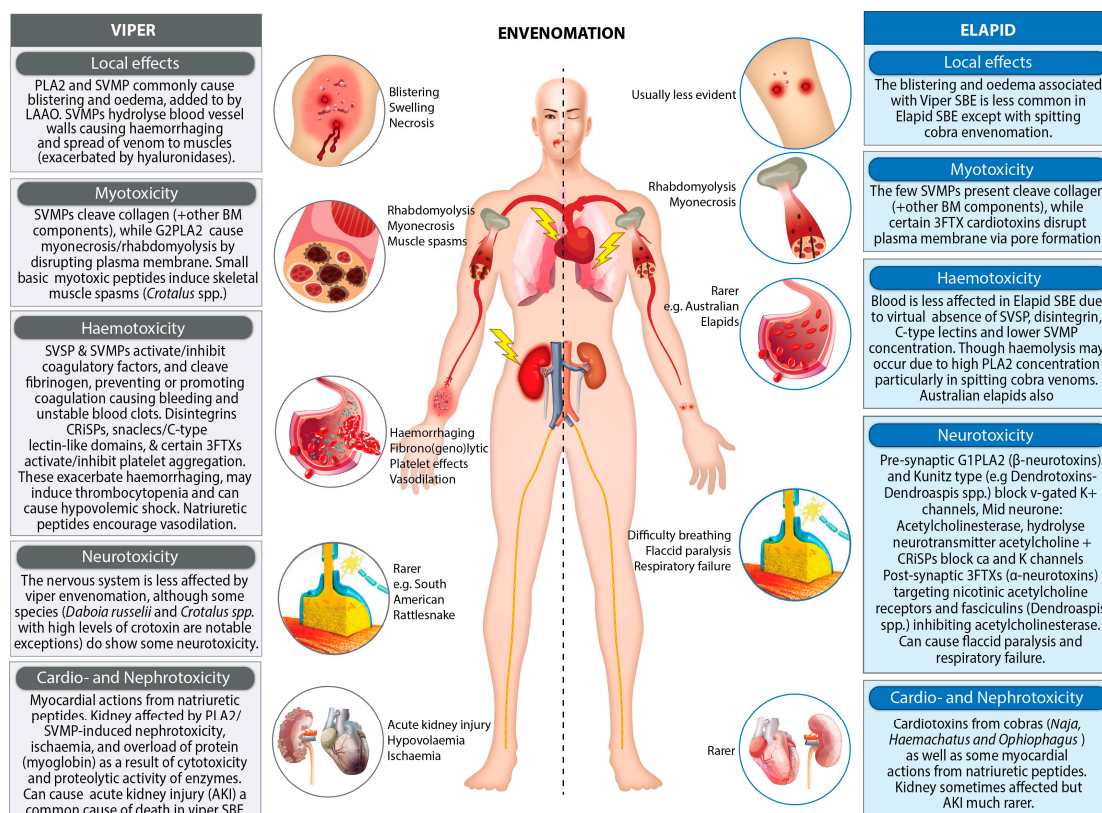


Figure 2. Generalised effects of viper and elapid snakebite envenomation and toxins causing these effects. Inspired by Gutiérrez et al. (2017) [16]. Abbreviations: PLA₂—Phospholipase A₂, SVMP—Snake venom metalloprotease, G2PLA₂—Group 2 PLA₂, SVSP—Snake venom serine protease, CRiSPs—Cysteine rich secretory proteins, Snakecys—Snake c-type lectins, 3FTXs—Three finger toxins, SBE—snakebite envenoming, BM—basement membrane.

A large number of protein families exist within snake venoms: there are four dominant protein families (phospholipase A₂, metalloproteases, serine proteases, and three-finger toxins), and six secondary protein families (Cysteine-rich secretory proteins, L-amino acid oxidases, kunitz peptides, C-type lectins, disintegrins and natriuretic peptides) as well as over 36 rarer protein families [56]. These dominant and secondary families form the bulk of snake venoms and are largely to blame for the incredibly broad symptomatology and pathology associated with SBE (Table 2).

Table 2. The major enzymatic (grey) and non-enzymatic (blue) proteins found in snake venoms and their primary functions. The table was adapted from Warrell (2010) [30] and abundance data were created using data from 132 snake species (42 members of Elapidae, 20 Viperinae and 65 Crotalinae). These data were provided in Tasoulin & Isbister (2017) [56] and data were used with the authors' permission.

Venom Component	Approximate Abundance (%) (±SD))			Major Described Functions
	Elapidae	Viperinae	Crotalinae	
Phospholipase A ₂ (PLA ₂)	31 (±24)	22 (±17)	22 (±20)	Presynaptic neurotoxicity (β-neurotoxins), membrane phospholipolysis, haemolysis, myotoxicity, necrosis and inhibition/activation of platelets
Snake venom metalloprotease (SVMP)	3 (±3)	35 (±20)	36 (±20)	Haemorrhaging, fibrin(ogen)olytic activity, endothelial damage and myotoxicity

Snake venom serine protease (SVSP)	1 (\pm 1)	12 (\pm 9)	16 (\pm 14)	Hypotension, fibrin(ogen)olytic activity and bleeding
L-amino acid oxidase (LAAO)	1 (\pm 2)	2 (\pm 2)	5 (\pm 4)	Apoptosis, oedema, cytotoxicity via products and anticoagulant effects via inhibition factor IX
Three-finger toxin (3FTX)	55 (\pm 27)	NA	NA	Postsynaptic neurotoxicity via binding of cholinergic receptors (α -neurotoxins), cardiotoxicity, myotoxicity and cytotoxicity
Kunitz type serine protease inhibitors (KSPi)	4 (\pm 10)	3 (\pm 6)	NA	Neurotoxicity via binding of voltage gated potassium channels or anticoagulopathic effects due to serine protease inhibition
Cysteine rich secretory protein (CRiSP)	2 (\pm 3)	4 (\pm 4)	2 (\pm 2)	Smooth muscle inhibition via blocking of calcium channels
Natriuretic peptides	1 (\pm 1)	1 (\pm 3)	7 (\pm 9)	Promote excretion of sodium by kidneys causing hypotension and cardiotoxicity
Snake C-type lectins (Snaclec)	NA	9 (\pm 6)	6 (\pm 8)	Platelet inhibition and activation via an array of receptors
Disintegrin	NA	6 (\pm 5)	2 (\pm 4)	Binding of integrins causing inhibition of platelet aggregation

2.1. Enzymatic Components

PLA₂ are a group of esterolytic enzymes present in snake venoms that typically catalyse the breakdown of glycerophospholipids, the main component of biological membranes, into lysophospholipids and a fatty acid (which may be involved with the oxidation of haemoglobin [57]). However, within snake venoms, many members of this group have lost most of their enzymatic activity and instead bind to various receptors. The snake venom PLA₂s are split into two groups, group I PLA₂s are found predominantly in elapid and some colubrid snakes, while group II are found only within Viperidae. Group I are generally β -neurotoxins which act pre-synaptically, sometimes binding to voltage gated potassium channels [58], although multiple mechanisms exist [59,60]. After binding, neurotoxic PLA₂s can sometimes hydrolyze nerve terminal phospholipids causing permanent neurotoxicity [61]. This has the effect of causing paralysis, while group II PLA₂s tend to act cytotoxically, predominantly as myotoxins, causing myonecrosis via the disruption of the plasma membrane [62]. Sometimes after hydrolysing membrane phospholipids, non-enzymatic PLA₂ homologues cause damage to the sarcolemma via hydrophobic interactions [63]. PLA₂s have further diverse pharmacological functions, however, haemotoxicity [64], postsynaptic neurotoxicity as well as the inhibition and activation of platelet aggregation, cardiotoxicity and anticoagulant effects have also been reported [65,66].

Snake venom metalloproteases (SVMPs) are the most abundant venom enzymes in vipers (also present to a lesser extent in elapids), and include both coagulants (e.g., activation of prothrombin or factor X), and anticoagulants (comprising of integrin shedding and fibrinolytic enzymes [67]). Importantly, they also frequently induce haemorrhaging due to hydrolysis of the endothelial cell basement membrane components around blood capillaries [68]. These also affect muscle fibres impairing their regeneration [69]. These enzymes are in themselves a highly diverse family, and are separated into four groups depending on the domains present: P-I/Group I comprise just a metalloprotease domain, present in all groups. In the venom gland it exists as a zymogen with a pro-peptide domain that is cleaved before activation; P-II/Group II has an additional disintegrin domain, which have been found to be liberated as free disintegrins after processing in some venoms [70]; P-III/Group III has additional disintegrin-like and Cysteine rich domains and P-IV as P-III but with two C-type lectin-like domains attached via disulphide bonds [52,71]. These additional domains afford SVMPs a wide variety of different functions. For example, the disintegrin domains bind integrins blocking their functions in platelets and endothelial cells [72] and have the potential to bind the

integrins in muscle cells, colocalising and exacerbating myotoxic effects [69]. Cysteine-rich domains have also been found to inhibit collagen induced platelet aggregation as well as to play a key role in the onset of inflammation [73]. Finally, C-type lectin-like domains, which amongst other functions of SVMs, are involved in the activation of platelets by the clustering of tyrosine kinase dependent receptors [74].

Snake venom serine proteases (SVSPs) mainly affect the haemostasis of victims by proteolytically degrading the blood components (e.g., fibrinogen) as well as modulating various coagulatory factors (e.g., factor V and plasminogen) [75]. Despite the variety of processes SVSPs can affect, the primary function of the majority of studied SVSPs is to cleave fibrinogen, promoting coagulation, but they can also prevent coagulation through dysfibrinogenemia. These are called ‘thrombin-like’ enzymes due to their mimicking of thrombin’s primary function, although SVSPs rarely activate factor XIII which thrombin does in order to cross-link the soluble fibrin clot into an insoluble clot [76]. There are additional SVSPs described as ‘kallikrein-like’ (bradykinin releasing and blood vessel dilating) [77,78], factor V activators (consequently prothrombin activating) [79] and platelet aggregators (via cleavage of protease activated receptors PAR1 & PAR4 [80]) that cause alterations in blood pressure or cause blood to clot [81]. Anticoagulant SVSPs also exist with some found to activate protein C, a proenzyme involved in negatively regulating the coagulation cascade via inactivation of factors V and VIII [82,83], and degrading blood clots by conversion of plasminogen to plasmin.

L-amino acid oxidases (LAAOs) are not an abundant enzyme family, they are, however, found fairly ubiquitously in both elapid and viper venoms [56]. They are glycoproteinaceous flavoenzymes and catalyse the oxidative deamination of L-amino acids. This produces an α -keto acid, ammonia and hydrogen peroxide, all of which can have cytotoxic effects. The hydrogen peroxide produced may additionally lead to the oxidation of haemoglobin seen as a result of some viper venoms [84,85]. They may also induce oedema [86] and apoptosis [87], as well as acting as anti-coagulants via the inhibition of factor IX [88]. These enzymes are, however, still poorly understood, and thought to play some roles in the stabilisation of venom components within the gland or ducts [89] or aid in digestion.

Other enzymes found in much lower quantities in venoms include; acetylcholinesterase, a serine hydrolase which functions synaptically, hydrolysing the neurotransmitter acetylcholine [90]; and hyaluronidases which are known as the spreading factors [91] due to their facilitation of the diffusion of other toxins across the body tissues as well as causing oedema via hydrolysing the hyaluronic acid barrier in the interstitial space [92]. The remaining groups of venom enzymes are thought to be involved more in digestion rather than the immobilisation of prey, and are consequently considered non-toxic by many researchers [93]. However, ignoring the hidden functions of these “non-toxic” components could be imprudent, for example, the ability of nucleases to liberate purines (adenosine in particular) which can act as multifunctional toxins [94].

2.2. Non-Enzymatic Components

As well as enzymes, there are also a whole host of non-enzymatic venom components, which carry out a variety of different functions. *Three-finger toxins* are characterised by a three-finger fold made up of three loops which protrude from a hydrophobic core [95]. They are found predominantly in elapid venoms, some viper venoms (only via transcriptomics [96]) and also certain colubrid venoms [97,98]. Despite their common structure, they bind to many different receptors and elicit a variety of biological effects [99]. They are typically neuro- or cytotoxic. The α -neurotoxins, one important group of three finger toxins, bind post-synaptically, to nicotinic acetylcholine receptors found in the skeletal muscle of vertebrates [98], blocking neuromuscular transmission, causing flaccid paralysis and respiratory failure in some cases [100]. Three-finger toxins also include κ -bungarotoxins and haditoxin which operate similarly to the α -neurotoxins [99]; as well as acetylcholinesterase inhibitors—the *fasciculins* of the *Dendroaspis* genus [101]; cytolytic, ion pore forming cardiotoxins (cytolysins) found in cobra venoms [102] and L-type calcium channel blockers and platelet aggregation inhibiting three-finger toxins as well [99].

Cysteine-rich secretory proteins (CRISPs) are single chain polypeptides widely distributed within venoms, and have been found in the venoms of all the three main families of venomous snakes [68]

as well as in some lizard venoms [103]. Like three-finger toxins, CRISPs have a scaffold that is highly conserved and is stabilised via disulphide linkages and exert a wide range of pharmacological activities. Helothermine, a CRISP isolated from the venom of the lizard, *Heloderma horridum horridum* has been found to block calcium [104] and potassium [105] currents in neurons and to lower body temperature in mice [106]. CRISPs have also been documented to inhibit smooth muscle contraction via the blocking of Ca^{2+} channels [107,108] and to block cyclic nucleotide gated ion channels which are significant in many modes of sensory transduction [106].

Kunitz-type proteinase inhibitors are small proteins that are found in a range of viper and elapid venoms [109]. While some act to inhibit serine proteases, others have been found to block a large range of ion channels despite high homology. One notable neurotoxic group of Kunitz peptides are called the dendrotoxins, and form the largest component of mamba (*Dendroaspis spp.*) venoms before α -neurotoxins [110]. These proteins have no protease activity and instead interact with voltage gated potassium channels [110,111]. This potentiates the effect of acetylcholine, facilitating its release at the presynaptic nerve terminal causing excitation resulting in involuntary muscle contractions [112]. Synergism between components within venoms is well known [110,113], and some PLA₂s are even known to act as heterodimers with Kunitz peptides potentiating their combined effects as in β -bungarotoxin from *Bungarus multicinctus* [114] and MitTX from *Micrurus tener tener* [115].

In mammalian systems, C-type lectins typically bind to calcium and sugar residues. However, in snake venoms they are known as *Snake C-type lectin-like proteins* or *snaclecs* and they rarely have the binding loop responsible for this mammalian function but instead bind to a variety of receptors on platelets [74], as well as coagulation factors IX/X [116] and endothelial cells [117]. They have been reported to both inhibit [118] and activate [119] via a number of receptors on platelets including $\alpha_2\beta_1$, GPIb, GPVI and CLEC-2 [89,120], sometimes causing thrombocytopenia as a result [16,74].

The *disintegrins* are a family of polypeptides present in viper venoms, some of which are released from SVMPs while others have independent genes. The majority of disintegrins rely on an RGD (Arg-Gly-Asp) motif, (a tripeptide recognised and used by integrins in cell membrane binding) to inhibit integrin function. Disintegrins are not to be confused with the disintegrin-like domains within certain metalloproteases which instead rely on an ECD (Glu-Cys-Asp) motif [72]. They inhibit collagen induced platelet activation via integrin $\alpha_2\beta_1$ [121] and can competitively inhibit the binding of collagen to the α_1 domain of $\alpha_1\beta_1$ [122] along with targets on a wide range of other disintegrins [123]. They are predominantly potent inhibitors of platelet aggregation [67], acting primarily upon integrin $\alpha\text{IIb}\beta_3$, the fibrinogen receptor. Others that do not inhibit platelet aggregation have also been characterised [124].

Natriuretic peptides have been found in both elapid and viper venoms, although they are found in much higher abundance in viper venoms, occasionally making up as much as 30% of venoms such as within the bushmasters; *Lachesis* genus [125]. These peptides promote natriuresis, that is to say the excretion of sodium into urine by the kidneys, which affects inotropic (speed and force of contractions) and lusitropic (rate of relaxation) myocardial actions, as well as promoting vasodilation causing hypotension [126,127].

There are many other non-enzymatic venom components which have been described as minor protein families [56] these include bradykinin-potentiating peptides (BPPs) which both inhibit angiotensin converting enzyme as well as cleaving bradykinin giving potent hypotensive effects [128]. The presence of growth factors including nerve growth factor (NGF) and endothelial growth factor (EGF) in venom is poorly understood but may be involved in prey incapacitation, with NGFs purportedly causing mast cells to release a mass of chemical mediators and increasing vascular permeability aiding the dispersal of other venom toxins [129]. There are an additional 40 or more rare and unique protein families [56]. These rare families frequently exert only mild, if any, toxic effects such as the *lipocalins* whose function is currently unknown [130]. Others of these families have extremely limited taxonomic distribution within snake venoms such as the *sarafotoxins*, which are a toxic form of the vasoconstrictive endothelins and are only found in the *Atractaspis* genus [95,131]. Small basic myotoxic peptides (also referred to as defensins [56]) which are found in a limited number of *Crotalus spp.* induce muscle spasms and necrosis [16,30] and other proteins such as waglerin which

is a neurotoxin found only in *Tropidolaemus* spp. [40]. Venoms are all associated with such different toxin combinations which in some cases work synergistically causing SBE to be an incredibly complex disease to treat.

Hence, the currently accepted antivenom therapy has numerous drawbacks, and thus, novel strategies are being employed worldwide to improve the treatment of this disease. Real improvements to the treatment will to some extent depend upon better diagnostic methods.

3. Antivenom (Anti-Snake Venom/Venin/ASV) and Its Associated Problems

Antivenom is the only effective and accepted treatment for systemic SBE yet to stand up to rigorous scientific testing and has single-handedly saved the lives of those suffering SBE for over a century [132].

Despite this, there are a number of major problems associated with antivenom: poor stability in liquid form, adverse reactions, often poor efficacy and great difficulties associated with production, which is frequently too expensive for those most in need. Antivenoms are made via the hyper-immunisation of an animal, typically large mammals e.g., horses and rare instances of manufacturers using sheep and donkeys [133]. The size of these animals means that large volumes of plasma can be collected, allowing larger volumes of antivenom to be generated [134]. This is produced by exposing the animal's immune system to a single venom leading to the creation of monovalent/monospecific antivenoms, or multiple venoms to produce polyvalent/polyspecific antivenoms. The animal's immune system responds by raising antibodies (particularly immunoglobulin G [IgG] in mammals) that bind specifically to immunogenic antigens present in the venom/s [135]. The plasma is then separated from the blood by centrifugation or sedimentation procedures and erythrocytes can then be reinfused into the animal [132]. Further purification then occasionally takes place to reduce non-immunoglobulin serum proteins in some antivenoms (CroFab) reducing non-selective effects. Non-specific immunoglobulins are sometimes also removed via affinity chromatography, and digestion by pepsin or papain is sometimes used to remove the Fc regions resulting in F(ab')₂ or Fab fragments respectively which are used by the majority of western antivenom producers, though whole IgG is also used [133].

3.1. Reproducibility Issues Associated with Antivenom Production

In reality, antivenoms are challenging to produce. Not only do the very same species causing the life-threatening bites have to be milked for their venoms—a high risk task for the personnel involved, but this toxic secretion then has to be injected into an animal at a safe (non-lethal) dose or detoxified in a way so as not to lose immunogenicity. These aforementioned issues cause antivenom generation to be inherently problematic, and can cause stress for the animal, the upkeep of which is already expensive without stress threatening poor immune responses and consequential yields of antivenom [136,137]. The process of production is not only extremely time consuming with low yields, but is also associated with huge batch-to-batch variability [138,139], unsurprising when injecting venoms, which vary greatly, into animals, whose immune systems will have hugely varied responses to the antigen. In order to mitigate these difficulties it is suggested that pooled venoms from at least 20–50 specimens from the same geographical location are used [132]. These can, where available, be compared to national reference venoms for quality control and undergo biochemical characterisation (SDS-PAGE, HPLC, enzymatic activities, etc.) as evidence of consistency. Antivenoms are prepared from pooled plasma/serum and then require rigorous testing to find the median effective dose (ED₅₀), i.e., the volume of antivenom required to protect 50% of a population injected with the venom [132].

3.2. Relative Instability of Antivenom

The instability of liquid antivenom reduces its availability in the remote regions of developing countries where it is most needed and lyophilised preparations are problematic. In liquid form, antivenom requires preservatives, as well as, and more problematically, refrigeration at between 4

°C and 6 °C to maintain its potency. Lyophilised or freeze-dried products are also available, but to minimise cost and maximise ease of use, some are distributed in liquid form [140]. Moreover, warmer temperatures can lead to the formation of protein aggregates in liquid antivenom, which increase the chances of adverse reactions [141]. The relative instability results in antivenom being sold with expiry dates and warnings for avoiding the use of antivenom that has undergone multiple freeze-thaw cycles, despite there being some evidence that neither of these have significant effects on antivenom efficacy [142]. Where antivenom shortages have been identified, such as for the North American Coral Snake antivenom, shelf life extension programs (SLEP) have validated stability over that predicted extending their usage period [143]. This prevents the local distribution of antivenom and contributes to over two thirds of snakebite victims preferentially choosing traditional healers over hospital treatment in several parts of the world, where snakebite is a major concern [144].

There have also been some studies suggesting that as well as being less prone to triggering adverse reactions, camelid immunoglobulins may belong to a more thermally stable subclass of IgGs [145] which could help to overcome the need for refrigeration [146]. Despite improved thermostability, this study was not really designed to replicate the variation in temperature that antivenom would undergo over the course of several years in a tropical country.

3.3. Adverse Reactions to Antivenom

Antivenom invariably contains immunogenic proteins, which activate the immune system of patients, and causes them to suffer from adverse reactions. These are split into two types: acute (anaphylactoid or pyrogenic) and delayed ‘serum’ sickness (now plasma as most antivenoms are plasma-derived) type reactions [147]. Early reactions may be triggered immediately but can take up to an hour for onset of the symptoms. They are associated with mild symptoms such as urticaria (hives), coughing, vomiting, diarrhoea, headaches and nausea, though severe systemic anaphylaxis can also develop, and is associated with bronchospasm, hypotension and angioedema [148]. Pyrogenic reactions may also occur in response to endotoxins from bacterial contaminants of the antivenom [149]. They are characterised by fever, vasodilation, reduction in blood pressure and shaking chills. Late reactions usually occur several days after the initial dose of antivenom and are a form of type III hypersensitivity, which is caused by a build-up of immune complexes inadequately cleared by the immune system [149]. They give similar symptoms to early reactions, but additional symptoms include joint pain, adenopathy, albuminuria and rare cases of encephalopathy. Anaphylactic reactions are frequently treated successfully using prophylactic drugs such as adrenaline and hydrocortisone [150] which serves to reduce capillary permeability and bronchospasm in people suffering from early adverse reactions [148].

The frequency and nature of adverse reactions depends in part on the level of antivenom purification. Crude first generation antivenom has caused adverse reactions in up to 54% of patients [151], but it can be affinity purified to produce second generation antivenoms (pure immunoglobulin mixes without any plasma proteins), consisting of just the whole immunoglobulins (IgG), which some studies have found to decrease adverse reactions to less than 25% of patients [152].

By removing the Fc (fragment crystallisable, or tail) regions of these antibodies enzymatically with pepsin or papain, third generation antivenoms are created. The use of papain breaks the hinge regions resulting in Fab fragments (these portions bind the toxin epitopes) [153] while pepsin will initially leave the hinge region intact forming F(ab')₂ fragments, although prolonged digestion could result in Fv fragments (fragments containing the variable region) which may only bind to antigens temporarily [154]. The removal of Fc regions is assumed to result in fewer adverse reactions [16], with Fab causing only minor adverse reactions when compared to IgG or F(ab')₂ [154].

Indeed, despite all the stages of purification, complete neutralisation by antivenom is rarely achieved [155] and a large percentage of IgG found in antivenom may not be therapeutically useful [146]. In addition to the enhanced stability of camelid immunoglobulins mentioned above [156,157], their immunoglobulins lack the light chains that are present in ovine and equine antibodies [158] and have also been found to bind to epitopes not bound by other mammalian IgGs [159]. However, all these developments into antivenom over the years still fail to address two of the treatment's biggest

drawbacks: stability and cost, which together seriously limit the availability of antivenoms to those most in need.

3.4. Expense of Antivenom

In addition to animal maintenance, when the level of immunoglobulin purification increases, the price of treatment also increases. Although the more expensive and effective generations of antivenoms are of some use in the western world where they are mostly affordable, in third world countries where snakebites are most prevalent, these extortionate antivenoms can cause victims to be financially as well as physically crippled from a snakebite, the financial burden of which can often extend to their friends and family [160]. In India, treatment can cost up to US\$5000, more than double India's GDP per capita and representative of over ten years salary for a typical farm worker [160]. Likewise in the USA, treatment (including antivenom) costing as much as US\$153,000 has been reported [161] though more expensive treatments are likely to have taken place. This does not mean it is impossible to make a cheap antivenom, as an effective antivenom is reported to have been developed from a Nigeria/UK collaboration that is available at just US\$40 per treatment, at which price antivenom is considered one of the most cost effective treatments in the world [136]. However, after the expense of clinical trials and hospital charges, treatment in some countries may have cost 1000 times the production cost of one vial of antivenom [161].

The majority of snakebites occur in rural settings, these are areas far from the hospitals and where electricity is required for refrigerating and administering antivenom [30]. The instability of antivenom means that keeping supplies in the unrefrigerated but most needed regions is impossible, and even if it were possible, the difficulty of administration combined with high probability of adverse reactions would render it of little use to untrained individuals without adequate tertiary care facilities. The dosage is complex, with hugely different mean effective doses depending on venoms targeted and quantity of venom delivered. Mean effective doses from 47 mL [162] to 180 mL [163] of antivenom have been reported and there is some evidence that larger doses can be less effective [164]. There are frequently drugs co-administered with antivenom such as broad-spectrum antibiotics to treat wound infections around the bite site which may occur due to the oral flora present in the mouths of snakes being introduced into bite victims [165,166], which may also lead to sepsis if untreated. There is also growing evidence that venom glands from many species contain a viable microbiome which may directly contribute to wound infection [167].

Such an expensive and complex medicine will always be difficult to distribute widely enough to give protection to the millions of people living alongside potentially deadly snakes. The dangerously low supplies of antivenom have been described as a 'crisis' [168] and available supplies are insufficient in both quantity and quality with limited—if any—preclinical assessment data available [137]. A more practical alternative therapeutic approach would therefore be of great merit, particularly to the developing world. Preventative measures such as wearing rubber boots [169] when harvesting and sleeping under mosquito nets [170] are also important to reduce reliance on therapy alone, though the purchase and distribution to all those in need is unrealistic.

Despite the issues with antivenom, as of yet it is the only medicine proven in the treatment of SBE in humans. The cases where it has been ineffective should not detract from its ability to save people even in the late stages of envenomation [171]. Indeed many of the problems arising from the use of antivenom can be minimised by adhering to the WHO guidelines for the management of snakebite [148]. Guidelines which could also serve to reduce the administration of dangerously large doses of antivenom, with reports of doses of 200 vials or two litres of antivenom in some rare cases [172].

4. Diagnosis of Snakebites

For a long time, the diagnosis of snakebites has relied almost entirely on the symptomatology as well as a detailed clinical history of the symptoms, and of the offending snake. For rapid assessment, five brief questions to help with this have been described [16]:

1. Where were you bitten? Leading to examination of bite site.

2. When were you bitten? In recent bites symptoms may be absent.
3. What were you doing when you were bitten? Activity may be diagnostic.
4. Where is the snake that bit you or what did it look like? Actual snake or photo can aid in diagnosis.
5. How are you feeling now? Check for further symptoms of envenoming.

In some situations, notably bites from the *Bungarus* genus, victims may wake paralysed as this genus frequently bites people indoors, at ground level, during the night [173]. In these sorts of situations there is no way of verbally confirming a bite and clinical or laboratory diagnosis have to be employed. Improvements to snakebite diagnostics would not only rule out administration of antivenom in cases of dry bites and bites from species not covered by the antivenom or non-venomous but may also begin to quantify the scale of envenoming and quantity of antivenom required, as well as paving the way to more case-specific treatments.

4.1. Clinical Diagnosis

The clinical symptoms to be seen first in viper envenomation are blistering, swelling, bleeding, necrosis and pain. While the first signs of neurotoxicity from elapid envenomation is ptosis caused by ophthalmoplegia (paralysis of facial and extraocular muscles) which can descend into cyanosis and a decrease in ventilatory capacity in the run up to flaccid paralysis. Further diagnosis relies on the presence of multiple markers, and systemic envenoming can be confirmed by peripheral neutrophil leucocytosis (an increase in the number of neutrophils in response to the venom), or abnormal haematocrit (ratio of red blood cells to blood) which can be an indicator of haemorrhaging (low haematocrit) or haemoconcentration due to plasma leakage from increased permeability of capillaries (high haematocrit) [16]. Incoagulable blood after bites from vipers, certain elapids and colubrids have caused the 20-min whole blood clotting test to be the mainstay of snakebite diagnostics for decades. This involves leaving a small sample of victim's blood in a glass tube for 20 min and then ascertaining whether it has clotted. This can be a good indicator of consumption coagulopathy and usually the presence of procoagulant [30] proteins in the venom of the offending snake [173,174]. Despite being worthy of acting as a diagnostic tool in some settings [175], it is primitive and there are instances of it providing false information [174] and hence, better diagnostics are undoubtedly required [176].

4.2. Venom Detection Kits

The Australian Commonwealth serums laboratory snake venom detection kit (CSL-SVDK) [177] which relies on an enzyme-linked immunoassay procedure is currently the only SBE detection device commercially available. This kit is less of a snake identification device than a tool for matching one of Australia's five monovalent antivenoms—Tiger snake (*Notechis*), Brown snake (*Pseudonaja*), Black snake (*Pseudechis*), Death adder (*Acanthophis*) or Taipan (*Oxyuranus*)—to the envenomation. For example, the tiger snake immunotype will also neutralise a range of other species including Lowland Copperhead (*Austrelaps superbus*) as well as some *Pseudechis*, *Tropidechis* and *Hoplocephalus* species [177]. The major problem with snakebite diagnostics is the cross reactivity seen between venoms, as some of the proteins in each venom overlap, detection devices are rarely species specific and will detect a range of species when using immunological techniques. This problem is especially evident with the CSL-SVDK which has been recorded giving false positives with bites from species considered completely non-venomous [178,179]. More specific molecular methods are being developed, but are inappropriate as point of care devices, although potentially beneficial in corroborating reliability in more appropriate point of care devices [180]. The production of lateral flow assays (LFA) which can quickly and qualitatively differentiate between bites allowing more specific antivenoms to be used is necessary. Research is well under way on the use of lateral flow devices to detect snakebites, and a device capable of differentiating between Indian cobra, *Naja naja* and Russell's Viper, *Daboia russelii*, envenomation in India has been developed [181]. Similarly, in Taiwan an LFA device to detect either haemorrhagic bites (*Trimeresurus stejnegeri* & *Protobothrops mucrosquamatus*) or neurotoxic bites (*Bungarus multicinctus* and *Naja atra*) and discriminating between

which of the two bivalent Taiwanese antivenoms to use has also been reported [182], which is progress from the enzyme-linked immunosorbent assay currently in use and single band LFA previously reported [183].

4.3. Improving the Diagnosis of SBE

A large percentage of snakebites are considered dry bites; where a venomous species has delivered no venom or bites from non-venomous species. Alternatively, bites from venomous species with a venom that has mild or non-lethal effects on humans, but has instead evolved to defeat amphibian, reptilian, ichtian or avian prey can lead to confusion regarding the state of envenomation [184]. These bites may still be presented to hospitals, using antivenoms unnecessarily, taking hospital beds and the time of healthcare professionals. A basic device simply able to differentiate between someone suffering a life-threatening bite or a dry bite would therefore provide confidence for clinicians including the less experienced personnel in rural regions and overcome the problems associated with lack of experience in administration of antivenom. A simple device may enable victims to confirm SBE and seek prompt hospital treatment instead of resorting to traditional healers.

In the case of true envenoming, that is to say the injection of a potentially life-threatening venom, immediate transfer to hospital and administration of the correct antivenom saves countless lives [16]. However, choosing the correct antivenom is frequently not an option, as there is often only one choice. In many of the problem areas the antivenom used is polyvalent; in India an antivenom raised against the ‘Big Four’—Indian Cobra (*Naja naja*), Russell’s Viper (*Daboia russelii*), Indian krait (*Bungarus caeruleus*) and Saw-scaled viper (*Echis carinatus*)—is used [185]. Similarly, the most widely used antivenom in Africa is polyvalent (SAVP) and is raised against 11 species: Black mamba (*Dendroaspis polylepis*), Green mamba (*Dendroaspis angusticeps*), Jameson’s mamba (*Dendroaspis jamesoni*), Cape cobra (*Naja nivea*), Snouted cobra (*Aspidelaps lubricus*), Egyptian cobra (*Naja haje*), Forest cobra (*Naja melanoleuca*), Gaboon viper (*Bitis gabonica*), Mozambique spitting cobra (*Naja mossambica*), Puff adder (*Bitis arietans*) and Rinkhals (*Haemachatus hemachatus*) [186], meaning a small fraction of the antibodies is specific for each snake bite. With typically just one choice of antivenom, clinicians have the binary choice of whether or not to administer the only antivenom available. A point of care test would prevent unwarranted and wasteful administration of this life-saving medicine, which despite new antivenoms being produced is still in very short supply (~2.5% of projected needs) [187]. It could also enable doctors to become less reliant on presented symptoms, and to be more conclusive in identifying the offending snake, depending on a device’s specificity for different taxa (families, genera, species, etc.). After the development of diagnostical devices, the many emerging possibilities for alternative treatments can be used with confidence and reliable epidemiological data can be gathered, allowing more rational distribution of antivenoms or novel treatments.

5. Future Treatment Approaches for SBE

Current animal-derived antivenoms are clearly antiquated, as are the huge number of ineffective herbal remedies still used and sought around the world [188] but the difficulties in evolving from this treatment are endless. That said, around the world a lot of research into future strategies is taking place and they have been reviewed in detail [189–192] as have the design considerations [193] which should be carefully considered by health care authorities before plunging forwards with unrealistic solutions. The majority can be split into small molecular inhibitors and protein or nucleic acid-based technologies.

5.1. Small Molecular Therapeutics (SMTs)

As mentioned previously, a large proportion of venoms (particularly viperidae) are made up of enzymatic components, with specific active sites, that frequently depend on just three amino acids—the catalytic triad. Therefore, compounds that can block this site prevent the enzymatic function of that venom component. A number of different small molecular therapeutics have been causing

excitement in recent years. The use of such compounds can be expedited by molecular docking studies and promising results have been obtained in this manner [194]. The foremost SMTs are varespladib and its orally available prodrug methyl-varespladib which are repurposed drugs for treating acute coronary syndrome, which shows potent inhibition of the secreted PLA₂ found in a range of snake venoms [195]. Although an inhibitor of just one venom enzyme family, it has been shown to improve survival in a large range of experimental envenomations. This has been shown to inhibit the anticoagulant and haemorrhagic aspects [196,197], as well as the myotoxicity caused by Group I and II PLA₂ [198]. As has been previously noted, however, many snake venoms are devoid of PLA₂ (notable is the black mamba *Dendroaspis polylepis*, with <0.1% PLA₂ [110]), and varespladib is unlikely to be efficacious against bites from these species [190]. The second most abundant enzymatic group after PLA₂ are the SVMPs (see Table 2), for which the matrix metalloprotease inhibitor batimastat and orally available prodrug marimastat have been shown to effectively abrogate the haemorrhagic and necrotic effects of these enzymes [194,199]. Both these SMTs, varespladib and batimastat/marimastat have side-effects however, significantly increasing the incidence of myocardial infarction [200] and inhibiting vascular growth [201], respectively. This causes unnecessary administration to be inadvisable and corroboratory diagnostics to be an important first step prior to administration. Acetylcholinesterase inhibitors such as neostigmine and atropine have also come under investigation with promising results in reducing mortality from some elapid venoms [202–204]. Nanoparticles (particles <100 nm) are also under investigation [205], and C60 fullerene (a spheroidal carbon molecule) has shown some antivenom properties in an insect model [206] although of course this is a far cry from the mammalian system involved in human SBE.

5.2. Protein, Peptide and Oligomer Based Technologies

In addition to antivenoms, other large biomolecular therapies are being investigated. Monoclonal human single chain variable fragments (scFvs) [207] as well as full monoclonal human IgGs [112] (known to have longer half-lives and different Fc-dependent effector functions) have also both been developed. Fewer adverse reactions and promises of cost competitiveness [208] indicate these technologies could be key in the inhibition of various components of snake venoms in the future. This research has highlighted the huge potential of recombinantly expressed oligoclonal mixtures in the neutralisation of venom toxins [112]. The large size of these molecules is a double-edged sword, however, and although their half-lives are prolonged compared to small molecules, their speed of distribution is reduced. Thus, reduced tissue penetration impacts the ability to reach areas affected by the tissue damage and necrosis associated with viper bites [209]. The single domain antibodies (sdAb), specifically those based on heavy chain variable domains, have begun to receive some attention. This research has predominantly focused on the V_HH fragments from camelids (nanobodies). These nanobodies are small, specific, stable and show high affinity for their epitopes making them a promising lead in potential future antivenoms [210]. The possibility of further improving their thermostability is also interesting [211]. Diabodies which are antibody-based dimers which bind antigens divalently and are composed of two single chain fragments [212], have been shown to neutralise neurotoxins [213] and benefit from retaining the benefits of an IgG molecule—with two binding sites, but being approximately one third of the size.

The use of aptamers, which are short sequences of DNA or RNA that bind to specific targets also show promise and have been shown to inhibit toxins from cone snails [214] as well as α -bungarotoxin and cardiotoxins [215]. Research is also being carried out on a large range of alternative binding scaffolds (ABscaffs) which due to low cost of production, high stability and engineerability could play a key role in future therapeutics for SBE [216].

A number of ABscaff proteins have been put forward as having potential in venom toxin neutralisation including affimers based on phytocystatins; adnectins (monobodies) based on a fibronectin domain and affibodies based on an Fc-binding staphylococcal domain, amongst many others [216]. Although yet to be put to use as antivenoms, these ABscaffs hold huge potential. They mostly rely on diversifiable loop regions, the insertion of peptide or nucleotide sequences into which allow molecular recognition and flexibility in binding regions. The major problem with these

scaffolds arises with their very short half-lives and all suffering from rapid clearance by the kidneys. The *in vivo* half-life of aptamers can be as low as two minutes [217] though PEG-ylation can increase this as can fusion to antibodies [218] which has the potential to increase half-lives and turn these scaffolds into realistic treatments. Such PEG-ylation and fusion to larger molecules defeats their foremost advantage: their small size, and would inevitably have cost implications.

The Fc domains found on antibodies are markers, allowing these proteins to be recycled back into the blood stream: proteins not possessing this region required for interaction with the neonatal Fc receptor are subjected to catabolism via lysosomal degradation [219,220], therefore, conjugation of promising ABScaffs to Fc domains has the potential to increase the half-lives of lead compounds.

6. Diagnostics Feeding into Treatment

Improved diagnostics are essential in not only differentiating between diverse venoms but allowing clinicians to act before symptoms of SBE develop and expediting the use of standard protocols rather than being forced to rely on their own judgement as is too frequently the case [172]. Hence, simple diagnostics would boost the production of more specific treatments. At the animal-derived antivenom level: monovalent, bivalent and genus specific antivenoms could be produced and used with confidence. Family specific detection devices, differentiating between a viper and elapid bite, could allow the two major polyvalent antivenoms (for Africa and India) to be divided, at least by family. The 'Big Four' antivenom could become two bivalent antivenoms; with one raised against saw-scaled viper, *E. carinatus*, and Russell's viper, *D. russelii*, venoms and the other against Indian cobra, *N. naja*, and Indian krait, *B. caeruleus* venoms. Similarly, African antivenoms could potentially be split into an elapid and viper antivenom. This would mean a higher proportion of each vial would be specific to the family-specific envenomation effects suffered by the patient.

Increasing advancement of kits able to detect specific toxins, could allow the envenoming species to be inferred, allowing treatments to begin targeting toxins present in the blood and those local toxins associated with the bite from a species. The cheap and heat stable SMTs could be made available locally in areas of high risk, allowing pre-hospital adjunctive treatments to be administered after ascertaining envenomation that could lower risk of paralysis and tissue damage [189]. Further surveillance and secondary treatment at hospital may then be sought, with more specific monoclonal, ABScaff or any other improved treatments administered (Figure 3).

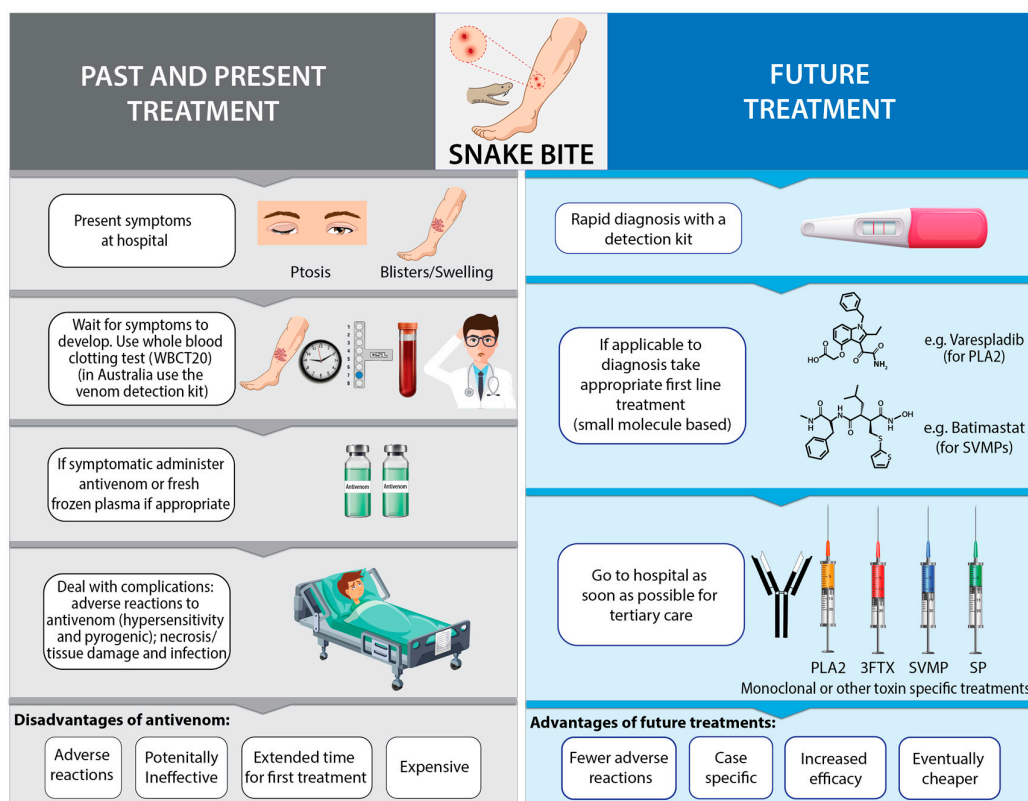


Figure 3. Comparison of current and future events involved in the diagnosis and treatment of snakebite envenoming.

7. Conclusion

SBE continues to be one of the most neglected tropical diseases, associated with one of the largest annual burdens of all the NTDs (over 1 million people in sub-Saharan Africa alone [221]) and one of the highest mortality rates. We need novel strategies in the diagnosis and treatment of SBE. Although they are required, are they realistic? Improved diagnosis involves fewer hurdles and will have a direct impact on patient outcomes, but the development and licencing of a superior therapy to treat snakebites other than antivenom will take time. The World Health Organisation's SBE working group has recently been developing a new strategy "WHO snakebite envenoming road map" [222] which aims primarily to augment antivenom production, the only available treatment for snakebite. The stockpiling of antivenoms by the WHO will increase affordability and access to this lifesaving drug worldwide while scientists continue to improve potential future therapies. However, diagnostics are in immediate need of improvement to prevent inappropriate administration of a drug which in much of its range is a precious resource [137]. The strategy appreciates that a focus on new treatments and effective diagnosis also needs to be made and that the acceleration of preclinical and clinical testing of treatments such as Varespladib may well improve hospital survival [222].

With climate change, the overlap between humans and venomous snakes seems likely to increase, as tropical margins also increase [223]. Added to which, poor waste management and the unrelenting rise of rodents alongside the continued expansion of humans into snake territory promises to support the rise of SBE throughout the Anthropocene unless something is done. Understanding the risk factors contributing to SBE is already leading to simple and cheap methods of prevention such as wearing boots and sleeping under mosquito nets. This needs to continue as we need to learn to live alongside the natural world, working with it rather than against it; for example, despite the dangers of electricity, it has become an essential part of our life. Similarly, even though SBE is dangerous, we have to learn to live with snakes to maintain natural biodiversity. While the complete eradication of SBE would require an impossible and unethical worldwide extermination of

all venomous snake species, the disease can be mitigated. Reducing predators like this will bring further problems from increased pest species and disease vectors. The SBE working group has a strategy that has the potential to carry out its promise of halving deaths by 2030 [222], by which time a non-animal-derived antivenom might just have been approved. Although with reports of drug development and approval taking over 15 years and costing up to USD\$12 billion, this is by no means a foregone conclusion [224]. Novel strategies are undoubtedly emerging and are indeed required if this disease is ever to cease being a frequently deadly medical emergency.

Author Contributions: Authors H.F.W., H.J.L., T.V., K.P., A.B.B., S.A.T., and S.V. wrote the paper. Authors H.F.W. and T.V. developed the figures.

Funding: This research received no external funding.

Conflicts of Interest: The authors declare no conflict of interest.

References

1. Harrison, R.A.; Hargreaves, A.; Wagstaff, S.C.; Faragher, B.; Lalloo, D.G. Snake envenoming: A disease of poverty. *PLoS Negl. Trop. Dis.* **2009**, *3*, e569.
2. WHO. Neglected Tropical Diseases. Available online: http://www.who.int/neglected_diseases/diseases/en/ (20 June 2019).
3. Williams, D.; Gutiérrez, J.M.; Harrison, R.; Warrell, D.A.; White, J.; Winkel, K.D.; Gopalakrishnakone, P. The global snake bite initiative: An antidote for snake bite. *Lancet* **2010**, *375*, 89–91.
4. Hernandez, H.W.; Soeung, M.; Zorn, K.M.; Ashoura, N.; Mottin, M.; Andrade, C.H.; Caffrey, C.R.; de Siqueira-Neto, J.L.; Ekins, S. High throughput and computational repurposing for neglected diseases. *Pharm. Res.* **2019**, *36*, 27.
5. Welton, R.E.; Liew, D.; Braitberg, G. Incidence of fatal snake bite in Australia: A coronial based retrospective study (2000–2016). *Toxicon* **2017**, *131*, 11–15, doi:10.1016/j.toxicon.2017.03.008.
6. Chippaux, J.P. Snake-bites: Appraisal of the global situation. *Bull. World Health Org.* **1998**, *76*, 515.
7. Kasturiratne, A.; Wickremasinghe, A.R.; de Silva, N.; Gunawardena, N.K.; Pathmeswaran, A.; Premaratna, R.; Savioli, L.; Lalloo, D.G.; de Silva, H.J. The global burden of snakebite: A literature analysis and modelling based on regional estimates of envenoming and deaths. *PLoS Med.* **2008**, *5*, e218.
8. Mohapatra, B.; Warrell, D.A.; Suraweera, W.; Bhatia, P.; Dhingra, N.; Jotkar, R.M.; Rodriguez, P.S.; Mishra, K.; Whitaker, R.; Jha, P. Snakebite mortality in India: A nationally representative mortality survey. *PLoS Negl. Trop. Dis.* **2011**, *5*, e1018.
9. Ralph, R.; Sharma, S.K.; Faiz, M.A.; Ribeiro, I.; Rijal, S.; Chappuis, F.; Kuch, U. The timing is right to end snakebite deaths in South Asia. *Bmj* **2019**, *364*, k5317.
10. Chippaux, J.-P. Incidence and mortality due to snakebite in the Americas. *PLoS Negl. Trop. Dis.* **2017**, *11*, e0005662, doi:10.1371/journal.pntd.0005662.
11. Abubakar, S.B.; Habib, A.G.; Mathew, J. Amputation and disability following snakebite in Nigeria. *Trop. Dr.* **2010**, *40*, 114–116, doi:10.1258/td.2009.090266.
12. Williams, S.S.; Wijesinghe, C.A.; Jayamanne, S.F.; Buckley, N.A.; Dawson, A.H.; Lalloo, D.G.; de Silva, H.J. Delayed psychological morbidity associated with snakebite envenoming. *PLoS Negl. Trop. Dis.* **2011**, *5*, e1255, doi:10.1371/journal.pntd.0001255.
13. Habib, A.G.; Kuznik, A.; Hamza, M.; Abdullahi, M.I.; Chedi, B.A.; Chippaux, J.-P.; Warrell, D.A. Snakebite is under appreciated: Appraisal of burden from West Africa. *PLoS Negl. Trop. Dis.* **2015**, *9*, e0004088, doi:10.1371/journal.pntd.0004088.
14. O’neal, C.J.; Jobling, M.G.; Holmes, R.K.; Hol, W.G. Structural basis for the activation of cholera toxin by human ARF6-GTP. *Science* **2005**, *309*, 1093–1096.
15. Sorobetea, D.; Svensson-Frej, M.; Grecis, R. Immunity to gastrointestinal nematode infections. *Mucosal Immunol.* **2018**, *11*, 304.
16. Gutiérrez, J.M.; Calvete, J.J.; Habib, A.G.; Harrison, R.A.; Williams, D.J.; Warrell, D.A. Snakebite envenoming. *Nat. Rev. Dis. Prim.* **2017**, *3*, 17063.
17. Sack, D.A.; R Bradley Sack, S. Getting serious about cholera. *N. Engl. J. Med.* **2006**, *355*, 649.

18. Aagaard-Hansen, J.; Chaignat, C.L. Neglected tropical diseases: Equity and social determinants. In *Equity, social determinants and public health programmes*. Blas, E., Kurup, A.S., Eds.; WHO Press: Geneva, Switzerland, **2010**; p. 135.
19. Hotez, P.J.; Molyneux, D.H.; Fenwick, A.; Kumaresan, J.; Sachs, S.E.; Sachs, J.D.; Savioli, L. Control of neglected tropical diseases. *N. Engl. J. Med.* **2007**, *357*, 1018–1027.
20. Wang, H.; Naghavi, M.; Allen, C.; Barber, R.M.; Bhutta, Z.A.; Carter, A.; Casey, D.C.; Charlson, F.J.; Chen, A.Z.; Coates, M.M. Global, regional, and national life expectancy, all-cause mortality, and cause-specific mortality for 249 causes of death, 1980–2015: A systematic analysis for the global burden of disease study 2015. *Lancet* **2016**, *388*, 1459–1544.
21. Ali, M.; Lopez, A.L.; You, Y.; Kim, Y.E.; Sah, B.; Maskery, B.; Clemens, J. The global burden of cholera. *Bull. World Health Org.* **2012**, *90*, 209–218.
22. De Silva, N.R.; Brooker, S.; Hotez, P.J.; Montresor, A.; Engels, D.; Savioli, L. Soil-transmitted helminth infections: Updating the global picture. *Trends Parasitol.* **2003**, *19*, 547–551.
23. Bethony, J.; Brooker, S.; Albonico, M.; Geiger, S.M.; Loukas, A.; Diemert, D.; Hotez, P.J. Soil-transmitted helminth infections: Ascariasis, trichuriasis, and hookworm. *Lancet* **2006**, *367*, 1521–1532.
24. Ottesen, E.A.; Hooper, P.J.; Bradley, M.; Biswas, G. The global programme to eliminate lymphatic filariasis: Health impact after 8 years. *PLoS Negl. Trop. Dis.* **2008**, *2*, e317.
25. Ottesen, E.A. Lymphatic filariasis: Treatment, control and elimination. *Adv. Parasitol.* **2006**, *61*, 395–441.
26. Basáñez, M.-G.; Sébastien, D.; Churcher, T.S.; Breitling, L.P.; Little, M.P.; Boussinesq, M. River blindness: A success story under threat? *PLoS Med.* **2006**, *3*, e371.
27. Smith, W.C.; van Brakel, W.; Gillis, T.; Saunderson, P.; Richardus, J.H. The Missing Millions: A Threat to the Elimination of Leprosy. *PLoS Negl. Trop. Dis.* **2015**, *9*, e0003658, doi:10.1371/journal.pntd.0003658.
28. Hopkins, D.R.; Ruiz-Tiben, E.; Eberhard, M.L.; Weiss, A.; Withers, P.C., Jr.; Roy, S.L.; Sienko, D.G. Dracunculiasis eradication: Are we there yet? *Am. J. Trop. Med. Hyg.* **2018**, *99*, 388–395.
29. Modahl, C.M.; Saviola, A.J.; Mackessy, S.P. Venoms of colubrids. *Venom Genom. Proteom.* **2016**, *2016*, 51–79.
30. Warrell, D.A. Snake bite. *Lancet* **2010**, *375*, 77–88.
31. Warrell, D.A. Venomous bites, stings, and poisoning: An update. *Infect. Dis. Clin.* **2019**, *33*, 17–38, doi:10.1016/j.idc.2018.10.001.
32. Tilbury, C.R.; Verster, J. A fatal bite from the burrowing asp *atractaspis corpulenta* (Hallowell 1854). *Toxicon* **2016**, *118*, 21–26, doi:10.1016/j.toxicon.2016.04.035.
33. Kardong, K.; Weinstein, S.; Smith, T.; Mackessy, S. Reptile venom glands: Form, function, and future. In *Handbook of venoms and toxins of reptiles*. Mackessy, S.P., Ed.; CRC Press Inc.: London, UK, **2009**; pp. 65–91.
34. Chara, K.; Baccouche, N.; Turki, O.; Regaig, K.; Chaari, A.; Bahloul, M.; Bouaziz, M. A rare complication of viper envenomation: Cardiac failure. A case report. *Med. Sante Trop.* **2017**, *27*, 52–55, doi:10.1684/mst.2016.0636.
35. El Zahran, T.; Kazzi, Z.; Chehadeh, A.A.; Sadek, R.; El Sayed, M.J. Snakebites in Lebanon: A descriptive study of snakebite victims treated at a tertiary care center in Beirut, Lebanon. *J. Emerg. Trauma Shock* **2018**, *11*, 119–124, doi:10.4103/jets.Jets_141_16.
36. Vikrant, S.; Jaryal, A.; Parashar, A. Clinicopathological spectrum of snake bite-induced acute kidney injury from India. *World J. Nephrol.* **2017**, *6*, 150–161, doi:10.5527/wjn.v6.i3.150.
37. Silva, A.; Kuruppu, S.; Othman, I.; Goode, R.J.; Hodgson, W.C.; Isbister, G.K. Neurotoxicity in Sri Lankan Russell's viper (*Daboia russelii*) envenoming is primarily due to U1-viperitoxin-Dr1a, a pre-synaptic neurotoxin. *Neurotox. Res.* **2017**, *31*, 11–19.
38. Segura, A.; Herrera, M.; Reta Mares, F.; Jaime, C.; Sanchez, A.; Vargas, M.; Villalta, M.; Gomez, A.; Gutierrez, J.M.; Leon, G. Proteomic, toxicological and immunogenic characterization of Mexican west-coast rattlesnake (*Crotalus basiliscus*) venom and its immunological relatedness with the venom of central American rattlesnake (*Crotalus simus*). *J. Proteom.* **2017**, *158*, 62–72, doi:10.1016/j.jpro.2017.02.015.
39. Gillissen, A.; Theakston, R.D.G.; Barth, J.; May, B.; Krieg, M.; Warrell, D.A. Neurotoxicity, haemostatic disturbances and haemolytic anaemia after a bite by a Tunisian saw-scaled or carpet viper (*Echis 'pyramidum'*-complex): Failure of antivenom treatment. *Toxicon* **1994**, *32*, 937–944.
40. Tan, C.H.; Tan, K.Y.; Yap, M.K.K.; Tan, N.H. Venomics of *tropidolaemus wagleri*, the sexually dimorphic temple pit viper: Unveiling a deeply conserved atypical toxin arsenal. *Sci. Rep.* **2017**, *7*, 43237, doi:10.1038/srep43237.

41. Kalita, B.; Singh, S.; Patra, A.; Mukherjee, A.K. Quantitative proteomic analysis and antivenom study revealing that neurotoxic phospholipase A2 enzymes, the major toxin class of Russell's viper venom from southern India, shows the least immuno-recognition and neutralization by commercial polyvalent antivenom. *Int. J. Boil. Macromol.* **2018**, *118*, 375–385.
42. Maduwage, K.; Isbister, G.K. Current treatment for venom-induced consumption coagulopathy resulting from snakebite. *PLoS Negl. Trop. Dis.* **2014**, *8*, e3220, doi:10.1371/journal.pntd.0003220.
43. Fry, B.G. Structure–function properties of venom components from Australian elapids. *Toxicon* **1999**, *37*, 11–32, doi:10.1016/S0041-0101(98)00125-1.
44. Reyes-Velasco, J.; Card, D.C.; Andrew, A.L.; Shaney, K.J.; Adams, R.H.; Schield, D.R.; Casewell, N.R.; Mackessy, S.P.; Castoe, T.A. Expression of venom gene homologs in diverse python tissues suggests a new model for the evolution of snake venom. *Mol. Biol. Evolut.* **2014**, *32*, 173–183, doi:10.1093/molbev/msu294.
45. Kardong, K.V. 'Protovipers' and the evolution of snake fangs. *Evolution* **1979**, 433–443.
46. Deufel, A.; Cundall, D. Functional plasticity of the venom delivery system in snakes with a focus on the poststrike prey release behavior. *Zool. Anz. A J. Comp. Zool.* **2006**, *245*, 249–267.
47. Uetz, P.; Hallermann, J. The Reptile Database. Available online: <http://reptile-database.reptarium.cz> (accessed on: 20 June 2019).
48. Chippaux, J.-P.; Williams, V.; White, J. Snake venom variability: Methods of study, results and interpretation. *Toxicon* **1991**, *29*, 1279–1303.
49. Shashidharamurthy, R.; Kemparaju, K. Region-specific neutralization of Indian cobra (*Naja naja*) venom by polyclonal antibody raised against the eastern regional venom: A comparative study of the venoms from three different geographical distributions. *Int. Immunopharmacol.* **2007**, *7*, 61–69.
50. Tsai, I.-H.; Tsai, H.-Y.; Wang, Y.-M.; Warrell, D.A. Venom phospholipases of Russell's vipers from myanmar and eastern India—Cloning, characterization and phylogeographic analysis. *Biochim. Biophys. Acta (BBA)-Proteins Proteom.* **2007**, *1774*, 1020–1028.
51. Fry, B.G.; Winkel, K.D.; Wickramaratna, J.C.; Hodgson, W.C.; Wüster, W. Effectiveness of snake antivenom: Species and regional venom variation and its clinical impact. *J. Toxicol. Toxin Rev.* **2003**, *22*, 23–34.
52. Chatrath, S.T.; Chapeaurouge, A.; Lin, Q.; Lim, T.K.; Dunstan, N.; Mirtschin, P.; Kumar, P.P.; Kini, R.M. Identification of novel proteins from the venom of a cryptic snake *Drysdalia coronoides* by a combined transcriptomics and proteomics approach. *J. Proteome Res.* **2011**, *10*, 739–750.
53. Watt, G.; Padre, L.; Tuazon, L.; Theakston, R.; Laughlin, L. Bites by the philippine cobra (*Naja naja philippinensis*): Prominent neurotoxicity with minimal local signs. *Am. J. Trop. Med. Hyg.* **1988**, *39*, 306–311.
54. Warrell, D.A. Tropical snake bite: Clinical studies in south-east Asia. *Toxicon* **1986**, *23*, 25–45.
55. Wüster, W.; McCarthy, C.J. Venomous Snake Systematics: Implications for Snake Bite Treatment and Toxinology. Bon, C., Goyffon, M., Eds.; In *Envenomings and their Treatments*. Fondation Mérieux: Lyon, France, 1996; pp. 13–23.
56. Tasoulis, T.; Isbister, G.K. A Review and database of snake venom proteomes. *Toxins* **2017**, *9*, 290.
57. Williams, H.F.; Hayter, P.; Ravishankar, D.; Baines, A.; Layfield, H.J.; Croucher, L.; Wark, C.; Bicknell, A.B.; Trim, S.; Vaiyapuri, S. Impact of *Naja nigricollis* venom on the production of methaemoglobin. *Toxins* **2018**, *10*, 539.
58. Pungerčar, J.; Križaj, I. Understanding the molecular mechanism underlying the presynaptic toxicity of secreted phospholipases A2. *Toxicon* **2007**, *50*, 871–892.
59. Prasarnpun, S.; Walsh, J.; Awad, S.; Harris, J. Envenoming bites by kraits: The biological basis of treatment-resistant neuromuscular paralysis. *Brain* **2005**, *128*, 2987–2996.
60. Vulfius, C.A.; Kasheverov, I.E.; Kryukova, E.V.; Spirova, E.N.; Shelukhina, I.V.; Starkov, V.G.; Andreeva, T.V.; Faure, G.; Zouridakis, M.; Tsetlin, V.I.; et al. Pancreatic and snake venom presynaptically active phospholipases A2 inhibit nicotinic acetylcholine receptors. *PLoS ONE* **2017**, *12*, e0186206, doi:10.1371/journal.pone.0186206.
61. Paoli, M.; Rigoni, M.; Koster, G.; Rossetto, O.; Montecucco, C.; Postle, A.D. Mass spectrometry analysis of the phospholipase A2 activity of snake pre-synaptic neurotoxins in cultured neurons. *J. Neurochem.* **2009**, *111*, 737–744.
62. Dixon, R.W.; Harris, J.B. Myotoxic activity of the toxic phospholipase, notexin, from the venom of the Australian tiger snake. *J. Neuropathol. Exp. Neurol.* **1996**, *55*, 1230–1237.
63. Gutiérrez, J.M.; Ownby, C.L. Skeletal muscle degeneration induced by venom phospholipases A2: Insights into the mechanisms of local and systemic myotoxicity. *Toxicon* **2003**, *42*, 915–931.

64. Fuly, A.; Machado, O.; Alves, E.; Carlini, C. Mechanism of inhibitory action on platelet activation of a phospholipase A2 isolated from *Lachesis muta* (Bushmaster) snake venom. *Thromb. Haemost.* **1997**, *78*, 1372–1380.
65. Tzeng, M.-C.; Yen, C.-H.; Hseu, M.-J.; Dupureur, C.M.; Tsai, M.-D. Conversion of bovine pancreatic phospholipase A at a single site into a competitor of neurotoxic phospholipases A by site-directed mutagenesis. *J. Biol. Chem.* **1995**, *270*, 2120–2123.
66. Kini, R.M. Excitement ahead: Structure, function and mechanism of snake venom phospholipase A2 enzymes. *Toxicon* **2003**, *42*, 827–840.
67. Ramos, O.; Selistre-de-Araujo, H. Snake venom metalloproteases—Structure and function of catalytic and disintegrin domains. *Comp. Biochem. Physiol. Part C Toxicol. Pharmacol.* **2006**, *142*, 328–346.
68. Mackessy, S.P. *Handbook of Venoms and Toxins of Reptiles*; CRC Press: Boca Raton, FL, USA, 2010.
69. Williams, H.F.; Mellows, B.A.; Mitchell, R.; Sfyri, P.; Layfield, H.J.; Salamah, M.; Vaiyapuri, R.; Collins-Hooper, H.; Bicknell, A.B.; Matsakas, A.; et al. Mechanisms underpinning the permanent muscle damage induced by snake venom metalloprotease. *PLoS Negl. Trop. Dis.* **2019**, *13*, e0007041, doi:10.1371/journal.pntd.0007041.
70. Siigur, E.; Siigur, J. Purification and characterization of lebetase, a fibrinolytic enzyme from *Vipera lebetina* (snake) venom. *Biochim. Biophys. Acta (BBA) Gene. Subj.* **1991**, *1074*, 223–229.
71. Fox, J.W.; Serrano, S.M.T. Structural considerations of the snake venom metalloproteinases, key members of the M12 repolysin family of metalloproteinases. *Toxicon* **2005**, *45*, 969–985, doi:10.1016/j.toxicon.2005.02.012.
72. Ferreira, B.A.; Deconte, S.R.; de Moura, F.B.R.; Tomiosso, T.C.; Clissa, P.B.; Andrade, S.P.; Araújo, F.d.A. Inflammation, angiogenesis and fibrogenesis are differentially modulated by distinct domains of the snake venom metalloproteinase jararhagin. *Int. J. Biol. Macromol.* **2018**, *119*, 1179–1187, doi:10.1016/j.ijbiomac.2018.08.051.
73. Clissa, P.B.; Lopes-Ferreira, M.; Della-Casa, M.S.; Farsky, S.H.P.; Moura-da-Silva, A.M. Importance of jararhagin disintegrin-like and cysteine-rich domains in the early events of local inflammatory response. *Toxicon* **2006**, *47*, 591–596, doi:10.1016/j.toxicon.2006.02.001.
74. Clemetson, K.J. Snaclecs (snake C-type lectins) that inhibit or activate platelets by binding to receptors. *Toxicon* **2010**, *56*, 1236–1246.
75. Serrano, S.M.; Maroun, R.C. Snake venom serine proteinases: Sequence homology vs. substrate specificity, a paradox to be solved. *Toxicon* **2005**, *45*, 1115–1132.
76. Stocker, K.; Fischer, H.; Meier, J. Thrombin-like snake venom proteinases. *Toxicon* **1982**, *20*, 265–273.
77. Xiong, S.; Huang, C. Synergistic strategies of predominant toxins in snake venoms. *Toxicol. Lett.* **2018**, *287*, 142–154, doi:10.1016/j.toxlet.2018.02.004.
78. Vaiyapuri, S.; Sunagar, K.; Gibbins, J.; Jackson, T.; Reeks, T.; Fry, B. Kallikrein enzymes. In *Venomous Reptiles and Their Toxins: Evolution, Pathophysiology and Biodiscovery*; Fry, B.G., Ed.; Oxford University Press: Oxford, UK, 2015; pp. 267–280.
79. Kisiel, W. Effect of snake venoms on factor V. *Handb. Nat. Toxins Reptil. Venom. Toxins* **2018**, *2018*, 253–264.
80. Santos, B.F.; Serrano, S.M.; Kuliopulos, A.; Niewiarowski, S. Interaction of viper venom serine peptidases with thrombin receptors on human platelets. *FEBS Lett.* **2000**, *477*, 199–202.
81. Vaiyapuri, S.; Thiagarajan, N.; Hutchinson, E.G.; Gibbins, J.M. Sequence and phylogenetic analysis of viper venom serine proteases. *Bioinformation* **2012**, *8*, 763–772.
82. Sanchez, E.F.; Santos, C.I.; Magalhaes, A.; Diniz, C.R.; Figueiredo, S.; Gilroy, J.; Richardson, M. Isolation of a proteinase with plasminogen-activating activity from *Lachesis muta muta* (bushmaster) snake venom. *Arch. Biochem. Biophys.* **2000**, *378*, 131–141.
83. Kisiel, W.; Kondo, S.; Smith, K.; McMullen, B.; Smith, L. Characterization of a protein C activator from *Agkistrodon contortrix* venom. *J. Biol. Chem.* **1987**, *262*, 12607–12613.
84. Meléndez-Martínez, D.; Muñoz, J.M.; Barraza-Garza, G.; Cruz-Peréz, M.S.; Gatica-Colima, A.; Alvarez-Parrilla, E.; Plenge-Tellechea, L.F. Rattlesnake *Crotalus molossus nigrescens* venom induces oxidative stress on human erythrocytes. *J. Venom. Anim. Toxins Incl. Trop. Dis.* **2017**, *23*, 24, doi:10.1186/s40409-017-0114-y.
85. Sharma, R.D.; Katkar, G.D.; Sundaram, M.S.; Paul, M.; NaveenKumar, S.K.; Swethakumar, B.; Hemshekhar, M.; Girish, K.S.; Kemparaju, K. Oxidative stress-induced methemoglobinemia is the silent killer during snakebite: A novel and strategic neutralization by melatonin. *J. Pineal Res.* **2015**, *59*, 240–254.

86. Izidoro, L.F.M.; Ribeiro, M.C.; Souza, G.R.; Sant'Ana, C.D.; Hamaguchi, A.; Homs-Brandeburgo, M.I.; Goulart, L.R.; Belebony, R.O.; Nomizo, A.; Sampaio, S.V. Biochemical and functional characterization of an L-amino acid oxidase isolated from Bothrops pirajai snake venom. *Bioorg. Med. Chem.* **2006**, *14*, 7034–7043.
87. Ande, S.R.; Kommoju, P.R.; Draxl, S.; Murkovic, M.; Macheroux, P.; Ghisla, S.; Ferrando-May, E. Mechanisms of cell death induction by L-amino acid oxidase, a major component of ophidian venom. *Apoptosis* **2006**, *11*, 1439–1451.
88. Sakurai, Y.; Shima, M.; Matsumoto, T.; Takatsuka, H.; Nishiya, K.; Kasuda, S.; Fujimura, Y.; Yoshioka, A. Anticoagulant activity of M-LAO, l-amino acid oxidase purified from agkistrodon halys blomhoffii, through selective inhibition of factor IX. *Biochim. Biophys. Acta (BBA)-Proteins Proteom.* **2003**, *1649*, 51–57.
89. de Queiroz, M.R.; de Sousa, B.B.; da Cunha Pereira, D.F.; Mamede, C.C.N.; Matias, M.S.; de Moraes, N.C.G.; de Oliveira Costa, J.; de Oliveira, F. The role of platelets in hemostasis and the effects of snake venom toxins on platelet function. *Toxicon* **2017**, *133*, 33–47.
90. Schetinger, M.R.; Rocha, J.B.T.; Ahmed, M.; Morsch, V.M. Snake venom acetylcholinesterase. In *Handbook of venoms and toxins of reptiles*. Mackessy, S.P., Ed.; CRC Press Inc.: London, UK, **2009**; pp. 207–219.
91. Isoyama, T.; Thwaites, D.; Selzer, M.G.; Carey, R.I.; Barbucci, R.; Lokeshwar, V.B. Differential selectivity of hyaluronidase inhibitors toward acidic and basic hyaluronidases. *Glycobiology* **2006**, *16*, 11–21.
92. Suwansrinon, K.; Khow, O.; Mitmoonpitak, C.; Daviratanasilpa, S.; Chaiyabutr, N.; Sitprija, V. Effects of Russell's viper venom fractions on systemic and renal hemodynamics. *Toxicon* **2007**, *49*, 82–88.
93. Dhananjaya, B.L.; Vishwanath, B.S.; D'Souza, C.J. Snake venom nucleases, nucleotidases, and phosphomonoesterases. *Handb. Venom. Toxins Reptil.* **2010**, *155*, 171.
94. Aird, S.D. Ophidian envenomation strategies and the role of purines. *Toxicon* **2002**, *40*, 335–393.
95. Fry, B.G. *Venomous Reptiles and Their Toxins: Evolution, Pathophysiol. and Biodiscovery*; Oxford University Press: Oxford, UK, 2015.
96. Aird, S.D.; Watanabe, Y.; Villar-Briones, A.; Roy, M.C.; Terada, K.; Mikheyev, A.S. Quantitative high-throughput profiling of snake venom gland transcriptomes and proteomes (Ovophis okinavensis and Protobothrops flavoviridis). *BMC Genom.* **2013**, *14*, 790, doi:10.1186/1471-2164-14-790.
97. Pawlak, J.; Mackessy, S.P.; Fry, B.G.; Bhatia, M.; Mourier, G.; Fruchart-Gaillard, C.; Servent, D.; Ménez, R.; Stura, E.; Ménez, A. Denmotoxin, a three-finger toxin from the colubrid snake Boiga dendrophila (Mangrove Catsnake) with bird-specific activity. *J. Biol. Chem.* **2006**, *281*, 29030–29041.
98. Heyborne, W.H.; Mackessy, S.P. Identification and characterization of a taxon-specific three-finger toxin from the venom of the green vinesnake (Oxybelis fulgidus; family Colubridae). *Biochimie* **2013**, *95*, 1923–1932, doi:10.1016/j.biochi.2013.06.025.
99. Kini, R.M.; Doley, R. Structure, function and evolution of three-finger toxins: Mini proteins with multiple targets. *Toxicon* **2010**, *56*, 855–867.
100. Nirthanan, S.; Gwee, M.C.E. Three-Finger & alpha;-Neurotoxins and the Nicotinic Acetylcholine Receptor, Forty Years On. *J. Pharmacol. Sci.* **2004**, *94*, 1–17, doi:10.1254/jphs.94.1.
101. Palud, D.; Soiolata, A.; Haw, C.; Mugnier, L.; Jarrosson, F.; Tarbe, M.; Mollet, C.; de Pomyers, H.; Gignes, D.; Mabrouk, K. Isolation and characterization of Fasciculin II: From Dendroaspis angusticeps snake venom and from chemical synthesis. *Toxicon* **2018**, *149*, 94–95.
102. Harvey, A.L. Cardiotoxins from cobra venoms. In *Handbook of Natural Toxins*; Routledge: London, UK, 2018; pp. 85–106.
103. Fry, B.G.; Vidal, N.; Norman, J.A.; Vonk, F.J.; Scheib, H.; Ramjan, S.R.; Kuruppu, S.; Fung, K.; Hedges, S.B.; Richardson, M.K. Early evolution of the venom system in lizards and snakes. *Nature* **2006**, *439*, 584.
104. Nobile, M.; Noceti, F.; Prestipino, G.; Possani, L.D. Helothermine, a lizard venom toxin, inhibits calcium current in cerebellar granules. *Exp. Brain Res.* **1996**, *110*, 15–20.
105. Nobile, M.; Magnelli, V.; Lagostena, L.; Mochca-Morales, J.; Possani, L.; Prestipino, G. The toxin helothermine affects potassium currents in newborn rat cerebellar granule cells. *J. Membr Biol.* **1994**, *139*, 49–55.
106. Suzuki, N.; Yamazaki, Y.; Brown, R.L.; Fujimoto, Z.; Morita, T.; Mizuno, H. Structures of pseudetoxin and pseudocin, two snake-venom cysteine-rich secretory proteins that target cyclic nucleotide-gated ion channels: Implications for movement of the C-terminal cysteine-rich domain. *Acta Crystallogr. Sect. D: Biol. Crystallogr.* **2008**, *64*, 1034–1042.
107. Yamazaki, Y.; Morita, T. Structure and function of snake venom cysteine-rich secretory proteins. *Toxicon* **2004**, *44*, 227–231.

108. Yamazaki, Y.; Koike, H.; Sugiyama, Y.; Motoyoshi, K.; Wada, T.; Hishinuma, S.; Mita, M.; Morita, T. Cloning and characterization of novel snake venom proteins that block smooth muscle contraction. *Eur. J. Biochem.* **2002**, *269*, 2708–2715.
109. Yuan, C.-H.; He, Q.-Y.; Peng, K.; Diao, J.-B.; Jiang, L.-P.; Tang, X.; Liang, S.-P. Discovery of a distinct superfamily of Kunitz-type toxin (KTT) from tarantulas. *PLoS ONE* **2008**, *3*, e3414, doi:10.1371/journal.pone.0003414.
110. Laustsen, A.H.; Lomonte, B.; Lohse, B.; Fernández, J.; Gutiérrez, J.M. Unveiling the nature of black mamba (*Dendroaspis polylepis*) venom through venomomics and antivenom immunoprofiling: Identification of key toxin targets for antivenom development. *J. Proteom.* **2015**, *119*, 126–142.
111. Harvey, A.L. Twenty years of dendrotoxins. *Toxicon* **2001**, *39*, 15–26, doi:10.1016/S0041-0101(00)00162-8.
112. Laustsen, A.H.; Karatt-Vellatt, A.; Masters, E.W.; Arias, A.S.; Pus, U.; Knudsen, C.; Osoez, S.; Slavny, P.; Griffiths, D.T.; Luther, A.M.; et al. In vivo neutralization of dendrotoxin-mediated neurotoxicity of black mamba venom by oligoclonal human IgG antibodies. *Nat. Commun.* **2018**, *9*, 3928, doi:10.1038/s41467-018-06086-4.
113. Laustsen, A.H. Toxin synergism in snake venoms. *Toxin Rev.* **2016**, *35*, 165–170.
114. Kwong, P.D.; McDonald, N.Q.; Sigler, P.B.; Hendrickson, W.A. Structure of β 2-bungarotoxin: Potassium channel binding by Kunitz modules and targeted phospholipase action. *Structure* **1995**, *3*, 1109–1119, doi:10.1016/S0969-2126(01)00246-5.
115. Bacongus, I.; Bohlen, Christopher, J.; Goehring, A.; Julius, D.; Gouaux, E. X-Ray structure of acid-sensing Ion channel 1–Snake toxin complex reveals open state of a Na⁺-selective channel. *Cell* **2014**, *156*, 717–729, doi:10.1016/j.cell.2014.01.011.
116. Ebner, S.; Sharon, N.; Ben-Tal, N. Evolutionary analysis reveals collective properties and specificity in the C-type lectin and lectin-like domain superfamily. *Proteins Struct. Funct. Bioinform.* **2003**, *53*, 44–55.
117. Vaiyapuri, S.; Hutchinson, E.G.; Ali, M.S.; Dannoura, A.; Stanley, R.G.; Harrison, R.A.; Bicknell, A.B.; Gibbins, J.M. Rhinocetin, a venom-derived integrin-specific antagonist inhibits collagen-induced platelet and endothelial cell functions. *J. Biol. Chem.* **2012**, *287*, 26235–26244.
118. Clemetson, K.J.; Lu, Q.; Clemetson, J.M. Snake C-type lectin-like proteins and platelet receptors. *Pathophysiol. Haemost. Thromb.* **2005**, *34*, 150–155.
119. Du, X.-Y.; Navdaev, A.; Clemetson, J.M.; Magnenat, E.; Wells, T.N.; Clemetson, K.J. Bilinixin, a snake C-type lectin from *Agkistrodon bilineatus* venom agglutinates platelets via GPIb and α 2 β 1. *Thromb. Haemost.* **2001**, *86*, 1277–1283.
120. Suzuki-Inoue, K.; Fuller, G.L.; García, Á.; Eble, J.A.; Pöhlmann, S.; Inoue, O.; Gartner, T.K.; Hugan, S.C.; Pearce, A.C.; Laing, G.D. A novel Syk-dependent mechanism of platelet activation by the C-type lectin receptor CLEC-2. *Blood* **2006**, *107*, 542–549.
121. Markland, F.S. Snake venoms and the hemostatic system. *Toxicon* **1998**, *36*, 1749–1800.
122. Nymalm, Y.; Puranen, J.S.; Nyholm, T.K.; Käpylä, J.; Kidron, H.; Pentikäinen, O.T.; Airenne, T.T.; Heino, J.; Slotte, J.P.; Johnson, M.S. Jararhagin-derived RKKH peptides induce structural changes in α II domain of human integrin α 1 β 1. *J. Biol. Chem.* **2004**, *279*, 7962–7970.
123. Calvete, J.J.; Marcinkiewicz, C.; Monleón, D.; Esteve, V.; Celda, B.; Juárez, P.; Sanz, L. Snake venom disintegrins: Evolution of structure and function. *Toxicon* **2005**, *45*, 1063–1074.
124. Marcinkiewicz, C.; Calvete, J.J.; Marcinkiewicz, M.M.; Raida, M.; Vijay-Kumar, S.; Huang, Z.; Lobb, R.R.; Niewiarowski, S. EC3, a novel heterodimeric disintegrin from *Echis carinatus* venom, inhibits α 4 and α 5 integrins in an RGD-independent manner. *J. Biol. Chem.* **1999**, *274*, 12468–12473.
125. Madrigal, M.; Sanz, L.; Flores-Díaz, M.; Sasa, M.; Núñez, V.; Alape-Girón, A.; Calvete, J.J. Snake venomomics across genus *Lachesis*. Ontogenetic changes in the venom composition of *Lachesis stenophrys* and comparative proteomics of the venoms of adult *Lachesis melanocephala* and *Lachesis acrochorda*. *J. Proteom.* **2012**, *77*, 280–297, doi:10.1016/j.jprot.2012.09.003.
126. Lainchbury, J.G.; Burnett Jr, J.C.; Meyer, D.; Redfield, M.M. Effects of natriuretic peptides on load and myocardial function in normal and heart failure dogs. *Am. J. Physiol. Heart Circ. Physiol.* **2000**, *278*, H33–H40.
127. Collins, E.; Bracamonte, M.P.; Burnett Jr, J.C.; Miller, V.M. Mechanism of relaxations to dendroaspis natriuretic peptide in canine coronary arteries. *J. Cardiovasc. Pharmacol.* **2000**, *35*, 614–618.
128. Sciani, J.M.; Pimenta, D.C. The modular nature of bradykinin-potentiating peptides isolated from snake venoms. *J. Venom. Anim. Toxins Incl. Trop. Dis.* **2017**, *23*, 45.

129. Sunagar, K.; Fry, B.G.; Jackson, T.N.; Casewell, N.R.; Undheim, E.A.; Vidal, N.; Ali, S.A.; King, G.F.; Vasudevan, K.; Vasconcelos, V.; et al. Molecular evolution of vertebrate neurotrophins: Co-option of the highly conserved nerve growth factor gene into the advanced snake venom arsenal. *PLoS ONE* **2013**, *8*, e81827, doi:10.1371/journal.pone.0081827.
130. Wei, C.; Chen, J. A novel lipocalin homologue from the venom gland of *Deinagkistrodon acutus* similar to mammalian lipocalins. *J. Venom. Anim. Toxins Incl. Trop. Dis.* **2012**, *18*, 16–23.
131. Bdolah, A.; Ducancel, F.; Sunagar, K.; Jackson, T.; Fry, B. Sarafotoxin peptides. *Venomous reptiles and their toxins: Evolution, pathophysiology and biodiscovery*. Oxford University Press: New York, NY, USA, **2015**; p. 341.
132. The World Health Organization. *WHO Guidelines for the Production, Control and Regulation of Snake Antivenom Immunoglobulins*; WHO: Geneva, Switzerland, **2010**; pp. 1–134.
133. Gutiérrez, J.M. Global availability of antivenoms: The relevance of public manufacturing laboratories. *Toxins* **2018**, *11*, 5.
134. Zolfagharian, H.; Mohammadpour Dounighi, N. Progress and improvement of the manufacturing process of snake antivenom. *Arch. Razi Inst.* **2016**, *68*, 1–10.
135. Abbas, A.K.; Lichtman, A.H.; Pillai, S. *Cellular and Molecular Immunology*; Elsevier Health Sciences: Philadelphia, PA, USA, 2011.
136. Brown, N.; Landon, J. Antivenom: The most cost-effective treatment in the world? *Toxicon* **2010**, *55*, 1405–1407.
137. Williams, D.J.; Gutiérrez, J.-M.; Calvete, J.J.; Wüster, W.; Ratanabanangkoon, K.; Paiva, O.; Brown, N.I.; Casewell, N.R.; Harrison, R.A.; Rowley, P.D. Ending the drought: New strategies for improving the flow of affordable, effective antivenoms in Asia and Africa. *J. Proteom.* **2011**, *74*, 1735–1767.
138. Herrera, M.; Paiva, O.K.; Pagotto, A.H.; Segura, A.; Serrano, S.M.; Vargas, M.; Villalta, M.; Jensen, S.D.; León, G.; Williams, D.J. Antivenomic characterization of two antivenoms against the venom of the taipan, *Oxyuranus scutellatus*, from Papua New Guinea and Australia. *Am. J. Trop. Med. Hyg.* **2014**, *91*, 887–894.
139. Segura, Á.; Herrera, M.; Villalta, M.; Vargas, M.; Gutiérrez, J.M.; León, G. Assessment of snake antivenom purity by comparing physicochemical and immunochemical methods. *Biologicals* **2013**, *41*, 93–97.
140. Al-Abdulla, I.; Garnvwa, J.M.; Rawat, S.; Smith, D.S.; Landon, J.; Nasidi, A. Formulation of a liquid ovine Fab-based antivenom for the treatment of envenomation by the nigerian carpet viper (*Echis ocellatus*). *Toxicon* **2003**, *42*, 399–404.
141. Rojas, G.; Espinoza, M.; Lomonte, B.; Gutiérrez, J. Effect of storage temperature on the stability of the liquid polyvalent antivenom produced in Costa Rica. *Toxicon* **1990**, *28*, 101–105.
142. O'Leary, M.A.; Kornhauser, R.S.; Hodgson, W.C.; Isbister, G.K. An examination of the activity of expired and mistreated commercial Australian antivenoms. *Trans. R. Soc. Trop. Med. Hyg.* **2009**, *103*, 937–942.
143. American College of Medical, T.; American Academy of Clinical, T. Antidote shortages in the USA: Impact and response. *J. Med. Toxicol* **2015**, *11*, 144–146, doi:10.1007/s13181-013-0372-1.
144. Snow, R.; Bronzan, R.; Roques, T.; Nyamawi, C.; Murphy, S.; Marsh, K. The prevalence and morbidity of snake bite and treatment-seeking behaviour among a rural Kenyan population. *Ann. Trop. Med. Parasitol.* **1994**, *88*, 665–671.
145. Omidfar, K.; Rasaee, M.J.; Kashanian, S.; Paknejad, M.; Bathaie, Z. Studies of thermostability in *Camelus bactrianus* (Bactrian camel) single-domain antibody specific for the mutant epidermal-growth-factor receptor expressed by *Pichia*. *Biotechnol. Appl. Biochem.* **2007**, *46*, 41–49.
146. Harrison, R.A.; Cook, D.A.; Renjifo, C.; Casewell, N.R.; Currier, R.B.; Wagstaff, S.C. Research strategies to improve snakebite treatment: Challenges and progress. *J. Proteom.* **2011**, *74*, 1768–1780.
147. Gutiérrez, J.M.; Theakston, R.D.G.; Warrell, D.A. Confronting the neglected problem of snake bite envenoming: The need for a global partnership. *PLoS Med.* **2006**, *3*, e150.
148. The World Health Organisation. *Guidelines for the Management of Snakebite*; WHO: Geneva, Switzerland, 2016.
149. Morais, V.; Massaldi, H. Snake antivenoms: Adverse reactions and production technology. *J. Venom. Anim. Toxins Incl. Trop. Dis.* **2009**, *15*, 2–18.
150. de Silva, H.A.; Pathmeswaran, A.; Ranasinha, C.D.; Jayamanne, S.; Samarakoon, S.B.; Hittharage, A.; Kalupahana, R.; Ratnatilaka, G.A.; Uluwatthage, W.; Aronson, J.K.; et al. Low-Dose adrenaline, promethazine, and hydrocortisone in the prevention of acute adverse reactions to antivenom following

- snakebite: A randomised, double-blind, placebo-controlled trial. *PLoS Med.* **2011**, *8*, e1000435, doi:10.1371/journal.pmed.1000435.
151. Malasit, P.; Warrell, D.A.; Chanthavanich, P.; Viravan, C.; Mongkolsapaya, J.; Singthong, B.; Supich, C. Prediction, prevention, and mechanism of early (anaphylactic) antivenom reactions in victims of snake bites. *Br. Med. J.* **1986**, *292*, 17–20.
 152. Otero, R.; Gutiérrez, J.; Rojas, G.; Núñez, V.; Díaz, A.; Miranda, E.; Uribe, A.; Silva, J.; Ospina, J.; Medina, Y. A randomized blinded clinical trial of two antivenoms, prepared by caprylic acid or ammonium sulphate fractionation of IgG, in bothrops and porthidium snake bites in Colombia: Correlation between safety and biochemical characteristics of antivenoms. *Toxicon* **1999**, *37*, 895–908.
 153. Lomonte, B.; León, G.; Hanson, L.Å. Similar effectiveness of Fab and F (ab')₂ antivenoms in the neutralization of hemorrhagic activity of viper a berus snake venom in mice. *Toxicon* **1996**, *34*, 1197–1202.
 154. Theakston, R.D.G.; Warrell, D.; Griffiths, E. Report of a WHO workshop on the standardization and control of antivenoms. *Toxicon* **2003**, *41*, 541–557.
 155. Warrell, D. The global problem of snake bite: Its prevention and treatment. *Recent Adv. Toxinol. Res.* **1992**, *1*, 121–153.
 156. Cook, D.A.; Owen, T.; Wagstaff, S.C.; Kinne, J.; Wernery, U.; Harrison, R.A. Analysis of camelid IgG for antivenom development: Serological responses of venom-immunised camels to prepare either monospecific or polyspecific antivenoms for West Africa. *Toxicon* **2010**, *56*, 363–372.
 157. Darvish, M.; Ebrahimi, S.A.; Shahbazzadeh, D.; Bagheri, K.-P.; Behdani, M.; Shokrgozar, M.A. Camelid antivenom development and potential in vivo neutralization of hottentotta saulcyi scorpion venom. *Toxicon* **2016**, *113*, 70–75.
 158. Hamers-Casterman, C.; Atarhouch, T.; Muyldermans, S.; Robinson, G.; Hammers, C.; Songa, E.B.; Bendahman, N.; Hammers, R. Naturally occurring antibodies devoid of light chains. *Nature* **1993**, *363*, 446–448.
 159. De Genst, E.; Silence, K.; Decanniere, K.; Conrath, K.; Loris, R.; Kinne, J.; Muyldermans, S.; Wyns, L. Molecular basis for the preferential cleft recognition by dromedary heavy-chain antibodies. *Proc. Natl. Acad. Sci. USA* **2006**, *103*, 4586–4591.
 160. Vaiyapuri, S.; Vaiyapuri, R.; Ashokan, R.; Ramasamy, K.; Nattamaisundar, K.; Jeyaraj, A.; Chandran, V.; Gajjeraman, P.; Baksh, M.F.; Gibbins, J.M. Snakebite and its socio-economic impact on the rural population of Tamil Nadu, India. *PLoS ONE* **2013**, *8*, e80090.
 161. Boyer, L.V. On 1000-fold pharmaceutical price markups, and why drugs cost more in the US than in Mexico. *Am. J. Med.* **2015**, *128*, 1265–1267.
 162. Seth, A.; Varma, P.; Pakhetra, R. Randomised control trial on the effective dose of anti-snake venom in cases of snake bite with systemic envenomation. *J. Assoc. Physicians India* **2000**, *48*, 756–756.
 163. Vijeth, S.; Dutta, T.; Shahapurkar, J.; Sahai, A. Dose and frequency of anti-snake venom injection in treatment of Echis carinatus (saw-scaled viper) bite. *J. Assoc. Physicians India* **2000**, *48*, 187–191.
 164. Paul, V.; Pratibha, S.; Prahlad, K.; Earali, J.; Francis, S.; Lewis, F. High-dose anti-snake venom versus low-dose anti-snake venom in the treatment of poisonous snake bites-a critical study. *J. Assoc. Physicians India* **2004**, *52*, 14–17.
 165. Panda, S.K.; Padhi, L.; Sahoo, G. Oral bacterial flora of Indian cobra (Naja naja) and their antibiotic susceptibilities. *Heliyon* **2018**, *4*, e01008, doi:10.1016/j.heliyon.2018.e01008.
 166. Blaylock, R. Normal oral bacterial flora from some southern African snakes. *Onderstepoort J. Vet. Res.* **2001**, *68*, 175–182.
 167. Esmaeilishirazifard, E.; Usher, L.; Trim, C.; Denise, H.; Sangal, V.; Tyson, G.H.; Barlow, A.; Redway, K.; Taylor, J.D.; Kremmyda-Vlachou, M. Microbial adaptation to venom is common in snakes and spiders. *bioRxiv* **2018**, 348433, doi:10.1101/348433.
 168. Habib, A.G.; Brown, N.I. The snakebite problem and antivenom crisis from a health-economic perspective. *Toxicon* **2018**, *150*, 115–123, doi:10.1016/j.toxicon.2018.05.009.
 169. Mahmood, M.A.; Halliday, D.; Cumming, R.; Thwin, K.T.; Myitzu, M.; White, J.; Alfred, S.; Warrell, D.A.; Bacon, D.; Naing, W.; et al. Inadequate knowledge about snakebite envenoming symptoms and application of harmful first aid methods in the community in high snakebite incidence areas of myanmar. *PLoS Negl. Trop. Dis.* **2019**, *13*, e0007171, doi:10.1371/journal.pntd.0007171.
 170. Chappuis, F.; Sharma, S.K.; Jha, N.; Loutan, L.; Bovier, P.A. Protection against snake bites by sleeping under a bed net in southeastern Nepal. *Am. J. Trop. Med. Hyg.* **2007**, *77*, 197–199.

171. Isbister, G.K. Antivenom efficacy or effectiveness: The Australian experience. *Toxicology* **2010**, *268*, 148–154.
172. Williams, H.F.; Vaiyapuri, R.; Gajjeraman, P.; Hutchinson, G.; Gibbins, J.M.; Bicknell, A.B.; Vaiyapuri, S. Challenges in diagnosing and treating snakebites in a rural population of Tamil Nadu, India: The views of clinicians. *Toxicon* **2017**, *130*, 44–46.
173. Warrell, D.A.; Theakston, R.D.G.; Sheriff, M.; Ariaratnam, C.A. Distinctive epidemiologic and clinical features of common krait (*Bungarus caeruleus*) bites in Sri Lanka. *Am. J. Trop. Med. Hyg.* **2008**, *79*, 458–462.
174. Stone, R.; Seymour, J.; Marshall, O. Plastic containers and the whole-blood clotting test: Glass remains the best option. *Trans. R. Soc. Trop. Med. Hyg.* **2006**, *100*, 1168–1172.
175. Gaus, D.P.; Herrera, D.F.; Troya, C.J.; Guevara, A.H. Management of snakebite and systemic envenomation in rural Ecuador using the 20-minute whole blood clotting test. *Wilderness Environ. Med.* **2013**, *24*, 345–350, doi:10.1016/j.wem.2013.08.001.
176. Theakston, R.D.G.; Laing, G.D. Diagnosis of snakebite and the importance of immunological tests in Venom research. *Toxins* **2014**, *6*, 1667.
177. CSL, C.S.L. Snake venom detection Kit (SVDK)—detection and identification of snake venom. *Clin. Toxinol. Clin. Toxinol.* **2007**, 1–19.
178. Steuten, J.; Winkel, K.; Carroll, T.; Williamson, N.A.; Ignjatovic, V.; Fung, K.; Purcell, A.W.; Fry, B.G. The molecular basis of cross-reactivity in the Australian snake venom detection kit (SVDK). *Toxicon* **2007**, *50*, 1041–1052.
179. Jelinek, G.A.; Tweed, C.; Lynch, D.; Celenza, T.; Bush, B.; Michalopoulos, N. Cross reactivity between venomous, mildly venomous, and non-venomous snake venoms with the commonwealth serum laboratories venom detection kit. *Emerg. Med.* **2004**, *16*, 459–464.
180. Sharma, S.K.; Kuch, U.; Höde, P.; Bruhse, L.; Pandey, D.P.; Ghimire, A.; Chappuis, F.; Alirol, E. Use of molecular diagnostic tools for the identification of species responsible for snakebite in Nepal: A pilot study. *PLoS Negl. Trop. Dis.* **2016**, *10*, e0004620.
181. Pawade, B.S.; Salvi, N.C.; Shaikh, I.K.; Waghmare, A.B.; Jadhav, N.D.; Wagh, V.B.; Pawade, A.S.; Waykar, I.G.; Potnis-Lele, M. Rapid and selective detection of experimental snake envenomation—Use of gold nanoparticle based lateral flow assay. *Toxicon* **2016**, *119*, 299–306.
182. Liu, C.-C.; Yu, J.-S.; Wang, P.-J.; Hsiao, Y.-C.; Liu, C.-H.; Chen, Y.-C.; Lai, P.-F.; Hsu, C.-P.; Fann, W.-C.; Lin, C.-C. Development of sandwich ELISA and lateral flow strip assays for diagnosing clinically significant snakebite in Taiwan. *PLoS Negl. Trop. Dis.* **2018**, *12*, e0007014.
183. Hung, D.Z.; Lin, J.H.; Mo, J.F.; Huang, C.F.; Liao, M.Y. Rapid diagnosis of *Naja atra* snakebites. *Clin. Toxicol.* **2014**, *52*, 187–191, doi:10.3109/15563650.2014.887725.
184. Naik, B.S. “Dry bite” in venomous snakes: A review. *Toxicon* **2017**, *133*, 63–67.
185. Pore, S.M.; Ramanand, S.J.; Patil, P.T.; Gore, A.D.; Pawar, M.P.; Gaidhankar, S.L.; Ghanghas, R.R. A retrospective study of use of polyvalent anti-snake venom and risk factors for mortality from snake bite in a tertiary care setting. *Indian J. Pharmacol.* **2015**, *47*, 270–274, doi:10.4103/0253-7613.157117.
186. Litschka-Koen, T.; Williams, D. Snake antivenoms in southern Africa. *Contin. Med. Educ.* **2011**, *29*, 75.
187. Brown, N.I. Consequences of Neglect: Analysis of the sub-Saharan African snake antivenom market and the global context. *PLoS Negl. Trop. Dis.* **2012**, *6*, e1670, doi:10.1371/journal.pntd.0001670.
188. Gupta, Y.; Peshin, S. Do herbal medicines have potential for managing snake bite envenomation? *Toxicol. Int.* **2012**, *19*, 89.
189. Bulfone, T.C.; Samuel, S.P.; Bickler, P.E.; Lewin, M.R. Developing small molecule therapeutics for the initial and adjunctive treatment of snakebite. *J. Trop. Med.* **2018**, 2018.
190. Knudsen, C.; Laustsen, A. Recent advances in next generation snakebite antivenoms. *Trop. Med. Infect. Dis.* **2018**, *3*, 42.
191. Laustsen, A.; Solà, M.; Jappe, E.; Oscoz, S.; Lauridsen, L.; Engmark, M. Biotechnological trends in spider and scorpion antivenom development. *Toxins* **2016**, *8*, 226.
192. H. Laustsen, A.; Engmark, M.; Milbo, C.; Johannesen, J.; Lomonte, B.; Maria Gutierrez, J.; Lohse, B. From fangs to pharmacology: The future of snakebite envenoming therapy. *Current Pharm. Des.* **2016**, *22*, 5270–5293.
193. Knudsen, C.; Ledsgaard, L.; Dehli, R.I.; Ahmadi, S.; Sørensen, C.V.; Laustsen, A.H. Engineering and design considerations for next-generation snakebite antivenoms. *Toxicon* **2019**, doi:10.1016/j.toxicon.2019.06.005.

194. Arias, A.S.; Rucavado, A.; Gutiérrez, J.M. Peptidomimetic hydroxamate metalloproteinase inhibitors abrogate local and systemic toxicity induced by *Echis ocellatus* (saw-scaled) snake venom. *Toxicon* **2017**, *132*, 40–49, doi:10.1016/j.toxicon.2017.04.001.
195. Lewin, M.; Samuel, S.; Merkel, J.; Bickler, P. Varespladib (LY315920) Appears to Be a potent, broad-spectrum, inhibitor of snake venom Phospholipase A2 and a possible pre-referral treatment for envenomation. *Toxins* **2016**, *8*, 248.
196. Bittenbinder, M.A.; Zdenek, C.N.; Op den Brouw, B.; Youngman, N.J.; Dobson, J.S.; Naude, A.; Vonk, F.J.; Fry, B.G. Coagulotoxic cobras: Clinical implications of strong anticoagulant actions of African spitting *Naja* venoms that are not neutralised by antivenom but are by LY315920 (Varespladib). *Toxins* **2018**, *10*, 516, doi:10.3390/toxins10120516.
197. Wang, Y.; Zhang, J.; Zhang, D.; Xiao, H.; Xiong, S.; Huang, C. Exploration of the inhibitory potential of varespladib for snakebite envenomation. *Molecules* **2018**, *23*, 391, doi:10.3390/molecules23020391.
198. Bryan-Quiros, W.; Fernandez, J.; Gutierrez, J.M.; Lewin, M.R.; Lomonte, B. Neutralizing properties of LY315920 toward snake venom group I and II myotoxic phospholipases A2. *Toxicon* **2019**, *157*, 1–7, doi:10.1016/j.toxicon.2018.11.292.
199. Escalante, T.; Franceschi, A.; Rucavado, A.; Gutiérrez, J.M.a. Effectiveness of batimastat, a synthetic inhibitor of matrix metalloproteinases, in neutralizing local tissue damage induced by BaP1, a hemorrhagic metalloproteinase from the venom of the snake *Bothrops asper*. *Biochem. Pharmacol.* **2000**, *60*, 269–274.
200. Nicholls, S.J.; Kastelein, J.J.; Schwartz, G.G.; Bash, D.; Rosenson, R.S.; Cavender, M.A.; Brennan, D.M.; Koenig, W.; Jukema, J.W.; Nambi, V. Varespladib and cardiovascular events in patients with an acute coronary syndrome: the VISTA-16 randomized clinical trial. *Jama* **2014**, *311*, 252–262.
201. Zhu, W.-H.; Guo, X.; Villaschi, S.; Nicosia, R.F. Regulation of vascular growth and regression by matrix metalloproteinases in the rat aorta model of angiogenesis. *Lab. Invest.* **2000**, *80*, 545.
202. Shah, S.; Naqvi, S.S.; Abbas, M.A. Use of neostigmine in black mamba snake bite: A case report. *Anaesth. Pain Intensive Care* **2016**, *20*, 77–79.
203. Faiz, M.A.; Ahsan, M.F.; Ghose, A.; Rahman, M.R.; Amin, R.; Hossain, M.; Tareq, M.N.; Jalil, M.A.; Kuch, U.; Theakston, R.D.G. Bites by the monocled cobra, *Naja kaouthia*, in chittagong division, bangladesh: Epidemiology, clinical features of envenoming and management of 70 identified cases. *Am. J. Trop. Med. Hyg.* **2017**, *96*, 876–884.
204. Lewin, M.R.; Samuel, S.P.; Wexler, D.S.; Bickler, P.; Vaiyapuri, S.; Mensh, B.D. Early treatment with intranasal neostigmine reduces mortality in a mouse model of *Naja naja* (Indian Cobra) envenomation. *J. Trop. Med.* **2014**, *2014*, doi:10.1155/2014/131835.
205. O'Brien, J.; Lee, S.-H.; Onogi, S.; Shea, K.J. Engineering the protein corona of a synthetic polymer nanoparticle for broad-spectrum sequestration and neutralization of venomous biomacromolecules. *J. Am. Chem. Soc.* **2016**, *138*, 16604–16607.
206. Karain, B.D.; Lee, M.K.H.; Hayes, W.K. C60 Fullerenes as a novel treatment for poisoning and envenomation: A proof-of-concept study for snakebite. *J. Nanosci. Nanotechnol.* **2016**, *16*, 7764–7771.
207. Silva, L.C.; Pucca, M.B.; Pessenda, G.; Campos, L.B.; Martinez, E.Z.; Cerni, F.A.; Barbosa, J.E. Discovery of human scFvs that cross-neutralize the toxic effects of *B. jararacussu* and *C. d. terrificus* venoms. *Acta Trop.* **2018**, *177*, 66–73, doi:10.1016/j.actatropica.2017.09.001.
208. Laustsen, A.H.; Johansen, K.H.; Engmark, M.; Andersen, M.R. Recombinant snakebite antivenoms: A cost-competitive solution to a neglected tropical disease? *PLoS Negl. Trop. Dis.* **2017**, *11*, e0005361.
209. Gutierrez, J.M.; Rucavado, A. Snake venom metalloproteinases: Their role in the pathogenesis of local tissue damage. *Biochimie* **2000**, *82*, 841–850.
210. Cook, D.A.; Samarasekera, C.L.; Wagstaff, S.C.; Kinne, J.; Wernery, U.; Harrison, R.A. Analysis of camelid IgG for antivenom development: Immunoreactivity and preclinical neutralisation of venom-induced pathology by IgG subclasses, and the effect of heat treatment. *Toxicon* **2010**, *56*, 596–603, doi:10.1016/j.toxicon.2010.06.004.
211. Anderson, G.P.; Liu, J.H.; Zabetakis, D.; Liu, J.L.; Goldman, E.R. Thermal stabilization of anti- α -cobratoxin single domain antibodies. *Toxicon* **2017**, *129*, 68–73, doi:10.1016/j.toxicon.2017.02.008.
212. Laustsen, A.H.; Gutiérrez, J.M.; Knudsen, C.; Johansen, K.H.; Bermúdez-Méndez, E.; Cerni, F.A.; Jürgensen, J.A.; Ledsgaard, L.; Martos-Esteban, A.; Øhlenschläger, M. Pros and cons of different therapeutic antibody formats for recombinant antivenom development. *Toxicon* **2018**, *146*, 151–175.

213. Aubrey, N.; Devaux, C.; Sizaret, P.-Y.; Rochat, H.; Goyffon, M.; Billiald, P. Design and evaluation of a diabody to improve protection against a potent scorpion neurotoxin. *Cell. Mol. Life Sci. CMLS* **2003**, *60*, 617–628.
214. El-Aziz, T.M.A.; Ravelet, C.; Molgo, J.; Fiore, E.; Pale, S.; Amar, M.; Al-Khoury, S.; Dejeu, J.; Fadl, M.; Ronjat, M. Efficient functional neutralization of lethal peptide toxins in vivo by oligonucleotides. *Sci. Rep.* **2017**, *7*, 7202.
215. Chen, Y.-J.; Tsai, C.-Y.; Hu, W.-P.; Chang, L.-S. DNA Aptamers against Taiwan banded krait α -bungarotoxin recognize Taiwan cobra cardiotoxins. *Toxins* **2016**, *8*, 66.
216. Jenkins, T.P.; Fryer, T.; Dehli, R.I.; Jürgensen, J.A.; Fuglsang-Madsen, A.; Føns, S.; Laustsen, A.H. Toxin neutralization using alternative binding proteins. *Toxins* **2019**, *11*, 53.
217. Griffin, L.C.; Tidmarsh, G.F.; Bock, L.C.; Toole, J.J.; Leung, L. In vivo anticoagulant properties of a novel nucleotide-based thrombin inhibitor and demonstration of regional anticoagulation in extracorporeal circuits. *Blood* **1993**, *81*, 3271–3276.
218. Wuellner, U.; Klupsch, K.; Buller, F.; Attinger-Toller, I.; Santimaria, R.; Zbinden, I.; Henne, P.; Grabulovski, D.; Bertschinger, J.; Brack, S. Bispecific CD3/HER2 targeting FynomAb induces redirected T cell-mediated cytotoxicity with high potency and enhanced tumor selectivity. *Antibodies* **2015**, *4*, 426–440.
219. Roopenian, D.C.; Akilesh, S. FcRn: The neonatal Fc receptor comes of age. *Nat. Rev. Immunol.* **2007**, *7*, 715.
220. Akilesh, S.; Christianson, G.J.; Roopenian, D.C.; Shaw, A.S. Neonatal FcR expression in bone marrow-derived cells functions to protect serum IgG from catabolism. *J. Immunol.* **2007**, *179*, 4580–4588.
221. Halilu, S.; Iliyasu, G.; Hamza, M.; Chippaux, J.-P.; Kuznik, A.; Habib, A.G. Snakebite burden in Sub-Saharan Africa: Estimates from 41 countries. *Toxicon* **2019**, *159*, 1–4, doi:10.1016/j.toxicon.2018.12.002.
222. Williams, D.J.; Faiz, M.A.; Abela-Ridder, B.; Ainsworth, S.; Bulfone, T.C.; Nickerson, A.D.; Habib, A.G.; Junghanss, T.; Fan, H.W.; Turner, M.; et al. Strategy for a globally coordinated response to a priority neglected tropical disease: Snakebite envenoming. *PLoS Negl. Trop. Dis.* **2019**, *13*, e0007059, doi:10.1371/journal.pntd.0007059.
223. Bouazza, A.; El Hidan, M.A.; Aimrane, A.; Kahime, K.; Lansari, A.; Laaradia, M.A.; Lahouaoui, H.; Moukrim, A. Climate change effects on venomous snakes: Distribution and snakebite epidemiology. In *Handbook of Research on Global Environmental Changes and Human Health*; IGI Global: Hershey, PA, USA, 2019; pp. 475–490.
224. Kannt, A.; Wieland, T. Managing risks in drug discovery: Reproducibility of published findings. *Naunyn-Schmiedeberg's Arch. Pharmacol.* **2016**, *389*, 353–360, doi:10.1007/s00210-016-1216-8.



© 2019 by the authors. Licensee MDPI, Basel, Switzerland. This article is an open access article distributed under the terms and conditions of the Creative Commons Attribution (CC BY) license (<http://creativecommons.org/licenses/by/4.0/>).

2.2 Challenges in diagnosing and treating snakebites in a rural population of Tamil Nadu, India: The views of clinicians

Harry F. Williams¹, Rajendran Vaiyapuri², Prabu Gajjerman³, Gail Hutchinson⁴, Jonathon M. Gibbins⁴, Andrew B. Bicknell⁴ and Sakthivel Vaiyapuri¹

¹School of Pharmacy, University of Reading, Reading, UK

²School of Pharmacy, University of Reading Malaysia, Johor, Malaysia

³Department of Biotechnology, Karpagam University, Coimbatore, Tamil Nadu, India

⁴Institute for Cardiovascular and Metabolic Research, School of Biological Sciences, University of Reading, Reading, UK

Toxicon 2017 - Reprinted with permission from Elsevier

Conclusion of this chapter

This chapter analyses the views of South Indian clinicians who come into regular contact with snakebite victims. They typically expect to see an increase in cases over the rainy season and all treated patients using polyvalent antivenom, with an initial dose of ten vials. Shockingly, 200 vials were used in one instance, a dosage associated with almost certain adverse effects, and highly unlikely to be necessary. The majority of clinicians found identifying the snake of importance, though others indicated that due to the lack of specific treatments knowledge of the snake was unnecessary. They highlighted the need for diagnostical methods to be developed and more efficacious treatments to be made available to them. More efficacious treatment will require a better understanding of all the underlying effects, particularly surrounding local tissue damage, oxidative stress and the resulting permanent sequelae.

Contribution to this chapter

General contribution (50%)

- Analysis and interpretation of data
- Writing of the manuscript

***data collection took place before the start of this doctorate by authors other than HFW**



Short communication

Challenges in diagnosing and treating snakebites in a rural population of Tamil Nadu, India: The views of clinicians



Harry F. Williams^a, Rajendran Vaiyapuri^b, Prabu Gajjeraman^c, Gail Hutchinson^d,
Jonathan M. Gibbins^d, Andrew B. Bicknell^d, Sakthivel Vaiyapuri^{a,*}

^a School of Pharmacy, University of Reading, Reading, UK

^b School of Pharmacy, University of Reading Malaysia, Johor, Malaysia

^c Department of Biotechnology, Karpagam University, Coimbatore, Tamil Nadu, India

^d Institute for Cardiovascular and Metabolic Research, School of Biological Sciences, University of Reading, Reading, UK

ARTICLE INFO

Article history:

Received 12 December 2016

Received in revised form

20 February 2017

Accepted 21 February 2017

Available online 24 February 2017

Keywords:

Snakebite

Venom

Anti-venom

ASV

Big four

ABSTRACT

Snakebites cause death, disability and economic devastation to their victims, people who live almost exclusively in rural areas. Annually an estimated two million venomous bites cause as many as 100,000 deaths worldwide as well as hundreds of thousands of deformities and amputations. Recent studies suggest that India has the highest incidence of snakebite and associated deaths worldwide. In this study, we interviewed 25 hospital-based clinicians who regularly treat snakebites in Tamil Nadu, India, in order to gauge their opinions and views on the diagnostic tools and treatment methods available at that time, the difficulties encountered in treating snakebites and improvements to snakebite management protocols they deem necessary. Clinicians identified the improvement of community education, training of medical personnel, development of standard treatment protocols and improved medication as priorities for the immediate future.

© 2017 Elsevier Ltd. All rights reserved.

1. Introduction

Snakebites are one of the major neglected tropical medical challenges affecting rural populations worldwide with several million bites (White, 2000) and around 100,000 deaths each year (Kasturiratne et al., 2008). India is one of the countries where snake envenomation is most prevalent, however snakebites in this country are poorly characterised (White, 2000; Kasturiratne et al., 2008; Chippaux, 1998; Warrell, 2010; Vaiyapuri et al., 2013). The medically important snakes in India are considered to be the 'big four': the Russell's viper (*Daboia russelii*), saw-scaled viper (*Echis carinatus*), Indian cobra (*Naja naja*) and the common krait (*Bungarus caeruleus*), although other medically important snakes have also been reported (Kochar et al., 2007; Simpson and Norris, 2007; Sharma et al., 2008; Joseph et al., 2007).

The complexity of snake venoms and their combined action in victims pose considerable challenges to the treatment of bites. Currently, the only available treatment in rural India is polyvalent

anti-snake venom (ASV) raised in either horses or sheep against the venoms of the big four. The efficacy of this ASV against the venom of snakes that are not one of the big four and big four individuals from different geographical locations is unclear. Moreover, the administration of ASV from horses and sheep regularly leads to dangerous anaphylactic reactions and problems relating to hypersensitivity that can last for several days. In India, there are no specific diagnostic tools to confirm snakebite occurrence in victims or to identify the source snake species or family. There is therefore a need to improve diagnostic methods for snakebites, allowing the family of the offending snake to be known, appropriate quantities of ASV to be delivered and the dangers associated with the administration of ASV by inexperienced individuals to be minimised.

In order to better understand the available diagnostic techniques, treatment methods, difficulties encountered in treating snakebites and improvements required to current protocols, we conducted face to face interviews with clinicians who regularly treat snakebites and present their views in this article.

2. Methods

This study was conducted along with a population survey aimed

* Corresponding author.

E-mail address: s.vaiyapuri@reading.ac.uk (S. Vaiyapuri).

at understanding snakebite incidence and its socio-economic impacts on the rural population of Tamil Nadu, India (Vaiyapuri et al., 2013). Interviews were conducted with 25 clinicians based in 20 private multi-specialty hospitals in the Indian state of Tamil Nadu. All the clinicians interviewed had been treating snakebites for at least six years and nine had more than 20 years of experience. A standard questionnaire was used to collect their views on snakebite incidence, diagnosis and treatment. The School of Biological Sciences Ethical Committee review panel at the University of Reading approved this study and the questionnaire. After obtaining written consent, the interviews were recorded either in the local language or in English and later translated by the authors. The appropriateness of translation was checked prior to the interviews. The authors performed the interviews and all data were anonymised prior to analysis.

3. Results and discussion

The clinicians in private hospitals were interviewed between 2010 and 2012 to gauge their opinions about current management and treatment of snakebites, the difficulties they have experienced and their views on how snakebite treatment could be improved in the future. On average, each clinician interviewed, evaluated and treated 50 snakebite victims per year with some of the referral hospital physicians seeing more than 100 victims each year (Table 1). Seventy-five percent of clinicians reported an increase in hospitalised snakebite cases during the rainy seasons, an observation that was stable over the years, while 25% observed no seasonal variations. In all cases, the clinical examination included analysing symptoms such as vomiting, nausea, bleeding gums, swelling/infection/bleeding at the bite site, and other physical symptoms. All the clinicians attempted to find out the time of bite, snake species and treatments received either from traditional healers or other medical professionals.

Following whole blood clotting time (WBCT) test and clinical observations, all clinicians used polyvalent ASV to treat the bites. Typically, treatment would start with ten vials of ASV, but as many as 200 vials were used in some cases (Table 1). The typical cost for a single vial was Rs 400–550. Antibiotics and anti-histamine were the most common additional treatments reported, and the duration of a patients stay in hospital ranged from 2 days up to 35 days during this treatment (Table 1). The clinicians estimated the cost of treatment to range from Rs 5,000 to Rs 200,000. We found 67% of clinicians to consider identification of the offending snake important in order to determine whether it was likely to have more haemotoxic or neurotoxic effects. The remaining clinicians felt that identifying the snake was unimportant; mainly due to the lack of species-specific treatment.

The clinicians reported a range of time intervals between the

snakebite and the arrival of a victim at hospital. Forty percent of victims arrived within 30 min and a further 30% of victims arrived within a few hours of the bite (Table 1). Many also commented that some patients (approximately 30%) did not come to hospital until several days after the bite due to treatments sought from locally available traditional healers. Delays in arrival were considered to lead to increased envenomation effects and complications, particularly pulmonary bleeding, renal failure, necrosis, septicemia, cerebral bleeding and respiratory failure. In some cases, the delay in obtaining correct treatments resulted in severe complications leading to surgery to remove or graft the affected areas. Despite this, less than five per cent of envenomed patients died in hospitals. Clinicians were frequently unable to save the lives of snakebite victims who had cerebral bleeding and pulmonary bleeding, and this was associated with 80% mortality due to increased complications. When clinicians were asked to report any unusual snakebite cases, two reported early morning neuromuscular syndrome. The clinicians infused ASV assuming that this may have been due to a krait bite, and the victims recovered after 24 h and confirmed that they had suffered from snakebite.

Clinicians were asked for their opinions on the treatments currently available and their views on how snakebite prevention and management could be improved in the future. Each, without exception, emphasized that current treatments lack efficacy since knowledge of the snakebite is normally limited, with nothing known about the species or dose of venom the victim is suffering from. They also suggested that diagnostic methods for snakebites should be improved to aid in the identification of snakebite, particularly in the case of krait bites. The clinicians recommended that tools must be developed to analyse the pharmacokinetics of venom activity in victims, and to monitor the rate of its release from the bite site into circulation. Developing appropriate diagnostic tools to identify specific snakebites would improve snakebite treatment.

Eighty percent of clinicians interviewed considered the use of polyvalent ASV to be a satisfactory approach, although considered improvements desirable, particularly to reduce side effects. We found 70% of clinicians to also recommend further ASV purification, which could reduce anaphylactic reactions in response to contaminants such as albumin and endotoxins. A few clinicians also recommended the introduction of monovalent ASV, although confident identification of snake species would be necessary for this to be effective. Clinicians unanimously recommended that a standard protocol should be made available and followed. This has been recommended by others (Alirol et al., 2010; Gutierrez et al., 2006) and there are recently updated (2016) WHO guidelines which can be found at apps.who.int/pds_docs/B5255.pdf and should be made available to all clinicians coming into regular contact with snakebite victims the world over, as there is a clear

Table 1

Summary of clinicians' interview on complications associated with the diagnosis and treatment of snakebites.

Complications associated with the diagnosis and treatment of snakebites	
Number of years involved in treating snakebites	6 - >30 years
Number of patients seen in each hospital	20 - 150 cases/year
Seasonal variations in snakebites	Most of the bites occurred in rainy seasons
Preclinical diagnostic methods	Vomiting, nausea, bleeding, swelling, infections at the bite site and first aid received
Main treatment method	ASV
Number of vials used for treatment	Minimum 10 and maximum up to 200
Costs of ASV	Rs 400 - Rs 550/vial
Additional treatment options	Broad spectrum antibiotics, anti-histamines and blood or plasma transfusion
Hospital stay during treatment	Minimum 2 days and maximum 35 days
Treatment costs	Minimum Rs 5,000 to maximum Rs 200,000 (went up to Rs 1,000,000 when surgery was required)
Extreme complications seen with snakebites	Pulmonary bleeding, cerebral bleeding, acute renal failure and uncontrolled breathing
Percentage of victims that died in hospitals	0–<5%

lack of knowledge in this area, as displayed by the delivery of up to 200 vials of ASV in some cases (Table 1). Even in private hospitals, clinicians found there to be no snakebite protocols available. The production and circulation of protocols could at the very least prevent such dangerous over-doses and wastage of ASV.

Half of the clinicians recommended that the government should raise awareness of the dangers of snakebite among the general population, suggesting the use of advertisements in the local media and awareness camps in rural areas. Several clinicians wanted to see better training for those working in rural areas in order to avoid the unnecessary use of ASV for non-venomous bites and to enable local practitioners to treat the victims with confidence rather than referring them to distant hospitals. The clinicians also suggested that snakebite management should be introduced into the curriculum for medical students.

When asked what advice they had given to victims, clinicians reported to have given guidance about prevention of future bites by wearing protective clothing, particularly shoes, taking extra care when outside, and that patients should avoid home treatments and instead go straight to hospital. These preventive measures have also been suggested by other researchers (Warrell, 2010; Alirol et al., 2010), and the WHO's latest guidelines for the management of snakebite in South East Asia recognise that community education is the best approach to prevent snakebites (WHO, 2016).

4. Conclusions

In summary, this study emphasizes the difficulties associated with the currently followed diagnostic and treatment methods from the clinicians' point of view. This highlights that there is a need to develop specific diagnostic tools for the confirmation of venomous snakebites and identification of the source snake family. Research should be initiated to develop monovalent ASV to specific snake species, or may be bivalent ASV for the viper and elapid sides of the big four. We believe that this article could help the government officials in Tamil Nadu and India, as well as researchers working in this area to understand the complications associated with snakebites and to design strategies to improve the diagnosis and treatment of snakebites in India.

Ethical statement

This research was conducted according to the Declaration of Helsinki and the ethical guidelines of the Indian Council of Medical Research. The research and the consent forms and questionnaire for

clinicians were approved by the research ethics committee at the School of Biological Sciences, University of Reading. Surveys were conducted between 2010 and 2012 in India. The aims of the research were explained to the participants in local languages or English and informed written consent was obtained from all study participants. All data were anonymised prior to analysis.

Acknowledgements

We would like to thank all the clinicians who participated in this study for their time and for sharing their expertise. We are also very grateful to Dr Robert Harrison at Liverpool School of Tropical Medicine, UK for his advice and critical evaluation during the preparation of this manuscript.

Transparency document

Transparency document related to this article can be found online at <http://dx.doi.org/10.1016/j.toxicon.2017.02.025>.

References

- Alirol, E., et al., 2010. Snake bite in South Asia: a review. *PLoS Negl. Trop. Dis.* 4 (1), e603.
- Chippaux, J.P., 1998. Snake-bites: appraisal of the global situation. *Bull. World Health Organ* 76, 513–524.
- Gutierrez, J.M., Theakston, R.D., Warrell, D.A., 2006. Confronting the neglected problem of snake bite envenoming: the need for a global partnership. *PLoS Med.* 3 (6), e150.
- Joseph, J.K., et al., 2007. First authenticated cases of life-threatening envenoming by the hump-nosed pit viper (*Hypnale hypnale*) in India. *Trans. R. Soc. Trop. Med. Hyg.* 101 (1), 85–90.
- Kasturiratne, A., et al., 2008. The global burden of snakebite: a literature analysis and modelling based on regional estimates of envenoming and deaths. *PLoS Med.* 5 (11), e218.
- Kochar, D.K., et al., 2007. Rediscovery of severe saw-scaled viper (*Echis sochureki*) envenoming in the Thar desert region of Rajasthan, India. *Wilderness Environ. Med.* 18 (2), 75–85.
- Sharma, L.R., Lal, V., Simpson, I.D., 2008. Snakes of medical significance in India: the first reported case of envenoming by the Levantine viper (*Macrovipera lebetina*). *Wilderness Environ. Med.* 19 (3), 195–198.
- Simpson, I.D., Norris, R.L., 2007. Snakes of medical importance in India: is the concept of the "Big 4" still relevant and useful? *Wilderness Environ. Med.* 18 (1), 2–9.
- Vaiyapuri, S., et al., 2013. Snakebite and its socio-economic impact on the rural population of Tamil Nadu, India. *PLoS One* 8 (11), e80090.
- Warrell, D.A., 2010. Snake bite. *Lancet* 375 (9708), 77–88.
- White, J., 2000. Bites and stings from venomous animals: a global overview. *Ther. Drug Monit.* 22, 65–68.
- WHO, 2016. Guidelines for the Management of Snakebite. Regional Office for South-East Asia, p. 22.

3. Aims and objectives of experimental chapters

1. Impact of *Naja nigricollis* Venom on the Production of Methaemoglobin

Hypothesis: Snake venoms can oxidise haemoglobin to produce toxic methaemoglobin.

Aims: Ascertain the ability for venoms to oxidise haemoglobin, assess the diversity of snake venoms showing potential for oxidising haemoglobin to methaemoglobin and establish whether this is a proteolytic effect

Experimental system: Full wavelength scans using haemoglobin peaks and methaemoglobin peaks to assess approximate scale of oxidation

Chapter connection: *This is likely to be a compounding factor to a range of the pathologies associated with snakebite envenomation. This effect will be most prominent at the local bite site, exacerbating skeletal muscle regeneration and potentially having similar effects on myoglobin.*

2. Mechanisms underpinning the permanent muscle damage induced by snake venom metalloprotease

Hypothesis: Snake venom metalloproteases cause attenuated regeneration via direct effects on the basement membrane

Aims: Uncover the exact mechanisms by which snake venom metalloproteases cause muscle damage and impair regeneration compared to pore-forming three-finger toxins

Experimental system: protein purification and characterisation *in vitro*, injection of toxins *in vivo*, immunostaining and imaging of cryosections

Chapter connection: *Muscle damage is a common side effect of snakebite envenomation (especially from vipers). The proposed matrix metalloprotease inhibitors batimastat and marimastat are one potential option to mitigate this.*

3. Effects of batimastat and marimastat on a group I metalloprotease from the venom of *Crotalus atrox*

Hypothesis: Commercially available inhibitors can prevent the collagenolytic effects of a P-I snake venom metalloprotease *in vitro*

Aims: Characterise a P-I snake venom metalloprotease and assess the ability for proposed inhibitors and chelators to abrogate its collagenolytic effects

Experimental system: protein purification and characterisation of inhibitors *in vitro*; enzymatic and *ex vivo* cell-based assays

Chapter connection: *Proposed adjunctive or alternative therapies such as matrix metalloprotease inhibitors (to counteract SVMPs) or melatonin (against oxidative stress and methaemoglobin) are likely to be effective in certain envenomations. However, in the case of dry bites, or bites from species whose effects are exacerbated by these compounds, they may do more harm than good. Therefore, diagnostic tools need to be developed and made available to ensure administration only when beneficial.*

4. The detection of snake venom serine proteases using a peptide-based approach

Hypothesis: Using multiple sequence alignment to identify conserved regions in proteins can allow the production of toxin-specific antibodies for detection of venoms

Aims: Develop antibodies with which to detect snake venom serine proteases based on specific regions of the toxin

Experimental system: injection of synthetic KLH-conjugated peptides into sheep; antibody purification; enzyme linked immunosorbent assays

Chapter connection: *Synthetic peptides are one possible means of developing toxin specific antibodies, but the artificial choosing of epitopes may have caused issues with steric hindrance. Therefore, the use of whole proteins to develop toxin-specific antibodies may provide sufficient epitopes for two-site assays to be possible, allowing for development into a lateral flow assay configuration.*

5. Toxin-specific antibodies for the detection of snake venom metalloproteases in clinical samples obtained from snakebite victims

Hypothesis: Purified proteins from venom can be used in the production of antibodies for broad ranging detection of viper venoms

Aims: Purify proteins and develop antibodies with which to detect snake venom metalloproteases in two-site assays and lateral flow assays

Experimental system: protein purification; enzyme linked immunosorbent assays (ELISA) and lateral flow assays (LFA)

Chapter connection: *Whole purified proteins provide a means by which to develop antibodies specific to that group of proteins and diagnose envenomations including this group of toxins. This could indicate treatment with adjunctive small molecular therapeutics, the rapid administration with which would reduce muscle damage, haemorrhaging, ischaemia and hypoxia. Over time such protocols for the treatment of snakebites will decrease morbidity among envenomations and prevent unnecessary administration of drugs and any consequential financial burden or adverse effects.*

4. Experimental Chapters

4.1 Impact of *Naja nigricollis* Venom on the Production of Methaemoglobin

Harry F. Williams*, Paul Hayter*, Divyashree Ravishankar, Anthony Baines, Harry J. Layfield, Lorraine Croucher, Catherine Wark, Andrew B. Bicknell, Steven Trim* and Sakthivel Vaiyapuri

Toxins 2018

4.2 Mechanisms underpinning the permanent muscle damage induced by snake venom metalloprotease

Harry F. Williams*, Ben A. Mellows*, Robert Mitchell*, Peggy Syfri, Harry J. Layfield, Maryam Salamah, Rajendran Vaiyapuri, Henry Collins-Hooper, Andrew B. Bicknell, Antonios Matsakas, Ketan Patel* and Sakthivel Vaiyapuri

PLoS Neglected Tropical Diseases 2019

4.3 Effects of batimastat and marimastat on a group I metalloprotease from the venom of *Crotalus atrox*

Harry F. Williams*, Harry J. Layfield*, Divyashree Ravishankar, Thomas M. Vallance and Sakthivel Vaiyapuri

In Preparation

4.4 The detection of snake venom serine proteases using a peptide-based approach

Harry F. Williams, Harry J. Layfield, Andrew B. Bicknell, Steven Trim and Sakthivel Vaiyapuri

In Preparation

4.5 Toxin-specific antibodies for the detection of snake venom metalloproteases in clinical samples obtained from snakebite victims

Harry F. Williams, Harry J. Layfield, Andrew B. Bicknell, Steven Trim and Sakthivel Vaiyapuri

In Preparation

*Authors contributed equally to this work

4.1 Impact of *Naja nigricollis* Venom on the Production of Methaemoglobin

Harry F. Williams^{*1}, Paul Hayter^{2*}, Divyashree Ravishankar¹, Anthony Baines³, Harry J. Layfield¹, Lorraine Croucher⁴, Catherine Wark⁴, Andrew B. Bicknell⁵, Steven Trim^{2*} and Sakthivel Vaiyapuri

¹School of Pharmacy, University of Reading, Reading, United Kingdom

²Venomtech Private Limited, Sandwich, United Kingdom

³School of Biosciences, University of Kent, Kent, United Kingdom

⁴BMG LabTech, Buckinghamshire, United Kingdom

⁵School of Biological Sciences, University of Reading, Reading, United Kingdom

Toxins 2018 - Open Access

Conclusion of this chapter

Part of the high morbidity associated with snakebites is the lack of proper understanding of all of the pathologies which can be caused by SBE. This chapter looks at the oxidation of haemoglobin to methaemoglobin with a range of snake venoms and hopes to highlight this as a common side effect of envenomation. The hypoxia and oxidative stress caused by methaemoglobin production will undoubtedly exacerbate local tissue damage and cause further detriment in muscle and other tissues already suffering from the direct action of various toxins as well as haemorrhage induced ischaemia and lack of blood flow. Added to which, the potential for this effect to also be present in myoglobin - the muscular oxygen storage protein - is likely to add to the extensive muscle damage associated with snakebites from certain species. Melatonin is one suggested treatment for this condition but will rely on accurate diagnosis to ensure efficacious administration.

Contribution to this chapter

General contribution (60%)

- Study design
- Analysis and interpretation of data
- Writing of the manuscript
- Preparation of the figures
- Performance of experiments and data collection



Experimental contribution

Figure 2 A-D Full wavelength scans and concentration dependence analysis

Figure 3 A-C SDS-PAGE and analysis of effects of DTT and heat treatment of venom

Article

Impact of *Naja nigricollis* Venom on the Production of Methaemoglobin

Harry F. Williams ^{1,†}, Paul Hayter ^{2,†}, Divyashree Ravishankar ¹, Anthony Baines ³,
Harry J. Layfield ¹, Lorraine Croucher ⁴, Catherine Wark ⁴, Andrew B. Bicknell ⁵, Steven Trim ^{2,*}
and Sakthivel Vaiyapuri ^{1,*}

¹ School of Pharmacy, University of Reading, Reading RG6 6UB, UK; h.f.williams@pgr.reading.ac.uk (H.F.W.); d.ravishankar@reading.ac.uk (D.R.); h.j.layfield@reading.ac.uk (H.J.L.)

² Venomtech, Discovery Park, Sandwich, Kent CT13 9ND, UK; paul.hayter@talktalk.net

³ School of Biosciences, University of Kent, Kent CT2 7NZ, UK; a.bains@venomtech.co.uk

⁴ BMG LabTech, Buckinghamshire HP19 8JR, UK; lorraine.croucher@bmglabtech.com (L.C.); catherine.wark@bmglabtech.com (C.W.)

⁵ School of Biological Sciences, University of Reading, Reading RG6 6UB, UK; a.b.bicknell@reading.ac.uk

* Correspondence: s.trim@venomtech.co.uk (S.T.); s.vaiyapuri@reading.ac.uk (S.V.)

† Authors contributed equally to this work.

Received: 19 October 2018; Accepted: 14 December 2018; Published: 15 December 2018



Abstract: Snakebite envenomation is an affliction currently estimated to be killing upwards of 100,000 people annually. Snakebite is associated with a diverse pathophysiology due to the magnitude of variation in venom composition that is observed worldwide. The haemolytic (i.e., lysis of red blood cells) actions of snake venoms are well documented, although the direct impact of venoms on haemoglobin is not fully understood. Here we report on the varied ability of a multitude of snake venoms to oxidise haemoglobin into methaemoglobin. Moreover, our results demonstrate that the venom of an elapid, the black necked spitting cobra, *Naja nigricollis*, oxidises oxyhaemoglobin (Fe²⁺) into methaemoglobin (Fe³⁺) in a time- and concentration-dependent manner that is unparalleled within the 47 viper and elapid venoms evaluated. The treatment of venom with a reducing agent, dithiothreitol (DTT) is observed to potentiate this effect at higher concentrations, and the use of denatured venom demonstrates that this effect is dependent upon the heat-sensitive proteinaceous elements of the venom. Together, our results suggest that *Naja nigricollis* venom appears to promote methaemoglobin production to a degree that is rare within the Elapidae family, and this activity appears to be independent of proteolytic activities of venom components on haemoglobin.

Keywords: Snakebite; venom; methaemoglobin; haemoglobin; neglected tropical disease; spitting cobra

Key Contribution: We demonstrate the impact of *Naja nigricollis* (the black necked spitting cobra) venom in the oxidation of haemoglobin to methaemoglobin, which is a toxic species capable of causing a range of additional issues to envenomed victims.

1. Introduction

Snakebite envenomation is considered to be a major neglected tropical disease. It is estimated to affect nearly five million people and result in approximately 100,000 deaths annually [1]. It is a crisis that predominantly impacts upon people living in rural areas of developing nations, and can induce major socio-economic ramifications [2,3]. Despite the significant impact on the health and well-being of humans, much remains unknown about the different toxic proteins and peptides that are the major components of snake venoms [4]. Venomous snakes have been classified into several

families and sub families, but the vast majority of deaths occur as a result of bites from those found in Viperidae (Vipers) and Elapidae (Elapids). These two families are very different; vipers are typically ambush predators that inject a venom composed mainly of large proteins that predominantly affect haemostasis, while elapids are generally more active hunters, with venoms containing fewer of these haemotoxic components but instead dominated by neurotoxic and cytotoxic proteins and peptides [5]. Thus elapids are less commonly associated with haemostatic disturbances.

A range of biological activities have been found to be induced by snake venom components, with many of these proteins targeting the blood, haemostasis and cardiovascular system [6,7]. Serine proteases and metalloproteases are the most abundant proteins found in viper venoms and they exhibit various haemotoxic effects. Metalloproteases are able to affect the basement membrane of blood vessels via collagenolytic activity [8], and several other venom components inhibit or activate platelets by different mechanisms [9–11]. As well as interacting with platelets and blood vessels, many venom proteins affect the blood coagulation cascade via coagulatory or anti-coagulatory effects [12]. An array of different proteins capable of causing haemolysis also exist within snake venoms, for example, the enzymatic phospholipase A2 (PLA2) which directly cleave the phospholipid bilayer, and the hydrophobic three-finger toxins, which can bind to the cell membrane to promote lysis [13]. Indeed, haemolysis can take place to such a degree that haemolytic anaemia has developed in some recorded cases of snakebites [14]. Haemolysis is a well-known effect of several snake venoms, although their direct effects on red blood cells (RBCs) and their components are not fully understood, especially given the oxidative stress typically observed as a secondary effect of certain snake bites [15–17].

In addition to natural intra- or extravascular haemolysis (approximately 10% of RBCs will lyse as a consequence of wear and tear) and direct lysis by venom components, haemolysis also takes place as a result of the venom-induced local tissue damage which produces reactive oxygen (ROS) and nitrogen species that contribute to oxidative damage and further lysis of cells [16]. The release of haemoglobin (Hb) into the plasma following haemolysis triggers inflammation and oxidative stress as well as impairing endothelial function. Excessive plasma Hb levels is called haemoglobinemia and it can induce extreme nitric oxide consumption and clinical sequelae including haemolysis-associated vasculopathies and endothelial dysfunction [18]. Free plasma Hb is bound rapidly by haptoglobin in order to inhibit its oxidative activity, and this complex is rapidly removed by the mononuclear phagocytic system, particularly the spleen [19]. After plasma haptoglobin is saturated, the excessive Hb is filtered out by the kidneys. Frequently, during envenomation these organs are already under pressure due to decreased renal blood flow as a result of ischaemia, thrombotic microangiopathy and rhabdomyolysis. These in turn cause myoglobin deposits in renal tubules [4] and together lead to acute kidney injury, which is a main systemic complication and is frequently the cause of death in viper bites [20].

RBCs are essential for the transportation of oxygen to the tissues and delivery of CO₂ (or dissolved HCO₃[−]) to the lungs; they are entirely dependent upon the oxygen transport protein, Hb. This protein relies on a prosthetic ferrous (Fe²⁺) haem group, the ferric oxidation of which renders the protein (termed as methaemoglobin (MetHb)) unable to transport oxygen (Fe³⁺), a process which has already been observed in specific snake venoms [21]. This process takes place at a very low rate naturally, and MetHb is maintained at <1% by rapid reduction to the ferrous form, a process catalysed by the enzyme methaemoglobin reductase [22]. Through this reaction, a superoxide free radical is generated but is quickly dismutated via the enzyme superoxide dismutase forming H₂O₂ and O₂ [23]. Methaemoglobinemia occurs when the levels of MetHb occur above 2% and serious neurological and cardiovascular symptoms can develop as a result of hypoxia with levels of approximately 15% and above [24].

Venom-induced oxidative stress appears to be an effect of envenomation that anti-snake venom (ASV) (the only available treatment for snakebite envenoming) fails to ameliorate [25], and may actually exacerbate [21]. These effects are reduced by the co-administration of melatonin, an anti-oxidant agent, along with ASV, and there is evidence to suggest a reduction in methaemoglobinemia as a result [16,21]. However, the scale of oxidative stress and other effects of venom components on the functions of RBCs

and Hb are yet to be studied in detail. Here, we report the screening of a large number of snake venoms and specifically characterise the effect of the venom of *Naja nigricollis* (*N. nigricollis*) to determine its impact on the production of MetHb.

2. Results

2.1. A Range of Snake Venoms Induce the Oxidation of Hb

The ability of venoms to oxidise Hb into MetHb has been reported within the family of Viperidae [15–17,26]. Here, we screened 47 different viper (30) and elapid (17) venoms from the targeted venom discovery array for the cardiovascular system (T-VDA^{CV}) in order to determine the impact of these on MetHb production. The venoms (0.2 mg/mL) were mixed with an equal volume of ovine Hb (the supernatant of lysed ovine RBCs) and incubated for 16 h prior to measuring the absorbance at 500 nm and 630 nm (i.e., absorbance maxima for MetHb). An overnight period of 16 h was used in the experiments in order to determine the maximum impact of venom on MetHb production. The data suggest that Hb oxidising activity is common among several viper venoms but this is a rare phenomenon for an elapid snake venom (Figure 1). Notably, the large increase in absorbance observed in many viper venoms was only evident in the venom of one elapid, *N. nigricollis*. As this is a unique feature observed in *N. nigricollis* venom, we have analysed this effect in greater detail.

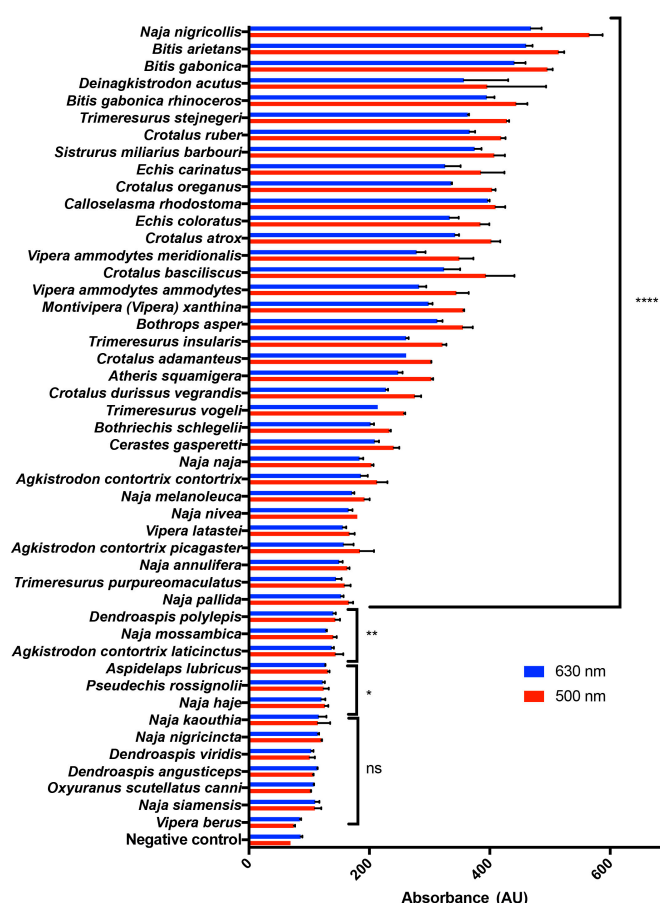


Figure 1. Impact of T-VDA^{CV} venom array on MetHb production. Whole snake venoms (0.2 mg/mL) from the T-VDA^{CV} array (Venomtech Limited, UK) targeting the cardiovascular system were dispensed into 96-well micro titre plates, mixed with an equal volume of ovine Hb, and incubated at 37 °C for 16 h. The absorbance was measured at 500 nm and 630 nm (i.e., the peaks typically observed for MetHb) by spectrofluorimetry (FLUOstar Optima, BMG Labtech) at 16 h. Data represent mean ± SEM ($n = 3$), and the p values (all the values were compared to the negative control [PBS]) were calculated by One-way ANOVA followed by post-hoc Tukey's test using GraphPad Prism (* $p < 0.05$, ** $p < 0.01$, and **** $p < 0.0001$).

2.2. *Naja Nigricollis* Venom Is Significantly Increasing MetHb Production

To determine the effect of *N. nigricollis* venom on MetHb production, additional experiments were performed using ovine Hb. *N. nigricollis* venom (10 mg/mL was used to achieve a maximum response) was incubated with ovine Hb and the level of absorbance for Hb and MetHb was measured every 2 h for 16 h. The venom displayed a time-dependent decrease in absorbance at 540 nm and 570 nm (i.e., peaks observed for Hb) with a corresponding time-dependent increase in absorbance at 500 nm and 630 nm (i.e., peaks typical of MetHb) (Figure 2A,B). Similarly, the increasing concentrations of *N. nigricollis* venom suggest that this venom-induced impact on MetHb production is also concentration-dependent (Figure 2C,D). Therefore, an optimal concentration of 0.2 mg/mL venom was used in other experiments in this study. Together these results suggest that the *N. nigricollis* venom is promoting the oxidation of oxyhaemoglobin to MetHb in a time- and concentration-dependent manner.

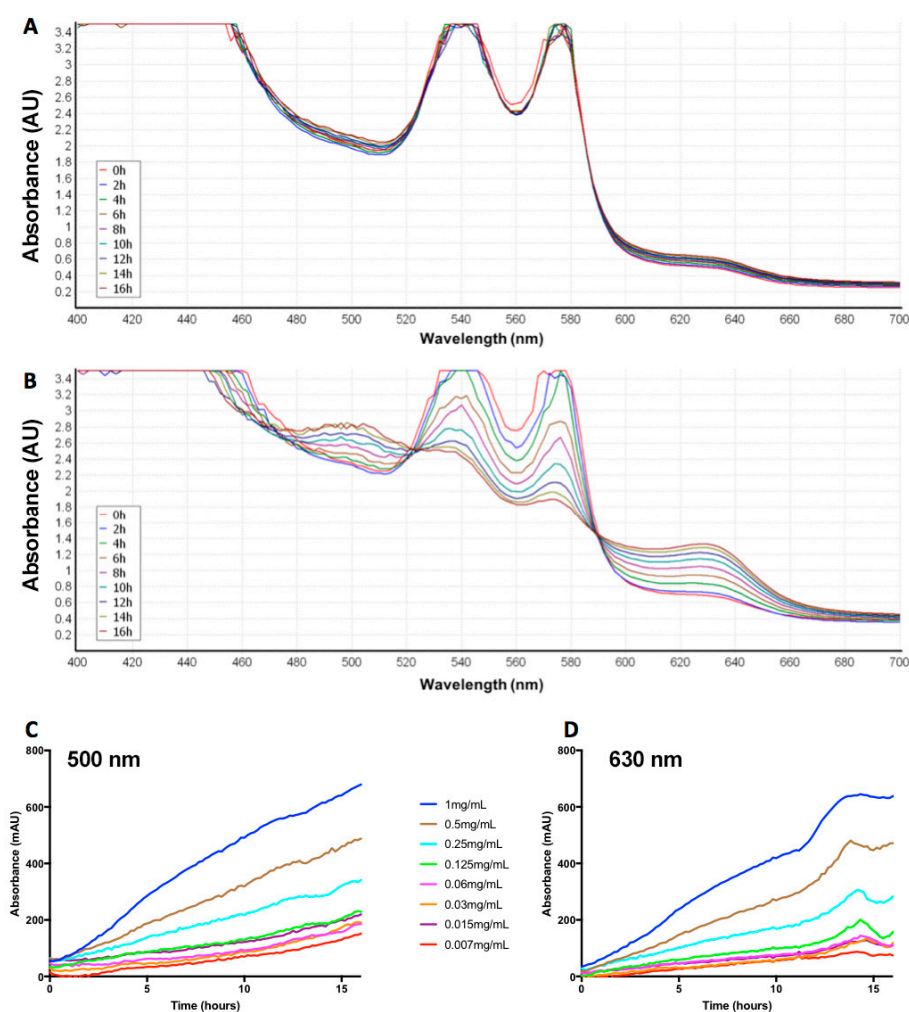


Figure 2. Time- and concentration-dependent changes in absorbance for MetHb over 16 h. Ovine Hb was incubated with a control (PBS) (A) or *N. nigricollis* venom (10 mg/mL to achieve maximum MetHb production) (B) at 37 °C in a plate reader (PHERAStar, BMG Labtech). The absorbance between 400 nm and 700 nm was measured every 2 h. The peaks typical of oxygenated Hb are at 540 nm and 570 nm, and those of MetHb are at 500 nm and 630 nm. Furthermore, the *N. nigricollis* venom was serially diluted from 1 mg/mL to 0.007 mg/mL and mixed with an equal volume of ovine Hb. It was then incubated for 16 h at 37 °C in a plate reader (FLUOStar Optima, BMG Labtech) and the absorbance was measured every 2 h at 500 nm (C) and 630 nm (D). The traces shown are representative of three separate experiments, and they were selected to clearly demonstrate the changes in absorbance for Hb and MetHb over a period of 16 h.

2.3. Heat-Denaturation of *N. nigricollis* Venom Reduces Its Effect on MetHb Production

In order to determine whether the ability of *N. nigricollis* venom on MetHb production is dependent on proteins, this venom was heat-denatured prior to using in the assay. The venom was incubated at two different temperatures, 65 °C and 95 °C for 10 min and then cooled to room temperature prior to use in the assay with ovine Hb. Notably, the heat-denatured venom exhibited significantly reduced MetHb production at 16 h (Figure 3A). This data suggest that MetHb production may be mediated through proteins that are present in the venoms and they are sensitive to heat denaturation.

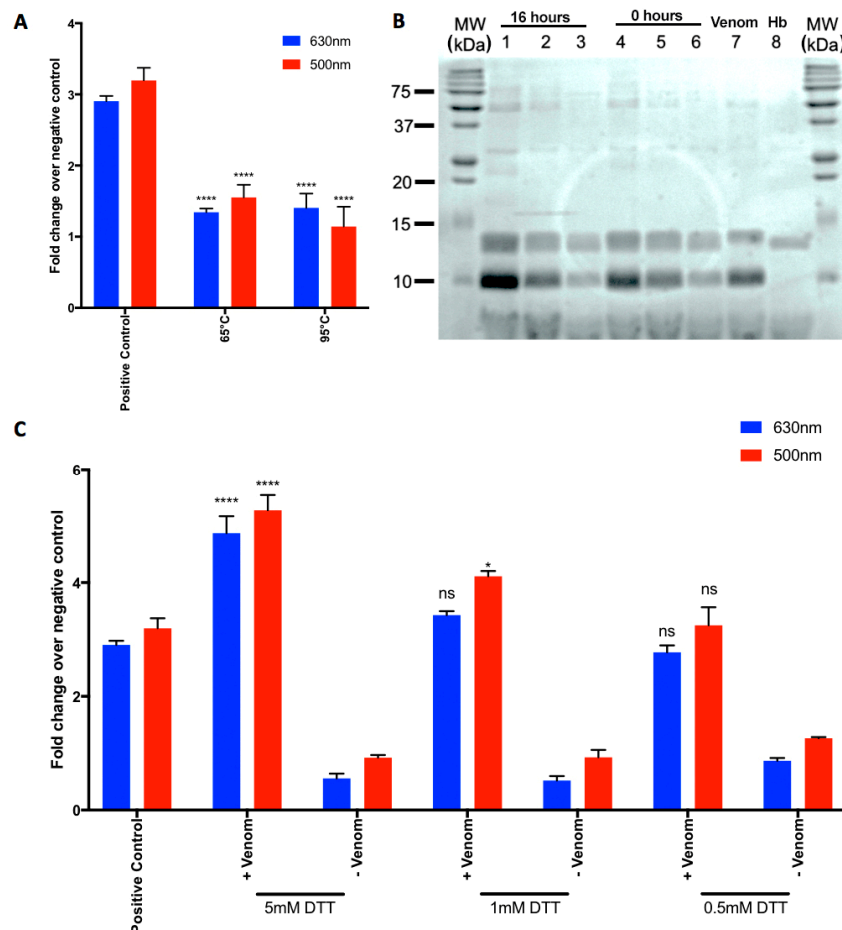


Figure 3. Effect of heat, proteolytic activity of venom and a reducing agent (DTT) on MetHb production. (A) *N. nigricollis* venom was heat treated at 65 °C or 95 °C for 10 min prior to cooling the venom to room temperature and mixing with ovine Hb. The level of absorbance at 500 nm and 630 nm was measured after 16 h. (B) SDS-PAGE (Coomassie stained) gel showing the protein profile of Hb before (as a control) and after incubation with different concentrations of *N. nigricollis* venom for 16 h. Lanes, MW—molecular weight marker, Lane 1 and 4: Venom (12 µg) + haemoglobin (3 µg). Lane 2 and 5: Venom (6 µg) + haemoglobin (3 µg). Lane 3 and 6: Venom (3 µg) + haemoglobin (3 µg). Lanes 1-3; after 16 h incubation and lanes 4-6; as controls at 0 h. Lane 7: *N. nigricollis* venom (3 µg) alone and Lane 8: Hb (3 µg) alone. The image shown is representative of three separate experiments. (C) *N. nigricollis* venom was treated with various concentrations (0.5 mM, 1 mM or 5 mM) of reducing agent, DTT for 10 min prior to mixing with ovine Hb and incubating for another 16 h. The level of absorbance was measured as shown above. Data represent mean \pm SEM ($n = 3$). The p values shown were as calculated by two-way ANOVA followed by post-hoc Tukey's test using GraphPad Prism 7 (* $p < 0.05$, ** $p < 0.01$, *** $p < 0.001$ and **** $p < 0.0001$). The heated (A) or DTT (C)-treated samples were all compared with the respective positive controls (untreated venom), and the negative control used was PBS.

2.4. *N. nigricollis* Venom Does Not Exert Direct Proteolytic Activity on Hb

To determine whether the MetHb production occurs due to proteolytic actions of *N. nigricollis* venom on Hb, different concentrations of the venom were incubated with 3 µg Hb overnight along with controls, and these samples were analysed by SDS-PAGE. As shown in Figure 3B, the venom does not have any direct proteolytic activity on Hb as the bands for this protein are intact and unaffected by increasing concentrations of venom over 16 h compared to the controls. These data suggest that *N. nigricollis* venom-induced effects on MetHb production are not dependent on direct proteolytic actions of this venom on Hb, although we cannot rule out the possibilities of the effects of this venom on other components that regulate MetHb production.

2.5. A Reducing Agent Increases the *N. nigricollis* Venom-Induced MetHb Production

To assess the impact of a reducing agent on the *N. nigricollis* venom-induced production of MetHb, 1,4-dithiothreitol (DTT) was used in the assay. The venom was pre-treated with different concentrations of DTT [we chose a range of concentrations (low to high) including 0.5 mM, 1 mM and 5 mM in order to analyse the maximum impact of this reducing agent on venom-induced MetHb production] and then incubated with ovine Hb. The presence of DTT failed to prevent the oxidation of Hb, and indeed increased the production of MetHb at the highest concentration (5 mM), although at lower concentrations this increase was not significant (Figure 3C). These data suggest that venom-induced MetHb production is not diminished by reducing agents such as DTT.

3. Discussion

The proteins found within the snake venoms have a multitude of pharmacological actions including direct effects on cells. These include cell lysis or blockade of their functions via binding to a range of receptors and ion channels. They also affect the blood coagulation cascade that is required for effective haemostasis and the cholinergic disruptions to nerve transmission [27,28]. Moreover, a number of snake venoms have been reported to induce direct haemolysis and lead to ischemia [29,30]. In this study, we have investigated the effects of a selection of snake venoms on the oxidation of Hb. Most of the snake venoms tested caused at least a minor increase of absorbance at the selected wavelength maxima for MetHb, although the elapids' absorption generally increased to a much lesser extent than the vipers. Despite this, compared to the other viper and elapid venoms, the largest shift observed was for the venom of an elapid, *N. nigricollis*.

In a previous study [21], *Naja naja* (Indian Cobra) venom was found to have a greater ability to produce MetHb than two other Indian vipers (*Echis carinatus* and *Daboia russelii*). Those results are inconsistent with the findings from this study where many of the viper venoms including *Echis carinatus* had more pronounced effects than *Naja naja* venom. Although the reasons for these discrepancies are not entirely clear, they have used human whole blood in their experiments, whereas we have used ovine Hb. Therefore, their experiments may relate more to the ability of venoms to lyse RBCs (as Hb would be much more accessible after lysis) than to directly oxidise Hb. We can postulate that single or multiple venom components may act either directly on Hb or potentially on MetHb reductase to prevent the equilibrium found under healthy natural conditions. A schematic diagram of our working hypothetical model of the impact of venom components on the production of MetHb is shown in Figure 4.

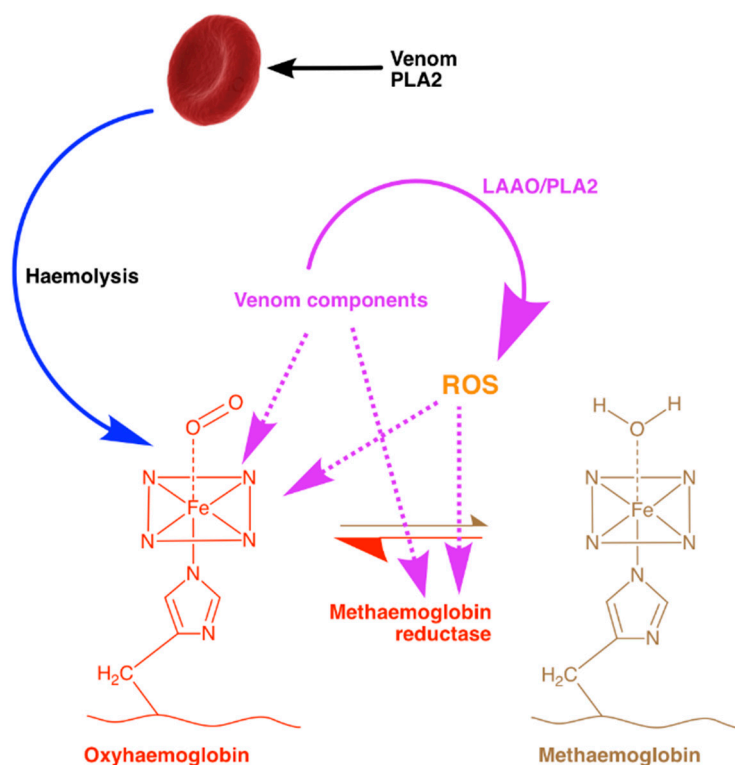


Figure 4. A schematic diagram hypothesising the impact of venom on MetHb production. Haemolysis (the lysing of RBCs) by phospholipase A2 (PLA2) and other venom components is a common effect of snakebite envenoming. In a healthy human, the oxidation of Hb to MetHb is constantly combated by an enzyme, MetHb reductase. After certain venomous snakebites, this equilibrium is shifted in favour of MetHb, a toxic species that is also known to be pro-inflammatory. This shift may be a result of the ROS, which is generated as a metabolite of L-amino acid deamination [via L-amino acid oxidases (LAAO)] or lipid peroxidation (via PLA2) present in various venoms. The potential mechanisms for venom-induced changes in MetHb production are shown in the figure as dotted magenta lines.

A previous study using *Crotalus molossus nigrescens* venom reported that high concentrations of this venom cause some level of proteolytic degradation to Hb [26]. The same study postulated that the venom's conversion of Hb to MetHb is due to the oxidative stress induced by H_2O_2 which is produced by venom LAAO [26]. It may be possible that following this, H_2O_2 then reacts with the ferrous Hb producing further reactive species via the Fenton reaction [31]. However, *N. nigricollis* is a snake with potentially cytotoxic venom that lacks LAAOs and is composed largely of three-finger toxins (73.3%) and PLA2 (21.9%) [32]. These proteins typically bind to cell membrane components or directly affect the phospholipid bilayer which leads to cell lysis, although they have not been documented interacting directly with Hb. The lack of LAAO and the abundance of PLA2 in *N. nigricollis* venom supports the theory that the phospholipase activity could be indirectly causing this effect as a result of its oxidative product, arachidonic acid. However, members of the genus *Agkistrodon* screened for their Hb oxidising ability (Figure 1) were found to have little or no effects on Hb despite having a high percentage (31–46%) of PLA2 [33], more than half of which are enzymatic [34]. There is a very small percentage of group III metalloproteases (2.4%) and cysteine-rich secretory proteins (CRiSPs) (0.2%) found in *N. nigricollis* venom [32], components that are also found in viper venoms and are more typically associated with this oxidative effect. The metalloproteases cause multiple pathologies which contribute to oxidative stress including haemorrhage, thereby inducing spontaneous haemolysis, liberating Hb and free iron. Metalloproteases are also able to induce necrosis [35], releasing myoglobin which has implications on the redox balance. After the degradation of the extra-cellular matrix by metalloproteases, damage-associated molecular patterns

(DAMPs) are likely to be released, and these can induce further oxidative stress and inflammation [25]. Given the lack of proteases in *N. nigricollis* venom, the highly cytotoxic PLA₂ found in this venom is more likely to be the primary cause of this oxidation. Hydrolysis of the sn-2 acyl bond of plasma membrane glycerophospholipids by PLA₂ releases free fatty acids such as arachidonic acid as well as lysophospholipids and lysophosphatidylcholine, and potentially toxic, ROS [25]. The increase in polyunsaturated fatty acids has also been postulated to cause an increase in lipid peroxidation following administration of a viper (*Echis carinatus*) venom, and it may be possible that similar peroxidation takes place as a result of *N. nigricollis* venom.

The time- (Figure 2A,B) and concentration- (Figure 2C,D) dependent shift in the absorbance of Hb/MetHb by *N. nigricollis* venom demonstrates that the components of this venom are able to promote the oxidation of Hb. The increase in MetHb production observed over 16 h and at higher venom concentrations suggests that this effect may increase over time in snakebite victims, and is dependent on the volume of venom injected by the snake. The increase in MetHb production observed with the venom that was treated with the highest concentration of DTT suggests that this effect is actually improved by the addition of a redox reagent. However, at lower concentrations of DTT, this increase was not observed. We originally hypothesised that the addition of a redox reagent such as DTT would prevent the production of ROS, and consequently MetHb by taking the place of antioxidants such as glutathione found naturally in the plasma [36]. The thiol groups of glutathione act as reducing agents in order to prevent the damage to cellular components by ROS. Therefore, the surprising increase in MetHb production with the highest concentration of DTT could be due to the reduction of the tetrameric structure of Hb and consequently, its enhanced oxidation. The decrease in activity seen with heat treatment of venom provides evidence to suggest that this effect may be due to the proteins present in the venom. The incubation of venom with purified bovine Hb and further analysis suggest that this effect is not a result of proteolytic degradation of the Hb. However, the results of a previous study using a protease-rich viper venom show that high venom concentrations can lead to proteolytic degradation of Hb. The SDS-PAGE presented here suffers from large protein bands (~16 kDa) in the crude venom overlapping with the Hb monomer (16.1 kDa), although it is clear that Hb is still present. Further investigation using non-reducing or native protein electrophoresis is required to ascertain if there is any degree of proteolysis with *N. nigricollis* venom on Hb and to further scrutinise the mechanism of action of this venom on MetHb production.

Venom-induced neurological and coagulation pathologies have long been the two major areas of interest for scientists to investigate snakebite pathophysiology due to their prominence as the most immediately life-threatening aspects of a snakebite. However, the morbidity is gaining interest recently as estimates of as many as 15,000 people annually suffering amputations as a result of snakebites in sub-Saharan Africa alone [37]. Hence, the disability adjusted life years (DALYs) and loss to any snakebite-afflicted region's work force are of serious importance. ASV is currently the only therapy for snakebite envenoming [4], and while it is effective in saving lives when administered appropriately, it frequently fails to address some of the long-term damage induced by snake venom components. This includes myotoxicity and skeletal muscle damage [38,39] as well as oxidative stress [25], which puts undue pressure on the body that is already suffering from an array of potentially fatal venom-induced health consequences. Following haemolysis caused either directly by the lysis of RBCs or as a result of ROS produced by venom components, Hb levels are elevated in the blood. As a result, this reduces the oxygen-carrying ability of the blood and decreases its ability to meet the oxygen demand of vital organs. Furthermore, the elevated levels of Hb cause a reduction in free-haptoglobin levels and can overwhelm the mononuclear phagocytic system, the spleen and eventually the kidneys, which may lead to acute kidney injury [40]. The additional complication of conversion to MetHb could potentially allow this toxic Hb species to build up and affect the efficiency of the systems in place to reduce free Hb. These complications to the blood would then undoubtedly have further effects on haemostasis and exacerbate existing ischaemic areas, contributing in turn to tissue damage, necrosis and long-term damage from snakebites.

In conclusion, we have demonstrated that a wide variety of venoms possess Hb-modifying activity among a range of viper and elapid snakes. From the venoms tested, we have observed a significantly higher activity for *N. nigricollis* venom for the production of MetHb. This effect is likely to be a result of proteins present in the venom, although further fractionation and characterisation is required to identify the exact proteins causing these changes. Moreover, most of the experiments performed in this study used ovine Hb due to availability. However, future experiments will be performed using human RBCs and Hb. The clinical significance of venoms on MetHb production and its contribution to envenomation will also be determined in the future. The work highlighting co-administration of melatonin with ASV is worth pursuing further [21], and the use of antioxidants in vivo could potentially be developed further to ascertain whether the oxidative stress can be reduced using flavonoids and their derivatives [41]. Although it may be a less important effect of snakebite envenomation than the immediately life-threatening elements, the reduction of oxidative stress on internal organs and tissues following a snakebite is likely to improve recovery and potentially reduce some of the long-term damage and morbidity as a result.

4. Materials and Methods

4.1. Materials

The cardiovascular targeted-venom discovery array (Catalogue code: T-VDA^{CV}) of whole snake venoms was from Venomtech Limited (Sandwich, UK) and ovine blood was obtained from Envigo (UK) Ltd. (Oxon, UK). Clear 96- and 384-well plates were purchased from Greiner (Gloucestershire, UK), and DTT, purified bovine Hb, and all other chemicals were from Sigma Aldrich (Dorset, UK).

4.2. Ovine RBC Lysis and Hb Production

Ovine blood was lysed by the addition of two volumes of ultrapure water followed by centrifugation ($5000\times g$), and the clear supernatant was collected and used in further assays as ovine Hb. Although this supernatant is likely to have other components from RBCs, the presence of a prominent Hb band was confirmed by SDS-PAGE prior to using this as a Hb source in further functional assays.

4.3. Screening of Venoms for MetHb Producing Activity

The whole snake venoms from the T-VDA^{CV} array were diluted in $1\times$ PBS (Fisher Scientific, Loughborough, UK) (0.2 mg/mL) and mixed with an equal volume of ovine Hb (diluted 1:2 in $1\times$ PBS) with a final assay volume of 100 μ L in a 96-well micro titre plate. These samples were then incubated at 37 °C and the absorbance at 500 nm and 630 nm was measured at 16 h by spectrofluorimetry (FLUOstar Optima, BMG Labtech, Aylesbury, UK).

4.4. Time- and Concentration-Dependent Effect of *N. nigricollis* Venom on MetHb Production

Ovine Hb diluted (1:2) in $1\times$ PBS was incubated with *N. nigricollis* venom (at 10 mg/mL or a range of concentrations between 1 mg/mL and 0.007 mg/mL) or PBS (a negative control) in a 384-well plate. Plates were incubated at 37 °C in a plate reader (PHERAStar, BMG Labtech, Aylesbury, UK) and the absorbance spectrum between 400 nm and 700 nm was measured at 2-h intervals over 16 h. After this time, maximum Hb oxidation appeared to be reached, and therefore, this time point was chosen for other experiments in this study. Moreover, to determine the impact of heat and a reducing agent, venom was heat-treated (65 °C or 95 °C in a dry bath) or treated with a reducing agent, DTT (0.5 mM, 1 mM or 5 mM) prior to using them in assays. The temperatures (65 °C or 95 °C) were determined based on our previous experience in denaturing venom proteins and using them in functional assays. DTT was specifically selected as this is a less toxic and volatile compared to β -mercaptoethanol; moreover, DTT prevents the reoxidation of disulfide bonds in proteins.

4.5. Sodium Dodecyl Sulfate-Polyacrylamide (SDS-PAGE) Gel Electrophoresis

The SDS-PAGE analysis was performed according to standard procedures as described previously [42]. The samples were taken before and after incubating a range of concentrations of venom with purified bovine Hb (Sigma Aldrich, Dorset, UK) at 37 °C for 16 h. Samples taken prior to 16-h incubation were used as controls to compare the impact of venom on Hb before and after the incubation. These samples were mixed with reducing sample treatment buffer (Bio-Rad, Watford, UK) and run on a pre-made (Bio-Rad, Watford, UK) 10% SDS-PAGE gel for 40 min at 150 constant volts. Gels were then stained with Coomassie brilliant blue (Bio-Rad, Watford, UK) for approximately 1 h on a rocker, before destaining overnight (10% acetic acid/10% methanol/80% H₂O).

4.6. Statistical Analysis

All statistical analyses were performed using GraphPad Prism 7. *p*-Values were calculated using one-way or two-way ANOVA followed by Tukey's post-hoc multiple comparisons test.

Author Contributions: Conceptualization, P.H., S.T. and S.V.; Data Curation, H.F.W., P.H., D.R., A.B., H.J.L., L.C. and C.W.; Formal Analysis, H.F.W., D.R., H.J.L. and S.V.; Investigation, P.H., A.B., L.C. and C.W.; Methodology, S.T.; Software, S.V.; Supervision, A.B.B., S.T. and S.V.; Writing-Original Draft, H.W., S.T. and S.V.; Writing-Review & Editing, H.F.W., P.H., A.B.B., S.T. and S.V.

Funding: This research received no external funding.

Acknowledgments: The authors would like to thank the British Heart Foundation for their funding support for author, Divyashree Ravishankar.

Conflicts of Interest: The authors declare no conflict of interest.

References

1. Kasturiratne, A.; Wickremasinghe, A.R.; de Silva, N.; Gunawardena, N.K.; Pathmeswaran, A.; Premaratna, R.; Savioli, L.; Lalloo, D.G.; de Silva, H.J. The global burden of snakebite: A literature analysis and modelling based on regional estimates of envenoming and deaths. *PLoS Med.* **2008**, *5*, e218. [[CrossRef](#)] [[PubMed](#)]
2. Williams, H.F.; Vaiyapuri, R.; Gajjeraman, P.; Hutchinson, G.; Gibbins, J.M.; Bicknell, A.B.; Vaiyapuri, S. Challenges in diagnosing and treating snakebites in a rural population of Tamil Nadu, India: The views of clinicians. *Toxicon* **2017**, *130*, 44–46. [[CrossRef](#)] [[PubMed](#)]
3. Vaiyapuri, S.; Vaiyapuri, R.; Ashokan, R.; Ramasamy, K.; Nattamaisundar, K.; Jeyaraj, A.; Chandran, V.; Gajjeraman, P.; Baksh, M.F.; Gibbins, J.M. Snakebite and its socio-economic impact on the rural population of Tamil Nadu, India. *PLoS ONE* **2013**, *8*, e80090. [[CrossRef](#)] [[PubMed](#)]
4. Gutiérrez, J.M.; Calvete, J.J.; Habib, A.G.; Harrison, R.A.; Williams, D.J.; Warrell, D.A. Snakebite envenoming. *Nat. Rev. Dis. Primers* **2017**, *3*, 17063. [[CrossRef](#)] [[PubMed](#)]
5. Warrell, D.A. Snake bite. *Lancet* **2010**, *375*, 77–88. [[CrossRef](#)]
6. Yamazaki, Y.; Morita, T. Snake venom components affecting blood coagulation and the vascular system: Structural similarities and marked diversity. *Curr. Pharm. Des.* **2007**, *13*, 2872–2886. [[CrossRef](#)] [[PubMed](#)]
7. Markland, F.S., Jr.; Swenson, S. Snake venom metalloproteinases. *Toxicon* **2013**, *62*, 3–18. [[CrossRef](#)]
8. Herrera, C.; Escalante, T.; Voisin, M.-B.; Rucavado, A.; Morazán, D.; Macêdo, J.K.A.; Calvete, J.J.; Sanz, L.; Nourshargh, S.; Gutiérrez, J.M. Tissue localization and extracellular matrix degradation by PI, PII and PIII snake venom metalloproteinases: Clues on the mechanisms of venom-induced hemorrhage. *PLoS Negl. Trop. Dis.* **2015**, *9*, e0003731. [[CrossRef](#)]
9. de Queiroz, M.R.; de Sousa, B.B.; da Cunha Pereira, D.F.; Mamede, C.C.N.; Matias, M.S.; de Moraes, N.C.G.; de Oliveira Costa, J.; de Oliveira, F. The role of platelets in hemostasis and the effects of snake venom toxins on platelet function. *Toxicon* **2017**, *133*, 33–47. [[CrossRef](#)]
10. Vaiyapuri, S.; Roweth, H.; Ali, M.S.; Unsworth, A.J.; Stainer, A.R.; Flora, G.D.; Crescente, M.; Jones, C.I.; Moraes, L.A.; Gibbins, J.M. Pharmacological actions of nobletin in the modulation of platelet function. *Br. J. Pharmacol.* **2015**, *172*, 4133–4145. [[CrossRef](#)]

11. Vaiyapuri, S.; Hutchinson, E.G.; Ali, M.S.; Dannoura, A.; Stanley, R.G.; Harrison, R.A.; Bicknell, A.B.; Gibbins, J.M. Rhinocetin, a venom-derived integrin-specific antagonist inhibits collagen-induced platelet and endothelial cell functions. *J. Biol. Chem.* **2012**, *287*, 26235–26244. [[CrossRef](#)] [[PubMed](#)]
12. Kini, R.M.; Koh, C.Y. Metalloproteases affecting blood coagulation, fibrinolysis and platelet aggregation from snake venoms: Definition and nomenclature of interaction sites. *Toxins* **2016**, *8*, 284. [[CrossRef](#)] [[PubMed](#)]
13. Donghui, M.; Armugam, A.; Jeyaseelan, K. Cytotoxic potency of cardiotoxin from naja sputatrix: Development of a new cytolytic assay. *Biochem. J.* **2002**, *366*, 35–43.
14. Gillissen, A.; Theakston, R.D.G.; Barth, J.; May, B.; Krieg, M.; Warrell, D.A. Neurotoxicity, haemostatic disturbances and haemolytic anaemia after a bite by a tunisian saw-scaled or carpet viper (echis 'pyramidum'-complex): Failure of antivenom treatment. *Toxicon* **1994**, *32*, 937–944. [[CrossRef](#)]
15. Santhosh, M.S.; Sundaram, M.S.; Sunitha, K.; Kemparaju, K.; Girish, K.S. Viper venom-induced oxidative stress and activation of inflammatory cytokines: A therapeutic approach for overlooked issues of snakebite management. *Inflamm. Res.* **2013**, *62*, 721–731. [[CrossRef](#)] [[PubMed](#)]
16. Katkar, G.D.; Sundaram, M.S.; Hemshekhar, M.; Sharma, D.R.; Santhosh, M.S.; Sunitha, K.; Rangappa, K.S.; Girish, K.S.; Kemparaju, K. Melatonin alleviates echis carinatus venom-induced toxicities by modulating inflammatory mediators and oxidative stress. *J. Pineal. Res.* **2014**, *56*, 295–312. [[CrossRef](#)] [[PubMed](#)]
17. Sebastin Santhosh, M.; Hemshekhar, M.; Thushara, R.M.; Devaraja, S.; Kemparaju, K.; Girish, K.S. Vipera russelli venom-induced oxidative stress and hematological alterations: Amelioration by crocin a dietary colorant. *Cell Biochem. Funct.* **2013**, *31*, 41–50. [[CrossRef](#)]
18. Rother, R.P.; Bell, L.; Hillmen, P.; Gladwin, M.T. The clinical sequelae of intravascular hemolysis and extracellular plasma hemoglobin: A novel mechanism of human disease. *JAMA* **2005**, *293*, 1653–1662. [[CrossRef](#)]
19. Mebius, R.E.; Kraal, G. Structure and function of the spleen. *Nat. Rev. Immunol.* **2005**, *5*, 606. [[CrossRef](#)]
20. Alves, E.C.; Sachett, J.D.A.G.; Sampaio, V.S.; Sousa, J.D.D.B.; Oliveira, S.S.D.; Nascimento, E.F.D.; Santos, A.D.S.; da Silva, I.M.; da Silva, A.M.M.; Wen, F.H.; et al. Predicting acute renal failure in bothrops snakebite patients in a tertiary reference center, western brazilian amazon. *PLoS ONE* **2018**, *13*, e0202361. [[CrossRef](#)]
21. Sharma, R.D.; Katkar, G.D.; Sundaram, M.S.; Paul, M.; NaveenKumar, S.K.; Swethakumar, B.; Hemshekhar, M.; Girish, K.S.; Kemparaju, K. Oxidative stress-induced methemoglobinemia is the silent killer during snakebite: A novel and strategic neutralization by melatonin. *J. Pineal Res.* **2015**, *59*, 240–254. [[CrossRef](#)] [[PubMed](#)]
22. Costa, T.R.; Burin, S.M.; Menaldo, D.L.; de Castro, F.A.; Sampaio, S.V. Snake venom L-amino acid oxidases: An overview on their antitumor effects. *J. Venom. Anim. Toxins* **2014**, *20*, 23. [[CrossRef](#)] [[PubMed](#)]
23. Lim, S.-K.; Ferraro, B.; Moore, K.; Halliwell, B. Role of haptoglobin in free hemoglobin metabolism. *Redox Rep.* **2001**, *6*, 219–227. [[CrossRef](#)]
24. Moseley, M.J.; Oenning, V.; Melnik, G. Methemoglobinemia. *AJN* **1999**, *99*, 47. [[CrossRef](#)] [[PubMed](#)]
25. Sunitha, K.; Hemshekhar, M.; Thushara, R.; Santhosh, M.S.; Sundaram, M.S.; Kemparaju, K.; Girish, K. Inflammation and oxidative stress in viper bite: An insight within and beyond. *Toxicon* **2015**, *98*, 89–97. [[CrossRef](#)] [[PubMed](#)]
26. Meléndez-Martínez, D.; Muñoz, J.M.; Barraza-Garza, G.; Cruz-Peréz, M.S.; Gatica-Colima, A.; Alvarez-Parrilla, E.; Plenge-Tellechea, L.F. Rattlesnake crotalus molossus nigrescens venom induces oxidative stress on human erythrocytes. *J. Venom. Anim. Toxins* **2017**, *23*, 24. [[CrossRef](#)]
27. Mackessy, S.P. *Handbook of Venoms and Toxins of Reptiles*; CRC Press: Boca Raton, FL, USA, 2010.
28. Fry, B.G. *Venomous Reptiles and Their Toxins: Evolution, Pathophysiology and Biodiscovery*; Oxford University Press: New York, NY, USA, 2015.
29. Fernandez, M.L.; Quartino, P.Y.; Arce-Bejarano, R.; Fernandez, J.; Camacho, L.F.; Gutierrez, J.M.; Kuemmel, D.; Fidelio, G.; Lomonte, B. Intravascular hemolysis induced by phospholipases a2 from the venom of the eastern coral snake, micrurus fulvius: Functional profiles of hemolytic and non-hemolytic isoforms. *Toxicol. Lett.* **2018**, *286*, 39–47. [[CrossRef](#)]
30. Lenske, E.; Padula, A.M.; Leister, E.; Boyd, S. Severe haemolysis and spherocytosis in a dog envenomed by a red-bellied black snake (pseudechis porphyriacus) and successful treatment with a bivalent whole equine igg antivenom and blood transfusion. *Toxicon* **2018**, *151*, 79–83. [[CrossRef](#)]
31. Winterbourn, C.C. Toxicity of iron and hydrogen peroxide: The fenton reaction. *Toxicol. Lett.* **1995**, *82*, 969–974. [[CrossRef](#)]

32. Petras, D.; Sanz, L.; Segura, Á.; Herrera, M.; Villalta, M.; Solano, D.; Vargas, M.; León, G.; Warrell, D.A.; Theakston, R.D.G. Snake venomomics of african spitting cobras: Toxin composition and assessment of congeneric cross-reactivity of the pan-african echitab-plus-icp antivenom by antivenomics and neutralization approaches. *J. Proteome Res.* **2011**, *10*, 1266–1280. [[CrossRef](#)]
33. Lomonte, B.; Tsai, W.-C.; Ureña-Díaz, J.M.; Sanz, L.; Mora-Obando, D.; Sánchez, E.E.; Fry, B.G.; Gutiérrez, J.M.; Gibbs, H.L.; Sovic, M.G.; et al. Venomomics of new world pit vipers: Genus-wide comparisons of venom proteomes across agkistrodon. *J. Proteomics* **2014**, *96*, 103–116. [[CrossRef](#)] [[PubMed](#)]
34. Jia, Y.; Ermolinsky, B.; Garza, A.; Provenzano, D. Phospholipase A₂ in the venom of three cottonmouth snakes. *Toxicon* **2017**, *135*, 84–92. [[CrossRef](#)] [[PubMed](#)]
35. Gutiérrez, J.M.A.; Romero, M.; Núñez, J.; Chaves, F.; Borkow, G.; Ovadia, M. Skeletal muscle necrosis and regeneration after injection of BaH1, a hemorrhagic metalloproteinase isolated from the venom of the snake *Bothrops asper* (Terciopelo). *Exp. Mol. Pathol.* **1995**, *62*, 28–41. [[CrossRef](#)] [[PubMed](#)]
36. Finkel, T.; Holbrook, N.J. Oxidants, oxidative stress and the biology of ageing. *Nature* **2000**, *408*, 239. [[CrossRef](#)] [[PubMed](#)]
37. Chippaux, J.-P. Estimate of the burden of snakebites in sub-saharan africa: A meta-analytic approach. *Toxicon* **2011**, *57*, 586–599. [[CrossRef](#)]
38. Gutiérrez, J.M.; León, G.; Rojas, G.; Lomonte, B.; Rucavado, A.; Chaves, F. Neutralization of local tissue damage induced by *bothrops asper* (Terciopelo) snake venom. *Toxicon* **1998**, *36*, 1529–1538. [[CrossRef](#)]
39. Jayawardana, S.; Gnanathasan, A.; Arambepola, C.; Chang, T. Chronic musculoskeletal disabilities following snake envenoming in sri lanka: A population-based study. *PLoS Negl. Trop. Dis.* **2016**, *10*, e0005103. [[CrossRef](#)]
40. Kumar, K.G.S.; Narayanan, S.; Udayabhaskaran, V.; Thulaseedharan, N.K. Clinical and epidemiologic profile and predictors of outcome of poisonous snake bites – an analysis of 1,500 cases from a tertiary care center in malabar, north kerala, india. *Int. J. General Med.* **2018**, *11*, 209–216. [[CrossRef](#)]
41. Sachetto, A.T.A.; Rosa, J.G.; Santoro, M.L. Rutin (quercetin-3-rutinoside) modulates the hemostatic disturbances and redox imbalance induced by *bothrops jararaca* snake venom in mice. *PLoS Negl. Trop. Dis.* **2018**, *12*, e0006774. [[CrossRef](#)]
42. Vaiyapuri, S.; Harrison, R.A.; Bicknell, A.B.; Gibbins, J.M.; Hutchinson, G. Purification and functional characterisation of rhinocerase, a novel serine protease from the venom of *bitis gabonica* rhinoceros. *PLoS ONE* **2010**, *5*, e9687. [[CrossRef](#)]



© 2018 by the authors. Licensee MDPI, Basel, Switzerland. This article is an open access article distributed under the terms and conditions of the Creative Commons Attribution (CC BY) license (<http://creativecommons.org/licenses/by/4.0/>).

4.2 Mechanisms underpinning the permanent muscle damage induced by snake venom metalloprotease

Harry F. Williams^{*1}, Ben A. Mellows^{*2}, Robert Mitchell^{*2}, Peggy Syfri³, Harry J. Layfield, Maryam Salamah, Rajendran Vaiyapuri⁴, Henry Collins-Hooper², Andrew B. Bicknell², Antonios Matsakas³, Ketan Patel^{2*} and Sakthivel Vaiyapuri¹

¹School of Pharmacy, University of Reading, Reading, United Kingdom

²School of Biological Sciences, University of Reading, Reading, United Kingdom

³Molecular Physiology Laboratory, Centre for Atherothrombotic and Metabolic Disease, Hull York Medical School, Hull, United Kingdom

⁴School of Pharmacy, University of Reading Malaysia, Johor, Malaysia

PLoS Neglected Tropical Diseases 2019 - Open Access

Conclusion of this chapter

In bites from most vipers as well as a large number of elapids, extensive tissue damage surrounding the bite site is common. This is frequently due to the action of snake venom metalloproteases which are not only haemorrhagic, but also attack the basement membrane surrounding myofibres causing long lasting damage. This is due largely to the destruction of the basement membrane, attenuating the properties of satellite cells, which are essential to effective muscle regeneration. The hypoxia caused by ischaemia from haemorrhaging, combined with potential oxidative stress from methaemoglobin production then exacerbate the effects of basement membrane degradation on satellite cell functionality. Small molecular therapeutics have been proposed as means of mitigating the local tissue damage by inhibition or chelation of the snake venom metalloproteases. However, the use of non-specific compounds which also inhibit endogenous proteins means proper diagnosis and ascertaining the requirement of such treatments is essential. This will ensure the envenoming involved an SVMP-containing venom and prevent the associated adverse effects in cases of dry-bites or bites from species without SVMP-containing venoms.

Contribution to this chapter

General contribution (65%)

- Performance of experiments and data collection
- Analysis and interpretation of data
- Writing of the manuscript
- Preparation of the figures

Experimental contribution

Figure 1 A-G Purified protein, carried out SDS-PAGE, prepared sample for mass spectrometry, prepared figures

Figure 2 A-E Carried out all functional assays, analysed data, prepared figures

Figure 4 A-W Carried out cryosectioning, H&E, immunostaining for IgG/MYH3 and imaging for day 5 and control treatments

Figure 5 A-R Carried out cryosectioning, immunostaining for collagen IV, production of CAMP antibodies

Figure 6 A-H Isolated myofibres, immunostaining, imaging and analysis of cells, clusters, differentiation and proliferation

RESEARCH ARTICLE

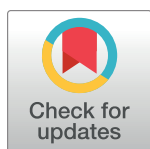
Mechanisms underpinning the permanent muscle damage induced by snake venom metalloprotease

Harry F. Williams¹ , Ben A. Mellows² , Robert Mitchell² , Peggy Sfyri³, Harry J. Layfield¹, Maryam Salamah¹, Rajendran Vaiyapuri⁴, Henry Collins-Hooper², Andrew B. Bicknell², Antonios Matsakas³, Ketan Patel^{2*} , Sakthivel Vaiyapuri^{1*} 

1 School of Pharmacy, University of Reading, Reading, United Kingdom, **2** School of Biological Sciences, University of Reading, Reading, United Kingdom, **3** Molecular Physiology Laboratory, Centre for Atherothrombotic and Metabolic Disease, Hull York Medical School, Hull, United Kingdom, **4** School of Pharmacy, University of Reading Malaysia, Johor, Malaysia

 These authors contributed equally to this work.

* ketan.patel@reading.ac.uk (KP); s.vaiyapuri@reading.ac.uk (SV)



OPEN ACCESS

Citation: Williams HF, Mellows BA, Mitchell R, Sfyri P, Layfield HJ, Salamah M, et al. (2019) Mechanisms underpinning the permanent muscle damage induced by snake venom metalloprotease. PLoS Negl Trop Dis 13(1): e0007041. <https://doi.org/10.1371/journal.pntd.0007041>

Editor: Ana M. Moura-da-Silva, Instituto Butantan, BRAZIL

Received: September 19, 2018

Accepted: November 30, 2018

Published: January 29, 2019

Copyright: © 2019 Williams et al. This is an open access article distributed under the terms of the [Creative Commons Attribution License](https://creativecommons.org/licenses/by/4.0/), which permits unrestricted use, distribution, and reproduction in any medium, provided the original author and source are credited.

Data Availability Statement: All the raw data used in this paper are available from Zenodo (URL: <https://zenodo.org/record/2271873> and DOI: [10.5281/zenodo.2271873](https://doi.org/10.5281/zenodo.2271873))

Funding: We would like to thank the Biotechnology and Biological Sciences Research Council, BBSRC (Grant number: J016454/1) for their funding support. <https://bbsrc.ukri.org/> The funders had no role in study design, data collection and analysis, decision to publish, or preparation of the manuscript.

Abstract

Snakebite is a major neglected tropical health issue that affects over 5 million people worldwide resulting in around 1.8 million envenomations and 100,000 deaths each year. Snakebite envenomation also causes innumerable morbidities, specifically loss of limbs as a result of excessive tissue/muscle damage. Snake venom metalloproteases (SVMPs) are a predominant component of viper venoms, and are involved in the degradation of basement membrane proteins (particularly collagen) surrounding the tissues around the bite site. Although their collagenolytic properties have been established, the molecular mechanisms through which SVMPs induce permanent muscle damage are poorly understood. Here, we demonstrate the purification and characterisation of an SVMP from a viper (*Crotalus atrox*) venom. Mass spectrometry analysis confirmed that this protein is most likely to be a group III metalloprotease (showing high similarity to VAP2A) and has been referred to as CAMP (*Crotalus atrox* metalloprotease). CAMP displays both collagenolytic and fibrinogenolytic activities and inhibits CRP-XL-induced platelet aggregation. To determine its effects on muscle damage, CAMP was administered into the tibialis anterior muscle of mice and its actions were compared with cardiotoxin I (a three-finger toxin) from an elapid snake (*Naja pallida*) venom. Extensive immunohistochemistry analyses revealed that CAMP significantly damages skeletal muscles by attacking the collagen scaffold and other important basement membrane proteins, and prevents their regeneration through disrupting the functions of satellite cells. In contrast, cardiotoxin I destroys skeletal muscle by damaging the plasma membrane, but does not impact regeneration due to its inability to affect the extracellular matrix. Overall, this study provides novel insights into the mechanisms through which SVMPs induce permanent muscle damage.

Competing interests: The authors have declared that no competing interests exist.

Author summary

Snakebite is a major neglected tropical disease that affects thousands of people in the rural areas of developing countries. As well as the deaths, snakebites result in a significant number of disabilities including permanent loss of limbs that alter the lifestyle of the victims. Snake venom is a mixture of different proteins with diverse functions; one of these major protein groups present in viper venoms are metalloproteases that primarily induce muscle damage. The mechanisms behind the development of snakebite (metalloprotease)-induced permanent muscle damage are poorly studied. Here, we have purified a metalloprotease (CAMP) from the venom of the Western diamondback rattlesnake, and characterised its function in mice. To determine the actions of CAMP in the development of permanent muscle damage, it was injected into the muscle of mice in a parallel comparison with cardiotoxin I (from the venom of the Red spitting cobra). The effects of these proteins on muscle regeneration were analysed at 5 and 10 days after injection. The results demonstrate that through a combination of effects on the structural scaffolds surrounding the tissues, blood vessels and regeneration, CAMP significantly affects the muscles, thereby leading to permanent muscle damage.

Introduction

Snakebite envenomation is a recently reinstated neglected tropical disease [1] that causes around 100,000 deaths annually [2, 3] and innumerable permanent disabilities predominantly on the rural population living in the lower income regions of the world [4–6]. The significant rate of mortality and morbidity occurs due to the difficulties associated with the treatment of snakebites [7], which vary depending on the species [8], geographical location [9], age of the offending snake [10, 11], the quantity of venom injected, correct diagnosis and mode of treatment [12]. Snake venoms contain proteins and small peptides with diverse functional effects [12]. Medically important snakes are generally found in two main families; Elapidae, a family with venoms mainly composed of smaller, neurotoxic proteins such as phospholipase A2 (PLA2) and three finger toxins, and Viperidae, a family with generally larger proteins such as serine and metalloproteases that primarily affect the cardiovascular and musculoskeletal systems. Snake venom serine proteases (SVSPs) mainly cause systemic envenomation effects such as the alteration of blood pressure, activation or inhibition of coagulation factors and degradation of fibrinogen [13, 14]. However, snake venom metalloproteases (SVMPs) primarily induce local envenomation effects such as swelling, necrosis and extensive tissue/muscle damage as well as the activation of certain coagulation factors and degradation of fibrinogen. SVMP-induced muscle damage is often difficult to treat due to the delay in obtaining appropriate medical treatment and poor outcome of anti-snake venom (ASV) treatment in the local tissues [15, 16]. Hence, extensive tissue damage is frequently treated by fasciotomy, a surgical procedure to remove the damaged tissues, cleaning the affected areas followed by skin graft or amputation of affected limbs or fingers when fasciotomy fails to suffice [7]. This results in permanent disabilities for victims, and significantly affects their socio-economic status following snakebites. For example, long term (persisting for over 13 years) musculoskeletal disabilities were found in over 3% of snakebite victims in a rural population of Sri Lanka and of these over 15% had to undergo amputations [17].

Skeletal muscle is composed of myofibres surrounded by the collagen-rich basement membrane. This tissue is imbued with a resident stem cell population called satellite cells (SCs), located under that basement membrane (BM), which are able to regenerate a functional tissue even after extensive damage [18]. The BM plays a key role in muscle repair by orientating the

regenerating myofibres, a process mediated by SCs and acting as a scaffold for fibres to grow parallel to the existing fibres [19]. The majority of the direct myotoxic effects of venoms are attributed to PLA2 [20]. They can induce either local or systemic effects depending on their specificity to muscle cells (systemic effects) or a broader range of cells (local effects) through hydrolysis of phospholipids in plasma membrane. Other myotoxic venom components include sodium channel-blocking myotoxins [21] and muscle fibre depolarising cardiotoxins [22]. SVMPs are enzymatic proteins that primarily attack the collagenous structures and various other important components of BM to induce muscle damage. It has recently been reported that SVMPs induce haemorrhage by cleaving components of the BM and extracellular matrix surrounding the smaller blood vessels [23] although as multi-domain proteins, they are capable of binding to and cleaving a range of different proteins [24, 25].

SVMPs are generally classified into four groups based on the additional domains present in their structure: PI/Group I—contains only a metalloprotease domain; PII/Group II—contains a metalloprotease and disintegrin domain, and in some cases the disintegrin domain has been reported to be processed and liberated as a free disintegrin; PIII/Group III—contains a metalloprotease, a disintegrin-like and cysteine-rich domains; PIV/Group IV—contains two lectin-like domains connected by disulphide bonds to the other domains that are found in PIII SVMPs [26]. Although disintegrin-like domains show high sequence identity to disintegrins, they lack the typical RGD motif found in the venom disintegrins, which inhibit platelet aggregation via selectively blocking integrins. Both disintegrin-like and cysteine-rich domains have been found to inhibit collagen-induced platelet aggregation and induce early events of acute inflammation [27]. Notably, disintegrin-like domains were reported to contain an ECD motif that interacts with integrins and block their functions [28]. The non-proteinase domains play key roles in determining the diverse pharmacological effects of PII, PIII and PIV classes of SVMPs including the activation of coagulation factor X [29] and prothrombin [30] amongst others. These domains have also been found to co-localise in muscles, facilitating the hydrolysis of collagen and other BM components by the metalloprotease domain and promoting its accumulation in the BM [24], exerting haemotoxic activities. Moreover, SVMPs are also known to cause ischaemia in the local tissues due to poor blood supply as a result of their haemotoxic effects [31], which may prevent phagocytic removal of necrotic debris and reduce the supply of oxygen and nutrients needed for regeneration [32]. Given the complexity of their actions, a better understanding of the molecular mechanisms through which SVMPs induce permanent muscle damage may pave the way to the development of improved therapeutic strategies for snakebites. In this study, we demonstrate novel insights into the mechanisms by which a PIII/group III metalloprotease isolated from the venom of a North American viper, the western diamondback rattlesnake, *Crotalus atrox* triggers permanent muscle damage. Our results establish that this SVMP induces muscle damage and also prevents muscle regeneration by acting on the BM, myofibres, blood supply and SCs.

Materials and methods

Materials

Lyophilised *C. atrox* venom was purchased from Sigma Aldrich (UK) and the purified Cardiotoxin 1 (CTX), a three-finger toxin from the venom of *Naja pallida* was obtained from Latoxan (France).

Protein purification

C. atrox venom (10mg) was dissolved in 1mL of 20mM Tris.HCl buffer (pH 7.6) and centrifuged at 5000g for 5 minutes before applying to a pre-made 1mL HiTrap™ Q HP Sepharose

anion exchange column. Protein elution was performed at a rate of 1mL/min using 1M NaCl/20mM Tris.HCl gradient (up to 60%) by an ÄKTA purifier system (GE Healthcare, UK) over 20 minutes. The collected fractions were analysed by SDS-PAGE using standard protocols as described previously [33] and fractions with the protein of interest were pooled. The pooled fractions were then concentrated using a Vivaspin centrifugal filter and applied to a gel filtration column (Superdex 75, 1.6cm x 70cm). Protein elution was performed at a rate of 1mL/min using 20mM Tris.HCl (pH 7.6). Following SDS-PAGE analysis, the fractions containing the protein of interest were pooled and concentrated before running through the same gel filtration column again for further purification. Finally, the fractions containing the pure protein were pooled, concentrated and stored at -80°C until further use. Protein estimation was performed using Coomassie plus protein assay reagent (ThermoFisher Scientific, UK) and bovine serum albumin as standards.

Mass spectrometry

The purified protein was subjected to SDS-PAGE, and a gel section containing the pure protein was subjected to tryptic digestion and analysed by mass spectrometry at AltaBioscience (Birmingham, UK). The extracted protein (10µg) from the gel slice was added to 100mM ammonium bicarbonate (pH 8). This was then incubated with dithiothreitol (10mM) at 56°C for 30 minutes. After cooling to room temperature, the cysteine residues were alkylated using iodoacetamide (50mM). Trypsin gold (Promega, UK) was subsequently added and the samples were incubated overnight at 37°C. The digested peptides were concentrated and separated using an Ultimate 3000 HPLC series (Dionex, USA). Samples were then trapped on an Acclaim PepMap 100 C18 LC column, 5µm, 100A 300µm i.d. x 5mm (Dionex, USA), then further separated in Nano Series Standard Columns 75µm i.d. x 15 cm. This was packed with C18 PepMap100 (Dionex, USA) and a gradient from 3.2% - 44% (v/v) solvent B (0.1% formic acid in acetonitrile) over 30 minutes was used to separate the peptides. The digested peptides were eluted (300nL/min) using a traversa nanomate nanospray source (Advion Biosciences, USA) into a LTQ Orbitrap Elite Mass Spectrometer (ThermoFisher Scientific, Germany). The MS and MS/MS data were then searched against Uniprot using Sequest algorithm and the partial sequence was then compared to the other similar protein sequences available in the protein database.

Fibrinogenolytic assay

Human plasma fibrinogen (100µg/mL) was incubated with different concentrations of the whole venom or the purified protein, and a small volume of digested samples were removed at 30, 60, 90 and 120 minutes and mixed with reducing sample treatment buffer [4% (w/v) SDS, 10% (v/v) β-mercaptoethanol, 20% (v/v) Glycerol and 50mM Tris.HCl, pH 6.8]. The samples were then analysed by 10% SDS-PAGE and stained with Coomassie brilliant blue to determine the fibrinogenolytic activity of venom and the purified protein.

Enzymatic assays

The metalloprotease activity of both *C. atrox* whole venom and the purified protein was assessed using a fluorogenic substrate, DQ-gelatin (ThermoFisher Scientific, UK). Briefly, the whole venom or purified protein (10µg/mL) was mixed in phosphate buffered saline (PBS, pH 7.4) with DQ gelatin (10µg/mL). The reaction mix was incubated at 37°C and the level of fluorescence was measured at 60 minutes using an excitation wavelength of 485nm and emission wavelength of 520nm by spectrofluorimetry (FLUOstar OPTIMA, Germany).

Similarly, the serine protease activity was measured using a selective substrate, N α -Benzoyl-L-Arginine-7-Amido-4-methylcoumarin hydrochloride (BAAMC) (Sigma Aldrich, UK). The whole venom or the purified protein (10 μ g/mL) was incubated with BAAMC (2 μ M) at 37°C and the level of fluorescence was measured at an excitation wavelength of 380nm and emission wavelength of 440nm by spectrofluorimetry.

Ethical statement

The University of Reading Research Ethics Committee has approved the procedures for blood collection from healthy human volunteers and the consent forms used to obtain written consent. Experiments with mice were performed in line with the principles and guidelines of the British Home Office and the Animals (Scientific Procedures) Act 1986 (PPL70/7516). All the procedures were approved by the University Research Ethics Committee (License number: UREC 17/17).

Platelet aggregation

Human blood was obtained from healthy volunteers in vacutainers with 3.2% (w/v) sodium citrate as an anti-coagulant and the platelet-rich plasma (PRP) was prepared as described previously [34–36]. Platelet aggregation assays were performed by optical aggregometry using 0.5 μ g/mL cross-linked collagen related peptide (CRP-XL) as an agonist in the presence and absence of different concentrations of the purified protein.

Administration of CTX or the purified protein in mice

The C57BL/6 mice (8 weeks old) were obtained from Envigo, UK. Mice were anaesthetised with 3.5% (v/v) isoflurane in oxygen before maintaining at 2% for the procedure. They were then injected intramuscularly with 30 μ L of either PBS (undamaged control), 50 μ M CTX, and 8 or 16 μ M of the purified protein into their right tibialis anterior muscle. Mice were then allowed to recuperate for either 5 or 10 days before sacrificing by carbon dioxide asphyxiation and cervical dislocation.

Dissection of tibialis anterior (TA) and extensor digitorum longus (EDL)

The TA muscles from mice were dissected, weighed and frozen on liquid nitrogen cooled isopentane prior to storage at -80°C. The EDL muscle was dissected from the undamaged contralateral hind limb of experimental mice and immediately placed in a 2mg/mL collagenase solution (Sigma Aldrich, UK) and incubated at 37°C with 5% CO₂ for 2 hours to isolate the single fibres as previously described [37].

Proliferation and migration of satellite cells

To determine the proliferation of SCs and myogenic differentiation, isolated single fibres were cultured for up to 48 hours at 37°C with 5% CO₂ in single fibre culture medium (SFCM—DMEM, 10% (v/v) horse serum, 1% (v/v) penicillin-streptomycin and 0.5% (v/v) chick embryo extract) supplemented with either 0, 0.3, 1 or 3 μ M of the purified protein prior to fixation in 2% (w/v) paraformaldehyde in PBS and maintained in PBS prior to immunocytochemistry.

The migration of muscle fibre SCs was analysed as described previously [37]. Briefly, the isolated single fibres were cultured for 24 hours in SFCM before transferring to SFCM containing 0, 0.3, 1 or 3 μ M of the purified protein and monitoring by a phase contrast microscope at 37°C with 5% CO₂ using a 10X objective. A time-lapse video was captured at a rate of 1 frame every 15 minutes for a 24-hour period and analysed to determine the rate of migration.

Immunohistochemistry

The collected TA muscles were mounted in Tissue-TEK[®] OCT compound in an orientation allowing the transverse sections of 13µm thickness to be obtained using a cryo microtome. The tissue sections were incubated in permeabilisation buffer [20mM HEPES, 3mM MgCl₂, 50mM NaCl, 0.05% (w/v) sodium azide, 300mM sucrose and 0.5% (v/v) Triton X-100] for 15 minutes at room temperature. To remove the excess permeabilisation buffer, 3 x 5 minute washes were performed using PBS before the application of wash buffer [PBS with 5% fetal bovine serum (v/v), 0.05% (v/v) Triton X-100] for 30 minutes at room temperature.

Primary antibodies were pre-blocked in wash buffer for 30 minutes prior to application onto muscle sections overnight at 4°C. In order to remove the primary antibodies, muscle sections were washed three times (5 minutes each) in wash buffer. The sections were then incubated with species-specific secondary antibodies that were conjugated with Alexa Fluor 488 or 594. The secondary antibodies were pre-blocked in wash buffer for minimum of 30 minutes before their application onto the slides and incubated for 1 hour in the dark at room temperature. Thereafter, the muscle sections were washed 3 x 5 minutes in PBS to remove the unbound secondary antibodies. Finally, the slides were mounted in fluorescent mounting medium, and the myonuclei were visualised using 4, 6-diamidino-2-phenylindole (DAPI) (2.5µg/mL). The images of sections were obtained using a fluorescence microscope (Zeiss AxioImager) and analysed using ImageJ. Macrophages were detected by F4.80 staining using the Vector Laboratories ImmPRESS Excel Staining Kit. A list of antibodies used in this study is provided in [S1 Table](#).

Statistical analysis

All the statistical analyses were performed using GraphPad Prism 7 and the P-values were calculated using one-way ANOVA followed by Dunnett's post hoc multiple comparisons test.

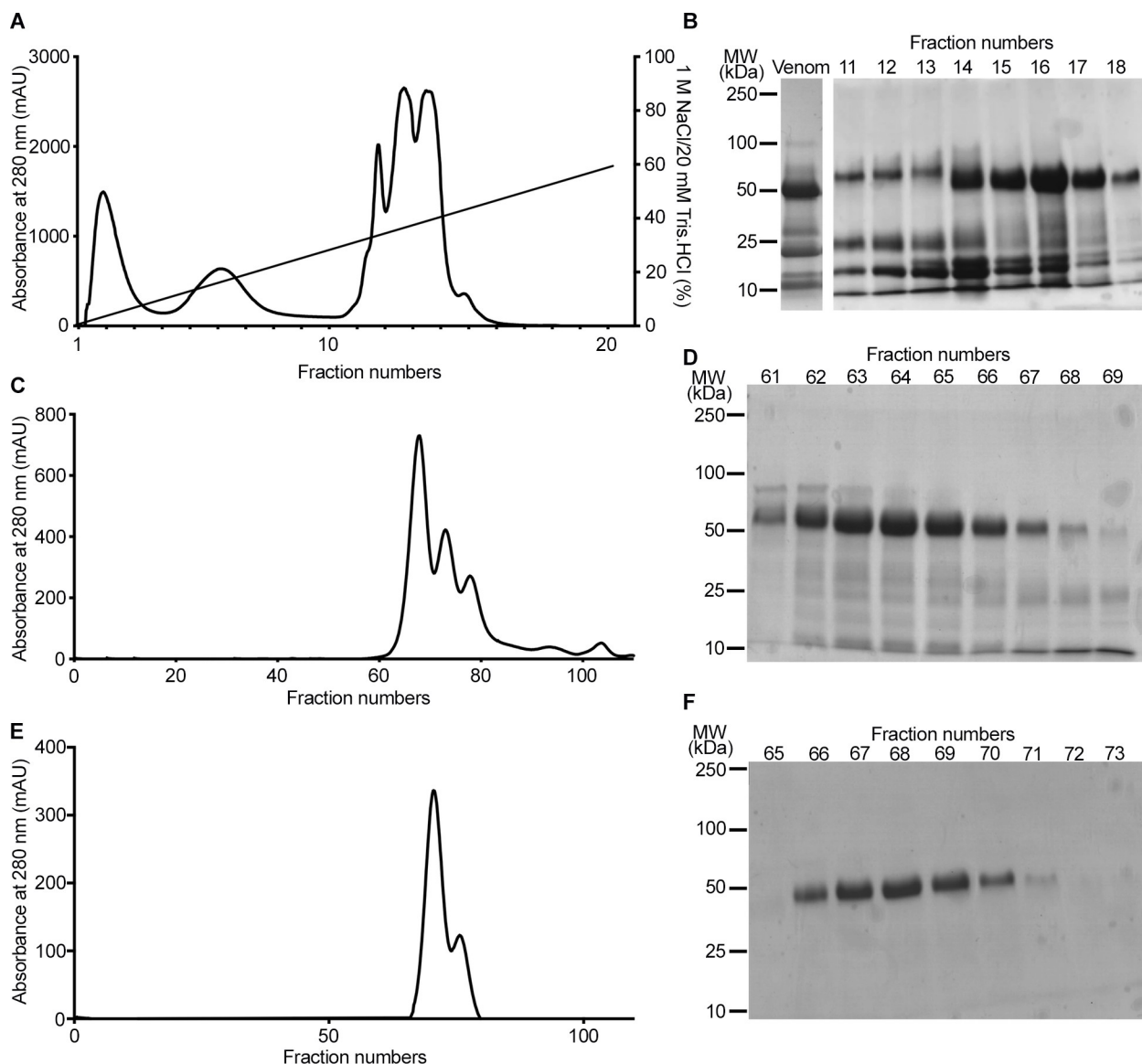
Results

Protein purification and identification

In order to purify a protein with a molecular weight of around 50kDa (as predicted for group III SVMs) from the venom of *C. atrox*, a two-dimensional chromatography approach was employed. Following the initial fractionation of venom via anion exchange chromatography ([Fig 1A and 1B](#)), the selected fractions (14–18) with a highly abundant protein at approximately 50kDa were pooled and run through a gel filtration chromatography column ([Fig 1C and 1D](#)). The fractions (62–67) were pooled and run through the same gel filtration column again to refine the purification ([Fig 1E and 1F](#)). Finally, a pure protein with a molecular weight of around 50kDa was isolated. Mass spectrometry characterisation of the tryptic digested peptides of this protein and further Mascot analysis confirmed it to be a similar or identical protein to vascular apoptosis inducing proteins (VAP) such as VAP2, a protein with a molecular weight of 55kDa (an identical molecular weight to the purified protein) [38], which is a group III metalloprotease ([Fig 1G](#)). The identified peptide sequences of the purified protein covered around 43% of the sequence of VAP2A (highlighted in red in [Fig 1G](#)). The purified protein has been referred to as 'CAMP' to denote *C. atrox* metalloprotease throughout this article.

Fibrinolytic and collagenolytic activities of CAMP

By using fluorogenic substrates, the protease activity of CAMP was analysed in comparison to the whole venom. CAMP displayed no serine protease activity as it failed to cleave a serine protease selective fluorogenic substrate, BAAMC although the whole venom displayed significant



G

1 miqvlvtic laafpyqgss iilesgnvnd yeivyrprkvt alpkgavqpk yedamqyelk
61 vngepvvlhl eknkqlfskd ysethyspdg reittypive dhcyyhgrie ndadstasis
121 acnglkghfk lqgemyliep lklsdseaha vykyenveke deapkmcgv t qnwksyepik
181 kasqlvvtæ hqkynpfrfv elvlvdkam vtnngdldk iktrmyelan tvndiyrmy
241 ihvalvglei wsnedkitvk peadytlnaf gewrktldlt rkkhdnaql taidldrvig
301 layvgsmchp krstgiiqdy spinlvvavi mahemghnlg inhdr gycsc gdyacimrpe
361 ispepstffs ncsyfdcwdf itnhnpeciv neplgtidis ppvegnelle vgeecdogtp
421 encneccda atcklksqsq cghgdceeqc kfsksgtecr asmsecdpæ hctgqssecp
481 advfhknqgp eldnygyngn epimyhqcyd lfgadvyeæ dscfernqkg nygygerken
541 gnkipcaped vkcgrlyckd nspgqnsck mfysnedehk gmvlpgtkca dgkvcnghc
601 vdvatay

Fig 1. Purification of CAMP from the venom of *C. atrox*. A, A chromatogram demonstrates the purification profile of 10mg of whole *C. atrox* venom by anion exchange chromatography. B, a Coomassie stained gel displays the protein profile of whole *C. atrox* venom and fractions 11–18 of anion exchange chromatography. A chromatogram (C) and Coomassie stained gel (D) show the purification profile of fractions 14–18 of anion exchange chromatography by gel filtration. E, a chromatogram of the second step of gel filtration for fractions 62–67 from the previous step and (F) a Coomassie stained gel shows the purified protein at approximately 50kDa. G, the tryptic digested samples of the purified protein were analysed by mass spectrometry and the identified peptide sequences match (via Mascot search) with the known sequence of VAP2A (coverage 43%; the mass spectrometry-identified peptide sequences of the purified protein are shown in red) and confirms that the purified protein is most likely to be VAP, a group III metalloprotease. The purified protein was named as CAMP to represent *C. atrox* metalloprotease.

<https://doi.org/10.1371/journal.pntd.0007041.g001>

serine protease activity (Fig 2A). However, it showed high levels (similar to the whole venom) of collagenolytic activity (Fig 2B). Furthermore, the ability of CAMP to digest fibrinogen was analysed by incubating it with human plasma fibrinogen. The SDS-PAGE analysis of samples that were taken at different points of incubation confirmed that CAMP is capable of cleaving A α and B β chains of fibrinogen although it was unable to cleave the γ chain (Fig 2C). The digestion of fibrinogen with CAMP appears to be rapid as the levels of A α and B β chains of fibrinogen were reduced significantly as early as 30 minutes of incubation. These results corroborate CAMP as an SVMP with collagenolytic and fibrinogenolytic activities, which may affect the collagen in the BM around the local tissues at the bite site and fibrinogen in the blood.

CAMP inhibits human platelet aggregation

The ability of CAMP to inhibit agonist-induced platelet activation was analysed using human platelet-rich plasma (PRP) by optical aggregometry. The pre-treatment of human platelets (PRP) with CAMP (50 μ g/mL) has significantly inhibited 0.5 μ g/mL CRP-XL-induced platelet aggregation (Fig 2D and 2E). This data confirms the ability of CAMP to affect human platelet activation.

CAMP induces haemorrhage and fluctuations in muscle size in mice

In order to determine the mechanisms through which SVMPs induce permanent muscle damage, CAMP was used as a tool to determine its pathological effects in TA muscle of mice in comparison with CTX. The intramuscular injection of CAMP induced haemorrhage in the damaged muscles and thereby, caused swelling and increase in muscle weight after five days of administration (Fig 3A and 3B). However, CTX did not induce haemorrhage or swelling although the muscle weight was reduced compared to the controls at the same time point. In contrast, after ten days of administration, muscle weight in CAMP-treated mice was decreased similar to CTX-treated muscle (Fig 3A and 3C). These data demonstrate that CAMP is capable of inducing haemorrhage and swelling and thereby, increases in muscle weight initially although it decreases at a later time point.

Attenuated regeneration in CAMP-damaged muscle

We examined the cellular processes underpinning the morphology of skeletal muscle and assessed muscle regeneration after damage induced by CAMP. Haematoxylin (H) and eosin (E) staining facilitates the identification of cellular organisation within a tissue and also the presence of fibres containing centrally located nuclei (CLN), which is an indicator of muscle regeneration. Five days after tissue damage, muscles treated with CTX contained many large fibres with CLN (Fig 4A). Furthermore, there were regions of high cell density between fibres displaying CLN. In contrast, 5 days after CAMP damage the number of fibres with CLN was less abundant and smaller than in CTX damaged muscle (Fig 4A and 4B). Additionally, there were areas of sparsely populated regions between fibres. Ten days after CTX damage, large

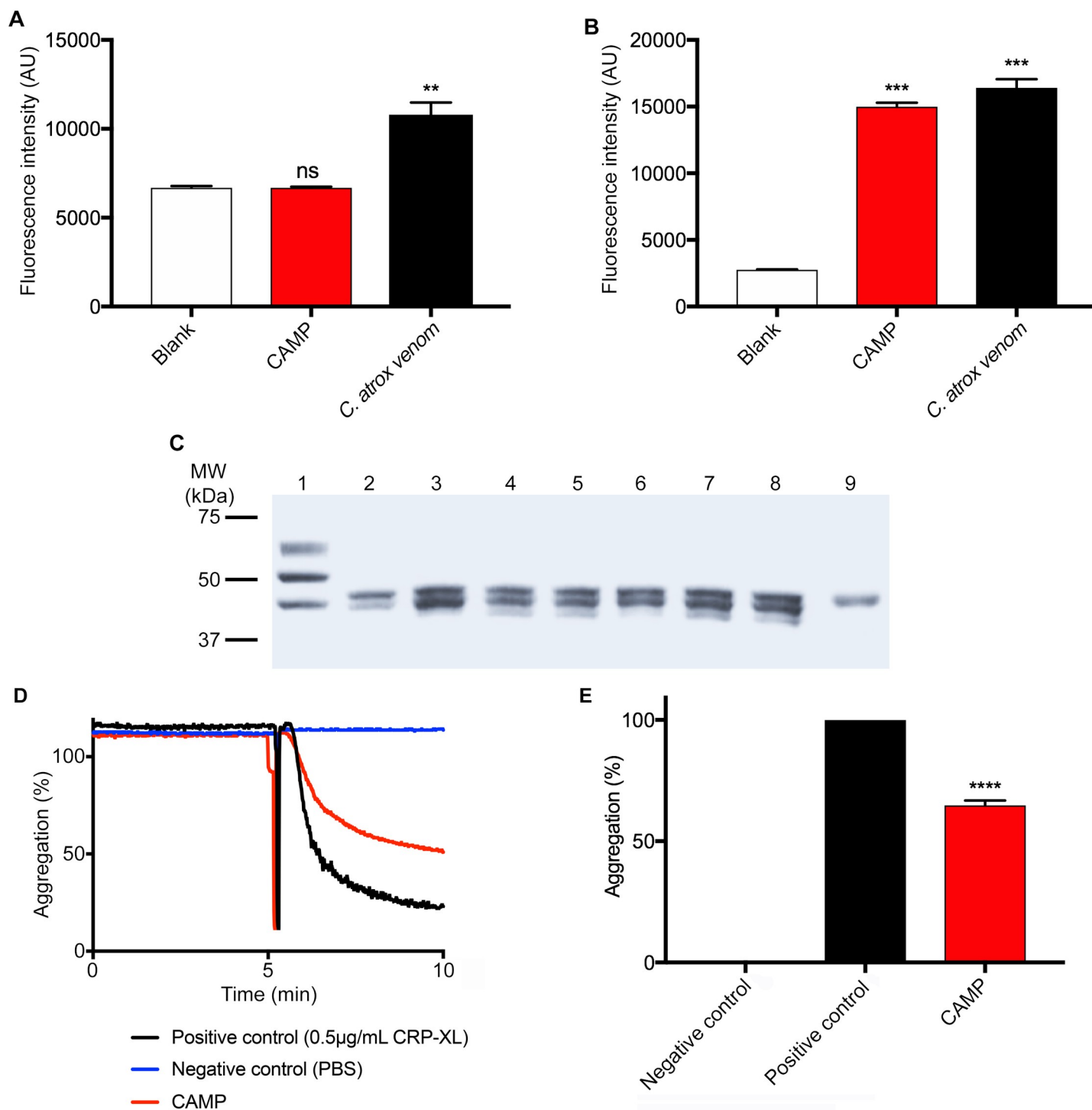


Fig 2. The functional characterisation of CAMP. A, the serine protease activity of 10µg/mL whole venom or CAMP was analysed using a fluorogenic substrate, Nα-Benzoyl-L-Arginine-7-Amido-4-methylcoumarin hydrochloride (BAAMC) by spectrofluorimetry. Similarly, (B) the metalloprotease activity of 10µg/mL whole venom or CAMP was analysed using DQ-gelatin, a specific fluorogenic substrate for collagenolytic enzymes and the level of fluorescence was measured by spectrofluorimetry. C, a Coomassie stained gel demonstrates the fibrinogenolytic activity of CAMP in comparison with whole *C. atrox* venom. Lanes, 1—undigested fibrinogen, 2—fibrinogen incubated with whole venom (100µg/mL), fibrinogen incubated with CAMP (100µg/mL) after 30 (3), 60 (4) and 90 (5) minutes, fibrinogen incubated with CAMP (50µg/mL) after 30 (6), 60 (7) and 90 (8) minutes, and CAMP alone (9). Representative aggregation traces (D) and data (E) demonstrate the impact of CAMP on cross-linked collagen related peptide (CRP-XL)-induced human platelet (PRP) aggregation. Data represent mean ± S.D. (n = 3). The p values shown are as calculated by One-way ANOVA followed by post hoc Tukey's test using GraphPad Prism (**p<0.01, ***p<0.001 and ****p<0.0001).

<https://doi.org/10.1371/journal.pntd.0007041.g002>

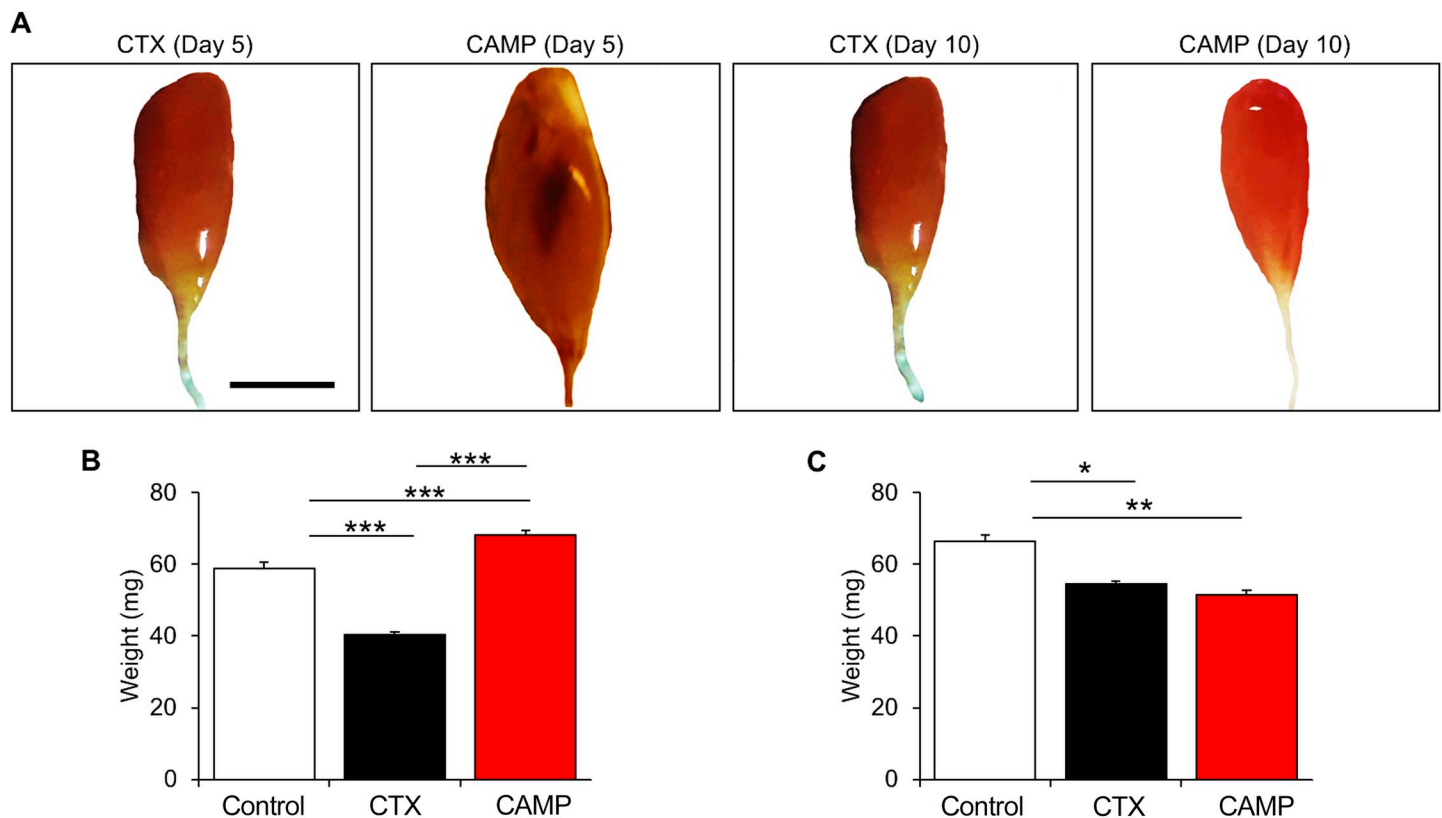


Fig 3. Macrostructure of tibialis anterior muscle after CAMP treatment. A, representative images of muscles treated with either CTX or CAMP for 5 or 10 days. Quantification of TA weight at 5 (B) and 10 (C) days post administration. Scale bar represents 5 mm. Data represent mean \pm S.D. (n = 5 for each cohort). The *p* values shown are as calculated by One-way ANOVA followed by post hoc Tukey's test using GraphPad Prism (**p* < 0.05, ***p* < 0.01 and ****p* < 0.001).

<https://doi.org/10.1371/journal.pntd.0007041.g003>

fibres with CLN were evident with very little space between muscle fibres (Fig 4C and 4D). The fibres appeared to be regular in terms of shape and size, evidencing robust muscle regeneration. Whereas, at the same time point, muscle damaged with CAMP displayed smaller fibres with CLN and inter-fibre regions populated with cells were prominent (Fig 4C and 4D). Next, we documented the profile of dying muscle fibres, facilitating the infiltration of circulating immunoglobulins (Ig) into the damaged fibres. Five days after CTX injection, low density of small calibre fibres displayed the infiltration by IgG (Fig 4E–4G). In contrast, at the same time point, CAMP treatment resulted in not only a higher density of fibres with infiltrated IgG, but they were also of larger size (Fig 4E–4G). By day 10, very few dying fibres were present in CTX treated muscle, however dying fibres were prominent in CAMP treated muscles (Fig 4H and 4I). We then examined the presence of regenerating muscle fibres, facilitated through the expression of embryonic myosin heavy chain protein (MYH3). Muscle regeneration was clearly evident in muscles damaged by CTX at day 5 (Fig 4J and 4K). Large numbers of evenly sized fibres expressing MYH3 featured in CTX-damaged tissue (Fig 4J and 4L). In contrast to CTX treatment, the number of regenerating fibres in CAMP-treated muscle was lower and when present were of heterogeneous size (Fig 4J–4L). By Day 10, the expression of MYH3 has been cleared in CTX-damaged muscle and when present was in very large fibres (Fig 4M–4O). In contrast, MYH3 expression was clearly evident at day 10 in CAMP-damaged muscle but in smaller, non-uniform fibres (Fig 4M–4O). Next, we examined the impact of CAMP and CTX on blood vessels through immunostaining with the endothelial cell specific antibody, CD31.

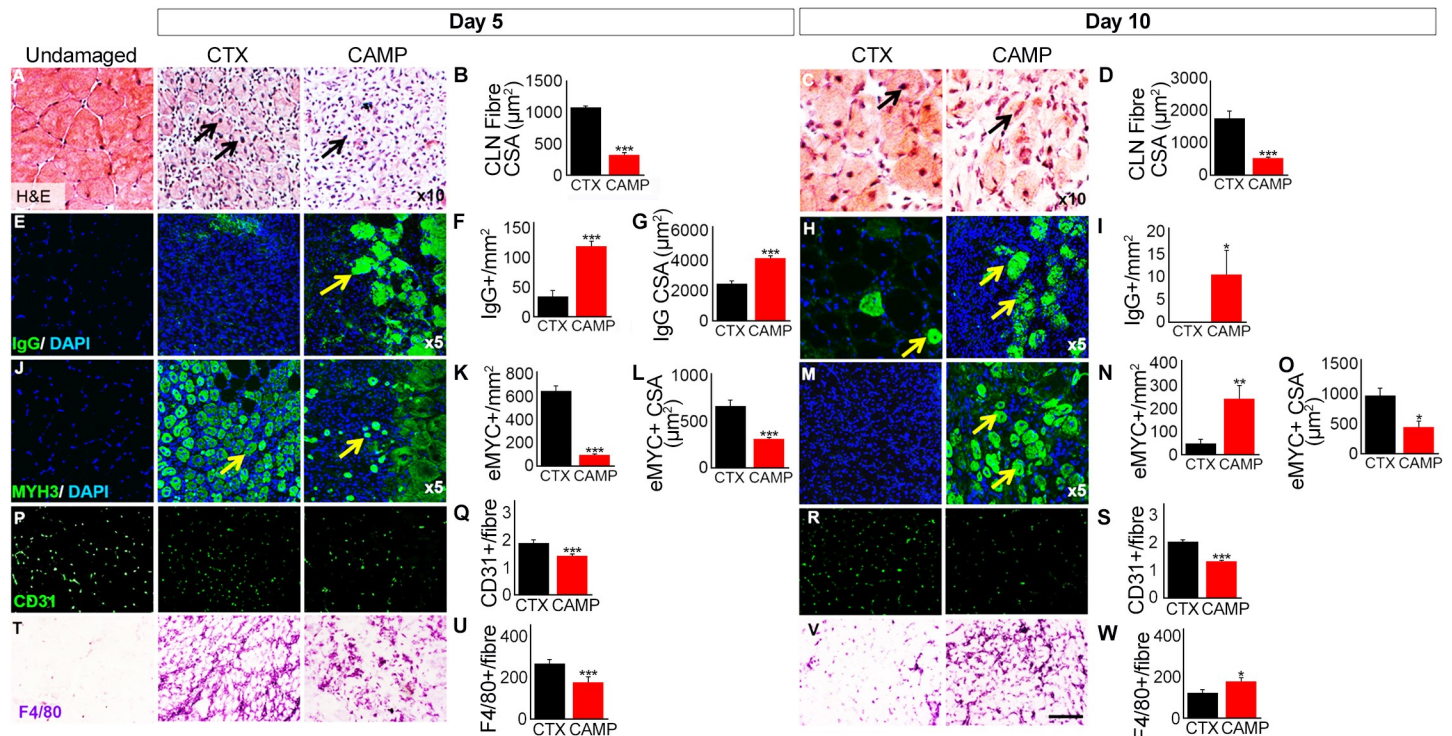


Fig 4. Analysis of tibialis anterior muscle regeneration after administration of CAMP or CTX. A, H and E staining of muscle identifying centrally located fibre nuclei (CLN) (arrows) and (B) quantification of centrally located muscle fibre size 5 days post administration. C, H and E staining of muscle (arrows) and (D) quantification of centrally located muscle fibre size 10 days post administration. E, intra-fibre IgG localisation for necrotic muscle fibres (arrows) and quantification of necrotic fibre density (F) and size (G) 5 days post administration. H, intra-fibre IgG localisation for necrotic fibres (arrows) and (I) quantification of necrotic fibre density 10 days post administration. J, identification of regenerating muscle fibres through the expression of MYH3 (arrows) and quantification of regenerating muscle fibre density (K) and size (L) 5 days post administration. M, identification of regenerating muscle fibres through the expression of MYH3 (arrows) and quantification of regenerating muscle fibre density (N) and size (O) 10 days post administration. P, Localisation of endothelial marker CD31 and (Q) quantification of capillaries per regenerating muscle fibre 5 days post administration. R, localisation of endothelial marker CD31 and (S) quantification of capillaries per regenerating muscle fibre 10 days post administration. T, immunostaining with antibody F4/80 and (U) its density quantification in damaged region 5 days post administration. V, immunostaining with antibody F4/80 and (W) its density quantification in damaged region 10 days post administration. Data represent mean \pm S.D. (n = 5 for each cohort). The p values shown are as calculated by two-tailed Student's T test for independent variables using GraphPad Prism (*p<0.05, **p<0.01 and ***p<0.001).

<https://doi.org/10.1371/journal.pntd.0007041.g004>

At both 5 and 10 days, the number of capillaries serving each regenerating fibre was greater in the CTX treated sample compared to CAMP (Fig 4P–4S). Importantly, the number of capillaries serving each regenerating fibre in the CTX treated sample was identical to the undamaged sample. Moreover, the degree of macrophage infiltration into the damaged area was analysed, as these cells are key to effective muscle regeneration. The density of macrophages in damaged muscle was greater in the CTX treated muscle compared to CAMP at day 5 (Fig 4T and 4U). However, by day 10, the situation was reversed; there was a greater density of macrophages in the CAMP treated samples compared to CTX (Fig 4V and 4W).

CAMP extensively damages the extracellular matrix (ECM) surrounding the myofibres

Efficient regeneration of skeletal muscle following acute damage is contingent on stem cells capable of replacing damaged tissue and their highly ordered formation into myotubes/fibres, a process orchestrated by the ECM. The organisation of collagen IV, a major BM component of muscle fibres was analysed as described previously [39]. A thin circle of collagen IV surrounding muscle fibre was evident 5 days after CTX treatment (Fig 5A). In contrast, at an

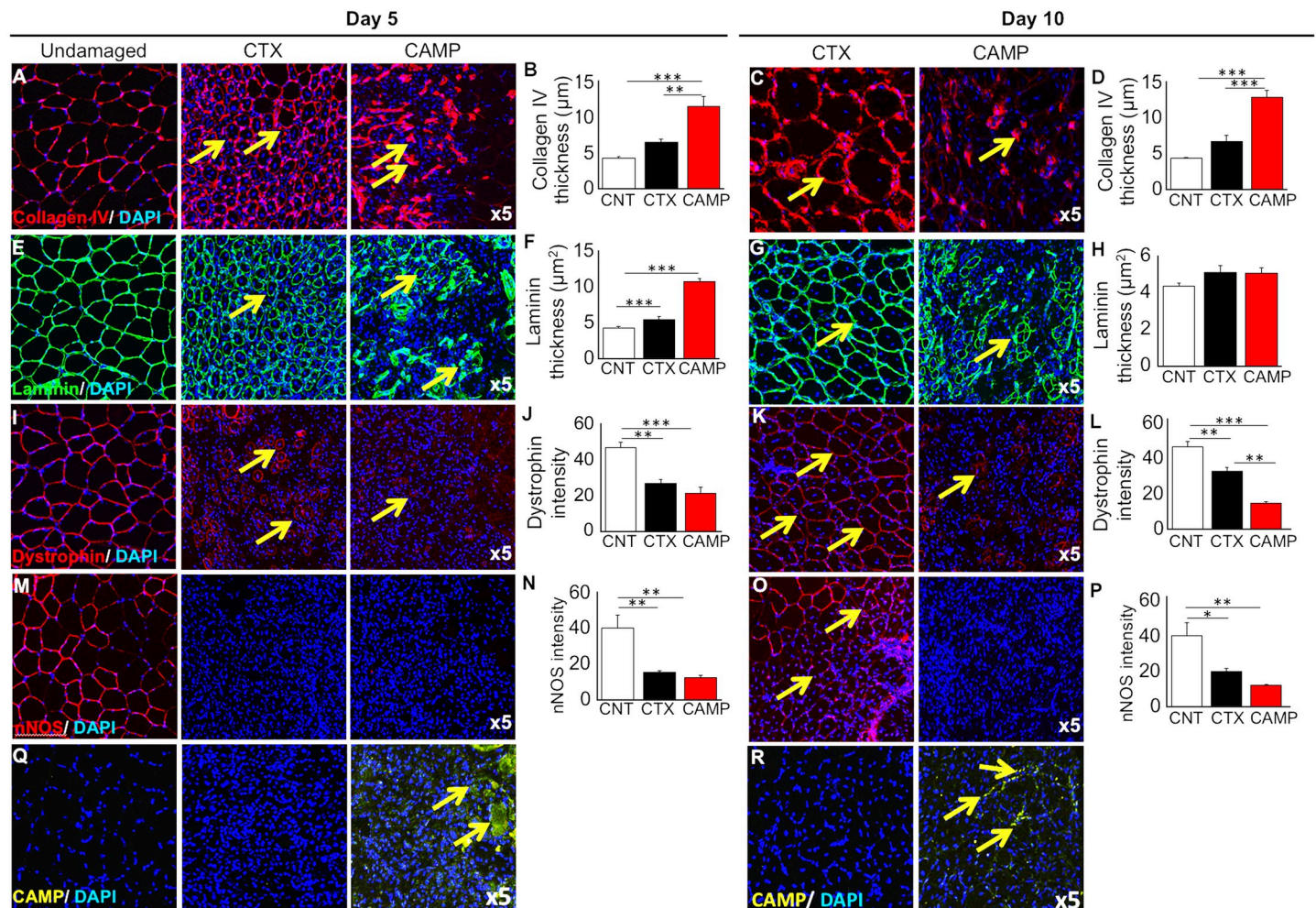


Fig 5. Immunohistochemical analysis of muscle extracellular matrix and associated proteins after tibialis anterior damage with CAMP or CTX. Localisation (arrows) (A) and thickness (B) of collagen IV 5 days post administration. Similarly, localisation (arrows) (C) and thickness (D) of collagen IV 10 days post injury. *Note:* CTX damaged tissues show circumferential collagen compared to foci in CAMP treatment. Localisation (arrows) (E) and thickness (F) of laminin 5 days post injury. Localisation (arrows) (G) and thickness (H) of laminin 10 days post injury. I, localisation of dystrophin 5 days post injury (arrows). *Note:* dystrophin around centrally located nuclei in CTX-treated muscle. In contrast, incomplete dystrophin domain around CAMP-damaged muscle. J, intensity of dystrophin 5 days post injury. Localisation (arrows) (K) and intensity (L) of dystrophin 10 days post injury. M, localisation of nNOS 5 days post injury (no circumferential nNOS was detectable at day 5) and (N) thickness of nNOS 5 days post injury. O, localisation of nNOS 10 days post administration (arrows). *Note:* circumferential nNOS was only detectable in CTX-treated muscle and (P) intensity of nNOS 10 days post injury. Localisation of CAMP in damaged region at day 5 (Q) and 10 (R) (arrows). Data represent mean \pm S.D. ($n = 5$ for each cohort). The p values shown are as calculated by One-way ANOVA followed by post hoc Tukey's test using GraphPad Prism (* $p < 0.05$, ** $p < 0.01$ and *** $p < 0.001$). CNT represents control.

<https://doi.org/10.1371/journal.pntd.0007041.g005>

identical time after CAMP treatment, muscle displayed large irregular, thick depositions of collagen IV (Fig 5A and 5B) but by day 10, the picture was even more polarised, as CTX-damaged muscle showed a relatively normal distribution of collagen IV (Fig 5C and 5D). In contrast, very few fibres from CAMP-treated muscle (at day 10) displayed a ring of collagen IV, and instead this protein was localised at thick foci (Fig 5C and 5D). A near-identical pattern was documented for the distribution of laminin, another major component of the muscle fibre ECM (Fig 5E–5H).

Furthermore, the impact of CTX and CAMP on molecules that are associated with linking the contractile apparatus to the ECM was investigated. Dystrophin is normally localised under the sarcolemma of mature muscle fibres. Its expression was evident around some of the larger

regenerating muscle fibres 5 days after CTX damage (Fig 5I). Whereas, very few fibres expressing dystrophin were detected at a similar time point in CAMP-treated muscles (Fig 5I). However, when present, the thickness of the dystrophin expression domain was similarly reduced by the two treatments (Fig 5J). At day 10, most of the fibres from CTX-treated muscle displayed a continuum of dystrophin expression, although at a lower thickness compared to undamaged tissue (Fig 5K and 5L). However, very few fibres with a ring of dystrophin were present in CAMP-treated muscles at day 10 (Fig 5K). Furthermore, the domain, when present was thinner than both control as well as CTX treated muscles (Fig 5L). Then, the distribution of nNOS, a protein that localises to a sub-sarcolemmal position which is dependent on its binding to dystrophin was assessed. At 5 days after treatment, very little nNOS was present in either CTX or CAMP-damaged muscles (Fig 5M and 5N). By day 10, a thin band of nNOS was evident in CTX-treated muscle but not in the muscle damaged by CAMP (Fig 5O and 5P). Lastly, the muscles were analysed to determine the presence of remaining CAMP in damaged tissues. The immunohistological profiling showed that CAMP was clearly present at both 5 and 10 days after its administration (Fig 5Q and 5R). These results show that CAMP treatment damages not only the ECM of muscle fibres but also affects intracellular components that link it to the contractile machinery.

CAMP affects the functions of satellite cells (SCs)

The role of SCs adjacent to the muscle fibres is critical for muscle regeneration. In order to determine the impact of CAMP on SCs, we have isolated myofibres from intact EDL muscles and exposed them to a range of concentrations of CAMP. As early as 24 hours after CAMP treatment, it was evident that there was a concentration dependent disturbance to the collagen component of the ECM around muscle fibres. A uniform layer of collagen expression was detected in untreated fibres (Fig 6A). At the lower concentration, CAMP caused a localised denuding of the myofibre (Fig 6B), whereas the higher concentration resulted in the absence of collagen from most parts of the fibres and caused it to concentrate in specific locations (Fig 6C). The cell growth, proliferation and migration were monitored on the isolated single muscle myofibres over a 48 hour time period. SCs were immunostained using the myogenic transcription factors, Pax7 (uncommitted cells) and MyoD (activated cells) in order to monitor the progression of cells through myogenesis. The concentrations of above 0.3μM of CAMP induced hypercontraction, which is indicative of extensive fibre damage. At 0.3μM, viable fibres were present, and revealed that CAMP significantly decreased the number of associated SCs (Fig 6D). Furthermore, the number of SC clusters was reduced per fibre (Fig 6E), although each cluster at the lower concentration had more cells than untreated fibres (Fig 6F). Analysis of differentiation was only possible at the lowest concentration of CAMP (Fig 6G) as at higher concentrations, hypercontraction prevented this analysis. The migration speed was calculated between 24 and 48 hours and was found to decrease significantly as the concentration of CAMP increased (Fig 6H). These data demonstrate that CAMP is able to affect both the proliferation and migration of SCs but not the differentiation.

Discussion

The swelling and necrosis at the bite site as well as permanent muscle damage are common effects of snakebite envenomation (particularly viper bites). These effects frequently lead to amputation and therefore disable victims, which adds to their inability to earn money, and exacerbates the poverty that is already experienced by the vast majority of snakebite victims [4]. Here we have purified a metalloprotease from one of the most studied venomous snake species, *C. atrox*. Although deaths from this snake are now uncommon, disfigurement is still a

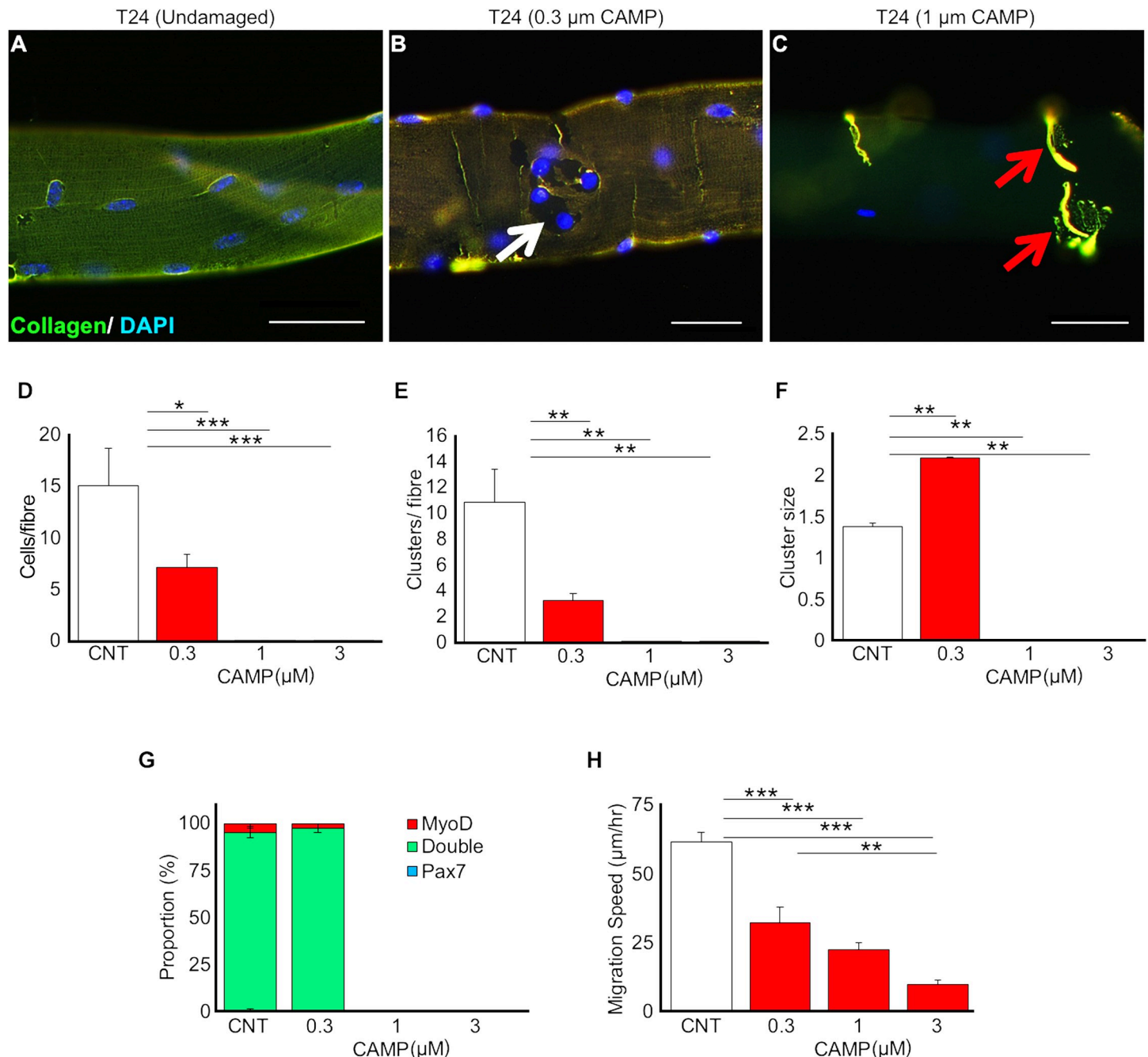


Fig 6. CAMP treatment affects proliferation and migration of satellite cells. (A–C) Increasing concentrations of CAMP change the distribution of collagen IV. Satellite cell proliferative characteristics following CAMP treatment were analysed. For example, satellite cell number per fibre (D), satellite cell clusters per fibre (E) and cluster size per fibre (F) were quantified. G, myogenic characteristics of satellite cells following CAMP treatment. H, migration rate of satellite cells. Scale bar represents 20 μ m. Data represent mean \pm S.D. (n = 20 fibres for each cohort). The p values shown are as calculated by One-way ANOVA followed by post hoc Tukey's test using GraphPad Prism (*p<0.05, **p<0.01 and ***p<0.001). CNT represents control.

<https://doi.org/10.1371/journal.pntd.0007041.g006>

prevalent side effect for survivors. SVMPs are a predominant component in viper venoms that are involved in inducing the local envenomation effects including muscle damage. The ability of SVMPs to degrade collagen has been established, but its impact on permanent muscle damage under *in vivo* settings has not been previously demonstrated in sufficient detail. Therefore,

we deployed a metalloprotease from the venom of *C. atrox* and analysed its impact on skeletal muscle damage in comparison to a three-finger toxin, CTX from the venom of *Naja pallida*. Mass spectrometry analysis of the purified protein suggests it to be a group III metalloprotease, which possess a metalloprotease domain as well as a disintegrin-like and cysteine-rich domains [40]. Based on the peptide sequences identified by the mass spectrometry, the purified protein is likely to be VAP2 or one of its heterodimers; VAP2A or VAP2B, both of which are vascular apoptosis inducing proteins (38) that are known to be haemorrhagic [41] and in the case of VAP2B to inhibit collagen-induced platelet activation [42]. Due to the limited peptide sequences identified by mass spectrometry for the purified protein, we are unable to conclude whether the purified protein (CAMP) is identical to VAP2 or either of its heterodimers. CAMP was characterised to be a collagenolytic and fibrinogenolytic enzyme. It also inhibited CRP-XL-induced platelet aggregation; group III metalloproteases are known to interact with the integrin $\alpha_2\beta_1$, binding to the α_2 subunit and causing the shedding of β_1 subunits [43]. However, VAP2B (a protein described from *C. atrox*) has been reported to inhibit collagen induced platelet aggregation by binding to collagen [44], although whether the SECD sequence found in disintegrin-like domains is able to bind CRP-XL in the same way, is unknown.

In order to determine the impact of SVMs in stimulating permanent muscle damage, different concentrations of CAMP were administered in mice along with CTX and control groups and the effects were analysed at five and ten days after the administration. We suggest that this occurs at two levels; by breaking down the ECM which normally acts as a scaffold for the formation of new muscle fibres and around existing blood vessels and secondly attenuating properties of resident stem cells that are essential to effective tissue repair. SVMs are known for their collagenolytic activities and for targeting various components of the BM in the vasculature and inducing haemorrhage [45]. In line with previous studies, here we demonstrate that CAMP induces haemorrhage and affects the architecture of collagen and laminin. The destruction of the collagen based ECM may be the key to long-term tissue destruction wrought by CAMP. The disintegrin-like and cysteine-rich domains have already been identified as essential to the haemorrhagic activity and ECM degradation attributed to the PIII metalloproteases [46]. This is in contrast to myotoxic PLA2 and three-finger toxins that are well documented in causing membrane permeabilisation and consequentially myonecrosis via the hydrolysis of membrane phospholipids or imbedding directly into the membrane respectively [47–49]. Our data emphasise that CAMP in comparison to CTX significantly hindered the regeneration of skeletal muscle fibres most probably by disturbing the organisation of the ECM. The elevated levels of necrosis seen five days after administration with CAMP improved after ten days, although it was still evident. However, it must be noted that at day 10, the CTX treated muscles had almost completely regenerated with healthy fibres. Moreover, very low levels of MYH3 were detected five days after CAMP treatment. In CTX-treated muscles, this marker of regenerating fibres was clearly evident and present at a high level. This indicates that the initiation of the regeneration process was attenuated by CAMP in comparison to CTX. Muscle regeneration is dependent on blood supply and clearance of damaged fibres. We show here that both these cellular compartments are affected in a detrimental manner by CAMP. We found that the number of capillaries serving each regenerating muscle fibre was smaller in CAMP treated muscle compared to CTX. Importantly the number of capillaries serving each fibre in damaged CTX muscle was the same as in undamaged regions. These results show that capillaries as well as muscle fibres are damaged by CAMP whereas it is only the latter in CTX treated tissue. Additionally, we show that there was a greater influx of macrophages into the CTX damaged muscle compared to regions affected by CAMP. Furthermore, the density of macrophages decreased in CTX treated muscle over time, attesting to regeneration. In contrast, the density of macrophages in CAMP treated muscle was lower at day 5 compared to CTX, possibly

indicating an attenuated clearance process. Importantly the density of macrophages did not change in the CAMP treated muscle over 10 days suggesting on-going muscle damage. Although the abundance of MYH3 increased in CAMP-treated muscles by day 10, its expression in CTX-injured muscles was almost undetectable, signifying advanced regeneration. This was reflected in the appearance of dystrophin and nNOS at their normal sub-sarcolemmal position. In keeping with the notion that CAMP treatment not only affects the degree of regeneration but also its timing, we showed that very few fibres expressed dystrophin in its normal position and a significantly reduced expression of nNOS was observed even at day 10. Most importantly we show that CAMP is still present at the site of injury even 10 days after its administration and that it profoundly disorganises the ECM.

The single fibre experiments highlight another aspect to explain the attenuated muscle regeneration following CAMP-mediated muscle damage. We demonstrate that the proliferation and migration of SCs was significantly reduced by CAMP treatment. Both of these factors are key in promoting muscle regeneration. Therefore, CAMP may bring about permanent impairment of muscle organisation and function by firstly destroying muscle fibres, secondly breaking down the organisation of the ECM. This is required by the SCs in order to align and fuse in a coordinated manner and lastly by diminishing the ability for SCs to expand their numbers and migrate to the site of injury to enact efficient regeneration. It is clear that current ASV treatment is not effective at preventing muscle damage. Although translating the results of this study into therapeutics might be difficult, these will improve the understanding of SVMP-induced permanent muscle damage. The ability of group III metalloproteases to bind components of the BM and prolong muscle exposure to their myotoxic effects suggests a therapeutic agent that is capable of interacting with these enzymes and non-enzymatic domains and preventing the longevity of these proteins in the area surrounding fibres may be able to speed up the rate of regeneration considerably. Moreover, any drugs aimed at treating this aspect of snakebite envenomation may struggle to reach it intravenously, and therefore, they may have to be administered via multiple local injections considering the widespread damage to microvasculature [32] and consequential lack of blood supply to affected tissues.

ASV is the only effective treatment for systemic envenoming, however local venom pathology is largely unaffected by ASV when treatment is not immediately administered [50]. ASV is composed of large immunoglobulins that appear to struggle to reach the areas affected by SVMPs. The combination of small vessel destruction combined with BM cleavage results in a poor blood supply and therefore weak neutralisation by intravenously administered ASV. Local injections of ASV have also been found to be of no benefit to the snakebite victims [51]. However, there are a range of matrix metalloprotease inhibitors that have undergone testing for their specificity to SVMPs and some promising compounds have been identified [52]. The small molecule inhibitors aimed at the metalloprotease domain such as batimastat [53] have been tested extensively and they were found to abrogate the haemorrhagic effects of venom if administered immediately after envenoming. Given their haemorrhagic effects are largely dependent upon collagen degradation, it is reasonable to postulate that this prevention of haemorrhagic effects may also apply to muscle damage. Moreover, metal chelating agents such as EDTA have also been tested *in vivo* at non-toxic doses and found to prevent venom-induced lethality [54].

The need for immediate administration is of course unrealistic with conventional ASV but small stable inhibitors have the potential to be spread and made available to those in areas with a high density of snakebites. Multiple local injections do bring the potential for delivery directly to the bite site and administering to multiple sites may overcome the problematic spread of drug through a site of damaged muscles and vessels. Future experiments should aim to investigate the effect of these drugs on BM components, using both pre-incubation with

drugs and post envenomation delivery models. Overall, the complete destruction or loss of a range of BM and dystrophin-glycoprotein complex components as well as the effect of this SVMP on muscle regeneration highlights the significant difficulties involved in treating the necrosis and muscle damage associated with snakebite envenomation. Hence, this study provides greater insights into the understanding of SVMP-induced permanent muscle damage and local snakebite envenomation effects.

Supporting information

S1 Table. The list of antibodies used in the immunohisto- and cytochemistry analyses. (DOCX)

Author Contributions

Conceptualization: Robert Mitchell, Ketan Patel, Sakthivel Vaiyapuri.

Formal analysis: Harry F. Williams, Ben A. Mellows, Peggy Sfyri, Rajendran Vaiyapuri, Henry Collins-Hooper, Antonios Matsakas.

Investigation: Harry F. Williams, Ben A. Mellows, Robert Mitchell, Peggy Sfyri, Harry J. Layfield, Maryam Salamah, Rajendran Vaiyapuri, Henry Collins-Hooper, Antonios Matsakas.

Methodology: Andrew B. Bicknell, Ketan Patel, Sakthivel Vaiyapuri.

Supervision: Andrew B. Bicknell, Antonios Matsakas, Ketan Patel, Sakthivel Vaiyapuri.

Visualization: Ketan Patel, Sakthivel Vaiyapuri.

Writing – original draft: Harry F. Williams, Ketan Patel, Sakthivel Vaiyapuri.

Writing – review & editing: Harry F. Williams, Ben A. Mellows, Robert Mitchell, Ketan Patel, Sakthivel Vaiyapuri.

References

1. WHO. Neglected tropical diseases 2017 [Available from: http://www.who.int/neglected_diseases/diseases/en/].
2. Kasturiratne A, Wickremasinghe AR, de Silva N, Gunawardena NK, Pathmeswaran A, Premaratna R, et al. The global burden of snakebite: a literature analysis and modelling based on regional estimates of envenoming and deaths. *PLoS Med.* 2008; 5(11):e218. <https://doi.org/10.1371/journal.pmed.0050218> PMID: 18986210
3. Chippaux JP. Snake-bites: appraisal of the global situation. *Bulletin of the World Health organization.* 1998; 76(5):515. PMID: 9868843
4. Harrison RA, Hargreaves A, Wagstaff SC, Faragher B, Laloo DG. Snake envenoming: a disease of poverty. *PLoS neglected tropical diseases.* 2009; 3(12):e569. <https://doi.org/10.1371/journal.pntd.0000569> PMID: 20027216
5. Chippaux J-P. Estimate of the burden of snakebites in sub-Saharan Africa: a meta-analytic approach. *Toxicon.* 2011; 57(4):586–99. <https://doi.org/10.1016/j.toxicon.2010.12.022> PMID: 21223975
6. Vaiyapuri S, Vaiyapuri R, Ashokan R, Ramasamy K, Nattamaisundar K, Jeyaraj A, et al. Snakebite and its socio-economic impact on the rural population of Tamil Nadu, India. *PLoS one.* 2013; 8(11):e80090. <https://doi.org/10.1371/journal.pone.0080090> PMID: 24278244
7. Williams HF, Vaiyapuri R, Gajjeraman P, Hutchinson G, Gibbins JM, Bicknell AB, et al. Challenges in diagnosing and treating snakebites in a rural population of Tamil Nadu, India: The views of clinicians. *Toxicon.* 2017; 130:44–6. <https://doi.org/10.1016/j.toxicon.2017.02.025> PMID: 28238804
8. Casewell NR, Wagstaff SC, Wüster W, Cook DA, Bolton FM, King SI, et al. Medically important differences in snake venom composition are dictated by distinct postgenomic mechanisms. *Proceedings of the National Academy of Sciences.* 2014; 111(25):9205–10.

9. Fry BG, Winkel KD, Wickramaratna JC, Hodgson WC, Wüster W. Effectiveness of snake antivenom: species and regional venom variation and its clinical impact. *Journal of Toxicology: Toxin Reviews*. 2003; 22(1):23–34.
10. Modahl CM, Mukherjee AK, Mackessy SP. An analysis of venom ontogeny and prey-specific toxicity in the Monocled Cobra (*Naja kaouthia*). *Toxicon*. 2016; 119:8–20. <https://doi.org/10.1016/j.toxicon.2016.04.049> PMID: 27163885
11. Wray KP, Margres MJ, Seavy M, Rokyta DR. Early significant ontogenetic changes in snake venoms. *Toxicon*. 2015; 96:74–81. <https://doi.org/10.1016/j.toxicon.2015.01.010> PMID: 25600640
12. Gutiérrez JM, Calvete JJ, Habib AG, Harrison RA, Williams DJ, Warrell DA. Snakebite envenoming. *Nature Reviews Disease Primers*. 2017; 3:nrdp201763.
13. Vaiyapuri S, Wagstaff SC, Harrison RA, Gibbins JM, Hutchinson EG. Evolutionary analysis of novel serine proteases in the venom gland transcriptome of *Bitis gabonica* rhinoceros. *PLoS One*. 2011; 6(6): e21532. <https://doi.org/10.1371/journal.pone.0021532> PMID: 21731776
14. Vaiyapuri S, Harrison RA, Bicknell AB, Gibbins JM, Hutchinson G. Purification and functional characterisation of rhinocerase, a novel serine protease from the venom of *Bitis gabonica* rhinoceros. *PLoS One*. 2010; 5(3):e9687. <https://doi.org/10.1371/journal.pone.0009687> PMID: 20300193
15. Silva A, Johnston C, Kuruppu S, Kneisz D, Maduwage K, Kleinfeld O, et al. Clinical and Pharmacological Investigation of Myotoxicity in Sri Lankan Russell's Viper (*Daboia russelii*) Envenoming. *PLoS neglected tropical diseases*. 2016; 10(12):e0005172. <https://doi.org/10.1371/journal.pntd.0005172> PMID: 27911900
16. Gutiérrez JM, Rucavado A, Chaves F, Díaz C, Escalante T. Experimental pathology of local tissue damage induced by *Bothrops asper* snake venom. *Toxicon*. 2009; 54(7):958–75. <https://doi.org/10.1016/j.toxicon.2009.01.038> PMID: 19303033
17. Jayawardana S, Gnanathanan A, Arambepola C, Chang T. Chronic musculoskeletal disabilities following snake envenoming in Sri Lanka: a population-based study. *PLoS neglected tropical diseases*. 2016; 10(11):e0005103. <https://doi.org/10.1371/journal.pntd.0005103> PMID: 27814368
18. Collins CA, Olsen I, Zammit PS, Heslop L, Petrie A, Partridge TA, et al. Stem cell function, self-renewal, and behavioral heterogeneity of cells from the adult muscle satellite cell niche. *Cell*. 2005; 122(2):289–301. <https://doi.org/10.1016/j.cell.2005.05.010> PMID: 16051152
19. Caldwell C, Matthey D, Weller R. Role of the basement membrane in the regeneration of skeletal muscle. *Neuropathology and applied neurobiology*. 1990; 16(3):225–38. PMID: 2402330
20. Gutiérrez JMa, Ownby CL. Skeletal muscle degeneration induced by venom phospholipases A 2: insights into the mechanisms of local and systemic myotoxicity. *Toxicon*. 2003; 42(8):915–31. <https://doi.org/10.1016/j.toxicon.2003.11.005> PMID: 15019491
21. Ownby CL, Cameron D, Tu A. Isolation of myotoxic component from rattlesnake (*Crotalus viridis viridis*) venom. Electron microscopic analysis of muscle damage. *The American journal of pathology*. 1976; 85(1):149. PMID: 970437
22. Duchon L, Excell BJ, Patel R, Smith B. Changes in motor end-plates resulting from muscle fibre necrosis and regeneration: a light and electron microscopic study of the effects of the depolarizing fraction (cardiotoxin) of *Dendroaspis jamesoni* venom. *Journal of the neurological sciences*. 1974; 21(4):391–417. PMID: 4822123
23. Bjarnason JB, Fox JW. Hemorrhagic metalloproteinases from snake venoms. *Pharmacology & therapeutics*. 1994; 62(3):325–72.
24. Baldo C, Jamora C, Yamanouye N, Zorn TM, Moura-da-Silva AM. Mechanisms of vascular damage by hemorrhagic snake venom metalloproteinases: tissue distribution and in situ hydrolysis. *PLoS neglected tropical diseases*. 2010; 4(6):e727. <https://doi.org/10.1371/journal.pntd.0000727> PMID: 20614020
25. Pinto AF, Terra RM, Guimaraes JA, Fox JW. Mapping von Willebrand factor A domain binding sites on a snake venom metalloproteinase cysteine-rich domain. *Archives of biochemistry and biophysics*. 2007; 457(1):41–6. <https://doi.org/10.1016/j.abb.2006.10.010> PMID: 17118332
26. Fox JW, Serrano SMT. Structural considerations of the snake venom metalloproteinases, key members of the M12 repolysin family of metalloproteinases. *Toxicon*. 2005; 45(8):969–85. <https://doi.org/10.1016/j.toxicon.2005.02.012> PMID: 15922769
27. Clissa PB, Lopes-Ferreira M, Della-Casa MS, Farsky SHP, Moura-da-Silva AM. Importance of jararhagin disintegrin-like and cysteine-rich domains in the early events of local inflammatory response. *Toxicon*. 2006; 47(5):591–6. <https://doi.org/10.1016/j.toxicon.2006.02.001> PMID: 16564063
28. Ferreira BA, Deconte SR, de Moura FBR, Tomiosso TC, Clissa PB, Andrade SP, et al. Inflammation, angiogenesis and fibrogenesis are differentially modulated by distinct domains of the snake venom

- metalloproteinase jararhagin. *International Journal of Biological Macromolecules*. 2018; 119:1179–87. <https://doi.org/10.1016/j.ijbiomac.2018.08.051> PMID: 30102981
29. Siigur E, Tonismagi K, Trummel K, Samel M, Vija H, Subbi J, et al. Factor X activator from *Vipera lebetina* snake venom, molecular characterization and substrate specificity. *Biochimica et biophysica acta*. 2001; 1568(1):90–8. PMID: 11731090
30. Yamada D, Sekiya F, Morita T. Prothrombin and factor X activator activities in the venoms of viperidae snakes. *Toxicon*. 1997; 35(11):1581–9. PMID: 9428105
31. Gleason ML, Odell GV, Ownby CL. Isolation and biological activity of viriditoxin and a viriditoxin variant from *Crotalus viridis viridis* venoms. *Journal of Toxicology: Toxin Reviews*. 1983; 2(2):235–65.
32. Hernández R, Cabalceta C, Saravia-Otten P, Chaves A, Gutiérrez JM, Rucavado A. Poor regenerative outcome after skeletal muscle necrosis induced by *Bothrops asper* venom: alterations in microvasculature and nerves. *PLoS One*. 2011; 6(5):e19834. <https://doi.org/10.1371/journal.pone.0019834> PMID: 21629691
33. Vaiyapuri S, Hutchinson EG, Ali MS, Dannoura A, Stanley RG, Harrison RA, et al. Rhinocetin, a venom-derived integrin-specific antagonist inhibits collagen-induced platelet and endothelial cell functions. *Journal of Biological Chemistry*. 2012; 287(31):26235–44. <https://doi.org/10.1074/jbc.M112.381483> PMID: 22689571
34. Ravishankar D, Salamah M, Attina A, Pothi R, Vallance TM, Javed M, et al. Ruthenium-conjugated chrysin analogues modulate platelet activity, thrombus formation and haemostasis with enhanced efficacy. *Scientific reports*. 2017; 7(1):5738. <https://doi.org/10.1038/s41598-017-05936-3> PMID: 28720875
35. Vaiyapuri S, Roweth H, Ali MS, Unsworth AJ, Stainer AR, Flora GD, et al. Pharmacological actions of nobiletin in the modulation of platelet function. *British journal of pharmacology*. 2015; 172(16):4133–45. <https://doi.org/10.1111/bph.13191> PMID: 25988959
36. Vaiyapuri S, Sage T, Rana RH, Schenk MP, Ali MS, Unsworth AJ, et al. EphB2 regulates contact-dependent and independent signalling to control platelet function. *Blood*. 2014; blood-2014–06-585083.
37. Otto A, Schmidt C, Luke G, Allen S, Valasek P, Muntoni F, et al. Canonical Wnt signalling induces satellite-cell proliferation during adult skeletal muscle regeneration. *Journal of cell science*. 2008; 121(17):2939–50.
38. Masuda S, Hayashi H, Araki S. Two vascular apoptosis-inducing proteins from snake venom are members of the metalloprotease/disintegrin family. *European journal of biochemistry*. 1998; 253(1):36–41. PMID: 9578458
39. Allamand V, Briñas L, Richard P, Stojkovic T, Quijano-Roy S, Bonne G. ColVI myopathies: where do we stand, where do we go? *Skeletal muscle*. 2011; 1(1):30.
40. Igarashi T, Araki S, Mori H, Takeda S. Crystal structures of catrocollastatin/VAP2B reveal a dynamic, modular architecture of ADAM/adamalsin/reprolysin family proteins. *FEBS letters*. 2007; 581(13):2416–22. <https://doi.org/10.1016/j.febslet.2007.04.057> PMID: 17485084
41. Kikushima E, Nakamura S, Oshima Y, Shibuya T, Miao JY, Hayashi H, et al. Hemorrhagic activity of the vascular apoptosis-inducing proteins VAP1 and VAP2 from *Crotalus atrox*. *Toxicon*. 2008; 52(4):589–93. <https://doi.org/10.1016/j.toxicon.2008.06.027> PMID: 18657564
42. Zhou Q, Smith J, Grossman M. Molecular cloning and expression of catrocollastatin, a snake-venom protein from *Crotalus atrox* (western diamondback rattlesnake) which inhibits platelet adhesion to collagen. *Biochemical Journal*. 1995; 307(2):411–7.
43. De Luca M, Ward CM, Ohmori K, Andrews RK, Berndt MC. Jararhagin and jaracetin: novel snake venom inhibitors of the integrin collagen receptor, alpha 2 beta 1. *Biochemical and biophysical research communications*. 1995; 206(2):570–6. PMID: 7530003
44. Zhou Q, Smith JB, Grossman MH. Molecular cloning and expression of catrocollastatin, a snake-venom protein from *Crotalus atrox* (western diamondback rattlesnake) which inhibits platelet adhesion to collagen. *The Biochemical journal*. 1995; 307 (Pt 2):411–7.
45. Herrera C, Escalante T, Voisin M-B, Rucavado A, Morazán D, Macêdo JKA, et al. Tissue localization and extracellular matrix degradation by PI, PII and PIII snake venom metalloproteinases: clues on the mechanisms of venom-induced hemorrhage. *PLoS neglected tropical diseases*. 2015; 9(4):e0003731. <https://doi.org/10.1371/journal.pntd.0003731> PMID: 25909592
46. Moura-da-Silva AM, Ramos OH, Baldo C, Niland S, Hansen U, Ventura JS, et al. Collagen binding is a key factor for the hemorrhagic activity of snake venom metalloproteinases. *Biochimie*. 2008; 90(3):484–92. <https://doi.org/10.1016/j.biochi.2007.11.009> PMID: 18096518
47. Lomonte B, Gutiérrez J. Phospholipases A2 From Viperidae Snake Venoms: How do They Induce Skeletal Muscle Damage? 2011. 647–59 p. PMID: 24061112

48. Dubovskii PV, Utkin YN. Cobra cytotoxins: structural organization and antibacterial activity. *Acta naturae*. 2014; 6(3):11–8. PMID: [25349711](#)
49. O'Brien J, Lee S-H, Gutiérrez JM, Shea KJ. Engineered nanoparticles bind elapid snake venom toxins and inhibit venom-induced dermonecrosis. *PLoS neglected tropical diseases*. 2018; 12(10):e0006736–e. <https://doi.org/10.1371/journal.pntd.0006736> PMID: [30286075](#)
50. Gutiérrez JM, León G, Rojas G, Lomonte B, Rucavado A, Chaves F. Neutralization of local tissue damage induced by *Bothrops asper* (terciopelo) snake venom. *Toxicon*. 1998; 36(11):1529–38. PMID: [9792169](#)
51. Chen J, Liaw S, Bullard M, Chiu T. Treatment of poisonous snakebites in northern Taiwan. *Journal of the Formosan Medical Association = Taiwan yi zhi*. 2000; 99(2):135–9. PMID: [10770028](#)
52. Howes J-M, Theakston RDG, Laing G. Neutralization of the haemorrhagic activities of viperine snake venoms and venom metalloproteinases using synthetic peptide inhibitors and chelators. *Toxicon*. 2007; 49(5):734–9. <https://doi.org/10.1016/j.toxicon.2006.11.020> PMID: [17196631](#)
53. Rucavado A, Escalante T, Gutiérrez JMa. Effect of the metalloproteinase inhibitor batimastat in the systemic toxicity induced by *Bothrops asper* snake venom: understanding the role of metalloproteinases in envenomation. *Toxicon*. 2004; 43(4):417–24. <https://doi.org/10.1016/j.toxicon.2004.01.016> PMID: [15051405](#)
54. Ainsworth S, Slagboom J, Alomran N, Pla D, Alhamdi Y, King SI, et al. The paraspecific neutralisation of snake venom induced coagulopathy by antivenoms. *Communications Biology*. 2018; 1(1):34.

4.3 Effects of batimastat and marimastat on a group I metalloprotease from the venom of *Crotalus atrox*

Harry F. Williams¹, Harry J. Layfield¹, Divyashree Ravishankar¹, Thomas M. Vallance¹
Steven Trim² and Sakthivel Vaiyapuri¹

¹School of Pharmacy, University of Reading, Reading, United Kingdom

²Venomtech Private Limited, Sandwich, United Kingdom

In Preparation

Conclusion of this chapter

Some of the wide variety of complications involved in snakebite envenomings, including skeletal muscle damage caused by snake venom metalloproteases, could be inhibited using commercially available inhibitors. These inhibitors are able to completely inhibit snake venom metalloprotease activity *in vitro*, as are metal chelators. These potential future therapeutics do also have negative consequences however, affecting endogenous systems, so certainty (in the form of improved diagnostics) is essential when administering such potentially harmful drugs. Such diagnostical products do not currently exist however, an issue covered in the further chapters.

Contribution to this chapter

General contribution (65%)

- Study design
- Analysis and interpretation of data
- Writing of the manuscript
- Preparation of the figures
- Supervised or performed all experiments

Experimental contribution

Figure 1 A-G Supervised and oversaw all experimental work, prepared sample for mass spectrometry

Figure 2 A-D Carried out all functional assays, analysed data, prepared figures

Figure 3 A-D Supervised experiments, analysed data, prepared figure

Figure 4 A-F Supervised experiments, analysed data, prepared figure

Figure 5 A-D Supervised experiments, analysed data, prepared figure

Effects of batimastat and marimastat on a group I metalloprotease from the venom of *Crotalus atrox*

Harry F. Williams^{1#}, Harry J. Layfield^{1#}, Divyashree Ravishankar¹, Thomas M. Vallance¹, Kahdr Alatawi¹, Steven A. Trim², Andrew B. Bicknell³, Ketan Patel³ and Sakthivel Vaiyapuri^{1*}

¹School of Pharmacy, University of Reading, Reading, United Kingdom

²Venomtech Private Limited, Sandwich, United Kingdom

³School of Biological Sciences, University of Reading, Reading, United Kingdom

*Correspondence to: Dr Sakthivel Vaiyapuri, School of Pharmacy, University of Reading, Reading, RG6 6UB, UK. Email: s.vaiyapuri@reading.ac.uk

#Contributed equally to this paper.

Abstract: As a painful and expensive cause of death for over 100,000 people predominantly in developing countries, snakebite envenomation is one of the most lethal of the neglected tropical diseases. It is also associated with an incredibly complex pathophysiology due to the vast number of different proteins and peptides found in the 600 or more venomous snake species around the world. Here, we report the purification and characterisation of a group I metalloprotease (CA2) from the venom of the western diamondback rattlesnake, *Crotalus atrox* and its sensitivity to matrix metalloprotease inhibitors such as batimastat and marimastat. CA2 shows high sequence homology to atroxase from the venom of *C. atrox* and exhibits collagenolytic, fibrinogenolytic, haemolytic and cytotoxic activities. It delays blood clotting and exerts a mild inhibitory effect on agonist-induced platelet aggregation. Its collagenolytic activity is largely inhibited by batimastat and marimastat as well as zinc chloride, while being partially potentiated by calcium chloride. This study demonstrates the impact of matrix metalloprotease inhibitors in the modulation of group I snake venom metalloprotease activities compared to the whole venoms. Through improved understanding of each of the components found within snake venoms and their sensitivity to small molecule inhibitors, we can pave the way to the development of improved treatment strategies with reduced side effects for snakebite envenoming.

Keywords: *Crotalus atrox*; metalloprotease; snake venom; neglected tropical disease; rattlesnake; batimastat; marimastat

1. Introduction

In 2017, snakebite envenomation (SBE) was reinstated to the list of neglected tropical diseases by the World Health Organisation (WHO) [1-3]. SBE is estimated to occur in at least 1.8-2.7

million people worldwide per year, resulting in an estimated 80,000-137,000 deaths and 400,000 amputations per year [4-6]. The distribution of these fatalities is primarily located in rural tropical areas, including some of the world's poorest and most hospital deprived communities [2,7,8]. Prompt access to antivenom and appropriate medical facilities is crucial in order to protect the victims' lives and from extensive injuries caused by snakebites in their limbs. The currently used antivenom is considered to be less effective in accessing the affected local areas and preventing the venom-induced tissue damage. Hence, the development of small molecules that are able to neutralise the impact of venom components would be highly beneficial in treating SBE.

Snake venom is a complex mixture of bioactive proteins and peptides, which have evolved to assist in subduing and killing prey as quickly as possible, as well as having a secondary role in prey digestion [9]. The clinical effects of SBE range from mild local effects to more serious life threatening systemic complications depending on a variety of variables including the size, species and locality of snake [10,11], ontogeny [12,13], size and health of the victim and the total volume of venom injected [14]. Snake venoms are composed of both enzymatic and non-enzymatic components. The most abundant enzymatic components from viper venoms are the snake venom metalloproteases (SVMPs), serine proteases and phospholipase A₂ (PLA₂) [15]. Whereas non-enzymatic components include three finger toxins, C-type lectins and disintegrins amongst many others. The western diamondback rattlesnake, *Crotalus atrox* (*C. atrox*) is a Crotaline or pit viper that belongs to the genus *Crotalus*. This is known as an aggressive snake and likely to be responsible for the majority of SBE fatalities in Northern Mexico. *C. atrox* venom has an abundance of two major protein families; SVMPs and serine proteases, which account for approximately 69.5% of the total protein content found within the venom [16].

SVMPs are zinc-dependent enzymes that vary in molecular mass from approximately 20 kDa to 100 kDa and are responsible for the haemorrhagic effects characterised by envenomation from vipers [9,17]. SVMPs are classified into P-I to P-IV depending on their additional domains. The simplest class, P-I, contains only a metalloprotease domain; P-II contain a metalloprotease domain followed by a disintegrin domain. P-III consist of a metalloprotease domain, as well as disintegrin-like and cysteine-rich domains [18] and P-IV have the same groups as P-III along with two additional C-type lectin like domains (snaclecs). SVMPs are known to play multiple roles including the degradation of collagen, laminin, fibrinogen, certain receptors and the basement membrane of muscles and blood capillaries. Hence, better understanding of their broad spectrum of activities and sensitivity to small

molecule chemical inhibitors will aid in the development of improved therapeutic strategies for SBE or selectively for venom-induced tissue damage. Endogenous matrix metalloproteases (MMPs) also exist in humans and are involved in, amongst many other things, angiogenesis, via the degradation of vascular basement membrane and remodelling of the extracellular matrix [19]. This facilitation of angiogenesis has made MMPs a key target of inhibition in the treatment of certain cancers which rely on angiogenesis to proliferate [20]. Two such MMP inhibitors (MMPI), batimastat and marimastat, despite failing in clinical trials against cancer in the 90s, show some evidence of being effective inhibitors of SVMPs [21-24].

SVMPs in *C. atrox* venom account for 49.7% of total venom; which breaks down further to 22.4% PI- SVMP and 27.3% PIII-SVMP. In order to determine the therapeutic potential of batimastat and marimastat against P-I SVMPs, here, we report the purification and functional characterisation of a P-I SVMP with a molecular weight of around 23kDa from the venom of *C. atrox*. The purified protein was inhibited by batimastat and marimastat as well as the whole *C. atrox* venom. These data will lead to the further evaluation of these molecules against the broad spectrum of pathological effects induced by SVMPs and venoms in general.

2. Materials and Methods

2.1 Protein purification

Lyophilized *C. atrox* venom was purchased from Sigma Aldrich (UK). The lyophilized venom (50 mg) was dissolved in 1 mL of 20 mM TRIS.HCl (pH 7.6) and after centrifugation at 5000 rpm for 5 minutes the supernatant was applied to a 5 mL HiTrap™ Sepharose (SP) HP cation exchange chromatography column (GE Healthcare, UK) and fractionated using an Akta Purifier (GE Healthcare, UK). Fractions were collected at a rate of 1 mL/min using 20 mM TRIS.HCl pH 7.6 (Buffer A) and 20 mM TRIS.HCl pH 7.6 + 1 M NaCl (Buffer B) using a gradient reaching 60% buffer B over 20 minutes (gradient 20). UNICORN v3 software was used to run the Akta Purifier system. Fractions were immediately put on ice to prevent protein denaturation. A small aliquot was taken from each peak to undergo a Bradford protein assay and sodium dodecyl sulphate polyacrylamide gel electrophoresis (SDS-PAGE) analysis using standard protocols. The Bradford Protein assay was run according to the manufacturers protocol (ThermoScientific, USA). The intensity of the colour change from brown to blue was measured at 600 nm using an Emax spectrophotometer (Molecular Devices, UK). Bovine serum albumin (BSA) was used as standards. All fractions containing the target protein were pooled

together and concentrated using Vivaspin 6 Ultrafiltration tubes (Sartorius, UK). A size exclusion chromatography column (Superdex 75 100 cm) was used to separate the pooled sample of proteins. Fractions were collected at a rate of 1 mL/min using 20 mM TRIS.HCl (pH 7.6). As soon as protein peaks emerged (280 nm), they were immediately placed on ice to prevent protein denaturation. SDS-PAGE was again used to analyse the fractions and those containing the purified protein of interest were again pooled and concentrated before storing at -80°C before further use.

2.2 SDS-PAGE

SDS-PAGE was used to analyse the proteins contained within each 1 mL fraction that was collected from columns. Proteins were denatured using reducing sample treatment buffer (RSTB) [10% (w/v) SDS, 10% (v/v) β -mercaptoethanol, 1% (w/v) bromophenol blue, 50% (v/v) glycerol and stacking buffer, nanopure water] and heated at 90°C for 10 minutes. Samples were loaded (30 μ L) into precast gradient (4-15%) Mini-PROTEAN® TGX™ gels (Biorad, UK) alongside the dual colour protein ladder (Precision Plus Biorad, UK) and resolved using a Mini-Protean II apparatus (Biorad, UK). Gels were immersed in a staining solution [0.1% (w/v) Coomassie Brilliant blue R250 (ThermoScientific, UK), 10% (v/v) acetic acid, 40% (v/v) methanol and 50% (v/v) deionized water] for 1 hour on a plate shaker, washed 3x with deionised H₂O for 5 minutes and destained [10% (v/v) acetic acid, 40% (v/v) methanol and 50% deionized water] for 3 hours or until protein bands became clear.

2.3 Fluorogenic assays

Metalloprotease activity was analysed using the fluorogenic substrate, DQ™ gelatin (ThermoScientific, UK). A range of concentrations of CA2 (1, 2, 5, 10 and 15 μ g/mL) were added to a black 96 well-plate in triplicate along with PBS as a negative control and whole *C. atrox* venom as a positive control. The DQ gelatin (10 μ g/mL in PBS) was added to each well. The 96-well plate was placed on a plate shaker for five minutes, incubated and read at 10, 30, 60 and 120 minutes using a FLUOstar OPTIMA (BMG Labtech, Germany) spectrofluorimeter. Metalloprotease activity was measured at an excitation wavelength of 485 nm and emission wavelength of 520 nm. In addition to testing for metalloprotease activity, effect of treatment with marimastat, batimastat, zinc chloride and calcium chlorides (12.5, 25, 50 and 200 μ M) as well as EDTA at three concentrations (25, 50 and 200 μ M), were also analysed using the same method and a fixed concentration of 2 μ g/mL of CA2.

To determine PLA₂ activity an EnzChek™ Phospholipase A2 Assay Kit (ThermoFisher Scientific, UK) was used in accordance to the manufacturer's instructions. CA2 was diluted to 2 µg/mL in PBS and treated in duplicate with chlorides MMP inhibitors and EDTA in 96 well black plates and incubated at 37°C. Readings were taken after 10, 30 and 60 minutes of incubation by FLUOstar OPTIMA (BMG Labtech, Germany) spectrofluorimeter using an excitation wavelength of 485 nm and emission wavelength of 520 nm.

2.4 Mass Spectrometry analysis

CA2 was subject to tryptic digestion and mass spectrometry using a gel slice containing the purified CA2 from SDS-PAGE and was analysed by Alta Bioscience (Birmingham, UK). The trypsin digestion was performed using 10 µL of sample (purified protein band from SDS-PAGE) and 40 µL of 100 mM ammonium bicarbonate (pH 8), added to 50 µL of 10 mM dithiothreitol (DTT) and incubated at 56°C for 30 minutes. The sample was then cooled to room temperature and cysteines alkylated with the addition of 50 µL 50 mM iodoacetamide and mixed and incubated at room temperature in the dark for 30 minutes. 25 µL of trypsin gold (Promega, Southampton, Hampshire, UK, 6 ng/µL) was subsequently added to the sample and left to incubate overnight at 37°C overnight. An UltiMate® 3000 HPLC series (Dionex, Sunnyvale, CA USA) was used for peptide separation and concentration. Samples were trapped on uPrecolumn Cartridge Acclaim PepMap 100 C18, 5 µM, 100A 300µm i.d. x 5mm (Dionex, Sunnyvale, CA USA) and separated in Nano Series™ Standard Columns 75 µm i.d. x 15 cm, packed with C18 PepMap100, 3 µm, 100Å (Dionex, Sunnyvale, CA USA). A gradient from 3.2% to 44% solvent B (0.1% formic acid in acetonitrile) for 30 minutes was used. Peptides were eluted directly (~ 300 nL min⁻¹) via a Triversa Nanomate nanospray source (Advion Biosciences, NY) into an LTQ Orbitrap Elite mass spectrometer (ThermoFisher Scientific, Germany). The mass spectrometer alternated between a full FT-MS scan (m/z 380 – 1800) and subsequent collision-induced dissociation (CID) MS/MS scans of the eight most abundant ions. The data-dependent scanning acquisition was controlled by Xcalibur 2.1 software. Survey scans were acquired in the Orbitrap at a resolution of 120,000 at m/z 400 and automatic gain control (AGC) 1 x 10⁶. Precursor ions were isolated and subjected to CID in the linear ion trap with AGC 1 x 10⁵. Collision activation for the experiment was performed in the linear trap using helium gas at normalized collision energy to precursor m/z of 35% and activation Q 0.25. The precursor isolation window was 2 m/z and only multiply-charged precursor ions were selected for MS/MS. MS and MS/MS scans were cross

referenced against the Uniprot database using Sequest algorithm (Thermo fisher PD 1.4). Variable modifications were deamidated (N and Q), oxidation (M) and phosphorylation (S, T and Y). Carbamidomethyl (C) modification was for fixed modification. The precursor mass tolerance was 10 ppm and the MS/MS mass tolerance was 0.8 Da. Two missed cleavage was allowed and were accepted as a real hit protein with at least two high confidence peptides.

2.5 Fibrinogenolytic assay

A solution containing CA2 (0.1 mg/mL) or venom (0.1mg/mL), fibrinogen (1 mg/mL) and PBS was prepared and incubated at 37°C. Samples (50 μ L) were taken at time intervals of 0, 10, 30 and 60 minutes and then again after 12 hours and immediately mixed with 25 μ L of RSTB before dry boiling at 90°C for 10 minutes. Each sample was then analysed by SDS-PAGE to determine their digestion pattern.

2.6 Human blood collection and platelet preparation

Blood samples from healthy volunteers were obtained in accordance to the approved procedures by the University of Reading Research Ethics Committee and the platelets were prepared as described previously [25,26]. Blood was collected using venipuncture into vacutainers containing 3.2% (w/v) citrate. For the preparation of platelet-rich-plasma (PRP), blood samples were centrifuged at 102 RCF for 20 minutes at 20 °C. PRP was rested for 30 minutes before use at 30 °C in a water bath (Clifton, UK) in a 50 mL falcon tube. For isolated/washed platelets (WP), the PRP was carefully retrieved from the LP4 tubes using a transfer pipette and placed into a 50 mL falcon tube, after adding 3 mL acid citrate dextrose (ACD, sodium citrate 2.5% (w/v), 2% glucose, 1.5% citric acid) and 10 μ L prostacyclin (PG12, stock 125 μ g/mL in Ethanol) and mixed gently by inversion and centrifuged at 1413 RCF. After this 1 mL of modified tyrodes-HEPES buffer (with 5 mM glucose) and 150 μ L of ACD was added to the platelet pellet which was then resuspended with 24 mL of 37°C tyrodes. A further 3 mL ACD and 10 μ L prostacyclin was added and the falcon tube gently inverted. Finally, the platelets were spun once more at 1413 RCF for 10 minutes at 20 °C, the supernatant was discarded, and the platelets were resuspended in modified tyrodes-HEPES buffer. Platelet-poor plasma (PPP) was obtained by centrifuging PRP at 1413 RCF for 10 minutes.

2.7 Platelet aggregation

A stock solution of 0.5 µg/mL cross-linked collagen-related peptide [CRP-XL, from Professor Richard Farndale (University of Cambridge, UK)] was used as a positive control and PBS as a negative control in platelet aggregation assays using an optical aggregometer (Chrono-log model 700). Two concentrations of CA2 and venom (3 and 10 µg/mL) were tested from three separate donors. After incubating the platelets with CA2/venom for five minutes, CRP-XL was added and aggregation traces were used to calculate inhibition.

2.8 Haemolytic Assay

Human erythrocytes were collected from the dense red blood cells found in the bottom of vacutainers following centrifugation for collection of PRP. These erythrocytes were then mixed with an equal volume of PBS, mixed and centrifuged at 1413 RCF for 2 minutes, the supernatant was discarded. This was repeated three times. Haemolytic activity was measured using these washed human erythrocytes (10%) suspended in PBS. The erythrocytes were then treated with 2.5 µg/mL of CA2 or the whole venom. Triton X-100 detergent (1%) was used as a positive control and PBS as a negative control. Samples were centrifuged at 1413 RCF for two minutes and 50 µL of supernatant was dispensed into a 96-well plate and the absorbance (at 540 nm) was measured using a spectrophotometer (Emax precision plate reader, UK). Samples from the erythrocyte CA2/venom mixtures were incubated at 37°C and haemolysis was measured after 6, 12, 24 and 48 hours.

2.9 Blood clotting assay

Untreated (without any anti-coagulants) whole human blood was mixed with CA2, whole venom or PBS in glass cuvettes. The solutions were then gently mixed once a minute until clotting was apparent. This was again done in three donors.

2.10 Lactate Dehydrogenase (LDH) cytotoxicity assay

An LDH cytotoxicity assay was used to determine whether CA2 had any cytotoxic effects on platelets. An LDH Cytotoxicity Assay Kit (ThermoFisher UK) was used in accordance to the manufacturer's instructions. Briefly, human PRP was incubated at 37°C for 30 minutes prior to incubation with different concentrations of venom protein or a vehicle control (deionised water) for five minutes. The substrate mix from the kit was added to the platelets and incubated for another 30 minutes and subsequently stopped using the stop solution provided. Absorbance was read at 490 nm

and 650 nm using Fluostar Optima s (BMG Labtech, Germany) Spectrofluorimeter. Absorbance was measured in triplicates using platelets obtained from three individual donors.

2.16 Statistical analysis

All statistical analysis was performed using GraphPad Prism V.7.00 statistical software.

3. Results

3.1 Purification of P-I SVMP

With the aim of purifying a P-I SVMP from *C. atrox* venom, we deployed a two-dimensional chromatography approach. Initially, 50 mg of whole *C. atrox* venom was applied to a cation-exchange (HiTrap, SP HP) chromatography column (Figure 1A). Following the analysis of acquired fractions by SDS-PAGE (Figure 1B), the fractions containing a protein of semi-purified protein of approximately the correct (23kDa) molecular weight (6-9) were further separated by gel filtration (Superdex-75) chromatography (Figure 1C). The selected fractions were analysed by SDS-PAGE (Figure 1D) and fractions with the protein of interest (67-70) were further run through the same gel filtration column to remove any impurities (Figure 1E-F). After these three stages of chromatography, a pure protein with a molecular weight of approximately 23 kDa was isolated (fractions 74-77) which we henceforth refer to as CA2 (denoting the second SVMP that we have isolated from the venom of *C. atrox*).

3.2 Mass spectrometry of CA2

The purified protein was then analysed by mass spectrometry using the peptides resulting from tryptic digestion (Figure 1G). Mascot analysis of the sequences confirmed the high sequence similarity (52.2% coverage) of isolated protein to atroxase, a 23kDa SVMP from the venom of *C. atrox* [27]. Although CA2 is likely to be atroxase, we are unable to conclude this in the absence of complete sequence for CA2. However, these data confirm that the purified protein is an SVMP with a molecular weight of 23kDa, and therefore is highly likely to be a P-I SVMP similar or identical to atroxase.

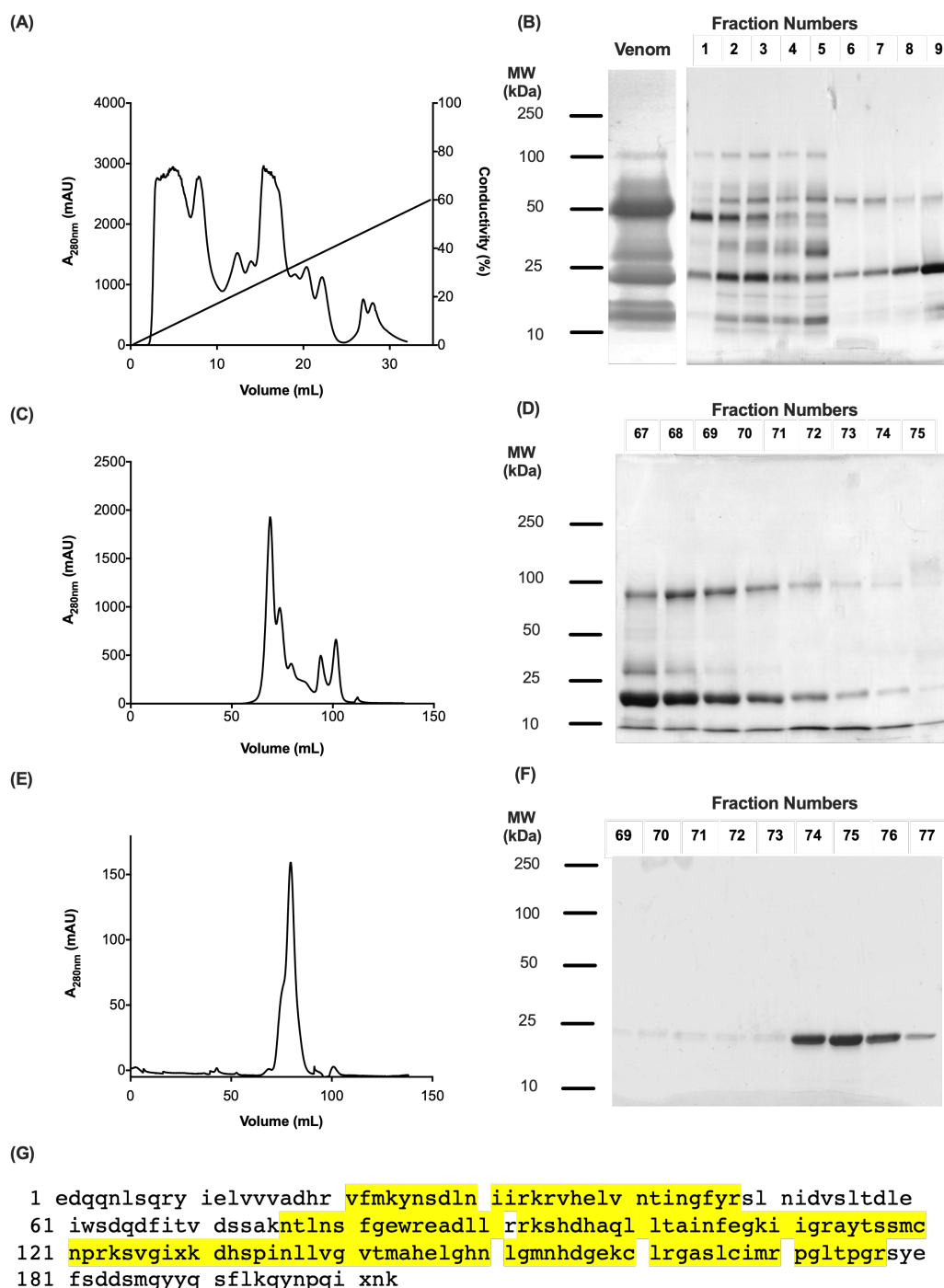


Figure 1. Purification and characterisation of CA2. A, 50 mg of whole *C. atrox* venom was fractionated using a cation exchange column chromatography and the collected fractions were analysed by SDS-PAGE (B). C, a chromatogram showing the gel filtration chromatography of fractions 6 to 9 collected from the cation exchange column. D, SDS-PAGE analysis of fractions resulting from the gel filtration chromatography. E, the chromatogram from the second run of gel filtration chromatography for selected fractions from the previous step, and SDS-PAGE analysis showing the purified protein (F). G, tryptic digested peptides from the purified protein were analysed by mass spectrometry and found to show 52.2% similarity to atroxase (mass spectrometry-identified peptide sequences are shown in yellow).

3.3 Fibrinogenolytic and collagenolytic activities of CA2

A range of functional assays were employed to determine the functions of CA2 compared to the whole venom. Fluorogenic substrates were used to assess the ability for CA2 to digest gelatin (polymerised collagen) (Figure 2A & B) and a PLA₂-specific substrate (Figure 2C). CA2 exhibited strong collagenolytic activity and no PLA₂ activity. This data suggests that CA2 is an SVMP and free of enzymatic PLA₂ impurities. One of the natural substrates for SVMPs, fibrinogen, was also incubated with CA2, before the digestion pattern was analysed by SDS-PAGE (Figure 2D). The results showed high specificity for the A α chain of fibrinogen, digesting this within 10 minutes although over a longer time CA2 also began to degrade the B β band and γ bands.

3.5 CA2 exerts cytotoxic activity

In order to assess whether CA2 has any cytotoxic effects on different cell types, we performed LDH cytotoxicity assays using platelets, whole blood and erythrocytes. Using the production of lactate dehydrogenase as a marker for platelet cytotoxicity, we found CA2 to be cytotoxic to platelets only at the highest concentration tested, 12.5 μ g/mL (Figure 2E), similarly it caused mild haemolysis but only after five hours of incubation at 2.5 μ g/mL (Figure 2F). This suggests it is able to cleave some element of the plasma membrane causing cell lysis.

3.4 Batimastat and marimastat inhibit CA2

After confirming that CA2 is an SVMP, we utilised MMPi, batimastat and marimastat to deduce the inhibitory properties of these compounds on CA2. We used the fluorogenic substrate, DQ gelatin, to analyse whether these compounds reduce the SVMP activity of CA2. Marimastat (Figure 3A & B) and batimastat (Figure 3C & D) caused almost complete inhibition of SVMP activity of both the whole *C. atrox* venom and CA2.

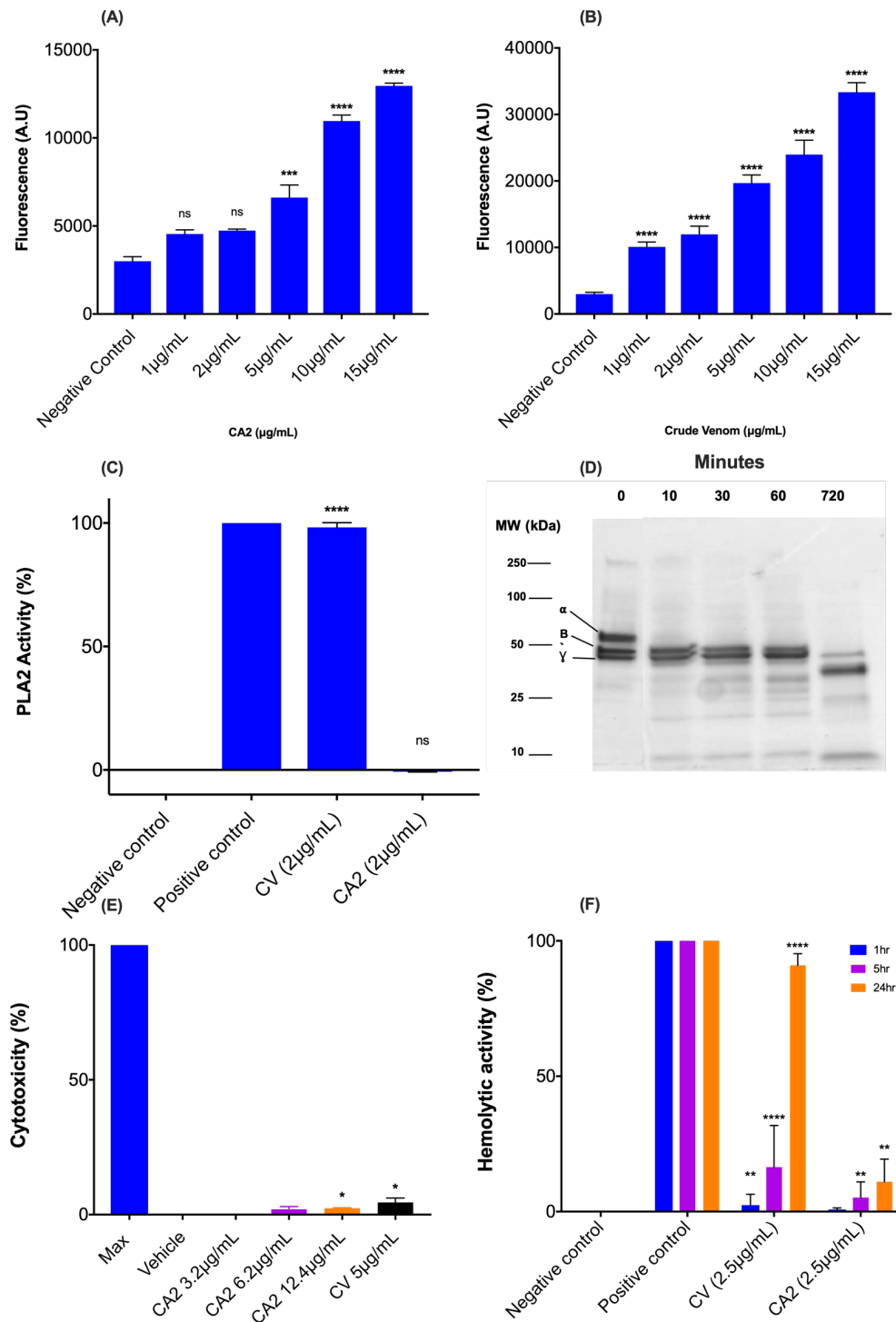


Figure 2. Functional characterisation of CA2. The SVMP activity of purified SVMP, CA2 (A) or the crude/whole venom (B) using a fluorogenic substrate, DQ gelatin. PLA₂ activity of whole venom (CV), bee venom (positive control) and CA2 using enzcheck PLA₂ substrate (C). D, SDS-page analysis of fibrinogen digestion by CA2 from 0 – 720 minutes. The cytotoxicity (E) of CA2 and whole venom as found via the measurement of lactate dehydrogenase release and ability for CA2 and whole venom to lyse red blood cells (F). Data were analysed in Graphpad Prism and represent mean \pm S.D. (n=3). The P-values shown are as calculated using one-way ANOVA followed by Tukey's post hoc multiple comparisons test. For this, the proteins were compared to negative control values, and all the values were normalised using a blank and positive control. (*P \leq 0.05, ** P \leq 0.01, *** P \leq 0.001 and **** P \leq 0.0001).

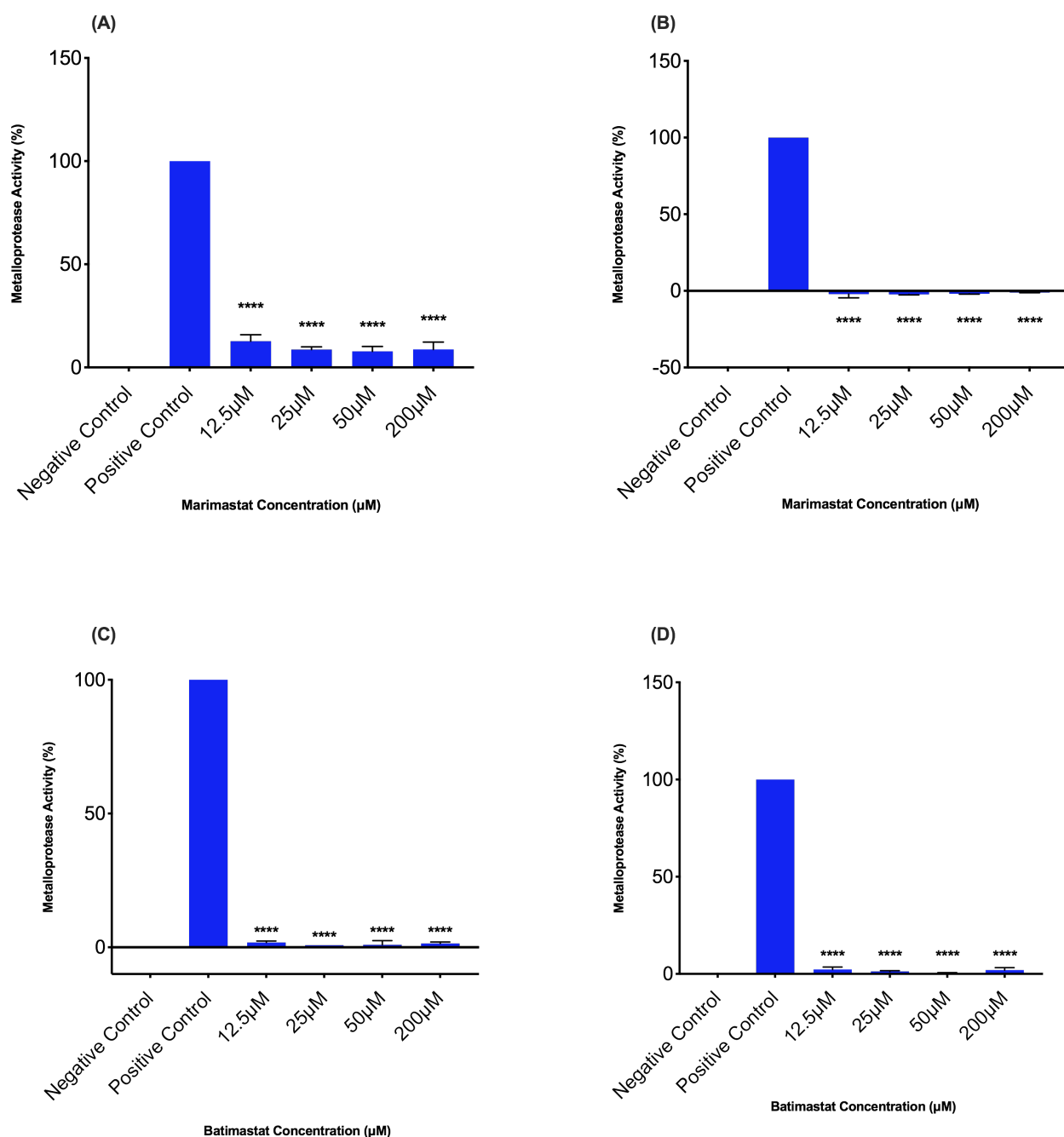


Figure 3. Effect of matrix metalloprotease inhibitors on collagenolytic activity of CA2 and whole venom. The inhibitory effect of marimastat on CA2 (A) or whole venom (B) and batimastat on CA2 (C) and whole venom (D), the protein or venom were treated with the inhibitors before the addition of a fluorogenic substrate, DQ-gelatin. Data were analysed in Graphpad Prism and represent mean \pm S.D. (n=3). The P-values shown are as calculated using one-way ANOVA followed by Tukey's post hoc multiple comparisons test. For this, the proteins were compared to positive control values, and all the values were normalised using negative and positive controls. (* $P \leq 0.05$, ** $P \leq 0.01$, *** $P \leq 0.001$ and **** $P \leq 0.0001$).

3.6 Chlorides have differing effects on metalloprotease activity

As zinc-dependent proteases rely heavily on free calcium for catalysis, metal chlorides can affect their ability to cleave a substrate. Varied concentrations of both zinc and calcium chloride were utilised to assess how they would modulate the SVMP activities of CA2 and whole venom. It was found that while zinc chloride significantly reduced the SVMP activity seen in both the whole venom and CA2 (Figure 4A & 4B), calcium chloride potentiated their SVMP activities (Figure 4C & 4D). These data confirm that CA2 is an SVMP which is relying on calcium ions for their activity.

3.7 Metal chelators inhibit the activity of CA2

A metal chelator (EDTA) was then employed to assess its ability to inhibit the activities of the SVMPs present in whole venom as well as CA2. The fluorogenic assay described previously for SVMPs was performed with the addition of ethylenediaminetetraceticacid (EDTA - a divalent cationic chelator) in order to determine its impact on CA2 activity. The metalloprotease activity of both whole venom and CA2 was strongly inhibited by EDTA (Figure 4E & 4F). These data corroborate this enzyme as a metalloprotease, given EDTA is a metal chelator and would inhibit via the chelation of zinc found in SVMPs which is essential to their catalytic activity.

3.8 CA2 inhibits platelet aggregation

Platelets were isolated from fresh human whole blood in the forms of platelet rich plasma and isolated platelets. These two preparations allowed us to see the effects of CA2 on platelets both directly, using isolated platelets and any indirect effects that could be a result of the enzyme on other plasma proteins using platelet-rich plasma. In platelet-rich plasma CA2 had little or no effect (Figure 5B) but in washed platelets CA2 had a statistically significant inhibitory effect (Figure 5A). The whole venom caused a strong activation in isolated platelets (Figure 5C) which was lesser in PRP (Figure 5D). The activation could be the result of cell lysis while the inhibition is likely to be a result of cleavage of membrane proteins.

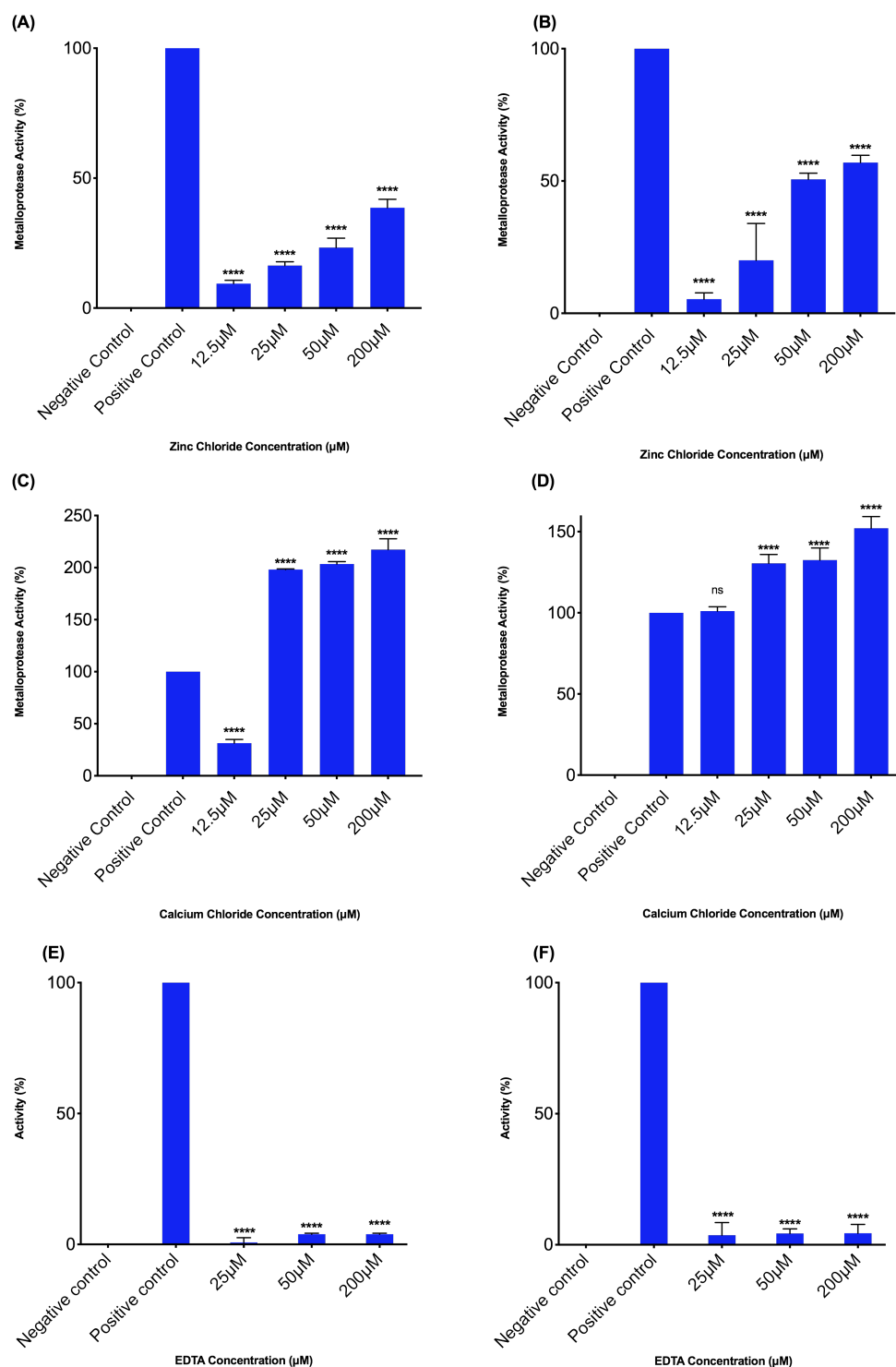


Figure 4. Effects of chlorides and a chelator on whole venom and CA2. Two chlorides, zinc chloride [on CA2 (A) whole venom (B)] and calcium chloride [on CA2 (C) or whole venom (D)] were used to assess their inhibitory or potentiatory effects as well as a metal chelator, EDTA [on CA2 (E) whole venom (F)]. Data were analysed in Graphpad Prism and represent mean \pm S.D. (n=3). The P-values shown are as calculated using one-way ANOVA followed by Tukey's post hoc multiple comparisons test. For this, the proteins were compared to positive control values, and all the values were normalised using negative and positive controls. (* $P \leq 0.05$, ** $P \leq 0.01$, *** $P \leq 0.001$ and **** $P \leq 0.0001$).

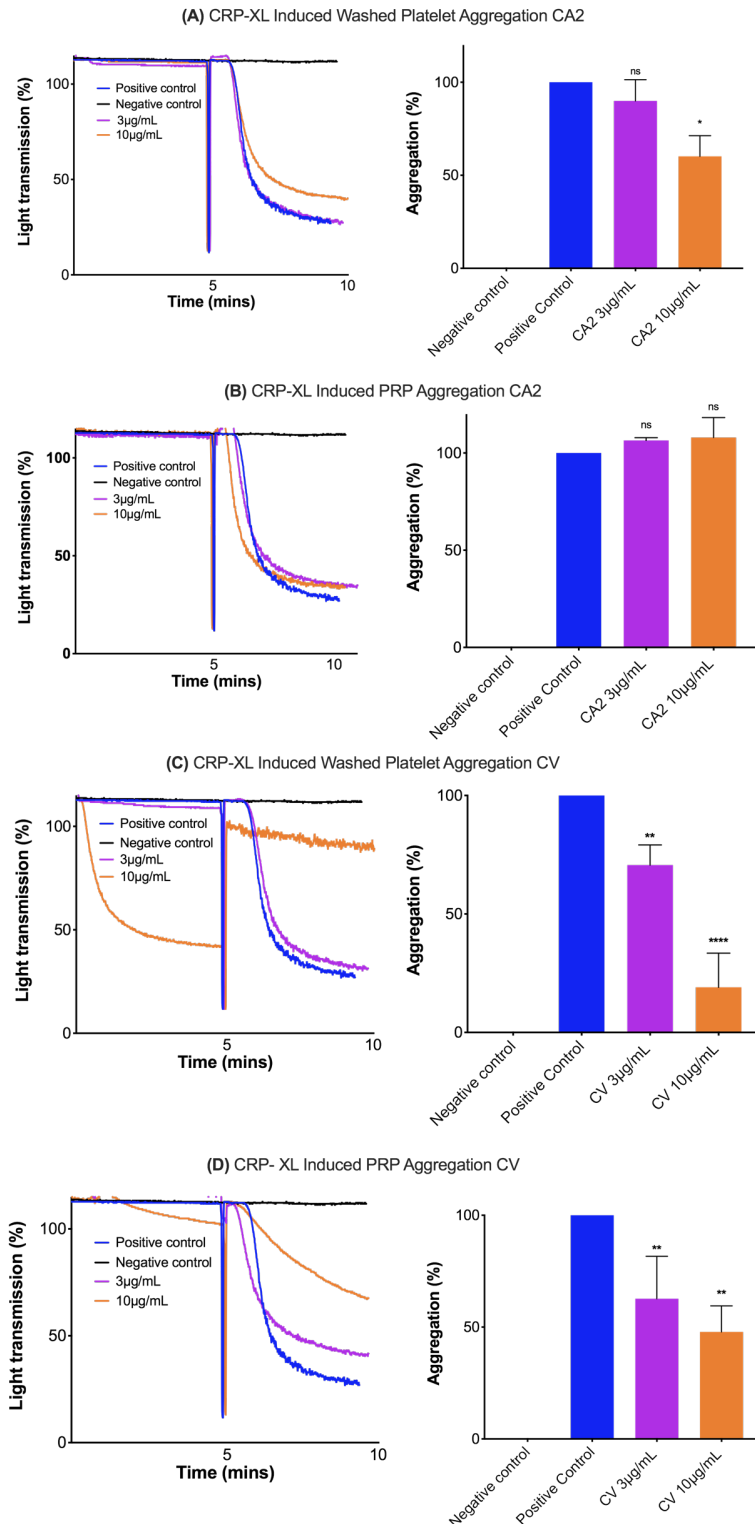


Figure 5. Effects of CA2 on platelets. The effect of CA2 on washed platelets (A) and platelet rich plasma (B) and whole venom on washed platelets (C) and platelet rich plasma (D). Representative aggregation traces and data demonstrate the impact of CA2 on cross-linked collagen related peptide (CRP-XL)-induced human platelet aggregation. Data were analysed in graphpad prism and represent mean \pm S.D. ($n = 3$). The p values shown are as calculated by One-way ANOVA followed by post hoc Tukey's test using GraphPad Prism (* $P \leq 0.05$, ** $P \leq 0.01$, *** $P \leq 0.001$ and **** $P \leq 0.0001$).

4. Discussion

SVMPs play important roles in the overall pathophysiology of viper envenoming by inducing local and systematic haemorrhage along with tissue damage, which is primarily attributed to their potential to degrade BM components in blood capillaries [28-31]. SVMPs activate two key coagulation factors; Factor X and prothrombin to exhibit their procoagulant effects [9,17,29-33]. SVMPs exhibit activities through activation of zymogens, coagulation factors and precursors of integrins or receptors [29], rendering blood uncoagulable [34]. This is due to their ability to cleave fibrinogen into fibrinopeptides without the induction of clotting [35]. The venom contains two different types of fibrinogenolytic enzymes; those that cleave the A α chain of fibrinogen and those which cleave both the A α and the B β chain [34,36]. The time course assay illustrated that CA2 primarily cleaved the A α chain, and cleavage of the B β chain occurred much more slowly (30 minutes later), whilst the γ chain remained almost intact (Figure 2D).

Given that SVMPs both directly [37] and indirectly [38] mediate local tissue damage, inhibition of these enzymes would reduce the local tissue damage typically associated with viper bites [28]. CA2 was treated with commercially available matrix metalloproteinase inhibitors (MMPi), batimastat and marimastat, which have already had promising research done into their use *in vivo* for snakebite envenomation [22-24]. Figure 3 (A-D) show both whole venom and CA2 enzyme activity were almost entirely inhibited when subjected to the MMPi. There is a high degree of structural and functional homology between SVMPs and their matrix-based relatives (MMPs) [28]. This suggests that substrate/inhibitor interactions between these subfamilies are likely to be analogous [28]. Marimastat is a hydroxamic acid derivative designed to exert broad-range MMP inhibition by mimicking the cleavage site of collagen substrates [28]. Although these MMPi's are likely to inhibit all SVMP domains, the additional domains found in P-II, P-III and P-IV SVMPs could potentially be unaffected despite inhibition of the protease domain, they may continue to exert anti-platelet or other effects. Antivenom on the other hand is likely to contain antibodies capable of binding all of these domains as well as the metalloprotease domain. Antivenom is made up of large immunoglobulins which, even when administered rapidly, struggle to reach the local bite-site in time to prevent tissue damage. Multiple injections of these smaller MMPi have been suggested [39], however the repercussions from inhibiting MMPs occurring naturally in the body are yet to be fully elucidated although effects on angiogenesis and vascular growth are to be expected [40].

SVMPs are zinc-containing endopeptidases [28] that are dependent on the presence of zinc [41] and calcium ions [42] to ensure enzymatic activity and stability as shown in Figure 4C-4F. The use of EDTA showed this metal chelator can abrogate entirely the collagenolytic activity of these enzymes (Figure 4A-4B), though the use of such broad-range metal chelators *in vivo* raises questions as to unwanted effects on endogenous metal-dependent physiology. Both whole venom and CA2 demonstrated a haemolytic effect on red blood cells (Figure 2F). It is likely that the mechanism of action for haemolysis for whole venom is similar to other species of *Crotalidae* and largely PLA₂ dependent [43], though SVMPs have the potential to lyse red blood cells via the hydrolysis of the many membrane proteins responsible for transport and adhesion of the cell, or somehow interacting with the underlying skeletal proteins such as spectrin [44].

The purification and characterisation of CA2 further demonstrates the breadth of SVMPs inhibited by MMPis and EDTA. The reality of their use on victims of SBE and the long-term damage associated with their use is yet to be elucidated, but with frequent amputations and long-term muscle damage as a result of viper bites it seems likely these small molecular therapeutics (SMT) are the lesser of two evils. The development of a drug able to inhibit SVMPs while leaving endogenous MMPs to function is the long term goal, but such specificity is likely to take time and amputations are occurring on a daily basis [45]. If morbidity is to be reduced to the same extent as the WHO intend to reduce mortality, SVMPs are a target in need of immediate inhibition [46]. The purification of individual venom components allows us to see their unadulterated effect and by comparison to the whole venom, this study somewhat highlights the contradictory nature of venoms; with CA2 inhibiting platelet aggregation while whole venom activates, or lyses platelets. In order to fully disentangle the web of effects that is found within a venom, each thread must first be understood. This study showed that the major P-I SVMP in *C. atrox*, has a range of effects, including inhibition of platelets and proteolytic effects, all of which are likely to be prevented by the SMTs currently being discussed as an adjunctive treatment for SBE [47].

Acknowledgments: This work received no external funding.

References

1. Hifumi, T.; Sakai, A.; Kondo, Y.; Yamamoto, A.; Morine, N.; Ato, M.; Shibayama, K.; Umezawa, K.; Kiri, N.; Kato, H., et al. Venomous snake bites: clinical diagnosis

- and treatment. *Journal of Intensive Care* **2015**, 3, 16, doi:10.1186/s40560-015-0081-8.
2. Williams, D.; Gutierrez, J.M.; Harrison, R.; Warrell, D.A.; White, J.; Winkel, K.D.; Gopalakrishnakone, P.; Global Snake Bite Initiative Working, G.; International Society on, T. The Global Snake Bite Initiative: an antidote for snake bite. *Lancet* **2010**, 375, 89-91, doi:10.1016/S0140-6736(09)61159-4.
 3. WHO. Neglected tropical diseases. Available online: http://www.who.int/neglected_diseases/diseases/en/ (accessed on
 4. White, J. Bites and Stings From Venomous Animals: A Global Overview. *Therapeutic Drug Monitoring* **2000**, 22, 65-68.
 5. Williams, D.; Gutiérrez, J.M.; Harrison, R.; Warrell, D.A.; White, J.; Winkel, K.D.; Gopalakrishnakone, P. The Global Snake Bite Initiative: an antidote for snake bite. *The Lancet* **2010**, 375, 89-91, doi:[https://doi.org/10.1016/S0140-6736\(09\)61159-4](https://doi.org/10.1016/S0140-6736(09)61159-4).
 6. Kasturiratne, A.; Wickremasinghe, A.R.; de Silva, N.; Gunawardena, N.K.; Pathmeswaran, A.; Premaratna, R.; Savioli, L.; Lalloo, D.G.; de Silva, H.J. The Global Burden of Snakebite: A Literature Analysis and Modelling Based on Regional Estimates of Envenoming and Deaths. *PLOS Medicine* **2008**, 5, e218, doi:10.1371/journal.pmed.0050218.
 7. Williams, H.F.; Vaiyapuri, R.; Gajjeraman, P.; Hutchinson, G.; Gibbins, J.M.; Bicknell, A.B.; Vaiyapuri, S. Challenges in diagnosing and treating snakebites in a rural population of Tamil Nadu, India: The views of clinicians. *Toxicon* **2017**, 130, 44-46.
 8. Vaiyapuri, S.; Vaiyapuri, R.; Ashokan, R.; Ramasamy, K.; Nattamaisundar, K.; Jeyaraj, A.; Chandran, V.; Gajjeraman, P.; Baksh, M.F.; Gibbins, J.M. Snakebite and its socio-economic impact on the rural population of Tamil Nadu, India. *PloS one* **2013**, 8, e80090.
 9. Takeda, S.; Takeya, H.; Iwanaga, S. Snake venom metalloproteinases: Structure, function and relevance to the mammalian ADAM/ADAMTS family proteins. *Biochimica et Biophysica Acta (BBA) - Proteins and Proteomics* **2012**, 1824, 164-176, doi:<https://doi.org/10.1016/j.bbapap.2011.04.009>.
 10. Sunagar, K.; Undheim, E.A.B.; Scheib, H.; Gren, E.C.K.; Cochran, C.; Person, C.E.; Koludarov, I.; Kelln, W.; Hayes, W.K.; King, G.F., et al. Intraspecific venom variation in the medically significant Southern Pacific Rattlesnake (*Crotalus oreganus helleri*): Biodiscovery, clinical and evolutionary implications. *Journal of Proteomics* **2014**, 99, 68-83, doi:<https://doi.org/10.1016/j.jprot.2014.01.013>.
 11. Fry, B.G.; Winkel, K.D.; Wickramaratna, J.C.; Hodgson, W.C.; Wüster, W. Effectiveness of snake antivenom: species and regional venom variation and its clinical impact. *Journal of Toxicology: Toxin Reviews* **2003**, 22, 23-34.
 12. Pla, D.; Sanz, L.; Sasa, M.; Acevedo, M.E.; Dwyer, Q.; Durban, J.; Pérez, A.; Rodriguez, Y.; Lomonte, B.; Calvete, J.J. Proteomic analysis of venom variability and ontogeny across the arboreal palm-pitvipers (genus *Bothriechis*). *Journal of Proteomics* **2017**, 152, 1-12, doi:<https://doi.org/10.1016/j.jprot.2016.10.006>.

13. Modahl, C.M.; Mukherjee, A.K.; Mackessy, S.P. An analysis of venom ontogeny and prey-specific toxicity in the Monocled Cobra (*Naja kaouthia*). *Toxicon* **2016**, *119*, 8-20.
14. Juckett, G.; Hancox, J.G. Venomous snakebites in the United States: management review and update. *American family physician* **2002**, *65*, 1367-1374.
15. Williams, H.F.; Layfield, H.J.; Vallance, T.; Patel, K.; Bicknell, A.B.; Trim, S.A.; Vaiyapuri, S. The Urgent Need to Develop Novel Strategies for the Diagnosis and Treatment of Snakebites. *Toxins* **2019**, *11*, 363.
16. Calvete, J.J.; Fasoli, E.; Sanz, L.; Boschetti, E.; Righetti, P.G. Exploring the venom proteome of the western diamondback rattlesnake, *Crotalus atrox*, via snake venomomics and combinatorial peptide ligand library approaches. *Journal of proteome research* **2009**, *8*, 3055-3067.
17. Gutiérrez, J.M.; Rucavado, A. Snake venom metalloproteinases: Their role in the pathogenesis of local tissue damage. *Biochimie* **2000**, *82*, 841-850, doi:[https://doi.org/10.1016/S0300-9084\(00\)01163-9](https://doi.org/10.1016/S0300-9084(00)01163-9).
18. Fox, J.W.; Serrano, S.M.T. Structural considerations of the snake venom metalloproteinases, key members of the M12 repolysin family of metalloproteinases. *Toxicon* **2005**, *45*, 969-985, doi:<https://doi.org/10.1016/j.toxicon.2005.02.012>.
19. Rundhaug, J.E. Matrix metalloproteinases and angiogenesis. *Journal of cellular and molecular medicine* **2005**, *9*, 267-285.
20. Jabłońska-Trypuć, A.; Matejczyk, M.; Rosochacki, S. Matrix metalloproteinases (MMPs), the main extracellular matrix (ECM) enzymes in collagen degradation, as a target for anticancer drugs. *Journal of enzyme inhibition and medicinal chemistry* **2016**, *31*, 177-183.
21. Arias, A.S.; Rucavado, A.; Gutiérrez, J.M. Peptidomimetic hydroxamate metalloproteinase inhibitors abrogate local and systemic toxicity induced by *Echis ocellatus* (saw-scaled) snake venom. *Toxicon* **2017**, *132*, 40-49, doi:<https://doi.org/10.1016/j.toxicon.2017.04.001>.
22. Rucavado, A.; Escalante, T.; Gutiérrez, J.M.a. Effect of the metalloproteinase inhibitor batimastat in the systemic toxicity induced by *Bothrops asper* snake venom: understanding the role of metalloproteinases in envenomation. *Toxicon* **2004**, *43*, 417-424.
23. Rucavado, A.; Escalante, T.; Franceschi, A.; Chaves, F.; León, G.; Cury, Y.; Ovadia, M.; Gutiérrez, J.M. Inhibition of local hemorrhage and dermonecrosis induced by *Bothrops asper* snake venom: effectiveness of early in situ administration of the peptidomimetic metalloproteinase inhibitor batimastat and the chelating agent CaNa₂EDTA. *The American journal of tropical medicine and hygiene* **2000**, *63*, 313-319.
24. Escalante, T.; Franceschi, A.; Rucavado, A.; Gutiérrez, J.M.a. Effectiveness of batimastat, a synthetic inhibitor of matrix metalloproteinases, in neutralizing local tissue damage induced by BaP1, a hemorrhagic metalloproteinase from the venom of the snake *Bothrops asper*. *Biochemical pharmacology* **2000**, *60*, 269-274.

25. Vaiyapuri, S.; Ali, M.S.; Moraes, L.A.; Sage, T.; Lewis, K.R.; Jones, C.I.; Gibbins, J.M. Tangeretin Regulates Platelet Function Through Inhibition of Phosphoinositide 3-Kinase and Cyclic Nucleotide Signaling. *Arteriosclerosis, Thrombosis, and Vascular Biology* **2013**, *33*, 2740-2749, doi:doi:10.1161/ATVBAHA.113.301988.
26. Vaiyapuri, S.; Hutchinson, E.G.; Ali, M.S.; Dannoura, A.; Stanley, R.G.; Harrison, R.A.; Bicknell, A.B.; Gibbins, J.M. Rhinocetin, a venom-derived integrin-specific antagonist inhibits collagen-induced platelet and endothelial cell functions. *The Journal of biological chemistry* **2012**, *287*, 26235-26244, doi:10.1074/jbc.M112.381483.
27. Willis, T.W.; Tu, A.T. Purification and biochemical characterization of atroxase, a nonhemorrhagic fibrinolytic protease from western diamondback rattlesnake venom. *Biochemistry* **1988**, *27*, 4769-4777, doi:10.1021/bi00413a028.
28. Howes, J.M.; Theakston, R.D.; Laing, G.D. Neutralization of the haemorrhagic activities of viperine snake venoms and venom metalloproteinases using synthetic peptide inhibitors and chelators. *Toxicon* **2007**, *49*, 734-739, doi:10.1016/j.toxicon.2006.11.020.
29. Kini, R.M.; Koh, C.Y. Metalloproteases Affecting Blood Coagulation, Fibrinolysis and Platelet Aggregation from Snake Venoms: Definition and Nomenclature of Interaction Sites. *Toxins* **2016**, *8*, 284, doi:10.3390/toxins8100284.
30. Siigur, J.; Tõnismägi, K.; Trummal, K.; Aaspõllu, A.; Samel, M.; Vija, H.; Subbi, J.; Kalkkinen, N.; Siigur, E. Vipera lebetina Venom Contains All Types of Snake Venom Metalloproteases. *Pathophysiology of Haemostasis and Thrombosis* **2005**, *34*, 209-214, doi:10.1159/000092426.
31. Tasoulis, T.; Isbister, G.K. A Review and Database of Snake Venom Proteomes. *Toxins (Basel)* **2017**, *9*, doi:10.3390/toxins9090290.
32. Matsui, T.; Fujimura, Y.; Titani, K. Snake venom proteases affecting hemostasis and thrombosis. *Biochimica et Biophysica Acta (BBA) - Protein Structure and Molecular Enzymology* **2000**, *1477*, 146-156, doi:[https://doi.org/10.1016/S0167-4838\(99\)00268-X](https://doi.org/10.1016/S0167-4838(99)00268-X).
33. Kini, R.M.; Rao, V.S.; Joseph, J.S. Procoagulant Proteins from Snake Venoms. *Pathophysiology of Haemostasis and Thrombosis* **2001**, *31*, 218-224, doi:10.1159/000048066.
34. Pandya, B.V.; Rubin, R.N.; Olexa, S.A.; Budzynski, A.Z. Unique degradation of human fibrinogen by proteases from western diamondback rattlesnake (Crotalus atrox) venom. *Toxicon* **1983**, *21*, 515-526, doi:[https://doi.org/10.1016/0041-0101\(83\)90129-0](https://doi.org/10.1016/0041-0101(83)90129-0).
35. Kim, C.H.; McBride, D.W.; Raval, R.; Sherchan, P.; Hay, K.L.; Gren, E.C.K.; Kelln, W.; Lekic, T.; Hayes, W.K.; Bull, B.S., et al. Crotalus atrox venom preconditioning increases plasma fibrinogen and reduces perioperative hemorrhage in a rat model of surgical brain injury. *Scientific reports* **2017**, *7*, 40821-40821, doi:10.1038/srep40821.

36. Pandya, B.V.; Budzynski, A.Z. Anticoagulant proteases from western diamondback rattlesnake (*Crotalus atrox*) venom. *Biochemistry* **1984**, *23*, 460-470, doi:10.1021/bi00298a010.
37. Gutierrez, J.M.; Rucavado, A. Snake venom metalloproteinases: their role in the pathogenesis of local tissue damage. *Biochimie* **2000**, *82*, 841-850.
38. Bernardoni, J.L.; Sousa, L.F.; Wermelinger, L.S.; Lopes, A.S.; Prezoto, B.C.; Serrano, S.M.T.; Zingali, R.B.; Moura-da-Silva, A.M. Functional Variability of Snake Venom Metalloproteinases: Adaptive Advantages in Targeting Different Prey and Implications for Human Envenomation. *PLOS ONE* **2014**, *9*, e109651, doi:10.1371/journal.pone.0109651.
39. Williams, H.F.; Mellows, B.A.; Mitchell, R.; Sfyri, P.; Layfield, H.J.; Salamah, M.; Vaiyapuri, R.; Collins-Hooper, H.; Bicknell, A.B.; Matsakas, A., et al. Mechanisms underpinning the permanent muscle damage induced by snake venom metalloprotease. *PLOS Neglected Tropical Diseases* **2019**, *13*, e0007041, doi:10.1371/journal.pntd.0007041.
40. Zhu, W.-H.; Guo, X.; Villaschi, S.; Nicosia, R.F. Regulation of vascular growth and regression by matrix metalloproteinases in the rat aorta model of angiogenesis. *Laboratory Investigation* **2000**, *80*, 545.
41. Jagadeesha, D.K.; Shashidhara murthy, R.; Girish, K.S.; Kemparaju, K. A non-toxic anticoagulant metalloprotease: purification and characterization from Indian cobra (*Naja naja naja*) venom. *Toxicon* **2002**, *40*, 667-675, doi:[https://doi.org/10.1016/S0041-0101\(01\)00216-1](https://doi.org/10.1016/S0041-0101(01)00216-1).
42. Gong, W.; Zhu, X.; Liu, S.; Teng, M.; Niu, L. Crystal structures of acutolysin A, a three-disulfide hemorrhagic zinc metalloproteinase from the snake venom of *Agkistrodon acutus* Edited by R. Huber. *Journal of Molecular Biology* **1998**, *283*, 657-668, doi:<https://doi.org/10.1006/jmbi.1998.2110>.
43. Rael, E.D.; Rivas, J.Z.; Chen, T.; Maddux, N.; Huizar, E.; Lieb, C.S. Differences in fibrinolysis and complement inactivation by venom from different northern blacktailed rattlesnakes (*Crotalus molossus molossus*). *Toxicon* **1997**, *35*, 505-513, doi:[https://doi.org/10.1016/S0041-0101\(96\)00139-0](https://doi.org/10.1016/S0041-0101(96)00139-0).
44. Mohandas, N.; Gallagher, P.G. Red cell membrane: past, present, and future. *Blood* **2008**, *112*, 3939-3948, doi:10.1182/blood-2008-07-161166.
45. Chippaux, J.-P. Estimate of the burden of snakebites in sub-Saharan Africa: a meta-analytic approach. *Toxicon* **2011**, *57*, 586-599.
46. Williams, D.J.; Faiz, M.A.; Abela-Ridder, B.; Ainsworth, S.; Bulfone, T.C.; Nickerson, A.D.; Habib, A.G.; Junghanss, T.; Fan, H.W.; Turner, M., et al. Strategy for a globally coordinated response to a priority neglected tropical disease: Snakebite envenoming. *PLOS Neglected Tropical Diseases* **2019**, *13*, e0007059, doi:10.1371/journal.pntd.0007059.
47. Bulfone, T.C.; Samuel, S.P.; Bickler, P.E.; Lewin, M.R. Developing Small Molecule Therapeutics for the Initial and Adjunctive Treatment of Snakebite. *Journal of tropical medicine* **2018**, *2018*.

4.4 The detection of snake venom serine proteases using a peptide-based approach

Harry F. Williams¹, Harry J. Layfield¹, Rufaida Ahamed¹, Andrew B. Bicknell², Steven Trim³ and Sakthivel Vaiyapuri¹

¹School of Pharmacy, University of Reading, Reading, United Kingdom

²School of Biological Sciences, University of Reading, Reading, United Kingdom

³Venomtech Private Limited, Sandwich, United Kingdom

In Preparation

Conclusion of this chapter

In order for future therapeutics including small molecular inhibitors such as batimastat/marimastat to be of real use and administered only when of net benefit to victims, diagnostic methods need to be developed. The future of diagnostics will undoubtedly, to some extent have to mirror therapeutics, with tools to indicate the administration of each suggested therapeutic. Here we develop a method for the identification of conserved regions in a protein family, from which to have peptides synthesised and specific antibodies to be developed for potential use in the diagnosis and indication of toxin-specific treatments. Such toxin-specific diagnostic platforms will empower clinicians to be able to treat victims of snakebite with confidence and pave the way for more specific treatment strategies.

Contribution to this chapter

General contribution (80%)

- Performed experiments
- Analysis and interpretation of data
- Writing of the manuscript
- Preparation of the figures

Experimental contribution

Figure 1 Collected sequence data, aligned sequences, assisted in identifying appropriate peptides, prepared figure

Figure 2 Used pyMOL to highlight regions covered by peptides, prepared figure

Figure 3 Prepared immunogens, separated serum from blood, carried out ELISA, prepared figure

Figure 4 Performed experiments, analysed data, prepared figure

Figure 5 Performed experiments, analysed data, prepared figure

Figure 6 Supervised experiments, analysed blot, prepared figure

The detection of snake venom serine proteases using a peptide-based approach

Harry F. Williams¹, Harry J. Layfield¹, Rufaida Ahamed¹, Andrew B. Bicknell², Steven Trim³ and Sakthivel Vaiyapuri^{1*}

¹School of Pharmacy, University of Reading, Reading, UK

²School of Biological Sciences, University of Reading, Reading, UK

³Venomtech, Discovery Park, Sandwich, Kent, UK

***Corresponding author**

Dr Sakthivel Vaiyapuri

E-mail: s.vaiyapuri@reading.ac.uk

Abstract

Snakebite envenomation (SBE) is a priority neglected tropical disease associated with mortality and morbidity of epic proportions and this is primarily concentrated in developing nations. One of the best methods to improve snakebite treatment is by developing robust diagnostic tools. Notably, improving diagnostical methods is essential to guide more specific and prompt treatments, as well as giving indication to the need for appropriate pre-hospital management for certain snake bites. Snake venom serine proteases (SVSPs) are predominantly present in viper venoms, and they share several structural features. Hence, we sought to identify the well conserved regions among SVSPs and utilise them for the detection of snake venoms towards developing a diagnostic test. Using a sequence and structural analysis, we have identified specific regions (at the N- and C-terminal ends) common to SVSPs. These regions were then modified to improve their stability and immunogenicity, and synthesised into unique region peptides (URPs) and used to raise antibodies in sheep. One site enzyme-linked immunosorbent assays (ELISA) were then used to analyse their specificity to a range of different snake venoms, those indicating the likely presence of serine proteases in the venom and consequential associated haemotoxic pathologies. This method effectively identified a range of venoms, with a preference for vipers over elapids, as would be expected given the low abundance of SVSPs in non-viper venoms. However, these antibodies were unable to detect venoms in two-site immunoassays which may be due to poor antibody binding or issues related to the steric hindrance on 3D structures of SVSPs.

1. Introduction

Snakebite envenomation (SBE), a recently reinstated priority neglected tropical disease [1] is estimated to kill up to 125,000 people annually [2, 3] and cause permanent muscular, psychological and financial issues to millions of people living predominantly in the poorest areas of the world [4, 5]. The high mortality and morbidity arise in part from the difficulties associated in treating this disease, which can vary hugely in its nature depending on the species [6], locality [7] and age [8, 9] of the offending snake, as well as the quantity of venom injected, correct diagnosis and treatment of bite. Therefore, a diagnostic kit capable of differentiating between SBE and dry bites would be pivotal in the indication of treatment and transitioning to more case-specific treatments.

Snake venoms are largely made up of enzymatic and non-enzymatic proteins and peptides, each of which has a different effect or range of effects on the human body [10]. Medically important snakes are generally found in two main families; Elapidae (elapids), a family with venoms composed mainly of smaller, more neurotoxic proteins such as phospholipase A2 (PLA2) and three finger toxins, and Viperidae (vipers), a family with generally larger venom components that attack the cardiovascular system, such as snake venom serine- and metalloproteases (SVSPs and SVMPS respectively) [11]. SVSPs are one of the most abundant families in viper venoms, making up approximately 15% of viper venoms [12], although ranging from nearly 60% in *Crotalus horridus* [13] to less than 1% in *Bothrops colombiensis* [14]. This is in contrast to elapids, where this protein family is virtually absent, with a few exceptions including *Notechis scutatus* [15] and most of the other Australian elapids [16] along with some species from the *Bungarus* genus [17] although SVSPs make up less than 6% of the venom in most of these cases.

SVSPs are well documented to affect haemostasis in a number of ways, including via pro-coagulant effects; e.g. 'thrombin-like' fibrinogen clotting enzymes, factor V activators, and platelet activators as well as anticoagulant effects: e.g. fibrinolytic, plasminogen and protein C activating enzymes [18, 19]. The snake venom 'thrombin-like' enzymes (SVTLEs) typically cleave fibrinogen (causing them to be called 'venombins'), preferentially releasing either

fibrinopeptide A (subdivided as 'venombins A') or fibrinopeptide B ('venombins B') or both ('venombins AB'), hence promoting coagulation via the conversion of fibrinogen to fibrinopeptides, which are essential to the formation of clots [20]. The SVTLEs differ from thrombin in their general inability to activate coagulation factor XIII, the lack of all the exosites present on the surface of thrombin, release of mostly a single fibrinopeptide, and the consequential lack of crosslinking formed by these fibrin monomers leads to the rapid dispersal of unstable and dangerous clots [21]. Other SVSPs occasionally activate coagulation factor V, a part of the prothrombinase complex which activates prothrombin to generate thrombin and are consequently procoagulant [22]. As well as the 'thrombin-like' enzymes, there are also 'kallikrein-like' SVSPs which release bradykinin from plasma kininogen, thus dilating blood vessels and consequently altering the blood pressure [23]. Some SVSPs also have effects on platelets, inducing platelet aggregation via the cleavage of protease activated receptors (specifically PAR1 & PAR4) [24].

Some of the anticoagulatory SVSPs are documented to activate protein C [25], which then deactivates factor Va and VIIIa with consequential anticoagulatory effects. Certain SVSPs are anticoagulatory, capable of activating the zymogen plasminogen, to form plasmin, an endogenous serine protease which degrades fibrin clots [20] as well as directly fibrinolytic SVSPs such as ancrod. The angiotensin degrading (and reduction to vasoconstriction) activity of some SVSPs [26] contributes to the hypotension and vascular shock seen particularly in viper envenomation.

Snakebite envenomation is a medical emergency, and it is generally the cardiovascular system (in bites from vipers – in part due to SVSPs) or the nervous system (in bites from elapids) that are the primary concern in saving a victim's life. Being able to discern which snake family has caused the bite, and indeed whether venom has been injected, would allow the victims to seek prompt hospital treatment and empower the clinicians to initiate appropriate treatment without waiting for the onset of clinical symptoms.

Antivenoms, the animal-derived immunoglobulins are the only available treatment for SBE. These are either monovalent when raised against a single venom, or polyvalent, when raised

against multiple venoms [27]. Most antivenoms are polyvalent and consequently only a fraction of the antibodies will be specific for the venom of offending snake. Being able to diagnose the species responsible for a bite would accelerate more specific treatment regimes, increasing the number of monovalent antivenoms being produced and reduce the wasteful injection of polyvalent antivenoms composed largely of redundant immunoglobulins. After hospitalisation, clinicians rely on seeing the actual snake specimen or an account of the snake as well as any local symptoms surrounding the bite site, and the traditional 20-minute whole-blood clotting test (WBCT20) [10]. However, there is a significant incidence of “dry-bites”, where a victim is bitten by a venomous snake, but no venom is injected [28], therefore the making of decisions based on a victim's account and bitemarks alone can be flawed. By the time symptoms are in evidence, such as severe swelling, internal bleeding, myoglobinuria, ptosis, haematuria, breathing difficulties, etc, the patient's condition may have become critical, therefore an assay enabling the rapid assessment of envenomation and identification of the species responsible, would not only save lives, but could trigger a paradigm shift in the treatment and management of SBE.

Despite clear recognition that we are in need of better snakebite diagnostics [29], advances in this field have been almost non-existent. The commonwealth serum laboratory snake venom detection kit (CSL-SVVK) is still, after over three decades the only available product in this field, the use of which is limited to Australasia. The CSL-SVVK relies on the enzyme-linked immunosorbent assay (ELISA) principle, which is relatively slow, and not without some difficulties involved in its use. The currently accepted technique for a simple point of care device giving rapid diagnosis is the lateral flow assay (LFA) and, in both India and Taiwan, the applications of LFA devices for SBE have been explored in scientific research [30, 31]. These are based on the use of monovalent and polyvalent antibodies respectively and seem able to identify the snake or snakes responsible for a bite within a very narrow range and are only of real use in these specific countries. However, in the future when more toxin specific treatments become available [32, 33] diagnostical devices able to detect individual toxins rather than species may be of greater use. Here, we identify, design and develop

antibodies for two unique regions found on viper venom serine proteases (unique region peptides – URPs) for use in detecting this group of enzymes in venoms, with a hope for uses in clinical diagnostics in the future. We used a sequence-structure-function and phylogenetic analysis to identify these peptides and screened the ability for corresponding antibodies to detect a range of different venoms.

2. Methods

In order to determine if SVSPs would be beneficial in developing a diagnostic method for SBE, URPs were designed based on viper venom serine proteases and antibodies were raised against these URPs in sheep to be used in the detection of these proteins in clinical samples from snakebite victims, and consequently corroborate envenomation from species containing these proteins.

2.1 Peptide design

The URPs were designed based on multiple sequence analysis previously carried out using 196 SVSP sequences [34] available on PubMed (<https://www.ncbi.nlm.nih.gov/protein/>). The basic local alignment search tool (BLAST) (<https://blast.ncbi.nlm.nih.gov/Blast.cgi>) was used in order to compare the sequences of all the proteins matching our search term “snake venom serine protease” and sequences were aligned using Clustal Omega [35]. Following the removal of signal and activation peptides, the mature protein sequences were compared between the SVSPs, as well as other protein families (including human serine proteases e.g. trypsin) to minimise cross reactivity with other groups. Highly conserved regions on these proteins were located at the N-terminal and C-terminal ends, and two URPs were designed: VIGGDECNINEHR (N-terminus/B) and KGNTDATCPP (C-terminus/A). The A-URP was slightly altered and the first alanine was exchanged for a lysine in order to increase solubility and provide a moiety that is amenable to modification. Similar sequence alignments can be seen in Vaiyapuri *et al.* (2012) [35], Ullah *et al.* (2018) [25] and Serrano & Maroun (2005) [20]. The crystal structures of the original SVSPs (available on Protein data bank <https://www.rcsb.org/>) were then viewed in PyMOL [36] in order to ensure that the conserved regions identified would be on the protein’s surface and freely accessible for antibodies. These

peptides were then slightly modified by adding a lysine to the A-URP to improve stability and solubility before being custom-synthesised by Sigma Aldrich (Merck, UK).

2.2 Antibody production

The URPs were conjugated to a carrier protein; maleimide activated keyhole limpet haemocyanin (KLH) in order to increase their immunogenicity. This carrier protein can bind to more than 200 haptens per KLH molecule, which increases the half-life of the URP and immunogenicity of the peptide by eliciting T helper and B cell responses, improving antibody production, yield and affinity. The KLH conjugation was achieved by mixing the maleimide activated KLH with the peptide at a molar ratio of 1:200 in phosphate buffered saline (PBS) (0.01 M phosphate buffer, 0.0027 M potassium chloride and 0.137 M sodium chloride, pH 7.4). After incubating at room temperature for sixty minutes, the solution was run through a PD-10 column (GE Healthcare, UK) in order to desalt and remove the EDTA. The desalted peptide-KLH conjugates were stored in -80°C freezer until further use.

2.3 Immunisation of sheep

The procedures used for immunisation and antibody production were approved by the British Home Office in accordance with the Animal (Scientific Procedures) Act 1986. Two sheep were injected with 50 µg of peptide-KLH conjugate each month via intradermal injections using GERBU P as an adjuvant as a scheduled immunisation programme for seven months. Before immunising, 10 mL of blood was taken from each sheep, the serum from which acted as a pre-immune serum control. Two weeks after each injection (with the exception of the first immunisation) approximately 500 mL (calculated based on the weight of the animal) of blood was taken from each sheep. The blood was allowed to clot overnight and the serum was then separated from any remaining blood cells and debris by centrifugation at 4000 RCF for 10 minutes at room temperature.

2.4 Immunoglobulin G (IgG) precipitation

Sodium sulfate was slowly added to the serum up to 18% under stirring conditions over 60 minutes. The serum was then centrifuged at 5000 RCF for 30 minutes at room temperature.

The supernatant was discarded and the pellet was suspended in PBS. The suspension was then dialysed against 0.1% (w/v) saline overnight, followed by PBS for 3 hours before storing the IgG at -20°C prior to affinity purification.

2.5 Affinity purification of URP-specific antibodies

Following precipitation, the antibodies were selectively purified by using URP-specific affinity chromatography. Two columns were prepared by coupling each of the two URPs (2 mg) used for immunisations to Ultralink® Iodoacetyl resin as per the manufacturer's instructions (Pierce, UK) [37]. Briefly, the lyophilised peptide (1 mg/mL) was dissolved in coupling buffer (50 mM Tris/5 mM EDTA pH 8.5) and was immediately added to Ultralink iodoacetyl gel prewashed with coupling buffer and incubated for 30 minutes at room temperature. After washing the unbound peptides with coupling buffer, non-specific binding sites were blocked using 50 mM β -mercaptoethanol in coupling buffer. The column was then washed again thoroughly with the coupling buffer before use. Alternating between high and low pH five times using 50 mM sodium acetate/20% (v/v) acetonitrile pH 6 and pH 3.5.

After washing the resin with PBS, dialysed antibodies from 50 mL of serum were diluted in 1L PBS and slowly applied to the column via siphon. The column was then washed again with PBS, followed by 0.5 M sodium acetate and 50 mM sodium acetate/20% acetonitrile pH 6. Fractions of 1 mL were then eluted using 50 mM sodium acetate/20% acetonitrile pH 3.5 directly into saturated sodium bicarbonate to promptly neutralise the acid. The fractions containing proteins were identified using Pierce Bradford Coomassie protein reagent (Thermofisher, UK) and those containing proteins were pooled and quantified using direct UV at 280 nm.

2.6 One-site enzyme-linked immunosorbent assay (ELISA)

To determine the immune response of the sheep and analyse the specificity of antibodies produced to different venoms, one-site ELISAs were carried out: a 96-well microtitre plate was coated with either 100 μ L 0.1 M sodium bicarbonate to act as a blank control or 100 μ L of the URPs (100 ng/mL) (to monitor immune response) or venoms (1 μ g/mL) (to analyse the cross

reactivity of antibodies to different venoms) diluted in 0.1 M sodium bicarbonate and incubated overnight at 4 °C. The plate was then blocked with 200 µL of assay buffer [1% (w/v) BSA in 0.05% (v/v) PBS-Tween20] for one hour. Following washing four times using 0.05% PBS-T with a plate washer (Denley Wellwash 4 Mk 2, USA), 100 µL of either diluted serum (1/500 for monitoring immune response) or affinity purified IgG (at 1 µg/mL for cross reactivity analysis) diluted in assay buffer were added to the wells, and the plate was then incubated for a further two hours at room temperature. Following four further washes 100 µL (0.5 µg/mL) of rabbit anti-sheep horseradish peroxidase (Invitrogen, UK) were added and incubated at room temperature for one hour. The plate was then washed four more times before adding 200 µL of 3,3',5,5'-Tetramethylbenzidine (TMB) substrate (Europa Bioproducts, UK) and incubating at room temperature for approximately 15 minutes or until the colour developed. The reaction was then stopped using 50 µL of 0.5 M HCl. The level of absorbance was measured at 450 nm using a microplate reader (EMax precision plate reader, UK).

2.7 Antibody biotinylation

The affinity purified antibodies were biotinylated as per the manufacturer's instructions. Briefly, EZ Link N-hydroxysuccinimido biotin (NHS-biotin) (ThermoFisher, UK) was dissolved in dimethyl sulfoxide (DMSO) and subsequently added to IgG in PBS at a 20 × molar excess. NHS-biotin is an ester of biotin which reacts readily with primary amine groups, forming amide bonds and labelling the antibody with biotin allowing for fast and specific detection with streptavidin, a high affinity binding partner for biotin. After mixing in the dark at room temperature for two hours, the unbound biotin was quenched using ethanolamine. The unbound biotin/ethanolamine was then removed using a G-10 desalting column (GE Healthcare, UK), and the desalted biotin-IgG conjugates were stored at -20 °C after quantification by measuring the absorbance at 280 nm by spectrophotometry.

2.8 Two-site/Sandwich ELISA

The 96-well microtitre plates were coated with the capture (non-biotinylated) antibody (5 µg/mL) (for either A & B URPs) for 16 hours at 4 °C, before blocking for one hour with assay

buffer before washing. Following this 100 μ L of venoms were added (in a range of 2 – 20 μ g per well) and incubation for up to 5 hours at room temperature. After further washing, biotinylated detection antibodies were added (1 μ g/mL) and incubated for two hours at room temperature. Following washing four times with PBS-T, streptavidin-HRP conjugate (0.5 μ g/mL) was added and incubated for one hour at room temperature prior to washing a further four times with PBS-T. TMB (250 μ L) was then added to each well and the plate was then incubated until the development of colour (up to one hour). The reaction was stopped using 0.5 M HCl and the absorbance was read at 450 nm using ELISA reader.

2.9 Immunoblotting analysis

The venoms (30 μ g) from various snakes were dissolved in PBS and then mixed with reducing sample treatment buffer [10% (w/v) SDS, 10% (v/v) β -mercaptoethanol, 1% (w/v) bromophenol blue, 50% (v/v) glycerol and stacking gel buffer (0.5 M tris, 0.4% (w/v) SDS pH 6.8)] and heated at 90°C for 10 minutes before being subjected to SDS-PAGE using 4-20% pre-made gels (Bio-Rad, UK). The proteins were then transferred from the gel to polyvinylidene difluoride (PVDF) membranes by semi-dry transfer system (Bio-Rad, UK) at 15 V (constant) for 90 minutes. The membrane was then blocked in 5% (w/v) BSA/PBS-T for 60 minutes at room temperature. After blocking, the membrane was incubated for 16 hours with URP-specific antibodies (0.25 μ g/mL) in 5% BSA/PBS-T. The membrane was then washed six times in 0.05% PBS-T before incubating with anti-sheep HRP (0.2 μ g/mL) diluted in 5% BSA/PBS-T for one hour. The membrane was then washed six times again before adding Pierce™ ECL Western Blotting Substrate (Thermo Scientific™, UK) and imaging using an ImageQuant LAS 4000 mini (GE Healthcare, UK).

2.10 Statistical analysis

All the data analysed were normalised, and statistical significance was calculated using GraphPad Prism 7 software [38]. One-way ANOVA was carried out before performing a post hoc Dunnett's multiple comparisons test in order to calculate p-values.

3. Results

3.1 Peptide design

The sequences of 196 SVSPs were previously aligned [34] and used in this study in order to identify the conserved regions for use in the development of two URPs (a subset shown in Figure 1). The signal (18 amino acids) and activation (6 amino acids) peptides are cleaved upon secretion of venom through the fangs, this activates the zymogenic, inactive form of enzymes found in the venom primary duct via proteolytic enzymes found in the secondary venom duct prior to injection into the prey or victim [39]. These signal and activation peptides from the SVSP sequences were consequently removed and the mature sequences were realigned before two highly conserved regions among viper SVSPs were identified; one at the N-terminus end: VIGGDECNINEHR (henceforth A-URP: highlighted in red in line 1 in Figure 1) the other at the C-terminus end: KGNTDATCPP (henceforth B-URP: highlighted in blue in line 241 in Figure 1). We ensured the regions contained sulfhydryl groups (cysteines) in order for conjugation to both maleimide activated KLH and the iodoacetyl gel resin that is required for affinity purification and added a lysine to the A-URP to increase solubility. In addition, the structure of a number of SVSPs were analysed using PyMOL [36] to ensure the URPs were on the exterior of the protein's 3D structure and freely accessible for antibody binding (Figure 2).

DA	VIGGNECDINEHRFLVAFFNT--TGFFCGGTLINPEWVVTAAHCDSTDFQMQLGVHSHKKV	82
PM	VIGGDECNINEHRSLVVFNS--SGIFCGGTLINKEWVLTAAACDSKNFQMMFGVHSHKKI	82
TS	VFGGDECNINEHRSLVVLFS--NGFLCGGTLINQDWVVTAAHCDSDNNFQLLFGVHSHKKI	82
EC	VTGGAECDINEHFLVALHTARSKRFHCTGTLIDNQWVLTAAACDRKNIRIKVGVHNKNK	84
VA	VIGGDECNINEHRSLALMYNSTSMKFHCSGTLINQEWVLTAAHCDMENMQIHLGVHDVSL	84
CA	VIGGDECNINEHRFLALMNS---DRFQCGGTLINEEWVVTAAHCDLKYMHYILGVHNVNV	81
GU	IIGGDECNINEHRFLVALYTSRSTRFYCGGTLINQEWVLTAAHCDRKNIRIKLGMHSEKV	84
AP	VIGGDECNRNEHRFLVALYNA--DKFLCGGTLNNEEWVLTAAHCDRRNIRIKLGMHSEKV	82
SC	IIGGDECNINEHRFLALVYS---DGNQCGGTLINEEWVLTAAHCEGNKMKIHLGMHSHKKV	81
	: ** *: *** *. . . * ***: : **:***: : : : .*: . .	
DA	LNEDQTRNPKEKFICPNKNNNEVLDDKIMLIKLDKPISNSKHIAPLSLPSSPPSVGSVC	142
PM	LNEDQTRDPKEKFICPNKKDDKNDKIMLIRLDSSVSNSEHIAPLSLPSSPPSVGSVC	142
TS	LNEDQTRDPKEKFFCPNRKKDDEVDDKIMLIKLDSSVSNSEHIAPLSLPSSPPSVGSVC	142
EC	RNKDEMMRVPKAEKFFCASSKTYTRWDKIMLIRLKRPNVNGSTHIAPLSLPSPASVDSEC	144
VA	PNKDEKRRVAKEKFFCLSSKSYTLWNKDIMLIKLNRPVITYSTHIAPLSLPSSPPSVGSVC	144
CA	KYDDEQRRFPKKKYFCLSSSNYTKGDKIMLIRLNRPVRNSAHIVPLSLPSSPPSVGSVC	141
GU	PNEDAQTRVPKEKFFCLSSKTYTKWDKIMLMRLKRPVNNSTHIAPVSLPSPSVGSVC	144
AP	PNEDQTRVPKEKFFCLSSKNYTLWDKIMLIRLDSPVSNSEHIAPLSLPSSPPSVGSDC	142
SC	PNKDKQTRVPKEKFFCVSSKNYTFWDKIMLIRLDRPVGNSEHIAPLSLPSSPPSVGSVC	141
	. * * :*: . . :*****: . : * **.*:****.* *. * *	
DA	RIMGWGSITPVKETFPDVPYCANINLLDHAVCQAGYPE--LLAEYRTLCAGIVQGGKDTCT	202
PM	RVMGWGAITSPQETYPDVPHCANINILDHAVCRAAYPE--LREKSKTLCAGILQGGKDSC	178
TS	RIMGWGKTIPTKEIYPDVPHCANINILDHAVCRTAYSW--RQVANTTLCAGILQGGRTCT	178
EC	RIMGWGTITTTKVITYPDVPHCANIKIFDYSVCREAYRK--LPEKSRTLCAGILEGGIDSC	180
VA	RIMGWGAITSPNETYPDVPHCANINILNYAVCRAENPW--LPAQSRTLCAGILQGGIDTC	180
CA	RVMGWGTITSPNVTFPDVPHCANINILDYEVCRAYPE--LPATRRTLCAGIMEGSKDSC	177
GU	RVMGWGTITSPQETYPDVPHCANINILDYEVCAAH--GGLPATSRRLCAGILKGGKDSC	180
AP	RIMGWGRISPSKETYPNVPHCANINILNYEVCLAAYPEYMLPATSRRLCAGILEGGKDSC	178
SC	RIMGWGTISPTKVILPDVPHCANINLLNYSVCRAAYPEYGLPATSRRLCAGILEGGKDTCT	177
	*:**** : *:***.**: : : * * :*****: . *: *	
DA	GGDSGGPLICNGQFQGIVSYGAHPCGQGPKEGIYTNVFDYTDWIQRNIAGNTDATCPP	258
PM	LVDSSGGPLICNGQVQGIVSDGGYPCGQPREPGVYTNVFDHLDWMKSIAGNTDATCPP	258
TS	HFDSGGPLICNGIFQGIVSWGHPGCGQPGEPGVYTKVFDYLDWIKSIAGNKDATCPP	258
EC	KADTGGPLICNGQFQGIASWGGKPCAQLKPALYTNVFDYNDWIKSIAGNTDATCPP	260
VA	KGDSGGPLICNGQIQGIVSWGDSPCAQLNPGHYTKVFDYTDWISIIAGNTNATCPP	260
CA	DGDSGGPLICNGQFQGIASWGADTCAQPREPGLYTKVFDYTDWISIIAGNTDATCPP	257
GU	KGDSGGPLICNGQFQGIASWGAHPCGQSLKPGVYTKVFDYTEWISIIAGNTDATCPP	260
AP	KGDSGGPLICNGQFQGILSWGDDPCGYVLQPALYTRVFDHLDWISIIAGNTDATCPP	260
SC	VGDSGGPLICNGQFQGIASWGSPNCGYVREPGLYTKVFDHLDWISIIAGNTDATCPP	259
	*:***** .*** * * * :*. **.**: :*: *****:*****	

Figure 1. Multiple sequence alignment used to identify conserved regions within viper venom serine proteases. The sequences of several SVSPs (including vipers and elapids) were aligned in order to identify the conserved regions from which to design peptides for use in the production of antibodies. Highlighted regions show areas used to design the peptides: in red VIGGDECNINEHR (N-terminus/B) and in blue KGNTDATCPP (C-terminus/A). Snake species and accession numbers of SVSPs: DA: *Deinagkistrodon acutus* (Q918X1), PM: *Protobothrops mucrosquamatus* (XP_015671555), TS: *Trimeresurus stejnegeri* (Q91516), EC: *Echis coloratus* (ADI47560), VA: *Vipera ammodytes ammodytes* (AMB36345), CA: *Crotalus atrox* (AUS82485), GU: *Gloydius ussuriensis* (Q8UVX1), AP: *Agkistrodon piscivorus* (AUS82476) and SC: *Sistrurus catenatus edwardsi* (ABG26968). All the FASTA sequences were obtained from NCBI Protein database and aligned using Clustal omega.



Figure 2. 3D structure of ACC-C (Accession number: P09872), a protein C activating venom serine protease from *Agkistrodon contortrix contortrix* with the unique region peptides highlighted in blue (A-URP) and red (B-URP). PyMOL was used to analyse the 3D structure of venom serine proteases and ensure that the unique regions we identified were available on the outer surface of the proteins and consequently accessible for antibody binding. Here one example from the southern copperhead, *Agkistrodon contortrix contortrix* is shown.

3.2 Immune response to the URPs

Over the course of five months, sheep were immunised with 50 µg of KLH-peptide (URP) conjugates and the serum was collected at regular intervals. Using one-site ELISAs, the immune response was monitored using diluted serum (1/100). From the results shown in Figure 3, the A-URP (C-terminus end) appeared to be mildly less immunogenic when

compared to the B-URP (N-terminus end). Although it is not entirely clear on the reasons for the slightly poorer immune response from the A-UPR, this could be partially due to the slightly smaller size compared to the B-URP: 10 amino acids for the A-URP compared with 13 amino acids for B-URP. Added to which, the B-URP also has a greater abundance of antigenic amino acids which can be associated with improved responses (lysine, arginine, glutamic acid, aspartic acid, glutamine, asparagine, etc [40]).

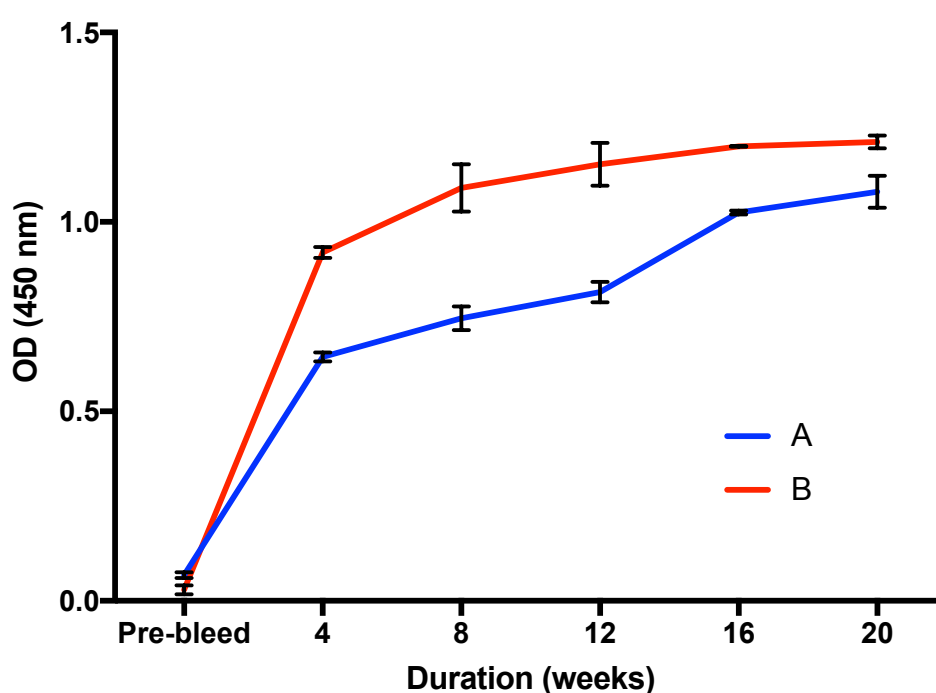


Figure 3. Immune responses against A-URP (C-terminus) and B-URP (N-terminus) of snake venom serine protease. Blood was taken from sheep every four weeks and the serum was used in one-site enzyme linked immunosorbent assays (ELISA) to monitor immune responses to these antigens. High binding microtitre plates were coated in a single concentration of URPs (1 $\mu\text{g/mL}$), before being washed and then incubated with different concentrations of sheep serum. The unbound serum was washed off prior to the addition of anti-sheep IgG antibodies conjugated to horseradish peroxidase (HRP). All unbound HRP was then washed off and a HRP substrate (tetramethylbenzidine) was added allowing the quantification of binding by measuring the absorbance of the product. Data were analysed in Graphpad Prism and represent mean \pm S.D. (n=3).

3.3 Standard curves using *Crotalus atrox* venom

In order to gauge the detection limits of URP-specific antibodies to detect a venom in one-site ELISA, *C. atrox* venom (as a best example) at concentrations from 20 $\mu\text{g/mL}$ to 10 ng/mL was coated onto a high binding plate, before following the one-site ELISA protocol outlined as above. Figure 4 shows the differences in sensitivity between the two URP-specific IgGs. B-URP specific antibodies are more sensitive to *C. atrox* venom than the A-URP antibodies. The A-URP antibodies stop detecting at approximately 80 ng/mL , while the B-URP antibodies detect (though to a very low degree) all the way down to 10 ng/mL . These differences could in part, be due to the length, immunogenicity and antigenicity of the peptide.

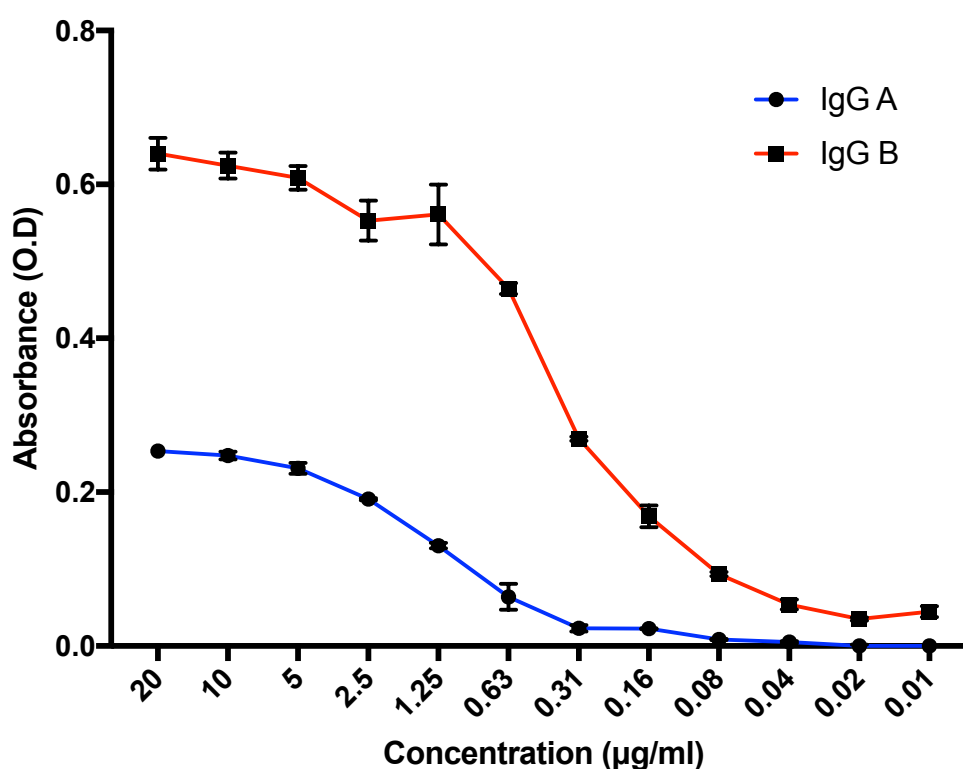


Figure 4. Standard curves for URP-specific antibodies using *Crotalus atrox* venom. One-site enzyme-linked immunosorbent assay (ELISA) was used to determine the detection limits of antibodies raised against KLH-conjugated unique region peptides (URPs) based on viper venom serine proteases. High binding microtitre plates were coated in different concentrations of *Crotalus atrox* venom, before being washed and then incubated with URP antibodies. The unbound antibodies were washed off prior to the addition of anti-sheep IgG antibodies conjugated to horseradish peroxidase (HRP). All unbound HRP was then washed off and a HRP substrate (tetramethylbenzidine) was added allowing the quantification of binding by measuring the absorbance of the product. Data were analysed in Graphpad Prism and represent mean \pm S.D. ($n=3$).

3.3 Immune reactivity against venoms in one-site ELISA

After production and purification of IgG from sheep immunised against URPs based on two different regions of SVSPs, a range of snake and invertebrate venoms were screened for their ability to be detected by these antibodies using one-site ELISA. The antibodies raised against the A-URP (Figure 5A) were able to detect most viper venoms screened, to a significant level, although certain species of Elapidae, notably *Dendroaspis polylepis*, were also detected to a lower extent. However, the responses obtained were considerably lower than the URPs used. Notably, the B-URP detected all vipers to a much higher level (Figure 5B), although *D. polylepis* was also detected to a significant level but to a smaller extent. These URPs generally seem to favour species from the subfamily Crotalinae over Viperinae, with *Atheris squamigera*, *Bitis gabonica rhinoceros* and *Echis carinatus* seeing the lowest levels of detection from within the vipers. One possible cause for the poorer A-URP antibodies is the two proline residues which can undergo cis/trans isomerisation reducing peptide purity and specificity of resulting antibodies.

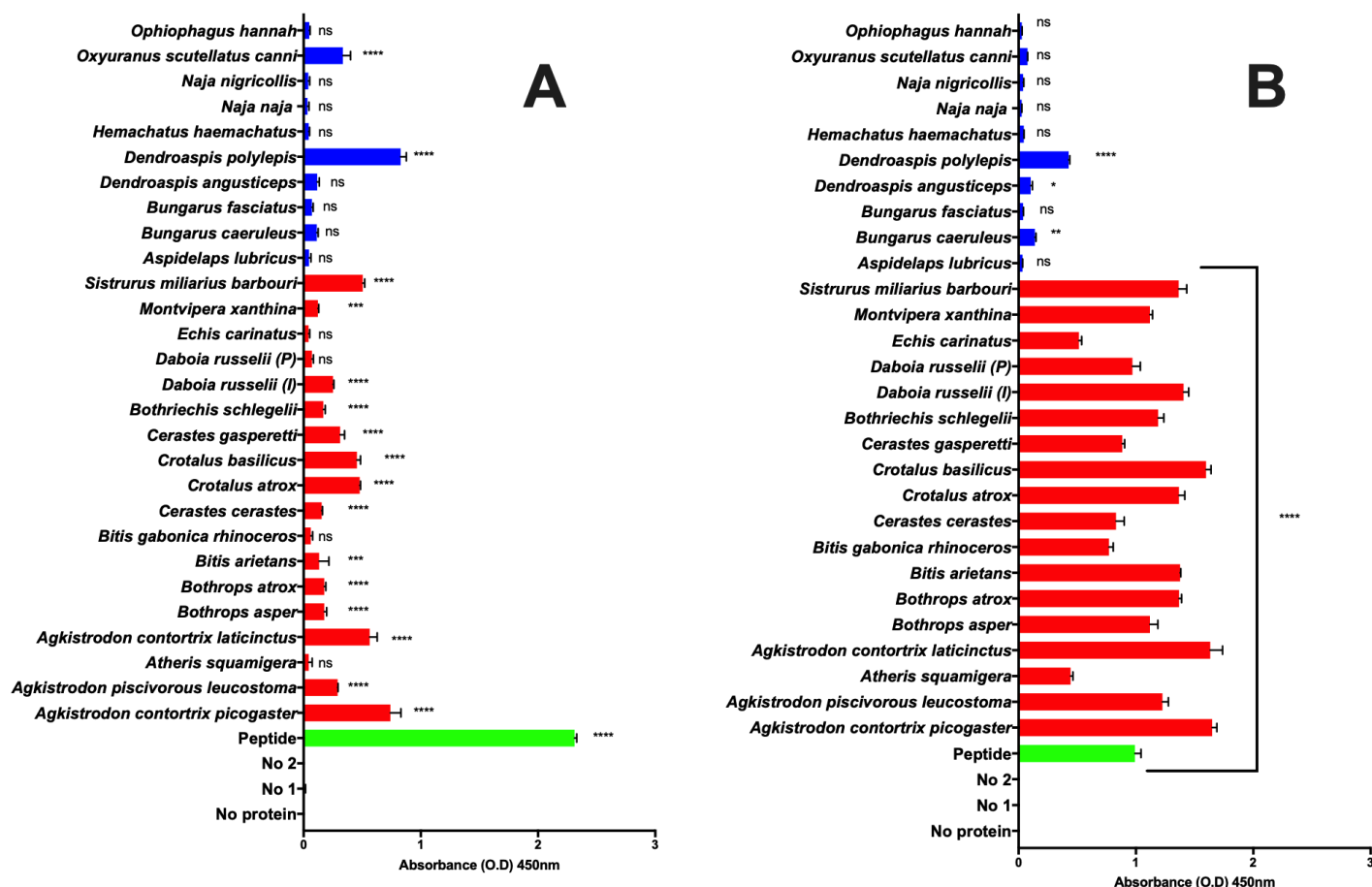


Figure 5. Specificity of URP antibodies to different viper (red) and elapid (blue) venoms. One-site enzyme-linked immunosorbent assay (ELISA) was used to determine the binding affinity of antibodies from sheep immunised with custom made KLH-conjugated peptides (URPs) to different snake venoms. High binding microtitre plates were coated in venoms (20 $\mu\text{g/mL}$), before being washed and then incubated with URP antibodies. The unbound antibodies were washed off prior to the addition of anti-sheep IgG antibodies conjugated to horseradish peroxidase (HRP). All unbound HRP was then washed off and a HRP substrate (tetramethylbenzidine) was added allowing the quantification of binding by measuring the absorbance of the product. It shows the binding affinity of antibodies raised against peptides designed based on two conserved sequences in viper venom serine proteases, one at the C-terminus end (A) and the other at the N-terminus end (B). Data were analysed in Graphpad Prism and represent mean \pm S.D. (n=3). The P-values shown are as calculated using one-way ANOVA followed by Tukey's post hoc multiple comparisons test. For this, the purified antibodies were compared to blank values, and all the values were normalised using a blank control. (* $P \leq 0.05$, ** $P \leq 0.01$, *** $P \leq 0.001$ and **** $P \leq 0.0001$).

3.4 Immunoblotting to assess venom proteins being bound by these antibodies

Immunoblotting was undertaken in order to visualise the individual protein bands which the antibodies bind to in some elapid and viper venoms. Figure 6 shows the differences in binding between the A-URP IgG and B-URP IgG. Both antibodies bind well to proteins of

approximately 30 kDa in *Agkistrodon*, *Crotalus* and *Daboia russelii* venoms, however much lesser bands are seen in *Echis carinatus*. The two elapid venoms used, *Bungarus fasciatus* and *Naja naja* were also bound to by a much lesser extent, although a band representing a small protein of less than 10 kDa is bound in *N. naja* venom.

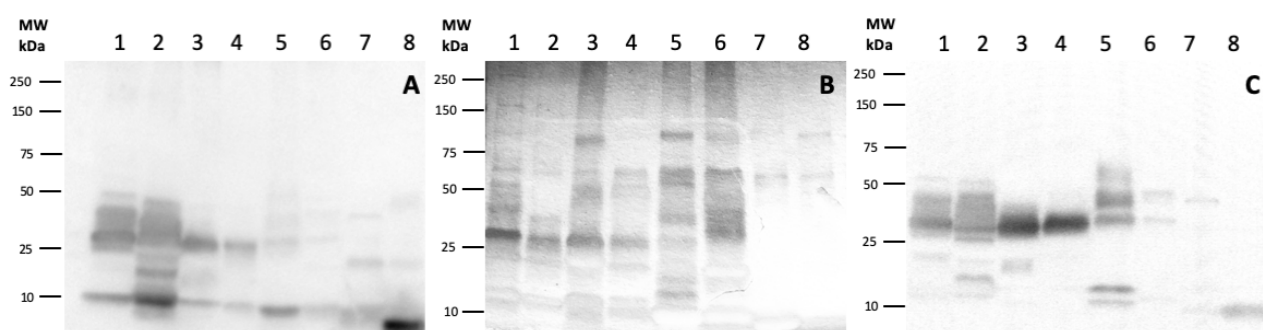


Figure 6. Immunoblots showing venom proteins bound to A-URP (A) and B-URP (C) antibodies and a silver stained gel (B). Venoms were treated with reducing sample treatment buffer and boiled at 90 °C for 10 minutes. These were then analysed by 10% SDS-PAGE at 150V for 45 minutes. The proteins were then transferred to a PVDF membrane before incubation with biotinylated IgG (0.25 µg/mL). The membrane was then washed before the addition of streptavidin-HRP (0.1 µg/mL). This was then washed again before a chemiluminescent substrate was used to visualise the areas where the antibodies had bound. **B**, a gel of crude venoms was silver stained by first fixing [40% (v/v) methanol, 10% (v/v) Acetic acid] then sensitising [5% (w/v) sodium thiosulphate, 6.4% (w/v) sodium acetate, 30% ethanol (v/v)] before priming with 2.5% (v/v) silver nitrate and developing [6.125% (w/v) sodium carbonate, 0.04% (v/v) formaldehyde]. In all images: lane 1, *Agkistrodon piscivorus leucostoma*, 2, *Agkistrodon contortrix laticinctus*, 3, *Crotalus basilicus*, 4, *Crotalus atrox*, 5, *Daboia russelii* 6, *Echis carinatus* 7, *Bungarus fasciatus* 8, *Naja naja*.

4. Discussion

The development of snakebite diagnostics would allow clinicians the world over to have a reliable method by which to determine whether a patient has become envenomed and potentially in the future, quantify the amount of venom and individual toxins present in the circulation of victims. Instead of relying on clinical experience with snakebites, which not all clinicians have, using a robust diagnostic method, they can corroborate snakebite envenomation and validate the treatment with an expensive and sometimes dangerously immunogenic drug, antivenom. By producing antibodies against specific venom proteins for diagnostic applications, these proteins, and consequently the whole venoms or similar species or family members, may be detected in biological fluids of snakebite victims. This study

demonstrates a novel peptide-based approach to produce toxin-specific antibodies. These can be used in diagnostical devices to deduce the snake species inflicting a bite and go on to direct treatment regimes.

The peptide-specific approach allows specific proteins to be targeted, based on published details about their sequences. This allows the diversity of species detected to be somewhat pre-determined and specific taxa to be targeted. This can however be impeded by unexpected sequence homology to other proteins, causing binding and detection to other proteins. The antibodies raised against the two URPs designed and detailed in this study showed a level of specificity for snake venoms which are typically more associated with SVSP contents, predominantly members of Viperidae with their characteristic haemo-/coagulotoxic venoms. The A-URP IgG gave a lower level of detection in ELISA relative to the B-URP, with both detecting both viper and elapid venoms, the B-URP also showed a more statistically significant preference for viper venoms. Notably, the highest detection was observed with *Dendroaspis polylepis* venom, a venom known to be devoid of SVSPs [41] is intriguing. The detection of *D. polylepis* venom to such a degree by both peptides may be due to the ATCP section of the A-URP sequence, which is also found in various adrenergic (accession number: P80495.1) and muscarinic toxins (~7 kDa, Accession number: P80494.1) in *D. polylepis* venom. Likewise, a similar GDRCN (compared to GDECN in B-URP) is found in various proteins in *D. polylepis* venom such as Calciseptine (~7 kDa, Accession number: P22947.1). The binding in ELISA to a small protein in Elapid venoms is corroborated by the low molecular weight band seen in *N. naja* venom via western blotting. The lack of SVSPs previously found in *D. polylepis* venom is likely to be based on a small potentially captive bred population and limited specimens. It could be that our source of venom is from a lineage with SVSPs in the venom. Venoms from multiple species should therefore be analysed, along with the protein content to determine the reliability of this SVSP absence.

Western blotting indicated these antibodies show a far greater preference for proteins in viper venoms, found in the 25 – 35 kDa range, which is consistent with reported molecular weights of SVSPs. Though several bands below the 10 kDa mark are present for both vipers

and elapids, this is particularly prominent in the A-URP, which again is likely to be due to short homologous regions found in other toxins.

Similarly several venoms such as *Bitis* species known to be rich in SVSPs, where these proteins comprise more than 20% of the venom showed very low levels of detection [42]. For the A-URP IgG, *Echis carinatus*, a species for which SVSPs make up between 2 – 5% of the venom was non-significant, along with *Atheris squamigera* which also has a low percentage of SVSPs in its venom [43].

In contrast to the A-URP antibodies, the antibodies against B-URP detected all viper venoms to a significant level as well as only one elapid venom again, *D. polylepis*, detecting several venoms to a level even greater than the peptide (used as a positive control). In line with the results from the A-URP, the least well detected species were *E. carinatus* and *A. squamigera*, although both detected to a high level of significance with the B-URP IgG. This improved specificity for SVSP-containing venoms could be due to the increased length of the B-URP (13 amino acids compared to just 10 for the A-URP). This larger B-URP also appears to be more conserved, with fewer SVSPs having substitutions in this region compared to the A-URP. Although these antibodies were produced based on the peptides with linear sequences, the ELISAs have confirmed that they can detect proteins in the native state in whole venoms. The slightly larger size could potentially give rise to an extra epitope and a wider variety of antibodies to be produced.

Despite experimenting with extreme variations in conditions, a two-site ELISA using the A and B IgG was not achieved. Proteins as large as full IgG (150 kDa) binding to SVSPs (~30 kDa) are also in danger of steric hindrance, as such large molecules could prevent both capture and detection antibodies accessing respective binding sites at the same time. Attempts to incorporate these same antibodies into a lateral flow device have also failed, suggesting the fundamental issues with the suitability of antibodies for LFA and 3D structure of SVSPs could be a problem. This issue has the potential to be overcome by the use of antibody fragments (Fab/F(ab)₂) or raising the capture antibody off the plate surface using anti-sheep antibodies, although this would introduce more cross reactivity.

The antibodies detailed herein were purified against the original URPs, however future work could attempt antibody purification using whole venoms. This could have the benefit of reducing the number of redundant 'wrap around' antibodies. These are antibodies which could target the ends of the URPs, wrapping around the ends of the peptides rather than the entire length of the hapten and are consequently unlikely to bind properly to the native SVSPs. This method could, however, also reduce specificity, with antibodies being given the opportunity to bind any proteins found in the venom used for purification. Another possible solution is the use of longer URPs, with potential increases to the number of epitopes and consequentially better detection and possibilities for a two-site assay. Increases in reactive epitopes have been linked to sensitivity improvements [44] and would undoubtedly have an effect on the outcome of a two-site assays. Although the diversity of serine proteases detected might be reduced due to the lesser sequence homology seen outside the unique regions used for these peptides.

The standard curves further show the lower specificity of the A-IgG but were only done against one venom and could look different for each venom. The relatively poor detection limits may also suggest detection from clinical samples such as blood or plasma would not be versatile, these limits would be unlikely to detect SVSPs in victims of SBE suffering only mild envenomation, though in some venoms this could be sufficient for detrimental effects.

Despite the lack of success in converting promising one-site antibodies into a two-site assay, the peptide-based approach shows much promise. The ability to detect specific toxins using synthetic peptides overcomes many of the limitations of using whole venoms and proteins, such as cross-reactivity and purity issues.

Snakebite treatment is on the cusp of moving into toxin-specific therapeutics, rather than the broad spectrum polyvalent antivenoms currently available. Small molecular therapeutics are available for snake venom PLA₂ [45] and metalloproteases [46], monoclonal human antivenoms have been produced against dendrotoxins [32] but alternative therapies for the SVSP-induced effects are still not advancing. The URP epitopes described here may also hold the ability for the broad-scale neutralisation of SVSPs: such specific epitopes holding

the key to neutralising an entire family of toxic venom proteins has implications in terms of a specific and efficacious therapeutic against serine-protease rich snake venoms and bites. These URPs could be used to develop human monoclonal antibodies, nanobodies or in the discovery of SVSP specific alternative binding scaffolds.

At the forefront of improving therapeutics of SBE are reliable diagnostics with which to corroborate envenoming and justify the administration of any future treatments. The potential for adverse reactions, even with future treatments, is still there, and eliminating unwarranted and potentially harmful administration of antivenoms is essential. Methods such as that described here could give reliable, toxin-specific diagnostics and could form the primary platform for future SBE diagnostics.

5. References

1. WHO. *Neglected tropical diseases*. 2017; Available from: http://www.who.int/neglected_diseases/diseases/en/.
2. Kasturiratne, A., et al., *The global burden of snakebite: a literature analysis and modelling based on regional estimates of envenoming and deaths*. PLoS Med, 2008. **5**(11): p. e218.
3. Chippaux, J.P., *Snake-bites: appraisal of the global situation*. Bulletin of the World Health organization, 1998. **76**(5): p. 515.
4. Harrison, R.A., et al., *Snake envenoming: a disease of poverty*. PLoS neglected tropical diseases, 2009. **3**(12): p. e569.
5. Chippaux, J.-P., *Estimate of the burden of snakebites in sub-Saharan Africa: a meta-analytic approach*. Toxicon, 2011. **57**(4): p. 586-599.
6. Casewell, N.R., et al., *Medically important differences in snake venom composition are dictated by distinct postgenomic mechanisms*. Proceedings of the National Academy of Sciences, 2014. **111**(25): p. 9205-9210.
7. Fry, B.G., et al., *Effectiveness of snake antivenom: species and regional venom variation and its clinical impact*. Journal of Toxicology: Toxin Reviews, 2003. **22**(1): p. 23-34.
8. Modahl, C.M., A.K. Mukherjee, and S.P. Mackessy, *An analysis of venom ontogeny and prey-specific toxicity in the Monocled Cobra (Naja kaouthia)*. Toxicon, 2016. **119**: p. 8-20.
9. Wray, K.P., et al., *Early significant ontogenetic changes in snake venoms*. Toxicon, 2015. **96**: p. 74-81.
10. Gutiérrez, J.M., et al., *Snakebite envenoming*. Nature Reviews Disease Primers, 2017. **3**: p. nrdp201763.
11. Warrell, D.A., *Snake bite*. The Lancet, 2010. **375**(9708): p. 77-88.

12. Tasoulis, T. and G.K. Isbister, *A Review and Database of Snake Venom Proteomes*. Toxins, 2017. **9**(9): p. 290.
13. Rokyta, D.R., K.P. Wray, and M.J. Margres, *The genesis of an exceptionally lethal venom in the timber rattlesnake (Crotalus horridus) revealed through comparative venom-gland transcriptomics*. BMC Genomics, 2013. **14**: p. 394.
14. Calvete, J.J., et al., *Snake venomomics and antivenomics of Bothrops colombiensis, a medically important pitviper of the Bothrops atrox-asper complex endemic to Venezuela: Contributing to its taxonomy and snakebite management*. J Proteomics, 2009. **72**(2): p. 227-40.
15. Tan, C.H., K.Y. Tan, and N.H. Tan, *Revisiting Notechis scutatus venom: on shotgun proteomics and neutralization by the "bivalent" Sea Snake Antivenom*. J Proteomics, 2016. **144**: p. 33-8.
16. Fry, B.G., *Structure–function properties of venom components from Australian elapids*. Toxicon, 1999. **37**(1): p. 11-32.
17. Rusmili, M.R., et al., *Proteomic characterization and comparison of Malaysian Bungarus candidus and Bungarus fasciatus venoms*. J Proteomics, 2014. **110**: p. 129-44.
18. Serrano, S.M.T., *The long road of research on snake venom serine proteinases*. Toxicon, 2013. **62**: p. 19-26.
19. Vaiyapuri, S., et al., *Purification and functional characterisation of rhinocerase, a novel serine protease from the venom of Bitis gabonica rhinoceros*. PLoS One, 2010. **5**(3): p. e9687.
20. Serrano, S.M. and R.C. Maroun, *Snake venom serine proteinases: sequence homology vs. substrate specificity, a paradox to be solved*. Toxicon, 2005. **45**(8): p. 1115-1132.
21. Stocker, K., H. Fischer, and J. Meier, *Thrombin-like snake venom proteinases*. Toxicon, 1982. **20**(1): p. 265-273.
22. Kisiel, W., *Effect of snake venoms on factor V*. Handbook of Natural Toxins: Reptile Venoms and Toxins, 2018.
23. Xiong, S. and C. Huang, *Synergistic strategies of predominant toxins in snake venoms*. Toxicology Letters, 2018. **287**: p. 142-154.
24. Santos, B.F., et al., *Interaction of viper venom serine peptidases with thrombin receptors on human platelets*. FEBS letters, 2000. **477**(3): p. 199-202.
25. Ullah, A., et al., *Thrombin-like enzymes from snake venom: Structural characterization and mechanism of action*. International Journal of Biological Macromolecules, 2018. **114**: p. 788-811.
26. Hung, C.-C. and S.-H. Chiou, *Fibrinogenolytic proteases isolated from the snake venom of Taiwan Habu: serine proteases with kallikrein-like and angiotensin-degrading activities*. Biochemical and Biophysical Research Communications, 2001. **281**(4): p. 1012-1018.
27. World Health Organization, W., *WHO guidelines for the production, control and regulation of snake antivenom immunoglobulins*. Geneva: WHO, 2010. **134**.
28. Naik, B.S., *"Dry bite" in venomous snakes: A review*. Toxicon, 2017. **133**: p. 63-67.
29. Williams, D.J., et al., *Strategy for a globally coordinated response to a priority neglected tropical disease: Snakebite envenoming*. PLOS Neglected Tropical Diseases, 2019. **13**(2): p. e0007059.

30. Pawade, B.S., et al., *Rapid and selective detection of experimental snake envenomation—Use of gold nanoparticle based lateral flow assay*. Toxicon, 2016. **119**: p. 299-306.
31. Liu, C.-C., et al., *Development of sandwich ELISA and lateral flow strip assays for diagnosing clinically significant snakebite in Taiwan*. PLoS neglected tropical diseases, 2018. **12**(12): p. e0007014.
32. Laustsen, A.H., et al., *In vivo neutralization of dendrotoxin-mediated neurotoxicity of black mamba venom by oligoclonal human IgG antibodies*. Nat Commun, 2018. **9**(1): p. 3928.
33. Laustsen, A.H., et al., *In vivo neutralization of dendrotoxin-mediated neurotoxicity of black mamba venom by oligoclonal human IgG antibodies*. Nature Communications, 2018. **9**(1): p. 3928.
34. Vaiyapuri, S., et al., *Sequence and phylogenetic analysis of viper venom serine proteases*. Bioinformation, 2012. **8**(16): p. 763-772.
35. Sievers, F., et al., *Fast, scalable generation of high-quality protein multiple sequence alignments using Clustal Omega*. Molecular systems biology, 2011. **7**: p. 539-539.
36. LLC, S., *The PyMOL Molecular Graphics System*.
37. ThermoScientific. *UltraLink® Iodoacetyl Gel*. 11/06/2019]; Available from: https://assets.thermofisher.com/TFS-Assets/LSG/manuals/MAN0011278_UltraLnk_Iodoacetyl_Gel_UG.pdf.
38. Ivashchenko, R., et al., *Prism 7 for Mac OS X-Version 7.0c, March 1, 2017*. 2017.
39. Mackessy, S.P. and L.M. Baxter, *Bioweapons synthesis and storage: the venom gland of front-fanged snakes*. Zoologischer Anzeiger-A Journal of Comparative Zoology, 2006. **245**(3-4): p. 147-159.
40. Lee, B.S., et al., *Antibody Production with Synthetic Peptides*. Methods Mol Biol, 2016. **1474**: p. 25-47.
41. Laustsen, A.H., et al., *Unveiling the nature of black mamba (*Dendroaspis polylepis*) venom through venomomics and antivenom immunoprofiling: Identification of key toxin targets for antivenom development*. Journal of proteomics, 2015. **119**: p. 126-142.
42. Calvete, J.J., J. Escolano, and L. Sanz, *Snake venomomics of *Bitis* species reveals large intragenus venom toxin composition variation: application to taxonomy of congeneric taxa*. Journal of proteome research, 2007. **6**(7): p. 2732-2745.
43. Wang, H., et al., *Comparative Profiling of Three *Atheris* Snake Venoms: *A. squamigera*, *A. nitschei* and *A. chlorechis**. The Protein Journal, 2018. **37**(4): p. 353-360.
44. Costa, M.M., et al., *Improved Canine and Human Visceral Leishmaniasis Immunodiagnosis Using Combinations of Synthetic Peptides in Enzyme-Linked Immunosorbent Assay*. PLOS Neglected Tropical Diseases, 2012. **6**(5): p. e1622.
45. Bryan-Quiros, W., et al., *Neutralizing properties of LY315920 toward snake venom group I and II myotoxic phospholipases A2*. Toxicon, 2019. **157**: p. 1-7.
46. Arias, A.S., A. Rucavado, and J.M. Gutiérrez, *Peptidomimetic hydroxamate metalloproteinase inhibitors abrogate local and systemic toxicity induced by *Echis ocellatus* (saw-scaled) snake venom*. Toxicon, 2017. **132**: p. 40-49.

4.5 Toxin-specific antibodies for the detection of snake venom metalloproteases in clinical samples obtained from snakebite victims

Harry F. Williams¹, Harry J. Layfield¹, Andrew B. Bicknell², Steven Trim³ and Sakthivel Vaiyapuri¹

¹School of Pharmacy, University of Reading, Reading, United Kingdom

²School of Biological Sciences, University of Reading, Reading, United Kingdom

³Venomtech Private Limited, Sandwich, United Kingdom

In Preparation

Conclusion of this chapter

The identification of toxin-specific peptides and raising of toxin-specific antibodies using such peptides shows one way in which a diagnostical method can be developed. An alternative method is to purify the toxin itself from whole snake venom. In this chapter we use purified snake venom metalloproteases to raise antibodies and assess the range of detection possible with these antibodies. The conserved nature of these proteins mean a wide range of viper and elapid venoms can be detected with these antibodies, and once developed into a lateral flow assay configuration, provide a rapid, point of care device through which clinicians can justify not only antivenom administration, but any future therapies developed to combat SVMP-induced pathologies.

Contribution to this chapter

General contribution (80%)

- Performed experiments
- Analysis and interpretation of data
- Writing of the manuscript
- Preparation of the figures

Experimental contribution

Figure 1 Prepared immunogens, separated serum from blood, carried out ELISA, prepared figure

Figure 2 Performed experiments, analysed data, prepared figure

Figure 3 Performed experiments, analysed data, prepared figure

Figure 4 Performed experiments, analysed data, prepared figure

Figure 5 Performed experiments, analysed data, prepared figure

Toxin-specific antibodies for the detection of snake venom metalloproteases in clinical samples obtained from snakebite victims

Harry F. Williams¹, Harry J. Layfield¹, Thomas M. Vallance¹, Andrew B. Bicknell², Steven Trim^{3,4} and Sakthivel Vaiyapuri^{1*}

¹ School of Pharmacy, University of Reading, Reading, UK

² School of Biological Sciences, University of Reading, Reading, UK

³ VenomTech, Discovery Park, Sandwich, Kent

⁴ Canterbury Christ Church University, Kent

*Corresponding Author: Dr Sakthivel Vaiyapuri, School of Pharmacy, University of Reading, Reading, RG6 6UB, UK. E-mail address: s.vaiyapuri@reading.ac.uk

Abstract

Snakebite envenoming (SBE) is an affliction which primarily effects the impoverished people of the rural tropics. Over 100,000 people are estimated to be killed via SBE annually and it is only in 2019 that health authorities worldwide have realised the severity of the situation. Improvements to the treatment of this disease are primarily focussed on toxin-specific approaches, however such methods will require better diagnostical tools capable of identifying toxins actually present in the blood of snakebite victims. Since our approach using snake venom serine proteases was not successful in developing a two-site ELISA for the detection of snake venoms in clinical samples, here we have used snake venom metalloproteases as a target for the identification of venoms as these are larger proteins and more abundant in viper venoms compared to serine proteases. In this chapter, we report the purification of a P-I and a P-III metalloprotease from the venom of *Crotalus atrox*, the western diamondback rattlesnake, and production of antibodies against these in sheep. These have then been used in the detection of metalloproteases in a range of venoms using enzyme-linked immunosorbent assays (ELISA) before being applied to lateral flow assay devices and used in clinical samples obtained from snakebite victims. This method shows promise in the detection of venoms in plasma, but currently faces sensitivity issues which need to be improved before such a device can be used by medical professionals in improving the diagnosis and future treatment for SBE. Overall, it appears that snake venom metalloproteases may be a potential candidate for the development of diagnostic tools for viper venoms.

Keywords: snakebite envenoming; diagnostics; lateral flow assay; point of care; enzyme-linked immunosorbent assay

1. Introduction

After decades of neglect, snakebite envenoming (SBE) is finally being taken seriously by the World Health Organisation [1]. SBE alongside cholera, yellow fever, Chagas' disease, Leishmaniasis and many others, is recognised by the World Health Organisation as a neglected tropical disease (NTD) [2] and has recently been made a WHO priority. It affects predominantly impoverished people in the tropics, inhabitants of rural communities far from western medicine and hospital facilities. Hence, these victims frequently rely on herbal/traditional medicines and consequently die without any official record of snakebite as the cause. The mortality and morbidity from this disease is consequently expected to be hugely greater than current numbers suggest [3]. From estimates, deaths could match those from many of the other NTDs combined [4], and recent estimates suggest snakebite induced mortality could be as high as 94,000 every year [5].

A large part of the snakebite problem stems from the diversity of venomous snakes across the world. Venomous snakes are mainly distributed in two families of strictly venomous snakes: Elapidae (elapids: include cobras, kraits, mambas and sea snakes) and Viperidae (vipers: include rattlesnakes, puff adders and saw-scaled vipers) as well as two families with both venomous and non-venomous species: Colubridae and Lamprophiidae [6-8]. Venomous snake species are thought to number more than 600 [9], approximately 20% of the total number of snakes worldwide and therefore snakebite is far from synonymous with envenomation, although this can be difficult to determine. Deaths from SBE come almost exclusively via the bites of vipers and elapids. These families while both potentially deadly, have very different venoms. Viper venoms being composed typically of haemotoxic serine [10-12] and metalloproteases [13, 14] along with other minor components while elapid venoms are typically more neurotoxic relying on non-enzymatic nerve-binding PLA2s [15] and three-finger toxins to paralyse victims [16, 17].

A venomous snakebite should be treated as a medical emergency, and it is generally the cardiovascular system (in bites from vipers) and nervous system (in bites from elapids) that are of primary concern in saving a victim's life. Elapid bites can lead to flaccid paralysis and respiratory failure [6, 18] while bites from vipers can lead to hypovolemic shock and kidney or heart failure along with severe local tissue damage [19, 20]. Being able to discern which snake family has caused the

bite, and indeed whether venom has been injected (dry bites are commonplace), would allow appropriate pre-hospital care to be given. The use of PLA2 inhibitors such as varespladib [21, 22] or acetylcholinesterase inhibitors such as neostigmine or atropine in cases of elapid bites [23-25]; and in viper bites, the debatable administration of fresh frozen plasma when coagulopathy is suspected [26-28] and use of matrix metalloprotease inhibitors such as batimastat to reduce the effects of SVMs – muscle damage and haemotoxicity [29, 30] are all currently being investigated for treating snakebite victims. Again for such treatment, the identity of the offending snake should be confirmed using a proper diagnostic device/method.

Antivenom is still, over a century after its first development, the only treatment for SBE [31]. It is made up of polyclonal antibodies, raised against a single venom (monovalent) or multiple venoms (polyvalent) in large mammals, typically horses [32]. The majority of antivenom is polyvalent, and therefore a large proportion of the antivenom delivered will not only be specific to the offending snake. Better diagnostical methods of SBE could therefore allow monovalent antivenoms to be used, reduce adverse reactions and prevent the wastage of non-specific immunoglobulins. The delivery of antivenom is usually based on the victim's account of the snake, examination of the bitten area, presenting symptoms and the 20-minute whole-blood clotting test [6]. However, there is a significant incidence of “dry-bites”, where a victim is bitten by a venomous snake, but no venom is injected [33], therefore making decisions based on a victim's account and bite marks is flawed, and waiting until symptoms start to show is commonly practised, despite the additional time between the bite and antivenom administration causing significant endangerment to the victim. By the time symptoms are in evidence crucial time is wasted, hence, making rapid accurate assessment of envenomation is critical in the improvement of SBE treatment. In cases of dry bites, the victims may still go to hospital and be treated for SBE, which not only wastes expensive and valuable antivenom, but puts themselves in a position to suffer the side effects of antivenom, including type III hypersensitivity, anaphylaxis, and pyrogenic reactions [6]. The ability to diagnose the presence of envenomation categorically would therefore not only stop the unnecessary use of antivenom, but minimise the adverse effects and treatment cost as well.

It has been well established that not all the components in a venom are toxic or associated with the clinical symptoms. Therefore, toxin-specific treatment approaches are currently under

development. The production of monoclonal antibodies (mAbs) and small molecule inhibitors to target specific venom components [34] is currently being investigated by several researchers. This would supersede the antiquated polyclonal plasma-derived therapy that is currently the only option for victims of snakebite. In order for these future therapies to be of proper use, improvements must first be made to the diagnosis of SBE. A snakebite victim or their relative is unlikely to be able to ascertain conclusively the offending snake species, and even if they are able to identify the species, the huge intraspecific variability in venom composition observed based on the ontogeny [35], geographic location [36, 37], habitat type [38] as well as distinct sexual dimorphism in venom composition in some species [39] make clinical suppositions as to the nature of venom unwise. Assumptions made based solely on species have caused a “clinician’s nightmare” with the Southern Pacific Rattlesnake, *Crotalus oreganus helleri* [38]. A more case-specific treatment regimen would be possible given the mAb, small molecular inhibitors, anti-toxin libraries and improved diagnostics that the future strives to bring us.

Currently, the development of diagnostics for snakebite has been slow. Notably, the commonwealth serum laboratory snake venom detection kit (CSL-SVDK) is the only commercially available product in this field, and is only suitable for venomous genera present in Australasia. Despite its first production in 1988, and various problems relating to cross-reactivity with saliva of non-venomous species [40], it is still considered to be a “globally unique tool in snakebite management” [41] and is used as standard procedure across Australia. Australia is estimated to suffer just 2-4 deaths from snakebite annually [5], yet the technology that has aided the country in minimising deaths, is yet to be available in the areas that really need it: South Asia and sub-Saharan Africa.

There has been some research into the use of gold nanoparticle-conjugated venom-based antibodies in lateral flow assays for the detection of snakebites [42, 43]. These enable incredibly rapid detection of venoms, faster than the CSL-SVDK which relies on enzyme-linked immunosorbent assays (ELISA) and requires more time to acquire results. They have so far relied on antibodies raised against individual snake species (monovalent antivenom), and are therefore of little use at a global scale, although at a local level they have the potential to revolutionise the treatment of SBE.

Here, we use a novel sequence-structure-function approach to develop a family level diagnostic device specifically for most of the medically important vipers. Based on previous analyses, we have identified SVMPs as a good target for viper venom detection as these proteins are the most abundant in viper venoms [8]. Hence, by purifying and raising antibodies against a P-I and P-III metalloprotease from the venom of the western diamondback rattlesnake, *Crotalus atrox*, we assessed the ability of these antibodies to detect a range of different viper and elapid venoms via one-site and two-site ELISA. Later, a combination of suitable antibodies was used for the development of lateral flow assay device and tested using clinical samples obtained from snakebite victims.

2. Methods

2.1 Materials

Lyophilised *Crotalus atrox* venom was purchased from Sigma Aldrich (UK). The whole venoms used in the ELISAs were provided by Venomtech Limited (UK).

2.2 Protein purification

The whole *C. atrox* venom (50 mg) was dissolved in 20 mM Tris·HCl pH 7.6, and centrifuged at 5000 x g for 5 minutes. The supernatant was then applied to either a 1 mL Sepharose Q HP anion exchange column (henceforth CA1 though previously named CAMP [44]) or a 1 mL Sepharose SP HP cation exchanger (protein named CA2) and eluted using 1 M NaCl/20 mM Tris·HCl pH 7.6 via a gradient up to 60%. The fractions with proteins (based on the absorbance) were analysed by SDS-PAGE using standard methods [44] and the fractions containing the protein of interest were then pooled and concentrated using Vivaspinn centrifugal filters before being applied to a superdex 75 gel filtration chromatography column. The collected fractions were analysed by SDS-PAGE and the fractions with the protein of interest were concentrated (same as above) before once again being applied to a superdex 75 column to reduce contaminating proteins. After identifying fractions with CA1 (~50 kDa SVMP) and CA2 (~23 kDa SVMP) in pure form, they were dialysed before dilution to requisite concentrations for immunising the animals.

2.3 Production of antibodies

Solutions containing 50µg (500 µL of 100 µg/mL in PBS) of the purified proteins were injected

into sheep via intradermal injections using GERBU P as the adjuvant (500 µL). This procedure was carried out in accordance with British Home Office regulations. Immunisations were repeated on a monthly basis and ten weeks after the first injection, 250 ml of blood was collected, allowed to clot, and serum was then separated from cellular debris by centrifugation at 4000 RCF for 10 minutes. This serum was then precipitated by gradual addition of sodium sulfate (up to 18%), before centrifugation at 4000 RCF for 10 minutes and resuspension in PBS. This was then filtered through syringe filters (0.45 µm) and diluted 1: 10 in PBS before affinity purification against the whole venom.

2.4 Preparation of affinity column with venom

Crude *C. atrox* venom (10 mg) was dissolved in 1 mL sepharose coupling buffer (0.1 M NaHCO₃/0.5 M NaCl pH 8.3-8.5). Cyanogen bromide-activated-sepharose 4B resin (Sigma Aldrich, UK) was then swelled in cold 1 mM HCl for 1 hour, after which the supernatant was discarded and an empty column was packed with this sepharose-venom conjugate. The column was then washed with deionised water and then sepharose coupling buffer before adding the dissolved whole venom. These were incubated at room temperature in a roller mixer for two hours. The unbound venom was then washed away using sepharose coupling buffer and unreacted groups were quenched using 0.2 M glycine. Blocking buffer was then removed by five alternate washes with coupling buffer followed by 0.1 M acetate buffer, containing 0.5 M NaCl, pH 3.5. The column was then equilibrated with PBS and stored at 4°C in 0.05% (w/v) sodium azide.

2.5 Affinity purification of antibodies

After applying 1 L of the diluted antibodies to the column over 10 hours, the column was equilibrated with 20 mL PBS, followed by 10 mL 500 mM sodium acetate buffer pH 8 and 50 mM sodium acetate buffer/20% acetonitrile(v/v) pH 6. The fractions of 1 ml were then collected manually using 50 mM sodium acetate buffer/20% acetonitrile (v/v) pH 3.5 to elute the IgG into saturated sodium bicarbonate buffer which was used to neutralise the pH, which was assessed using litmus pH paper. The fractions containing IgG were identified using Coomassie Plus (Bradford) assay reagent (ThermoFisher, UK). These fractions were then pooled, dialysed, and concentrated before the protein content was estimated by UV spectrophotometry (280 nm). The antibodies were then aliquotted and stored at -80 °C prior to use.

2.6 Biotinylation of antibodies

N-hydroxysuccinimidobiotin (NHS-biotin) was dissolved in dimethyl sulfoxide (DMSO) before being used to label the purified IgG. NHS-biotin was added to the affinity purified IgG (in PBS) at a 20 x molar excess. After mixing in the dark for two hours at room temperature, ethanolamine was used to quench any unbound biotin. Unbound biotin/ethanolamine was then removed via a PD-10 desalting column, and the resulting biotin-IgG conjugate was stored at -20°C after protein quantification by direct measurement of O.D at 280 nm by UV spectrophotometry.

2.7 One-site ELISA

To assess the range of venoms these antibodies were able to cross react with, one-site ELISAs were carried out: 96-well high-binding microtitre plates (Corning, UK) were coated with either 100 µl of 0.1 M sodium bicarbonate to act as a blank control or 100 µl of a range of venoms (10 µg/mL) in 0.1 M sodium bicarbonate and incubated overnight at 4°C. The plates were then emptied and blocked with 200 µl of assay buffer [0.5% BSA (w/v) in PBS/0.05% (w/v) tween-20 (PBS-T)] for one hour. Following washing four times using a plate washer (Denley Wellwash 4 Mk 2, UK) and wash buffer (0.05% PBS-T (v/v)), 100 µl of toxin-specific IgG (250 ng/mL) in assay buffer was added to the wells, and the plate was then incubated for a further one hour at room temperature. Following further washing (4 times), 100 µl of rabbit anti-sheep horseradish peroxidase conjugated IgG (250 ng/mL) was added and incubated at room temperature for one hour. The plate was then washed four more times with wash buffer before adding 200 µl of 3,3',5,5'-Tetramethylbenzidine (TMB) substrate (Europa Bioproducts, UK) and incubating at room temperature for 15 minutes or until the colour developed. The reaction was then stopped using 50 µl of 0.5 M HCl. Absorbance was measured at 450 nm using a microplate reader (EMax precision plate reader, UK).

2.8 Two-site ELISA

High-binding microtitre plates were coated with a capture (un-labelled with biotin) antibody (5 µg/mL) overnight and blocked using assay buffer for one hour following this. A range of different venoms (100 µl of 10 µg/mL venoms) were then added and incubated for 2 hours at room temperature. After further washing, biotinylated detection antibodies (0.5 µg/mL) were added and incubated for two hours. After washing four times, 100 µL of streptavidin-HRP conjugate (0.5 µg/mL) was added and after 30 minutes washed off. TMB was then added and incubated until the

development of colour (approximately 15 minutes). The reaction was stopped using 0.5 M HCl and the absorbance was read at 450 nm using a microplate reader.

2.9 Synthesis of colloidal gold

Gold nanoparticles of approximately 40 nm were prepared for use in lateral flow assays in collaboration with UBIO PLC (Cochin, India). Briefly, gold chloride solution [0.01% HAuCl₄ (v/v)] was boiled in the dark for five minutes. Trisodium citrate (2 mL of 1% Na₃C₆H₅O₇) was then added with continuous stirring and the solution was boiled until a blue and then dark red colour was produced. The solution was then stabilised at room temperature and stored at 4 °C while protected from light using foil coated glassware.

2.10 Colloidal gold probe preparation

The CA1 and CA2 antibodies purified previously were diluted to 2 µg/mL in 0.1 M citrate buffer, pH 6.8 and added to a solution of the colloidal gold nanoparticles synthesised previously. The solution was stirred for 60 minutes to allow conjugation, BSA was then added (up to 0.02%) to stabilise the conjugates. A resuspension buffer (0.01% BSA (w/v) , 0.001% sodium azide (v/v), 10mM sodium phosphate pH 7.5) was then used to dilute the solution before the application of conjugates onto the conjugate pad (at 60 µg/mL) and drying by dehumidification for 30 minutes. These were then stored in azide (0.02% (w/v) at 4 °C before use in conjugate pad in lateral flow assay (LFA) development.

2.11 Preparation of LFA devices

The CA1 or CA2 capture (unlabelled) antibodies (2 mg/mL) were coated in test lines on the nitrocellulose membrane and goat anti-mouse antibodies (Whatmann, India) were coated as control line (2 mg/mL). The strips were then blocked with 0.02% BSA (w/v) in PBS before being dried by dehumidification. A commercially available glass fibre conjugate pad was prepared and coated in gold-antibody conjugates (both CA antibodies and gold conjugated mouse antibodies for control) mixed with conjugate spray buffer (0.01% (w/v) BSA, 0.05% (w/v) sodium azide, 0.01% (w/v) sucrose, 10mM sodium phosphate, pH 7.5) before drying by dehumidification. After assembly in appropriate plastic cassettes, the kits were assessed using dilutions of respective antigens, a range of venoms and plasma samples obtained from snakebite victims. Assembled kits were stored at room temperature away from sunlight and humidity.

2.12 Ethical statement and blood collection

TCR multispecialty hospital research ethics committee approved the procedures for blood collection from snakebite victims. Human blood was obtained from patients in vacutainers with 3.2% (w/v) sodium citrate as an anti-coagulant and spun at 3000 RCF for 5 minutes. Plasma was then separated and stored at -20 °C until testing with LFA.

2.13 Statistical analysis

All data were first normalised before calculating statistical significance using GraphPad Prism 7 software [45]. One-way and two-way ANOVAs (based on the data) were carried out before performing a post hoc Dunnett's multiple comparisons test in order to calculate the statistical significance.

3. Results

3.1 Immune responses to CA1 and CA2 metalloproteases

Sheep were injected once every four weeks with either whole CA1 (Group III SVMP) or CA2 (Group I SVMP) in order to produce antibodies specific for these two SVMPs. Despite CA1 being nearly double the molecular weight of CA2, both proteins generated a similar immune response which steadily increased during the first 8 weeks (Figure 1). After this point, the immune response appears to plateau.

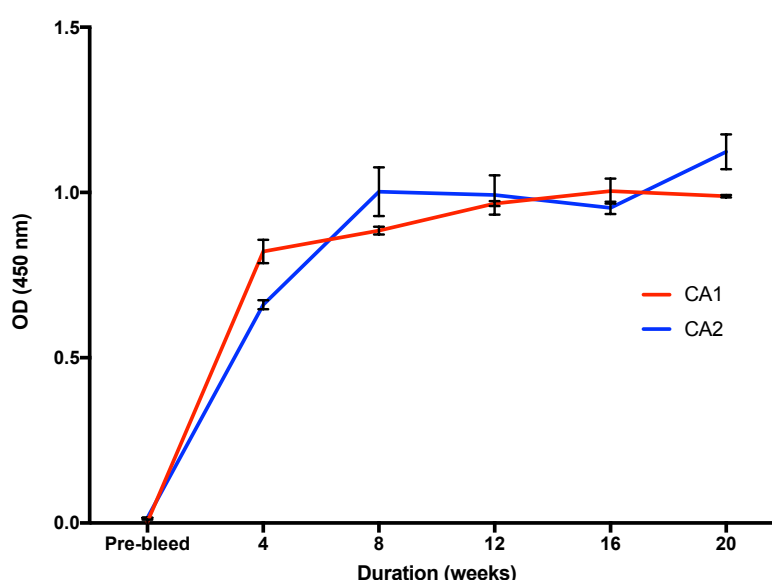


Figure 1: Sheep immune responses against purified metalloproteases: CA1 and CA2. Blood was taken from sheep every four weeks and the serum was used in one-site enzyme linked immunosorbent assays (ELISA) to monitor immune responses to the purified CA1 and CA2. The O.D values measured by spectrophotometry indicate the level of antibody binding and indicate the immune response over the 20 week immunisation schedule. Data were analysed in Graphpad Prism and represent mean \pm S.D. (n=3).

3.2 Specificity of toxin-specific IgG against a range of venoms using one-site ELISA

To ascertain the cross-reactivity of these antibodies to different venoms arrays of viper and elapid venoms were used, and detected using different combinations of antibodies. One-site ELISAs demonstrated that these antibodies detect a wide range of venoms, but are generally more viper specific, cross reacting to a lesser degree with elapid venoms. In one-site assays (Figure 2), CA1 antibodies show statistically significant cross reactivity with almost all the venoms (less specificity towards elapid venoms compared to vipers) used, while CA2 antibodies show a slightly greater specificity for viper venoms. Unsurprisingly *Crotalus atrox*, the snake from which these proteins originated is detected to the greatest degree, along with the purified proteins.

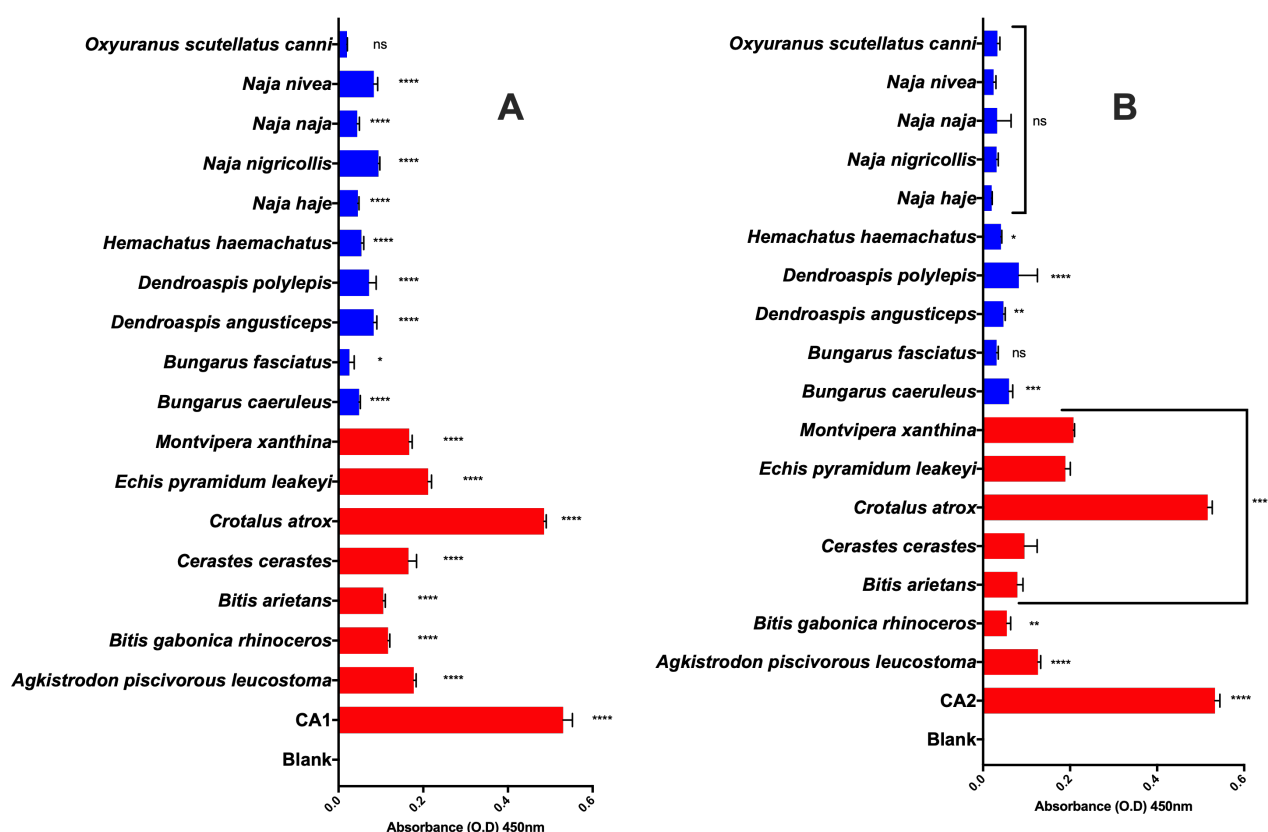


Figure 2: Specificity of CA1 (A) and CA2 (B) antibodies to different viper and elapid venoms by one-site ELISA. After affinity purification of toxin-specific IgG (CA1 and CA2), one-site ELISAs were carried out in order to assess their specificity against a range of venoms. High binding microtitre plates were coated with a range of different venoms in sodium bicarbonate buffer before washing, blocking with BSA and the addition of CA1 or CA2 antibodies. The unbound antibodies were then washed off before the addition of anti-sheep-HRP conjugate. Followed by further washing, trimethyl benzidine (TMB) was added and the level of absorbance was measured at 450 nm by spectrometry. Data were analysed in Graphpad Prism and represent mean \pm S.D. (n=3). The P-values shown are as calculated using one-way ANOVA followed by Tukey's post hoc multiple comparisons test. For this, the purified antibodies were compared to blank values, and all the values were normalised using a blank control. (*P \leq 0.05, ** P \leq 0.01, *** P \leq 0.001 and **** P \leq 0.0001).

3.3 Specificity of toxin-specific antibodies against a range of different venoms using two-site ELISA

Following one-site ELISA, CA1 and CA2 antibodies were biotinylated for use in two-site ELISA in order to determine their specificity without non-specific cross reactivity that was observed in one-site ELISA against elapid venoms. A range of venoms were screened using two-site ELISA and toxin-specific antibodies in different configurations: CA1 as both capture and detection antibody (CA1-CA1); CA1 as capture and CA2 as detection (CA1-CA2); CA2 as both capture and detection antibody (CA2-CA2) and CA2 as capture with CA1 as detection antibody (CA2-CA1). In contrast to the one-site assays, in two-site assays, there was much more specific binding of CA1 and CA2 for viper venoms, with very few elapid venoms being detected at a significant level (Figure 3). Detection does not differ significantly between the different genders (male and female) and morphologies (albino and normal) of *C. atrox* (Figure 3A-3D), although the closely related *Crotalus basilicus* is detected to a much lesser extent as are *Agkistrodon* species and *Bothriechis schlegelii* (Figure 3A-3D). The other members of Crotalinae (the pit vipers) including *Bothrops atrox*, *B. asper* and *Sistrurus miliarius barbouri* are all well detected. The Viperinae species: *Montivipera xanthina*, *Bitis arietans*, *Echis carinatus*, *E. pyramidum leakeyi* and *Atheris squamigera* are all also detected to a much lower but still significant level. All the elapid venoms only showed a very small degree of binding and most of these were insignificant. Due to minimising significant elapid detection and maximising vipers detected to significant level the CA1-CA2 combination was employed in further experiments.

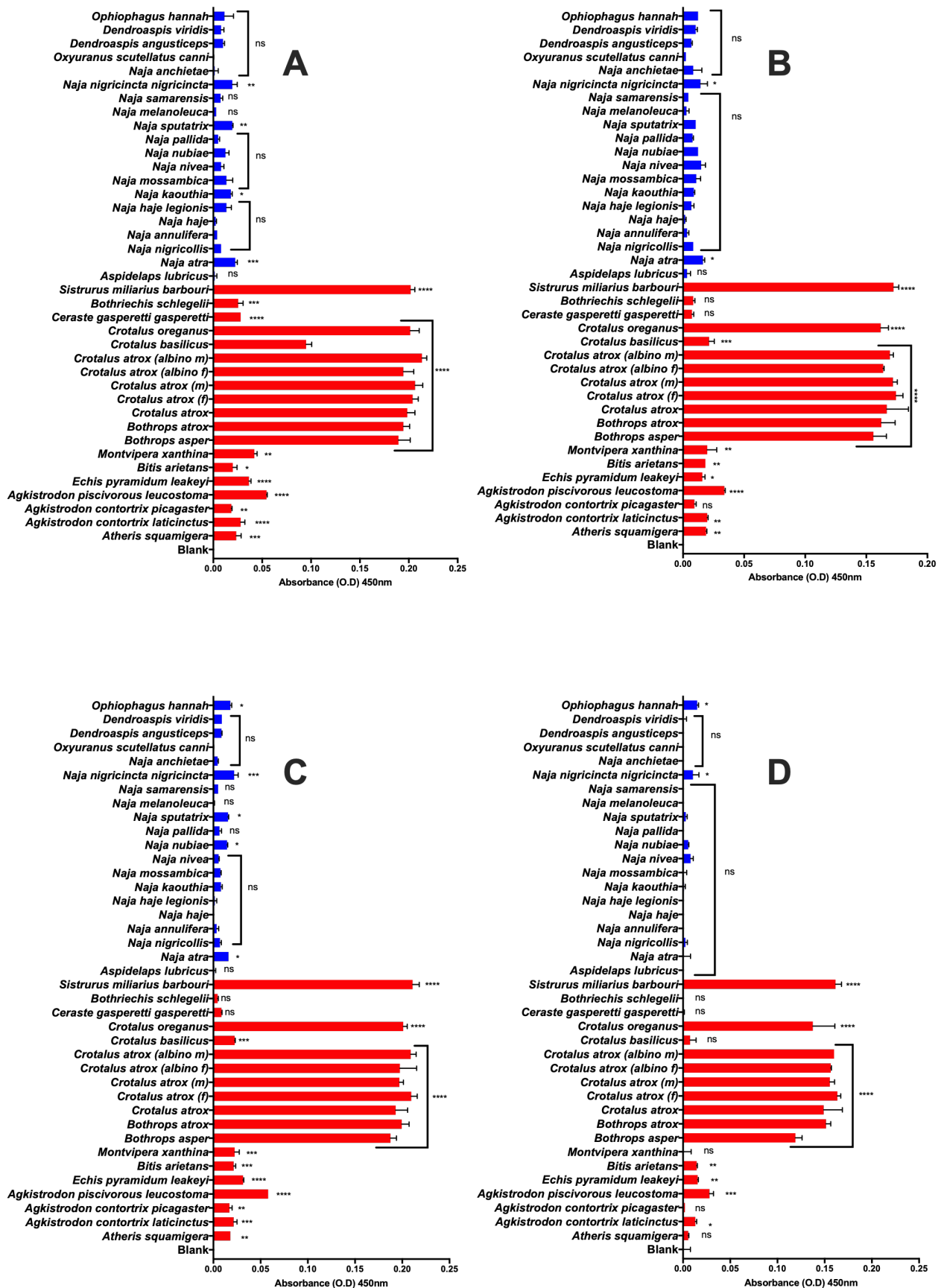


Figure 3. Two-site ELISA showing specificity of different combinations of CA1 and CA2 antibodies to different viper (red) and elapid (blue) venoms: CA1-CA1 (A), CA1-CA2 (B), CA2-CA1 (C) and CA2-CA2 (D) combinations were used. After affinity purification of toxin-specific IgG, two-site ELISAs were carried out in order to assess their specificity for a range of different venoms. High binding microtitre plates were coated with capture (as specified above) antibodies in sodium

bicarbonate before washing and the addition of different venoms (10 µg/mL). For detection, biotinylated CA1 or CA2 antibodies were then added. These were then washed off before the addition of streptavidin-HRP conjugate. Following further washing, colorimetric visualisation using trimethyl benzidine (TMB) was developed and measured the absorbance at 450 nm in a microplate reader. Data were analysed in Graphpad Prism and represent mean \pm S.D. (n=3). The P-values shown are as calculated using one-way ANOVA followed by Tukey's post hoc multiple comparisons test. For this, the purified antibodies were compared to blank values, and all the values were normalised using a blank control. (*P \leq 0.05, ** P \leq 0.01, *** P \leq 0.001 and **** P \leq 0.0001).

3.3 Detection of venom in spiked whole blood and urine samples by two-site ELISA

After assessing the ability for different combinations of CA1 and CA2 antibodies to detect a range of venoms in assay buffer, one combination (CA1-CA2) was then used to assess their ability to detect venoms in urine and plasma samples which had been spiked with venoms. The use of more complex mediums (biological fluids) decreased almost all the cross reactivity that was observed previously with elapid venoms in urine, although almost all viper venoms were clearly detected. In whole blood, slightly more detection of elapid venoms was seen when compared to urine but none to a significant level.

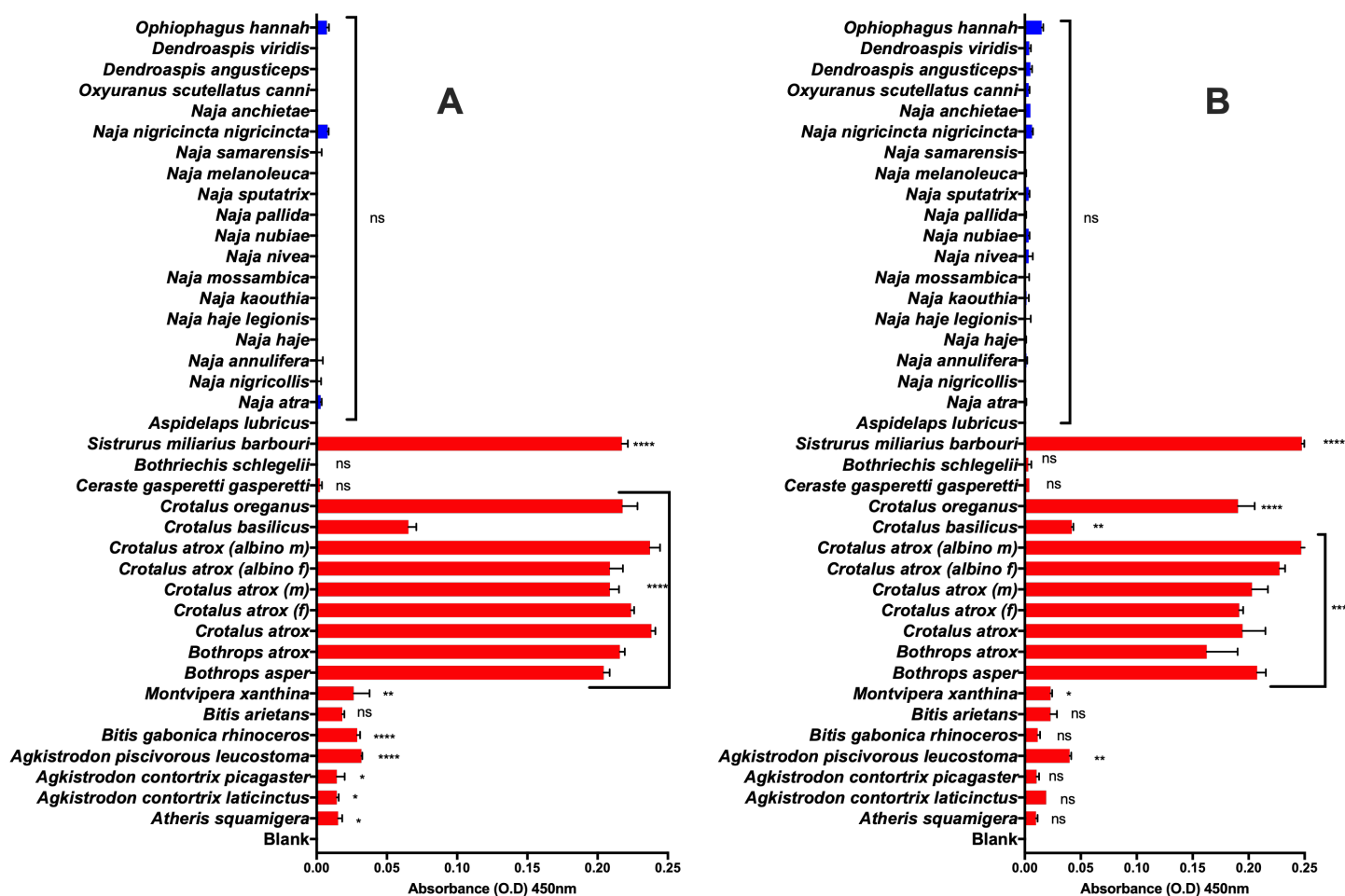


Figure 4: Two-site ELISA showing the detection of different viper (red) and elapid (blue) venoms in urine (A) and whole blood (B). After purification of toxin-specific antibodies, two-site ELISAs were carried out in order to assess their specificity for a range of different venoms in biological samples such as urine and blood. High binding microtitre plates were coated with CA1 capture antibodies (10 µg/mL) in sodium bicarbonate buffer before washing and the addition of different venoms (10 µg/mL) spiked in either human urine or whole blood. For detection, biotinylated CA2 antibodies were then added (0.5 µg/mL). These were then washed off before the addition of streptavidin-HRP conjugate. These were again washed off before colorimetric visualisation using trimethyl benzidine (TMB) and measuring absorbance at 450 nm in a microplate reader. Data were analysed in Graphpad Prism and represent mean \pm S.D. (n=3). The P-values shown are as calculated using one-way ANOVA followed by Tukey's post hoc multiple comparisons test. For this, the purified antibodies were compared to blank values, and all the values were normalised using a blank control. (*P \leq 0.05, ** P \leq 0.01, *** P \leq 0.001 and **** P \leq 0.0001).

3.4 Optimisation of ELISA using toxin-specific antibodies for the detection of Indian 'big four' snake venoms

Given the extremity of the SBE in India, particularly with the 'big four' snakes (Russell's viper, Indian cobra, Indian krait and saw-scaled viper), the toxin-specific antibodies were then assessed to determine their ability to detect these species venoms. Higher concentrations (1 and 2 $\mu\text{g/mL}$) of detection antibodies allowed detectability of 'big four' snake venoms, and some degree of detection in both urine and blood using all antibody concentrations (Figure 5). At both concentrations 1 $\mu\text{g/mL}$ (Figure 5A) and 2 $\mu\text{g/mL}$ (Figure 5B) and in both blood (Figure 5C) and urine (Figure 5D) the combination of CA1-CA1 gives the highest level of detection. In assay buffer *Naja naja* goes undetected then interestingly absorbance increases significantly in blood and urine. Likewise, *Echis carinatus* has the highest detection in buffer, but in blood and urine *Daboia russelii* does.

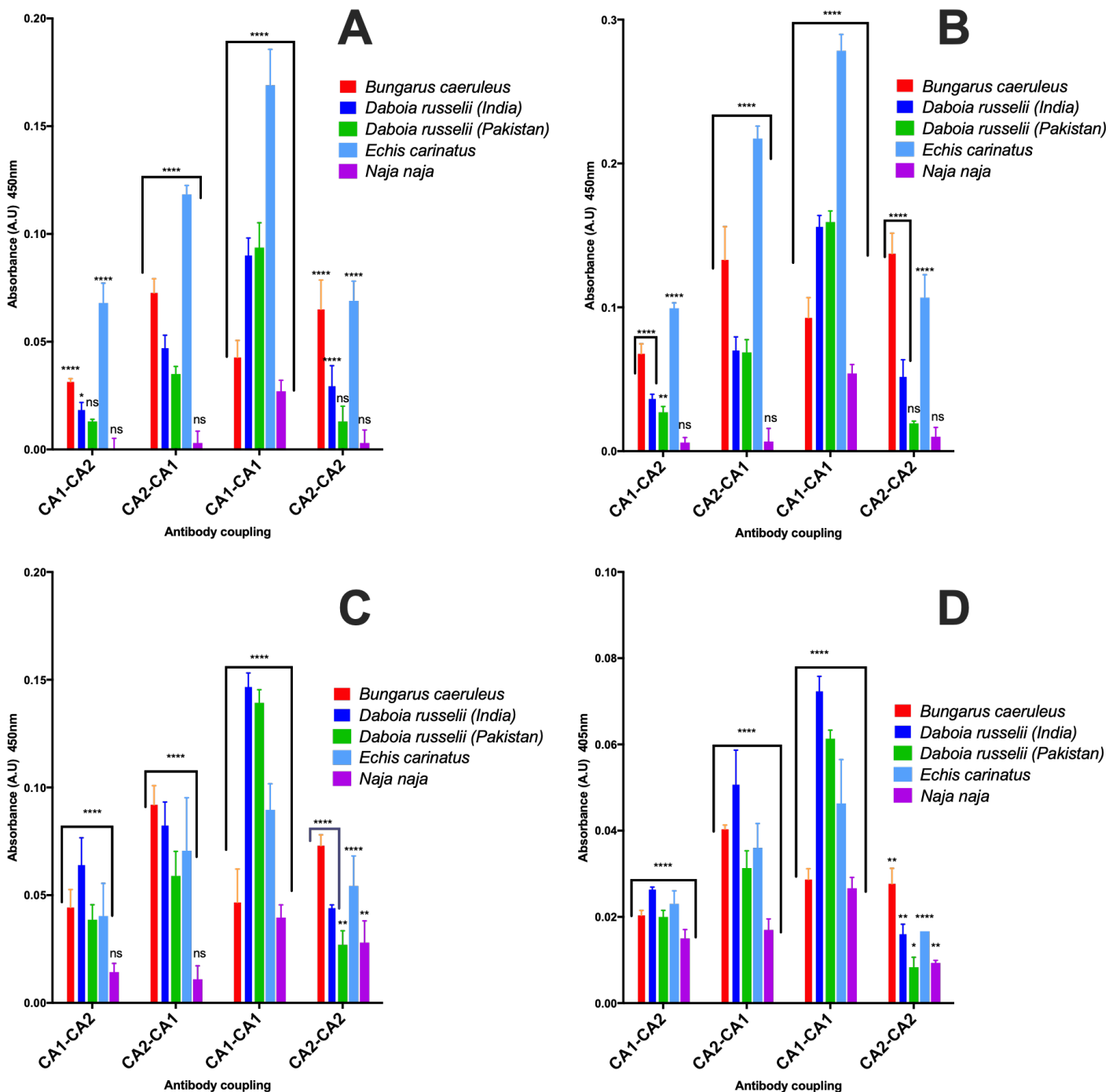


Figure 5: Two-site ELISA showing the ability of toxin-specific antibodies for the detection of the Indian 'big four' snake venoms: Indian Krait (*Bungarus caeruleus*), Russell's viper (*Daboia russelii* - Indian and Pakistani origin), Saw-scaled viper (*Echis carinatus*) and Indian Cobra (*Naja naja*). Different concentrations of capture and detection antibodies were used until specific concentrations for the detection of these species' venoms were identified. Concentrations of 1 $\mu\text{g/mL}$ (A) and 2 $\mu\text{g/mL}$ (B) were found to improve the detection of these species, and a concentration of 2 $\mu\text{g/mL}$ was then used in both blood (C) and urine (D) spiked with venoms. Data were analysed in Graphpad Prism and represent mean \pm S.D. (n=3). The P-values shown are as calculated using one-way ANOVA followed by Tukey's post hoc multiple comparisons test. For this, the purified antibodies were compared to blank values, and all the values were normalised using a blank control. (* $P \leq 0.05$, ** $P \leq 0.01$, *** $P \leq 0.001$ and **** $P \leq 0.0001$).

3.5 Lateral flow assays for the detection of snakebite envenomation in clinical samples

After optimising and analysing the cross reactivity of these CA antibodies using one- and two-site ELISAs, the most effective pairing on antibodies (CA1-CA2) were applied to lateral flow assay devices in order to work in a point of care setting and were trialled on snakebite patient samples. The LFA device was optimised used venoms in buffer and then spiked plasma before being tested on patient samples. In total 32 samples were tested, of which three were healthy human plasma controls (all of which gave negative results). In this different configuration and using clinical samples, detection proved broader than in ELISA, with samples from individuals thought to be bitten by Indian cobras, *Naja naja*, also giving positives, suggesting this LFA could have the potential to work as an SVMP detection device for elapids also. However, the strips were specific to snakebite with control samples from healthy human plasma showing no positives and those from a centipede bite also not giving results associated with SBE. *Daboia russelii* envenomed victim samples gave a high rate of detection with just two of 23 victim samples giving negative results (Figure 5C). This could be attributable to dry or mild bites, or juvenile snakes injecting a venom dose below the detection limit of the device.

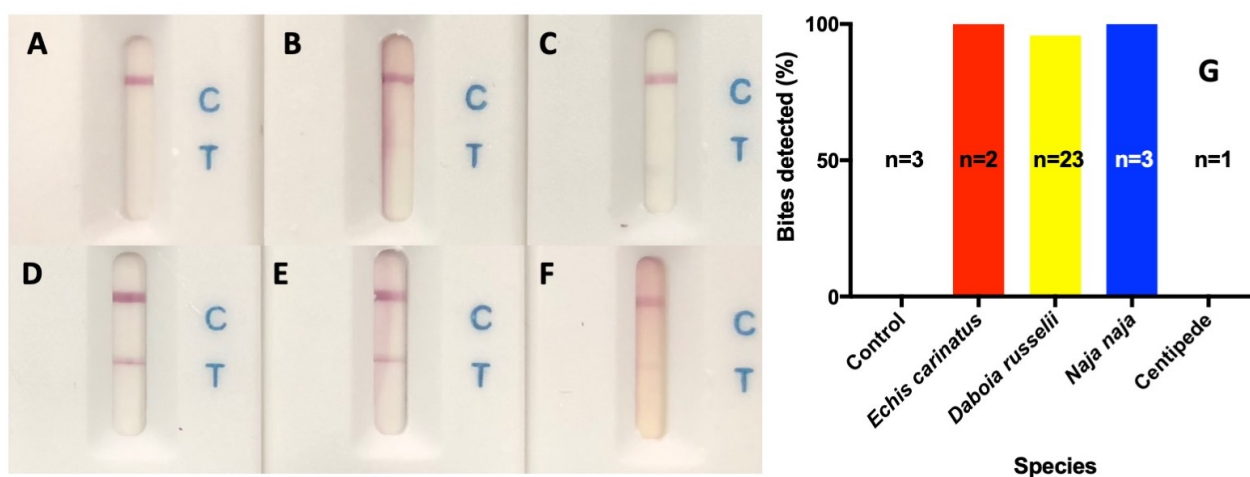


Figure 5: Lateral flow assay using CA1-CA2 antibodies on plasma samples from victims of envenomation (n=32: control=3, *Echis carinatus*=2, *Daboia russelii*=23, *Naja naja*=3, centipede=1). The CA antibodies were tried in various embodiments and found to respond most successfully in LFA configuration with the CA1-CA2 combination. These were then conjugated to gold nanoparticles before use in LFA devices. These were then used with 30 μ l of plasma samples from victims of envenomation and compared to a clinicians prediction of offending snake species using description of snake combined with presence of bite marks, blistering, ptosis and blood clotting time. **A**, control showing plasma from non-envenomed individual. **B**, lack of test line seen with plasma from victim of centipede envenomation (n=1). **C**, Lack of test line seen with false negative for *Daboia russelii* envenomation (n=1). **D**, solid line seen with heavy Russell's viper envenoming (n=5). **E**, fainter band seen with majority of snakebite envenomings (n=21) **F**, example of much

fainter band given by one sample from Russell's viper patient (n=1). The devices detected envenomation in 93% of snakebite victims (just 2 from 29 samples from envenomed patients undetected) (G).

4. Discussion

SBE is a brutal affliction, for which medical professionals have virtually no diagnostical devices and only one, sometimes dangerous, treatment option. A universal venom detection kit would allow clinicians the world over to have a reliable method by which to qualify whether a patient has become envenomed. In the future, the same method will be used, in conjunction with emerging devices [46] to also quantify the amount of venom or specific toxins present in the circulation of victims. This would reduce accountability on the clinicians part, speed up the treatment and direct more specific treatments as and when they become available. Instead of relying on experience with treating snakebites, clinicians would have a device with which to validate further treatment with an expensive and sometimes dangerously immunogenic drug: anti-venom. By producing antibodies specific for certain venoms/toxic proteins, these proteins, and consequently venoms containing these proteins, can then be detected in biological samples from victims, dictating toxin-specific treatments, thereby ensuring a need and efficacy of the treatment.

In this study we purified two metalloproteases from *Crotalus atrox*, in order to raise and purify antibodies for use in diagnosing SBE. SBE currently suffers from a chronic lack of reliable methods of affirming envenomation. Despite being from the same species and family of proteins, CA1 and CA2 are heterogeneous proteins: CA1 is a P-III SVMP, containing disintegrin-like as well as cysteine-rich domains as well as the metalloprotease domain and CA2, as a P-I SVMP and has just the metalloprotease domain. Using a Basic Local Alignment Search Tool (BLAST) analysis of their sequences shows that the sequence for CA1 (the larger SVMP) covers 51% of the sequence of CA2 and a much higher 68% are positives meaning the sequence is made up of either identical or similar amino acids. This somewhat explains the similarities in their detection of the different species, although the disintegrin-like and cysteine-rich domains could be expected to lead to greater differentiation, as these regions may contain a range of different epitopes.

The ELISA work ascertained that these SVMP-specific antibodies are successful in detecting most members of Crotalinae, the subfamily containing *Crotalus atrox* along with the most closely related species including some true vipers. Surprisingly, relatively poor reactivity (still highly

significant) with *C. basiliscus* was observed despite being closely related and its venom being composed of nearly 70% SVMPs [47]. Additionally, despite *Crotalus atrox* being evolutionarily more distant from *Bothrops* than *Agkistrodon* and *Bothriechis*, *Bothrops* species are detected to a much greater extent: seemingly SVMPs are well conserved within these genera despite more evolutionary distance [48], this may be attributable to similarities in preys.

Through ELISAs in assay buffer, many true vipers (members of Viperinae) were also detected to a significant level but to a much lesser extent than the Crotalids and very few elapids were detected. Upon switching the buffer to human fluids (urine and blood) almost all cross reactivity with elapid venoms and most significant detection of Viperinae was also removed (although minor detection was still observed), possibly in part due to better blocking of the plate with plasma proteins. Slightly improved specificity could also be due to any especially cross reactive antibodies binding to plasma proteins rather than venom proteins or capture antibodies. While an incredibly valuable tool *in vitro*, in a clinical setting ELISA is relatively complicated and time consuming, requiring a minimum of approximately 20 minutes to get results and giving somewhat qualitative results when compared to LFA which can deliver results in a matter of minutes and gives a binary result, minimising confusion for clinicians.

Translating these antibodies into an LFA configuration enabled the detection of Russell's viper, *Daboia russelii*, and saw-scaled vipers, *Echis carinatus*, as well as all three cases of an elapid bite from the Indian cobra, *Naja naja*. Although *N. naja* venom does have a small metalloprotease content of around 1% [49], these are likely to show high homogeneity to viper SVMPs. BLAST analysis of SVMPs from *Naja atra* (Atragin, accession: D3TTC2) and *Naja mossambica* (Mocarhagin, accession: Q10749) against CA1 gave 58% and 44% coverage of identities respectively (72% and 63% positives - identical and similar amino acids combined). Therefore, the ability for these antibodies to detect venoms from *Naja* is possible (despite results from ELISA), only unlikely given the very low percentage found in *N. naja* venom [49]. This percentage is likely to vary based on a range of factors such as locality, age and possibly gender and the South Indian phenotype could possibly express a larger percentage of SVMPs, though published percentages

vary little and those between 1.45% in Pakistan [50] and 0.85% in Rajasthan/Gujarat and 0.86% in Sri Lanka have been reported [51].

At the initial antibody concentrations used (0.5 $\mu\text{g/mL}$), few species from Viperinae and Elapidae were detected (Figure 3 & 4), but by increasing antibody concentrations in ELISA, and using an alternative platform (LFA) these more distantly related snake species and venoms were also detected (Figure 5). Although this study eventually yielded an LFA device with such high cross reactivity it was unable to differentiate between vipers and elapids. Further optimisation, and raising of antibodies in two different species could overcome these hurdles.

The major pitfall in assessing the LFA's reliability is reliance on a clinician's expert opinion to corroborate or refute the LFA results. Based on the local effects and other symptoms, description of snake or actual snake - in the case that the offending snake was killed and brought to hospital - clinicians can sometimes have a good idea of the offending snake. However, there are cases of these being very wrong and fear in victims can trigger misleading symptoms causing the administration of anti-venom in non-venomous bites, which can result in unnecessary anaphylaxis [52]. Even when correctly identifying the snake as a venomous species, the hugely varied levels of envenomation from dry bite to the near emptying of venom ducts into a victim cause a huge range of symptoms and pathologies to result. Therefore, the use of molecular techniques such as PCR-aided DNA sequencing to corroborate a clinician's interpretation of a bite in evaluating point of care devices would be beneficial. This has already been reported using DNA found on swabs from the bite site and comparing this with morphological identification of dead snakes [53]. The next generation of lateral flow devices will no doubt include multiple strips, each denoting a particular taxon, toxin or treatment type, whether the treatment be monovalent antivenoms or small molecule therapeutics. Whatever the future of snakebite therapeutics hold, diagnostic are in dire need of improvement as a priority.

While the differential identification between viper and elapid SBE proved unreliable via the current prototype LFA device, the presence of SVMPs in victim samples seems to be correctly implied. What is required is an accurate venom profile of the South Indian *N. naja* phenotype and sequencing of its SVMPs. A larger sample size including a larger range of species would aid in the

assessment of breadth of species detected and specificity for venoms with high SVMP content. The ability for this device to detect SVMPs could act as indication for rapid administration of SVMP-specific drugs or small molecule inhibitors such as batimastat/marimastat or other future treatments and significantly reduce SVMP-induced muscle damage and necrosis [8]. The negative effects of these broad spectrum metalloprotease inhibitors on angiogenesis [54] mean a definite indication is required before such potentially detrimental drugs are administered, and an LFA device such as that described here would be preferential than waiting for symptoms to develop. As novel, toxin-specific treatments become available, indicative diagnostics will become essential and a similar degree of specificity to respective treatments seems sensible. LFA devices currently provide the most rapid option for this and rapidity of treatment is essential when it comes to SBE-induced morbidities. As and when treatments become approved and available, similar devices also need to be developed in such a manner.

SBE continues to take an unnecessarily large toll on the underprivileged people of the tropics, this is hoped to be halved by 2030 by the WHO, but bold ideas will have to deliver approved diagnostic and therapeutic products if this is ever to become a reality.

References

1. Williams, D.J., et al., *Strategy for a globally coordinated response to a priority neglected tropical disease: Snakebite envenoming*. PLOS Neglected Tropical Diseases, 2019. **13**(2): p. e0007059.
2. WHO. *Neglected tropical diseases*. 2017; Available from: http://www.who.int/neglected_diseases/diseases/en/.
3. Chippaux, J.-P., *Estimating the global burden of snakebite can help to improve management*. PLoS medicine, 2008. **5**(11): p. e221.
4. Williams, D., et al., *The Global Snake Bite Initiative: an antidote for snake bite*. The lancet, 2010. **375**(9708): p. 89-91.
5. Kasturiratne, A., et al., *The global burden of snakebite: a literature analysis and modelling based on regional estimates of envenoming and deaths*. PLoS Med, 2008. **5**(11): p. e218.
6. Gutiérrez, J.M., et al., *Snakebite envenoming*. Nature Reviews Disease Primers, 2017. **3**: p. nrdp201763.
7. Warrell, D.A., *Snake bite*. The Lancet, 2010. **375**(9708): p. 77-88.
8. Williams, H.F., et al., *The Urgent Need to Develop Novel Strategies for the Diagnosis and Treatment of Snakebites*. Toxins, 2019. **11**(6): p. 363.
9. Fry, B.G., *Venomous reptiles and their toxins: evolution, pathophysiology and biodiscovery*. 2015.
10. Vaiyapuri, S., et al., *Sequence and phylogenetic analysis of viper venom serine proteases*. Bioinformation, 2012. **8**(16): p. 763-772.

11. Sanchez, E.F., et al., *Isolation of a proteinase with plasminogen-activating activity from Lachesis muta muta (bushmaster) snake venom*. Archives of biochemistry and biophysics, 2000. **378**(1): p. 131-141.
12. Kisiel, W., et al., *Characterization of a protein C activator from Agkistrodon contortrix contortrix venom*. Journal of Biological Chemistry, 1987. **262**(26): p. 12607-12613.
13. Ramos, O. and H. Selistre-de-Araujo, *Snake venom metalloproteases—structure and function of catalytic and disintegrin domains*. Comparative Biochemistry and Physiology Part C: Toxicology & Pharmacology, 2006. **142**(3): p. 328-346.
14. Mackessy, S.P., *Handbook of venoms and toxins of reptiles*. 2010: CRC Press.
15. Paoli, M., et al., *Mass spectrometry analysis of the phospholipase A2 activity of snake pre-synaptic neurotoxins in cultured neurons*. Journal of neurochemistry, 2009. **111**(3): p. 737-744.
16. Kini, R.M. and R. Doley, *Structure, function and evolution of three-finger toxins: mini proteins with multiple targets*. Toxicon, 2010. **56**(6): p. 855-867.
17. Nirthanan, S. and M.C.E. Gwee, *Three-Finger α-Neurotoxins and the Nicotinic Acetylcholine Receptor, Forty Years On*. Journal of Pharmacological Sciences, 2004. **94**(1): p. 1-17.
18. Bittenbinder, M.A., et al., *Coagulotoxic Cobras: Clinical Implications of Strong Anticoagulant Actions of African Spitting Naja Venoms That Are Not Neutralised by Antivenom but Are by LY315920 (Varespladib)*. Toxins (Basel), 2018. **10**(12).
19. Chara, K., et al., *A rare complication of viper envenomation: cardiac failure. A case report*. Med Sante Trop, 2017. **27**(1): p. 52-55.
20. El Zahran, T., et al., *Snakebites in Lebanon: A Descriptive Study of Snakebite Victims Treated at a Tertiary Care Center in Beirut, Lebanon*. J Emerg Trauma Shock, 2018. **11**(2): p. 119-124.
21. Wang, Y., et al., *Exploration of the Inhibitory Potential of Varespladib for Snakebite Envenomation*. Molecules, 2018. **23**(2).
22. Lewin, M., et al., *Varespladib (LY315920) Appears to Be a Potent, Broad-Spectrum, Inhibitor of Snake Venom Phospholipase A2 and a Possible Pre-Referral Treatment for Envenomation*. Toxins, 2016. **8**(9): p. 248.
23. Shah, S., S.S. Naqvi, and M.A. Abbas, *Use of neostigmine in black mamba snake bite: a case report*. Anaesth Pain & Intensive Care, 2016. **20**(1): p. 77-79.
24. Faiz, M.A., et al., *Bites by the monocled cobra, Naja kaouthia, in Chittagong division, Bangladesh: Epidemiology, clinical features of envenoming and management of 70 identified cases*. The American journal of tropical medicine and hygiene, 2017. **96**(4): p. 876-884.
25. Lewin, M.R., et al., *Early treatment with intranasal neostigmine reduces mortality in a mouse model of Naja naja (Indian Cobra) envenomation*. Journal of tropical medicine, 2014. **2014**.
26. Maduwage, K. and G.K. Isbister, *Current treatment for venom-induced consumption coagulopathy resulting from snakebite*. PLoS neglected tropical diseases, 2014. **8**(10): p. e3220.
27. Holla, S.K., et al., *The role of fresh frozen plasma in reducing the volume of anti-snake venom in snakebite envenomation*. Tropical doctor, 2018. **48**(2): p. 89-93.
28. Isbister, G., et al., *A randomized controlled trial of fresh frozen plasma for coagulopathy in Russell's viper (Daboia russelii) envenoming*. Journal of Thrombosis and Haemostasis, 2017. **15**(4): p. 645-654.
29. Escalante, T., et al., *Effectiveness of batimastat, a synthetic inhibitor of matrix metalloproteinases, in neutralizing local tissue damage induced by BaP1, a hemorrhagic*

- metalloproteinase from the venom of the snake Bothrops asper*. Biochemical pharmacology, 2000. **60**(2): p. 269-274.
30. Arias, A.S., A. Rucavado, and J.M. Gutiérrez, *Peptidomimetic hydroxamate metalloproteinase inhibitors abrogate local and systemic toxicity induced by Echis ocellatus (saw-scaled) snake venom*. Toxicon, 2017. **132**: p. 40-49.
 31. WHO. *Guidelines for the production, control and regulation of snake antivenom immunoglobulins*. World Health Organisation 2017; Available from: http://www.who.int/bloodproducts/snake_antivenoms/en/.
 32. World Health Organization, W., *WHO guidelines for the production, control and regulation of snake antivenom immunoglobulins*. Geneva: WHO, 2010. **134**.
 33. Naik, B.S., "Dry bite" in venomous snakes: A review. Toxicon, 2017. **133**: p. 63-67.
 34. Laustsen, A.H., *Guiding recombinant antivenom development by omics technologies*. New Biotechnology, 2017.
 35. Pla, D., et al., *Proteomic analysis of venom variability and ontogeny across the arboreal palm-pitvipers (genus Bothriechis)*. Journal of Proteomics, 2017. **152**: p. 1-12.
 36. Tsai, I.-H., et al., *Venom phospholipases of Russell's vipers from Myanmar and eastern India—Cloning, characterization and phylogeographic analysis*. Biochimica et Biophysica Acta (BBA)-Proteins and Proteomics, 2007. **1774**(8): p. 1020-1028.
 37. Shashidharamurthy, R. and K. Kemparaju, *Region-specific neutralization of Indian cobra (Naja naja) venom by polyclonal antibody raised against the eastern regional venom: A comparative study of the venoms from three different geographical distributions*. International immunopharmacology, 2007. **7**(1): p. 61-69.
 38. Sunagar, K., et al., *Intraspecific venom variation in the medically significant Southern Pacific Rattlesnake (Crotalus oreganus helleri): Biodiscovery, clinical and evolutionary implications*. Journal of Proteomics, 2014. **99**: p. 68-83.
 39. Amorim, F., et al., *Proteopectidomic, Functional and Immunoreactivity Characterization of Bothrops moojeni Snake Venom: Influence of Snake Gender on Venom Composition*. Toxins, 2018. **10**(5): p. 177.
 40. Jelinek, G.A., et al., *Cross reactivity between venomous, mildly venomous, and non-venomous snake venoms with the Commonwealth Serum Laboratories Venom Detection Kit*. Emergency Medicine, 2004. **16**(5-6): p. 459-464.
 41. Nimorakiotakis, V.B. and K.D. Winkel, *Prospective assessment of the false positive rate of the Australian snake venom detection kit in healthy human samples*. Toxicon, 2016. **111**: p. 143-146.
 42. Liu, C.-C., et al., *Development of sandwich ELISA and lateral flow strip assays for diagnosing clinically significant snakebite in Taiwan*. PLoS neglected tropical diseases, 2018. **12**(12): p. e0007014.
 43. Pawade, B.S., et al., *Rapid and selective detection of experimental snake envenomation—Use of gold nanoparticle based lateral flow assay*. Toxicon, 2016. **119**: p. 299-306.
 44. Williams, H.F., et al., *Mechanisms underpinning the permanent muscle damage induced by snake venom metalloprotease*. PLoS Neglected Tropical Diseases, 2019. **13**(1): p. e0007041.
 45. Ivashchenko, R., et al., *Prism 7 for Mac OS X-Version 7.0c, March 1, 2017*. 2017.
 46. Dunbar, J., A. Jehanli, and G. Hazell, *7 Evaluation of a new point of care quantitative cube reader for salivary analysis in the english premier league soccer environment*. 2015, BMJ Publishing Group Ltd and British Association of Sport and Exercise Medicine.
 47. Segura, A., et al., *Proteomic, toxicological and immunogenic characterization of Mexican west-coast rattlesnake (Crotalus basiliscus) venom and its immunological relatedness with*

- the venom of Central American rattlesnake (Crotalus simus)*. J Proteomics, 2017. **158**: p. 62-72.
48. Alencar, L.R.V., et al., *Diversification in vipers: Phylogenetic relationships, time of divergence and shifts in speciation rates*. Molecular Phylogenetics and Evolution, 2016. **105**: p. 50-62.
 49. Dutta, S., et al., *Proteomic analysis to unravel the complex venom proteome of eastern India Naja naja: Correlation of venom composition with its biochemical and pharmacological properties*. J Proteomics, 2017. **156**: p. 29-39.
 50. Wong, K.Y., et al., *Elucidating the biogeographical variation of the venom of Naja naja (spectacled cobra) from Pakistan through a venom-decomplexing proteomic study*. Journal of Proteomics, 2018. **175**: p. 156-173.
 51. Sintiprungrat, K., et al., *A comparative study of venomomics of Naja naja from India and Sri Lanka, clinical manifestations and antivenomics of an Indian polyspecific antivenom*. Journal of Proteomics, 2016. **132**: p. 131-143.
 52. Silveira, P.V.P. and S.d.A. Nishioka, *Non-venomous snake bite and snake bite without envenoming in a brazilian teaching hospital: analysis of 91 cases*. Revista do Instituto de Medicina Tropical de São Paulo, 1992. **34**(6): p. 499-503.
 53. Sharma, S.K., et al., *Use of molecular diagnostic tools for the identification of species responsible for snakebite in Nepal: a pilot study*. PLoS neglected tropical diseases, 2016. **10**(4): p. e0004620.
 54. Zhu, W.-H., et al., *Regulation of vascular growth and regression by matrix metalloproteinases in the rat aorta model of angiogenesis*. Laboratory Investigation, 2000. **80**(4): p. 545.

5. General Discussion

Snakebite envenoming (SBE) is perhaps the most toxicologically complex issue that a human can experience and one of the most difficult pathological complications humanity has ever attempted to overcome. A rapid and unexpected injection of a constantly evolving and highly diverse cocktail of hundreds of toxins and enzymatic proteins cause both rapidly deadly systemic neurotoxicity and coagulotoxicity as well as amputation-worthy local effects sometimes leading to lifetime sequelae. Overall, SBE is associated with detrimental effects on virtually every aspect of human physiology. The impossibility of appropriately solving this medical emergency has prevented any major breakthroughs in treatment for over a century. We are now seeing the true severity of the epidemiology associated with SBE and this thesis has added to the field in a number of small ways.

5.1 Main findings of this thesis

Snakebite envenomation is in urgent need of improvements to both diagnosis and treatment of bites. The diversity of toxins involved and consequential range of underlying pathophysiologies make improving upon current treatments difficult and this is further hindered by a lack of diagnostic methods (Williams *et al.*, 2019a). Clinicians are somewhat powerless in treating victims, with no way to corroborate envenomation but waiting for symptoms to develop, and even then usually have just one treatment option, polyvalent antivenoms, which they appreciate do little to abrogate the local effects and morbidity associated with bites (Williams *et al.*, 2017). A number of different venom components all work synergistically to worsen the state of victims. For example, the production of toxic, methaemoglobin is the result of a large range of venoms, this increases both hypoxia and oxidative stress (Williams *et al.*, 2018) which then further exacerbates tissue damage and is likely to impair muscle regeneration, which relies on a healthy blood supply. One of the main enzymes causing delayed muscle regeneration are the snake venom metalloproteases, these enzymes cause haemorrhaging and degrade the basement membrane hindering the ability for satellite cells

to regenerate (Williams *et al.*, 2019b). Matrix metalloprotease inhibitors batimastat and marimastat are suggested therapeutics for these SVMP-induced pathologies and have shown efficacy *in vitro* against a P-I metalloprotease. These also inhibit endogenous proteins however and require careful diagnosis before administration – as should all future therapeutics with any potential to worsen a victim's state with improper administration. Diagnostic approaches based on identifying conserved toxin sequences and the production of synthetic peptides or the purification of toxins from whole venom can both serve in raising toxin-specific antibodies with which to diagnose and more efficaciously treat snakebite envenoming. Such diagnostical platforms are required if clinicians are to be able to use the next generations of antivenom therapeutics and generally improve our understanding of the underlying pathophysiology with SBE.

5.2 Limitations of the studies

Snakebite envenomation is concentrated in the rural tropics where people are unequipped for regular contact with venomous snakes. This aspect of SBE means that, unlike diseases manifested in wealthier nations, it has undergone relatively little research, and the full scale of the epidemiology is still relatively unknown (Habib and Brown, 2018; Ralph *et al.*, 2019; Chippaux, 2017; Mohapatra *et al.*, 2011; Vaiyapuri *et al.*, 2013). While the major systemic effects leading to mortality such as the neurotoxicity (causing death by paralysis) and haemotoxicity (causing death by hypovolemic shock) are fairly well studied, the lesser effects which contribute hugely to the morbidity are still very poorly understood (Habib *et al.*, 2015; Williams *et al.*, 2011; Snow *et al.*, 1994). Research around SBE therefore suffers from a massive hole in the knowledge base required to gather a complete picture of the effects taking place. One significant unknown surrounds the different aspects leading to hypoxia and how significant this hypoxia is on the necrosis and damage local to the bite site. Unfortunately, basic information such as the volume of venom injected by different snake species and systemic concentrations of venom in the blood are all but unknown. Predictions can be made based on yields from milking venomous snakes (Hill and Mackessy, 1997; de Roodt *et al.*,

1998) combined with average blood volumes found in humans. However, this does not take into account the colocalization of certain venom components with tissues surrounding the local bite site, the higher concentrations of venom found closer to the bite site, reduced injection of venom by snakes in laboratory settings and the much smaller venom injections given by snakes following recent feeding alongside many other variables. Therefore, suitable concentrations for studying the effects of venoms are hard to agree upon and vary hugely in within the field. The varied nature of venoms both inter- and intraspecifically, by ontogeny, diet, gender, size and habitat (Williams et al., 2019a) all lead to such disparity in venoms which are all considered to be the same when from the same species, mean replicating studies is somewhat impossible unless using the exact same pooled venom sample. These cause great issues in diagnosis as well as making all generalisations most unwise when it comes to the conclusions.

The variations from one venom to the next mean data indicating a low level of proteases are not necessarily accurate and the actual venom may be much richer in these than suggested (Pla *et al.*, 2019). The numerous proteins found in venoms (frequently with several heterogenous proteins of the same molecular weight being found in one venom) make using SDS-PAGE a precarious procedure. The presence of multiple proteins of a similar molecular weight to haemoglobin, fibrinogen and many other endogenous proteins, make using techniques such as SDS-PAGE to display proteolysis somewhat inconclusive.

The incredibly rapid and potent collagenolytic activity by SVMPs mean their effect on muscles can be too destructive to allow scientific deconstruction of the full processes. With isolated myofibres, we found denuding of the basement membrane and hypercontraction of the fibres to take place so rapidly at higher concentrations that only the lowest concentration could be analysed for proliferative effects and effects on migration speed could only be studied over the first 24 hours (before hypercontraction had taken place) (Williams et al., 2019b). The lack of *in vivo* work with the small molecular therapeutics suggested therein and tested *in vitro* also add to reduced impact of this work.

Using synthetic peptides to mimic regions of whole proteins was proven to work in single site format but failed in two site formats. This suggests steric hindrance is preventing binding in some way. Despite this lack of evolution into a format of realistic use, this chapter does portray a methodology by which others can develop epitope specific antibodies and detect specific toxins. Using whole proteins caused a lack of specific detection, and the detection of such a broad range of species that it may be of limited use in the real world.

5.3 Potential synergism between methaemoglobin production and myotoxicity

Some of the effects of SBE appear to be well understood, for example the post- and pre-synaptic neurotoxicity which are generally associated more with elapid bites, however, despite intense studies still have a number of unanswered questions (Ranawaka *et al.*, 2013). Direct haemolysis of venom is a well-known function of cytotoxic phospholipase A₂ (PLA₂) (Gutiérrez *et al.*, 2017), but the consequential oxidation of the haemoglobin released from lysed erythrocytes has previously only been mentioned briefly and primarily only in a few viperids (Meléndez-Martínez *et al.*, 2017; Sharma *et al.*, 2015). The ability for elapid venoms devoid of L-amino acid oxidases (LAAO) to also produce methaemoglobin challenges the assumption that this is always an LAAO-mediated event and far more broad ranging than previously described (Williams *et al.*, 2018). This adds a new level of hypoxia to the challenges of SBE pathologies and additional complications to exacerbate envenomation effects. The lack of oxygen associated with methaemoglobinaemia is likely to starve cells and organs already in dire need of nutrients, thus exacerbating an already potentially critical condition and further delaying muscle regeneration in myotoxic envenomations (Moseley *et al.*, 1999). The inability for methaemoglobin to bind oxygen, combined with the stronger binding of haemoglobin to oxygen when the ferrous (Fe²⁺) ions of haem are oxidised to the ferric (Fe³⁺) state shifts the oxygen dissociation curve to the left and causes hypoxia as well as increased lactic acid production (Darling and Roughton, 1942; Banimahd *et al.*, 2016).

In addition to having this effect on haemoglobin, this oxidative effect is also likely to occur in myoglobin due to sharing high structural homology. Myoglobin is closely

related to haemoglobin and is an oxygen storage protein found specifically in muscles (Davies, 1990). By oxidising myoglobin, venoms would eradicate the muscular oxygen supply provided by healthy myoglobin, thereby intensifying the extensive muscle damage already seen with a large number of snake venoms (Gutiérrez and Ownby, 2003; Williams et al., 2019b; Gutiérrez *et al.*, 1995). The myotoxicity associated with SBE is also complex, with a range of components carrying out compounding effects. The phospholipid destruction associated with enzymatic PLA₂ (Gutiérrez and Ownby, 2003) and pore formation by non-enzymatic PLA₂ can cause systemic myotoxicity and acute kidney injury due to build-up of myoglobin in renal tubules (Sitprija and Sitprija, 2012). This release of myoglobin (and possibly metmyoglobin) into the vasculature following extensive venom-derived muscle damage is likely to worsen the hypoxia and oxidative stress caused by methaemoglobin production. Certain myotoxins can also cause acute skeletal muscle degeneration which due to the lack of disruption to the basement membrane (BM), is associated with relatively unimpeded regeneration due to the vasculature and extra-cellular matrix being relatively unaffected (Gutiérrez and Ownby, 2003). In contrast, venoms containing snake venom metalloproteases (SVMPs), have clearly shown their ability to cleave vasculature and BM components thereby hindering regeneration (Gutiérrez *et al.*, 2018). The added negative consequence on the speed of migration and proliferation of satellite cells that we have shown adds yet another level of complexity to the problem surrounding the treatment of SBE-associated muscular damage (Williams et al., 2019b) and suggests rapid treatment may be the only way to prevent toxin longevity in muscles along with the BM and vascular destruction associated with this family of enzymes.

The SVMP-induced effects of snake venoms have the proposed treatment with matrix metalloprotease inhibitors (Arias *et al.*, 2017; Rucavado *et al.*, 2004; Rucavado *et al.*, 2000), which undoubtedly inhibit the collagenolytic effects of these proteases and are likely to reduce haemorrhaging. This reduction in haemorrhaging may have the added benefit of increasing circulation, preventing such high venom concentrations in the local bite site, and diluting any methaemoglobin produced.

The negative connotations of these inhibitors on endogenous proteins first requires careful consideration and better diagnostics are necessary to reduce the misuse of such potentially detrimental drugs in the treatment of SBE. Likewise, the use of melatonin in the reduction of hypoxia and toxic methaemoglobin build up requires careful diagnosis to ensure effects associated with melatonin administration will not exacerbate the specific envenomation.

5.4 The necessity for treatments based on thorough diagnosis

The immediate administration of small molecular therapeutics such as the matrix metalloprotease inhibitors batimastat/marimastat or metal chelators such as EDTA, have proven to inhibit SVMPs both *in vitro* and *in vivo* (Arias et al., 2017; Rucavado et al., 2004; Rucavado et al., 2000; Escalante *et al.*, 2000) and we have shown a P-I metalloprotease to also be inhibited by these compounds (Williams et al., *in preparation*). It is a fair assumption to think all SVMPs, given their high sequence homogeneity, conserved active site and zinc dependence will be similarly affected by these compounds. The SVMP induced haemorrhaging, fibrinogenolytic activity, anti-platelet activity and delayed muscle regeneration are all likely to be prevented by these compounds. The question is at which point the administration of these compounds lose their merit and actually become detrimental? Within hours after envenomation the tissue damage and myotoxicity that these compounds aim to prevent will have already taken place. Administration after such a time may primarily have negative consequences: the prevention of angiogenesis - the formation of new vessels is necessary to replace venom-induced vasculature damage and muscle regeneration; morphogenesis and tissue repair. It is therefore of merit to develop a diagnostic tool to give sufficient indication for administration of such a drug in field or pre-hospital settings. There are similar concerns with melatonin administration and despite reducing oxidative stress, adding to hypotension in certain bites would undoubtedly worsen the victims state – development of diagnostics before alternative treatments become the normal treatment strategy is therefore essential.

The detection of snake venom components and corroboration of SBE has become a necessity. The large number of venom proteins show at least some level of similarity to endogenous proteins (SVSPs and endogenous serine proteases; SVMPs and matrix metalloproteases; PLA2 etc). Therefore, inhibitors broad ranging enough to inhibit all of a family of venom proteins are also likely to unnecessarily inhibit these endogenous proteins too, causing unknown damage. Therefore, thorough verification of envenoming and the presence of toxins is absolutely necessary before such administration takes place. Methods of developing appropriate diagnostic devices have been described in this thesis (Williams et al., *in preparation*, Williams et al., *in preparation*) and devices using such methods need immediate production to not only enable future therapies to be correctly administered, but antivenom to be used only in victims of SBE, not in dry and non-venomous bites. Diagnostical tools will also enable much needed accuracy in epidemiology of snakebites to be improved and clinicians to feel empowered in their confident administration of a potentially life-changing treatment – both in terms of debt and hypersensitivity.

5.5 Future Work

We have described a way in which to assess haemoglobin oxidation, however, fractionation and reassessment of the oxidising ability of specific toxins is required to identify the proteins responsible for this effect in LAAO-devoid venoms. The inhibition of such effects using antioxidants needs to be studied in more detail and the negative effects of melatonin need to be weighed up against its ability to ameliorate the associated hypoxia. The added burden of this effect in relation to neurotoxicity and coagulotoxicity needs to be quantified in order to appraise the need to address this frequently ignored side-effect of SBE. Myoglobin also needs to be assessed for its ability to be oxidised by various venoms and amelioration of the effects on both myoglobin and haemoglobin by melatonin need to be quantified. One fairly simple and non-invasive way of assessing whether venom oxidises myoglobin would be to compare the urine of those suffering myoglobinuria as a result of SBE with urine from someone suffering myoglobinuria from physical trauma. Using full wavelength scans as we described herein, the

two samples could be assessed for their myoglobin peaks which occur at 540 nm and 580 nm (compared with a single peak at 628 nm for metmyoglobin (Schenkman *et al.*, 1997)).

The *in vitro* efficacy of MMPi in the inhibition of SVMPs reported elsewhere has been corroborated, although the true effects of these under *in vivo* settings over an extended period is yet to be studied and will no doubt cast a shadow over what the snakebite community has hailed as a panacea for the SVMP-induced morbidities. What are the side-effects and long-term implications of MMPi use in snakebite victims?

There are still no snakebite diagnostical devices commercially available to indicate and direct treatment outside of Australasia. Future work needs to address this as a priority. Antivenoms themselves can quite simply be made into lateral flow devices instantly indicating the merit of that antivenom, preventing unnecessary adverse reactions and wastage of a medicine which is already in dangerously short supply (Habib and Brown, 2018). More specific devices can then be built upon this initial diagnostical platform. The use of specific toxins, or toxin-specific peptides has shown some promise towards developing diagnostic devices using toxin-specific antibodies. Further tweaking and optimisation is required if they are ever going to be of use in a clinical setting in order to improve the specificity and accuracy. Monovalent antivenom for use in such diagnostical devices around the world needs to be made available and diagnostics need greater heed taken of them before treatments become approved and available with no way of indicating them except the onset of symptoms – by which time the merit of administration is, while still essential, reduced.

5.6 Conclusion

A full understanding of the true complexity of SBE, with the secondary, as well as primary effects of each component being fully understood is potentially beyond the scope of humanity. The further we study each component the more functions and secondary effects become evident. There remain many mysteries to uncover, hidden in the infinite toxicological profile of snake venoms worldwide, but efforts need to concentrate on the major venom components.

Improvements to both therapeutics and diagnostics are a necessity if we are to meet the halving of SBE mortality by 2030 put forward by the WHO. We cannot allow another century passing where animal-derived immunoglobulins are the only acceptable treatment for a disease that promises to be only worsen in the future.

Improvements are urgently needed to the treatment and diagnosis of snakebite (Williams et al., 2019a). It kills more than many of the other neglected tropical diseases combined and has far greater complexity in terms of improving treatment.

The dramatic morbidity associated with SBE is seen worst in India where clinicians struggle to treat snakebite effectively due to a large range of challenges including a lack of diagnostics and available therapeutics (Williams et al., 2017). Despite there being suggested treatments for the oxidative stress (melatonin) and local tissue damage (varespladib and MMPis) these need thorough study and proper diagnostic options before administration to all those presenting symptoms of snakebite.

The presentation of a snakebite does not automatically indicate SBE, and assumptions based on species can highlight holes in the science. For example, methaemoglobin production was previously associated with only viper venoms but we found to be a secondary effect of elapid venoms also (Williams et al., 2018). This can exacerbate the oxidative stress and hypoxia, which in turn impacts on other venom-induced complications, including potential further delays to muscle regeneration. The effect seen with haemoglobin may even have similar impacts on myoglobin – causing even greater harm through further extension to the hypoxic conditions.

The hypoxia from oxidative stress and haemorrhagic ischaemia combines with the destruction of muscular basement membranes by snake venom metalloproteases (SVMP) to affect satellite cell function and persist within muscles for over ten days to cause prolonged effects and delayed regeneration (Williams et al., 2019b). Methaemoglobin production is likely

to exacerbate this, not only effecting blood supply, but potentially also oxygen stored in myoglobin.

Treatment of these SVMP-effects include matrix metalloprotease inhibitors such as batimastat/marimastat and metal chelators such as EDTA and were here found all able to inhibit the collagenolytic effects of one such SVMP (Williams et al., *in preparation*). The use of such drugs would potentially speed up muscle regeneration and reducing the haemorrhaging and hypoxia associated with these enzymes. Diagnostical tools are compulsory to prevent unnecessary and potentially dangerous administration of such drugs.

For the diagnosis of SBE, two methods are outlined: 1. Using multiple sequence alignment and 3D structures of proteins, toxin specific peptides have been designed and used to produce snake family-specific antibodies (Williams et al., *in preparation*), steric hindrance may prevent these specific antibodies ever being of use commercially however; 2. Antibodies raised against purified proteins have been used in the detection of a wide range of venoms and may give indication for further treatment (Williams et al., *in preparation*).

Together, these experimental chapters highlight the complexity of snakebite envenomation and the future of therapies based on diagnosis. There are compounding and synergistic factors to consider; hypoxia from the production of radicals and toxic molecules such as methaemoglobin act to further impede tissue regeneration from the directly cytotoxic effects of certain proteins. Certain compounds have been suggested to ameliorate the local tissue damage, hypoxia and even neurotoxicity, but without a thorough understanding of the venomous snakebites which they serve to treat and those they could further exacerbate it is hard for these therapeutics to be taken forwards. This requires diagnostics to be improved allowing the offending snake or toxins present in the venom to be ascertained. This will not only allow administration of appropriate drugs but improve research into snakebite envenomation, with effects unequivocally associated with diagnosed species or toxin group instead of assumptions being made based on guesswork.

References

- Arias, A. S., Rucavado, A. & Gutiérrez, J. M. (2017). Peptidomimetic hydroxamate metalloproteinase inhibitors abrogate local and systemic toxicity induced by *Echis ocellatus* (saw-scaled) snake venom. *Toxicon*, **132**, 40-49.
- Banimahd, F., Loo, T., Amin, M., Ahadiat, O. R., Chakravarthy, B. & Lotfipour, S. (2016). A Rare but Important Clinical Presentation of Induced Methemoglobinemia. *The western journal of emergency medicine*, **17**, 627-629.
- Chippaux, J.-P. (2017). Incidence and mortality due to snakebite in the Americas. *PLOS Neglected Tropical Diseases*, **11**, e0005662.
- Darling, R. C. & Roughton, F. (1942). The effect of methemoglobin on the equilibrium between oxygen and hemoglobin. *American Journal of Physiology-Legacy Content*, **137**, 56-68.
- Davies, M. J. (1990). Detection of myoglobin-derived radicals on reaction of metmyoglobin with hydrogen peroxide and other peroxidic compounds. *Free radical research communications*, **10**, 361-370.
- de Roodt, A. R., Dolab, J. A., Galarce, P. P., Gould, E., Litwin, S., Dokmetjian, J. C., Segre, L. & Vidal, J. C. (1998). A study on the venom yield of venomous snake species from Argentina. *Toxicon*, **36**, 1949-1957.
- Escalante, T., Franceschi, A., Rucavado, A. & Gutiérrez, J. M. a. (2000). Effectiveness of batimastat, a synthetic inhibitor of matrix metalloproteinases, in neutralizing local tissue damage induced by BaP1, a hemorrhagic metalloproteinase from the venom of the snake *Bothrops asper*. *Biochemical pharmacology*, **60**, 269-274.
- Gutiérrez, J. M., Calvete, J. J., Habib, A. G., Harrison, R. A., Williams, D. J. & Warrell, D. A. (2017). Snakebite envenoming. *Nature Reviews Disease Primers*, **3**, nrdp201763.
- Gutiérrez, J. M., Escalante, T., Hernández, R., Gastaldello, S., Saravia-Otten, P. & Rucavado, A. (2018). Why is Skeletal Muscle Regeneration Impaired after Myonecrosis Induced by Viperid Snake Venoms? *Toxins*, **10**, 182.
- Gutiérrez, J. M. a. & Ownby, C. L. (2003). Skeletal muscle degeneration induced by venom phospholipases A2: insights into the mechanisms of local and systemic myotoxicity. *Toxicon*, **42**, 915-931.
- Gutiérrez, J. M. a., Romero, M., Núñez, J., Chaves, F., Borkow, G. & Ovadia, M. (1995). Skeletal Muscle Necrosis and Regeneration after Injection of BaH1, A Hemorrhagic Metalloproteinase Isolated from the Venom of the Snake *Bothrops asper* (Terciopelo). *Experimental and Molecular Pathology*, **62**, 28-41.
- Habib, A. G. & Brown, N. I. (2018). The snakebite problem and antivenom crisis from a health-economic perspective. *Toxicon*, **150**, 115-123.
- Habib, A. G., Kuznik, A., Hamza, M., Abdullahi, M. I., Chedi, B. A., Chippaux, J.-P. & Warrell, D. A. (2015). Snakebite is Under Appreciated: Appraisal of Burden from West Africa. *PLOS Neglected Tropical Diseases*, **9**, e0004088.
- Hill, R. E. & Mackessy, S. P. (1997). Venom yields from several species of colubrid snakes and differential effects of ketamine. *Toxicon*, **35**, 671-678.
- Meléndez-Martínez, D., Muñoz, J. M., Barraza-Garza, G., Cruz-Peréz, M. S., Gatica-Colima, A., Alvarez-Parrilla, E. & Plenge-Tellechea, L. F. (2017). Rattlesnake *Crotalus molossus nigrescens* venom induces oxidative stress on human erythrocytes. *Journal of Venomous Animals and Toxins including Tropical Diseases*, **23**, 24.
- Mohapatra, B., Warrell, D. A., Suraweera, W., Bhatia, P., Dhingra, N., Jotkar, R. M., Rodriguez, P. S., Mishra, K., Whitaker, R. & Jha, P. (2011). Snakebite mortality in India: a nationally representative mortality survey. *PLoS neglected tropical diseases*, **5**, e1018.

- Moseley, M. J., Oenning, V. & Melnik, G. (1999). Methemoglobinemia. *AJN The American Journal of Nursing*, **99**, 47.
- Pla, D., Sanz, L., Quesada-Bernat, S., Villalta, M., Baal, J., Chowdhury, M. A. W., León, G., Gutiérrez, J. M., Kuch, U. & Calvete, J. J. (2019). Phylovenomics of *Daboia russelii* across the Indian subcontinent. Bioactivities and comparative in vivo neutralization and in vitro third-generation antivenomics of antivenoms against venoms from India, Bangladesh and Sri Lanka. *Journal of proteomics*, **207**, 103443.
- Ralph, R., Sharma, S. K., Faiz, M. A., Ribeiro, I., Rijal, S., Chappuis, F. & Kuch, U. (2019). The timing is right to end snakebite deaths in South Asia. *Bmj*, **364**, k5317.
- Ranawaka, U. K., Laloo, D. G. & de Silva, H. J. (2013). Neurotoxicity in Snakebite—The Limits of Our Knowledge. *PLOS Neglected Tropical Diseases*, **7**, e2302.
- Rucavado, A., Escalante, T., Franceschi, A., Chaves, F., León, G., Cury, Y., Ovadia, M. & Gutiérrez, J. M. (2000). Inhibition of local hemorrhage and dermonecrosis induced by *Bothrops asper* snake venom: effectiveness of early in situ administration of the peptidomimetic metalloproteinase inhibitor batimastat and the chelating agent CaNa₂EDTA. *The American journal of tropical medicine and hygiene*, **63**, 313-319.
- Rucavado, A., Escalante, T. & Gutiérrez, J. M. a. (2004). Effect of the metalloproteinase inhibitor batimastat in the systemic toxicity induced by *Bothrops asper* snake venom: understanding the role of metalloproteinases in envenomation. *Toxicon*, **43**, 417-424.
- Schenkman, K. A., Marble, D. R., Burns, D. H. & Feigl, E. O. (1997). Myoglobin oxygen dissociation by multiwavelength spectroscopy. *Journal of Applied Physiology*, **82**, 86-92.
- Sharma, R. D., Katkar, G. D., Sundaram, M. S., Paul, M., NaveenKumar, S. K., Swethakumar, B., Hemshekhar, M., Girish, K. S. & Kemparaju, K. (2015). Oxidative stress-induced methemoglobinemia is the silent killer during snakebite: a novel and strategic neutralization by melatonin. *Journal of pineal research*, **59**, 240-254.
- Sitprija, V. & Sitprija, S. (2012). Renal effects and injury induced by animal toxins. *Toxicon*, **60**, 943-53.
- Snow, R., Bronzan, R., Roques, T., Nyamawi, C., Murphy, S. & Marsh, K. (1994). The prevalence and morbidity of snake bite and treatment-seeking behaviour among a rural Kenyan population. *Annals of tropical medicine and parasitology*, **88**, 665-671.
- Sousa, I. D. L., Barbosa, A. R., Salvador, G. H. M., Frihling, B. E. F., Santa-Rita, P. H., Soares, A. M., Pessôa, H. L. F. & Marchi-Salvador, D. P. (2019). Secondary hemostasis studies of crude venom and isolated proteins from the snake *Crotalus durissus terrificus*. *International Journal of Biological Macromolecules*, **131**, 127-133.
- Vaiyapuri, S., Vaiyapuri, R., Ashokan, R., Ramasamy, K., Nattamaisundar, K., Jeyaraj, A., Chandran, V., Gajjeraman, P., Baksh, M. F. & Gibbins, J. M. (2013). Snakebite and its socio-economic impact on the rural population of Tamil Nadu, India. *PloS one*, **8**, e80090.
- Williams, H. F., Hayter, P., Ravishankar, D., Baines, A., Layfield, H. J., Croucher, L., Wark, C., Bicknell, A. B., Trim, S. & Vaiyapuri, S. (2018). Impact of *Naja nigricollis* Venom on the Production of Methaemoglobin. *Toxins*, **10**, 539.
- Williams, H. F., Layfield, H. J., Vallance, T., Patel, K., Bicknell, A. B., Trim, S. A. & Vaiyapuri, S. (2019a). The Urgent Need to Develop Novel Strategies for the Diagnosis and Treatment of Snakebites. *Toxins*, **11**, 363.
- Williams, H. F., Mellows, B. A., Mitchell, R., Sfyri, P., Layfield, H. J., Salamah, M., Vaiyapuri, R., Collins-Hooper, H., Bicknell, A. B., Matsakas, A., Patel, K. & Vaiyapuri, S. (2019b). Mechanisms underpinning the permanent muscle damage induced by snake venom metalloprotease. *PLOS Neglected Tropical Diseases*, **13**, e0007041.

- Williams, H. F., Vaiyapuri, R., Gajjeraman, P., Hutchinson, G., Gibbins, J. M., Bicknell, A. B. & Vaiyapuri, S. (2017). Challenges in diagnosing and treating snakebites in a rural population of Tamil Nadu, India: The views of clinicians. *Toxicon*, **130**, 44-46.
- Williams, S. S., Wijesinghe, C. A., Jayamanne, S. F., Buckley, N. A., Dawson, A. H., Lalloo, D. G. & de Silva, H. J. (2011). Delayed Psychological Morbidity Associated with Snakebite Envenoming. *PLOS Neglected Tropical Diseases*, **5**, e1255.

6. Appendix

A1. Questionnaire used in additional introductory chapter 2:

Challenges in diagnosing and treating snakebites in a rural population of Tamil Nadu, India: The views of clinicians.

A2. Coauthored papers:

A2.1 Ravishankar, D., Salamah, M., Attina, A., Pothi, R., Vallance, T., Javed, M., Williams, H. F., Alzahrani, E., Kabova, E., Vaiyapuri, R., Shankland, K., Gibbins, J., Strohfeld, K., Greco, F., Osborn, H., & Vaiyapuri, S. (2017) Ruthenium-conjugated chrysin analogues modulate platelet activity, thrombus formation and haemostasis with enhanced efficacy. *Scientific reports*

A2.2 Vallance, T. M., Zeuner, M. T., Williams, H. F., Widera, D., & Vaiyapuri, S. (2017). Toll-Like Receptor 4 Signalling and Its Impact on Platelet Function, Thrombosis, and Haemostasis. *Mediators of Inflammation*

A2.3 Ravishankar, D., Salamah, M., Akimbaev, A., Williams, H. F., Albadawi, D. A., Vaiyapuri, R., ... & Vaiyapuri, S. (2018). Impact of specific functional groups in flavonoids on the modulation of platelet activation. *Scientific Reports*

A2.4 Salamah, M. F., Ravishankar, D., Kodji, X., Moraes, L. A., Williams, H. F., Vallance, T. M., Albadawi, D., Vaiyapuri, R., Watson, K., Gibbins, J., Brain, S., Perretti, M., & Vaiyapuri, S. (2018). The endogenous antimicrobial cathelicidin LL37 induces platelet activation and augments thrombus formation. *Blood advances*

Doctor's questionnaire

Doctor's name:

Hospital name:

How long have you been treating snake bites?

How many snake bite patients do you see in a month? In a year?

In which month of the year do you receive most cases? Is this stable over the years?

What questions do you ask the victim or their relatives when they arrive?

What is the first treatment you give?

How important is it to know the identity of the snake?

If the snake is unknown how do you treat?

How long after the bite do patients arrive at the hospital?

What are the effects of this delay?

Do you use polyvalent anti-venom? Or mono valent for specific snake?

Who is the supplier of anti-venom to your hospital?

How much does it cost for a vial? How many do you normally use to treat the victim?

Do you use any other treatments for snake bite?

What would be the minimum and maximum costs to treat a snake bite victim?

Have you seen any extreme cases so far?

Can you describe what these were and how you treated them?

Have you seen anything which you would consider a medical miracle following a snake bite?

Have you seen any unusual envenomation effects?

Did you treat this effect successfully?

What is the percentage of snake bite victims who die in the hospital?

Is that because of their time delay to reach the hospital?

Do people die because of increased blood pressure and heart rate due to the threat?

Has anybody died because the snake was misidentified and treatment was given for the wrong snake?

What would you advise the victims after treatment?

How long do they normally stay in the hospital?

Would you be happy to show us the snake bite statistics recorded in your hospital?

Would you be happy to show us any extreme case reports?

Is there any snakebite victim admitted in your hospital now?

Can we meet them for a short interview?

What you think about the current treatments for snake bites?

How do you think we can improve the treatments?

What would you suggest researchers should investigate as a priority to treat snake bites better?

Do you think the government should take any specific actions in the treatments or in the prevention of snake bites? What would that be?

Would you be happy to answer any further questions in the future?

SCIENTIFIC REPORTS

OPEN

Ruthenium-conjugated chrysin analogues modulate platelet activity, thrombus formation and haemostasis with enhanced efficacy

Divyashree Ravishankar¹, Maryam Salamah¹, Alda Attina¹, Radhika Pothi¹, Thomas M. Vallance¹, Muhammad Javed¹, Harry F. Williams¹, Eman M. S. Alzahrani¹, Elena Kabova¹, Rajendran Vaiyapuri², Kenneth Shankland¹, Jonathan Gibbins³, Katja Strohfeldt¹, Francesca Greco¹, Helen M. I. Osborn¹ & Sakthivel Vaiyapuri¹

The constant increase in cardiovascular disease rate coupled with significant drawbacks of existing therapies emphasise the necessity to improve therapeutic strategies. Natural flavonoids exert innumerable pharmacological effects in humans. Here, we demonstrate the effects of chrysin, a natural flavonoid found largely in honey and passionflower on the modulation of platelet function, haemostasis and thrombosis. Chrysin displayed significant inhibitory effects on isolated platelets, however, its activity was substantially reduced under physiological conditions. In order to increase the efficacy of chrysin, a sulfur derivative (thio-chrysin), and ruthenium-complexes (Ru-chrysin and Ru-thio-chrysin) were synthesised and their effects on the modulation of platelet function were evaluated. Indeed, Ru-thio-chrysin displayed a 4-fold greater inhibition of platelet function and thrombus formation *in vitro* than chrysin under physiologically relevant conditions such as in platelet-rich plasma and whole blood. Notably, Ru-thio-chrysin exhibited similar efficacy to chrysin in the modulation of haemostasis in mice. Increased bioavailability and cell permeability of Ru-thio-chrysin compared to chrysin were found to be the basis for its enhanced activity. Together, these results demonstrate that Ru-thio-coupled natural compounds such as chrysin may serve as promising templates for the development of novel anti-thrombotic agents.

Cardiovascular diseases (CVDs) are collectively regarded as the number one killer worldwide, and notably, thrombosis is responsible for the majority of CVD-associated mortalities and morbidities^{1, 2}. Platelets (small circulating blood cells) play indispensable roles in haemostasis by preventing excessive blood loss upon vascular damage through blood clotting. However, inappropriate activation of platelets leads to thrombosis (formation of blood clots within blood vessels) under pathological conditions such as the rupture of atherosclerotic plaques³. Thrombosis reduces the blood supply to vital organs such as the heart and brain resulting in heart attacks and strokes, respectively. Hence, targeting platelets has been proven to be effective in the prevention and treatment of CVDs (primarily heart attacks and strokes)^{4, 5}. While the currently used anti-platelet drugs such as aspirin and clopidogrel demonstrate efficacy in many patients, they exert undesirable side effects such as bleeding complications and are ineffective in others⁵. Therefore, the development of safer, more effective therapeutic strategies for the prevention and treatment of thrombotic diseases is a pressing priority.

¹School of Pharmacy, University of Reading, Reading, UK. ²School of Pharmacy, University of Reading Malaysia, Johar, Malaysia. ³Institute for Cardiovascular and Metabolic Research, School of Biological Sciences, University of Reading, Reading, UK. Divyashree Ravishankar, Maryam Salamah, Helen M.I. Osborn and Sakthivel Vaiyapuri contributed equally to this work. Correspondence and requests for materials should be addressed to H.M.I.O. (email: h.m.i.osborn@reading.ac.uk) or S.V. (email: s.vaiyapuri@reading.ac.uk)

The direct relationships between dietary components and cardiovascular health have been established over the last few decades even though their underlying molecular mechanisms are not well understood^{6–9}. Although several genetic factors account for the development of CVD risks in multiple settings¹⁰, dietary components form an essential part of the disease progression. While a number of dietary molecules such as lipids are responsible for the development of CVDs, many small molecules including flavonoids that are present in various plant products exert beneficial effects in the prevention of such diseases^{11,12}. Individuals who consume diets with low levels of saturated fatty acids together with a substantial amount of fruits and vegetables have been shown to have reduced development of CVD risks^{13,14}. In particular, a number of dietary flavonoids such as quercetin¹⁵, tangeretin¹⁶, nobiletin¹⁷, luteolin and apigenin have been shown to exhibit inhibitory effects in platelets by modulating diverse signalling cascades¹⁸. However, several challenges are associated with using dietary components for the prevention and treatment of diseases. Some of these include malabsorption, poor bioavailability of desired compounds in the blood stream, poor metabolic stability as well as reduced lipophilicity to readily cross the cell membranes^{19–22}. Specific chemical modifications (e.g. addition of sulfur groups²³) to the fundamental structures of dietary flavonoids have been shown to improve their hydrophobic nature and enhance their biological activities. Indeed, all the natural flavonoids share a basic template structure which can be modified by the specific addition of various functional groups, affording a diverse array of biological activities^{18,22}.

In recent years, the therapeutic applications of organometallic complexes have been considered for numerous pathological conditions^{24–27}. For example, cisplatin, a platinum-based FDA-approved anti-cancer drug has substantially increased the survival rate of patients with testicular cancer²⁸ and it is being widely used to treat different types of cancer²⁹. The success of cisplatin, as well as the occurrence of dose-limiting side effects stimulated significant research in this area. Ruthenium-based organometallics are a very promising class of therapeutic compound, with two specific candidates, NAMI-A and KP1019 having entered clinical trials^{30,31}. There are three specific properties which make ruthenium an interesting metal for drug development: its range of oxidation states, its ability to mimic iron binding under physiological conditions and its low toxicity compared to platinum³². Hence, we hypothesised that ruthenium-based complexes of flavonoids may offer greater efficacy in target cell types by overcoming the problems associated with the natural flavonoids. In this study, we report the design, synthesis, chemical characterisation and biological evaluation of novel ruthenium complexes of chrysin, a natural flavonoid present in honey, honeycombs, propolis and passionflowers, as well as its synthesised thioflavone derivative for the modulation of platelet function, *in vitro* thrombus formation and haemostasis.

Results

Synthesis and chemical characterisation of the ruthenium complexes of chrysin and thio-chrysin.

Similar to a recent study³³, our initial experiments confirmed the inhibitory effects of chrysin in the activation of washed platelets in a concentration-dependent manner. Due to the limited knowledge of chrysin in the modulation of platelet function, thrombosis and haemostasis, this flavonoid was selected as a starting point for the chemical synthesis and biological evaluation of derivatives with additional chemical features in order to achieve enhanced platelet inhibitory effects under physiological conditions. In order to determine the relative potency of flavones versus thioflavones, thio-chrysin was chemically synthesised as reported by us previously²³. New methods were then developed in order to access the novel ruthenium-chrysin (Ru-chrysin) and ruthenium-thio-chrysin (Ru-thio-chrysin) complexes. Chrysin and thio-chrysin were initially deprotonated prior to reacting with the commercially available bis [dichlorido (η^6 -*p*-cymene)] ruthenium(II), as shown in the scheme (Fig. 1A). Optimisation of synthesis was performed to ensure efficient deprotonation of the phenolic hydroxyl group adjacent to the carbonyl residue prior to the addition of the organometallic reagents. Table S1 displays the range of conditions used with different bases and molar equivalents (eq.) of NaOMe (1.05 eq. to 2.00 eq.) to synthesise Ru-chrysin. Product isolation proved to be difficult in the presence of Hünig's base, triethyl amine, or DBU. Reactions with 1.10 eq., 1.25 eq. and 2.00 eq. of NaOMe yielded a mixture of products with the starting material (chrysin) being the primary contaminant. Purification of Ru-chrysin from these mixtures through recrystallisation was unsuccessful. ¹H NMR spectroscopic analysis of the reaction mixtures revealed a positive correlation between the percentage of uncomplexed chrysin and an increased molar equivalent of NaOMe. This indicated that the excess amount of NaOMe might be affecting the hydrolysis of the bis [dichlorido(η^6 -*p*-cymene)] ruthenium(II) reagent thus leading to a higher percentage of uncomplexed chrysin. Finally, complete conversion of chrysin to Ru-chrysin was achieved in the presence of 1.05 eq. of NaOMe with 0.55 eq. of bis [dichlorido(η^6 -*p*-cymene)] ruthenium(II). The product Ru-chrysin was purified by recrystallisation from EtOAc:CHCl₃ (9:1 v/v) and was isolated in a yield of 75%.

The conditions used for preparing Ru-chrysin (1.05 eq. of NaOMe with 0.55 eq. of bis [dichlorido(η^6 -*p*-cymene)] ruthenium(II)) yielded the Ru-thio-chrysin product but with a higher percentage of uncomplexed starting material, thio-chrysin. As illustrated above, an increased quantity of NaOMe was not beneficial in achieving a complete reaction conversion and therefore the synthesis of Ru-thio-chrysin was attempted with 0.90 eq. of bis [dichlorido (η^6 -*p*-cymene)] ruthenium(II) and 1.05 eq. of NaOMe. This reaction successfully yielded Ru-thio-chrysin and purification was achieved by recrystallisation from EtOAc:CHCl₃ (9:1 v/v) which resulted in access to the pure material in 65% yield. The loss of one proton in the ¹H NMR spectra of Ru-chrysin (Figure S1A) versus chrysin, and Ru-thio-chrysin (Figure S2) versus thio-chrysin, from the hydroxyl groups of chrysin and thio-chrysin, respectively, confirmed the formation of Ru-complexes. A range of further chemical characterisation methods including ¹³C-NMR spectroscopic analysis (Figure S1B), mass spectrometry and elemental analysis confirmed the formation of the Ru-complexes. Furthermore, the crystal structures of Ru-chrysin (Fig. 1B) and Ru-thio-chrysin (Fig. 1C) were solved from powder X-ray diffraction data (Figure S3, Table S2) using DASH^{34,35} and refined using TOPAS (Bruker, Germany), as only polycrystalline samples of both compounds could be obtained.

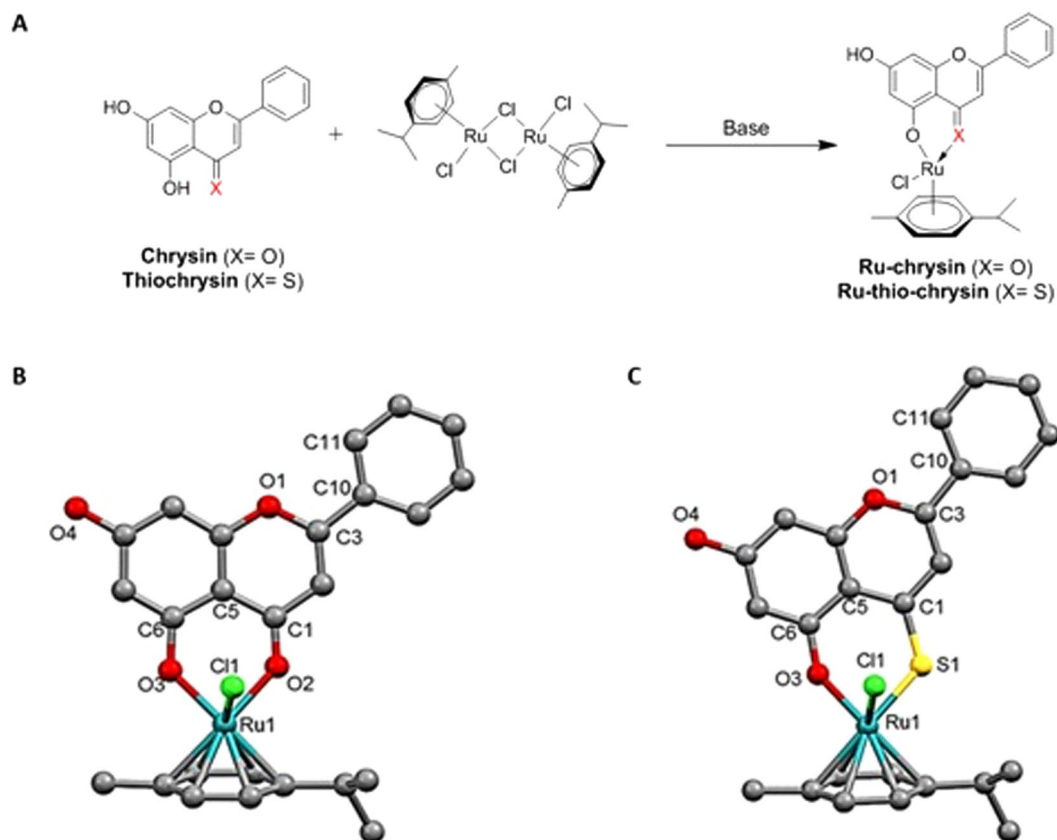


Figure 1. Synthesis scheme and molecular structures for Ru-chrysin and Ru-thio-chrysin. (A) Schematic diagram represents the synthesis of Ru-chrysin and Ru-thio-chrysin from chrysin and thio-chrysin, respectively *via* reaction with bis [dichlorido (η^6 -p-cymene)] ruthenium(II). The molecular structures of Ru-chrysin (B) and Ru-thio-chrysin (C) were determined by X-ray diffraction studies. The hydrogen bonds are not shown in the figures to enhance the clarity of the molecular images. The symbols C, O, Cl, S and Ru represent carbon, oxygen, chlorine, sulfur and ruthenium, respectively. The numbers shown indicate the position of respective carbon atoms.

Ru-chrysin and Ru-thio-chrysin display enhanced effects in platelet-rich plasma compared to washed platelets.

To determine the effects of chrysin and thio-chrysin and their Ru-complexes in the modulation of platelet activation, aggregation assays were performed using cross-linked collagen-related peptide (CRP-XL) as a platelet agonist, by optical aggregometry. Firstly, to determine the effects of chrysin and its derivatives on isolated platelets, aggregation assays were performed using human washed platelets (devoid of plasma proteins and other blood cells). Chrysin inhibited CRP-XL (0.5 μ g/mL)-induced aggregation in washed platelets in a concentration-dependent manner (Fig. 2A and B). A concentration of 6.25 μ M chrysin displayed approximately 80% reduction in CRP-XL (0.5 μ g/mL)-induced platelet aggregation. The addition of a thiol group to chrysin did not affect its inhibitory effects (Fig. 2C and D). While Ru-Cl failed to affect platelet aggregation in washed platelets (Figure S4A), Ru-chrysin (Fig. 2E and F) and Ru-thio-chrysin (Fig. 2G and H) inhibited CRP-XL-induced platelet aggregation in a concentration-dependent manner. The overall effects of Ru-thio-chrysin were significantly better than Ru-chrysin at least at lower concentrations such as 6.25 μ M, although higher concentrations resulted in similar effects. Together, these data demonstrate that the chemical modifications of chrysin did not affect its overall inhibitory activities in human washed platelets.

Plasma proteins such as albumin have been shown to bind small molecules including flavonoids and affect their bioavailability to target cells³⁶. Therefore, to determine the effects of various concentrations of chrysin and its derivatives in the presence of plasma proteins, aggregation assays were performed using human platelet-rich plasma (PRP) and 0.5 μ g/mL CRP-XL. In contrast to the results obtained with washed platelets, chrysin displayed reduced inhibitory effects on platelet aggregation in PRP. A concentration of 100 μ M chrysin displayed around 40% reduction in platelet aggregation upon activation with 0.5 μ g/mL CRP-XL, whilst the lower concentrations such as 6.25 μ M and 12.5 μ M did not exhibit significant effects (Fig. 3A and B). Thio-chrysin displayed similar inhibitory effects compared to chrysin in platelet aggregation (Fig. 3C and D). As with washed platelets, Ru-Cl failed to show any inhibitory effects in PRP (Figure S4B). While Ru-chrysin did not significantly affect the platelet aggregation at the concentrations of 6.25 μ M and 12.5 μ M (Fig. 3E and F), Ru-thio-chrysin displayed a significant effect at lower concentrations including 6.25 μ M compared to the control (Fig. 3G and H). In addition, Ru-thio-chrysin exhibited significantly more inhibitory effects compared to the respective concentrations of native chrysin. These data demonstrate that although chrysin exhibited enhanced inhibitory effects on platelet activation in washed platelets,

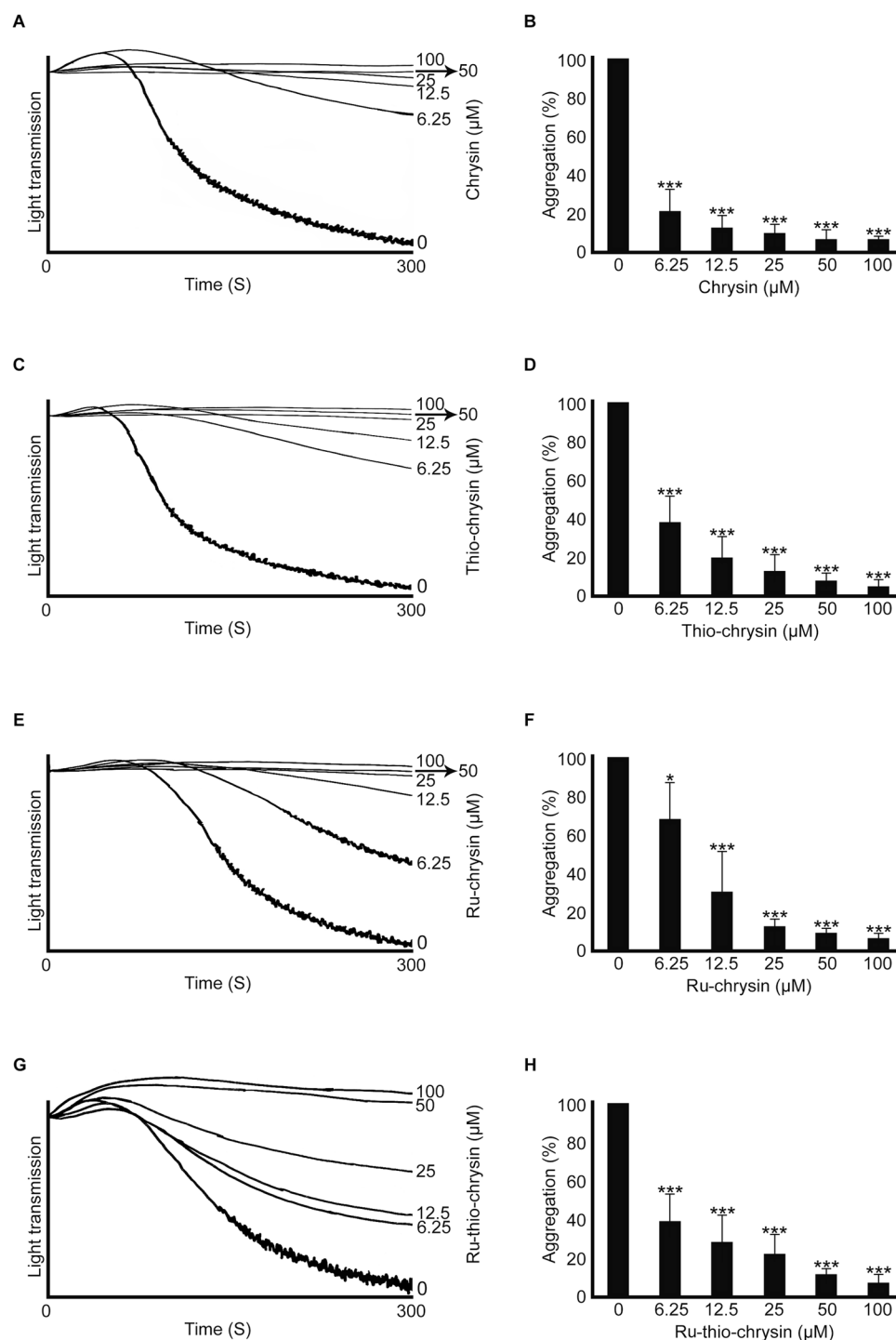


Figure 2. Effects of chrysin and its derivatives in washed platelet aggregation. Human washed platelets were incubated with a vehicle control [0.1% (v/v) DMSO] or different concentrations of chrysin (A,B), thio-chrysin (C,D), Ru-chrysin (E,F) and Ru-thio-chrysin (G,H) for 5 minutes prior to the addition of 0.5 μg/mL CRP-XL and the platelet aggregation was monitored for 5 minutes by optical aggregometry. The aggregation traces shown are representative of three separate experiments. The maximum aggregation obtained with vehicle control at 5 minutes was taken as 100% to calculate the level of aggregation for chrysin and its derivatives-treated samples. Cumulative data represent mean ± S.D. (n = 3). *Indicates significance with respect to controls and *p* values shown (**p* < 0.05, and ****p* < 0.001) are as calculated by one-way ANOVA using Graphpad Prism.

it failed to show similar levels of effects in PRP. However, Ru-chrysin and Ru-thio-chrysin displayed enhanced inhibitory effects on platelets even in PRP. The Ru-complex of thio-chrysin appeared to be more effective than others in the modulation of platelet activation in the presence of plasma proteins.

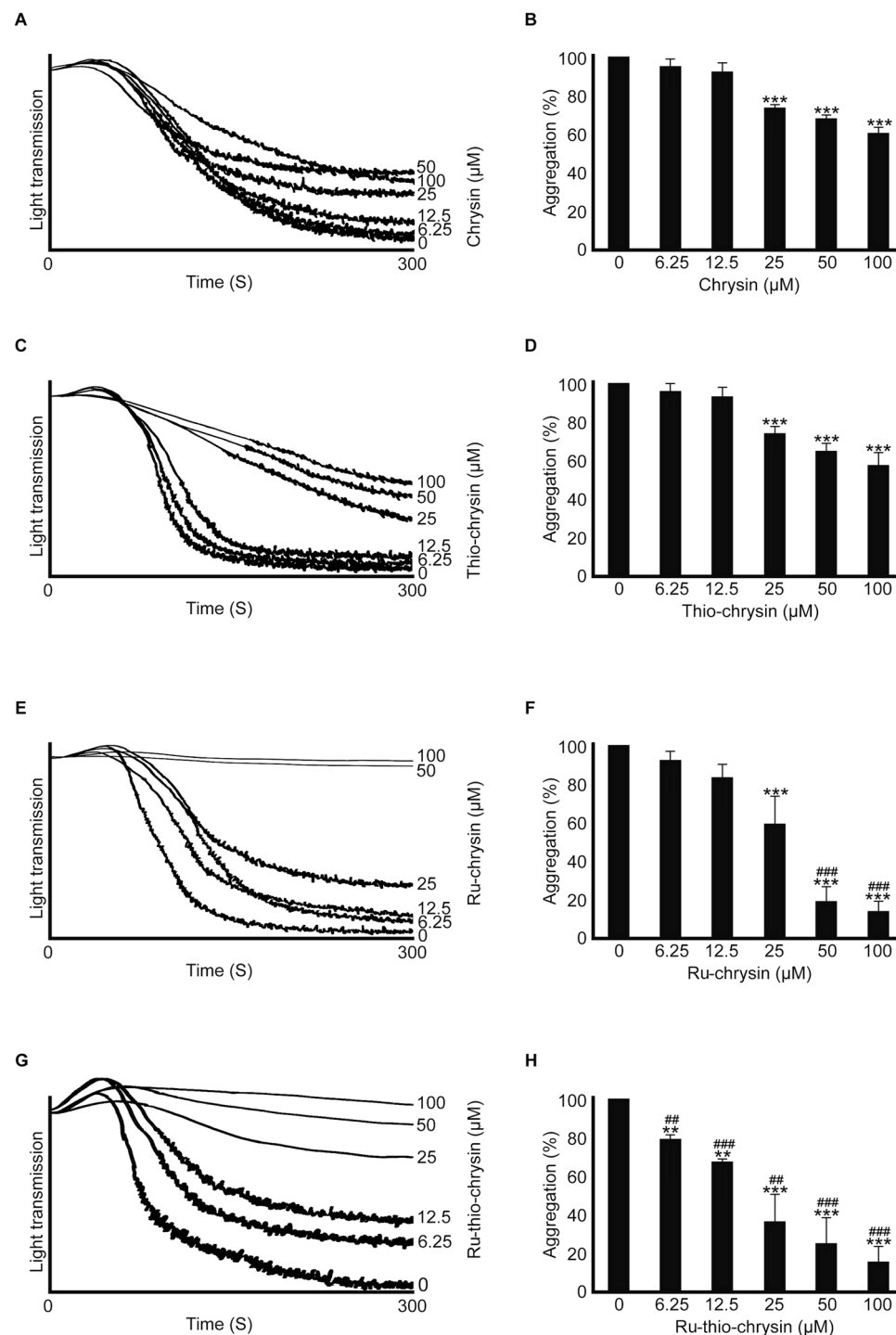


Figure 3. Impact of chrysin and its derivatives on platelet activation in platelet-rich plasma. Human platelet-rich plasma was treated with vehicle control [0.1% (v/v) DMSO] or a range of concentrations of chrysin (A,B), thio-chrysin (C,D), Ru-chrysin (E,F) and Ru-thio-chrysin (G,H) for 5 minutes prior to the addition of 0.5 μg/mL CRP-XL in an optical aggregometer. The platelet aggregation was monitored for 5 minutes. The traces shown are representative of three separate experiments. The maximum aggregation obtained with vehicle control at 5 minutes was taken as 100% to calculate the level of aggregation for chrysin and its derivatives-treated samples. Cumulative data represent mean ± S.D. (n = 3). *Indicates significance with respect to controls and # indicates significance with respect to the respective chrysin concentrations, *p* values shown (**,## *p* < 0.01 and ***,### *p* < 0.001) are as calculated by one-way ANOVA using Graphpad Prism.

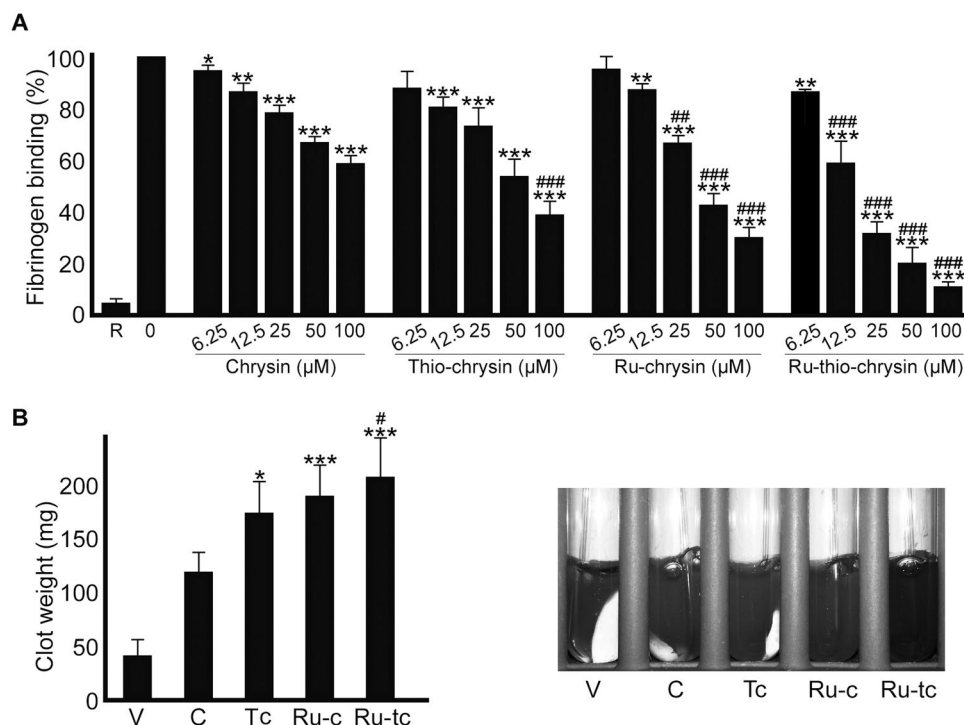


Figure 4. Chrysin and its derivatives inhibit inside-out and outside-in signalling in platelets. **(A)** human platelet-rich plasma was treated with vehicle [0.1% (v/v) DMSO] or diverse concentrations of chrysin, thio-chrysin, Ru-chrysin and Ru-thio-chrysin for 5 minutes prior to the addition of 0.5 μg/mL CRP-XL and incubation of 20 minutes at room temperature. The level of fibrinogen binding (as a marker for inside-out signalling to integrin αIIbβ3) was quantified using FITC-labelled anti-human fibrinogen antibodies by flow cytometry. The level of fluorescence obtained with vehicle control was taken as 100% to calculate the extent of inhibition in chrysin and its derivatives-treated samples. R represents ‘resting’ platelets. Cumulative data represent mean ± S.D. (n = 4). **(B)** human platelet-rich plasma was treated with vehicle (V) [0.1% (v/v) DMSO] or 50 μM of chrysin (C) or its derivatives, thio-chrysin (Tc), Ru-chrysin (Ru-c) and Ru-thio-chrysin (Ru-tc) for 5 minutes. Following incubation, clotting was initiated by the addition of 1 U/mL thrombin and the clot retraction was monitored for three hours. The remaining clot weight at three hours was measured to analyse the extent of retraction process. The image shown on the right is representative of four separate experiments. *Indicates significance with respect to controls and # indicates significance with respect to the respective chrysin concentrations; p values shown (*, #p < 0.05, **, #p < 0.01 and ***, #p < 0.001) are as calculated by one-way ANOVA using Graphpad Prism.

Chrysin and its derivatives affect inside-out signalling to integrin αIIbβ3. Since chrysin and its derivatives affected platelet aggregation, we hypothesised that they may affect inside-out signalling to integrin αIIbβ3, as this plays a critical role in the affinity modulation of this integrin and its subsequent binding to fibrinogen in order to facilitate platelet aggregation³. Hence, the level of fibrinogen binding on the platelet surface was measured as a marker for inside-out signalling to integrin αIIbβ3 using human PRP and FITC-labelled anti-fibrinogen antibodies by flow cytometry. Similar to aggregation assays, Ru-thio-chrysin showed significantly enhanced inhibitory effects on fibrinogen binding to the platelet surface upon activation with 0.5 μg/mL CRP-XL (Fig. 4A). While the concentration of 6.25 μM Ru-thio-chrysin showed around 15–20% inhibition, it inhibited the fibrinogen binding levels by almost 90% at 100 μM concentration. Notably, Ru-thio-chrysin (at concentrations of more than 12.5 μM) and Ru-chrysin (at concentrations of more than 25 μM) displayed significantly more effects compared to the respective concentrations of chrysin. Chrysin and thio-chrysin displayed similar inhibitory effects. Similar to the aggregation data, these results further emphasise the increased potential of Ru-complexes in exerting their target effects under these conditions.

Outside-in signalling driven by integrin αIIbβ3 is affected by chrysin and its derivatives. Following fibrinogen binding, integrin αIIbβ3 triggers signalling into the platelets in order to induce clot retraction and promote wound healing. This also represents a late downstream signalling event in the platelet activation process³⁷. To determine whether chrysin and its derivatives affect outside-in signalling by integrin αIIbβ3, a clot retraction assay was performed. The human platelets (PRP) were treated with different concentrations of chrysin, thio-chrysin, Ru-chrysin and Ru-thio-chrysin prior to the addition of thrombin and initiation of clot formation and subsequent retraction. At three hours, the clot obtained with the vehicle control [0.1% (v/v) DMSO] retracted to around 50 mg. Although chrysin did not show significant effects, its derivatives substantially inhibited the clot retraction process as the clot weights remained at more than 100 mg (Fig. 4B). Similar to other platelet functional assays, Ru-thio-chrysin displayed superior effects in comparison to native chrysin.

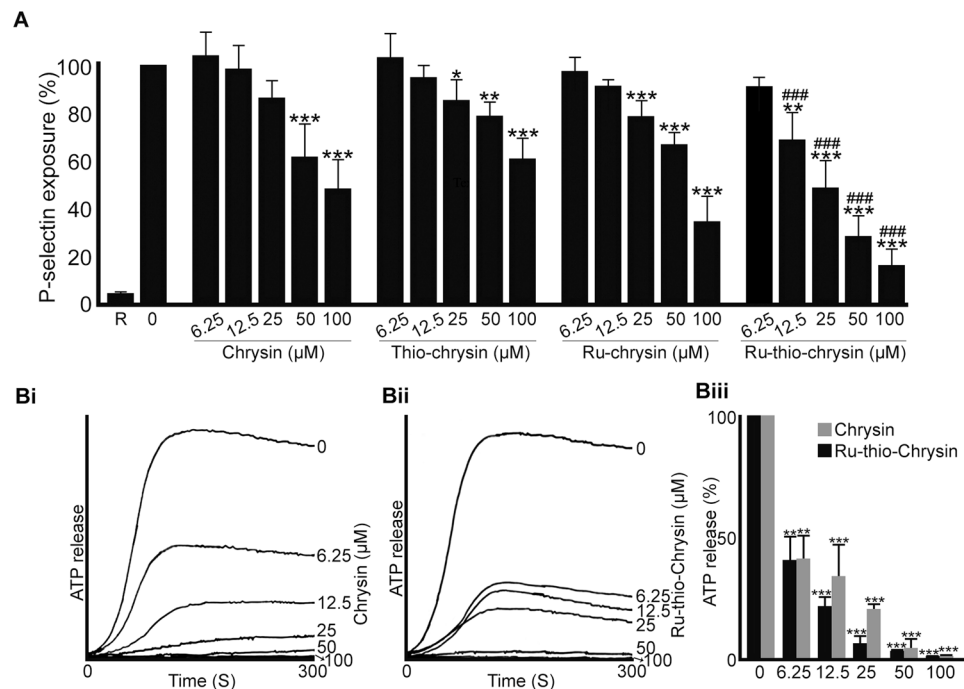


Figure 5. Chrysin and its derivatives affect granule secretion in platelets. **(A)** human platelet-rich plasma was treated with vehicle [0.1% (v/v) DMSO] or diverse concentrations of chrysin, thio-chrysin, Ru-chrysin and Ru-thio-chrysin for 5 minutes prior to the addition of 0.5 μg/mL CRP-XL and incubation of 20 minutes at room temperature. The level of P-selectin (as a marker for α-granule secretion) was quantified using PECy5-labelled anti-human P-selectin antibodies by flow cytometry. The level of fluorescence obtained with vehicle control was taken as 100% to calculate the extent of inhibition in chrysin and its derivatives-treated samples. R represents 'resting' platelets. Cumulative data represent mean ± S.D. (n = 4). **(B)** human washed platelets were mixed with luciferin-luciferase reagent for two minutes followed by incubation with a vehicle control [0.1% (v/v) DMSO] or different concentrations of chrysin **(i)** or Ru-thio-chrysin **(ii)** for another 5 minutes. Platelets were then activated with 0.5 μg/mL CRP-XL and the ATP release was monitored for 5 minutes by lumi-aggregometry. The traces shown are representative of three separate experiments. The maximum ATP release obtained with vehicle control was taken as 100% to calculate the level of inhibition in chrysin and Ru-thio-chrysin treated samples **(iii)**. Cumulative data represent mean ± S.D. (n = 3). *Indicates significance with respect to controls and * indicates significance with respect to the respective chrysin concentrations; p values shown (*p < 0.05, **p < 0.01 and ***p < 0.001) are as calculated by one-way ANOVA using Graphpad Prism.

Interestingly, thio-chrysin displayed significant inhibitory effect in clot retraction, suggesting that the chemical modification of 4-C=O (carbonyl) to 4-C=S (thiocarbonyl) may influence integrin αIIbβ3-mediated outside-in signalling. Together, these data establish a role for chrysin derivatives in the modulation of outside-in signalling by integrin αIIbβ3 in human platelets.

Effects of chrysin and its derivatives on granule secretion in platelets. Platelets primarily contain two types of granules (α- and dense granules) and the activation of platelets releases the granule contents to the external environment, where they play important roles in the stimulation of additional platelets and their recruitment to the growing thrombus³⁸. To establish whether chrysin and its derivatives affect α-granule secretion in platelets, the level of P-selectin on the platelet surface upon activation with 0.5 μg/mL CRP-XL was measured as a marker for α-granule secretion using human PRP and PECy5-labelled anti-P-selectin antibodies by flow cytometry. CRP-XL-induced α-granule secretion was inhibited significantly by Ru-thio-chrysin at the concentrations of 12.5 μM and above, with approximately 80% inhibition being achieved at 100 μM concentration (Fig. 5A). Ru-chrysin and thio-chrysin significantly affected platelet granule secretion at the concentrations of 25 μM and above. However, chrysin affected α-granule secretion only at a minimum concentration of 50 μM in platelets. Only Ru-thio-chrysin displayed more inhibitory effects on α-granule secretion compared to chrysin at concentrations from 12.5 μM in PRP.

Based on the above data, chrysin and Ru-thio-chrysin were selected to distinguish their modulatory effects on dense granule secretion and other platelet functions. ATP secretion was measured as a marker for dense granule secretion in washed platelets upon activation with 0.5 μg/mL CRP-XL in the presence and absence of different concentrations of chrysin and Ru-thio-chrysin using a luciferin-luciferase luminescence assay (Fig. 5B). Both chrysin and Ru-thio-chrysin significantly inhibited dense granule secretion at the concentrations tested (6.25–100 μM) with 100% inhibition observed at 100 μM concentration of both. These data demonstrate that chrysin and its derivatives significantly affect platelet granule secretion, which may influence the subsequent functions of platelets.

Chrysin and Ru-thio-chrysin do not affect platelet adhesion under static conditions. Integrins α Ib β 3 and α 2 β 1 play critical roles in platelet adhesion to different matrix proteins such as fibrinogen and collagen, respectively. To determine whether chrysin and Ru-thio-chrysin directly influence platelet adhesion by affecting the functions of integrins α Ib β 3 and α 2 β 1, the static platelet adhesion assay was performed on collagen, CRP-XL (a selective ligand for GPVI that is used to differentiate the binding effects of collagen to GPVI and integrin α 2 β 1) and fibrinogen-coated surfaces using human PRP in the presence and absence of various concentrations of chrysin and Ru-thio-chrysin. Moreover, to determine the linear impact of these compounds on integrin α Ib β 3, integrilin (4 μ M), an antagonist for integrin α Ib β 3 was also used in this assay prior to the treatment with different concentrations of chrysin and Ru-thio-chrysin. Chrysin and Ru-thio-chrysin did not affect platelet adhesion to collagen, CRP-XL or fibrinogen both in the presence and absence of integrilin (Figure S5). These data suggest that chrysin and Ru-thio-chrysin may not directly affect the functions of α Ib β 3 and α 2 β 1 on the platelet surface.

Effects of chrysin and Ru-thio-chrysin in the modulation of calcium signalling in platelets. Platelets contain a dense-tubular system to store calcium, and the activation of platelets allows the mobilisation of calcium from stores to the cytoplasm. Similarly, a substantial amount of calcium is also pumped from the external milieu into the cytoplasm during platelet activation. The elevated levels of calcium play major roles including the intracellular reorganisation of cytoskeleton to allow platelet spreading and subsequent thrombus formation³⁹. Based on the above results achieved in washed platelets and PRP, chrysin and Ru-thio-chrysin were tested to evaluate their effects on the modulation of calcium mobilisation. Chrysin displayed greater inhibitory effects on calcium mobilisation than Ru-thio-chrysin in washed platelets compared to the control (Fig. 6Ai and Aii). However, Ru-thio-chrysin exhibited significantly greater effects in PRP compared to chrysin at a concentration of 100 μ M (Fig. 6Bi and Bii). Similar to other assays performed using PRP, Ru-thio-chrysin showed enhanced reduction in calcium mobilisation in platelets with around 60% obtained at 100 μ M. Together, these results demonstrate the impact of chrysin and Ru-thio-chrysin in the modulation of calcium mobilisation in platelets.

Chrysin and Ru-thio-chrysin negatively regulate PI3K/AKT and Src signalling in platelets. Calcium mobilisation is associated with phosphoinositide 3-kinase (PI3K) signalling in platelets³⁹. Protein kinase B (AKT) is a downstream effector of PI3K and a key marker for the PI3K/AKT signalling pathway. A recent study has demonstrated the inhibitory effects of chrysin on the phosphorylation of AKT³³. In addition, chrysin has been reported to inhibit focal adhesion kinase (FAK) activation³³, which plays a key role in downstream signalling of integrins (outside-in signalling) that leads to platelet spreading⁴⁰ as well as Src kinases that are critical initiators of integrin signalling and platelet activation⁴¹. Therefore, to determine whether chrysin and Ru-thio-chrysin share similar molecular targets in platelets, the phosphorylation of AKT at S473, FAK at Y397 and Src at Y527 (inhibitory site) was measured using resting and 0.5 μ g/mL CRP-XL activated platelets in the presence and absence of different concentrations of chrysin and Ru-thio-chrysin by immunoblot analysis. The vehicle [0.1% (v/v) DMSO]-treated samples displayed a notable level of phosphorylation of AKT and FAK upon activation with CRP-XL, however, chrysin and Ru-thio-chrysin inhibited their phosphorylation in a concentration-dependent manner (Fig. 6C). Similarly, chrysin and Ru-thio-chrysin had a significant impact on the dephosphorylation of Src at Y527, which is an essential phenomenon for the activation of platelets. Together these data suggest that chrysin and Ru-thio-chrysin may share similar molecular targets in platelets, and their inhibitory effects on Src may directly or indirectly influence other signalling pathways that render the inhibition of platelet function.

Chrysin and Ru-thio-chrysin inhibit thrombus formation under arterial flow conditions. Platelet activation under arterial flow conditions culminates in the formation of thrombus at the damaged blood vessels and thereby reducing the blood supply to target tissues. Here, the effects of chrysin and Ru-thio-chrysin on thrombus formation under arterial flow conditions on collagen-coated surface were tested. DiOC6-labelled whole human blood treated with vehicle control or 100 μ M chrysin or Ru-thio-chrysin was perfused over collagen-coated surfaces of Vena8 biochips and thrombus formation was monitored for 10 minutes under arterial flow conditions (20 dynes/cm²). The control sample showed notable level of thrombus formation over a 10 minutes period (Fig. 7A). Chrysin inhibited the thrombus growth and volume by around 50% compared to the control (Fig. 7B and C). Notably, Ru-thio-chrysin at a concentration of 100 μ M significantly reduced the number of thrombi, rate of thrombus formation and volume with approximately 75% inhibition achieved at this concentration. These data corroborate the effects of Ru-thio-chrysin in whole blood (in the presence of plasma proteins and other blood cells), whereas chrysin did not exhibit similar effects.

Chrysin and Ru-thio-chrysin affect haemostasis in mice. To determine the effects of Ru-thio-chrysin in comparison to native chrysin in the modulation of haemostasis under physiological conditions in mice, a tail-bleeding assay was performed as described previously¹⁶. Mice were anaesthetised prior to infusing the vehicle control or chrysin or Ru-thio-chrysin (final concentration of 25 μ M) through femoral arteries. Following five minutes incubation, 1 mm of tail tip was dissected and the bleeding time was monitored. Chrysin-infused mice displayed extended bleeding time (average of 901 seconds) compared to the control group (average of 445 seconds) (Fig. 7D). Ru-thio-chrysin extended the bleeding time in mice to an average of 1096 seconds, although these effects do not significantly differ from chrysin. These data illustrate that Ru-thio-chrysin and chrysin affect haemostasis with similar efficacy in mice.

Ru-thio-chrysin possesses enhanced bioavailability. Similar to other natural flavonoids, chrysin displayed prominent inhibitory effects in isolated platelets but their inhibitory effects were reduced under physiological conditions when PRP or whole blood were used. We hypothesised that the inhibitory effects of chrysin were

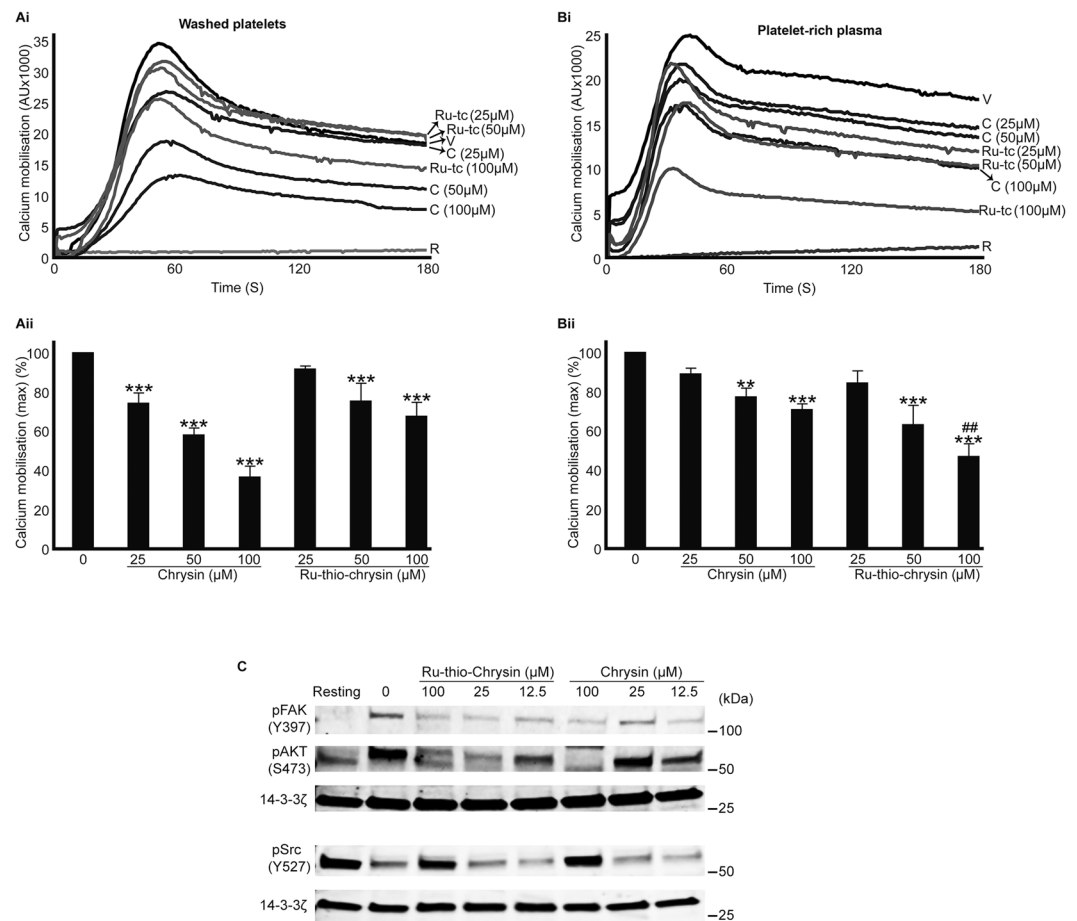


Figure 6. Chrysin and its derivatives influence the calcium mobilisation and phosphorylation of various signalling proteins in platelets. Fluo4 AM-dye labelled human washed platelets (**Ai,Aii**) and platelet-rich plasma (**Bi,Bii**) were treated with vehicle control (V) [0.1% (v/v) DMSO] or different concentrations of chrysin (C) or Ru-thio-chrysin (Ru-tc) for 5 minutes prior to the addition of 0.5 μg/mL CRP-XL and monitoring of calcium mobilisation for three minutes by fluorimetry. The calcium traces (**Ai** and **Bi**) shown are representative of three separate experiments. The maximum fluorescence obtained with each sample was converted into percentages to calculate the level of calcium mobilisation obtained with vehicle and chrysin or Ru-thio-chrysin treated samples. Cumulative data (**Aii** and **Bii**) represent mean ± S.D. (n = 3). *Indicates significance with respect to controls and # indicates significance with respect to the respective chrysin concentrations; *p* values shown (**, # *p* < 0.01 and *** *p* < 0.001) are as calculated by one-way ANOVA using Graphpad Prism. (**C**) Human washed platelets were treated with vehicle control or different concentrations of chrysin or Ru-thio-chrysin for 5 minutes prior to the addition of 0.5 μg/mL CRP-XL and incubation for another 5 minutes. The platelets were lysed and used for immunoblot analysis to detect the level of AKT phosphorylation at residue S473, FAK phosphorylation at Y397 and phosphorylation of Src at Y527. The level of 14-3-3ζ protein was detected as a loading control. The cropped images of the blots shown here are representative of three separate experiments. The uncropped full length blots are presented in Supplementary Information (Figure S8).

reduced due to greater binding to plasma proteins such as albumin and hence, poor bioavailability, and reduced lipophilicity in order to cross cell membranes. To determine the binding ability of chrysin and Ru-thio-chrysin to human serum albumin (HSA), the HSA binding assay was performed using TRANSIL^{XL} HSA binding kit according to the manufacturer's instructions. The binding affinities (K_d) of chrysin and Ru-thio-chrysin were determined to be 1.93 μM and 1.40 mM, respectively. Moreover, the fraction bound to plasma (fb) was found to be 99.7% for chrysin and <29.6% for Ru-thio-chrysin. These data confirm that chrysin possesses greater binding affinity towards plasma proteins, primarily albumin, than Ru-thio-chrysin.

To determine the level of uptake of chrysin and Ru-thio-chrysin in platelets, mass spectrometry-based analysis was performed. Washed human platelets were treated with chrysin or Ru-thio-chrysin (100 μM) for 5 minutes and the unbound compounds were washed prior to the quantification of the amount of chrysin and Ru-thio-chrysin present in platelets by LC-MS (Orbitrap, C8 column, Solvent system: 0.1% formic acid in water and 0.1% formic acid in acetonitrile). The uptake of Ru-thio-chrysin in platelets was found to be at 8.38 ± 1.07 μM whereas chrysin was found to be at 6.86 ± 0.27 μM as determined using standard curves (Figure S6). This indicates that Ru-thio-chrysin, which possesses higher hydrophobicity (CLogP = 7.94 as predicted using Chemdraw

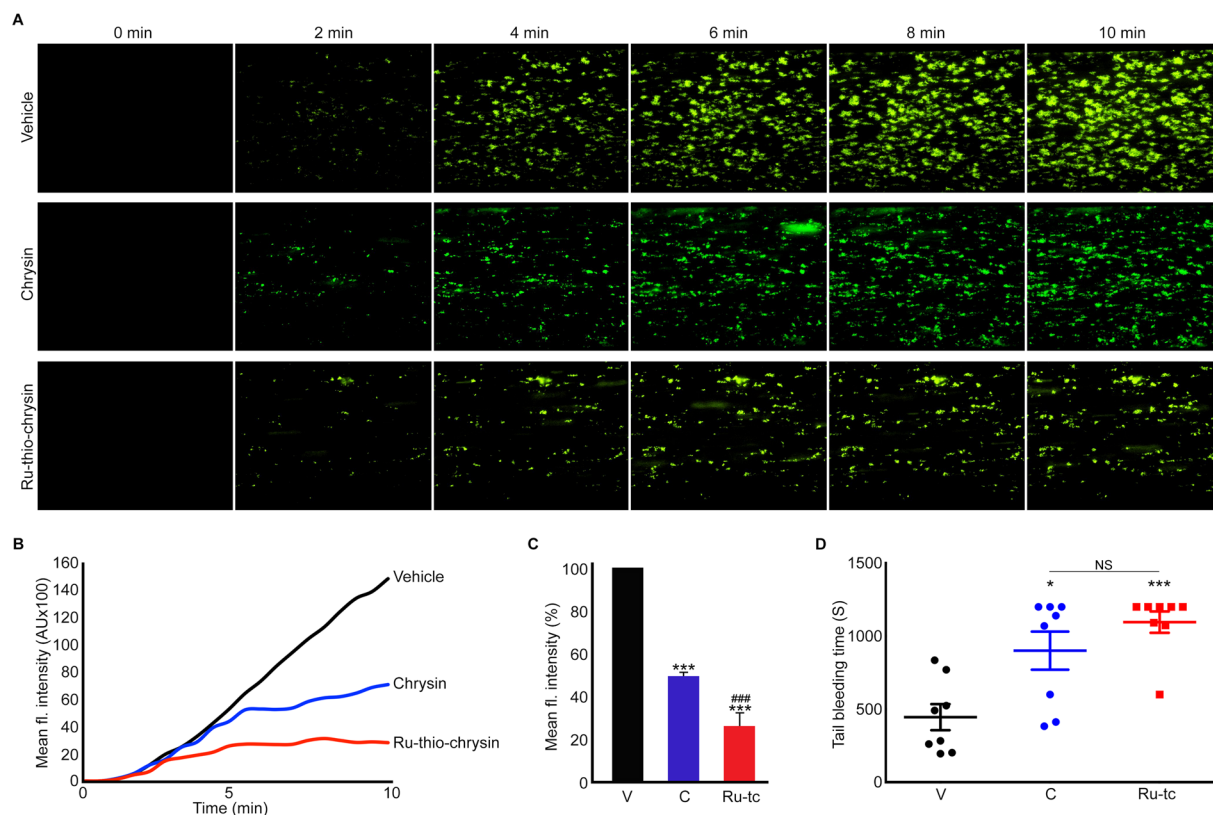


Figure 7. Differential effects of chrysin and Ru-thio-chrysin in the modulation of thrombus formation under arterial flow conditions and haemostasis in mice. DiOC6-labelled human whole blood was treated with vehicle control [0.1% (v/v) DMSO] or 100 μ M chrysin or Ru-thio-chrysin for 5 minutes prior to the perfusion over collagen-coated Vena8 biochips. Thrombus formation was monitored by capturing Z-stack fluorescent images at every 30 seconds over 10 minutes by fluorescence microscopy. The images shown (A) at different time points and traces (B) are representative of three separate experiments. (C) The mean fluorescence intensity obtained with vehicle control (V) at 10 minutes was taken as 100% to calculate the level of inhibition in chrysin (C) and Ru-thio-chrysin (Ru-tc)-treated samples. Data represent mean \pm S.D. (n = 3). *Indicates significance with respect to control and # indicates significance with respect to the respective chrysin concentration; p values shown (***, ### $p < 0.001$) are as calculated by one-way ANOVA using Graphpad Prism. (D) The effects of vehicle control [0.1% (v/v) DMSO] or 25 μ M of chrysin (C) or Ru-thio-chrysin (Ru-tc) in the modulation of haemostasis were analysed by tail bleeding assay in mice. Data represent \pm S.D. (n = 8 mice in each group). The p values shown (* $p < 0.05$ and *** $p < 0.001$) are as calculated by non-parametric Mann-Whitney test using Graphpad Prism.

16.0 software) than chrysin (CLogP = 3.04), has greater cellular permeability in platelets. These data confirm that the increased inhibitory effects observed for Ru-thio-chrysin are, indeed, due to its reduced binding to plasma proteins, greater bioavailability, and enhanced cell permeability when compared to chrysin.

Chrysin and its synthetic derivatives display no cytotoxic effects in platelets. In order to examine whether the native chrysin and its synthetic derivatives exert any cytotoxic effects in platelets at the concentrations used in this study, the lactate dehydrogenase (LDH) assay was performed using PRP. While the positive control displayed maximal effects in platelets, chrysin and its synthetic derivatives did not show significant cytotoxic effects in platelets at the concentrations used in this study (i.e. between 6.25 and 100 μ M) (Figure S7). These data confirm that the inhibitory effects of chrysin and its synthetic derivatives presented in this study were not due to the cytotoxic effects of these molecules.

Discussion

In this study, the effects of chrysin and its chemical derivatives on the modulation of platelet function, *in vitro* thrombus formation and haemostasis were determined. Similar to a number of other dietary flavonoids such as quercetin^{42–44}, tangeretin¹⁶, nobiletin¹⁷, luteolin and apigenin¹⁸, chrysin also exhibited inhibitory effects in various platelet functions. Chrysin affected CRP-XL-induced platelet aggregation, inside-out signalling to integrin α IIb β 3, granule secretion and integrin α IIb β 3 mediated outside-in signalling in platelets. Notably, chrysin reduced thrombus formation *in vitro* in human blood under arterial flow conditions and extended bleeding time in mice. Recently, Liu *et al.* (2016)³³ reported the anti-platelet properties of chrysin and its possible molecular targets in platelets. Chrysin has concentration-dependently inhibited platelet activation induced by various platelet

agonists including collagen, thrombin, U46619 and ADP. In addition, chrysin was found to inhibit the phosphorylation of numerous signalling proteins such as Syk, PLC γ 2, AKT, PKC, ERK1/2, FAK, GSK3 β and FC γ RIIa consistent with the ability of flavonoids to inhibit kinase signalling. Together the previous study concluded that chrysin is involved in the modulation of platelet function by inhibiting inside-out signalling to integrin α IIb β 3 and outside-in signalling driven by the same integrin molecule³³. Similarly, in the present study, chrysin was found to affect CRP-XL-induced inside-out signalling to integrin α IIb β 3 and phosphorylation of selective signalling molecules such as AKT, FAK and Src. In addition, chrysin was previously reported to affect platelet function *via* inhibition of cyclooxygenase activity and reduction of cAMP levels possibly by inhibiting adenylate cyclase⁴⁵. These results indicate that chrysin is likely to have several molecular targets in platelets and thereby it modulates diverse functions of platelets enabling it to control thrombosis and haemostasis.

In general, dietary flavonoids have been shown to affect platelet function by acting as pro-oxidants in order to induce the production of nitric oxide (NO) (a potent inhibitor of platelet function through the elevation of cGMP)⁴⁶, antioxidants by inhibiting reactive oxygen species (ROS) production, binding to cell surface receptors and affecting the integrity of the plasma membrane^{18,47}. Notably, a number of flavonoids have been shown to directly act as powerful inhibitors of numerous kinases (primarily tyrosine kinases) involved in diverse signalling pathways in platelets^{18,48}. In addition, flavonoids such as apigenin, genistein, luteolin and quercetin have also been shown to inhibit TXA₂ receptor on platelet surface and affect its signalling. Therefore, by using a range of cellular targets, dietary flavonoids enrich the anti-platelet properties. Hence, flavonoids act as templates for the design and synthesis of therapeutically valuable compounds with specific cellular targets, and they provide a basis to determine the molecular relationships between numerous cell surface receptors, intracellular signalling proteins and dietary components¹⁸.

Interestingly, several studies have highlighted the potential hindrances of using dietary flavonoids as therapeutically valuable compounds for the treatment and prevention of diseases. Some of these include poor bio-availability, enhanced binding to plasma proteins and decreased hydrophobicity/ lipophilicity to cross the cell membranes^{22,36}. Therefore, several researchers have attempted to chemically modify the natural flavonoids in order to overcome these issues^{23,49}. The previous studies published on the anti-platelet effects of chrysin have mainly used washed platelets to evaluate the functions of chrysin in platelets^{33,45}. In the present study, although chrysin inhibited platelet function significantly on isolated platelets, a substantial reduction in the effects of chrysin in platelets was observed when PRP and whole blood were used in experiments. These data indicate the potential binding of chrysin to plasma proteins in PRP and also other blood cells such as leukocytes and red blood cells in whole blood, and internalisation in these cell types. The addition of sulfur groups to flavonoids has previously been shown to improve their hydrophobicity and biological effects²³. Therefore, the present study was initiated in order to synthesise chemical derivatives of chrysin with enhanced anti-platelet effects by reducing their binding to plasma proteins and increasing their bio-availability. Initially, thio-chrysin was synthesised by replacing an oxygen molecule with a sulfur group in the basic structure of chrysin. A parallel comparison of thio-chrysin with native chrysin revealed no significant differences in their inhibitory effects when washed platelets or PRP were used in platelet aggregation assays.

In recent years, organometallic complexes have been widely considered as valuable compounds for a number of pathological conditions including cancer²⁷. Indeed, platinum-based chemical agents such as cisplatin, carboplatin and oxaliplatin are being used as effective drugs in the treatment of solid tumours e.g. for testicular and other cancer types^{28,50}. Due to increased associated toxicity, lack of selectivity and side effects such as nerve damage, nausea and hair loss of platinum-based drugs, a focus on other transition metals such as ruthenium, titanium, rhodium and iridium has been initiated^{24,30,50–53}. In order to understand the roles of ruthenium-based flavonoid complexes in the modulation of platelet function, for the first time, in this study we synthesised Ru-chrysin and Ru-thio-chrysin complexes and determined their effects on the modulation of platelet function. Interestingly, both complexes showed enhanced inhibitory effects in platelets in comparison to chrysin and thio-chrysin under physiological conditions such as in PRP and whole blood, although they exerted slightly reduced effects in washed platelets. A comparison of chrysin and Ru-thio-chrysin in thrombus formation under arterial flow conditions using whole blood has revealed the significance of ruthenium-based complexes in the modulation of platelet function under physiological conditions. Ru-thio-chrysin substantially reduced thrombus growth and volume, whilst chrysin at the same concentration only exhibited moderate reduction in thrombus volume. Notably, Ru-thio-chrysin showed similar effects in the modulation of haemostasis in mice compared to native chrysin. It appears that the combination of ruthenium with thio-chrysin exerts 10–25% greater effects compared to Ru-chrysin complex.

Since ruthenium is able to achieve several oxidation states (II, III and IV) at low energy levels under physiological conditions and interact with a range of biomolecules, it may facilitate efficient interaction of the small molecule present in the complex with its molecular targets, including targets that would normally be inaccessible for small molecules on their own^{24,50}. In addition, since ruthenium belongs to the same group within the periodic table as iron, ruthenium is known to mimic the nature of iron molecules, and therefore it has been shown to bind transferrin and thereby enhance the bioavailability of small molecules to a greater extent^{54–57}. Furthermore, some ruthenium-based organometallic complexes have displayed enhanced stability in water and air⁵⁰, which may be beneficial to exert prolonged effects of the target small molecule including chrysin. While the small molecules present in the ruthenium complexes bind to the target site, ruthenium may enhance its target-specific activities. Overall, ruthenium tends to have less severe side effects but enhanced biological properties compared to platinum-based drugs⁵⁰. In line with these observations, our results demonstrate that Ru-thio-chrysin exhibits reduced binding ability to plasma proteins, and increased cell permeability in comparison to native chrysin. In addition, Ru-thio-chrysin shares similar molecular targets to chrysin in platelets indicating that the mechanisms through which they inhibit platelet function are unlikely to be changed. Interestingly, Ru-thio-chrysin displayed similar effects to chrysin in the modulation of haemostasis in mice and there were no toxic effects observed in platelets with the concentrations of Ru-complexes used in this study.

Together with the numerous advantages of organometallic complexes, the results of this study demonstrate the importance of using ruthenium-based organometallic complexes in the development of novel anti-platelet agents for the prevention and treatment of thrombotic diseases. Preliminary analysis of signalling cascades in this study suggests that chrysin and Ru-thio-chrysin are likely to have similar targets in platelets. However, further studies are underway to determine the specific targets of chrysin and its ruthenium-complexes in platelets. In addition, the stability of the complexes in biological systems, their circulating plasma concentrations upon oral uptake and the nature of metabolites they produce in platelets must be determined.

Methods

Synthesis of ruthenium-chrysin derivatives (Ru-chrysin and Ru-thio-chrysin).

- a) Synthesis of chlorido [(5-oxo- κ O)-7-hydroxy-(2-phenyl)-4H-chromen-4-onato- κ O] (η 6-*p*-cymene)ruthenium(II) (Ru-chrysin)

To a solution of chrysin (0.10 g, 0.39 mmol) and NaOMe (0.02 g, 0.41 mmol, 1.05 eq.) in anhydrous methanol (10 mL), [Ru(η 6-*p*-cymene)Cl₂]₂ (0.13 g, 0.21 mmol, 0.55 eq.) in anhydrous dichloromethane (10 mL) was added under argon atmosphere. The reaction mixture was heated at reflux for 18 h and then the solvent was evaporated *in vacuo*. The obtained residue was dissolved in warm chloroform:methanol [9.0:1.0 v/v] (15 mL) and the solution was filtered to remove NaCl (by product) and other insoluble impurities. The solution was then concentrated (2–3 mL) and the compound was precipitated by the addition of EtOAc. The precipitated compound was filtered and recrystallized from EtOAc:CHCl₃ (9:1 v/v) to obtain the pure product (Ru-chrysin) as an orange red solid (0.15 g, 75%). The obtained compound was suitable for X-ray diffraction studies.

m.p.: 258–260 °C; **¹H NMR**: (DMSO-*d*₆, 400 MHz) 1.28, 1.30 (6H, 2 × *s*, 2 × CH₃_{cym}), 2.16 (3H, *s*, CH₃_{cym}), 2.89–2.91 (1H, *m*, CH_{cym}), 5.37 (2H, *d*, *J* = 8.0 Hz, H-2_{cym}, H-3_{cym}), 5.65 (2H, *d*, *J* = 8.0 Hz, H-5_{cym}, H-6_{cym}), 5.99 (1H, *s*, H-6), 6.05 (1H, *s*, H-8), 6.94 (1H, *s*, H-3), 7.54–7.58 (3H, *m*, H-3',4',5'), 8.01 (2H, *d*, *J* = 8.0 Hz, H-2',6'), 10.29 (1H, *s*, OH); **¹³C NMR**: (DMSO-*d*₆, 100 MHz) δ 17.55 (CH₃_{cym}), 22.02 (2 × CH₃_{cym}), 30.44 (CH_{cym}), 77.88 (C3), 82.54 (C8), 86.30 (C10), 90.06 (C9), 96.68 (C6), 98.12 (C3_{cym}, C5_{cym}), 102.41 (C2_{cym}), 104.02 (C1'), 105.81 (C6_{cym}), 126.22 (C3', C5'), 129.27 (C2', C6', C4'), 130.52 (C1_{cym}), 131.95 (C4_{cym}), 158.09 (C2), 159.71 (C5), 167.76 (C7), 177.07 (C=O); ***m/z* (FTMS + ESI)**: Observed as M-Cl (C₂₅H₂₃O₄Ru) requires 489.0634, found 489.0645. **Elemental analysis**: C₂₅H₂₃O₄ClRu, Calculated: C-57.31%, H-4.42%, Cl-6.77%, Ru-19.29%; found: C-57.44%, H-4.25%, Cl-6.74%, Ru-19.31%. **X-ray crystal structure obtained.**

- b) Synthesis of chlorido [(5-oxo- κ O)-7-hydroxy-(2-phenyl)-4H-chromen-4-thionato- κ S] (η 6-*p*-cymene)ruthenium(II) (Ru-thio-chrysin)

To a solution of thio-chrysin (0.10 g, 0.37 mmol) and NaOMe (0.02 g, 0.39 mmol, 1.05 eq.) in anhydrous methanol (10 mL), [Ru(η 6-*p*-cymene)Cl₂]₂ (0.20 g, 0.33 mmol, 0.90 eq.) in anhydrous dichloromethane (10 mL) was added under argon atmosphere. The reaction mixture was heated at reflux for 18 h and then the solvent was evaporated *in vacuo*. The obtained residue was dissolved in warm chloroform:methanol [9.5:0.5 v/v] (15 mL) and the solution was filtered to remove NaCl (by product) and other insoluble impurities. The solution was then concentrated (2–3 mL) and the compound was precipitated by the addition of EtOAc. The precipitated compound was filtered and recrystallized from EtOAc:CHCl₃ (9:1 v/v) to obtain the pure product (Ru-thio-chrysin) as a reddish brown solid (0.13 g, 65%). The obtained compound was suitable for X-ray diffraction studies.

m.p.: decomposes at 270 °C; **¹H NMR**: (DMSO-*d*₆, 400 MHz) 1.21, 1.23 (6H, 2 × *s*, 2 × CH₃_{cym}), 2.07 (3H, *s*, CH₃_{cym}), 2.71–2.74 (1H, *m*, CH_{cym}), 5.31–5.68 (2H, *m*, H-2_{cym}, H-3_{cym}), 6.21, 7.41 (2H, *m*, H-5_{cym}, H-6_{cym}), 6.36 (1H, *s*, H-6), 6.39 (1H, *s*, H-8), 7.52–7.64 (3H, *m*, H-3',4',5'), 7.89 (1H, *s*, H-3), 8.14, 8.16 (2H, *d*, *J* = 8.0 Hz, H-2',6'), 10.47 (1H, *s*, OH); **¹³C NMR**: Couldn't be obtained. ***m/z* (FTMS + ESI)**: Observed as M-Cl (C₂₅H₂₃O₃RuS) requires 505.0406, found 505.0407. **Elemental analysis**: C₂₅H₂₃O₃ClRuS, Calculated: C-55.60%, H-4.29%, Cl-6.58%, Ru-18.72%; S-5.94% found: C-55.73%, H-4.16%, Cl-6.56%, Ru-18.71%, S-6.00%. **X-ray crystal structure obtained.**

X-ray diffraction analysis and structure determination for Ru-chrysin and Ru-thio-chrysin.

Powder X-ray diffraction data for Ru-chrysin and Ru-thio-chrysin were collected on a Bruker D8 Advance (Cu K α 1, λ = 1.54056 Å) diffractometer operating in capillary transmission mode. The diffractometer was equipped with a LynxEye detector. Monochromatic Cu K α 1 is achieved with the use of a curved Johansson type primary monochromator. Furthermore, an 8 mm detector aperture slit and a metal knife edge collimator were used to minimise air scattering.

Both samples were lightly ground prior to packing into a 0.5 mm borosilicate capillary, and the data collection was carried out at room temperature (ca. 293 K). The powder diffraction data were indexed with DICVOL91⁵⁸ and solved using the simulated annealing (SA) approach implemented in DASH 3.3.2³⁴. Previously solved crystal structures were used to derive the starting models used in the SA optimisation; the CSD reference code BENZAX⁵⁹ was used for the Ru-coordinated cymene moiety whilst the dihydroxyflavone ligand was derived from the CSD reference code RAMGOB01⁶⁰. Both crystal structures were subsequently refined with TOPAS (Bruker, Germany). Further crystallographic information and CIF files are given in Table S2 and Table S3, respectively. The final Rietveld fits to the powder diffraction data are shown in Figure S3.

Human platelet preparation, aggregation assays and immunoblotting. The preparation of human platelets and aggregation assays were performed using standard protocols as described by us previously^{15, 16}.

Briefly, human blood was collected in 3.2% citrate containing vacutainers via venepuncture from healthy, aspirin-free individuals with informed consent in accordance with the methods approved by the University of Reading Research Ethics Committee. All methods were performed in accordance with the relevant institutional and national guidelines and regulations. Blood samples were centrifuged at 102 g for 20 minutes at room temperature to separate the PRP, which was used in aggregation, flow cytometry, static platelet adhesion, calcium mobilisation and clot retraction assays. For the preparation of washed platelets, 50 mL of blood samples were mixed with 7.5 mL of ACD (acid citrate dextrose) (20 g/L glucose, 25 g/L sodium citrate and 15 g/L citric acid) and centrifuged at 102 g for 20 minutes at room temperature. The PRP was carefully aspirated from the other blood cells prior to mixing with 3 mL of ACD and centrifuging at 1413 g for 10 minutes at room temperature. The resulting platelet pellet was re-suspended in modified Tyrodes-HEPES buffer (2.9 mM KCl, 134 mM NaCl, 0.34 mM $\text{Na}_2\text{HPO}_4 \cdot 12\text{H}_2\text{O}$, 1 mM MgCl_2 , 12 mM NaHCO_3 , 20 mM HEPES, pH 7.3) and washed by centrifuging again at 1413 g for 10 minutes. The resulting platelet pellet was suspended in modified Tyrodes-HEPES buffer at a density of 4×10^8 cells/mL for aggregation, dense granule secretion, cellular uptake studies and calcium mobilisation assays. Human platelet aggregation was performed using CRP-XL as an agonist in the presence and absence of various concentrations of chrysin and its synthetic derivatives by optical aggregometry. A vehicle control [DMSO at a concentration of less than 0.1% (v/v)] was included in all the experiments. Dense granule secretion in platelets was determined by measuring the ATP release using the luciferin-luciferase reagent by lumi-aggregometry (Chrono-Log, USA). SDS-PAGE and immunoblotting analysis were performed using standard protocols¹⁶. The rabbit anti-phospho-specific antibodies for human AKT pS473, FAK pY397 and Src pY527 were obtained from Abcam, UK and rabbit anti-human 14-3-3 ζ (Santa Cruz Biotechnology, USA) was used to detect protein 14-3-3 ζ as a loading control in immunoblot assays. The Cy5-conjugated goat anti-rabbit IgG (Life technologies, UK) was used as the secondary antibody.

Flow cytometry based assays. Fibrinogen binding (a marker for platelet inside-out signalling to integrin $\alpha\text{IIb}\beta_3$) and P-selectin exposure (a marker for α -granule secretion) were measured by flow cytometry (Accuri C6, BD Biosciences, UK). The platelets (PRP) were treated with a vehicle control [0.1% (v/v) DMSO] or with different concentrations of chrysin and its synthetic derivatives prior to activation with CRP-XL (0.5 $\mu\text{g}/\text{mL}$). The levels of fibrinogen binding and P-selectin exposure were measured using FITC-labelled anti-human fibrinogen antibodies (Dako, UK) and PECy5-labelled CD62P antibodies (BD Biosciences, UK), respectively. The median fluorescence intensity was used to assess the levels of fibrinogen binding and P-selectin exposure on the platelet surface. The level of fluorescence obtained with the vehicle control was taken as 100% when compared with the treated samples.

Intracellular calcium mobilisation. The intracellular calcium levels in platelets were measured using Fluo-4 AM calcium-sensitive dye by spectrofluorimetry. The PRP or washed platelets pre-incubated with Fluo-4 AM were treated with a vehicle control [0.1% (v/v) DMSO] or appropriate concentrations of chrysin or Ru-thio-chrysin prior to activating with 0.5 $\mu\text{g}/\text{mL}$ CRP-XL and measuring the fluorescence continuously for 3 minutes using an excitation wavelength of 485 nm and emission at 510 nm by a Fluostar Optima spectrofluorimeter (BMG Labtech, Germany). Data were analysed by calculating the maximum level of calcium released in each sample.

Clot retraction. PRP (200 μL) was mixed with 5 μL of red blood cells and the final volume was made to 950 μL with modified Tyrodes-HEPES buffer in the presence and absence of various concentrations of chrysin or its synthetic derivatives. Clot formation was initiated by adding 1 U/mL (50 μL) thrombin. A glass capillary was placed in middle of the tube and the clot retraction was observed over a period of 3 hours at room temperature. Clot weight was measured as a marker for clot retraction after 3 hours.

In vitro thrombus formation. Human citrated blood [labelled with DiOC₆ (Sigma Aldrich, UK)] was incubated with vehicle [0.1% (v/v) DMSO] or 100 μM of chrysin or Ru-thio-chrysin for 5 minutes and perfused over collagen coated Vena8 BioChips (Cellix Ltd, Ireland) at a shear rate of 20 dynes/cm². Z-stack images of thrombi were obtained every 30 seconds for up to 10 minutes using a Nikon eclipse (TE2000-U) microscope (Nikon Instruments, UK). The median fluorescence intensity and thrombus volume were calculated by analysing the images using ImageJ.

Tail bleeding assay. The University of Reading Local Ethical Review Panel and the British Home Office approved the tail-bleeding assay performed in this study. All methods were performed in accordance with the relevant guidelines and regulations. In brief, C57BL/6 mice (9 weeks old; Envigo, UK) were anaesthetized using ketamine (80 mg kg⁻¹) and xylazine (5 mg kg⁻¹) administered via intraperitoneal route 20 minutes prior to the experiment and placed on a heated pad (37 °C). The vehicle control [0.1% (v/v) DMSO] or 25 μM Chrysin (C) or Ru-thio-chrysin (Ru-tc) was injected via femoral artery 5 minutes prior to the dissection of 1 mm of tail tip using a scalpel blade. The tail tip was placed in sterile saline at 37 °C and the time to cessation of bleeding was measured up to 20 minutes.

Platelet uptake of chrysin and Ru-thio-chrysin. Washed human platelets were treated with chrysin or Ru-thio-chrysin (100 μM) for 5 minutes and the platelets were then washed twice with modified Tyrodes-HEPES buffer by centrifugation at 1413 g for 10 minutes to remove unbound flavonoids. The compounds taken up by the platelets were extracted with methanol (400 μL). The methanol extract was dried using vacuum centrifugation and reconstituted in 200 μL of methanol for mass spectrometry (LC-MS) analysis. The concentration of chrysin and Ru-thio-chrysin in platelets were extrapolated from the standard curves of chrysin and Ru-thio-chrysin, respectively (Figure S6).

HSA binding assay. HSA binding assay was performed using TRANSIL^{XL} binding kit (Sovicell, Germany) according to the manufacturer's protocol. Briefly, 15 µL of 16x concentration of chrysin or Ru-thio-chrysin was added (to obtain a final concentration of 50 µM) to a column of 8 wells of the room temperature equilibrated TRANSIL assay plate containing varying amount of HSA immobilised silica beads. The plate was then incubated on a plate shaker at 100 g for 12 minutes followed by centrifugation for 10 minutes at 750 g. The supernatant (100 µL) was analysed by LC-MS to determine the affinity of chrysin and Ru-thio-chrysin based on the concentration of the free compounds in the supernatant. The K_d values for chrysin and Ru-thio-chrysin were calculated according to the instructions and algorithms supplied by the manufacturer (Sovicell, User Guide TRANSIL PPB binding kit V2.01, 2017).

Static platelet adhesion assay. Micro titre plates (96 well) were coated with 1 µg/100 µL/well of fibrinogen, collagen or CRP-XL followed by incubation at 4 °C for overnight. Following the removal of unbound proteins/peptide, the wells were blocked with 1% bovine serum albumin in modified Tyrodes-HEPES buffer for 1 hour. The plates were then washed three times with modified Tyrode's-HEPES buffer prior to adding human PRP (1 × 10⁸ cells/mL, 50 µL/well) and incubated at room temperature for 1 hour. Non-adhered platelets were discarded and then the wells were washed with modified Tyrodes-HEPES buffer. Citrate lysis buffer (100 µL/well) was added and incubated for 1 hour at room temperature. Finally, 100 µL of 2 M NaOH was added to all the wells to stop the reaction and the absorbance was measured at 405 nm using a Fluostar Optima spectrofluorimeter (BMG Labtech, Germany). Experiments were performed both in the absence and presence of integrilin (4 µM) (an antagonist for integrin αIIbβ3).

LDH cytotoxicity assay. The LDH cytotoxicity assay was performed using the LDH Cytotoxicity Assay Kit (Pierce, Thermo Fisher, UK) according to the manufacturer's instructions. In brief, the PRP was incubated at 37 °C for 30 minutes. The vehicle [0.1% (v/v) DMSO] or different concentrations of chrysin and its synthetic derivatives were added to the PRP and incubated for 5 minutes. Following incubation, the reaction mixture (provided in the kit) was added to the PRP and incubated for 30 minutes. The reaction was then stopped using a stop solution provided in the kit. The absorbance of the mixture was measured at 490–650 nm using a Fluostar Optima spectrofluorimeter (BMG Labtech, Germany). Results provided represent duplicate absorbance measures from three separate donors.

Statistical analysis. The data obtained in this study are represented as mean ± S.D. The statistical significance between the controls and chrysin or its derivatives-treated samples was determined using one-way ANOVA. The data obtained from tail bleeding assay were analysed using a non-parametric Mann-Whitney test. All the statistical analyses were performed using GraphPad Prism 7 software (GraphPad Software Inc., USA).

Note. CCDC deposition number for Ru-chrysin: 1495422 and Ru-thio-chrysin: 1495423.

References

1. BHF Headline Statistics. *British Heart Foundation* (2016).
2. Davi, G. & Patrono, C. Platelet activation and atherothrombosis. *N Engl J Med* **357**, 2482–2494, doi:[10.1056/NEJMra071014](https://doi.org/10.1056/NEJMra071014) (2007).
3. Gibbins, J. M. Platelet adhesion signalling and the regulation of thrombus formation. *J Cell Sci* **117**, 3415–3425, doi:[10.1242/jcs.01325](https://doi.org/10.1242/jcs.01325) (2004).
4. Collaborative meta-analysis of randomised trials of antiplatelet therapy for prevention of death, myocardial infarction, and stroke in high risk patients. *Bmj* **324**, 71–86 (2002).
5. Barrett, N. E. *et al.* Future innovations in anti-platelet therapies. *Br J Pharmacol* **154**, 918–939, doi:[10.1038/bjp.2008.151](https://doi.org/10.1038/bjp.2008.151) (2008).
6. Symonds, M. E., Stephenson, T. & Budge, H. Early determinants of cardiovascular disease: the role of early diet in later blood pressure control. *Am J Clin Nutr* **89**, 1518S–1522S, doi:[10.3945/ajcn.2009.27113F](https://doi.org/10.3945/ajcn.2009.27113F) (2009).
7. Ravera, A. *et al.* Nutrition and Cardiovascular Disease: Finding the Perfect Recipe for Cardiovascular Health. *Nutrients* **8**, doi:[10.3390/nu8060363](https://doi.org/10.3390/nu8060363) (2016).
8. Badimon, L., Vilahur, G. & Padro, T. Systems biology approaches to understand the effects of nutrition and promote health. *Br J Clin Pharmacol*, doi:[10.1111/bcp.12965](https://doi.org/10.1111/bcp.12965) (2016).
9. Rees, K. *et al.* Dietary advice for reducing cardiovascular risk. *Cochrane Database Syst Rev*, Cd002128, doi:[10.1002/14651858.CD002128.pub5](https://doi.org/10.1002/14651858.CD002128.pub5) (2013).
10. Pranavchand, R. & Reddy, B. M. Current status of understanding of the genetic etiology of coronary heart disease. *J Postgrad Med* **59**, 30–41, doi:[10.4103/0022-3859.109492](https://doi.org/10.4103/0022-3859.109492) (2013).
11. Khurana, S., Venkataraman, K., Hollingsworth, A., Piche, M. & Tai, T. C. Polyphenols: benefits to the cardiovascular system in health and in aging. *Nutrients* **5**, 3779–3827, doi:[10.3390/nu5103779](https://doi.org/10.3390/nu5103779) (2013).
12. Liu, R. H. Dietary bioactive compounds and their health implications. *J Food Sci* **78**(Suppl 1), A18–25, doi:[10.1111/1750-3841.12101](https://doi.org/10.1111/1750-3841.12101) (2013).
13. Hertog, M. G., Feskens, E. J., Hollman, P. C., Katan, M. B. & Kromhout, D. Dietary antioxidant flavonoids and risk of coronary heart disease: the Zutphen Elderly Study. *Lancet* **342**, 1007–1011 (1993).
14. McCullough, M. L. *et al.* Flavonoid intake and cardiovascular disease mortality in a prospective cohort of US adults. *Am J Clin Nutr* **95**, 454–464, doi:[10.3945/ajcn.111.016634](https://doi.org/10.3945/ajcn.111.016634) (2012).
15. Mosawy, S., Jackson, D. E., Woodman, O. L. & Linden, M. D. Treatment with quercetin and 3',4'-dihydroxyflavonol inhibits platelet function and reduces thrombus formation *in vivo*. *Journal of Thrombosis and Thrombolysis* **36**, 50–57, doi:[10.1007/s11239-012-0827-2](https://doi.org/10.1007/s11239-012-0827-2) (2013).
16. Vaiyapuri, S. *et al.* Tangeretin regulates platelet function through inhibition of phosphoinositide 3-kinase and cyclic nucleotide signaling. *Arterioscler Thromb Vasc Biol* **33**, 2740–2749, doi:[10.1161/atvbaha.113.301988](https://doi.org/10.1161/atvbaha.113.301988) (2013).
17. Vaiyapuri, S. *et al.* Pharmacological actions of nobiletin in the modulation of platelet function. *Br J Pharmacol* **172**, 4133–4145, doi:[10.1111/bph.13191](https://doi.org/10.1111/bph.13191) (2015).
18. Wright, B., Spencer, J. P., Lovegrove, J. A. & Gibbins, J. M. Insights into dietary flavonoids as molecular templates for the design of anti-platelet drugs. *Cardiovasc Res* **97**, 13–22, doi:[10.1093/cvr/cvs304](https://doi.org/10.1093/cvr/cvs304) (2013).
19. Manach, C. & Donovan, J. L. Pharmacokinetics and metabolism of dietary flavonoids in humans. *Free Radic Res* **38**, 771–785 (2004).
20. Williamson, G., Barron, D., Shimoi, K. & Terao, J. *In vitro* biological properties of flavonoid conjugates found *in vivo*. *Free Radic Res* **39**, 457–469, doi:[10.1080/10715760500053610](https://doi.org/10.1080/10715760500053610) (2005).

21. Rechner, A. R. *et al.* The metabolic fate of dietary polyphenols in humans. *Free Radic Biol Med* **33**, 220–235 (2002).
22. Tsao, R. Chemistry and biochemistry of dietary polyphenols. *Nutrients* **2**, 1231–1246, doi:[10.3390/nu2121231](https://doi.org/10.3390/nu2121231) (2010).
23. Ravishanker, D., Watson, K. A., Greco, F. & Osborn, H. M. I. Novel synthesised flavone derivatives provide significant insight into the structural features required for enhanced anti-proliferative activity. *Rsc Adv* **6**, 64544–64556, doi:[10.1039/C6RA11041J](https://doi.org/10.1039/C6RA11041J) (2016).
24. Leung, C.-H., Lin, S., Zhong, H.-J. & Ma, D.-L. Metal complexes as potential modulators of inflammatory and autoimmune responses. *Chemical Science* **6**, 871–884, doi:[10.1039/C4SC03094J](https://doi.org/10.1039/C4SC03094J) (2015).
25. Wang, X., Wang, X. & Guo, Z. Functionalization of Platinum Complexes for Biomedical Applications. *Acc Chem Res* **48**, 2622–2631, doi:[10.1021/acs.accounts.5b00203](https://doi.org/10.1021/acs.accounts.5b00203) (2015).
26. Nardon, C., Boscutti, G. & Fregona, D. Beyond platinum: gold complexes as anticancer agents. *Anticancer Res* **34**, 487–492 (2014).
27. Kostova, I. & Balkansky, S. Metal complexes of biologically active ligands as potential antioxidants. *Curr Med Chem* **20**, 4508–4539 (2013).
28. Feldman, D. R., Bosl, G. J., Sheinfeld, J. & Motzer, R. J. Medical treatment of advanced testicular cancer. *Jama* **299**, 672–684, doi:[10.1001/jama.299.6.672](https://doi.org/10.1001/jama.299.6.672) (2008).
29. Dorcier, A. *et al.* In Vitro Evaluation of Rhodium and Osmium RAPTA Analogues: The Case for Organometallic Anticancer Drugs Not Based on Ruthenium. *Organometallics* **25**, 4090–4096, doi:[10.1021/om060394o](https://doi.org/10.1021/om060394o) (2006).
30. Bergamo, A. & Sava, G. Ruthenium anticancer compounds: myths and realities of the emerging metal-based drugs. *Dalton Trans* **40**, 7817–7823, doi:[10.1039/c0dt01816c](https://doi.org/10.1039/c0dt01816c) (2011).
31. Lentz, F. *et al.* Pharmacokinetics of a novel anticancer ruthenium complex (KP1019, FFC14A) in a phase I dose-escalation study. *Anticancer Drugs* **20**, 97–103, doi:[10.1097/CAD.0b013e3283222bc5](https://doi.org/10.1097/CAD.0b013e3283222bc5) (2009).
32. Strohfeldt, K. A. *Essentials of Inorganic Chemistry*. 2015 edn, (Wiley, 2015).
33. Liu, G. *et al.* Antiplatelet activity of chrysin via inhibiting platelet α IIb β 3-mediated signaling pathway. *Mol Nutr Food Res*, doi:[10.1002/mnfr.201500801](https://doi.org/10.1002/mnfr.201500801) (2016).
34. David, W. I. F. *et al.* DASH: a program for crystal structure determination from powder diffraction data. *Journal of Applied Crystallography* **39**, 910–915, doi:[10.1107/S0021889806042117](https://doi.org/10.1107/S0021889806042117) (2006).
35. I. F. David, W., Shankland, K., Shankland, K. & Shankland, N. Routine determination of molecular crystal structures from powder diffraction data. *Chemical Communications*, 931–932, doi:[10.1039/A800855H](https://doi.org/10.1039/A800855H) (1998).
36. Xiao, J. & Kai, G. A review of dietary polyphenol-plasma protein interactions: characterization, influence on the bioactivity, and structure-affinity relationship. *Crit Rev Food Sci Nutr* **52**, 85–101, doi:[10.1080/10408398.2010.499017](https://doi.org/10.1080/10408398.2010.499017) (2012).
37. Shattil, S. J. & Newman, P. J. Integrins: dynamic scaffolds for adhesion and signaling in platelets. *Blood* **104**, 1606–1615, doi:[10.1182/blood-2004-04-1257](https://doi.org/10.1182/blood-2004-04-1257) (2004).
38. Reed, G. L. Platelet secretory mechanisms. *Semin Thromb Hemost* **30**, 441–450, doi:[10.1055/s-2004-833479](https://doi.org/10.1055/s-2004-833479) (2004).
39. Bergmeier, W. & Stefanini, L. Novel molecules in calcium signaling in platelets. *J Thromb Haemost* **7**(Suppl 1), 187–190, doi:[10.1111/j.1538-7836.2009.03379.x](https://doi.org/10.1111/j.1538-7836.2009.03379.x) (2009).
40. Hitchcock, I. S. *et al.* Roles of focal adhesion kinase (FAK) in megakaryopoiesis and platelet function: studies using a megakaryocyte lineage-specific FAK knockout. *Blood* **111**, 596–604, doi:[10.1182/blood-2007-05-089680](https://doi.org/10.1182/blood-2007-05-089680) (2008).
41. Senis, Y. A., Mazharian, A. & Mori, J. Src family kinases: at the forefront of platelet activation. *Blood* **124**, 2013–2024, doi:[10.1182/blood-2014-01-453134](https://doi.org/10.1182/blood-2014-01-453134) (2014).
42. Jasuja, R. *et al.* Protein disulfide isomerase inhibitors constitute a new class of antithrombotic agents. *J Clin Invest* **122**, 2104–2113, doi:[10.1172/jci61228](https://doi.org/10.1172/jci61228) (2012).
43. Wright, B., Gibson, T., Spencer, J., Lovegrove, J. A. & Gibbins, J. M. Platelet-mediated metabolism of the common dietary flavonoid, quercetin. *PLoS One* **5**, e9673, doi:[10.1371/journal.pone.0009673](https://doi.org/10.1371/journal.pone.0009673) (2010).
44. Hubbard, G. P., Wolfram, S., Lovegrove, J. A. & Gibbins, J. M. Ingestion of quercetin inhibits platelet aggregation and essential components of the collagen-stimulated platelet activation pathway in humans. *J Thromb Haemost* **2**, 2138–2145, doi:[10.1111/j.1538-7836.2004.01067.x](https://doi.org/10.1111/j.1538-7836.2004.01067.x) (2004).
45. Landolfi, R., Mower, R. L. & Steiner, M. Modification of platelet function and arachidonic acid metabolism by bioflavonoids. Structure-activity relations. *Biochem Pharmacol* **33**, 1525–1530 (1984).
46. Freedman, J. E. *et al.* Select flavonoids and whole juice from purple grapes inhibit platelet function and enhance nitric oxide release. *Circulation* **103**, 2792–2798 (2001).
47. Prochazkova, D., Bousova, I. & Wilhelmova, N. Antioxidant and prooxidant properties of flavonoids. *Fitoterapia* **82**, 513–523, doi:[10.1016/j.fitote.2011.01.018](https://doi.org/10.1016/j.fitote.2011.01.018) (2011).
48. Grassi, D. *et al.* Flavonoids, vascular function and cardiovascular protection. *Curr Pharm Des* **15**, 1072–1084 (2009).
49. Yoon, H. *et al.* Design, synthesis and inhibitory activities of naringenin derivatives on human colon cancer cells. *Bioorg Med Chem Lett* **23**, 232–238, doi:[10.1016/j.bmcl.2012.10.130](https://doi.org/10.1016/j.bmcl.2012.10.130) (2013).
50. Page, S. Ruthenium compounds as anticancer agents. *Education in Chemistry* **49**, 26–29 (2012).
51. Dowling, C. M. *et al.* Antitumor activity of Titanocene Y in xenografted PC3 tumors in mice. *Lett Drug Des Discov* **5**, 141–144, doi:[10.2174/157018008783928463](https://doi.org/10.2174/157018008783928463) (2008).
52. Sweeney, N. J. *et al.* The synthesis and cytotoxic evaluation of a series of benzodioxole substituted titanocenes. *Appl Organomet Chem* **21**, 57–65, doi:[10.1002/aoc.1177](https://doi.org/10.1002/aoc.1177) (2007).
53. Sarsam, S. W., Nutt, D. R., Strohfeldt, K. & Watson, K. A. Titanocene anticancer complexes and their binding mode of action to human serum albumin: A computational study. *Metallomics* **3**, 152–161, doi:[10.1039/c0mt00041h](https://doi.org/10.1039/c0mt00041h) (2011).
54. Kostova, I. Ruthenium complexes as anticancer agents. *Curr Med Chem* **13**, 1085–1107 (2006).
55. Vincent, J. B. & Love, S. The binding and transport of alternative metals by transferrin. *Biochim Biophys Acta* **1820**, 362–378, doi:[10.1016/j.bbagen.2011.07.003](https://doi.org/10.1016/j.bbagen.2011.07.003) (2012).
56. Page, S. M., Boss, S. R. & Barker, P. D. Tuning heavy metal compounds for anti-tumor activity: is diversity the key to ruthenium's success? *Future Med Chem* **1**, 541–559, doi:[10.4155/fmc.09.25](https://doi.org/10.4155/fmc.09.25) (2009).
57. Pongratz, M. *et al.* Transferrin binding and transferrin-mediated cellular uptake of the ruthenium coordination compound KP1019, studied by means of AAS, ESI-MS and CD spectroscopy. *Journal of Analytical Atomic Spectrometry* **19**, 46–51, doi:[10.1039/B309160K](https://doi.org/10.1039/B309160K) (2004).
58. Boulton, A. & Louer, D. Powder pattern indexing with the dichotomy method. *J. Appl. Cryst.* **37**, 724–731, doi:[10.1107/s0021889804014876](https://doi.org/10.1107/s0021889804014876) (2004).
59. Kandioller, W. *et al.* Organometallic anticancer complexes of lapachol: metal centre-dependent formation of reactive oxygen species and correlation with cytotoxicity. *Chem. Comm* **49**, 3348–3350, doi:[10.1039/C3CC40432C](https://doi.org/10.1039/C3CC40432C) (2013).
60. Hibbs, D. E., Overgaard, J., Gatti, C. & Hambley, T. W. The electron density in flavones I. Baicalein. *New J. Chem.* **27**, 1392–1398, doi:[10.1039/B301740K](https://doi.org/10.1039/B301740K) (2003).

Acknowledgements

This work was greatly supported by funding from the British Heart Foundation, Wellcome Trust, Felix Trust, Royal Society, Physiological Society and the Saudi Arabian Cultural Bureau. We gratefully acknowledge the Chemical Analysis Facility at the University of Reading for providing access to mass spectrometry and powder diffraction facilities.

Author Contributions

D.R. designed the study, performed experiments, analysed data and wrote the paper; M.S. has performed experiments and analysed data; A.A. performed experiments and analysed data; R.P. performed experiments and analysed data; T.M.V. performed experiments and analysed data; M.J. performed experiments and analysed data; H.F.W. performed experiments and analysed data; E.M.S.A. performed experiments and analysed data; E.K. performed experiments and analysed data; R.V. performed experiments and analysed data; J.G. contributed towards the study design; K.S. contributed towards the study design; E.G. contributed towards the study design; H.M.I.O. designed the study and wrote the paper and S.V. designed the study, performed experiments, analysed data and wrote the paper.

Additional Information

Supplementary information accompanies this paper at doi:[10.1038/s41598-017-05936-3](https://doi.org/10.1038/s41598-017-05936-3)

Competing Interests: The authors declare that they have no competing interests.

Publisher's note: Springer Nature remains neutral with regard to jurisdictional claims in published maps and institutional affiliations.



Open Access This article is licensed under a Creative Commons Attribution 4.0 International License, which permits use, sharing, adaptation, distribution and reproduction in any medium or format, as long as you give appropriate credit to the original author(s) and the source, provide a link to the Creative Commons license, and indicate if changes were made. The images or other third party material in this article are included in the article's Creative Commons license, unless indicated otherwise in a credit line to the material. If material is not included in the article's Creative Commons license and your intended use is not permitted by statutory regulation or exceeds the permitted use, you will need to obtain permission directly from the copyright holder. To view a copy of this license, visit <http://creativecommons.org/licenses/by/4.0/>.

© The Author(s) 2017

Review Article

Toll-Like Receptor 4 Signalling and Its Impact on Platelet Function, Thrombosis, and Haemostasis

Thomas M. Vallance, Marie-Theres Zeuner, Harry F. Williams, Darius Widera, and Sakthivel Vaiyapuri

School of Pharmacy, University of Reading, Reading RG6 6UB, UK

Correspondence should be addressed to Darius Widera; d.widera@reading.ac.uk and Sakthivel Vaiyapuri; s.vaiyapuri@reading.ac.uk

Academic Editor: Elzbieta Kolaczowska

Copyright © 2017 Thomas M. Vallance et al. This is an open access article distributed under the Creative Commons Attribution License, which permits unrestricted use, distribution, and reproduction in any medium, provided the original work is properly cited.

Platelets are anucleated blood cells that participate in a wide range of physiological and pathological functions. Their major role is mediating haemostasis and thrombosis. In addition to these classic functions, platelets have emerged as important players in the innate immune system. In particular, they interact with leukocytes, secrete pro- and anti-inflammatory factors, and express a wide range of inflammatory receptors including Toll-like receptors (TLRs), for example, Toll-like receptor 4 (TLR4). TLR4, which is the most extensively studied TLR in nucleated cells, recognises lipopolysaccharides (LPS) that are compounds of the outer surface of Gram-negative bacteria. Unlike other TLRs, TLR4 is able to signal through both the MyD88-dependent and MyD88-independent signalling pathways. Notably, despite both pathways culminating in the activation of transcription factors, TLR4 has a prominent functional impact on platelet activity, haemostasis, and thrombosis. In this review, we summarise the current knowledge on TLR4 signalling in platelets, critically discuss its impact on platelet function, and highlight the open questions in this area.

1. Introduction

Platelets are small, anucleated, and short-lived blood cells with a range of important functions beyond their classical roles in haemostasis [1–3]. The function of platelets in haemostasis has been well documented and is linked to their capacity to respond to the damaged endothelium [4–6]. Following vessel damage and initial activation, platelets secrete a wide variety of small molecules and proteins from intracellular granules in order to activate and recruit more circulating platelets and immune cells, such as leukocytes [4]. In addition to these secretion events, platelets undergo dramatic shape changes that enable them to cover the site of injury and prevent bleeding [4]. Thrombosis (blood clot formation) mediated by platelets occurs in the arteries under pathological conditions and significantly obstructs the blood flow to major organs such as the heart and brain resulting in heart attacks and strokes, respectively [7]. In addition to their physiological functions, platelets can be involved in different

pathological conditions, for example, in atherosclerosis [8, 9]. If the atherosclerotic plaque ruptures, the exposure of the subendothelial matrix and release of procoagulatory matrix proteins, such as collagen, are sufficient to initiate the formation of a thrombus (blood clot) at this site [4, 10]. Thrombus poses a significant systemic risk because it is formed in a narrowed blood vessel and so has the potential to completely occlude the vessel and trigger a myocardial infarction or ischaemic stroke [10].

Platelets also have pivotal roles in the innate immune system, which includes cells that combat general infections (e.g., neutrophils), and is responsible for the eradication of pathogens to protect the body from infection [11, 12]. During the immune response, platelets have been shown to interact with and respond to many species of Gram-positive and Gram-negative bacteria through different receptors [13, 14]. Moreover, platelets are capable of internalising specific types of bacteria and viruses although the function of this phenomenon is poorly understood [15, 16]. The ability of platelets to

participate in such a wide range of functions and their ability to synthesise certain new proteins despite lacking a nucleus have generated significant scientific interest [2, 3, 17].

In addition, platelets play a role in the development of disseminated intravascular coagulation (DIC), a common complication observed in patients with sepsis [18–20]. During DIC, platelets are activated and form smaller thrombi in the microvasculature or aggregates that are sequestered in organs such as the lungs. Together, this leads to thrombocytopenia, a reduction in the number of circulating platelets. Mild thrombocytopenia is defined as less than 1.5×10^{11} platelets per litre of blood compared to between 1.5 and 4.0×10^{11} in healthy individuals, but more severe thrombocytopenia is defined as less than 0.5×10^{11} platelets per litre [6, 20, 21]. Furthermore, it has been discovered that platelets can promote the formation of neutrophil extracellular traps (NETs) which have cytotoxic actions on host cells beyond their beneficial antibacterial effects [22].

Notably, conditions such as sepsis and DIC have been suggested to be linked to several platelet receptors, especially Toll-like receptor (TLR) 4 [8, 18, 22, 23]. In human nucleated cells, especially in professional antigen-presenting cells, the binding of a ligand to TLR1, 2, 4, 5, 6, 7, 8, 9, and 10 results in the activation of the so called myeloid differentiation factor-88- (MyD88-) dependent pathway, whereas TLR3 activates the MyD88-independent pathway [12, 23, 24]. In contrast to most TLRs which signal exclusively through one of the two pathways, TLR4 is able to activate both MyD88-dependent and MyD88-independent signalling [12, 24].

Platelets contain all of the proteins (e.g., MyD88 and interferon regulatory factor 3 (IRF3)) that are required for signal transduction through TLR4 and so at first glance it would appear that platelets utilise the same mechanisms as in nucleated cells [2, 25]. However, as we will explain in more detail in the subsequent sections, this cannot be the case as both the MyD88-dependent and the MyD88-independent pathways culminate in the activation and nuclear translocation of transcription factors, and this step would not be applicable in anucleated cells like platelets [2, 12, 26]. Before examining the evidence for the TLR4 signalling pathways in platelets, it is worth reviewing the pathways in nucleated cells for use as a benchmark.

2. TLR4 Signalling in Nucleated Cells

2.1. TLR4 Ligands. Lipopolysaccharide (LPS) is a component of Gram-negative bacterial cell membranes and a powerful ligand for TLR4 [27, 28]. LPS is composed of a lipid A moiety (responsible for the molecule's interactions with TLR4), the core oligosaccharide, and the O-antigen polysaccharide [27, 29, 30]. The lipid A moiety is localised in the outer cell membrane and is formed from a 1,4-bis-phosphorylated diglucosamine molecule linked to variable acyl chains (e.g., six chains in *Escherichia coli* LPS) [27, 29]. The phosphate groups and acyl chains of LPS are important for interactions with TLR4, and alterations in these can shift the molecule from being an agonist to an antagonist [27, 31]. LPS may not be the only ligand for TLR4 as damage-associated

molecular patterns (DAMPs), such as high-mobility group box 1 (HMGB1) and heat shock proteins (HSPs), have also been suggested to be capable of inducing activation through this receptor [12, 32].

Although the immunogenic region of LPS is inside the bacterial cell membrane, it is capable of eliciting an immune response due to the presence of lipopolysaccharide-binding protein (LBP) [27, 29, 33]. LBP is a soluble protein that is synthesised by hepatocytes and found in the blood [28, 33]. It is capable of binding to areas rich in LPS (e.g., LPS aggregates and Gram-negative bacterial membranes) and promotes the exposure of the molecule's hydrophobic regions [34]. Subsequent to this, LPS monomers, via a process facilitated by albumin, can associate with CD14 (cluster of differentiation 14), a high affinity, horse shoe-shaped, glycosylphosphatidylinositol- (GPI-) anchored membrane protein [28, 31, 33–35]. CD14 forms a dimer with the dimerisation interface at the C-terminal end and LPS-binding pockets at the N-terminal end [33]. The transfer of LPS to TLR4 and the breakdown of LPS aggregates (micelles) into monomers are mediated by CD14 [28, 31, 33, 36]. Albumin can bind LPS, and other hydrophobic molecules, via hydrophobic interactions between domain III (on albumin) and the fatty acid chains of LPS [34]. Furthermore, albumin is capable of transferring LPS to TLR4 on its own although this requires approximately 10-fold higher concentrations of LPS compared to CD14 [34].

2.2. TLR4 Receptor. Similarly to CD14 (the molecule responsible for transferring LPS to TLR4), the ectodomains of TLR4 are horse shoe-shaped due to the presence of several leucine-rich repeats (LRRs) [33, 37]. Like other type I membrane-spanning proteins, the membrane-spanning domain of TLR4 is comprised of a single helix that serves to link the intracellular and extracellular domains [31]. The intracellular domain of TLRs contains a Toll/IL-1 receptor (TIR) domain common to all of the adaptor protein molecules involved at this stage of signalling [1, 31].

For signalling via TLR4 to occur, TLR4 requires heteromeric association with myeloid differentiation factor 2 (MD-2) [38, 39] (Figure 1). MD-2 is required because TLR4 does not bind LPS directly [27]. This is exemplified by the ability of human MD-2 to bind LPS in the absence of TLR4 [31]. MD-2 is constitutively associated with TLR4 through an interaction in the central region of TLR4 and may be responsible for the recognition of different LPS chemotypes [33, 39].

TLR4 has been detected on the plasma membrane and in intracellular compartments (such as the early endosome) of both nucleated cells and platelets [24, 40, 41]. In addition, TLR4 is capable of internalisation, as has been shown following prolonged exposure to LPS [24, 40–42]. The mechanisms behind the internalisation of TLR4 differ between cell types and may be required for MyD88-independent signalling [40, 43]. The intracellular forms of TLRs are not inactive as may be expected for an internalised extracellular receptor but are capable of recognising ligands (such as LPS) in endosomes, lysosomes, and endolysosomes [12, 43, 44]. Notably, plasma membrane localisation of TLR4 requires HSP

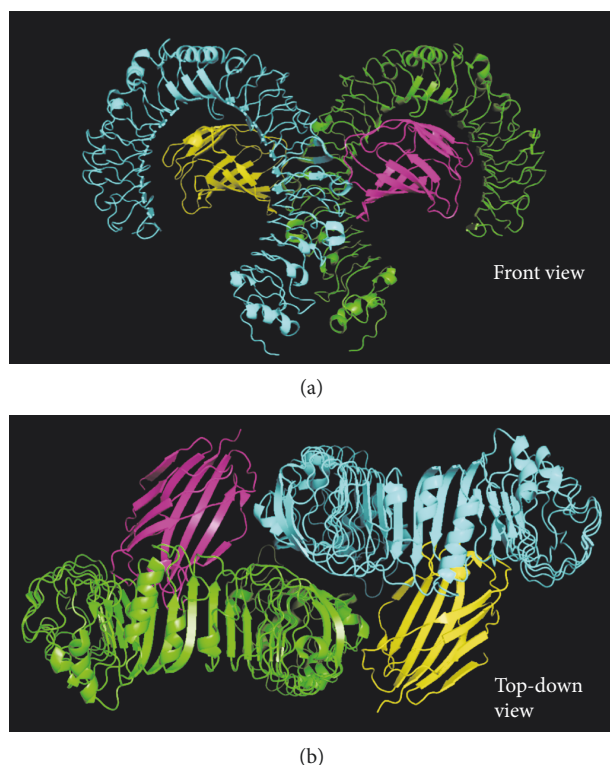


FIGURE 1: Structure of TLR4/MD-2 ectodomains, in a heterotetrameric form, as seen from (a) or (b). The TLR4 molecule (green) is constitutively bound to MD-2 (magenta), and the TLR4* (cyan) molecule is constitutively bound to MD-2* (yellow). Dimerisation interfaces form between TLR4 and MD-2* and vice versa. Images were created by adapting the structure of TLR4 (PDB code: 3FXI) using PyMOL [37].

90 kDa β member 1 (gp96) and protein associated with TLR4 (PRAT4A) acting as chaperones [44, 45]. Moreover, MD-2 has been reported to play a role in TLR4 localisation at the plasma membrane as its absence traps TLR4 in the Golgi apparatus [38].

2.3. TLR4 Activation. In order to activate the TLR4 signalling pathway, two receptor complexes need to dimerise to bring together the intracellular TIR domains (Figure 1) [31]. LPS and MD-2 (constitutively bound) binding to TLR4 is required for the TLR4 complex dimerisation to take place [27]. This dimerisation occurs due to the formation of a dimerisation domain that incorporates a hydrophobic patch on TLR4 and one of the acyl chains of LPS [33]. The remaining acyl chains are hidden in the hydrophobic cavity of MD-2 [27]. Ectodomain dimerisation leads to an interaction between the two intracellular domains of the TLR4 monomers [31]. This builds a platform onto which the intracellular signalling complexes can be formed [33]. At this stage, the two pathways diverge but there is still disagreement about what happens during this step [31].

2.4. The MyD88-Dependent Pathway. For the MyD88-dependent pathway, the TIR domain-containing adaptor protein (TIRAP), also known as MyD88 adaptor-like (Mal) protein, interacts with the TIR domain of the receptor

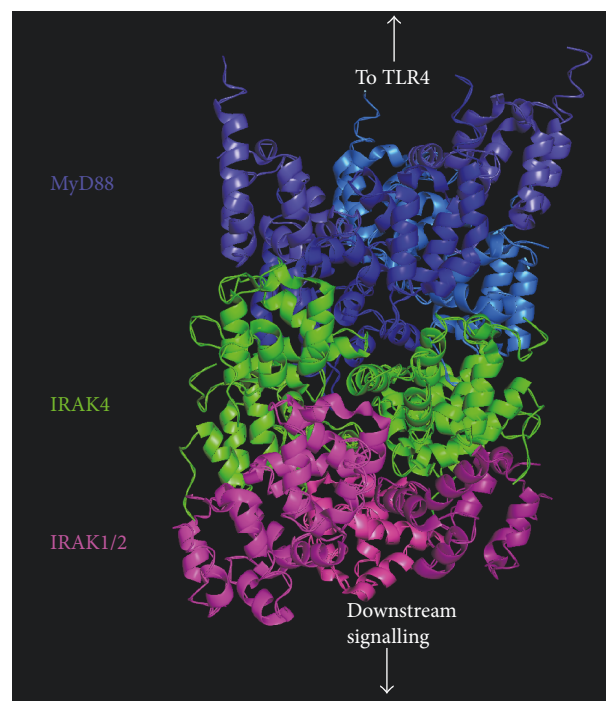


FIGURE 2: Structure of the Myddosome showing the protein death domains (DD). The Myddosome is formed of six MyD88 molecules, four IRAK4 molecules, and four IRAK1/2 molecules arranged in a single-stranded helix. MyD88 occupies the two layers closest to the plasma membrane whereas IRAK4 and IRAK1/2 form the two subsequent layers. The image was created by adapting the structure of the Myddosome (PDB code: 3MOP) using PyMOL [47].

enabling it to recruit MyD88 to the plasma membrane [31]. TIRAP presence at the plasma membrane is mediated by its phosphatidylinositol-4,5-bisphosphate- ($\text{PI}(4,5)\text{P}_2$ -) binding domain [43, 46]. It has been suggested that TIRAP may bind to TLR4's TIR domain using complementary charge distributions because of the observation that charges differ between TLR3 (cannot bind TIRAP) and TLR4 and TLR2 (can or only bind TIRAP, resp.). However, the exact details and structures involved during this binding have not been determined, partially due to the lack of a crystal structure for the TIR domain of TLR4 [31]. Once TIRAP has bound to the receptor, it recruits MyD88 via an interaction between their respective TIR domains [43, 46, 47].

MyD88 contains a death domain (DD) at its N-terminal end, which is crucial for the subsequent signalling cascade as it enables the construction of a large multimeric complex called the Myddosome (Figure 2) [47]. The Myddosome is formed of six MyD88, four interleukin- (IL-) 1 receptor-associated kinase 4 (IRAK4), and four IRAK1/2 molecules, all of which contain DDs, arranged in a single-stranded left-handed helix [24, 47]. As shown in Figure 2, this helix has multiple levels with the first two levels comprised solely of MyD88, IRAK4 is found in the third level, and IRAK1/2 is found in the fourth level [47]. Following assembly, IRAK4 undergoes an activating autophosphorylation process thereby enabling it to phosphorylate, and activate, IRAK1/2 [47]. Phosphorylation of IRAK1/2 stimulates disassociation

from the Myddosome and triggers polyubiquitination of tumour necrosis factor (TNF) receptor-associated factor (TRAF) 6 [47, 48]. TRAF6 interacts with TRAF-activated kinase 1 (TAK) and IRAK1/2, and this complex in turn interacts with NF- κ B essential modulator (NEMO) to stimulate the activating phosphorylation of I κ B kinase- (IKK-) β and the degradation of I κ B [24, 49–51]. Degradation of I κ B and the release of inhibition on NF- κ B permit it to translocate into the nucleus and enhance expression of proinflammatory cytokines including TNF α and IL-1 β [44, 50, 51]. The MyD88-dependent signalling downstream of LPS stimulation is dependent on TLR4 remaining at the plasma membrane as inhibition of internalisation increases NF- κ B activity [52].

Activation of mitogen-activated protein kinases (MAPKs) downstream of MyD88 and TAK1 is also involved in TLR4-mediated responses in nucleated cells [44, 48]. MAPKs include a range of proteins including extracellular signal-regulated kinase (ERK) 1 and 2, c-Jun N-terminal kinase (JNK) 1 and 2, and p38 [48]. These kinases are capable of activating the transcription factor, activator protein 1 (AP-1) [48]. This part of the MyD88-dependent pathway is dependent on the downregulation of TRAF3, via ubiquitination by cellular inhibitor of apoptosis (cIAP), near the plasma membrane where it has a negative regulatory role [48]. A summary of all the signalling pathways in nucleated cells is shown in Figure 3.

2.5. The MyD88-Independent Pathway. TRIF-related adaptor molecule (TRAM) is responsible for recruiting TIR domain-containing adaptor-inducing interferon- β (TRIF) in the MyD88-independent pathway [31]. Signalling through this pathway occurs following specific internalisation of the TLR4-MD-2 heterotetramer, its bound ligand, and CD14 [53–55]. The protein responsible for the internalisation (clathrin or caveolin) of TLR4 varies between cell types and with time although dynamin and CD14 are always necessary [40, 43, 52, 55]. Whereas CD14 is only required at low concentrations of LPS for MyD88-dependent pathway signalling (with other proteins such as albumin capable of transferring LPS to MD-2), CD14 is always necessary for MyD88-independent signalling [34, 55, 56]. As internalisation of TLR4 occurs, the decrease in PI(4,5)P₂ in the local area leads to a weakening of the interaction between TLR4 and TIRAP and thus propagates the breakdown of the Myddosome [24, 43]. Interestingly, endocytosis of TLR4 does not appear to be dependent on TLR4-mediated signalling, with cells lacking TIRAP, MyD88, TRAM, or TRIF retaining the capacity to internalise the receptor [55]. This has been suggested to be a result of phospholipase C γ 2 (PLC γ 2) and spleen-associated tyrosine kinase (Syk) activation in a CD14-dependent and TLR4-independent manner [55].

Upon internalisation, TLR4 enters the endosome, a region of the cell where TRAM and TRAF3 are present and from where MyD88-independent signalling can begin [24, 43, 48, 55]. When recruited to the TLR4-TRAM-TRIF complex by TRIF, TRAF3 is polyubiquitinated thus stimulating the activation of TRAF family member-associated NF- κ B

activator- (TANK-) binding kinase- (TBK-) 1 and IKK ϵ [48]. TBK1 and IKK ϵ are then free to phosphorylate IRF3, which is activated upon phosphorylation and dimerisation and stimulates the production of type I interferons [48, 56].

3. TLR4 Signalling in Platelets

3.1. Platelet Activation upon Vascular Damage. The response of platelets to “classical” agonists and the subsequent activation in haemostasis have been well defined [4–6]. During vascular injury, there is exposure of the subendothelial matrix and proaggregatory proteins, such as von Willebrand factor (vWF) and collagen, to the flow of blood. vWF is immobilised on collagen, and its association with GPIb-V-IX, a large glycoprotein (GP) complex, represents the initial interaction between platelets and the damaged vessel. This interaction slows down the platelets enabling them to interact with the exposed collagen via GPVI and platelet activation to ensue [57–59]. Binding of collagen to GPVI promotes an intracellular signalling cascade involving tyrosine kinase-mediated (e.g., Syk) activation of PLC γ 2. The degradation of PI(4,5)P₂ by PLC γ 2 into diacylglycerol (DAG) and inositol 1,4,5-trisphosphate (Ins(1,4,5)P₃, also known as IP₃) induces indirect activation of protein kinase C (PKC) [59].

Platelet activation induces shape change and modulation of integrin $\alpha_{IIb}\beta_3$ affinity to allow the formation of a platelet plug with fibrinogen used as a bridging molecule to surrounding platelets [5, 6]. Integrin activation is critical for a successful aggregation response. In resting platelets, integrin $\alpha_{IIb}\beta_3$ is in a low affinity state but a conformational change during platelet activation enables high-affinity binding of ligands. PKC activation has a key role in modulating integrin $\alpha_{IIb}\beta_3$ affinity [59, 60].

Furthermore, activation of platelets leads to degranulation and the secretion of adenosine diphosphate (ADP) and the synthesis and release of thromboxane A₂ (TxA₂), resulting in the activation of more platelets and recruitment of them to the thrombus [57–59]. Moreover, prothrombin is cleaved into thrombin following interactions involving tissue factor, factor VIIa, and factor Xa on the activated platelet surface. Thrombin is able to activate platelets through a cleavage of a region in the extracellular domains of protease-activated receptors (PARs) 1 and 4. Together, these agonists activate more circulating platelets and thus stimulate the formation of a platelet plug to seal the damaged region [5–7].

3.2. TLR4 Expression in Platelets. The presence of TLR4 on platelets is not disputed, and it was first identified on mouse and human platelets using flow cytometry by Andonegui et al. [36]. In addition, the same research group demonstrated that TLR4 displays functional effects in platelets. Furthermore, the discovery was backed up independently by Cognasse et al. in the same year, also through flow cytometry-based experiments [41]. Other research groups have also confirmed the presence of TLR4 on platelets through immunoblot analysis [42, 61, 62]. The amount of TLR4 expressed on the surface of platelets is variable, and an intracellular pool has also been identified [30, 41, 42].

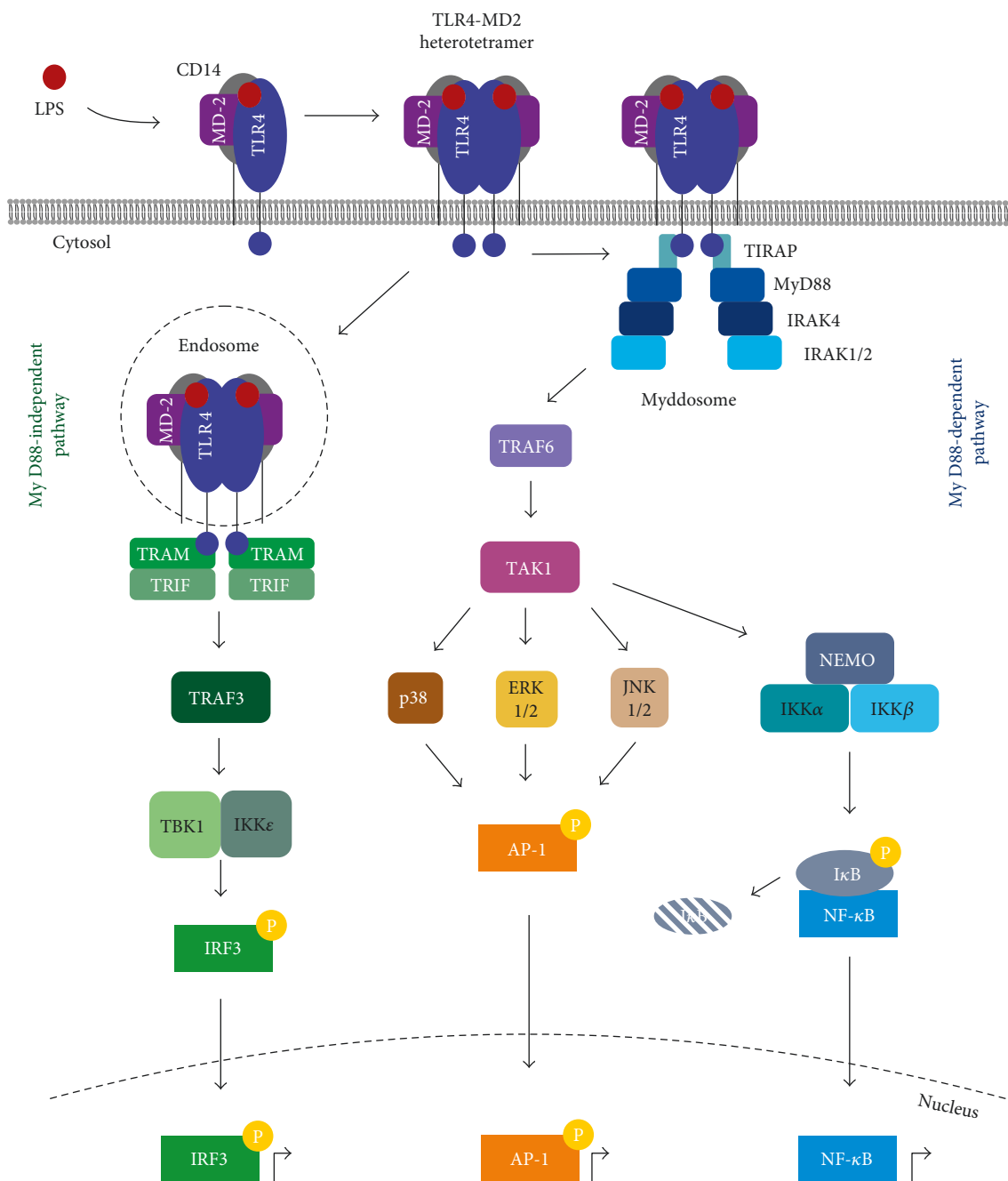


FIGURE 3: Summary of intracellular TLR4 signalling pathways in nucleated cells. LPS is transferred to CD14 (or albumin), via a process involving LBP and albumin, which transfers LPS to TLR4:MD-2 to complete the heterotetramerisation. There are two major signalling pathways, namely, the MyD88-dependent and -independent pathways, for TLR4 signalling. In the MyD88-dependent pathway, TIRAP (or Mal) enables MyD88 binding to TLR4 and formation of the Myddosome, which contains MyD88, IRAK4, and IRAK1/2. The kinases found at the base of the Myddosome activate TRAF6 and TAK1 followed by the activation of NEMO and its associated kinases. IKK β stimulates the degradation of inhibitory I κ B, which leads to nuclear translocation of NF- κ B and transcription of proinflammatory genes. In addition, TAK1 activates JNK1/2, ERK1/2, and p38, which can then stimulate the transcription factor AP-1. In the MyD88-independent pathway, following CD14-dependent internalisation into the endosomes, TRAM and TRIF are recruited to TLR4 before activating TRAF3. Activation of TRAF3 activates TBK1 and IKK ϵ , which phosphorylate and activate the transcription factor IRF3 that stimulates the transcription of anti-inflammatory cytokines.

A big difference in TLR4 signalling between platelets and nucleated cells is that although platelets contain the intracellular signalling proteins required for TLR signalling (Figure 4), they do not have all of the necessary extracellular

components (e.g., CD14) [2, 63, 64]. Membrane-bound CD14 is absent in platelets; however, this problem is overcome by high levels of soluble CD14 in the plasma [14, 30, 63, 65]. This may prevent “priming” of platelets

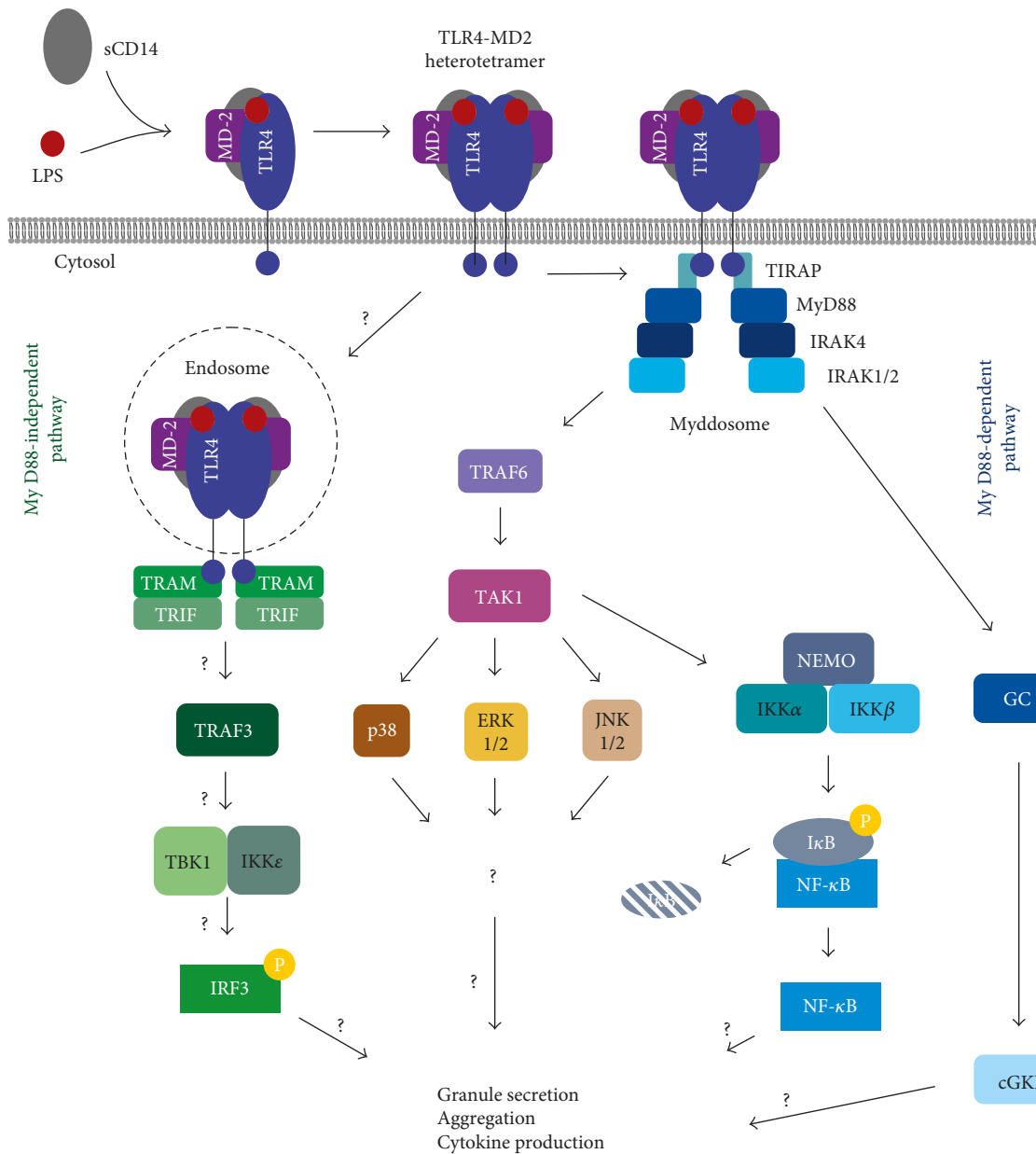


FIGURE 4: Summary of intracellular TLR4 signalling in platelets. Although the individual steps of the MyD88-dependent pathway have been observed, signalling in its entirety downstream of TLR4 has not been confirmed. Similar to nucleated cells, the proteins required for signalling through MyD88-dependent and -independent pathways are present in platelets but it is currently unclear how they mediate their effects. Signalling downstream of MyD88 can also be mediated by cGKI. The presences of TLR4, MyD88, IRAK1, TRAF6, TAK1, JNK, MAPK, $\text{I}\kappa\text{B}\alpha$, NF- κB , TRIF, TRAF3, TBK1, IKK ϵ , and IRF3 have all been confirmed by immunoblot analysis [2, 25]. Question marks (?) denote aspects of the pathway that have not been confirmed.

at low concentrations of LPS whilst responses at higher concentrations are not affected. Moreover, the requirement for higher concentrations of LPS could prevent NET formation in response to minor bacterial infections, thus protecting against unwarranted endothelial damage [22]. Furthermore, the absence of membrane-bound CD14 may also have an impact on MyD88-independent signalling which requires CD14 for the endocytosis of TLR4 and LPS [55]. The loss of CD14 caused by “washing” platelets appears to reduce the magnitude of the response to LPS although a response is still present [63, 66, 67].

3.3. TLR4 Activity in Platelets. A strong piece of evidence for TLR4 activity in platelets comes from experiments conducted by Clark et al. They demonstrated that high concentrations of LPS led to an interaction between platelets and neutrophils that stimulated the formation of NETs [22]. The researchers also linked this activity to sepsis, a disease that is commonly associated with platelet TLR4 [19]. This was achieved by determining the production of NETs in the blood samples of sepsis patients [22]. It is unclear whether it was the LPS in the blood or another substance that stimulated this response as certain proteins that may stimulate platelets in

a TLR4-dependent manner are also released into the blood during sepsis, for example, HMGB1 [22, 32]. Similarly, further evidence for the role of platelet TLR4 is provided by the observation that the levels of soluble cluster of differentiation 40 ligand (sCD40L) are raised following treatment of platelets with LPS [63, 66–69]. This is important because platelet α -granules are the largest source of sCD40L, and CD40L is involved in inflammatory responses elucidated by the endothelium and immune cells [1, 68–70]. Increases in sCD40L levels have been suggested to directly involve TLR4 [69].

Many attempts have been made to characterise the responses of platelets to LPS and other TLR4 agonists although there have been conflicting results. Evidence from different studies agree that exposure of platelets to LPS stimulates the release of tumour necrosis factor- (TNF-) α , a molecule that is produced downstream of the MyD88-dependent pathway in nucleated cells [42, 50, 71]. Although platelets lack genomic DNA, they still contain mRNA transcripts that can be processed and spliced following stimulation of platelets by LPS or thrombin [63, 72]. Transcripts that are affected include IL-1 β (a proinflammatory cytokine) and cyclooxygenase-2 (produces a platelet agonist, Tx $_A_2$) [63]. In addition, IL-1 β mRNA has been shown to be spliced in platelets in a TLR4-dependent manner with JNK and protein kinase B (PKB) (found downstream of the MyD88-dependent pathway) activity increasing during splicing [65]. Furthermore, splicing of IL-1 β was diminished in the presence of JNK or PKB inhibitors. However, the mechanism of action has not yet been elucidated [65]. Platelet shape change as a result of actin filament formation has also been suggested [63]. A comprehensive examination of cytokine release from platelets after treatment with LPS was conducted by Cognasse et al. [30]. They demonstrated that the expression of CD63 and release of sCD40L and platelet-activating factor 4 (PAF4) were increased; release of regulated upon activation, normally T-expressed, and presumably secreted (RANTES), angiogenin and platelet-derived growth factor- (PDGF-) AB were decreased (along with TLR4 expression); meanwhile, there was no change in the expression of soluble P-selectin, epidermal growth factor (EGF), transforming growth factor β (TGF β), or IL-8 [30]. Upregulation of P-selectin following LPS exposure is controversial with evidence both for [32, 61, 63] and against [26, 30, 66].

3.4. The Role of MyD88 in Platelets. It is unclear whether the traditional TLR4 pathways are responsible for all the effects mediated by TLR4 ligands on platelet function. MyD88 $^{-/-}$ mouse platelets have been used to demonstrate that this protein is necessary for the effects of LPS in enhancing aggregation and granule secretion in platelets. Some effects downstream of MyD88 have also been shown to be mediated by the cyclic guanosine monophosphate- (cGMP-) mediated signalling pathway [61].

In contrast, one research study demonstrates that there is virtually no role for MyD88 in modulating platelet function during Gram-negative (*Klebsiella pneumoniae*) bacterial infection [71]. Differences in responses were observed in systemic MyD88 $^{-/-}$ mice compared to the controls;

however, these differences could not be recovered by transfusing wild-type platelets into the MyD88 $^{-/-}$ mice. Furthermore, some changes in the secretion of TNF α and monocyte chemoattractant protein-1 (MCP-1) were observed that could be the result of deletion of platelet MyD88, thus suggesting that signalling to NF- κ B is still intact and functioning [71].

The results of this study are somewhat limited for several reasons. For example, the observed effects were not shown to be mediated by TLR4 as competitive antagonists, blocking antibodies for TLR4, and platelets derived from TLR4-deficient mice were not used in their experimental settings. Furthermore, this study did not use pure LPS (or other potential TLR4 ligands), but rather whole *Klebsiella pneumoniae* bacteria, which means that other bacterial components or exotoxins may have been able to influence cellular activities. More specifically, there was no investigation into the success of the platelet transfusions as the recipient mice were not depleted of their platelets and transfused platelets may have been sequestered in organs such as the lungs and spleen. The possibility of adaptive mechanisms in the MyD88-deficient mice was not investigated either; nor was an alternative signalling pathway suggested. Nevertheless, this study highlights the necessity for further research in order to confirm the significance of MyD88 in TLR4-mediated signalling in platelets.

3.5. Priming Platelets. There is evidence suggesting that LPS (and therefore TLR4-mediated signalling) has a “priming” role in platelets. LPS on its own is unable to induce aggregation in washed platelets, but it can potentiate agonist-induced aggregation responses. This was elucidated through the use of classical agonists such as collagen and thrombin [14, 26, 61]. Despite washed platelets being used, sCD14 was still detectable on platelets via flow cytometry [61]. Similar results have been obtained with platelet-rich plasma (PRP) using agonists such as adenosine diphosphate (ADP) [63]. The response was mediated by TLR4 as demonstrated through the use of TLR4 $^{-/-}$ mouse platelets [61]. An intriguing observation from this was that the different bacterial strains of LPS tested had different potencies [61]. This has also been observed with the LPS from *Rhodobacter sphaeroides* demonstrating its ability to act as a competitive TLR4 antagonist [63]. This priming behaviour in platelets is also supported by studies using NF- κ B and IKK β inhibitors [26, 73, 74].

The identification of TLR4:MyD88 coupling to the cGMP-dependent pathway is important as this pathway stimulates platelet aggregation from a subthreshold concentration of an agonist (0.02 U/mL of thrombin) [75]. Thus, there is a precedent for TLR4 to have a priming role in platelet aggregation. The response to cGMP-analogues was biphasic with an initial stimulatory response followed by an inhibitory response [75]. An interesting point to consider is that whilst cGMP-dependent kinase I (cGKI) inhibition affected aggregation and secretion to low agonist concentrations (excluding ADP), there was no effect on calcium mobilisation [76] and TLR4 is also incapable of modulating calcium mobilisation [77]. cGKI has been proposed to

be involved positively in the G_i -pathway, and so activation of cGKI could help amplify platelet responses in a similar manner to the $P2Y_{12}$ receptor [76].

3.6. NF- κ B in Platelets. Given that platelets lack a nucleus, it may appear that the presence of a signal transduction pathway that culminates in transcription factor activation would have no role in platelet function. This initially prompted some researchers to claim that TLR4 and its downstream signalling proteins in platelets were relics left over from their formation by megakaryocytes. Furthermore, certain experiments concluded that there were no responses mediated by TLR4 with specific bacterial species, lending support to this argument [78]. Other concerns arose from different LPS chemotypes derived from diverse bacterial species having diverse potencies when it comes to elucidating a response [61, 63, 66, 79]. NF- κ B, however, appears to have a role in platelet function, suggesting a nongenomic role, especially when the ability of NF- κ B inhibitors to reduce the proaggregatory effects of TLR4 is considered [26, 80].

Notably, IKK β is involved in the phosphorylation of soluble N-ethylmaleimide-sensitive factor attachment protein receptors (SNAREs), particularly synaptosomal-associated protein 23 (SNAP23), and thus, IKK β has an important role in granular secretion [73]. Phosphorylation of SNAREs is known to occur downstream of PKC when thrombin is used as an agonist [73]. This is relevant because IKK β is found downstream of both this classical agonist pathway and the MyD88-dependent pathway, suggesting a mechanism by which TLR4 activation could lead to the secretion of granules that has been shown in some studies [32, 51, 73]. Further investigations have revealed that IKK β activity occurs downstream of TAK1, found in the MyD88-dependent pathway [25]. This evidence points towards the ability of the MyD88-dependent pathway to promote SNARE complex formation and may explain some of the “priming” activity induced by TLR4 ligands. However, it is unclear whether IKK β directly phosphorylates SNAP23 or whether it occurs due to the activation of NF- κ B. It has been shown that NF- κ B activity is involved in modulating dense and α -granule secretion upon activation with low agonist doses by using inhibitors of I κ B α phosphorylation and ubiquitination (to indirectly inhibit NF- κ B activity) [74, 80]. Moreover, NF- κ B inhibition decreases binding of platelets to fibrinogen [80]. This suggests that NF- κ B is responsible for modulating secretion in this case although one of the inhibitors used is likely to directly inhibit IKK β . Inhibition of aggregation has also been seen to be mediated by NF- κ B inhibitors downstream of TLR4, suggesting that TLR4 and NF- κ B activity is connected in platelets [26].

3.7. Other Ligands. Although LPS has been the predominant ligand mentioned in this review, other ligands have also been suggested to bind to TLR4; however, this area is highly controversial [9, 67, 81, 82]. HMGB1 is one such possible ligand and has been shown to have effects in platelets in an autocrine and paracrine manner [32]. With a presence in the plasma and on NETs, the DNA-binding protein released from dead/dying cells or activated immune cells has

opportunities to interact with platelets in many conditions, for example, sepsis [22, 32, 83, 84]. HMGB1 has been reported to elicit similar responses in platelets compared to LPS, including the priming effects. These effects were also shown to involve TLR4, MyD88, and cGKI although there is not yet clear evidence indicating exactly how these proteins relate. ERK was another protein that had a change in its activity as a result of treatment with HMGB1 dependent on the presence of TLR4 [32]. HMGB1 has also been shown to have a role in tumour metastasis in a mechanism involving TLR4 [84]. Platelets are known to aid in cancer metastasis by forming protective thrombi around metastasising cells [85], and subsequent experiments by Yu et al. demonstrated that deletion of TLR4 in mice led to fewer metastatic tumours [84]. However, evidence from nucleated cells exists implying that HMGB1 acts solely as a TLR ligand-binding protein (e.g., LPS) and potentiates signalling through TLRs (alarmin effect) [86, 87]. Thus, the effects observed in the studies might be due to the binding of HMGB1-LPS colligation to TLR4 [87]. Moreover, recent studies have shown that, instead of direct binding to TLR4, HMGB1 directly exerts effects (such as activation of NF- κ B and MAPKs) on cells through binding to the receptor for advanced glycosylation end-products (RAGE) [88].

Another ligand that has been suggested to alter platelet activity in a TLR4-dependent manner is cellular fibronectin [9]. It has been shown that cellular fibronectin can modify platelet activity in a similar manner to LPS by potentiating aggregation induced by low doses of thrombin and increasing phosphorylation of NF- κ B and IKK α/β [9]. Furthermore, it was shown that the presence of TLR4 in mouse platelets significantly increased thrombus growth when treated with cellular fibronectin [9]. These findings suggest a possible effect of cellular fibronectin that may be mediated in a TLR4-dependent manner.

Histones have also been proposed to be ligands for TLR4 and are found in the blood during sepsis following release from neutrophils or necrotic cells [89–92]. They are important for the organisation of DNA in nucleated cells and, like HMGB1, appear in NETs [93]. Histones (especially H4) have interactions in the blood, and they have been reported to have a role in chemokine production in whole blood, platelet aggregation, and also thrombocytopenia in mice [89, 93]. However, these studies concluded that it was monocytes, and not platelets, that were responsible for the TLR4-dependent production of cytokines (even though histone H4 did associate with platelets) whereas the impact of TLR4 on histone-induced aggregation and thrombocytopenia was not examined [89, 93]. In contrast, it has been shown that histones can stimulate P-selectin exposure and thrombin generation on platelets in a TLR2- and TLR4-dependent manner [81].

Additionally, HSP60, a cell-stress marker, has been proposed to trigger TLR4-mediated signalling in a vascular smooth muscle cell line, with implications in atherosclerosis. However, the effects of this protein have not been tested on platelets despite an increased expression of HSP60 on endothelial cells in shear stress environments [94, 95]. Serum amyloid A (SAA) is a potential ligand for TLR4 that is

released, primarily from the liver, during an inflammatory response [96, 97]. Platelets have been shown to adhere to SAA in an integrin $\alpha_{IIb}\beta_3$ -dependent manner; however, it has not been determined whether or not this integrin is solely responsible for this behaviour as the research was conducted before the discovery of TLR4 on platelets [97]. Further research is required to determine whether these proposed ligands are having an effect due to direct binding to TLR4 or if it is the result of a more complex interaction, as has been suggested for HMGB1 [87].

4. TLR4 Signalling in Platelets: What Is Still to Discover?

Although many studies have linked TLR4 activity in platelets to immune responses, there have not been many studies to explore the signalling pathways downstream of TLR4 or MyD88 [26, 32, 61]. This is of particular interest as this receptor, with so many potential ligands and possible functions, operates through a pathway that classically results in gene transcription, but this end result is not achievable due to the lack of a nucleus in platelets. Moreover, the presence of all the signalling proteins in the pathways has been confirmed [2, 25] but whether the entirety of each pathway is functional, in platelets, has not been elucidated. Currently, individual steps of the MyD88-dependent pathway have been seen but not tied together downstream of TLR4. The MyD88-independent pathway in platelets also lacks considerable amounts of detail, including study of its activity. Furthermore, platelet TLR4 expression levels have been linked to more severe disease states in inflammatory responses [8, 9, 81, 84, 98–101]. This obviously makes TLR4 an interesting receptor to target for the prevention and/or treatment of cardiovascular diseases. However, it is challenging due to the important contribution of TLR4 to innate immunity. Determination of the effector proteins involved and their responses may lead to the discovery of novel pathways downstream of TLRs and present TLR4 as a novel therapeutic target for the treatment of cardiovascular diseases and other pathological settings such as inflammatory disease.

Abbreviations

ADP:	Adenosine diphosphate
AP-1:	Activator protein 1
CD63:	Cluster of differentiation 63
cGKI:	cGMP-dependent kinase I
cGMP:	Cyclic guanosine monophosphate
cIAP:	Cellular inhibitor of apoptosis
DAG:	Diacylglycerol
DAMPs:	Damage-associated molecular patterns
DD:	Death domain
DIC:	Disseminated intravascular coagulation
EGF:	Epidermal growth factor
ERK:	Extracellular signal-regulated kinase
GP:	Glycoprotein
gp96:	Heat shock protein 90 kDa β member 1
GPI:	Glycosylphosphatidylinositol
HSP60:	Heat shock protein 60

HMGB1:	High-mobility group box 1
HSP:	Heat shock protein
I κ B:	Inhibitor of NF- κ B
IKK:	I κ B kinase
IL:	Interleukin
Ins(1,4,5)P ₃ :	Inositol 1,4,5-trisphosphate
IRAK:	IL-1 receptor-associated kinase
IRF3:	Interferon regulatory factor 3
JNK:	c-Jun N-terminal kinase
LBP:	Lipopolysaccharide-binding protein
LPS:	Lipopolysaccharide
LRR:	Leucine-rich repeat
Mal:	MyD88 adaptor-like
MAPK:	Mitogen-activated protein kinases
MCP-1:	Monocyte chemoattractant protein-1
MD-2:	Myeloid differentiation factor-2
MyD88:	Myeloid differentiation factor 88
NEMO:	NF- κ B essential modulator
NET:	Neutrophil extracellular trap
NF- κ B:	Nuclear factor of κ -light-polypeptide-gene-enhancer in B cells
PAF4:	Platelet-activating factor 4
PAR:	Protease-activated receptor
PDGF-AB:	Platelet-derived growth factor-AB
PI(4,5)P ₂ :	Phosphatidylinositol-4,5-bisphosphate
PKB:	Protein kinase B
PKC:	Protein kinase C
PLCy2:	Phospholipase Cy2
PRAT4A:	Protein associated with TLR4
PRP:	Platelet-rich plasma
RAGE:	Receptor for advanced glycation end-products
RANTES:	Regulated upon activation, normally T-cell expressed, and presumably secreted
SAA:	Serum amyloid A
(s)CD14:	(Soluble) cluster of differentiation 14
sCD40L:	Soluble cluster of differentiation 40 ligand
SNAP23:	Synaptosomal-associated protein 23
SNARE:	Soluble N-ethylmaleimide-sensitive factor attachment protein receptor
Syk:	Spleen-associated tyrosine kinase
TAK1:	TRAF-activated kinase 1
TBK1:	TRAF family member-associated NF- κ B activator- (TANK-) binding kinase 1
TGF β :	Transforming growth factor β
TIR:	Toll/IL-1 receptor
TIRAP:	TIR domain-containing adaptor protein
TLR:	Toll-like receptor
TNF:	Tumour necrosis factor
TRAF:	TNF receptor-associated factor 3
TRAM:	TRIF-related adaptor molecule
TRIF:	TIR domain-containing adaptor-inducing interferon- β
TxA ₂ :	Thromboxane A ₂
vWF:	von Willebrand factor.

Conflicts of Interest

The authors declare that no conflicts of interest exist.

Authors' Contributions

The manuscript was written by Thomas M. Vallance, Darius Widera, and Sakthivel Vaiyapuri. The figures were created by Marie-Theres Zeuner and Thomas M. Vallance. Further contributions for the preparation of this manuscript were provided by Marie-Theres Zeuner and Harry F. Williams. Darius Widera and Sakthivel Vaiyapuri contributed equally to this work.

Acknowledgments

The authors would like to thank the British Heart Foundation for funding this research (Grant no. FS/16/65/32489).

References

- [1] P. Von Hundelshausen and C. Weber, "Platelets as immune cells: bridging inflammation and cardiovascular disease," *Circulation Research*, vol. 100, no. 1, pp. 27–40, 2007.
- [2] J. Berthet, P. Damien, H. Hamzeh-Cognasse, B. Pozzetto, O. Garraud, and F. Cognasse, "Toll-like receptor 4 signal transduction in platelets: novel pathways," *British Journal of Haematology*, vol. 151, no. 1, pp. 89–92, 2010.
- [3] A. A. Alhasan, O. G. Izuogu, H. H. Al-Balool et al., "Circular RNA enrichment in platelets is a signature of transcriptome degradation," *Blood*, vol. 127, no. 9, pp. e1–e11, 2016.
- [4] K. Jurk and B. E. Kehrel, "Platelets: physiology and biochemistry," *Seminars in Thrombosis and Haemostasis*, vol. 31, no. 4, pp. 381–392, 2005.
- [5] S. Offermanns, "Activation of platelet function through G protein-coupled receptors," *Circulation Research*, vol. 99, no. 12, pp. 1293–1304, 2006.
- [6] C. Deppermann and P. Kubes, "Platelets and infection," *Seminars in Immunology*, vol. 28, no. 6, pp. 536–545, 2016.
- [7] N. Mackman, "Triggers, targets and treatments for thrombosis," *Nature*, vol. 451, no. 7181, pp. 914–918, 2008.
- [8] K. M. Gurses, D. Kocyigit, M. U. Yalcin et al., "Enhanced platelet Toll-like receptor 2 and 4 expression in acute coronary syndrome and stable angina pectoris," *The American Journal of Cardiology*, vol. 116, no. 11, pp. 1666–1671, 2015.
- [9] P. Prakash, P. P. Kulkarni, S. R. Lentz, and A. K. Chauhan, "Cellular fibronectin containing extra domain A promotes arterial thrombosis in mice through platelet Toll-like receptor 4," *Blood*, vol. 125, no. 20, pp. 3164–3172, 2015.
- [10] P. Libby, "Inflammation in atherosclerosis," *Nature*, vol. 420, no. 6917, pp. 868–874, 2002.
- [11] L. M. Beaulieu and J. E. Freedman, "The role of inflammation in regulating platelet production and function: Toll-like receptors in platelets and megakaryocytes," *Thrombosis Research*, vol. 125, no. 3, pp. 205–209, 2010.
- [12] F. Cognasse, K. A. Nguyen, P. Damien et al., "The inflammatory role of platelets via their TLRs and Siglec receptors," *Frontiers in Immunology*, vol. 6, no. 83, pp. 1–15, 2015.
- [13] M. Arman, K. Krauel, D. O. Tilley et al., "Amplification of bacteria-induced platelet activation is triggered by FcγRIIA, integrin αIIbβ3, and platelet factor 4," *Blood*, vol. 123, no. 20, pp. 3166–3174, 2014.
- [14] A. L. Ståhl, M. Svensson, M. Mörgelin et al., "Lipopolysaccharide from enterohemorrhagic *Escherichia coli* binds to platelets through TLR4 and CD62 and is detected on circulating platelets in patients with hemolytic uremic syndrome," *Blood*, vol. 108, no. 1, pp. 167–176, 2006.
- [15] T. Youssefian, A. Drouin, J. M. Massé, J. Guichard, and E. M. Cramer, "Host defense role of platelets: engulfment of HIV and *Staphylococcus aureus* occurs in a specific subcellular compartment and is enhanced by platelet activation," *Blood*, vol. 99, no. 11, pp. 4021–4029, 2002.
- [16] J. W. Semple, R. Aslam, M. Kim, E. R. Speck, and J. Freedman, "Platelet-bound lipopolysaccharide enhances Fc receptor-mediated phagocytosis of IgG-opsonized platelets," *Blood*, vol. 109, no. 11, pp. 4803–4805, 2007.
- [17] I. C. Macaulay, P. Carr, A. Gusnanto, W. H. Ouwehand, D. Fitzgerald, and N. A. Watkins, "Platelet genomics and proteomics in human health and disease," *Journal of Clinical Investigation*, vol. 115, no. 12, pp. 3370–3377, 2005.
- [18] R. J. Stark, N. Aghakasiri, and R. E. Rumbaut, "Platelet-derived Toll-like receptor 4 (TLR-4) is sufficient to promote microvascular thrombosis in endotoxemia," *PLoS One*, vol. 7, no. 7, article e41254, 2012.
- [19] R. P. Davis, S. Miller-Dorey, and C. N. Jenne, "Platelets and coagulation in infection," *Clinical & Translational Immunology*, vol. 5, no. 7, article e89, 2016.
- [20] M. Levi and T. van der Poll, "Coagulation and sepsis," *Thrombosis Research*, vol. 149, pp. 38–44, 2017.
- [21] J. L. Chin, S. H. Hisamuddin, A. O'Sullivan, G. Chan, and P. A. McCormick, "Thrombocytopenia, platelet transfusion, and outcome following liver transplantation," *Clinical and Applied Thrombosis/Hemostasis*, vol. 22, no. 4, pp. 351–360, 2016.
- [22] S. R. Clark, A. C. Ma, S. A. Tavener et al., "Platelet TLR4 activates neutrophil extracellular traps to ensnare bacteria in septic blood," *Nature Medicine*, vol. 13, no. 4, pp. 463–469, 2007.
- [23] M. Zeuner, K. Bieback, and D. Widera, "Controversial role of Toll-like receptor 4 in adult stem cells," *Stem Cell Reviews and Reports*, vol. 11, no. 4, pp. 621–634, 2015.
- [24] A. F. McGettrick and L. A. O'Neill, "Localisation and trafficking of Toll-like receptors: an important mode of regulation," *Current Opinion in Immunology*, vol. 22, no. 1, pp. 20–27, 2010.
- [25] Z. A. Karim, H. P. Vemana, and F. T. Khasawneh, "MALT1-ubiquitination triggers non-genomic NF-κB/IKK signaling upon platelet activation," *PLoS One*, vol. 10, no. 3, article e0119363, 2015.
- [26] L. Rivadeneyra, A. Carestia, J. Etulain et al., "Regulation of platelet responses triggered by Toll-like receptor 2 and 4 ligands is another non-genomic role of nuclear factor-κB," *Thrombosis Research*, vol. 133, no. 2, pp. 235–243, 2014.
- [27] U. Ohto, K. Fukase, K. Miyake, and T. Shimizu, "Structural basis of species-specific endotoxin sensing by innate immune receptor TLR4/MD-2," *Proceedings of the National Academy of Sciences*, vol. 109, no. 19, pp. 7421–7426, 2012.
- [28] J. A. Gegner, R. J. Ulevitch, and P. S. Tobias, "Lipopolysaccharide (LPS) signal transduction and clearance. Dual roles for LPS binding protein and membrane CD14," *Journal of Biological Chemistry*, vol. 270, no. 10, pp. 5320–5325, 1995.
- [29] A. Steimle, I. B. Autenrieth, and J. S. Frick, "Structure and function: lipid A modifications in commensals and pathogens," *International Journal of Medical Microbiology*, vol. 306, no. 5, pp. 290–301, 2016.

- [30] F. Cognasse, H. Hamzeh-Cognasse, S. Lafarge et al., "Toll-like receptor 4 ligand can differentially modulate the release of cytokines by human platelets," *British Journal of Haematology*, vol. 141, no. 1, pp. 84–91, 2008.
- [31] J. M. Billod, A. Lacetera, J. Guzmán-Caldentey, and S. Martín-Santamaría, "Computational approaches to Toll-like receptor 4 modulation," *Molecules*, vol. 21, no. 8, p. 994, 2016.
- [32] S. Vogel, R. Bodenstein, Q. Chen et al., "Platelet-derived HMGB1 is a critical mediator of thrombosis," *Journal of Clinical Investigation*, vol. 125, no. 12, pp. 4638–4654, 2015.
- [33] Q. Yin, T. M. Fu, J. Li, and H. Wu, "Structural biology of innate immunity," *Annual Review of Immunology*, vol. 33, pp. 393–416, 2015.
- [34] G. A. Esparza, A. Teghanemt, D. Zhang, T. L. Gioannini, and J. P. Weiss, "Endotoxin-albumin complexes transfer endotoxin monomers to MD-2 resulting in activation of TLR4," *Innate Immunity*, vol. 18, no. 3, pp. 478–491, 2012.
- [35] T. L. Gioannini, D. Zhang, A. Teghanemt, and J. P. Weiss, "An essential role for albumin in the interaction of endotoxin with lipopolysaccharide-binding protein and sCD14 and resultant cell activation," *Journal of Biological Chemistry*, vol. 277, no. 49, pp. 47818–47825, 2002.
- [36] G. Andonegui, S. Kerfoot, K. McNaghy, K. Ebbert, K. Patel, and P. Kubes, "Platelets express functional Toll-like receptor-4 (TLR4)," *Blood*, vol. 106, no. 7, pp. 2417–2423, 2005.
- [37] B. S. Park, D. H. Song, H. M. Kim, B. S. Choi, H. Lee, and J. O. Lee, "The structural basis of lipopolysaccharide recognition by the TLR4-MD-2 complex," *Nature*, vol. 458, no. 7242, pp. 1191–1195, 2009.
- [38] Y. Nagai, S. Akashi, M. Nagafuku et al., "Essential role of MD-2 in LPS responsiveness and TLR4 distribution," *Nature Immunology*, vol. 3, no. 7, pp. 667–672, 2002.
- [39] R. Shimazu, S. Akashi, H. Ogata et al., "MD-2, a molecule that confers lipopolysaccharide responsiveness on Toll-like receptor 4," *The Journal of Experimental Medicine*, vol. 189, no. 11, pp. 1777–1782, 1999.
- [40] M. Pascual-Lucas, S. Fernandez-Lizarbe, J. Montesinos, and C. Guerri, "LPS or ethanol triggers clathrin- and rafts/caveolae-dependent endocytosis of TLR4 in cortical astrocytes," *Journal of Neurochemistry*, vol. 129, no. 3, pp. 448–462, 2014.
- [41] F. Cognasse, H. Hamzeh, P. Chavarin, S. Acquart, C. Genin, and O. Garraud, "Evidence of Toll-like receptor molecules on human platelets," *Immunology and Cell Biology*, vol. 83, no. 2, pp. 196–198, 2005.
- [42] R. Aslam, E. R. Speck, M. Kim et al., "Platelet Toll-like receptor expression modulates lipopolysaccharide-induced thrombocytopenia and tumor necrosis factor- α production in vivo," *Blood*, vol. 107, no. 2, pp. 637–642, 2006.
- [43] J. C. Kagan, T. Su, T. Horng, A. Chow, S. Akira, and R. Medzhitov, "TRAM couples endocytosis of Toll-like receptor 4 to the induction of interferon- β ," *Nature Immunology*, vol. 9, no. 4, pp. 361–368, 2008.
- [44] E. M. Moresco, D. LaVine, and B. Beutler, "Toll-like receptors," *Current Biology*, vol. 21, no. 13, pp. R488–R493, 2011.
- [45] F. Randow and B. Seed, "Endoplasmic reticulum chaperone gp96 is required for innate immunity but not cell viability," *Nature Cell Biology*, vol. 3, no. 10, pp. 891–896, 2001.
- [46] J. C. Kagan and R. Medzhitov, "Phosphoinositide-mediated adaptor recruitment controls Toll-like receptor signaling," *Cell*, vol. 125, pp. 943–955, 2006.
- [47] S. C. Lin, Y. C. Lo, and H. Wu, "Helical assembly in the MyD88:IRAK4:IRAK2 complex in TLR/IL-1R signalling," *Nature*, vol. 465, no. 7300, pp. 885–890, 2010.
- [48] H. Hacker, P. H. Tseng, and M. Karin, "Expanding TRAF function: TRAF3 as a tri-faced immune regulator," *Nature Reviews Immunology*, vol. 11, no. 7, pp. 457–468, 2011.
- [49] A. Płóciennikowska, A. Hromada-Judycka, K. Borzęcka, and K. Kwiatkowska, "Co-operation of TLR4 and raft proteins in LPS-induced pro-inflammatory signaling," *Cellular and Molecular Life Sciences*, vol. 72, no. 3, pp. 557–581, 2015.
- [50] M. T. Zeuner, C. L. Kruger, K. Volk et al., "Biased signalling is an essential feature of TLR4 in glioma cells," *Biochimica et Biophysica Acta*, vol. 1863, no. 12, pp. 3084–3095, 2016.
- [51] T. Kawai and S. Akira, "Signaling to NF- κ B by Toll-like receptors," *Trends in Molecular Medicine*, vol. 13, no. 11, pp. 460–469, 2007.
- [52] H. Husebye, Ø. Halaas, H. Stenmark et al., "Endocytic pathways regulate Toll-like receptor 4 signaling and link innate and adaptive immunity," *The EMBO Journal*, vol. 25, no. 4, pp. 683–692, 2006.
- [53] N. Tanimura, S. Saitoh, F. Matsumoto, S. Akashi-Takamura, and K. Miyake, "Roles for LPS-dependent interaction and relocation of TLR4 and TRAM in TRIF-signaling," *Biochemical and Biophysical Research Communications*, vol. 368, no. 1, pp. 94–99, 2008.
- [54] E. Latz, A. Visintin, E. Lien et al., "Lipopolysaccharide rapidly traffics to and from the Golgi apparatus with the Toll-like receptor 4-MD-2-CD14 complex in a process that is distinct from the initiation of signal transduction," *Journal of Biological Chemistry*, vol. 277, no. 49, pp. 47834–47843, 2002.
- [55] I. Zanoni, R. Ostuni, L. R. Marek et al., "CD14 controls the LPS-induced endocytosis of Toll-like receptor 4," *Cell*, vol. 147, no. 4, pp. 868–880, 2011.
- [56] Z. Jiang, P. Georgel, X. Du et al., "CD14 is required for MyD88-independent LPS signaling," *Nature Immunology*, vol. 6, no. 6, pp. 565–570, 2005.
- [57] Z. Sun, "Platelet TLR4: A critical link in pulmonary arterial hypertension," *Circulation Research*, vol. 114, no. 10, pp. 1551–1553, 2014.
- [58] J. D. McFadyen and Z. S. Kaplan, "Platelets are not just for clots," *Transfusion Medicine Reviews*, vol. 29, no. 2, pp. 110–119, 2015.
- [59] J. M. Gibbins, "Platelet adhesion signalling and the regulation of thrombus formation," *Journal of Cell Science*, vol. 117, no. 16, pp. 3415–3425, 2004.
- [60] B. Nieswandt, D. Varga-Szabo, and M. Elvers, "Integrins in platelet activation," *Journal of Thrombosis and Haemostasis*, vol. 7, Supplement 1, pp. 206–209, 2009.
- [61] G. Zhang, J. Han, E. J. Welch et al., "LPS stimulates platelet secretion and potentiates platelet aggregation via TLR4/MyD88 and the cGMP-dependent protein kinase pathway," *The Journal of Immunology*, vol. 182, no. 12, pp. 7997–8004, 2009.
- [62] K. Hashimoto, M. Jayachandran, W. G. Owen, and V. M. Miller, "Aggregation and microparticle production through Toll-like receptor 4 activation in platelets from recently

- menopausal women," *Journal of Cardiovascular Pharmacology*, vol. 54, no. 1, pp. 57–62, 2009.
- [63] P. N. Shashkin, G. T. Brown, A. Ghosh, G. K. Marathe, and T. M. McIntyre, "Lipopolysaccharide is a direct agonist for platelet RNA splicing," *The Journal of Immunology*, vol. 181, no. 5, pp. 3495–3502, 2008.
- [64] F. Liu, S. A. Morris, J. L. Epps, and R. C. Carroll, "Demonstration of an activation regulated NF-kappaB/I-kappaBalpha complex in human platelets," *Thrombosis Research*, vol. 106, no. 4–5, pp. 199–203, 2002.
- [65] G. T. Brown and T. M. McIntyre, "Lipopolysaccharide signaling without a nucleus: kinase cascades stimulate platelet shedding of proinflammatory IL-1 β -rich microparticles," *The Journal of Immunology*, vol. 186, no. 9, pp. 5489–5496, 2011.
- [66] J. Berthet, P. Damien, H. Hamzeh-Cognasse et al., "Human platelets can discriminate between various bacterial LPS isoforms via TLR4 signaling and differential cytokine secretion," *Clinical Immunology*, vol. 145, no. 3, pp. 189–200, 2012.
- [67] P. Damien, F. Cognasse, M.-A. Eyraud et al., "LPS stimulation of purified human platelets is partly dependent on plasma soluble CD14 to secrete their main secreted product, soluble-CD40-ligand," *BMC Immunology*, vol. 16, p. 3, 2015.
- [68] F. Cognasse, S. Lafarge, P. Chavarin, S. Acquart, and O. Garraud, "Lipopolysaccharide induces sCD40L release through human platelets TLR4, but not TLR2 and TLR9," *Intensive Care Medicine*, vol. 33, no. 2, pp. 382–384, 2007.
- [69] A. Assinger, M. Laky, S. Badrnya, A. Esfandeyari, and I. Volf, "Periodontopathogens induce expression of CD40L on human platelets via TLR2 and TLR4," *Thrombosis Research*, vol. 130, no. 3, pp. e73–e78, 2012.
- [70] P. André, L. Nannizzi-Alaimo, S. K. Prasad, and D. R. Phillips, "Platelet-derived CD40L: the switch-hitting player of cardiovascular disease," *Circulation*, vol. 106, no. 8, pp. 896–899, 2002.
- [71] S. F. de Stoppelaar, T. A. Claushuis, M. P. Jansen et al., "The role of platelet MyD88 in host response during gram-negative sepsis," *Journal of Thrombosis and Haemostasis*, vol. 13, no. 9, pp. 1709–1720, 2015.
- [72] M. M. Denis, N. D. Tolley, M. Bunting et al., "Escaping the nuclear confines: signal-dependent pre-mRNA splicing in anucleate platelets," *Cell*, vol. 122, pp. 379–391, 2005.
- [73] Z. A. Karim, J. Zhang, M. Banerjee et al., "I κ B kinase phosphorylation of SNAP-23 controls platelet secretion," *Blood*, vol. 121, no. 22, pp. 4567–4574, 2013.
- [74] E. Malaver, M. A. Romaniuk, L. P. D'atri et al., "NF- κ B inhibitors impair platelet activation responses," *Journal of Thrombosis and Haemostasis*, vol. 7, no. 8, pp. 1333–1343, 2009.
- [75] Z. Li, X. Xi, M. Gu et al., "A stimulatory role for cGMP-dependent protein kinase in platelet activation," *Cell*, vol. 112, no. 1, pp. 77–86, 2003.
- [76] Z. Li, G. Zhang, J. A. Marjanovic, C. Ruan, and X. Du, "A platelet secretion pathway mediated by cGMP-dependent protein kinase," *Journal of Biological Chemistry*, vol. 279, no. 41, pp. 42469–42475, 2004.
- [77] J. R. Ward, L. Bingle, H. M. Judge et al., "Agonists of Toll-like receptor (TLR)2 and TLR4 are unable to modulate platelet activation by adenosine diphosphate and platelet activating factor," *Thrombosis and Haemostasis*, vol. 94, no. 4, pp. 831–838, 2005.
- [78] S. F. de Stoppelaar, T. A. M. Claushuis, M. C. Schaap et al., "Toll-like receptor signalling is not involved in platelet response to *Streptococcus pneumoniae* in vitro or in vivo," *PLoS One*, vol. 11, no. 6, article e0156977, 2016.
- [79] S. W. Kerrigan and D. Cox, "Platelet-bacterial interactions," *Cellular and Molecular Life Sciences*, vol. 67, no. 4, pp. 513–523, 2010.
- [80] S. L. Spinelli, A. E. Casey, S. J. Pollock et al., "Platelets and megakaryocytes contain functional nuclear factor- κ B," *Arteriosclerosis, Thrombosis, and Vascular Biology*, vol. 30, no. 3, pp. 591–598, 2010.
- [81] F. Semeraro, C. T. Ammollo, J. H. Morrissey et al., "Extracellular histones promote thrombin generation through platelet-dependent mechanisms: involvement of platelet TLR2 and TLR4," *Blood*, vol. 118, no. 7, pp. 1952–1961, 2011.
- [82] M. Zeuner, T. Vallance, S. Vaiyapuri, G. S. Cottrell, and D. Widera, "Development and characterisation of a novel NF- κ B reporter cell line for investigation of neuro-inflammation," *Mediators of Inflammation*, vol. 2017, Article ID 6209865, 2017.
- [83] I. Mitroulis, K. Kambas, A. Chrysanthopoulou et al., "Neutrophil extracellular trap formation is associated with IL-1 β and autophagy-related signaling in gout," *PLoS One*, vol. 6, no. 12, article e29318, 2011.
- [84] L. X. Yu, L. Yan, W. Yang et al., "Platelets promote tumour metastasis via interaction between TLR4 and tumour cell-released high-mobility group box1 protein," *Nature Communications*, vol. 5, p. 5256, 2014.
- [85] L. J. Gay and B. Felding-Habermann, "Contribution of platelets to tumour metastasis," *Nature Reviews Cancer*, vol. 11, no. 2, pp. 123–134, 2011.
- [86] H. Hreggvidsdottir, T. Ostberg, H. Wähämaa et al., "The alarmin HMGB1 acts in synergy with endogenous and exogenous danger signals to promote inflammation," *Journal of Leukocyte Biology*, vol. 86, no. 3, pp. 655–662, 2009.
- [87] J. H. Youn, Y. J. Oh, E. S. Kim, J. E. Choi, and J. Shin, "High mobility group box 1 protein binding to lipopolysaccharide facilitates transfer of lipopolysaccharide to CD14 and enhances lipopolysaccharide-mediated TNF- α production in human monocytes," *The Journal of Immunology*, vol. 180, no. 7, pp. 5067–5074, 2008.
- [88] G. P. Sims, D. C. Rowe, S. T. Rietdijk, R. Herbst, and A. J. Coyle, "HMGB1 and RAGE in inflammation and cancer," *Annual Review of Immunology*, vol. 28, pp. 367–388, 2010.
- [89] J. Westman, P. Papareddy, M. W. Dahlgren et al., "Extracellular histones induce chemokine production in whole blood ex vivo and leukocyte recruitment in vivo," *PLoS Pathogens*, vol. 11, no. 12, article e1005319, 2015.
- [90] J. Xu, X. Zhang, M. Monestier, N. L. Esmon, and C. T. Esmon, "Extracellular histones are mediators of death through TLR2 and TLR4 in mouse fatal liver injury," *The Journal of Immunology*, vol. 187, no. 5, pp. 2626–2631, 2011.
- [91] J. Xu, X. Zhang, R. Pelayo et al., "Extracellular histones are major mediators of death in sepsis," *Nature Medicine*, vol. 15, no. 11, pp. 1318–1321, 2009.
- [92] C. T. Esmon, "Extracellular histones zap platelets," *Blood*, vol. 118, no. 13, pp. 3456–3457, 2011.
- [93] T. A. Fuchs, A. A. Bhandari, and D. D. Wagner, "Histones induce rapid and profound thrombocytopenia in mice," *Blood*, vol. 118, no. 13, pp. 3708–3714, 2011.

- [94] Y. Zhao, C. Zhang, X. Wei et al., "Heat shock protein 60 stimulates the migration of vascular smooth muscle cells via Toll-like receptor 4 and ERK MAPK activation," *Scientific Reports*, vol. 5, no. 1, article 15352, 2015.
- [95] B. Hochleitner, E. Hochleitner, P. Obrist et al., "Fluid shear stress induces heat shock protein 60 expression in endothelial cells in vitro and in vivo," *Arteriosclerosis, Thrombosis, and Vascular Biology*, vol. 20, pp. 617–623, 2000.
- [96] R. Ebert, P. Benisch, M. Krug et al., "Acute phase serum amyloid A induces proinflammatory cytokines and mineralization via Toll-like receptor 4 in mesenchymal stem cells," *Stem Cell Research*, vol. 15, no. 1, pp. 231–239, 2015.
- [97] S. Urieli-Shoval, G. Shubinsky, R. P. Linke, M. Fridkin, I. Tabi, and Y. Matzner, "Adhesion of human platelets to serum amyloid A," *Blood*, vol. 99, no. 4, pp. 1224–1229, 2002.
- [98] E. M. Bauer, R. S. Chanthaphavong, C. P. Sodhi, D. J. Hackam, T. R. Billiar, and P. M. Bauer, "Genetic deletion of Toll-like receptor 4 on platelets attenuates experimental pulmonary hypertension," *Circulation Research*, vol. 114, no. 10, pp. 1596–1600, 2014.
- [99] N. Ding, G. Chen, R. Hoffman et al., "TLR4 regulates platelet function and contributes to coagulation abnormality and organ injury in hemorrhagic shock and resuscitation," *Circulation: Cardiovascular Genetics*, vol. 7, no. 5, pp. 615–624, 2014.
- [100] P. Patrignani, C. Di Febbo, S. Tacconelli et al., "Reduced thromboxane biosynthesis in carriers of Toll-like receptor 4 polymorphisms in vivo," *Blood*, vol. 107, no. 9, pp. 3572–3574, 2006.
- [101] J. C. Tsai, Y. W. Lin, C. Y. Huang, F. Y. Lin, and C. S. Tsai, "Calpain activity and Toll-like receptor 4 expression in platelet regulate haemostatic situation in patients undergoing cardiac surgery and coagulation in mice," *Mediators of Inflammation*, vol. 2014, Article ID 484510, 12 pages, 2014.

SCIENTIFIC REPORTS

OPEN

Impact of specific functional groups in flavonoids on the modulation of platelet activation

Divyashree Ravishankar¹, Maryam Salamah¹, Angela Akimbaev¹, Harry F. Williams¹, Dina A. I. Albadawi¹, Rajendran Vaiyapuri², Francesca Greco¹, Helen M. I. Osborn¹ & Sakthivel Vaiyapuri¹

Received: 2 March 2018

Accepted: 5 June 2018

Published online: 22 June 2018

Flavonoids exert innumerable beneficial effects on cardiovascular health including the reduction of platelet activation, and thereby, thrombosis. Hence, flavonoids are deemed to be a molecular template for the design of novel therapeutic agents for various diseases including thrombotic conditions. However, the structure-activity relationships of flavonoids with platelets is not fully understood. Therefore, this study aims to advance the current knowledge on structure-activity relationships of flavonoids through a systematic analysis of structurally-related flavones. Here, we investigated a panel of 16 synthetic flavones containing hydroxy or methoxy groups at C-7,8 positions on the A-ring, with a phenyl group or its bioisosteres as the B-ring, along with their thio analogues possessing a sulfur molecule at the 4th carbon position of the C-ring. The antiplatelet efficacies of these compounds were analysed using human isolated platelets upon activation with cross-linked collagen-related peptide by optical aggregometry. The results demonstrate that the hydroxyl groups in flavonoids are important for optimum platelet inhibitory activities. In addition, the 4-C=O and B ring phenyl groups are less critical for the antiplatelet activity of these flavonoids. This structure-activity relationship of flavonoids with the modulation of platelet function may guide the design, optimisation and development of flavonoid scaffolds as antiplatelet agents.

Platelets are small circulating blood cells that play pivotal roles in the regulation of haemostasis upon vascular injury through blood clotting^{1,2}. However, unnecessary activation of platelets within the vasculature leads to pathological conditions such as thrombosis, which results in blockage or reduction of blood flow to major organs including heart and brain instigating heart attack and stroke, respectively^{3,4}. The currently used therapeutic options that involve the use of antiplatelet drugs such as clopidogrel, aspirin, and prasugrel are often linked with adverse side effects such as bleeding and are ineffective in some patients^{5–10}. As cardiovascular diseases remain the leading cause of death worldwide¹¹, the development of improved therapeutic strategies to prevent and treat thrombotic diseases remains a pressing priority.

Flavonoids, a group of polyphenolic plant metabolites, have been widely demonstrated to possess beneficial effects in the prevention of cardiovascular diseases^{12–14}. Epidemiological and clinical studies have established a prominent link between the regular consumption of dietary flavonoids and decreased incidences of cardiovascular diseases or their risk markers^{15–20}. Flavonoids have also been recognised as modulators of platelet function and their inhibitory activities can be attributed to their ability to inhibit reactive oxygen species (ROS) production^{21,22}, modify cytoskeletal proteins such as actin and tubulin that mediate degranulation^{23,24}, and to inhibit various kinases^{25–29} and receptors^{30,31} that play numerous roles in the regulation of platelet activation and thrombosis. The pharmacological potential of flavonoids is strongly related to their molecular structure, hence, the identification of key structural elements that are prerequisites for antiplatelet activity has provoked considerable interest in the area of drug discovery^{32,33}. With a view to develop flavonoids as potential anti-thrombotic agents, some studies have been carried out to identify the key structural features governing the antiplatelet activity of flavonoids³⁴. However, the current knowledge of structure-activity relationships (SARs) has mainly resulted from analyses involving different subclasses of natural flavonoids^{32,34}. In order to translate flavonoids into potential molecular templates for drug design, a better understanding of the SAR of flavonoids, and a careful comparison of

¹School of Pharmacy, University of Reading, Reading, UK. ²School of Pharmacy, University of Reading Malaysia, Johor, Malaysia. Correspondence and requests for materials should be addressed to S.V. (email: s.vaiyapuri@reading.ac.uk)

substitution pattern within a flavonoid subclass is necessary. Hence, to gain greater insights into the SAR of flavonoids with human platelets, this study has focused on assessing the effect of methoxylation, 4-C=S substitution, and different B-ring substitutions using a series of 16 synthetic flavones on the antiplatelet activities.

Materials and Methods

Flavones. The synthetic flavones used in this study are grouped into four main classes namely; hydroxy flavones with free -OH and 4-C=O, hydroxy 4-thioflavones with free -OH and 4-C=S, methoxy flavones with -OMe and 4-C=O and methoxy 4-thioflavones with -OMe and 4-C=S³⁵. The hydroxy flavones include 7,8-dihydroxy-2-phenyl-4H-chromen-4-one (F-1), 7,8-dihydroxy-2-(thiophen-2-yl)-4H-chromen-4-one (F-2), 2-(furan-2-yl)-7,8-dihydroxy-4H-chromen-4-one (F-3) and 7,8-dihydroxy-2-(pyridine-3-yl)-4H-chromen-4-one (F-4). The hydroxy 4-thioflavones include 7,8-dihydroxy-2-phenyl-4H-chromen-4-thione (TF-1), 7,8-dihydroxy-2-(thiophen-2-yl)-4H-chromen-4-thione (TF-2), 2-(furan-2-yl)-7,8-dihydroxy-4H-chromen-4-thione (TF-3) and 7,8-dihydroxy-2-(pyridine-3-yl)-4H-chromen-4-thione (TF-4). The methoxy flavones include 7,8-dimethoxy-2-phenyl-4H-chromen-4-one (CYC-1), 7,8-dimethoxy-2-(thiophen-2-yl)-4H-chromen-4-one (CYC-2), 2-(furan-2-yl)-7,8-dimethoxy-4H-chromen-4-one (CYC-3) and 7,8-dimethoxy-2-(pyridine-3-yl)-4H-chromen-4-one (CYC-4). The methoxy 4-thioflavones include 7,8-dimethoxy-2-phenyl-4H-chromen-4-thione (TCYC-1), 7,8-dimethoxy-2-(thiophen-2-yl)-4H-chromen-4-thione (TCYC-2), 2-(furan-2-yl)-7,8-dimethoxy-4H-chromen-4-thione (TCYC-3) and 7,8-dimethoxy-2-(pyridine-3-yl)-4H-chromen-4-thione (TCYC-4). Stock solutions of these flavones were prepared in dimethyl sulfoxide (DMSO) (100%) at 10 mg/mL concentration and the final required test concentrations were obtained by appropriately diluting these stocks. The final concentration of DMSO in platelets was maintained at 0.1% (v/v), which did not affect their function.

Human blood collection. All the experiments in this study were conducted in line with the appropriate institutional and national guidelines and regulations. Human blood was collected by venepuncture from aspirin free, healthy volunteers into vacutainers containing 3.2% (v/v) citrate after obtaining their informed consent. The procedures and consent forms used in this study were approved by the University of Reading Research Ethics Committee.

Preparation of human isolated platelets. Human isolated platelets were prepared by adding 7.5 mL of ACD [(acid citrate dextrose) (20 g/L glucose, 25 g/L sodium citrate and 15 g/L citric acid)] to 50 mL of blood prior to centrifugation at 100 g for 20 minutes at room temperature. The Platelet-Rich Plasma (PRP) was removed using wide bore pipette tips and mixed with 3 mL of ACD and centrifuged at 1400 g for 10 minutes at room temperature. The resulting platelet pellet was resuspended in modified Tyrodes-HEPES buffer (2.9 mM KCl, 134 mM NaCl, 0.34 mM Na₂HPO₄·12H₂O, 1 mM MgCl₂, 12 mM NaHCO₃, 20 mM HEPES, pH 7.3) and centrifuged again at 1400 g for 10 minutes²⁸. The final platelet pellet obtained was suspended in modified Tyrodes-HEPES buffer at a density of 4×10^8 cells/mL for aggregation assays and rested at 30 °C for 30 minutes before using in platelet functional assays.

Platelet aggregation assays. Platelet aggregation was performed using a platelet glycoprotein VI (GPVI)-selective agonist, CRP-XL (obtained from Professor Richard Farndale, University of Cambridge) in the presence or absence of a vehicle control [0.1% (v/v) DMSO] or different concentrations of flavone derivatives by optical aggregometry. Human isolated platelets (267 µL) taken in siliconised cuvettes were incubated with 3 µL of a vehicle control or various concentrations of flavone derivatives for 5 minutes at 37 °C. Following the incubation, 30 µL of CRP-XL (0.5 µg/mL) was added to platelets and the level of aggregation was measured for 5 minutes at 37 °C under constant stirring (1200 rpm). Data were analysed by calculating the percentage of maximum platelet aggregation at 5 minutes, and the level of aggregation obtained with the vehicle control was considered as 100% to quantify the impact of flavones on platelets.

Lactate dehydrogenase assay. The lactate dehydrogenase (LDH) assay was performed using a LDH Cytotoxicity Assay Kit (Pierce, Thermo Fisher) according to the manufacturer's instructions. Briefly, to 50 µL of human isolated platelets, 1 µL of a positive control [1% (v/v) Triton-X 100, provided in the kit] or a vehicle control [0.1% (v/v) DMSO] or various concentrations of flavone derivatives were added and incubated for 30 minutes at 37 °C. Then, 25 µL of the reaction mixture (provided in the kit) were added to the platelets and further incubated for 30 minutes in dark. Finally, the reaction was stopped by adding 25 µL of stop solution (provided in the kit). The absorbance was measured at 490 and 650 nm using a Fluostar Optima spectrofluorimeter (BMG Labtech, Germany). The level of LDH released with the positive control was considered as 100% to quantify the LDH release in flavone-treated samples.

Statistical analysis. The statistical significance between the vehicle controls and flavones-treated platelet samples was analysed by one-way ANOVA followed by Bonferroni *post-hoc* test. All the statistical analyses were performed using GraphPad Prism 7 (GraphPad Software Inc., USA).

Results

To determine the relationship between the specific functional groups in the structures of flavones and their antiplatelet activity, a series of hydroxy flavones, hydroxy 4-thioflavones, methoxy flavones and methoxy 4-thioflavones containing different B-ring (Figs 1A, 2A, 3A & 4A) were used in this study. These 16 flavones were synthesised based on the molecular template of 7,8-hydroxy flavone to systematically determine the influence of hydroxyl (-OH), methoxy (-OMe) and 4-thiocarbonyl (4-C=S) groups as well as the effects of phenyl group and its bioisosteres such as thiofuran, furanyl and pyridinyl moieties as B-ring on platelet activation/function.

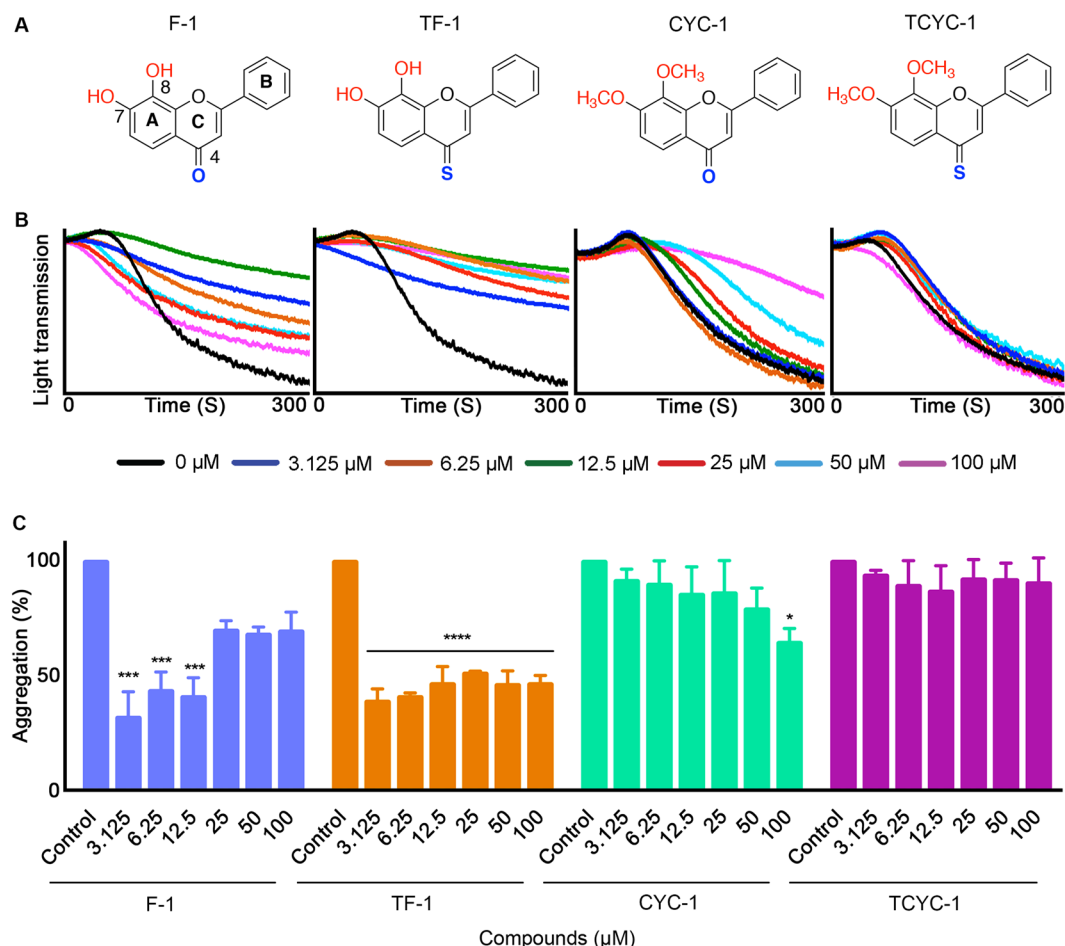


Figure 1. Effect of flavones with phenyl B-ring on human platelet activation. (A) Chemical structures of the flavones, F-1, TF-1, CYC-1 and TCYC-1. (B) Representative traces displaying the level of aggregation obtained when human isolated platelets were treated (for 5 minutes) with a vehicle control [0.1% (v/v) DMSO] or various concentrations of flavones, F-1, TF-1, CYC-1 and TCYC-1 (3.125–100 μM) and 0.5 μg/mL CRP-XL. (C) Bar graphs show the percentage of aggregation obtained in the presence and absence of different concentrations of flavones, F-1, TF-1, CYC-1 and TCYC-1. The data were normalised by considering the maximum aggregation observed for the vehicle control at 5 minutes as 100%, and the level of inhibition in flavone and its derivatives-treated platelet samples was calculated accordingly. Cumulative data denote mean ± S.D. (n = 3). The *p* values displayed (**p* < 0.05, ****p* < 0.001 and *****p* < 0.001) are as analysed by one-way ANOVA using Graphpad Prism.

The synthesis of these compounds from our laboratories has been previously reported³⁵ and the purities of compounds were analysed by reverse phase HPLC, and they were found to be >95%.

In order to determine the SAR of flavones with human platelets, the effects of 16 selected synthetic flavones on CRP-XL-stimulated platelet aggregation were evaluated by optical aggregometry. Human isolated platelets were treated with a vehicle [0.1% (v/v) DMSO] or diverse concentrations of flavones (3.125, 6.25, 12.5, 25, 50 and 100 μM) for 5 minutes prior to activation with 0.5 μg/mL CRP-XL for 5 minutes. None of the flavones exhibited activatory effects on platelets on their own, and the vehicle control containing 0.1% (v/v) DMSO did not affect platelet activation.

Flavones with phenyl B-ring. Hydroxy flavone (F-1) with free hydroxyls and carbonyl moiety significantly inhibited CRP-XL-stimulated platelet aggregation at lower concentrations such as 3.125, 6.25 and 12.5 μM but no significant inhibition was observed at concentrations higher than 12.5 μM. The hydroxy 4-thioflavone (TF-1) showed significant inhibitory effects at all the concentrations tested. However, the methoxy flavone (CYC-1) inhibited the aggregation significantly only at 100 μM and the methoxy 4-thioflavone (TCYC-1) did not show any inhibitory effects at any of the concentrations tested (Fig. 1A–C).

Flavones with thiofuran B-ring. Hydroxy flavone (F-2) displayed a similar inhibitory trend to F-1 with significant inhibition at lower concentrations up to 12.5 μM, whereas the hydroxy 4-thioflavone (TF-2) and the methoxy flavone (CYC-2) inhibited aggregation only at 100 μM. The methoxy 4-thioflavone (TCYC-2) of this group was found to possess no inhibitory activity on platelet aggregation (Fig. 2A–C).

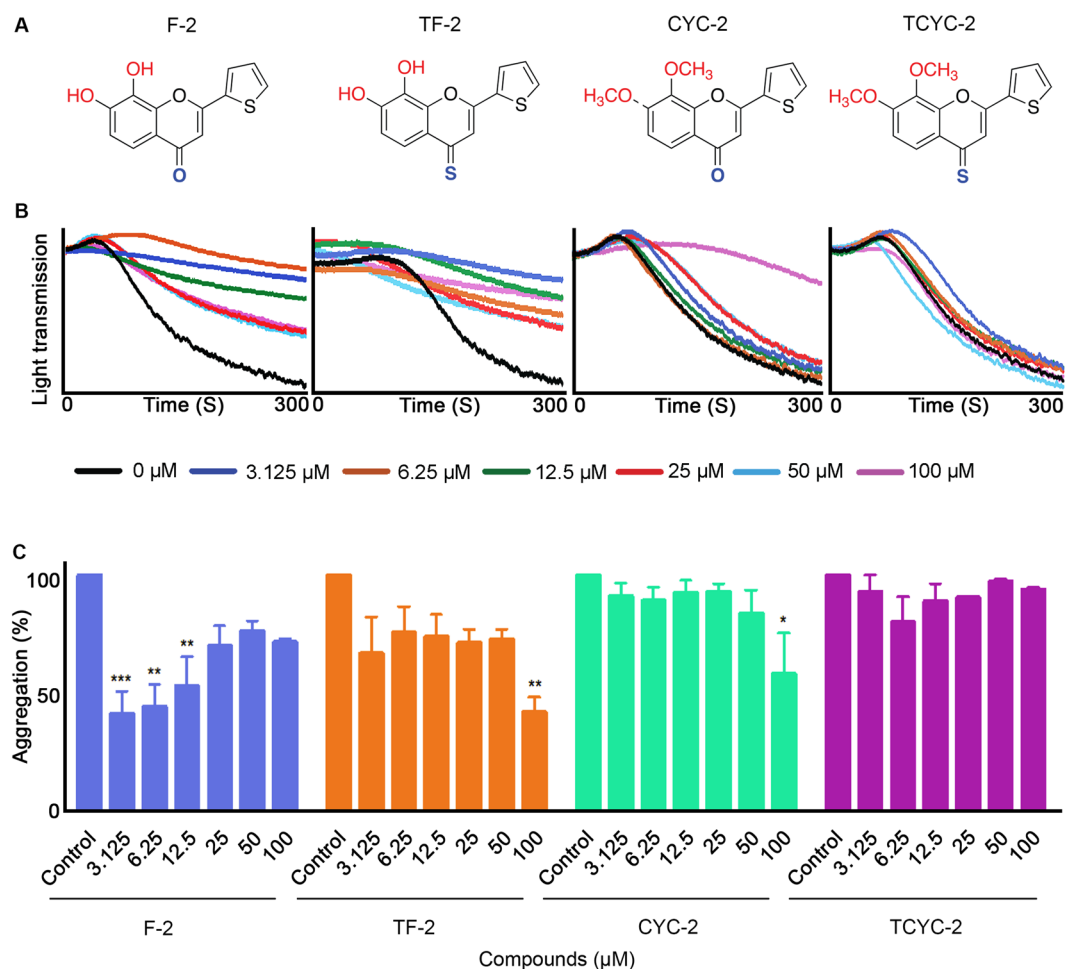


Figure 2. Effect of flavones with thiofuran B-ring on human platelet activation. (A) Chemical structures of the flavones, F-2, TF-2, CYC-2 and TCYC-2. (B) Representative traces showing the level of aggregation obtained when human isolated platelets were treated (for 5 minutes) with a vehicle control [0.1% (v/v) DMSO] or diverse concentrations of flavones, F-2, TF-2, CYC-2 and TCYC-2 (3.125–100 μM) and 0.5 μg/mL CRP-XL. (C) Bar graphs show the percentage of aggregation obtained in the presence and absence of various concentrations of flavones, F-2, TF-2, CYC-2 and TCYC-2. The data were normalised by considering the maximum aggregation observed for the vehicle control at 5 minutes as 100%, and the level of inhibition in flavone and its derivatives-treated platelet samples was calculated accordingly. Cumulative data denote mean ± S.D. (n = 3). The *p* values displayed (**p* < 0.05, ***p* < 0.01 and ****p* < 0.001) are as analysed by one-way ANOVA using Graphpad Prism.

Flavones with furan B-ring. Hydroxy flavone (F-3) and hydroxy 4-thioflavone (TF-3) inhibited the CRP-XL-induced platelet activation at all the concentrations tested, however, the methoxy flavone (CYC-3) and the methoxy 4-thioflavone (TCYC-3) failed to inhibit the aggregation (Fig. 3A–C).

Flavones with pyridine B-ring. None of the flavones with a pyridine B-ring displayed inhibitory effects on CRP-XL-stimulated platelet aggregation (Fig. 4A–C) at concentrations up to 100 μM.

It is interesting to note the impact of altering the B-ring on the platelet activity among the same class of flavones. For hydroxy flavones (with –OH and 4-C=O), changing the phenyl group (F-1) to a thiofuran group (F-2) did not affect the inhibitory potential as both compounds elicited the inhibitory activity up to 12.5 μM. Consistent inhibition (~65–70%) across the tested concentrations (3.125–100 μM) was observed when the phenyl group was replaced with a furan group (F-3). In contrast, substitution of the phenyl group with a pyridine group led to a complete abolition of inhibitory activity in platelets (F-4). A similar trend was observed for the hydroxy 4-thioflavones (with –OH and 4-C=S) when the B-ring phenyl group was replaced with its bioisosteres furan and pyridine. However, the substitution of thiofuran led to a reduction in the activity, for example, TF-2 showed ~50% inhibition only at 100 μM (Fig. 2) where its phenyl analogue, TF-1 elicited ~50% inhibition at all the concentrations used (Fig. 1).

The influence of B-ring modifications was not conspicuous among the methoxy flavones (with –OMe and 4-C=O) and methoxy 4-thioflavones (with –OMe and 4-C=S) as these two classes of flavones did not display any significant inhibitory activity on platelets in comparison to their hydroxyl analogues. Nevertheless, amongst the methoxy flavones, flavones with a B ring phenyl group (CYC-1) or thiofuran group (CYC-2) showed similar

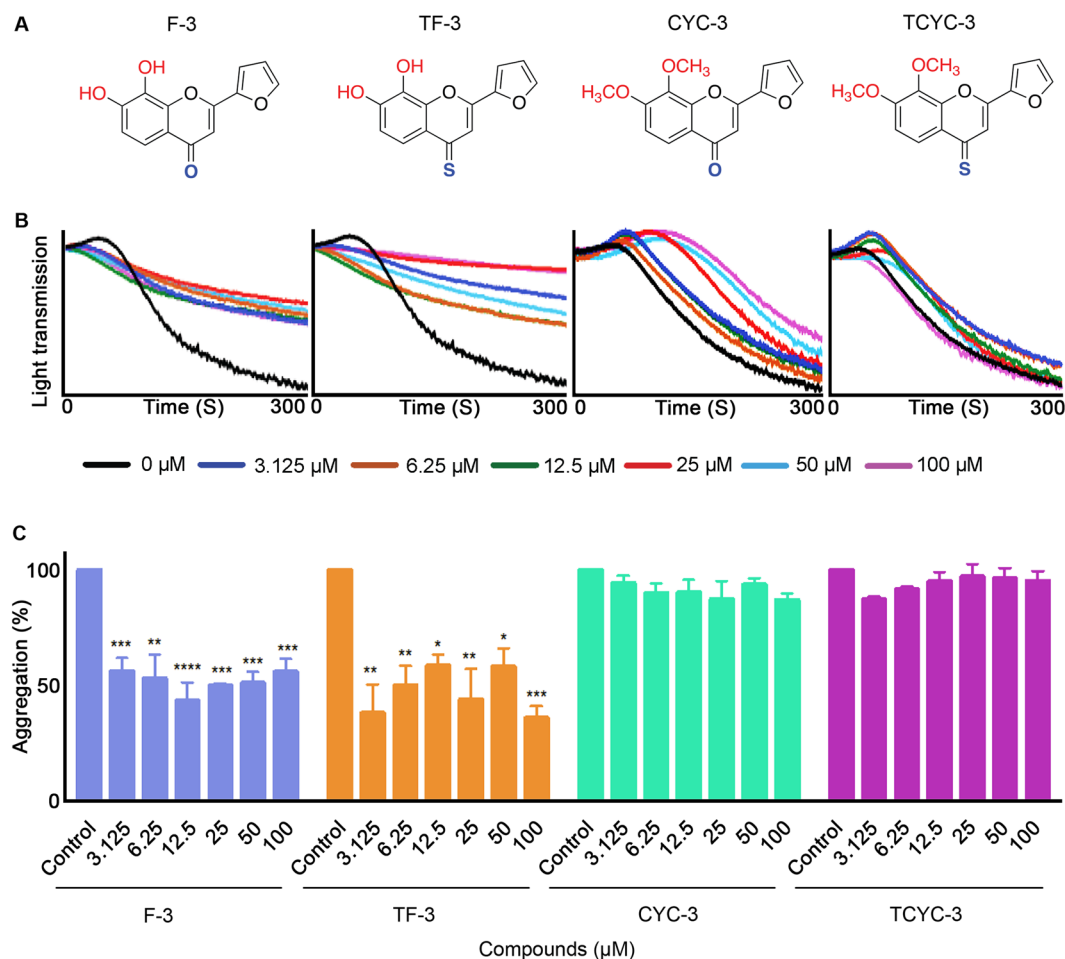


Figure 3. Effect of flavones with furan B-ring on human platelet activation. **(A)** Chemical structures of the flavones, F-3, TF-3, CYC-3 and TCYC-3. **(B)** Representative traces displaying the level of aggregation obtained when human isolated platelets were treated (for 5 minutes) with a vehicle control [0.1% (v/v) DMSO] or various concentrations of flavones, F-3, TF-3, CYC-3 and TCYC-3 (3.125–100 μ M) and 0.5 μ g/mL CRP-XL. **(C)** Bar graphs display the percentage of aggregation obtained in the presence and absence of diverse concentrations of flavones, F-3, TF-3, CYC-3 and TCYC-3. The data were normalised by considering the maximum aggregation observed for the vehicle control at 5 minutes as 100%, and the level of inhibition in flavone and its derivatives-treated platelet samples was calculated accordingly. Cumulative data denote mean \pm S.D. ($n = 3$). The p values displayed (* $p < 0.05$, ** $p < 0.01$, *** $p < 0.001$ and **** $p < 0.001$) are as analysed by one-way ANOVA using Graphpad Prism.

activities with inhibition only at 100 μ M. Methoxy 4-thioflavones (with –OMe and 4-C=S) did not exert any inhibitory effects on platelets.

To corroborate the above results, the effects of these flavones on another platelet activation marker, specifically fibrinogen binding (a marker for inside-out signalling to integrin α IIb β 3), were measured by flow cytometry. The results obtained from this experiment concur with the aggregation data where hydroxy flavones F-1 (at 3.125–12.5 μ M), F-2 (at 3.125–12.5 μ M) and F-3 (at all concentrations tested), as well as thiohydroxy flavones TF-1 (at all concentrations tested), TF-2 (at 100 μ M) and TF-3 (at all concentrations tested) significantly inhibited fibrinogen binding (Fig. S1), which is critical for subsequent platelet aggregation.

Finally, to determine whether the platelet inhibition observed was the result of a specific pharmacological effect of flavones rather than due to their cytotoxic effects, an LDH cytotoxicity assay was performed. For this, platelets were treated with a vehicle control [0.1% (v/v) DMSO] or diverse concentrations of flavones (3.125, 6.25, 12.5, 25, 50 and 100 μ M) and the release of LDH, a cytosolic enzyme, which is an indicator of cellular toxicity was measured. As shown in Fig. 5, a positive control showed the maximum level of cytotoxicity with a higher LDH release, whereas the flavones did not exert cytotoxic effects at the concentrations (3.125–100 μ M) used. These observations suggest that the inhibitory effects of flavones demonstrated in this study were not due to their cytotoxic effects on platelets.

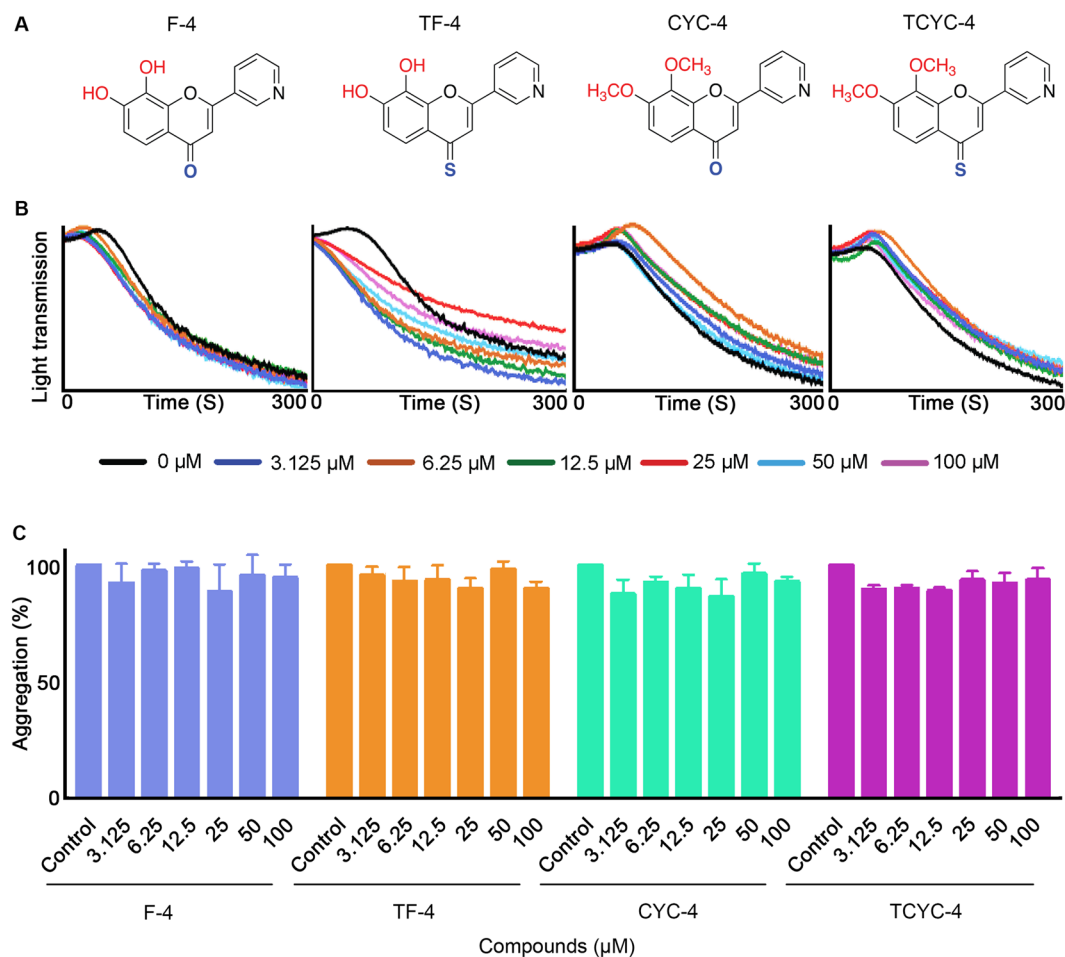


Figure 4. Effect of flavones with pyridyl B-ring on human platelet activation. **(A)** Chemical structures of the flavones, F-4, TF-4, CYC-4 and TCYC-4. **(B)** Representative traces showing the level of aggregation obtained when human isolated platelets treated (for 5 minutes) with a vehicle control [0.1% (v/v) DMSO] or various concentrations of flavones, F-4, TF-4, CYC-4 and TCYC-4 (3.125–100 μM) and 0.5 $\mu\text{g/mL}$ CRP-XL. **(C)** Bar graphs show the percentage of aggregation obtained with flavones, F-4, TF-4, CYC-4 and TCYC-4. The data were normalised by considering the maximum aggregation observed for the vehicle control at 5 minutes as 100%, and the level of inhibition in flavone and its derivatives-treated platelet samples was calculated accordingly. Cumulative data denote mean \pm S.D. (n = 3).

Discussion

Understanding the relationship between distinct functional groups within the structures of flavones and their influence on antiplatelet activity is critical for further development and modification of flavones in order to make them as more potent lead compounds for drug design. Such knowledge will aid in the development of improved therapeutic strategies for the prevention and treatment of cardiovascular diseases, specifically thrombosis. In the present study, the analysis and comparison of the inhibitory activities of a series of 16 structurally-related synthetic flavones on CRP-XL-stimulated human platelet activation highlighted the key structural features that are required for the inhibition of platelet function.

In general, comparison between different classes of flavones with the same B-ring moiety suggested that the hydroxy flavones (with free -OH groups) were more effective than their corresponding methoxy flavones (with -OCH₃ group). This highlighted that hydroxy groups, which are hydrogen bond donors, are essential for their inhibitory activities in platelets and that methoxy groups with hydrogen bond accepting profiles are less effective in this regard. However, the study by Bojić *et al.*³⁴ reports increased anti-aggregatory potencies of O-methylated derivatives in comparison to their hydroxy analogues. This disparity could possibly be due to the difference in the hydroxyl substitution pattern of the flavones studied which would affect the interaction with the molecular target. In addition, several previous studies reported the loss of biological activity of flavonoids upon complete methylation of their active hydroxy groups^{29,35,36}. Together with these previous studies, our data suggest that hydroxy groups are a key descriptor for the biological activity of flavonoids. It is worth highlighting that the hydroxy flavones used in this study possess hydroxyl groups at the C-7,8 position as opposed to the C-5,7 position in chrysin, a natural flavone that was previously reported to negatively modulate platelet activity³⁷. When comparing the activity between chrysin and its 7,8-hydroxy analogue (F-1), it can be deduced that the position of the hydroxyl groups also influences platelet function as chrysin exhibited dose-dependent inhibition of platelet

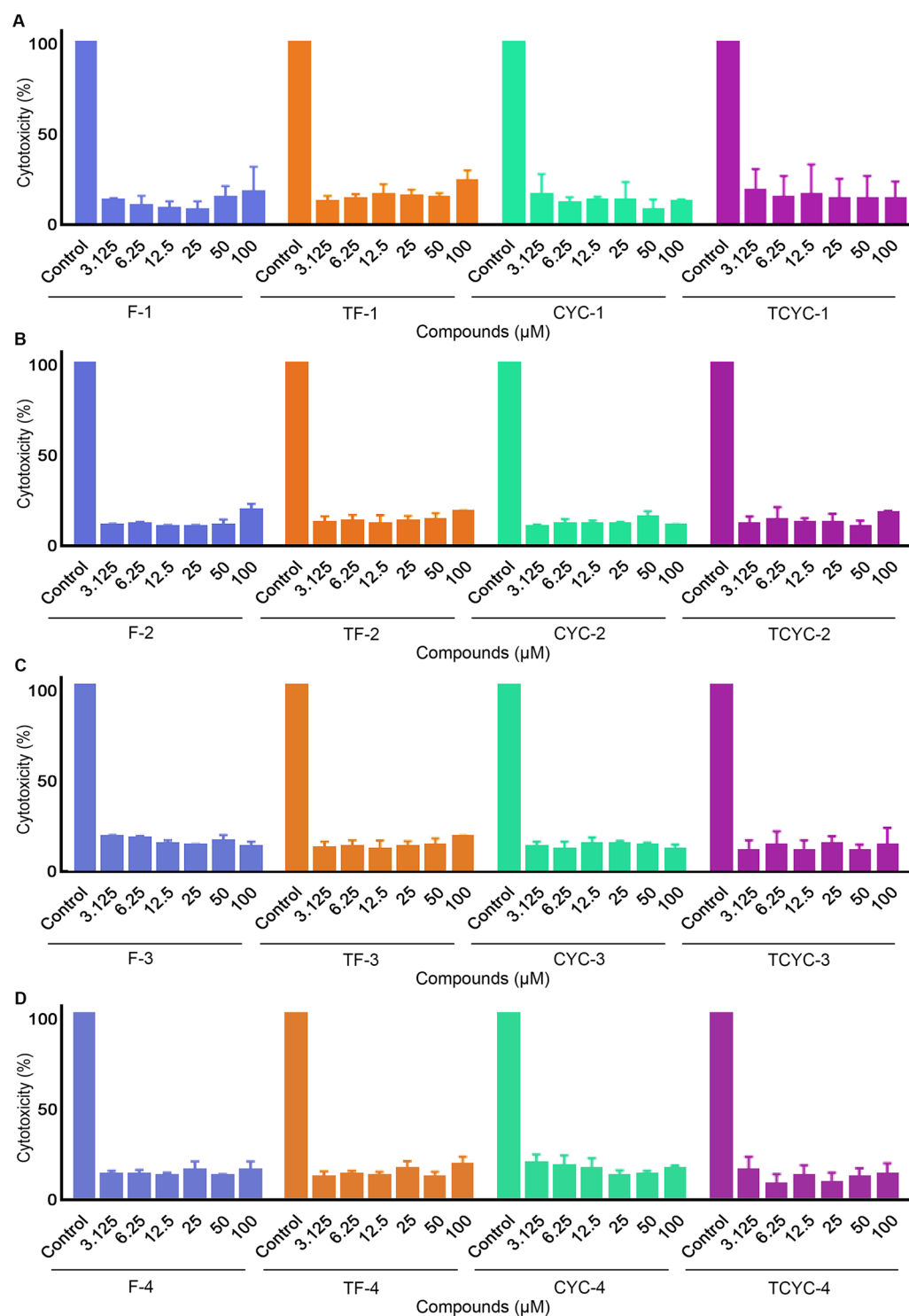


Figure 5. Cytotoxicity profile of flavones in human platelets. Human isolated platelets were treated with a positive control, or a vehicle control [0.1% (v/v) DMSO] or various concentrations (3.125–100 μM) of flavones, F-1, TF-1, CYC-1 and TCYC-1 (A), F-2, TF-2, CYC-2 and TCYC-2 (B), F-3, TF-3, CYC-3 and TCYC-3 (C) and F-4, TF-4, CYC-4 and TCYC-4 (D) for 30 minutes and the release of LDH, a marker for cytotoxicity was measured at 490 and 650 nm using spectrofluorimeter. The LDH release attained with the positive control was considered as 100%, and the levels of LDH release for flavone-treated samples were calculated. The data represent mean ± S.D. (n = 3). Statistical significance was analysed by one-way ANOVA using Graphpad Prism.

activity (6.25–100 μM)³⁸, whereas, 7,8- hydroxyl flavone showed inhibition only between 3.25–12.5 μM. Further studies are required to determine the reasons for the low inhibitory effects obtained from higher concentrations of hydroxyl flavones with phenyl and thiofuran B-rings.

A number of previous studies have reported the significance of 4-C=O in the C-ring of flavonoids for antiplatelet activities based on the comparison between flavonoids with and without 4-C=O^{32,34,39}. In this study, the influence of modification of 4-C=O to 4-C=S was also evaluated. Indeed, the replacement of 4-C=O with 4-C=S was well tolerated for flavones with free hydroxy groups (hydroxy flavones and hydroxy 4-thioflavones), however, no beneficial effects were observed for flavones with methoxy groups (methoxy flavones and methoxy 4-thioflavones). It is interesting to note that the influence of 4-C=S was also found to be dependent on the B-ring functionality as moderate loss of inhibitory activity was observed upon the replacement of 4-C=O with 4-C=S for flavones with a thiofuran B-ring. This demonstrates that the systematic analysis of flavones through careful correlation of effect of each substitution with respect to other functional groups is important for better optimisation of these compounds as molecular templates for drug design and discovery.

Natural flavonoids contain a phenyl group as the B-ring, hence, previous reports have focused on the influence of the position of the B-ring and its hydroxylation patterns. The present study involving synthetic flavonoids allowed the determination of the effect of incorporating bioisosteres of the phenyl group. It was found that replacing the phenyl group with a furan group was well tolerated for hydroxy flavones and hydroxy 4-thioflavones, whereas replacement of a phenyl group with a thiofuran group led to loss of inhibitory activities in platelets for hydroxy 4-thioflavones but was tolerated for hydroxy flavones. Conversely, replacement of the phenyl group with a pyridine group led to complete loss of inhibition in platelets. These observations suggest that the B-ring phenyl group is not critical for the antiplatelet activity, but the B-ring heteroatoms largely influence the activity. Furthermore, these observations suggest that the orientation and binding modes of the B-ring moieties might influence the interaction with their molecular targets. Hence, identification of the molecular targets for these flavones, and careful optimisation of the nature of the B-ring could lead to more efficacious flavone scaffolds for the development of novel antiplatelet agents. Furthermore, the hydroxy flavones and thiohydroxy flavones showed significant inhibitory effects on fibrinogen binding, a key marker for platelet activation via inside-out signalling to integrin $\alpha\text{IIb}\beta_3$. This suggests that these flavones specifically with free hydroxy groups may modulate distinctive functions of platelets. The LDH cytotoxicity assay showed that these flavones are not cytotoxic to platelets at the concentrations tested and hence the inhibitory effects observed are due to their pharmacological effects on platelet function.

In conclusion, a panel of 16 structurally-related hydroxy flavones, methoxy flavones and their 4-thio analogues were screened for their antiplatelet activity upon CRP-XL-induced activation in human platelets. SAR analysis of these flavones suggested that the free hydroxyl group is essential for antiplatelet activity. Moreover, the modification at 4-C=O to 4-C=S in the C-ring, and B-ring modifications of phenyl group into specific bioisostere such as furanyl group, are well tolerated without any significant loss of their inhibitory activities. The molecular targets and the impact of these synthetic flavones on specific signalling pathways in platelets were not investigated in this study. Since the natural flavonoids possess broad spectrum of binding affinities and inhibitory activities against numerous cellular targets, the synthetic flavones with higher specificity for selective targets may be beneficial in achieving targeted effects. Therefore, further studies will be required to underpin the impact of these synthetic flavones with specific functional groups on various molecular targets in platelets. Together, the results obtained in this study with synthetic flavones enhance the current understanding of the SAR of flavones with human platelets and may aid in the design and development of novel anti-thrombotic strategies using flavones as potential molecular templates.

References

- George, J. N. Platelets. *Lancet* **355**, 1531–1539 (2000).
- Ghoshal, K. & Bhattacharyya, M. Overview of platelet physiology: Its hemostatic and nonhemostatic role in disease pathogenesis. *Sci. World J.* **2014**, 16 (2014).
- Ruggeri, Z. M. Platelets in atherothrombosis. *Nat. Med.* **8**, 1227–1234 (2002).
- Willoughby, S., Holmes, A. & Loscalzo, J. Platelets and cardiovascular disease. *Eur. J. Cardiovasc. Nurs.* **1**, 273–288 (2002).
- Vane, J. R. & Botting, R. M. The mechanism of action of aspirin. *Thromb. Res.* **110**, 255–258 (2003).
- Mackman, N. Triggers, targets and treatments for thrombosis. *Nature* **451**, 914–918 (2008).
- Michelson, A. D. P2Y₁₂ Antagonism: Promises and Challenges. *Arterioscler. Thromb. Vasc. Biol.* **28**, s33–s38 (2008).
- Cattaneo, M. New P2Y₁₂ blockers. *Journal of Thrombosis and Haemostasis* **7**, 262–265 (2009).
- Angiolillo, D. J., Bates, E. R. & Bass, T. A. Clinical profile of prasugrel, a novel thienopyridine. *Am. Heart J.* **156** (2008).
- Jakubowski, J. A., Winters, K. J., Naganuma, H. & Wallentin, L. Prasugrel: A novel thienopyridine antiplatelet agent. A review of preclinical and clinical studies and the mechanistic basis for its distinct antiplatelet profile. *Cardiovascular Drug Reviews* **25**, 357–374 (2007).
- <http://www.who.int/mediacentre/factsheets/fs317/en/>; Date accessed: 2017-06-17.
- Hertog, M. G., Feskens, E. J., Hollman, P. C., Katan, M. B. & Kromhout, D. Dietary antioxidant flavonoids and risk of coronary heart disease: the Zutphen Elderly Study. *Lancet* **342**, 1007–1011 (1993).
- Wang, C.-Z., Mehendale, S. R., Calway, T. & Yuan, C.-S. Botanical flavonoids on coronary heart disease. *Am. J. Chin. Med.* **39**, 661–71 (2011).
- Hollenberg, N. K., Schmitz, H., McDonald, I. & Poulter, N. Cocoa, flavanols and cardiovascular risk. *Br. J. Cardiol.* **11**, 379–386 (2004).
- Knekt, P., Jarvinen, R., Reunanen, A. & Maatela, J. Flavonoid intake and coronary mortality in Finland: a cohort study. *BMJ* **312**, 478–481 (1996).
- Marjorie, M. *et al.* Flavonoid intake and cardiovascular disease mortality in a prospective cohort of {US} adults. *Am. J. Clin. Nutr.* **95**, 454–464 (2012).
- Ponzo, V. *et al.* Dietary flavonoid intake and cardiovascular risk: a population-based cohort study. *J. Transl. Med.* **13**, 218 (2015).
- McCullough, M. L. *et al.* Flavonoid intake and cardiovascular disease mortality in a prospective cohort of US adults. *Am. J. Clin. Nutr.* **95**, 454–64 (2012).
- Chiva-Blanch, G. *et al.* Differential effects of polyphenols and alcohol of red wine on the expression of adhesion molecules and inflammatory cytokines related to atherosclerosis: A randomized clinical trial. *Am. J. Clin. Nutr.* **95**, 326–334 (2012).
- Estruch, R. *et al.* Different effects of red wine and gin consumption on inflammatory biomarkers of atherosclerosis: A prospective randomized crossover trial: Effects of wine on inflammatory markers. *Atherosclerosis* **175**, 117–123 (2004).

21. Pignatelli, P. *et al.* The flavonoids quercetin and catechin synergistically inhibit platelet function by antagonizing the intracellular production of hydrogen peroxide. *Am. J. Clin. Nutr.* **72**, 1150–1155 (2000).
22. Pignatelli, P. *et al.* Polyphenols synergistically inhibit oxidative stress in subjects given red and white wine. *Atherosclerosis* **188**, 77–83 (2006).
23. Gupta, K. & Panda, D. Perturbation of microtubule polymerization by quercetin through tubulin binding: A novel mechanism of its antiproliferative activity. *Biochemistry* **41**, 13029–13038 (2002).
24. Böhl, M., Czupalla, C., Tokalov, S. V., Hoflack, B. & Gutzzeit, H. O. Identification of actin as quercetin-binding protein: An approach to identify target molecules for specific ligands. *Anal. Biochem.* **346**, 295–299 (2005).
25. Peluso, M. R. Flavonoids attenuate cardiovascular disease, inhibit phosphodiesterase, and modulate lipid homeostasis in adipose tissue and liver. *Exp. Biol. Med. (Maywood)*. **231**, 1287–1299 (2006).
26. Maeda-Yamamoto, M. *et al.* O-Methylated Catechins from Tea Leaves Inhibit Multiple Protein Kinases in Mast Cells. *J. Immunol.* **172**, 4486–4492 (2004).
27. Vaiyapuri, S. *et al.* Pharmacological actions of nobiletin in the modulation of platelet function. *Br. J. Pharmacol.* **172**, 4133–4145 (2015).
28. Vaiyapuri, S. *et al.* Tangeretin regulates platelet function through inhibition of phosphoinositide 3-kinase and cyclic nucleotide signaling. *Arterioscler. Thromb. Vasc. Biol.* **33**, 2740–2749 (2013).
29. Kumar, S. & Pandey, A. K. Flavonoids: Reviews Chemistry and Biological Activities of Flavonoids: An Overview. *Sci. world J.* **2013**, 17 (2013).
30. Hubbard, G. P. *et al.* Quercetin inhibits collagen-stimulated platelet activation through inhibition of multiple components of the glycoprotein VI signaling pathway. *J. Thromb. Haemost.* **1**, 1079–1088 (2003).
31. Holt, R. R., Actis-Goretti, L., Momma, T. Y. & Keen, C. L. Dietary flavanols and platelet reactivity. *Journal of Cardiovascular Pharmacology* **47** (2006).
32. Wright, B., Spencer, J. P. E., Lovegrove, J. A. & Gibbins, J. M. Insights into dietary flavonoids as molecular templates for the design of anti-platelet drugs. *Cardiovasc. Res.* **97**, 13–22 (2013).
33. Wright, B. *et al.* A structural basis for the inhibition of collagen-stimulated platelet function by quercetin and structurally related flavonoids. *Br. J. Pharmacol.* **159**, 1312–1325 (2010).
34. Bojić, M., Debeljak, Ž., Tomić, M., Medić-Šarić, M. & Tomić, S. Evaluation of antiaggregatory activity of flavonoid aglycone series. *Nutr. J.* **10**, 73 (2011).
35. Ravishankar, D., Watson, K. A., Greco, F. & Osborn, H. M. I. Novel synthesised flavone derivatives provide significant insight into the structural features required for enhanced anti-proliferative activity. *RSC Adv.* **6**, 64544–64556 (2016).
36. Xie, Y., Yang, W., Tang, F., Chen, X. & Ren, L. Antibacterial Activities of Flavonoids: Structure-Activity Relationship and Mechanism. *Curr. Med. Chem.* **22**, 132–149 (2014).
37. Liu, G. *et al.* Antiplatelet activity of chrysin via inhibiting platelet α Ib β 3-mediated signaling pathway. *Mol. Nutr. Food Res.* **60**, 1984–1993 (2016).
38. Ravishankar, D. *et al.* Ruthenium-conjugated chrysin analogues modulate platelet activity, thrombus formation and haemostasis with enhanced efficacy. *Sci. Rep.* **7** (2017).
39. Navarro-Núñez, L. *et al.* Thromboxane A2 receptor antagonism by flavonoids: Structure-activity relationships. *J. Agric. Food Chem.* **57**, 1589–1594 (2009).

Acknowledgements

The authors would like to thank the British Heart Foundation (Grant reference: PG/16/64/32311) and the Felix Trust (PhD studentship for Dr Ravishankar) for their funding support.

Author Contributions

D.R. and S.V. designed the biological aspects of this study, performed experiments, analysed data and wrote the paper; H.M.I.O., F.G. and D.R. designed the chemical aspects of this study; M.S., A.A., H.W., D.A.I.A. and R.V. have performed experiments and analysed data.

Additional Information

Supplementary information accompanies this paper at <https://doi.org/10.1038/s41598-018-27809-z>.

Competing Interests: The authors declare no competing interests.

Publisher's note: Springer Nature remains neutral with regard to jurisdictional claims in published maps and institutional affiliations.



Open Access This article is licensed under a Creative Commons Attribution 4.0 International License, which permits use, sharing, adaptation, distribution and reproduction in any medium or format, as long as you give appropriate credit to the original author(s) and the source, provide a link to the Creative Commons license, and indicate if changes were made. The images or other third party material in this article are included in the article's Creative Commons license, unless indicated otherwise in a credit line to the material. If material is not included in the article's Creative Commons license and your intended use is not permitted by statutory regulation or exceeds the permitted use, you will need to obtain permission directly from the copyright holder. To view a copy of this license, visit <http://creativecommons.org/licenses/by/4.0/>.

© The Author(s) 2018

The endogenous antimicrobial cathelicidin LL37 induces platelet activation and augments thrombus formation

Maryam F. Salamah,¹ Divyashree Ravishankar,^{1,*} Xenia Kodji,^{2,*} Leonardo A. Moraes,^{3,*} Harry F. Williams,¹ Thomas M. Vallance,¹ Dina A. Albadawi,¹ Rajendran Vaiyapuri,⁴ Kim Watson,⁵ Jonathan M. Gibbins,⁵ Susan D. Brain,² Mauro Perretti,⁶ and Sakthivel Vaiyapuri¹

¹School of Pharmacy, University of Reading, Reading, United Kingdom; ²Section of Vascular Biology & Inflammation, School of Cardiovascular Medicine & Research, King's College London, London, United Kingdom; ³Department of Physiology, National University of Singapore, Singapore; ⁴School of Pharmacy, University of Reading Malaysia, Johor, Malaysia; ⁵School of Biological Sciences, University of Reading, Reading, United Kingdom; and ⁶William Harvey Research Institute, London, United Kingdom

Key Points

- LL37 primes platelet function and augments thrombus formation.
- LL37 mainly acts through FPR2/ALX in platelets.

Platelet-associated complications including thrombosis, thrombocytopenia, and hemorrhage are commonly observed during various inflammatory diseases such as sepsis, inflammatory bowel disease, and psoriasis. Despite the reported evidence on numerous mechanisms/molecules that may contribute to the dysfunction of platelets, the primary mechanisms that underpin platelet-associated complications during inflammatory diseases are not fully established. Here, we report the discovery of formyl peptide receptor 2, FPR2/ALX, in platelets and its primary role in the development of platelet-associated complications via ligation with its ligand, LL37. LL37 acts as a powerful endogenous antimicrobial peptide, but it also regulates innate immune responses. We demonstrate the impact of LL37 in the modulation of platelet reactivity, hemostasis, and thrombosis. LL37 activates a range of platelet functions, enhances thrombus formation, and shortens the tail bleeding time in mice. By utilizing a pharmacological inhibitor and *Fpr2/3* (an ortholog of human FPR2/ALX)-deficient mice, the functional dependence of LL37 on FPR2/ALX was determined. Because the level of LL37 is increased in numerous inflammatory diseases, these results point toward a critical role for LL37 and FPR2/ALX in the development of platelet-related complications in such diseases. Hence, a better understanding of the clinical relevance of LL37 and FPR2/ALX in diverse pathophysiological settings will pave the way for the development of improved therapeutic strategies for a range of thromboinflammatory diseases.

Introduction

Platelets play pivotal roles in the regulation of hemostasis; however, their unwarranted activation under pathological conditions leads to the formation of blood clots (thrombosis) within the circulation, which is a major cause of premature death.¹⁻³ Platelets also play significant roles in the regulation of innate immunity, inflammatory responses, and microbial infection.^{4,5} The activation of platelets during inflammatory diseases induces the formation of blood clots or disseminated intravascular coagulation in capillaries, resulting in the blockage of blood supply to tissues.^{6,7} Moreover, platelet activation results in the aggregation and sequestration of platelets, instigating thrombocytopenia.^{8,9} Several mechanisms that contribute to platelet dysfunction under inflammatory diseases have been reported¹⁰; however, the primary molecular mechanisms that underpin platelet activation are not fully understood.

LL37 is the only cathelicidin known to be expressed in human cells.¹¹ It acts as a powerful antimicrobial peptide against bacteria,¹² fungi,¹³ and viral particles¹⁴ and modulates innate and adaptive immune responses predominantly through formyl peptide receptor 2 (FPR2/ALX).^{15,16} Despite detailed

research on the roles of LL37 in the modulation of inflammatory responses in various pathological settings,^{17,18} its effects in the regulation of thrombosis and other platelet-related complications remained unknown for a long time. Because the level of LL37 released during inflammation is significantly higher than normal,^{19,20} understanding its critical functions in the modulation of platelet reactivity will pave the way for determining fundamental mechanisms underlying platelet-related complications in various inflammatory diseases. Immediately prior to the submission of this manuscript, Pircher et al²¹ demonstrated the ability of LL37 to prime circulating platelets and induce thromboinflammation. Although they have established a significant functional impact of LL37 in platelets, its actions via FPR2/ALX were not determined. In this study, we report the effects of LL37 on a range of platelet functional assays and establish its roles in the modulation of platelet reactivity, thrombosis, and hemostasis. Moreover, by using pharmacological tools and *Fpr2/3*-deficient mice, we have established the functional dependence of LL37 on FPR2/ALX in platelets.

Methods

The University of Reading Research Ethics Committee approved all the experimental procedures using human blood from healthy volunteers. The mouse strains of *Fpr1*^{-/-}²² and *Fpr2/3*^{-/-}²³ on a C57BL/6 background obtained from William Harvey Research Institute (London, United Kingdom) and control C57BL/6 mice from Envigo (United Kingdom) were used in this study. Detailed methods for the preparation of platelets, immunoblotting, enzyme-linked immunosorbent assay (ELISA), immunocytochemistry, in vitro thrombus formation, tail bleeding, platelet aggregation, dense granule secretion, platelet spreading, calcium mobilization, cytotoxicity and flow cytometry-based assays, mass spectrometry, molecular docking, and statistical analyses are provided in the supplemental Methods.

Results

Platelets store LL37 and release it upon activation

The expression of LL37 has been reported in several cell types including neutrophils where it is mainly stored in granules.^{24,25} By using immunofluorescence microscopy, we determined the presence of LL37 in human platelets (Figure 1A). Furthermore, resting and cross-linked collagen-related peptide (CRP-XL) (a glycoprotein VI [GPVI]-selective agonist) (1 μ g/mL)-activated human platelets were centrifuged, and the supernatant and pellet were used in ELISA to determine the release of LL37 from platelets. In the resting state, the level of LL37 was significantly higher in the pellet (1559 ± 433 pM) compared with the supernatant (41 ± 12 pM) (Figure 1B). However, upon activation of platelets with CRP-XL, the presence of LL37 was significantly increased in the supernatant (1490 ± 581.7 pM) compared with the pellet (59 ± 7.6 pM). Similar results were obtained upon the activation of platelets with collagen (acts via GPVI and integrin $\alpha 2\beta 1$) or TRAP-6 (acts via PAR1). To corroborate these results, the release of LL37 in human platelet-poor plasma (PPP) or platelet-rich plasma (PRP) was investigated by mass spectrometry. The level of LL37 was stable and significantly increased in PRP compared with PPP over 2 hours, indicating its release; by contrast, the level of LL37 was significantly reduced in PPP (Figure 1C). Together, these data confirm the presence of LL37 in platelets (between picomolar and nanomolar concentrations) and its release upon platelet activation.

LL37 augments thrombus formation and affects hemostasis

To determine whether LL37 has a direct influence on thrombotic complications during inflammatory diseases, its effects on thrombus formation under arterial flow conditions were investigated.^{26,27} LL37 (10, 20, and 50 μ M) significantly increased the thrombus formation (Figure 1Di) and the mean fluorescence intensity in a concentration-dependent manner (Figure 1Dii). The highest concentration of LL37 (50 μ M) increased the thrombus intensity by $\sim 70\%$ compared with the vehicle-treated samples (Figure 1Diii). Moreover, LL37 affected hemostasis in mice as determined by a tail bleeding assay. A mean bleeding time of 370.8 ± 46.6 seconds was observed in the vehicle-treated group; however, the infusion of LL37 significantly shortened the bleeding time to a mean of 225.2 ± 18.8 seconds (Figure 1E).

LL37 induces platelet activation

To further determine the impact of LL37 in distinctive platelet functions, additional assays were performed. Human isolated platelets were treated with a vehicle or LL37 (5, 10, and 20 μ M), and the level of aggregation was monitored by optical aggregometry. LL37 directly induced platelet aggregation in a concentration-dependent manner, notably, 20 μ M LL37 induced 100% aggregation (Figure 1F). In line with a recent study,²¹ in our experiments, LL37 failed to induce aggregation in human PRP (supplemental Figure 1). Similarly, to determine whether LL37 influences inside-out signaling to integrin $\alpha \text{IIb}\beta 3$ and α -granule secretion, the level of fibrinogen binding and P-selectin exposure was measured respectively using human isolated platelets and PRP by flow cytometry. LL37 increased the level of fibrinogen binding in human isolated platelets (Figure 2Ai) and PRP (Figure 2Aii) in a concentration-dependent manner. Similarly, the level of P-selectin exposure was increased by LL37 in isolated platelets (Figure 2Bi) and PRP (Figure 2Bii). Moreover, the ability of LL37 to induce platelet spreading on immobilized fibrinogen (Figure 2C) was analyzed as a marker for integrin $\alpha \text{IIb}\beta 3$ -mediated outside-in signaling. LL37 (5, 10, and 20 μ M) significantly increased the number of adhered (Figure 2Ci) and spread (Figure 2Cii) platelets, and the relative surface area (Figure 2Ciii) compared with their controls. Furthermore, to assess the effects of LL37 in calcium mobilization, intracellular calcium levels were measured in human isolated platelets. LL37 induced calcium mobilization with a maximum level achieved with 50 μ M. The level of calcium release obtained with 50 μ M LL37 is similar to that obtained with CRP-XL (1 μ g/mL), although the initial kinetics of calcium release appeared to be faster for LL37 (Figure 2D). These data confirm that LL37 triggers distinctive platelet functions.

LL37 does not exhibit cytotoxic effects in platelets

A previous study²⁸ reported the inhibitory effects of LL37 in platelets at exceptionally high concentrations (0.1–1.2 mM). It has been shown previously that LL37 exhibits cytotoxic effects in neutrophils and monocytes at concentrations higher than 50 μ M.²⁹ To determine whether the concentrations of LL37 used in this study (≤ 50 μ M) exhibit any cytotoxic effects in platelets, lactate dehydrogenase cytotoxicity assay was performed. The concentrations of LL37 used here (1–50 μ M) failed to exert any cytotoxic effects in human isolated platelets, although 100 μ M LL37 displayed significant toxicity (Figure 2E). These results confirm that LL37 concentrations up to

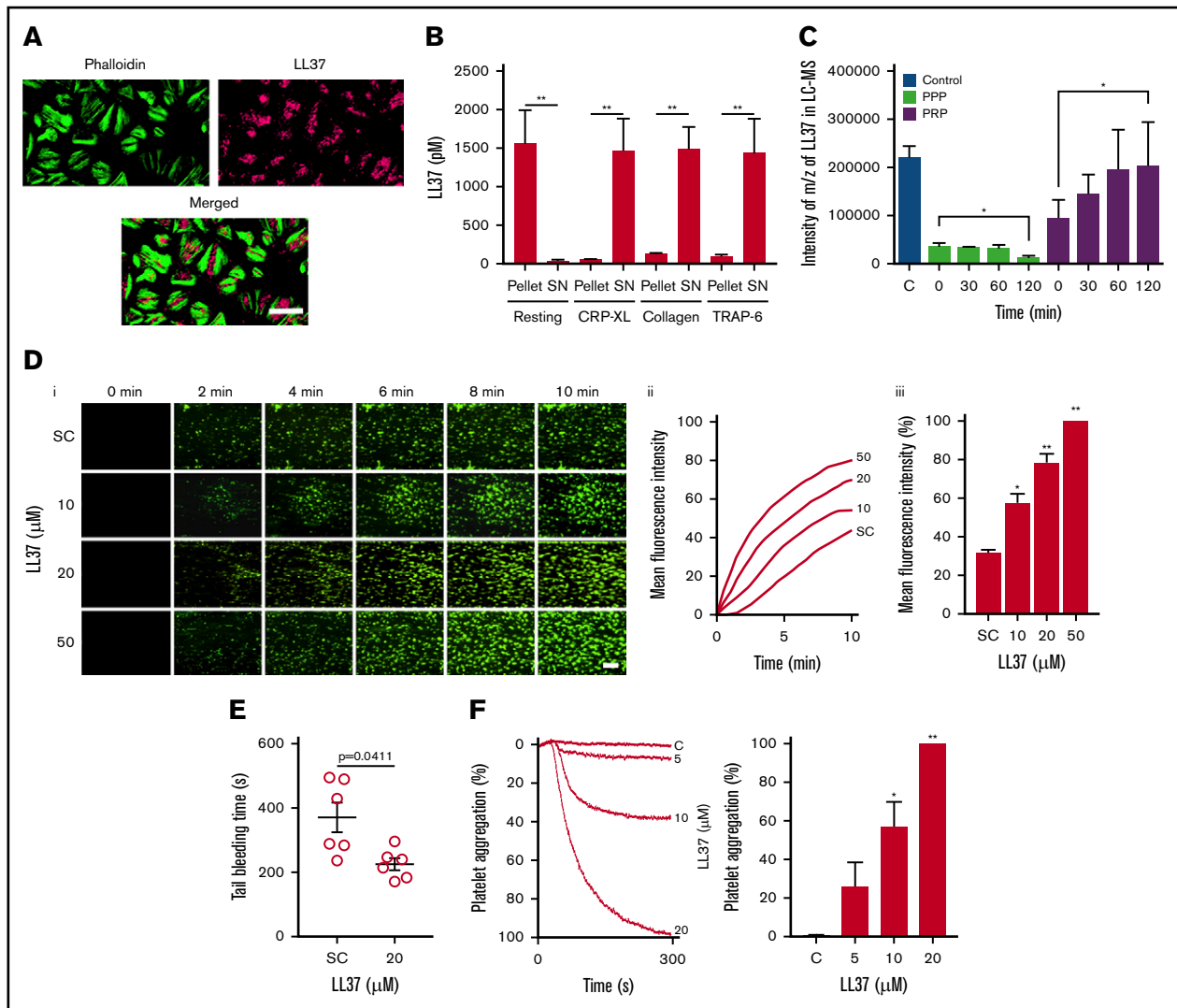


Figure 1. Presence of LL37 in platelets and its impact on thrombus formation, hemostasis, and platelet activation. (A) Human platelets were treated with primary antibodies against LL37 and appropriate fluorescent-labeled secondary antibodies (purple) and phalloidin (green) and analyzed by confocal microscopy (magnification $\times 100$; bar represents 10 μ m). Images shown are representative of 3 independent experiments. (B) the level of LL37 in resting and activated (1 μ g/mL CRP-XL, 1 μ g/mL collagen or 10 μ M thrombin receptor activator peptide 6 [TRAP-6]) platelet pellets and supernatants (SNs) was measured by ELISA using LL37-selective antibodies. Data represent mean \pm standard error of the mean (SEM) ($n = 5$). (C) The stability/release of LL37 in human plasma was analyzed by mass spectrometry (liquid chromatography mass spectrometry [LC-MS]). Graph represents the intensities of LL37 (100 μ g/mL) spiked in PRP and PPP at different time points over 120 minutes. Control represents the intensity of LL37 at 100 μ g/mL (unspiked). Data represent mean \pm SEM ($n = 3$). (D) The effects of LL37 in the modulation of thrombus formation. Human DiOC₆-labeled whole blood was preincubated with a scrambled peptide (SC) or LL37 (10, 20, and 50 μ M) for 10 minutes prior to perfusion over collagen-coated (400 μ g/mL) Vena8 Biochips. Images (i) (at 10 minutes) shown are representative of 3 separate experiments (magnification $\times 10$; bar represents 10 μ m). Data (ii-iii) represent mean \pm SEM ($n = 3$). (E) The impact of LL37 (20 μ M) on the modulation of hemostasis. C57BL/6 mice (10-12 weeks old) were anesthetized 20 minutes before the infusion of a scrambled peptide or LL37 (20 μ M) via femoral artery 5 minutes before the dissection of 1 mm of tail tip, and monitoring of time to cessation of bleeding. Data represent mean \pm SEM ($n = 6$ per group). (F) The effects of LL37 on platelet activation were measured by optical aggregometry using human isolated platelets. Data represent mean \pm SEM ($n = 6$). The statistical significance was established by 1-way analysis of variance (ANOVA) followed by Bonferroni's correction in most of the experiments except the data shown in panels B and E, which were analyzed by 2-tailed unpaired Student t test and nonparametric Mann-Whitney U test, respectively (* $P < .05$; ** $P < .01$).

50 μ M do not display any toxic effects in platelets, although higher concentrations may exhibit cytotoxic effects.

LL37 activates platelets selectively through FPR2/ALX

Numerous studies indicate that LL37 acts primarily through FPR2/ALX to exert its effects in immune cells.^{16,30,31} The expression of FPR2/ALX in megakaryocytes and human and mouse platelets at

the transcript level has been reported previously.^{32,33} Here, the presence of FPR2/ALX in human platelets remained unchanged in resting and CRP-XL (1 μ g/mL)-activated platelets as confirmed by immunoblots (Figure 3Ai), although the activation increased the surface level as determined by flow cytometry (Figure 3Aii). Moreover, the presence of *Fpr2/3* (an ortholog to human FPR2/ALX) in control, and its absence in *Fpr2/3*^{-/-} mouse platelets, was confirmed (Figure 3Aiii).

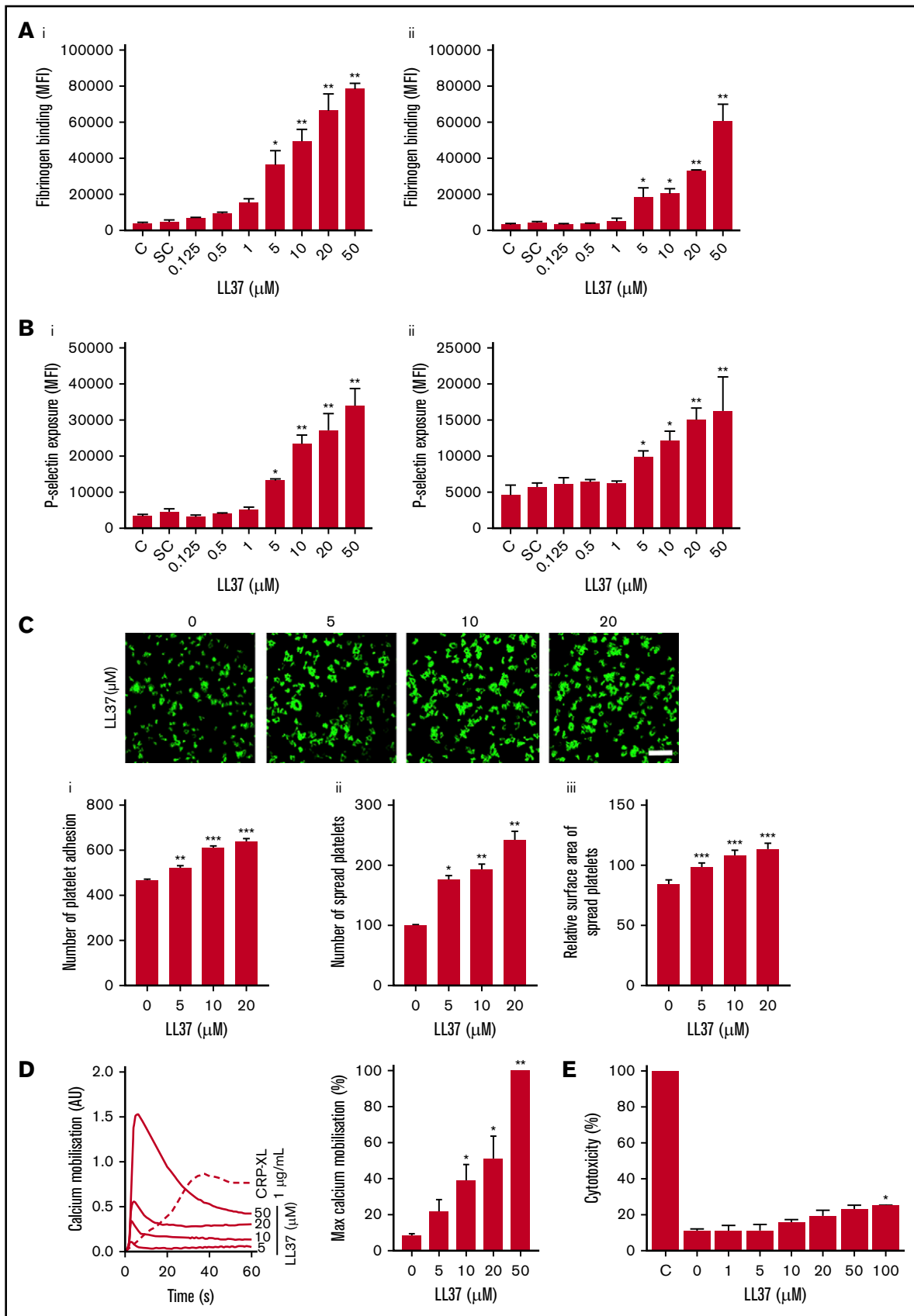


Figure 2.

To determine the functional dependence of LL37 on FPR2/ALX, the binding of LL37 to the platelet surface was confirmed using a fluorescently labeled LL37 (5-FAM-LC-conjugated LL37) by flow cytometry. 5-FAM-LL37 (20 μ M) displayed marked binding to the surface of human platelets compared with a fluorescently labeled scrambled LL37 (5-FAM-conjugated sc-LL37) (Figure 3Bi). Similarly, LL37 (20 μ M) binding was analyzed using platelets obtained from control, *Fpr1*^{-/-}, or *Fpr2/3*-deficient mice. The control and *Fpr1*^{-/-} mouse platelets exhibited significant binding to 5-FAM-LL37 compared with *Fpr2/3*^{-/-} (Figure 3Bii). In addition to LL37, mCRAMP (mouse ortholog of LL37) was also investigated for the binding to mouse platelets, and indeed, the level of mCRAMP binding was reduced in *Fpr2/3*^{-/-} mouse platelets compared with the controls (Figure 3Biii). The interactions between LL37 and FPR2/ALX were examined by molecular docking analysis, which predicted that LL37 peptide forms prominent hydrogen bonds with key residues such as Gln-89, Ser-182, Asn-285, and Gly-275 of FPR2/ALX that are identified as crucial for receptor activation (Figure 3Biv; Table 1).

The functional dependence of LL37 on FPR2/ALX was analyzed by using a range of platelet functional assays. The activatory effects of LL37 (5-50 μ M) were substantially reduced in *Fpr2/3*^{-/-} mouse platelets both in isolation (Figure 3Ci,Di) or whole blood (Figure 3Cii,Dii) compared with the controls as analyzed by fibrinogen binding and P-selectin exposure. Notably, the characterization of platelets obtained from *Fpr2/3*^{-/-} mice failed to display any defects in size and number of platelets or the levels of major platelet receptors such as GPVI (Figure 3Ei), glycoprotein Ib α (GPIb α) (Figure 3Eii), α IIb β 3 (Figure 3Eiii), and α 2 β 1 (Figure 3Eiv) compared with the control mouse platelets. To corroborate these results, platelet functional assays were performed in the presence of a selective FPR2/ALX antagonist, WRW₄ (WRW₄WWWW), in human and mouse platelets. The addition of WRW₄ (5 μ M) in human isolated platelets before activation with 20 μ M LL37 inhibited platelet aggregation by ~40% (Figure 3F). Similarly, the effects of LL37 (20 μ M) on fibrinogen binding (Figure 3Gi) and P-selectin exposure (Figure 3Gii) were significantly reduced in WRW₄ (5 μ M)-treated mouse platelets. These data demonstrate the involvement of FPR2/ALX in the regulation of LL37-mediated effects in platelets.

FPR2/ALX regulates normal platelet activation

To validate the importance of FPR2/ALX in the regulation of normal platelet activation, further experiments were performed using human isolated platelets in the presence or absence of WRW₄. CRP-XL (0.25 μ g/mL)-induced platelet aggregation was significantly reduced in the presence of WRW₄ (2.5-20 μ M). The inhibition of FPR2/ALX with WRW₄ (20 μ M) reduced the platelet aggregation by ~89% (Figure 4A). Similar results were obtained with adenosine 5'-diphosphate (ADP)-induced platelet aggregation, wherein WRW₄ (20 μ M) inhibited 75% of aggregation (Figure 4B). Moreover,

dense granule secretion (evidenced by adenosine triphosphate release) was significantly reduced in the presence of WRW₄ (Figure 4C). The platelet activation was also assessed using whole blood obtained from control and *Fpr2/3*^{-/-} mice upon stimulation with conventional platelet agonists such as CRP-XL, ADP, AY-NH₂ (activates protease activated receptor, PAR4), and U46619, an analog of thromboxane A₂ by measuring the levels of fibrinogen binding and P-selectin exposure. Similar to human platelets, the activation of platelets obtained from *Fpr2/3*^{-/-} mice upon stimulation with CRP-XL (Figure 4D), ADP (Figure 4E), AY-NH₂ (Figure 4F), and U46619 (Figure 4G) was significantly reduced compared with the controls. Additionally, preincubation of human platelets with WRW₄ (1.25-20 μ M) significantly decreased the number of adhered (Figure 5Ai) and spread (Figure 5Aii) platelets, and the relative surface area (Figure 5Aiii). The impact of *Fpr2/3* on the modulation of hemostasis in mice was determined by tail bleeding assay. A mean bleeding time of 428.5 \pm 64.8 seconds was observed in the control group; however, *Fpr2/3*-deficient mice significantly increased the bleeding time to a mean of 1128 \pm 71.9 seconds (Figure 5B). Together, these data emphasize the impact of FPR2/ALX on the regulation of normal platelet function through a positive feedback mechanism (may be through LL37), and thus the inhibition or deletion of this receptor results in diminished platelet function in general.

FPR2/ALX exerts its effects through cAMP-dependent signaling

FPRs are G_i-coupled receptors,³⁴ which are known to inhibit adenylate cyclase, reducing the level of cAMP, a known inhibitor of platelet function. Therefore, the deletion of G_i-coupled receptor genes in mice increases the basal cAMP levels in target cells.^{35,36} To investigate whether the inhibition of FPR2/ALX in human or deletion of *Fpr2/3* in mouse platelets is influenced by the cAMP-dependent signaling, the level of cAMP was quantified in platelets. The inhibition of FPR2/ALX with WRW₄ (20 μ M) significantly elevated the cAMP levels compared with the controls in human platelets (Figure 5Ci). Similarly, resting *Fpr2/3*^{-/-} mouse platelets exhibited elevated basal levels of cAMP compared with the controls (Figure 5Cii). In order to corroborate this data, we investigated the phosphorylation of the vasodilator-stimulated phosphoprotein (VASP), a substrate for protein kinase A that is involved in the regulation cAMP-mediated signaling. The treatment of platelets with an FPR2/ALX-selective inhibitor, WRW₄, increased the phosphorylation of Ser157-VASP (Figure 5Di). Similarly, *Fpr2/3*^{-/-} mouse platelets demonstrated increased phosphorylation of Ser157-VASP compared with control mouse platelets (Figure 5Dii).

Discussion

LL37 is a powerful antimicrobial peptide that plays substantial roles in the initiation of chemotaxis and subsequent inflammatory

Figure 2. The impact of LL37 on platelet activation, spreading, and calcium mobilization. (A) The level of fibrinogen binding was analyzed using fluorescein isothiocyanate-conjugated fibrinogen antibodies by flow cytometry in human isolated platelets (i) or PRP (ii). (B) Similarly, the level of P-selectin exposure was measured in human isolated platelets (i) or PRP (ii) using PE-Cy5-labeled P-selectin antibodies. Data represent mean \pm SEM (n = 3). (C) Platelet adhesion and spreading on immobilized fibrinogen was analyzed using platelets treated with LL37 (5, 10, and 20 μ M) by confocal microscopy (magnification \times 60; bar represents 10 μ m). The number of adhered (i) and spread (ii) platelets, and the relative surface area of spread platelets (iii) was determined via analyzing the images using ImageJ. Ten random fields of view were recorded and analyzed for each sample. Data represent mean \pm SEM (n = 3). (D) Ca²⁺ mobilization was measured using Fluo-4 AM dye-loaded human isolated platelets upon stimulation with LL37 by spectrofluorimetry. Data represent mean of maximum level of Ca²⁺ \pm SEM (n = 4). (E) The cytotoxic effects of LL37 were measured in human isolated platelets using a lactate dehydrogenase cytotoxicity assay kit. Data represent mean \pm SEM (n = 4). The statistical significance was established by 1-way ANOVA followed by Bonferroni's correction (*P < .05; **P < .01; ***P < .001).

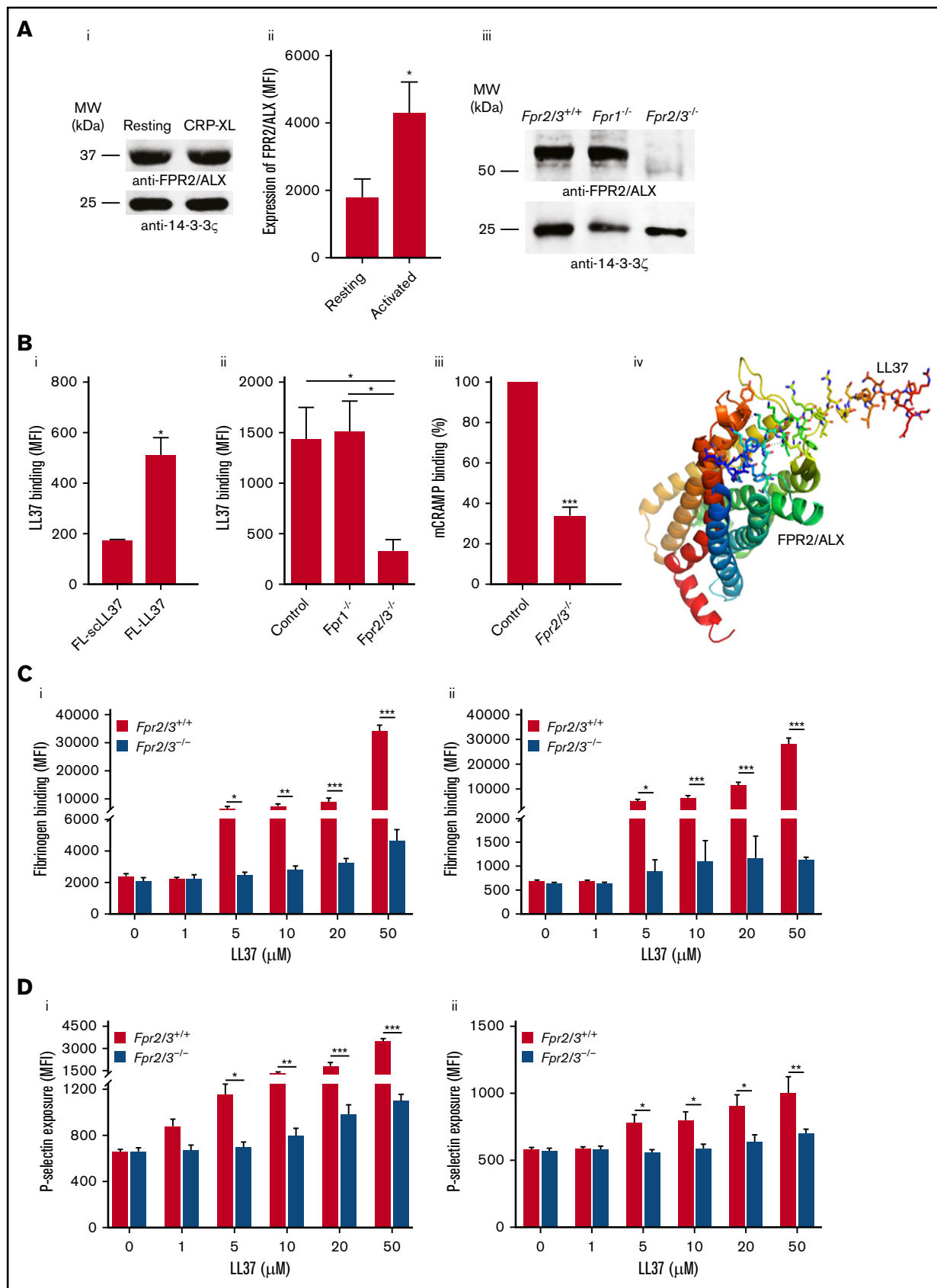


Figure 3.

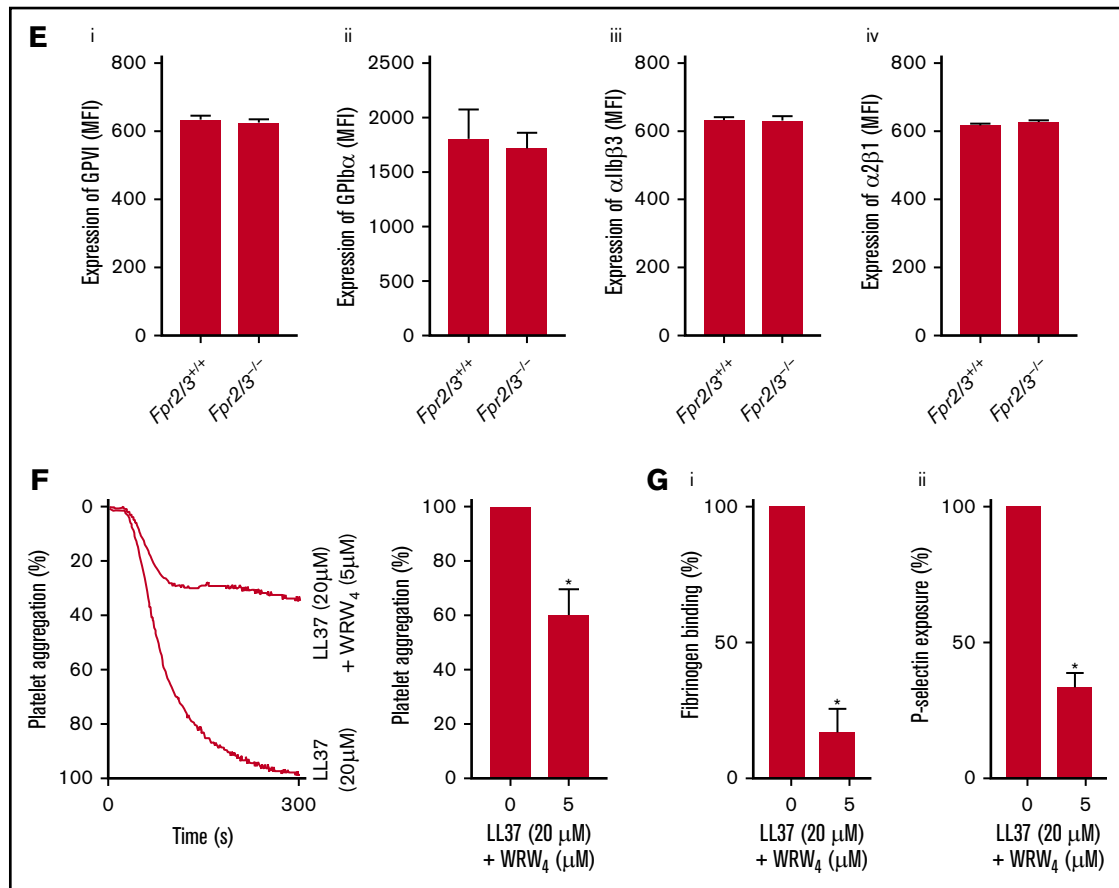


Figure 3. Expression of FPR2/ALX in platelets and its influence on LL37-mediated platelet activation. The presence of FPR2/ALX was confirmed in human (Ai) and mouse (Aiii) platelet lysates by immunoblot analysis using selective antibodies. The blots are representative of 3 separate experiments. The expression of FPR2/ALX on the surface of resting or activated (1 μg/mL CRP-XL) human platelets was analyzed using FPR2/ALX-selective and fluorescent-labeled secondary antibodies by flow cytometry (Aii). Data represent mean ± SEM (n = 4). The binding of LL37 to platelets was analyzed by flow cytometry. Human isolated platelets were incubated with 20 μM 5-FAM-LC-conjugated LL37 (FL-LL37) or scrambled LL37 (FL-scLL37), and the level of binding was analyzed by flow cytometry (Bi). Data represent mean ± SEM (n = 4). Similarly, platelets obtained from control, *Fpr2/3^{-/-}*, and *Fpr1^{-/-}* mice were analyzed with 20 μM 5-FAM-LC-conjugated LL37 or scrambled 5-FAM-LC-LL37 (Bii). Data represent mean ± SEM (n = 7). Similarly, platelets obtained from control or *Fpr2/3^{-/-}* mice were analyzed with 20 μM 5-FAM-conjugated mCRAMP or scrambled 5-FAM-mCRAMP (Biii). Data represent mean ± SEM (n = 4). The interactions between LL37 and FPR2/ALX were analyzed through structural modeling and molecular docking analysis (Biv). (C) The level of fibrinogen binding upon stimulation with LL37 in isolated platelets (i) or whole blood (ii) obtained from *Fpr2/3^{-/-}* or control mice was analyzed by flow cytometry. Data represent mean ± SEM (n = 10 for panel Ci; n = 8 for panel Cii). (D) Similarly, the level of P-selectin exposure was analyzed using isolated platelets (i) or whole blood (ii) from these mice. Data represent mean ± SEM (n = 10 for panel Di; n = 13 for panel Dii). (E) The expression levels of major platelet receptors such as GPVI (i), GPIbα (ii), αIIbβ3 (iii), and α2β1 (iv) in platelets obtained from *Fpr2/3^{-/-}* and control mice were analyzed by flow cytometry using selective fluorescent-labeled antibodies. Data represent mean ± SEM (n = 8 per group). (F) The effect of a selective inhibitor for FPR2/ALX, WRW₄ (5 μM), on LL37-induced platelet activation was measured by optical aggregometry. Data represent mean ± SEM (n = 3). (G) Mouse isolated platelets were stimulated with LL37 (20 μM) in the presence or absence WRW₄ (5 μM), and the level of fibrinogen binding (i) and P-selectin exposure (ii) were analyzed by flow cytometry. Data represent mean ± SEM (n = 4). The statistical significance was calculated using 1-way ANOVA followed by Bonferroni's correction in most of the experiments except for the data shown in panels Aii, B, and E-G, where a 2-tailed unpaired Student *t* test was used (**P* < .05; ***P* < .001; ****P* < .0001).

responses in immune cells including monocytes,¹⁶ mast cells,³⁷ eosinophils, and neutrophils.³⁸ Moreover, the involvement of LL37 in the development of pathological conditions such as sepsis, inflammatory bowel disease, psoriasis, and cystic fibrosis has been previously reported, and hence, its therapeutic potential has been analyzed in detail.³⁹ LL37 has also been found to play a role in the pathogenesis of atherosclerosis,^{40,41} wherein it leads to the development of lesions and recruitment of inflammatory cells at the site of injury.¹⁸ However, the role of LL37 in the modulation of thrombosis and hemostasis has not been investigated until recently.

Immediately prior to the submission of this manuscript, a recent study demonstrated the functional impact of LL37 in priming platelets and inducing thromboinflammatory conditions, although the molecular mechanisms that regulate such effects were not fully established.²¹ However, in this study, we have investigated the impact of LL37 in the modulation of platelet reactivity, thrombosis, and hemostasis under physiological conditions and uncovered the functional dependence of LL37 on FPR2/ALX in platelets.

The expression of LL37 has been reported in numerous cell types including epithelial cells and immune cells such as neutrophils

Table 1. Summary of polar contacts between LL37 and FPR2/ALX

Hydrogen bond interactions		
Interacting LL37 residues	Interacting FPR2/ALX residues	Average distance (Å)
Gly-3 (N)	Arg-26 (NH2)	2.76
Ser-9 (OG)	Glu-89 (OE1)	3.12
Ser-9 (O)	Glu-89 (OE2)	2.61
Lys-10 (N)	Glu-89 (OE2)	2.81
Ser-9 (OG)	Asn-171 (ND2)	3.00
Gln-22 (NE2)	Ser-182 (N)	3.20
Gln-22 (OE1)	Ser-182 (OG)	2.91
Gln-22 (NE2)	Ser-182 (OG)	3.14
Gln-22 (NE2)	Ser-182 (OG)	3.18
Glu-11 (OE2)	Gly-275 (N)	3.23
Lys-8 (NZ)	Lys-276 (O)	2.53
Arg-7 (NH1)	Asn-285 (OD1)	3.08
Arg-7 (NE)	Asn-285 (OD1)	3.29

and monocytes.⁴² Because platelets are also derived from the myeloid lineage,⁴³ we hypothesized that platelets may possess LL37, and indeed the presence of LL37 in platelets and its release to the external milieu upon activation were confirmed in this study. Similar to neutrophils, platelets may also contain LL37 in their granules and release it upon stimulation to increase its concentration at the local environment and enhance the secondary activation of platelets toward augmentation of thrombosis. A recent study²¹ also reported the elevated level of LL37 in the microenvironment of arterial thrombi in human and mice. Platelets are known to contain several antimicrobial peptides and release them upon activation during microbial infection.⁴⁴ Similarly, platelets may contribute to the release of LL37 upon activation to support the microbial clearance, activation of inflammatory responses, and modulation of thrombosis and hemostasis during pathological settings. Although the activation of platelets during inflammatory diseases is inevitable because of the presence of several molecules that activate platelets,⁴⁵ here we demonstrate LL37 as a major contributor to platelet activation and thrombus formation.

Thrombosis and subsequent bleeding are associated with various inflammatory diseases.⁴⁶ Similarly, disseminated intravascular coagulation, thrombosis in the microvasculature, and sequestration of platelets are some of the common clinical manifestations in sepsis.⁴⁷ The level of LL37 is significantly increased in psoriasis⁴⁸ and sepsis⁴⁹ patients compared with healthy individuals. In line with thrombosis in vasculature, LL37 augmented in vitro thrombus formation and shortened the bleeding time in mice. These data demonstrate a fundamental function for LL37 in the modulation of thrombosis and hemostasis. Similarly, LL37 induced platelet aggregation, fibrinogen binding, granule secretion, adhesion, spreading, and intracellular calcium mobilization in platelets. Pircher et al²¹ also demonstrated the functional impact of LL37 on arterial thrombosis and platelet granule secretion. In line with this previous study, we also did not observe the ability of LL37 to induce platelet aggregation in PRP, although it displayed aggregation in human

isolated platelets. Similarly, the previous study has failed to detect a response for LL37 on integrin $\alpha\text{IIb}\beta 3$ activation and platelet spreading on a fibrinogen-coated surface. In our study, however, we demonstrate the ability of LL37 to increase fibrinogen binding and platelet spreading. Surprisingly, the previous study failed to detect integrin $\alpha\text{IIb}\beta 3$ activation. However, we have directly measured the level of fibrinogen binding in isolated platelets, PRP, and whole blood with a range of concentrations of LL37 (ie, up to 50 μM), whereas they have measured PAC-1 binding in isolated platelets using LL37 concentrations of only up to 5 μM . It is unclear why these discrepancies occur between the previously reported data and our results, although it may be attributed in part to the differences in the methodologies used.

The concentrations used in this study (up to 50 μM) revealed the activatory effects of LL37 in platelets. A recent study reported the inhibitory effects of LL37 in platelets at concentrations between 0.1 and 1.2 mM.²⁸ These concentrations are not only substantially greater than those achievable in pathological conditions, but also exert cytotoxic effects in several cell types²⁹ including platelets (Figure 2E) at 100 μM . However, in severe psoriasis, a median concentration of 304 μM LL37 in psoriatic lesions has been reported,⁴⁸ which can exert cytotoxicity towards platelets at the local sites and reduce the number of functional platelets. During pulmonary infection, a concentration of 5 μM LL37 has been detected.⁵⁰ Notably, the normal plasma concentration of LL37 in healthy individuals is suggested to be ~ 1.2 μM ,⁵¹ which did not exert any effects on platelets. The LL37 concentrations used in this study are similar to those achievable during pathological conditions, such as sepsis,⁴⁹ and early stages of psoriasis. Hence, the LL37 inhibitory effects previously reported in platelets may well be because of cytotoxicity, although additional causes cannot be excluded. This perspective was also reflected in the recent study by Pircher et al.²¹ Together with the previous reports, our data demonstrate that LL37 induces platelet activation at the early stages of inflammatory diseases resulting in the initiation of thrombosis and modulation of hemostasis. However, at concentrations of 100 μM and above, LL37 may exert cytotoxicity, reducing the number and function of circulating platelets, which can ultimately lead to bleeding complications. Together with the modulation of thrombosis and hemostasis, LL37 may also induce other platelet-related complications (eg, thrombocytopenia and inflammation) during various inflammatory diseases where its level is elevated. Notably, the previous study²¹ has demonstrated the impact of LL37 in the augmentation of platelet-neutrophil interactions, cytokine release, release of extracellular nucleosomes, and reactive oxygen species.

LL37 has been reported to act mainly through FPR2/ALX in other cell types,^{16,24} although additional receptors such as Toll-like receptors, receptor tyrosine kinases, ligand-gated ion channel, CCR3, P2Y₁₁, and P2X₇ were shown to bind this peptide.⁵² To investigate the underlying molecular mechanisms through which LL37 modulates platelet function, the effects of LL37 in human platelets treated with WRW₄ and platelets obtained from *Fpr2/3*^{-/-} mice were analyzed. LL37-mediated activation was largely reduced by WRW₄ and in platelets obtained from *Fpr2/3*^{-/-} mice, confirming the functional dependence of LL37 primarily on FPR2/ALX. LL37 binding assays confirmed the substantial reduction in the binding of LL37 to *Fpr2/3*^{-/-} platelet surface compared with *Fpr1*^{-/-} and control mouse platelets. Additionally, we were able

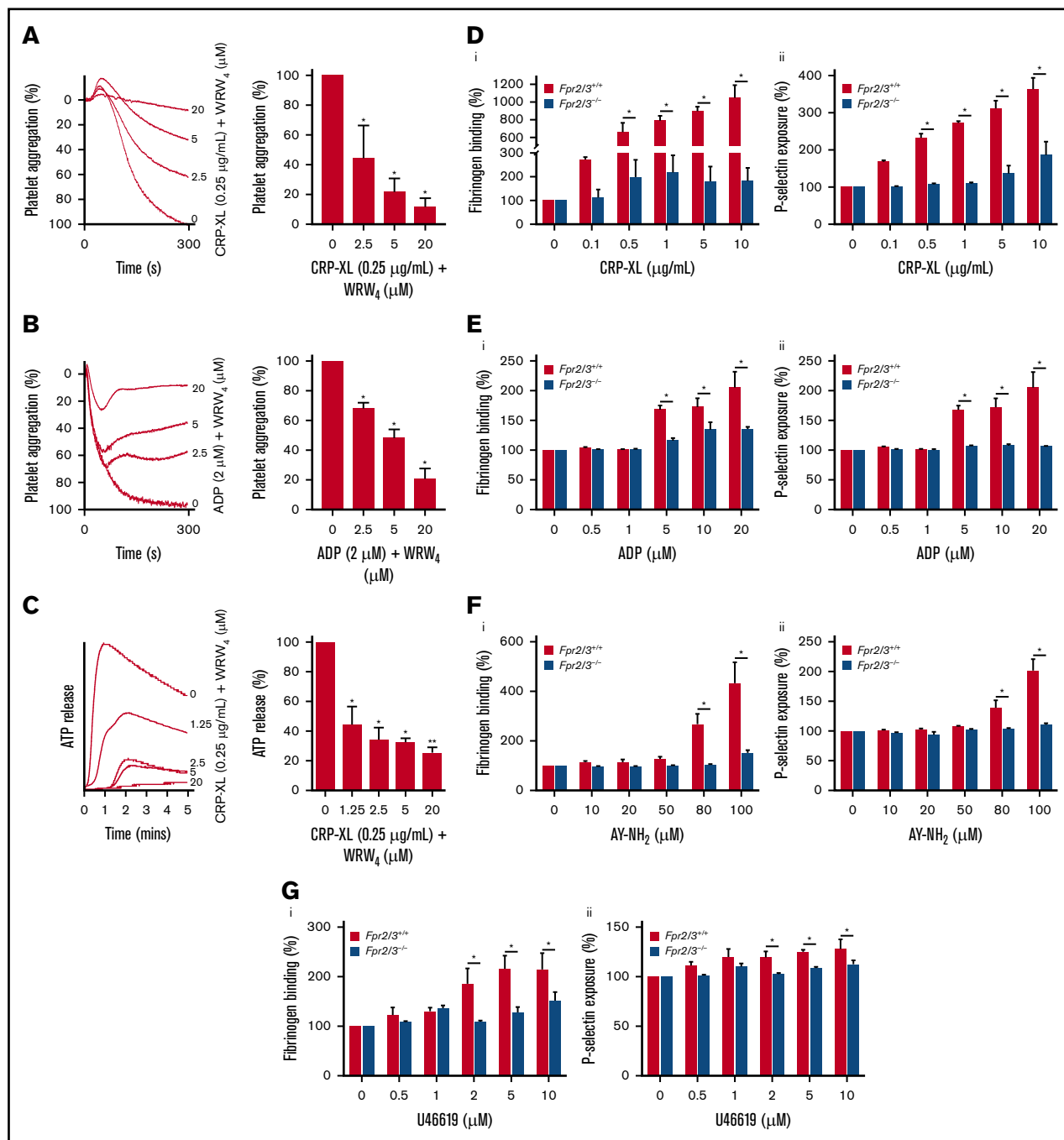


Figure 4. Positive feedback regulation of FPR2/ALX in platelets. The effects of different concentrations of WRW₄ on CRP-XL- (0.25 μ g/mL) (A) or ADP-induced (2 μ M) (B) human platelet aggregation was analyzed by optical aggregometry. (C) The level of adenosine triphosphate (ATP) secretion in human platelets (PRP) treated with WRW₄ prior to activation with CRP-XL (0.25 μ g/mL) was measured by lumi-aggregometry. The levels of fibrinogen binding (i) and P-selectin exposure (ii) were analyzed in platelets obtained from control or *Fpr2/3^{-/-}* mice upon stimulation with various concentrations of CRP-XL (D), ADP (E), AY-NH₂ (F), or U46619 (G) by flow cytometry. Data represent mean \pm SEM (n = 3). P values shown are as calculated by 2-way ANOVA followed by Bonferroni's correction in most of the experiments except for the data shown in panels A-C, which were analyzed by 1-way ANOVA followed by Bonferroni's correction (**P* < .05; ***P* < .01).

to demonstrate that FPR2/ALX inhibition in human platelets or deletion of *Fpr2/3* gene in mice lead to the elevation of cAMP levels, which is a major inhibitory molecule for platelet activation. This indicates the involvement of cAMP-dependent signaling

pathways in the regulation of FPR2/ALX in platelets. Nevertheless, the activation of platelets by LL37 through receptors other than FPRs cannot be excluded, and further investigations will be needed to explore the contributions of such receptors in the

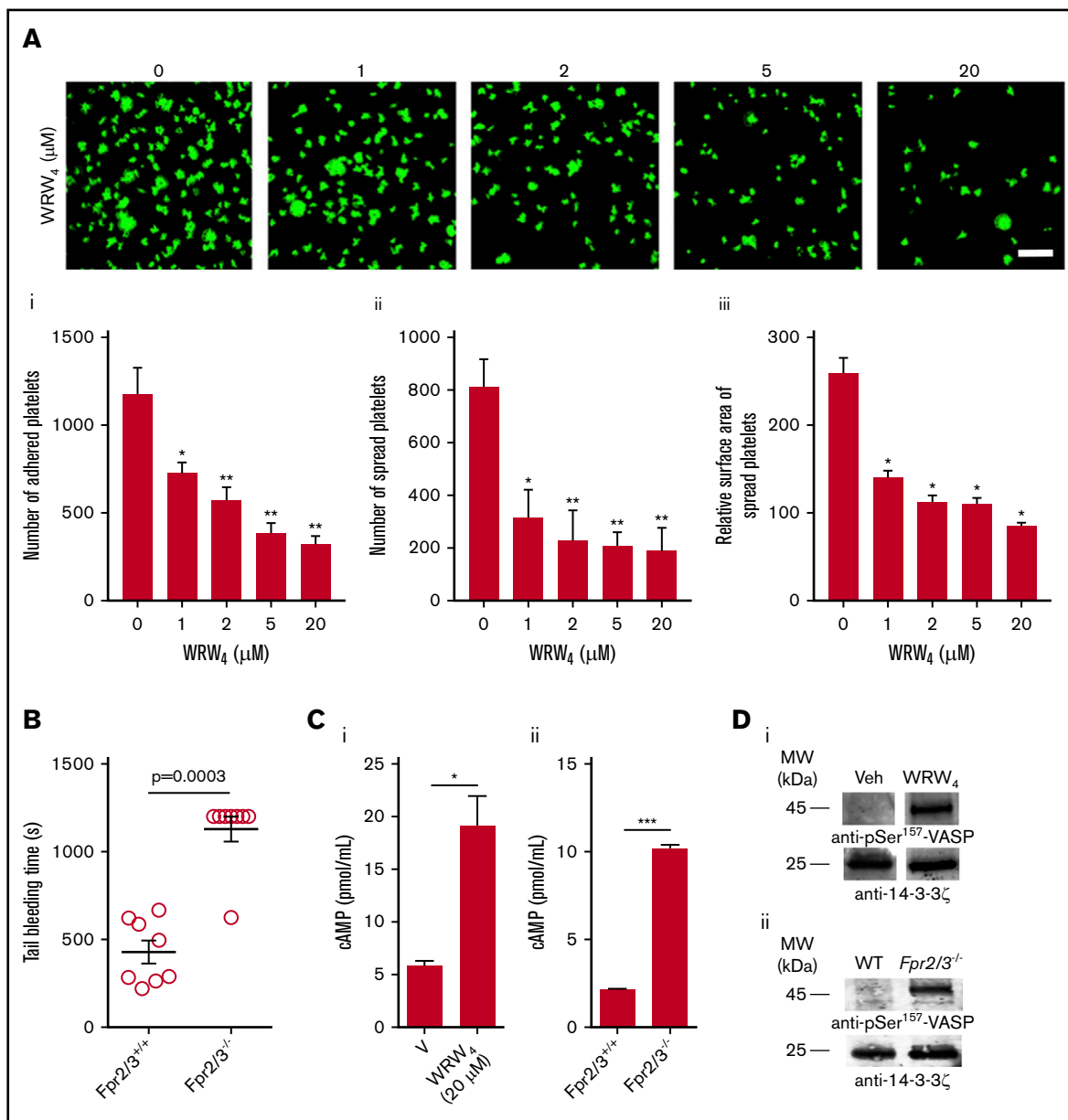


Figure 5. Impact of FPR2/ALX in platelet spreading, hemostasis, and cyclic adenosine monophosphate (cAMP)-mediated signaling. (A) Platelet adhesion and spreading on fibrinogen-coated glass surface was analyzed in the absence and presence of WRW₄ (1.25, 2.5, 5, and 20 μM) by confocal microscopy (magnification ×60; bar indicates 10 μm). The number of adhered (Ai) and spread (Aii) platelets and the relative surface area of spread platelets (Aiii) were determined by analyzing the images using ImageJ. Ten random fields of view were recorded for each sample. Data represent mean ± SEM (n = 3). (B) The impact of FPR2/ALX in the modulation of hemostasis was analyzed using tail bleeding assay in control or *Fpr2/3*^{-/-} mice. Data represent mean ± SEM (n = 8 in each group). (C) The level of cAMP in human isolated platelets in the presence or absence of WRW₄ (i) and control and *Fpr2/3*^{-/-} mouse platelets (ii) was analyzed using a cAMP assay kit. Data represent mean ± SEM (n = 4). (D) The phosphorylation of VASP at Ser-157 was analyzed in the presence of WRW₄ (i) and in platelets obtained from *Fpr2/3*^{-/-} mice (ii) by immunoblot analysis using selective antibodies. The blots are representative of 3 separate experiments. *P* values shown are as calculated by 1-way ANOVA followed by Bonferroni's correction in most of the experiments except for the data shown in panels B-C, where a nonparametric Mann-Whitney *U* test and a 2-tailed unpaired Student *t* test were used, respectively (**P* < .05; ***P* < .01; ****P* < .001).

modulation of platelet function upon ligation with LL37. Interestingly, the recent study²¹ has reported that LL37 is partially acting through the GPVI signaling pathway in platelets, but it does not have any impact on G protein-coupled receptor-mediated signaling specifically via FPR1 and FPR2/ALX using a single concentration of pharmacological inhibitors (Boc-MLF and

WRW₄) for these receptors. However, in the present study, we report the presence of FPR2/ALX (a G protein-coupled receptor) and its role in the regulation of LL37-mediated effects in platelets using a range of concentrations of these pharmacological inhibitors and platelets obtained from *Fpr2/3*^{-/-} mice in multiple experiments.

In conclusion, we demonstrate that LL37 is stored in platelets and secreted upon activation. Similar to a recent publication,²¹ we also report that LL37 promotes thrombus formation. LL37 induced a range of platelet function such as platelet aggregation, inside-out signaling to integrin $\alpha\text{IIb}\beta 3$ and outside-in signaling, granule secretion, calcium mobilization, and shortened tail bleeding time in mice. These effects were diminished in the presence of an FPR2/ALX pharmacological inhibitor and in platelets obtained from *Fpr2/3*^{-/-} mice confirming the functional dependence of LL37 primarily via this receptor in platelets. Additionally, we demonstrate an instrumental role for FPR2/ALX in the positive feedback regulation of platelet function, in which the deficiency or blockade of this receptor impaired hemostasis and the normal activation of platelets. The significant roles of LL37 and FPR2/ALX in the modulation of thrombosis and hemostasis renders them potential candidates for the exacerbation of platelet-related complications and immune responses in numerous inflammatory diseases where platelets play critical roles. Notably, the presence of FPRs in platelets opens up new avenues to investigate the involvement of a multiplicity of FPR ligands in the modulation of thrombosis, hemostasis, and other platelet-related complications during inflammatory responses. Based on the data presented in this study, both LL37 and FPRs can act as potential

therapeutic targets for cardiovascular and a range of inflammatory diseases.

Acknowledgments

This work was supported by grants from the Wellcome Trust (204389/Z/16/Z), the British Heart Foundation (PG/16/64/32311), the Royal Society, the British Pharmacological Society, the Physiological Society, and the Saudi Arabian Ministry of Higher Education.

Authorship

Contribution: M.F.S. and S.V. designed the study, performed experiments, analyzed data, and wrote the manuscript; D.R., X.K., L.A.M., H.F.W., T.M.V., D.A.A., R.V., and K.W. performed experiments and analyzed data; and J.M.G., S.D.B., and M.P. provided expertise and reagents for specific experiments and support during the preparation of the manuscript.

Conflict-of-interest disclosure: The authors declare no competing financial interests.

ORCID profile: S.V., 0000-0002-6006-6517.

Correspondence: Sakthivel Vaiyapuri, School of Pharmacy, University of Reading, Reading RG6 6UB, United Kingdom; e-mail: s.vaiyapuri@reading.ac.uk.

References

- Gibbins JM. Platelet adhesion signalling and the regulation of thrombus formation. *J Cell Sci*. 2004;117(16):3415-3425.
- Vaiyapuri S, Flora GD, Gibbins JM. Gap junctions and connexin hemichannels in the regulation of haemostasis and thrombosis. *Biochem Soc Trans*. 2015;43(3):489-494.
- Ravishankar D, Salamah M, Attina A, et al. Ruthenium-conjugated chrysin analogues modulate platelet activity, thrombus formation and haemostasis with enhanced efficacy. *Sci Rep*. 2017;7:5738.
- Hamzeh-Cognasse H, Damien P, Chabert A, Pozzetto B, Cognasse F, Garraud O. Platelets and infections - complex interactions with bacteria. *Front Immunol*. 2015;6:82.
- Rondina MT, Garraud O. Emerging evidence for platelets as immune and inflammatory effector cells. *Front Immunol*. 2014;5:653.
- Gisondi P, Girolomoni G. Psoriasis and atherothrombotic diseases: disease-specific and non-disease-specific risk factors. *Semin Thromb Hemost*. 2009;35(3):313-324.
- Santilli S, Kast DR, Grozdev I, et al. Visualization of atherosclerosis as detected by coronary artery calcium and carotid intima-media thickness reveals significant atherosclerosis in a cross-sectional study of psoriasis patients in a tertiary care center. *J Transl Med*. 2016;14(1):217.
- Tamagawa-Mineoka R, Katoh N, Kishimoto S. Platelet activation in patients with psoriasis: increased plasma levels of platelet-derived microparticles and soluble P-selectin. *J Am Acad Dermatol*. 2010;62(4):621-626.
- Tamagawa-Mineoka R, Katoh N, Ueda E, Masuda K, Kishimoto S. Elevated platelet activation in patients with atopic dermatitis and psoriasis: increased plasma levels of beta-thromboglobulin and platelet factor 4. *Allergol Int*. 2008;57(4):391-396.
- Vallance TM, Zeuner MT, Williams HF, Widera D, Vaiyapuri S. Toll-like receptor 4 signalling and its impact on platelet function, thrombosis, and haemostasis. *Mediators Inflamm*. 2017;2017:9605894.
- Larrick JW, Hirata M, Balint RF, Lee J, Zhong J, Wright SC. Human CAP18: a novel antimicrobial lipopolysaccharide-binding protein. *Infect Immun*. 1995;63(4):1291-1297.
- Jacobsen AS, Jenssen H. Human cathelicidin LL-37 prevents bacterial biofilm formation. *Future Med Chem*. 2012;4(12):1587-1599.
- Wong JH, Ng TB, Legowska A, Rolka K, Hui M, Cho CH. Antifungal action of human cathelicidin fragment (LL13-37) on *Candida albicans*. *Peptides*. 2011;32(10):1996-2002.
- Barlow PG, Svoboda P, Mackellar A, et al. Antiviral activity and increased host defense against influenza infection elicited by the human cathelicidin LL-37. *PLoS One*. 2011;6(10):e25333.
- Agier J, Efenberger M, Brzezińska-Błaszczak E. Cathelicidin impact on inflammatory cells. *Cent Eur J Immunol*. 2015;40(2):225-235.
- De Yang, Chen Q, Schmidt AP, et al. LL-37, the neutrophil granule- and epithelial cell-derived cathelicidin, utilizes formyl peptide receptor-like 1 (FPR1) as a receptor to chemoattract human peripheral blood neutrophils, monocytes, and T cells. *J Exp Med*. 2000;192(7):1069-1074.

17. Hwang YJ, Jung HJ, Kim MJ, et al. Serum levels of LL-37 and inflammatory cytokines in plaque and guttate psoriasis. *Mediators Inflamm*. 2014;2014:268257.
18. Kahlenberg JM, Kaplan MJ. Little peptide, big effects: the role of LL-37 in inflammation and autoimmune disease. *J Immunol*. 2013;191(10):4895-4901.
19. Sørensen O, Arnljots K, Cowland JB, Bainton DF, Borregaard N. The human antibacterial cathelicidin, hCAP-18, is synthesized in myelocytes and metamyelocytes and localized to specific granules in neutrophils. *Blood*. 1997;90(7):2796-2803.
20. Lowry MB, Guo C, Borregaard N, Gombart AF. Regulation of the human cathelicidin antimicrobial peptide gene by 1 α ,25-dihydroxyvitamin D3 in primary immune cells. *J Steroid Biochem Mol Biol*. 2014;143:183-191.
21. Pircher J, Czermak T, Ehrlich A, et al. Cathelicidins prime platelets to mediate arterial thrombosis and tissue inflammation. *Nat Commun*. 2018;9:1523.
22. Gao JL, Lee EJ, Murphy PM. Impaired antibacterial host defense in mice lacking the N-formylpeptide receptor. *J Exp Med*. 1999;189(4):657-662.
23. Dufton N, Hannon R, Brancalione V, et al. Anti-inflammatory role of the murine formyl-peptide receptor 2: ligand-specific effects on leukocyte responses and experimental inflammation. *J Immunol*. 2010;184(5):2611-2619.
24. Gordon YJ, Huang LC, Romanowski EG, Yates KA, Proske RJ, McDermott AM. Human cathelicidin (LL-37), a multifunctional peptide, is expressed by ocular surface epithelia and has potent antibacterial and antiviral activity. *Curr Eye Res*. 2005;30(5):385-394.
25. Agerberth B, Charo J, Werr J, et al. The human antimicrobial and chemotactic peptides LL-37 and α -defensins are expressed by specific lymphocyte and monocyte populations. *Blood*. 2000;96(9):3086-3093.
26. Ravishanker D, Salamah M, Akimbaev A, et al. Impact of specific functional groups in flavonoids on the modulation of platelet activation. *Sci Rep*. 2018;8:9528.
27. Vaiyapuri S, Sage T, Rana RH, et al. EphB2 regulates contact-dependent and contact-independent signaling to control platelet function. *Blood*. 2015;125(4):720-730.
28. Su W, Chen Y, Wang C, Ding X, Rwbisira G, Kong Y. Human cathelicidin LL-37 inhibits platelet aggregation and thrombosis via Src/PI3K/Akt signaling. *Biochem Biophys Res Commun*. 2016;473(1):283-289.
29. Johansson J, Gudmundsson GH, Rottenberg ME, Berndt KD, Agerberth B. Conformation-dependent antibacterial activity of the naturally occurring human peptide LL-37. *J Biol Chem*. 1998;273(6):3718-3724.
30. Wan M, Godson C, Guiry PJ, Agerberth B, Haeggström JZ. Leukotriene B4/antimicrobial peptide LL-37 proinflammatory circuits are mediated by BLT1 and FPR2/ALX and are counterregulated by lipoxin A4 and resolvin E1. *FASEB J*. 2011;25(5):1697-1705.
31. Iaccio A, Cattaneo F, Mauro M, Ammendola R. FPRL1-mediated induction of superoxide in LL-37-stimulated IMR90 human fibroblast. *Arch Biochem Biophys*. 2009;481(1):94-100.
32. Czapiga M, Gao JL, Kirk A, Lekstrom-Himes J. Human platelets exhibit chemotaxis using functional N-formyl peptide receptors. *Exp Hematol*. 2005;33(1):73-84.
33. Rowley JW, Oler AJ, Tolley ND, et al. Genome-wide RNA-seq analysis of human and mouse platelet transcriptomes. *Blood*. 2011;118(14):e101-e111.
34. Wenzel-Seifert K, Arthur JM, Liu HY, Seifert R. Quantitative analysis of formyl peptide receptor coupling to G(i)alpha(1), G(i)alpha(2), and G(i)alpha(3). *J Biol Chem*. 1999;274(47):33259-33266.
35. Yang J, Wu J, Jiang H, et al. Signaling through Gi family members in platelets. Redundancy and specificity in the regulation of adenylyl cyclase and other effectors. *J Biol Chem*. 2002;277(48):46035-46042.
36. Liu YF, Ghahremani MH, Rasenick MM, Jakobs KH, Albert PR. Stimulation of cAMP synthesis by Gi-coupled receptors upon ablation of distinct G α i protein expression. Gi subtype specificity of the 5-HT1A receptor. *J Biol Chem*. 1999;274(23):16444-16450.
37. Niyonsaba F, Iwabuchi K, Someya A, et al. A cathelicidin family of human antibacterial peptide LL-37 induces mast cell chemotaxis. *Immunology*. 2002;106(1):20-26.
38. Tjabringa GS, Ninaber DK, Drijfhout JW, Rabe KF, Hiemstra PS. Human cathelicidin LL-37 is a chemoattractant for eosinophils and neutrophils that acts via formyl-peptide receptors. *Int Arch Allergy Immunol*. 2006;140(2):103-112.
39. Fabisiak A, Murawska N, Fichna J. LL-37: cathelicidin-related antimicrobial peptide with pleiotropic activity. *Pharmacol Rep*. 2016;68(4):802-808.
40. Edfeldt K, Agerberth B, Rottenberg ME, et al. Involvement of the antimicrobial peptide LL-37 in human atherosclerosis. *Arterioscler Thromb Vasc Biol*. 2006;26(7):1551-1557.
41. Döring Y, Drechsler M, Wantha S, et al. Lack of neutrophil-derived CRAMP reduces atherosclerosis in mice. *Circ Res*. 2012;110(8):1052-1056.
42. Bandurska K, Berdowska A, Barczyńska-Felusiak R, Krupa P. Unique features of human cathelicidin LL-37. *Biofactors*. 2015;41(5):289-300.
43. Ogawa M. Differentiation and proliferation of hematopoietic stem cells. *Blood*. 1993;81(11):2844-2853.
44. Tang YQ, Yeaman MR, Selsted ME. Antimicrobial peptides from human platelets. *Infect Immun*. 2002;70(12):6524-6533.
45. Nording HM, Seizer P, Langer HF. Platelets in inflammation and atherogenesis. *Front Immunol*. 2015;6:98.
46. Ahlehoff O, Gislason GH, Lindhardsen J, et al. Psoriasis carries an increased risk of venous thromboembolism: a Danish nationwide cohort study. *PLoS One*. 2011;6(3):e18125.
47. Semeraro N, Ammollo CT, Semeraro F, Colucci M. Sepsis-associated disseminated intravascular coagulation and thromboembolic disease. *Mediterr J Hematol Infect Dis*. 2010;2(3):e2010024.
48. Ong PY, Ohtake T, Brandt C, et al. Endogenous antimicrobial peptides and skin infections in atopic dermatitis. *N Engl J Med*. 2002;347(15):1151-1160.

49. Berkestedt I, Herwald H, Ljunggren L, Nelson A, Bodelsson M. Elevated plasma levels of antimicrobial polypeptides in patients with severe sepsis. *J Innate Immun.* 2010;2(5):478-482.
50. Schaller-Bals S, Schulze A, Bals R. Increased levels of antimicrobial peptides in tracheal aspirates of newborn infants during infection. *Am J Respir Crit Care Med.* 2002;165(7):992-995.
51. Sørensen O, Cowland JB, Askaa J, Borregaard N. An ELISA for hCAP-18, the cathelicidin present in human neutrophils and plasma. *J Immunol Methods.* 1997;206(1-2):53-59.
52. Verjans ET, Zels S, Luyten W, Landuyt B, Schoofs L. Molecular mechanisms of LL-37-induced receptor activation: An overview. *Peptides.* 2016;85: 16-26.